

Energy Efficient Mobility Systems

2020 Annual Progress Report

Vehicle Technologies Office

(This page intentionally left blank)

Disclaimer

This report was prepared as an account of work sponsored by an agency of the United States government. Neither the United States government nor any agency thereof, nor any of their employees, makes any warranty, express or implied, or assumes any legal liability or responsibility for the accuracy, completeness, or usefulness of any information, apparatus, product, or process disclosed or represents that its use would not infringe privately owned rights. Reference herein to any specific commercial product, process, or service by trade name, trademark, manufacturer, or otherwise does not necessarily constitute or imply its endorsement, recommendation, or favoring by the United States government or any agency thereof. The views and opinions of authors expressed herein do not necessarily state or reflect those of the United States government or any agency thereof.

Acknowledgements

We would like to acknowledge and thank the lead authors of the SMART Mobility Capstone Reports for their tireless efforts, patience, and leadership in publishing the results of the SMART Mobility Consortium’s research through our six Capstone Reports: Eric Rask (ANL) for Connected and Automated Vehicles; John Smart (INL) for Advanced Fueling Infrastructure; David Smith (ORNL) for Multi-Modal Freight; Anna Spurlock (LBNL) for Mobility Decision Science; Stan Young (NREL) for Urban Science; and Aymeric Rousseau (ANL) for the SMART Mobility Modeling Workflow. SMART Mobility represents a cornerstone of the EEMS Program, and its success is due to the dedication of these individuals, as well as contributions from many other national lab staff members.

Additionally, we would like to thank Danielle Chou for her contributions to the EEMS Program in 2020. As an AAAS Mobility Research Fellow, Ms. Chou has been a tremendous asset to the EEMS team, providing valuable insight, perspective, and project management capabilities. We thank Danielle for the role she has played and acknowledge her service to DOE.

Finally, we would like to acknowledge all the researchers, participants, and stakeholders that contributed to and collaborated with the Energy Efficient Mobility Systems Program this past year. The global COVID-19 pandemic has impacted the lives of Americans—ourselves, as well as our friends, families, and colleagues—in immeasurable ways. The disruption not only affected the transportation system, leading to an urgent need to apply EEMS research capabilities to new challenges, but it also created new obstacles to the work we do. We acknowledge the creativity, resilience, and perseverance of those in the EEMS community who found new ways to accomplish the program’s goals.

Acronyms

A

AADT	Average Annual Daily Traffic
AC	Alternating Current
ACC	Adaptive Cruise Control
accel	Acceleration
ACES	Automated, Connected, Efficient Shared Mobility
ACS	Advanced Combustion Systems
AEO	Annual Energy Outlook
AER	All-electric range
AFI	Advanced Fueling Infrastructure
AFV	Alternative Fuel Vehicle
AMD	Automated Mobility District
AMT	Automated Mechanical Transmission
ANL	Argonne National Laboratory
ANN	Artificial Neural Network
AOI	Areas of Interest
APEC	Asia Pacific Economic Council
APRF	Advanced Powertrain Research Facility
APT	Pressure Sensor
ASD	Aftermarket Safety Device
AT	Autonomous Taxi
ATDM	Active Transportation Demand Management
ATW	Active Transmission Warm up
AVTE	Advanced Vehicle Testing and Evaluation

B

BaSc	Baseline and Scenario
Batt	Battery
BEAM	Framework for Behavior, Energy, Autonomy, and Mobility
BEB	Battery Next-Generation Electric Transit Bus
BET	Battery Electric Truck
BEV	Battery Electric Vehicle
BMW	Bayerische Motoren Werke AG
BSFC	Brake Specific Fuel Consumption
BSM	Basic Safety Message
BTE	Brake Thermal Efficiency

C

CAC	Charge Air Cooler
CACC	Cooperative Adaptive Cruise Control
CAE	Computer-Aided Engineering
CAEV	Connected and automated electric vehicles

CAFE	Corporate Average Fuel Economy
CAN	Controller Area Network
CAV	Connected and automated vehicles
CARB	California Air Resources Board
CBD	Central Business District
CCS	Combined Charging System
CW, CCW	Clockwise, Counter Clockwise
CD	Charge-Depleting
CERV	Conference on Electric Roads and Vehicles
CFD	Computational Fluid Dynamics
CFDC	Commercial Fleet Data Center
CFL	Combined Fluid Loop
CH ₄	Methane
CHTS	California Household Travel Survey
CRHTI	Chicago Regional Household Travel Inventory
CIP	Common Integration Platform
CMAP	Chicago Metropolitan Agency for Planning
Cm ³	Cubic
CNG	Compressed Natural Gas
CO	Carbon monoxide
CO ₂	Carbon Dioxide
COMM	Commuter
Conv	Conventional Vehicle
COP	Coefficient of Performance
CPT	Cumulative prospect theory
CRADA	Cooperative Research and Development Agreement
CS	Charge Sustaining
Cs	Cold start
CV	Conventional vehicle

D

D3	Downloadable Dynamometer Database
DC	Direct current
DCFC	Direct Current Fast Charge
DCT	Dual-clutch transmission
decel	Deceleration
DER	Distributed energy resource
DFGM	Digital Flux Gate Magnetometer
DFMEA	Design of Failure Modes Analysis
DOE	U.S. Department of Energy
DOHC	Dual overhead cam
DS	Down speeding
DSM	Distributed Security Module
DSM	Diagnostic Security Module
DSP	Digital Signal Processor

DSRC	Dedicated Short Range Communications
DTA	Dynamic traffic assignment
DWPT	Dynamic Wireless Power Transfer
dt	Change in time
dv	Change in velocity
Dyno	Dynamometer

E

EAD	Signal eco-approach and departure
EAVS	Electrically Assisted Variable Speed Supercharger
EC	European Commission
EDV	Electric Drive Vehicle
EDX	Energy dispersive x-ray spectroscopy
EERE	Energy Efficiency and Renewable Energy
EGR	Exhaust Gas Recirculation
EG/W	Ethylene glycol/water
EIA	Energy Information Agency
EOL	End of life
EPA	Environmental Protection Agency
ePATHS	Electrical PCM Assisted Thermal Heating System
EREV	Extended-Range Electric Vehicles
ESIF	Energy Systems Integration Facility
ESS	Energy Storage System
ETT	Electric Transportation Technologies
E-TREE	Electric Truck with Range Extending Engine
EUMD	End-Use Measurement Device
EV	Electric Vehicle
EVI-Pro	Electric Vehicle Infrastructure Projection Tool
EV2G	Electric Vehicle-to-Grid
eVMT	Electric Vehicle Miles Traveled
EVSE	Electric Vehicle Service Equipment
EXV	Electronic Expansion Valve

F

FAF	Freight Analysis Framework
FASTSim	Future Automotive Systems Technology Simulator
FC	Fuel cell
FC	Fast charge
FCons	Fuel consumption
FCTO	Fuel Cell Technologies Office
FCV	Fuel Cell Vehicle
FCR	Fuel consumption rate
FE	Fuel Economy
FEA	Finite Element Analysis
FEX	Front-end Heat Exchanger

FFLEET	Freight Fleet Level Energy Estimation Tool
FG	Fixed gear ratio
FGLD	Fine-grained location data
FHWA	Federal Highway Administration
FLNA	Frito-Lay North America
FM	Friction Modifier
FMEP	Friction Mean Effective Pressure
FOA	Funding Opportunity Announcement
FTIR	Fourier transform infrared spectroscopy
FTP	Federal Test Procedure
FWD	Four-wheel drive
FY	Fiscal year
G	
G	gram
GB	Gigabyte
GCEDV	Grid Connected Electrical Drive Vehicles
GEM	Gas Emissions Model
GGE	Gasoline gallon equivalent
GHG	Greenhouse Gas
GITT	Grid Interaction Tech Team
GM	General Motors
GMLC	Grid Modernization Lab Consortium
GnPs	Graphene nanoplatelets
GO	Graphene Oxide
GPRA	Government Performance and Results Act
GPS	Global Positioning System
GREET	Greenhouse gases, Regulated Emissions, and Energy use in Transportation
GSF1	Generic Speed Form 1
GSU	Grid side unit
GUI	Graphic User Interface
GVW	Gross Vehicle Weight
H	
h-APU	hybrid Auxiliary Power Unit
HC	Unburned hydrocarbons
HD	Heavy Duty
HEV	Hybrid-Electric Vehicle
HHDDT	Heavy Heavy-Duty Diesel Truck
HHV	Hydraulic Hybrid Vehicle
HIL	Hardware-In-the-Loop
HP	Heat Pump
Hp	Horsepower
HTML	HyperText Markup Language
HV	High Voltage

HVAC	Heating Ventilating and Air Conditioning
HWFET	Highway Fuel Economy Test
HPMS	Highway Performance Monitoring System
HVTB	High Voltage Traction Battery
HWY	Highway Program or Highway Fuel Economy Test Cycle
HPC	High Performance Computing
HTR	Heater
Hz	Hertz

I

I	Inertia
IC	Internal Combustion
ICDV	Internal Combustion Drive Vehicles
ICE	Internal Combustion Engine
ICTF	Intermodal Container Transfer Facility
ICU	Inverter-Charger Unit
IEB	Information Exchange Bus
IEC	International Electrotechnical Commission
IGBT	Insulated Gate Bipolar Transistors
IHX	Internal Heat Exchanger
INL	Idaho National Laboratory
IOT	Internet of Things
IR	Infrared Radiation
ISO	International Organization for Standardization
ITS	Intelligent Transportation Systems

J

JIT	Just-in-Time
-----	--------------

K

kg	Kilogram
km	Kilometer
kW	Kilowatt
kWh	Kilowatt hour

L

L	litre
L1	Level 1 benchmark
L2	Level 2 benchmark
Lbf	Pounds force
LCC	Liquid-Cooled Condenser
LCV	Long combination vehicle
LD	Light-duty
LH	line haul
Li	Lithium

LIB	Lithium-ion battery
LLNL	Lawrence Livermore National Laboratory
LTC	Lockport Technical Center
LV	Leading Vehicle
M	
M	Mass
MaaS	Mobility as a Service
MBSE	Model Based System Engineering
MEP	Mobility energy productivity (MEP)
MD	Medium Duty
MDCEV	Multiple Discrete-Continuous Extreme Value
MDS	Mobility Decision Science
mpg	Miles per gallon
MMTCE	Million Metric Tons of Carbon Equivalent
MIIT	Ministry of Industry and Information Technology
mi	Mile
MJ	Megajoules
MONLP	Multi-Objective Non-Linear Program
MORPC	Mid-Ohio Regional Planning Commission
MOSFET	Metal-Oxide Semiconductor Field-Effect Transistor
MNL	Multinomial Logit
mph	Miles per hour
MPGe	Miles per gallon equivalent, Miles per gallon gasoline equivalent
MTC	Metropolitan Transportation Commission
MTDC	Medium Truck Duty Cycle
MOVES	Motor Vehicle Emission Simulator
MPR	Market Penetration Rates
MRF	Moving Reference Frame
MURECP	Medium-Duty Urban Range Extended Connected Powertrain
MY	Model year
M ²	Meters squared
N	
NACFE	North American Council for Freight Efficiency
NCCP	Normalized cross-correlation power
NDA	Non-Disclosure Agreement
NETL	National Energy Technology Laboratory
NHTS	National Household Travel Survey
NHTSA	National Highway Transportation Safety Administration
NM	Newton meters
NO _x	Nitrogen oxides
NR	Natural Rubber
NRE	Non Recurring Engineering
NREL	National Renewable Energy Laboratory

NRT	National Retail Trucking
NVH	Noise, vibration, and harshness
NVUSD	Napa Valley Unified School District
NYSERDA	New York State Energy Research Development Authority

O

OBC	On-board charger
OCBC	Orange County Bus Cycle
OEM	Original Equipment Manufacturer
OneSAF	One Semi-Automated Forces
ORNL	Oak Ridge National Laboratories

P

P	Active Power
PC	Polycarbonate
PCM	Phase-Change Material
PCU	Power Control Unit
PCU	Powertrain Control Unit
PEEM	Power Electronics and Electric Motor
PEV	Plug-In Electric Vehicle
PFC	Power factor correction
PFI	Port fuel injection
PGW	Pittsburgh Glass Works
PHEV	Plug-in Hybrid Electric Vehicle
PHEV##	Plug-in hybrid electric vehicle with ## miles of all-electric range
PI	Principal Investigator
PID	Proportional+Integral+Derivative
PM	Permanent Magnet
PM	Particulate Matter
PMP	Pontryagin Minimum Principle
PMT	Passenger/Person Miles Traveled
ppm	Parts per Million
PTC	Positive Temperature Coefficient (Electric Heater)
PTO	Power Take-Off
PVP	Polyvinylpyrrolidone
PWWMD	Public Works and Waste Management Department
λ	Power Factor
ϕ	Power Angle

Q

Q	Reactive power
QA	Quality assurance
QC	Quality control

R

R2	Coefficient of Determination
R/D	Receiver / Dryer
REV	New York State's Reforming the Energy Vision Initiative
REx	Range Extending Engine
rGO	reduced graphene oxide
RH	Relative Humidity
RMS	Root Mean Square
ROL	Ring-On-Liner
rpm	Revolutions Per Minute
RSU	Road Side Unit
RTRP-	Random-Thresholds, Random-Parameters Hierarchical Ordered Probit
RWDC	Real-World Drive-Cycle

S

S	Apparent power
SAE	Society of Automotive Engineers
SAV	Shared Automated Vehicles
SCAG	Southern California Association of Governments
SCAQMD	South Coast Air Quality Management District
SCIG	Southern California International Gateway
SDO	Standards Definition Organizations
SI	Système International d'Unités
SI	Gasoline Spark Ignition
SMART	Systems and Modeling for Accelerated Research in Transportation
SNR	Sensor
SOC	State of Charge
SPaT	Signal phase and timing
SPRINGS	Statistical Planning for Resilience in Next Generation Systems
SPL	Sound Pressure Level
SR	Speed Ratio
SS	Steady State
S/S	Start/Stop
SPaT	Signal Phase and Timing
STELLA	Strongly-TypEd, Lisp-like LAnguage
StAR	Storage-Assisted Recharging
SVET	Smart vehicle energy technology
SVTrip	Stochastic Vehicle Trip Creator

T

T	Torque
TA	Technical Area
TA	Torque Assist
TC	Thermocouple
TAZ	Traffic Analysis Zone
TCO	Total cost of ownership

TE	Thermoelectric
TE	Transmission Error
TES	Thermal Energy Storage
TGA	Thermogravimetric analysis
THC	Total hydrocarbon emissions
TIM	Thermal Interface Materials
TLRP	Thermal Load Reduction Package
TN	Testing Network
TNC	Transportation Network Companies
TOU	Time-Of-Use
TRB	Transportation Research Board
TSDC	Transportation Secure Data Center
TSI	Turbocharged stratified injection
TTC	Time to Collision
TV	Trailing Vehicle
TXVs	Thermal Expansion Valves

U

U.S.	U.S. Driving Research and Innovation for Vehicle Efficiency and Energy Sustainability
UA	Transfer Coefficient
UC	Ultra-capacitor
UCR	University of California, Riverside
UDDS	Urban Dynamometer Driving Schedule
UM	University of Michigan
UN ECE	United Nations Economic Council for Europe
UNSW	University of New South Wales
UPS	United Parcel Service
URL	Uniform Resource Locator
US06	Environmental Protection Agency US06 or Supplemental Federal Test Procedure
USABC	United States Advanced Battery Consortium
USCAR	U.S. Council for Automotive Research
Util	Battery capacity utilization

V

V	Voltage
V2G	Vehicle-to-Grid
V2I	Vehicle-to-Infrastructure
V2V	Vehicle to Vehicle
VAr	Volt-Amp-reactive
VCC	Volvo Car Corp
VGI	Vehicle-Grid Integration
VGT	Variable Geometry Turbocharger
VHT	Vehicle hours traveled
VIP	Vacuum insulated panels
VKT	Vehicle kilometers traveled

VMT	Vehicle miles traveled
VOTT	Value-of-travel-time
VPPG	Virtual-Physical Proving Ground
VS	Vehicle Systems
VSATT	Vehicle Systems Analysis Technical Team
VSI	Vehicle Systems Integration
VSST	Vehicle Systems Simulation and Testing
VTIF	Vehicle Testing and Integration Facility
VTO	Vehicle Technologies Office

W

Dw	Change in Angle W
WCC	Water Cooled Condenser
WEC	World Endurance Championship
WEG	Water/Ethylene Glycol
Wh	Watt hour
WHR	Waste Heat Recovery
WPT	Wireless Power Transfer
WTP	Willingness to pay
WTW	Well-to-Wheels

X

XPS	X-ray photoelectron spectroscopy
-----	----------------------------------

Y

Z

ZI-HOPIT	Zero-Inflated Hierarchical Ordered Probit
ZOV	Zero-occupancy vehicle

Executive Summary

Our transportation system is changing. New, disruptive technologies such as connected and automated vehicles are being developed and introduced to the market. Innovative business models that provide car-sharing and ride-hailing services give new mobility options to consumers. Freight transport is evolving to meet the demands of a retail sector that is increasingly based on e-commerce. While this transition was already underway, the global COVID-19 pandemic significantly disrupted the daily lives and activities of Americans, causing dramatic changes in highway congestion, public transit use, online purchasing, and attitudes about shared mobility options. The permanence of these changes remains to be seen and their effects must be considered in the research, development, and deployment of new mobility solutions.

The shifting mobility landscape offers opportunities to improve the economic and energy productivity of the U.S. transportation sector, while advancing the safety, affordability, and accessibility of transportation for all Americans. The U.S. Department of Energy (DOE) Office of Energy Efficiency and Renewable Energy (EERE) Vehicle Technologies Office (VTO) created the Energy Efficient Mobility Systems (EEMS) Program to understand the range of mobility futures that could result from disruptive transportation technologies and services and to create solutions that improve mobility energy productivity (MEP), or energy efficiency, affordability, and access provided by the transportation system. Increases in MEP result from improvements in the quality or output of the transportation system and/or reductions in the energy and cost of transportation.

EEMS Program activities during FY 2020 focused on analytical research and large-scale modeling and simulation to understand the impacts that new mobility technologies and services will have at the vehicle-, traveler-, and overall transportation system-level. This research included the development of a multi-fidelity, end-to-end transportation system models and tools to evaluate the complex interactions among the various actors within the mobility landscape, analysis of empirical data to characterize which solutions may provide the largest benefits, and development of new control systems and algorithms that use vehicle connectivity and automation to improve the performance and efficiency of individual vehicles as well as the overall traffic system.

This document presents a brief overview of the EEMS Program and documents progress and results from projects within each of the EEMS activity areas. The Computational Modeling and Simulation key activity area summarizes work within the sub-areas of (1) the SMART (Systems and Modeling for Accelerated Research in Transportation) Mobility Lab Consortium, (2) Artificial Intelligence, High-Performance Computing, and Data Analytics, and (3) Core Simulation and Evaluation Tools. Additionally, the program's advanced R&D projects are summarized within (4) the Connectivity and Automation Technology key activity area. Each of the individual progress reports provide a project overview and highlights of the technical results.

Table of Contents

I	Computational Modeling and Simulation	13
I.1	SMART Mobility	13
I.1.1	Experimental Evaluation of Eco-Driving Strategies (LBNL)	13
I.1.2	Cooperative Adaptive Cruise Control (CACC)/Platooning Testing: Measuring Energy Savings, Interaction with Aerodynamics Changes and Impacts of Control Enhancements (LBNL)	20
I.1.3	Experimental Evaluation of Cooperative ACC for Passenger Cars – Development of CACC Capability for Cars with different Powertrains (LBNL and ANL) [Task 3.1.2]	37
I.1.4	Urban Science (National Renewable Energy Laboratory)	55
I.1.5	GPRA New Cities Modeling - POLARIS	71
I.1.6	Transportation System Modeling of Southeastern Michigan and Austin, TX Using BEAM	79
I.2	Artificial Intelligence, High Performance Computing, and Data Analytics	86
I.2.1	HPC-Enabled Artificial Intelligence for Connected and Automated Vehicle Development	86
I.2.2	Ubiquitous Traffic Volume Estimation through Machine Learning Procedures (NREL)	94
I.2.3	Transportation Data Analytics (Big Data Systems for Mobility (BDSM))	101
I.2.4	Transportation State Estimation Capability (PNNL)	111
I.2.5	Real-Time Data and Simulation for Optimizing Regional Mobility in the United States (ORNL, NREL)	122
I.3	Core Simulation and Evaluation Tools	133
I.3.1	Livewire Data Sharing Platform (NREL, PNNL, INL)	133
I.3.2	Core Modeling, Simulation and Evaluation (ANL)	141
I.3.3	Virtual and Physical Proving Ground for Development and Validation of Future Mobility Technologies (Oak Ridge National Laboratory)	148
I.3.4	DOE/DOT Automated, Connected, Efficient, and Shared (ACES) to Human-Centric Mobility Metrics -Identifying Common Metrics, Research Methodologies and Collaboration Opportunities across DOT-DOE Mobility Portfolios (NREL)	159
I.3.5	RoadRunner – A Simulation Tool for Energy-Efficient Connected and Automated Vehicle Control Development	175
II	Connectivity and Automation Technology	185
II.1.1	Energy-Efficient Maneuvering of Connected and Automated Vehicles (CAVs) with Situational Awareness at Intersections (SwRI)	185

II.1.2 CIRCLES: Congestion Impacts Reduction via CAV-in-the-loop Lagrangian Energy Smoothing (The Regents of the University of California)..... 199

II.1.3 Validating Connected, Automated, and Electric Vehicle Models and Simulation (American Center for Mobility) 217

II.1.4 Next Generation Intelligent Traffic Signals for the Multimodal, Shared, and Automated Future (Xtelligent, Inc.)..... 227

II.1.5 Developing an Eco-Cooperative Automated Control System (Virginia Tech)..... 233

II.1.6 Evaluating Energy Efficiency Opportunities from Connected and Automated Vehicle Deployments Coupled with Shared Mobility in California (UCR, NREL)..... 240

II.1.7 Boosting Energy Efficiency of Heterogeneous Connected and Automated Vehicle (CAV) Fleets via Anticipative and Cooperative Vehicle Guidance (Clemson University) 247

List of Figures

Figure 1 SMART Mobility Capstone Reports were published in FY2020.....	8
Figure 2 Hardware-in-the-Loop (HIL) Test Track.	8
Figure 3 Web Visualization of MEP Calculation.	9
Figure 4 Visualizations of Transit and MEP in Atlanta (left); Road Network and MEP in Austin (middle); and Activity Locations and MEP in Detroit (right)	9
Figure 5 Visualization of the travel time estimates obtained from TranSEC for Seattle.....	10
Figure 6 ORNL CAVE Lab with Vehicle-in-the-Loop Functionality	10
Figure 7 Space-time diagram of simulated a lane The dark region indicates segments where control is not applied. (Right) Wave formation is persistent. Left) Space-time diagram where 10% of the vehicles are controlled via RL.	11
Figure 8 Vehicle-in-the-Loop Simulations: physical vehicle integrated in a string of vehicles in VISSIM.....	11
Figure I.1.1.1 The Opportunities for Vehicles to Arrive at the End of Green Phase or at End of Red Phase.....	15
Figure I.1.1.2 Trajectories of Arriving Vehicles at Major and Minor Streets.....	15
Figure I.1.1.3 Statistics of Durations of Green, Yellow and Red Phases for the Major Approach.....	17
Figure I.1.2.1 The Concept of Operation for Integrated Traffic Signal Control and Cavs	22
Figure I.1.2.2 The Definition of Phase ID	23
Figure I.1.2.3 HIL Components for Evaluating the Cooperative Intersection Control.....	24
Figure I.1.2.4 Low-Level Control Layer for Reference Speed Tracking.....	25
Figure I.1.2.5 ACC Block Structure	26
Figure I.1.2.6 Headway Regions for Cruise Control and ACC Decision Algorithm.....	26
Figure I.1.2.7 Illustration of Implemented State Machine for CACC Operation.....	27
Figure I.1.2.8 Headway Regions for Cruise Control and ACC Decision Algorithm.....	27
Figure I.1.2.9 HIL Test Track.....	29
Figure I.1.2.10 Vehicle Trajectories Observed on the Major Road in the Baseline Case.....	31
Figure I.1.2.11 Vehicle Trajectories Observed on The Major Road in the Signal Optimization Plus Trajectory Planning Case	31
Figure I.1.2.12 Probability Density of Speed.....	33
Figure I.1.2.13 Probability Density of the Fuel Consumption for Car 1.....	34
Figure I.1.2.14 Probability Density of the Fuel Consumption for Car 2.....	34
Figure I.1.3.1 Software Architecture for the CACC Control Implementation.....	38
Figure I.1.3.2 CACC System Structure Represented as Block Diagram	39
Figure I.1.3.3 Low Level Block Structure for Speed Tracking	40
Figure I.1.3.4 Vehicle Lower-Level Properties and Available Command Systems	40
Figure I.1.3.5 Vehicle Throttle Pedal Map Surface in Function of Speed and Acceleration.....	41
Figure I.1.3.6 Time and Modelled Frequency Response (Left and Right) of Vehicles' Low-Level	41

Figure I.1.3.7 Illustration of Implemented State Machine for CACC Operation..... 42

Figure I.1.3.8 ACC Block Structure 43

Figure I.1.3.9 CACC Block Structure..... 43

Figure I.1.3.10 LPV Representation of Feedback Control Design 44

Figure I.1.3.11 Comparison Between CTG and VTG Spacing Policies on Time Gap (Left) and Spacing (Right) 44

Figure I.1.3.12 Feedforward Control Structure for High-Performance CACC 45

Figure I.1.3.13 Illustration of Time Sequence of Cutting-In Scenario (Left to Right) 45

Figure I.1.3.14 Planned Speed, Distance and Time Gap Profiles for Different Time Gap Values..... 46

Figure I.1.3.15 ACC Structure Testing on Highway Traffic 47

Figure I.1.3.16 Regular-CACC Testing. Speeds, Gap Error and Time Gap Variables..... 48

Figure I.1.33 Speed steps profile results of high-performance CACC testing..... 48

Figure I.1.3.17 Speed Variations Scenario Based on Jerk Steps Profile..... 49

Figure I.1.3.18 Multisine Scenario Testing for High-Performance CACC 50

Figure I.1.3.19 Cutting-In Vehicle Testing Scenario on CACC String 51

Figure I.1.3.20 CACC Vehicle Testing of Three Vehicles on Public Highway 52

Figure I.1.4.1 Truck Freight Flows for Chicago Area by Origin and Destination..... 57

Figure I.1.4.2 Spatial Representation of MEP Values Using the POLARIS/Chicago Typology Transfer Multiplier Matrix Applied to New York City 59

Figure I.1.4.3 Austin Red Line and Amds 62

Figure I.1.4.4 Spatial Coverage of MEP Calculations 63

Figure I.1.4.5 Web Visualization Prototype to Display MEP Scores 64

Figure I.1.4.6 Willingness to Pool and the Pooling Success Rate of Authorized Trips Over Time..... 65

Figure I.1.4.7 MEP Scores for Austin..... 66

Figure I.1.4.8 Comparison of Pixel-Level BEAM and POLARIS MEP Scores for Austin 66

Figure I.1.4.9 Temporal Mobility Pattern Shifts Resulting from COVID-19..... 67

Figure I.1.4.10 Sample Telematics Streams Providing Insight into Driving and Charging Behavior 69

Figure I.1.5.1 Visualizations of (A) Activity Locations in Detroit, (B) Road Network in Austin, and (C) Transit in Atlanta 73

Figure I.1.5.2 Behavior Model Calibration for (A) Activity Generation and (B) Departure Times 74

Figure I.1.5.3 Behavior Model Calibration for (A) Work Trip Length and (B) Mode Share 74

Figure I.1.5.4 (a) E-Commerce Demand and (b) Vehicle In-Network 75

Figure I.1.5.5 The Graph Depicts (a) Average Distance Per Activity Type and (b) Overall Mode Shares..... 75

Figure I.1.5.6 Austin Network Results Showing (a) Vehicles-In-Motion Over Time and (b) the Network Speeds Over Time..... 76

Figure I.1.5.7 Behavior Model Calibration for (a) Mode Shares, (b) Discretionary Trip Lengths, and (c) Departure Times 77

Figure I.1.5.8 Model Validation Results: (a) Passenger Vehicles in Network and (b) Link Traffic Counts Comparison.....	77
Figure I.1.5.9 MEP Results for: (a) Atlanta, (b) Austin, and (c) Detroit	78
Figure I.1.6.1 BEAM Deployment Pipeline, Involving Population Synthesis, Calibration of a Preliminary Model Including Discretionary Activities Generated in BEAM, and Then Calibration of a Final Implementation Using Discretionary Activities Generated in Activitysim	81
Figure I.1.6.2 Speed Calibration Values for Austin.....	83
Figure I.1.6.3 Speed Calibration Values for Detroit	84
Figure I.2.1.1 Synthetic Imagery Examples.....	89
Figure I.2.1.2 Canonical Structure of Reinforcement Learning.....	90
Figure I.2.1.3 Mixed Mode Simulation and Learning	91
Figure I.2.1.4 Simulation Domain	91
Figure I.2.1.5 Summary of Project Tools: NREL HPC-Cavs Simulator and RL Applications Spectrum.....	92
Figure I.2.2.1 Predicted Versus Observed Hourly Volumes for a Typical Week For (A) The Model Trained on NC and Tested on PA (Thus Displayed are PA Predicted Volumes), and (B) The Model Trained on PA and Tested on NC (Thus Displayed are NC Predicted Volumes).....	98
Figure I.2.2.2 Predicted Versus Observed Hourly Volumes for a Typical Week for the Model Trained on PA and Tested on NC (Thus Displayed are NC Predicted Volumes) with the Meta Model (PA+NC Train) and Test on NC.....	98
Figure I.2.3.1 Predicted Flow and Speed with Observed Flow and Speed Plotted in the Form of a Fundamental Traffic Flow Diagram, Demonstrating that the Model has Learned the Fundamental Diagram Behavior	104
Figure I.2.3.2 Hypothetical Incident Location in Red	105
Figure I.2.3.3 Simulation Parallel Scaling with 100% Active Vehicle Rerouting Penetration on Cori.....	106
Figure I.2.3.4 Traffic Flow without Rerouting	106
Figure I.2.3.5 Traffic Flow with Rerouting	106
Figure I.2.3.6 Preliminary Vehicles Assessed for Data-Driven Estimation Technique.....	107
Figure I.2.3.7 Example Speed Vs Time and Corresponding Tractive Force Vs Speed Plots for Two Example Drive Cycles	108
Figure I.2.3.8 Chevrolet Bolt Predicted Versus Actual Energy Consumption.....	108
Figure I.2.4.1 Comparing the Results of Estimated Distributions of Travel Times for 6 Randomly Chosen Links in the La Downtown Network With and Without Spatial Partitioning.....	113
Figure I.2.4.2. Illustrating the Estimated Speed Distributions on Weekdays for a Downtown La Arterial and a Freeway Link Along with their Respective Speed Limits	114
Figure I.2.4.3. Wasserstein Distance – Cumulative Distribution Function for Both Los Angeles (top) and Seattle (bottom).....	114
Figure I.2.4.4 Accuracy/Cost Trade-Off for Different Data Imputation Methods. Weekday 5am-10pm Using 5 Immediate Neighboring Sensors as Reference	115
Figure I.2.4.5 Data Imputation with Long-Short Term Memory (LSTM) Neural Networks Using Two Different Sensors with Short and a Long Data Window for Model Training	115
Figure I.2.4.6 Data Imputation Using a Regression Tree Algorithm.....	115

Figure I.2.4.7 Data Imputation Using a K-Nearest Neighbor (KNN) Algorithm 116

Figure I.2.4.8. (A) Original GPS Coordinates Reported by the Bus. (B) Corresponding Map-Matched Trajectory Using FMM..... 117

Figure I.2.4.9 Vehicle Detection/Counting Within a Predefined Area of Interest (Red Polygon)..... 117

Figure I.2.4.10 Travel Time Estimation Workflow 118

Figure I.2.4.11 Visualization of The Travel Time Estimates Obtained from Transec for the Whole LA Basin Area At 6pm on a Weekday..... 118

Figure I.2.4.12 Visualization of the Travel Time Estimates Obtained from Transec for Seattle and its Metropolitan Area During the Period of 4pm to 6pm..... 119

Figure I.2.4.13 Visualization of Congestion Patterns (Deviation with Respect to Free-Flow Travel Times) in Downtown LA 120

Figure I.2.5.1 Phased Workflow 124

Figure I.2.5.2 Various Interactive Charts Displaying Some Atspms 127

Figure I.2.5.3 Real-Time Traffic Signal Control System Structure 128

Figure I.2.5.4 Remote Setup of Control Experiment: VPN Tunnel into City of Chattanooga from Remote Desktop Interfaces to Run Control Algorithms in the Cloud and Obtain New Values to Send to On-Street Controllers 129

Figure I.3.1.1 Livewire Data Platform Search Page (<https://Livewire.Energy.Gov/Project-Search>) 135

Figure I.3.1.2 Livewire Data Platform File Upload (<https://Livewire.Energy.Gov/Project-Search>) 136

Figure I.3.1.3 Livewire Data Platform User and Group Management..... 136

Figure I.3.1.4 Livewire Data Platform Access Management Interface..... 137

Figure I.3.1.5 Livewire Data Platform Metadata 138

Figure I.3.2.1 The Energy for Transportation Workflow..... 143

Figure I.3.2.2 Main Tab of the Large-Scale Workflow 144

Figure I.3.2.3 A 2-Speed Gearbox Can Help Reduce the Motor Size and Still Meet the Performance Requirements 145

Figure I.3.2.4 Improved Data Acquisition and Control System with Heads-Up Control Touch Panel 145

Figure I.3.2.5 Realtime Visualization of BSM Packets 147

Figure I.3.3.1 Dspace ASM Virtual Vehicle-In-The-Loop (Left) Fully Integrated and Navigating a Handling Course Using Feedback from the Powertrain Under Test (Right)..... 152

Figure I.3.3.2 CAVE Lab Setup with Full Vehicle-In-The-Loop (VIL) Functionality, Including Steering, Integrated with Virtual Vehicle Environment..... 153

Figure I.3.3.3 Snapshot of Rviz Displaying Camera and Lidar Point Cloud Data from the Ego-Vehicle Operating in the CARLA Server. The Manual Control User Interface and Relevant Commands are Shown in the Bottom Right..... 154

Figure I.3.3.4 Left: The CARLA Server with an Ego Vehicle Making a Right Turn. Right: The Autoware Rviz Configuration Displays All the Relevant Sensor Data to Localize the Ego Vehicle and Follow the Green Waypoints 155

Figure I.3.3.5 Virtual Replica of the ACM Track in: A) VTD; B) IPG Carmaker; C) PTV VISSIM..... 156

Figure I.3.3.6 Communication Network Replica of ACM Track. Green Dots: Location of Rsus; Red Circle: Communication Range	156
Figure I.3.3.7 Diagram of IPG Carmaker and VISSIM Co-Simulation.....	157
Figure I.3.3.8 IPG Carmaker and VISSIM Co-Simulation on SCALEXIO Real-Time Control System	158
Figure I.3.4.1 Road Capacity for People.....	162
Figure I.3.4.2. Mean Occupancy Value for Trips by State (Left); and Mean Occupancy Value of Non-Household Members on Trips by State (Right) (NHTS, 2017)	165
Figure I.3.4.3 Below Shows a Comparison of a Traditional Vehicles Per Hour Per Lane (VPHPL) Metric Compared to a New Proposed Persons Per Hour Per Lane (PPHPL) Metric	166
Figure I.3.4.4. Diagram on VPHPL Versus PPHPL, Considering Key Parameters Shaping PPHPL	166
Figure I.3.4.5. Violin Plots of Road Capacity Metrics for Private Vehicles, Transit Bus and Walk/Bike	167
Figure I.3.4.6 Cumulative Distribution Function of PEIT by Increasing Vehicle Occupancy for Private Vehicles and Buses by One Standard Deviation.....	167
Figure I.3.4.7 Cumulative Distribution Function of PEIT by Increasing Mode Share of Walk/Bike and Bus by One Standard Deviation.....	168
Figure I.3.4.8 Cumulative Distribution Function of PEIT by Increasing Vehicle Energy Efficiency (or Fuel Economy) by One Standard Deviation for Private Vehicles and Buses	168
Figure I.3.4.9 Full Cost Per Mode Per Mile for the Three Efficiency Scenarios, Affordability Metric	171
Figure I.3.4.10 Direct Out-Of-Pocket Costs to a Traveler, Per Traveler Mile, for the Three Efficiency Scenarios, Affordability Metric	172
Figure I.3.4.11 Average Out of Pocket Cost Per Person Per Year for the Three Efficiency Scenarios, Affordability Metric.....	172
Figure I.3.5.1 Back and Forth Data Request Process Between Hyundai and Argonne	177
Figure I.3.5.2 Multi-Step Data Analysis Process in the Data Analytic Framework	177
Figure I.3.5.3 Schematic Diagram of a High-Fidelity Dynamic Human Driver Model	178
Figure I.3.5.4 Selected Areas of All Geographical Location Clusters: Metropolitan Areas (Left) and Rural Areas (Right)	178
Figure I.3.5.5 Definition of 102 Groups by 25 Areas and 6 Vehicle Modes	179
Figure I.3.5.6 UPSAI-Based Neighborhoods in Washtenaw County, MI (Left) and Statistical Data Analysis (Right).....	180
Figure I.3.5.7 Step-By-Step Bsna and Bna Situations Segmentation Algorithm.....	181
Figure I.3.5.8 Situation Segmentation Algorithm Test Result.....	181
Figure I.3.5.9 Acceleration Regime Calibration Example	182
Figure I.3.5.10 Roadrunner GUI in AMBER.....	183
Figure II.1.1.1 Program Objective	186
Figure II.1.1.2 Ego Vehicle Set	186
Figure II.1.1.3 Urban Corridor in Columbus, Ohio (High Street)	187
Figure II.1.1.4 Intelligent Intersection Concept.....	187
Figure II.1.1.5 Technology Approach.....	188

Figure II.1.1.6 Signal Phasing and Timing Pattern (High Street Corridor Sample) 189

Figure II.1.1.7 Vehicle Routing Decisions 190

Figure II.1.1.8 Camera Feed High Street..... 190

Figure II.1.1.9 Energy Estimation Framework 191

Figure II.1.1.10 Sample Output of the Energy Estimation Framework Summarizing Energy Consumption Based on Powertrain Mix, Driver Model and Cav Penetration 191

Figure II.1.1.11 Google Maps Estimation for High Street Nominal Speeds 192

Figure II.1.1.12 Trip Time Histogram of Vehicles in Traffic Simulation Navigating High Street Corridor.... 193

Figure II.1.1.13 Comparison Between Measured and Predicted Fuel Consumption and Delta SOC (Battery Usage) Across 17 Different Drive Cycles (Each Dot Represents a Drive Cycle) 195

Figure II.1.2.1 Images Taken from the Validation Phase of the I-24 Testbed..... 202

Figure II.1.2.2 Demonstration of Object Tracking with Bounding Boxes and Vehicle Speed Annotations 203

Figure II.1.2.3 Visualization of Both Fitted Simplified Models for Power Consumption as a Function of Instantaneous Vehicle Speed and Acceleration. Left: Priusev 1.0 Model for an Electric Vehicle. Right: Tacoma 1.0 for an Internal Combustion Engine Vehicle 205

Figure II.1.2.4 Speed Variance for Different Safety and Incentive Thresholds. Left: Without Control, Right: With Control 206

Figure II.1.2.5 (Left) Space-Time Diagram of a Lane in the I-210 in the Absence of Control. The Dark Region Indicates Segments Where Control is Not Applied. Wave Formation is Persistent. (Right) Space-Time Diagram Where 10% of the Vehicles are Controlled Via RL..... 208

Figure II.1.2.6 (Left) Ratio of System-Level MPG of RL-Controlled to System-Level MPG of the Uncontrolled Case as a Function of Penetration Rate. At All Studied Penetration Rates, We See a Significant Improvement Over the Uncontrolled Case. (Right) Ratio of System-Level MPG of RL-Controlled to System-Level MPG of the Uncontrolled Case as a Function of Max Speed of the Network. At Most Velocities, With the Exception of Speeds Where Cars are Essentially Stopped, We See a Significant Improvement Over the Uncontrolled Case..... 209

Figure II.1.2.7 Centralized and Decentralized Traffic Control Approaches Currently Being Explored by the RL Team 210

Figure II.1.2.8 Safe Set of the Followerstopper. The Safe Set is Defined in the Domain Where *Distance* is Positive, *Lead Speed* is Between 0 and 30, and *Follower Speed* is Between 0 and 30. The Red Surface Represents the Boundary of the Safety Set. The Safe Set is the Set of States Bounded by the Surface (I.E., All States Below the Surface) 212

Figure II.1.2.9 A Timeline of Control Strategy Scores. Each Dot Represents a Control Strategy Score Assuming 100% Toyota Tacomas (Blue) and 100% Toyota Prius Evs (Orange) on the Road. Scores are Plotted as Percentage Improvement Relative to the Baseline (Red), and Solid Blue and Orange Lines to Show the Best Scores to Date 213

Figure II.1.2.10 A Diagram Showing Where Libpanda, ROS, and the CAN Coach Fit in the Hardware/Software Stack 214

Figure II.1.3.1 Results Showing a Dynamic Test on the Bolt for a 0-30% APP Input with Comparisons of the Vehicle Dynamics Prediction/Model..... 220

Figure II.1.3.2 Results Showing Testing and Demonstration of Navigation-Based Speed Control on the ACM Highway Loop with a GM Volt..... 220

Figure II.1.3.3 Architecture of the ORNL Algorithms Implemented in Mixed Reality Simulation..... 221

Figure II.1.3.4 ORNL’s Speed Harmonization Algorithm Implementation In VTD.....	222
Figure II.1.3.5 Component Performance Maps for Chrysler Pacifica Integrated into Autonomie	223
Figure II.1.3.6 Vehicle Speed, Engine Power, and Cumulated Fuel Rate for the Chrysler Pacifica, in Test and Simulation (Left); Vehicle Speed, Motor Power, and SOC for the Chevrolet Bolt, in Test and Simulation....	223
Figure II.1.3.7 Configuration of the Controller Implementation for Development of a Digital Twin.....	225
Figure II.1.3.8 Five Test Plans Developed with Multiple Types of Mini-Scenarios	225
Figure II.1.4.1 Transportation Agency Pilot Sites	229
Figure II.1.4.2 Performance Improvement in Single (Non-Coordinated Intersections)*	230
Figure II.1.4.3 Performance Improvement from Free Mode Corridor Baseline	231
Figure II.1.4.4 Data Partner Current Evaluation Status	232
Figure II.1.5.1 Proposed Eco-CAC System	234
Figure II.1.5.2 Fuel/Energy Consumption and Travel Time for High -Congestion, Multi-Class Routing Options.....	235
Figure II.1.5.3 LA Network - Speed Harmonization Logic Test Network (LA Network)	236
Figure II.1.6.1 Model Framework.....	241
Figure II.1.6.2 Impact Evaluation on Travel Behavior	243
Figure II.1.6.3 Speed Histogram in a 3D View (Unit: Mph)	244
Figure II.1.6.4 Ride-Hail Waiting Time Histogram.....	244
Figure II.1.6.5 Energy Consumption for the City of Riverside Network (Unit: Kwh Per Capita)	245
Figure II.1.6.6 Statewide VMT And Energy Analysis	246
Figure II.1.7.1 Inverse Probability Density Function of Position	248
Figure II.1.7.2 Block Diagram of the Optimal Lane Selection NLP Distributed MPC Framework.....	249
Figure II.1.7.3 Vehicle-in-the-Loop Simulations: Physical Vehicle Integrated in a String of Vehicles in VISSIM.....	249
Figure II.1.7.4 Fuel Flow Dynamometer Test Setup	250
Figure II.1.7.5 Mean Fleet Fuel Efficiency Improvements Over the 0% CAV Case at Each Input Vehicle Volume/Hour	251
Figure II.1.7.6 Cell Density Plots Showing Dense Groups of Vehicles in the Network at 0%, 30% CAV Penetration. With the Introduction of Cavs, Shockwave Effects Were Dissipated	251
Figure II.1.7.7 Fleet Fuel Efficiency Improvements Over the 0% CAV Case at Each Input Vehicle Volume/Hour for an SUV-Sized Vehicle Electric Powertrain (Left) and Hybrid	251
Figure II.1.7.8 Simulated Energy and String Length of 8 Automated Electric Vehicles Trailing a Drive Cycle-Bound Lead Vehicle	252
Figure II.1.7.9 Percent Reduction in Fuel Consumption (Top) and Average Travel Time (Bottom) for the Rbls and Ols Methods Compared to the Baseline of 0% Cav Penetration. Note: T_b is the Average Travel Time for the Baseline Scenario.....	252
Figure II.1.7.10	253
Figure II.1.7.11 Nissan Leaf Tracking Performance.....	254
Figure II.1.7.12	254

List of Tables

Table I.1.2.1 VT-CPFM Model Parameters.....	30
Table I.1.2.2 Mobility and Vehicle Energy Efficiency of Simulated Vehicles.....	30
Table I.1.2.3 Mobility and Vehicle Energy Efficiency Performance Change Regarding the Baseline Scenario	30
Table I.1.2.4 Mobility and Vehicle Energy Efficiency Performance of Physical CAVs.....	32
Table I.1.2.5 K-S Test Results between Each Two Test Cases	35
Table I.1.3.1 Identified Low-Level Parameters and Acceleration Range for Each Platform	42
Table I.1.5.1 Data Sources used in Model Construction.....	72
Table I.1.5.2 Summary Results Comparison for All Cities	78
Table I.1.6.1 Summary Statistics in Austin and Detroit	84
Table I.1.6.2 Aggregate Mode Split in Austin and Detroit.....	84
Table I.2.1.1 Statistics of Synthetic Data Set collected for CARLA Town 1	88
Table I.2.2.1 Independent Model Results	96
Table I.2.2.2 Results from Spatial Transferability Exercises.....	97
Table I.3.4.1 Characterizing Current and Emerging Metrics for Integrated Mobility	163
Table I.3.4.2 Occupancy Goals of Selected U.S. Cities.....	164
Table I.3.4.3 Traditional vs Proposed Metrics for Review of Integrated Mobility, Energy, and Costs.....	165
Table I.3.4.4 Average Out of Pocket Costs Per Traveler Mile (Note: Annual Fixed Costs for Car and Bicycle Travel are Distributed Proportionately Across Annual Miles Traveled).....	169
Table I.3.4.5 Average Out of Pocket Costs Per Traveler Mile	169
Table I.3.4.6 Internal and External Costs Per Vehicle Mile Traveled and Per Person/Passenger Mile Traveled	170
Table II.1.1.1 Milestone Summary (as of Q4).....	188
Table II.1.1.2 Fuel Economy (Miles per Gallon) Comparison for Hyundai Elantra	193
Table II.1.1.3 NCCP Values for Dodge Charger Model.....	194
Table II.1.1.4 Fuel Economy (Miles per Gallon) Comparison for Chrysler 300.....	194
Table II.1.1.5 Energy Consumption Comparison for Kia Soul EV	196
Table II.1.1.6 NCCP Values for Kia Soul EV	196
Table II.1.1.7 Energy Consumption Comparison for Tesla Model 3.....	196
Table II.1.1.8 NCCP Values for Tesla Model 3.....	197
Table II.1.3.1 Chrysler Pacifica Validation	224
Table II.1.3.2 Chevrolet Bolt Validation	224
Table II.1.5.1 Average Freeway Benefits of Speed Harmonization Logic	236
Table II.1.5.2 Test Results of the Eco-CACC-I Controllers with Signal Optimization.....	237
Table II.1.5.3 Tested Platooning Configurations.....	237
Table II.1.5.4 Platooning Test Results with Multi-objective Routing	238

Table II.1.7.1 Fuel Flow in Chassis Dynamometer Testing	250
Table II.1.7.2 Combustion Mazda RX7 - Experimental Controller Performance	255
Table II.1.7.3 Electric Nissan Leaf - Experimental Controller Performance.....	255

Vehicle Technologies Office Overview

Vehicles move our national economy. Annually, vehicles transport 11 billion tons of freight—about \$35 billion worth of goods each day¹—and move people more than 3 trillion vehicle-miles.² Growing our economy requires transportation, and transportation requires energy. The transportation sector accounts for about 30% of total U.S. energy needs³ and the average U.S. household spends over 15% of its total family expenditures on transportation, making it the most expensive spending category after housing.⁴

The Vehicle Technologies Office (VTO) funds a broad portfolio of research, development, demonstration, and deployment (RDD&D) projects to develop affordable, efficient, and clean transportation options to tackle the climate crisis and accelerate the development and widespread use of a variety of innovative transportation technologies. The research pathways focus on electrification, fuel diversification, vehicle efficiency, energy storage, lightweight materials, and new mobility technologies to improve the overall energy efficiency and affordability of the transportation or mobility system. VTO leverages the unique capabilities and world-class expertise of the National Laboratory system to develop innovations in electrification, including advanced battery technologies; advanced combustion engines and fuels, including co-optimized systems; advanced materials for lighter-weight vehicle structures; and energy efficient mobility systems.

VTO is uniquely positioned to accelerate sustainable transportation technologies due to strategic public-private research partnerships with industry (e.g., U.S. DRIVE, 21st Century Truck Partnership) that leverage relevant expertise. These partnerships prevent duplication of effort, focus DOE research on critical RDD&D barriers, and accelerate progress. VTO focuses on research that supports DOE's goals of building a 100% clean energy economy, addressing climate change, and achieving net-zero emissions no later than 2050 to the benefit of all Americans.

Annual Progress Report

As shown in the organization chart (below), VTO is organized by technology area: Batteries & Electrification R&D, Materials Technology R&D, Advanced Engine & Fuel R&D, Energy Efficient Mobility Systems, and Technology Integration. Each year, VTO's technology areas prepare an Annual Progress Report (APR) that details progress and accomplishments during the fiscal year. VTO is pleased to submit this APR for Fiscal Year (FY) 2020. In this APR, each project active during FY 2020 describes work conducted in support of VTO's mission. Individual project descriptions in this APR detail funding, objectives, approach, results, and conclusions during FY 2020.

¹ Bureau of Transportation Statistics, Department of Transportation, Transportation Statistics Annual Report 2018, Table 4-1. <https://www.bts.gov/tsar>.

² Transportation Energy Data Book 37th Edition, Oak Ridge National Laboratory (ORNL), 2019. Table 3.8 Shares of Highway Vehicle-Miles Traveled by Vehicle Type, 1970-2017.

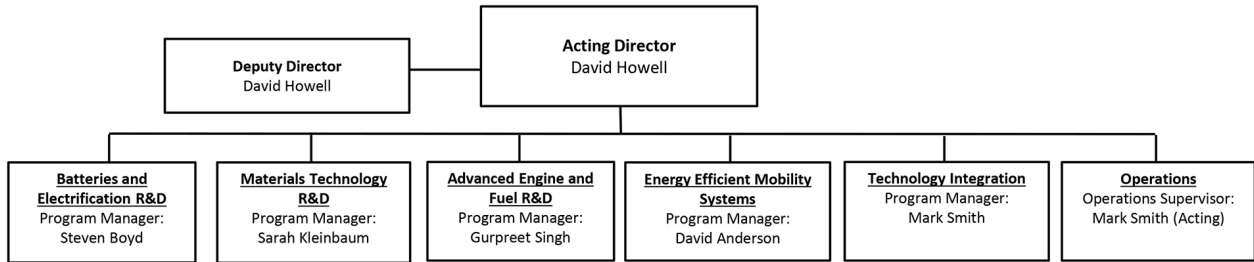
³ Ibid. Table 2.1 U.S. Consumption of Total Energy by End-use Sector, 1950-2018.

⁴ Ibid. Table 10.1 Average Annual Expenditures of Households by Income, 2016.

Organization Chart

Vehicle Technologies Office

March 2021



Energy Efficient Mobility Systems Program Overview

Introduction

On behalf of the Energy Efficient Mobility Systems (EEMS) Program of the U.S. Department of Energy's (DOE's) Office of Energy Efficiency and Renewable Energy (EERE) Vehicle Technologies Office (VTO), we are pleased to submit this Annual Progress Report (APR) for Fiscal Year (FY) 2020.

The introduction of disruptive transportation technologies and services, such as connected and automated vehicles, car-sharing, and ride-hailing services, provides new, low-cost mobility options for consumers. Additionally, the evolving retail sector, shaped by the convenience of online shopping, has resulted in not only a shift in how we transport and deliver goods, but it has also had ripple effects in personal transportation. This transforming mobility landscape presents a significant opportunity to improve economic and energy productivity and advance safety, affordability, and accessibility in the transportation sector. However, while these changes can provide benefits to the American public, they also present risks, challenges, and questions that must be addressed.

The mobility transformation was abruptly altered in 2020, as the global COVID-19 pandemic significantly disrupted the daily lives and activities of Americans, resulting in dramatic changes in highway congestion, public transit use, online purchasing, and attitudes about shared mobility options. The permanence of these changes remains to be seen and their effects must be considered in the research, development, and deployment of new mobility solutions.

DOE conducts research to understand how the changing mobility landscape will affect transportation energy consumption and identifies opportunities to create more efficient, affordable, reliable, accessible, and secure transportation options that enhance mobility for individuals and businesses. Within EERE, the EEMS Program is responsible for this research portfolio.

This APR describes work that the EEMS Program conducted during FY 2020 in support of the EEMS Program goals as described in the following section.

Mission and Goals

The EEMS Program supports VTO's mission to improve transportation energy efficiency through low-cost, secure, and clean energy technologies. EEMS conducts early-stage research and development (R&D) at the vehicle-, traveler-, and system-levels, creating knowledge, insights, tools, and technology solutions that increase *mobility energy productivity* for individuals and businesses. This multi-level approach is critical to understanding the opportunities that exist for optimizing the overall transportation system. The EEMS Program uses this approach to develop tools and capabilities to evaluate the energy impacts of new mobility solutions and to create new technologies that provide economic benefits to all Americans through enhanced mobility.

Through its SMART Mobility Laboratory Consortium, the EEMS Program developed an accessibility metric known as *mobility energy productivity*. Because EEMS aims not only to reduce the energy consumed in the transportation system, but also to reduce the time and cost associated with moving people and goods while improving access to mobility, a comprehensive metric that incorporates all three factors (energy, time, and cost) is required. Mobility energy productivity (MEP) is used as a lens through which the EEMS program can evaluate the mobility impacts that potential technologies and services may have and by which program success can be measured as it develops new mobility solutions.

The EEMS Program works towards achieving three strategic goals in order to reach the program's overall goal of *identifying critical pathways and developing innovative technology solutions to enable significant*

improvements in mobility energy productivity when adopted at scale. Each strategic goal is discrete, but all three goals are interrelated such that the success in any one goal furthers the achievement of the other two.

STRATEGIC GOAL #1: Develop new tools, techniques, and core capabilities to understand and identify the most important levers to improve the energy productivity of future integrated mobility systems.

STRATEGIC GOAL #2: Identify and support early-stage R&D to develop innovative technologies that enable energy efficient future mobility systems.

STRATEGIC GOAL #3: Share research insights, and coordinate and collaborate with stakeholders to support energy efficient local and regional transportation systems.

Program Organization

To achieve its programmatic goals, the EEMS Program implements four coordinated areas of focus, each with its own set of projects. Each of these four research areas directly supports at least one of the three EEMS strategic goals. The four research areas are:

- Systems & Modeling for Accelerated Research in Transportation (SMART) Mobility Laboratory Consortium
- Artificial Intelligence, High-Performance Computing, and Data Analytics
- Core Simulation and Evaluation Tools
- Connectivity and Automation Technology

The first three areas are grouped within the “Computational Modeling and Simulation” key activity, while the “Connectivity and Automation Technology” area represents its own key activity.

SMART Mobility Lab Consortium

The SMART Mobility Laboratory Consortium is a multi-year, multi-laboratory collaborative dedicated to further understanding the energy implications and opportunities of advanced mobility solutions. In FY2020, the EEMS Program concluded the first phase of research under SMART Mobility, which consisted of five coordinated research pillars: Connected and Automated Vehicles, Mobility Decision Science, Multi-Modal Freight, Urban Science, and Advanced Fueling Infrastructure.

Building upon the research results and insights from the first phase of SMART Mobility, EEMS launched “SMART Mobility 2.0” in FY2020, with increased emphasis on development, improvement, and deployment of the integrated SMART Mobility Modeling Workflow and a concentrated effort on research, development, and evaluation of connected and automated vehicle control algorithms. Additionally, SMART Mobility 2.0 includes several research projects on various aspects of the transportation system (e.g., micromobility, transit, curb management, and drones) that inform the integrated SMART Mobility modeling platform.

The SMART Mobility Laboratory Consortium is the EEMS program’s primary effort to create tools and generate knowledge about how future mobility systems may evolve and identify ways to reduce their energy intensity. The consortium also identifies R&D gaps that the EEMS Program may address through its research portfolio. Furthermore, the tools and insights created through the SMART Mobility Laboratory Consortium are shared with a variety of mobility stakeholders, including technology developers, automotive manufacturers, local governments, and transportation planning organizations.

Artificial Intelligence, High Performance Computing, and Data Analytics

The EEMS Program conducts research to develop and apply the National Laboratories' capabilities in artificial intelligence (AI), high-performance computing (HPC), and data analytics to various transportation problems. The use of these tools assists in the design, planning, and operation of future mobility systems at multiple scales. HPC helps manage, store, analyze, and visualize conclusions from big data. AI serves to recognize patterns and extract actionable information to answer transportation-related questions through predictive data analytics applied to both vehicle/infrastructure (i.e., physical) data and human decision-making (i.e. behavioral) data.

The program's efforts in this area include the development of scalable data science and HPC-supported computational frameworks needed to build next-generation transportation/mobility system models and operational analytics that leverage the availability of near-real-time data and run quickly. This includes multi-lab efforts focused on developing city/regional-scale "digital twins" of the transportation system, providing real-time awareness of the state of the highway system (e.g., traffic flow and volumes). These models can then be used to develop control systems that improve congestion and reduce energy consumption (e.g., by implementing adaptive traffic signal control or optimal routing of individual vehicles). Additionally, the EEMS Program supports research to apply deep-learning techniques for sensing, perception, and control of automated vehicles (AVs), expedite the development and increase the performance of AV control algorithms, and implement virtual test environments to support the development of resilient AV control systems.

The AI, HPC, and data analytics area merges large-scale transportation data sets from public and private entities with unparalleled computational and analytical resources at the National Laboratories to develop actionable solutions to specific transportation energy challenges faced by cities, states, and regions across the U.S. These solutions enable local stakeholders to plan and operate their transportation systems in a way that improves energy efficiency as their populations grow and new mobility options become available. In doing so, it directly supports all three EEMS strategic goals.

Core Simulation and Evaluation

VTO has successfully conducted hardware evaluations of component and vehicle technologies, developed vehicle systems models based on the results of these evaluations, and performed simulation and analysis of potential vehicle powertrain solutions built upon these models. The EEMS Program develops and maintains these critical capabilities within the National Laboratory system in order to test, evaluate, model, and simulate advanced components, powertrains, vehicles, and transportation systems. These capabilities include vehicle and component test procedure development, highly instrumented hardware evaluation, controls algorithm validation, high-fidelity physical simulation, and transportation data management and analysis. As individual vehicles become more connected (with each other and with transportation infrastructure) and increasingly automated, new evaluation capabilities such as anything-in-the-loop (XIL) test environments will be necessary to support the EEMS Program in evaluating the energy and mobility outcomes of future transportation systems and for other VTO R&D programs in quantifying the performance and efficiency benefits of specific powertrain technologies under development.

The suite of core VTO evaluation and simulation tools is critical to the EEMS Program's ability to understand the impacts of future mobility and is also important in identifying research opportunities and producing insights to share with mobility stakeholders.

Connectivity and Automation Technology

The EEMS Program's Connectivity and Automation Technology R&D focuses on innovative, early-stage, and scalable mobility projects and targeted system-level opportunities to reduce the energy intensity of the movement of people and goods through connected and automation transportation solutions. The program partners with industry and academia to research and develop technology solutions that lead to mobility improvements through advancements in hardware, software, control systems, advanced sensing and computing, and powertrain components. Competitive funding opportunity announcements (FOAs) solicit

project proposals to develop technology solutions that progress the state-of-the-art towards the EEMS Program's targets. Through cost-shared cooperative agreements, FOAs provide external stakeholders the opportunity to develop innovative and disruptive solutions that the private sector would not otherwise consider due to their risk or uncertainty of return-on-investment, but which could result in public benefits if successful. These solicitations may be broad in scope, calling for a wide variety of proposals for technology development efforts across a range of potential concepts, or may specifically target an explicitly defined research concept. Additionally, the EEMS Program solicits R&D proposals from the National Laboratories through periodic lab calls and directly initiate targeted projects with individual labs or lab consortia to leverage specific lab capabilities.

The Connectivity and Automation Technology portfolio directly supports EEMS strategic goals by developing innovative technology solutions for mobility – the results of which inform the analytical work to understand the impacts of these new technologies and are disseminated to the stakeholder community.

Coordination

The EEMS Program coordinates its activities with other programs within VTO, as well as with other federal agencies, industry stakeholders, and other members of the mobility research community.

VTO's Technology Integration Program works with cities and stakeholders to demonstrate and evaluate new mobility technologies in the field and collect data through "Living Labs" pilot projects. These projects are an important feedback mechanism to EEMS R&D and provide a source of real-world data to test, validate, and improve models, simulations, software, and hardware. The EEMS Program coordinates with the Technology Integration Program, collaborating with stakeholders to support city and regional efforts to develop energy efficient transportation systems through key elements of an implementation strategy: stakeholder engagement, demonstration projects, and technical assistance.

Coordination between EEMS and other federal programs focused on connected, automated, and efficient transportation systems is critically important. DOE was a key contributor to *Ensuring American Leadership in Automated Vehicle Technologies – Automated Vehicles 4.0*, a multi-agency report published by the National Science and Technology Council and the U.S. Department of Transportation (USDOT) in January 2020.⁵ EEMS also participates in planning discussions with various modal administrations within USDOT, including the Federal Highway Administration (FHWA), Federal Transit Administration (FTA), and the Intelligent Transportation Systems Joint Program Office (ITS-JPO). Coordination with USDOT is important due to the linkage between VTO's R&D activities to create efficient, secure, and sustainable transportation technologies, and USDOT's mission to ensure our nation has the safest and most efficient and modern transportation system in the world.⁶

In addition to intergovernmental collaboration with the USDOT, the EEMS Program coordinates with industry partners. For example, U.S. DRIVE (Driving Research and Innovation for Vehicle efficiency and Energy sustainability) is a non-binding and voluntary government-industry partnership focused on advanced automotive and related energy infrastructure technology R&D.⁷ EEMS participates in U.S. DRIVE through the Vehicle and Mobility Systems Analysis Technical Team (VMSATT) to identify the most promising areas of pre-competitive mobility research of interest to the government, automotive industry, energy sector, and utility company partners. Additionally, the EEMS Program coordinates with the medium- and heavy-duty trucking and freight industry through the 21st Century Truck Partnership (21CTP)⁸, by pursuing collaborative R&D to realize its vision for our nation's trucks and buses to safely and cost-effectively move larger volumes of freight

⁵ <https://www.transportation.gov/sites/dot.gov/files/docs/policy-initiatives/automated-vehicles/360956/ensuringamericanleadershipav4.pdf>

⁶ <https://www.transportation.gov/about>

⁷ <https://www.energy.gov/eere/vehicles/us-drive>

⁸ <https://www.energy.gov/eere/vehicles/21st-century-truck-partnership>

and greater numbers of passengers while emitting little or no pollution. The EEMS Program is directly involved with the Freight Operational Efficiency Technical Team within the truck partnership.

The EEMS Program continually seeks additional high-value opportunities to engage with relevant stakeholders in order to share EEMS-funded research results and learn from other mobility-related efforts. For example, the EEMS Program is a governmental sponsor and member of the National Academies/Transportation Research Board Forum on Preparing for Automated Vehicles and Shared Mobility⁹, which brings together public, private, and other research organizational partners to share perspectives about how the deployment of automated vehicles and shared mobility services may dramatically increase safety, reduce congestion, improve access, enhance sustainability, and spur economic development. The SMART Mobility Laboratory Consortium also convened an Executive Advisory Board, comprised of experts and decision-makers representing the automotive industry, technology companies, academia, non-governmental organizations, non-profits, and other transportation-related associations. This board provides input and review to the research conducted by the Consortium and helps ensure the work performed is aligned with a variety of mobility stakeholders. As the Consortium focuses on completing and deploying its integrated modeling workflow during SMART Mobility 2.0, it will continue to pursue collaborations and partnerships with local city governments, transportation planning organizations, and other stakeholders to inform transportation policy making.

Project Funding

VTO selects and funds critical research through a combination of competitive funding opportunity announcement (FOA) selections, and direct funding to its National Laboratories. Competitive FOA projects are fully funded through the duration of the project in the year that the funding is awarded. Funding for direct funded and competitive award projects are contingent on annual Congressional budget appropriations.

Research Highlights

In FY2020, the Energy Efficient Mobility Systems Program's SMART Mobility Laboratory Consortium completed its first phase and initiated its second phase of research. EERE published a series of six Capstone reports summarizing the results, findings, and insights generated during the first phase: one report for each of the five research pillars (Connected and Automated Vehicles, Mobility Decision Science, Multi-Modal Freight, Urban Science, and Advanced Fueling Infrastructure), and an additional report on the development of the multi-fidelity, end-to-end modeling workflow that captures the complex interactions among mobility decision-making, technology implementation, mobility service models and modes, land use, and electric vehicle (EV) charging infrastructure. Because FY2020 was a transition year between the two phases of SMART Mobility, focus was placed on creating the final reports and establishing new projects for SMART Mobility 2.0. Therefore, there are relatively few projects summarized in the SMART Mobility section of this Annual Project Report (APR). New projects developed and initiated under SMART Mobility's second phase will be included in the FY2021 APR.

In addition to SMART Mobility, nine new projects were awarded within EEMS's Connectivity and Automation Technology R&D portfolio in FY2020, and research in the AI, HPC, and Data Analytics research area made significant progress. Meanwhile, advancements were made in the modeling, simulation, evaluation, and data management tools that support the EEMS Program and VTO more broadly. Results, insights, and progress from these four areas are described in detail through the remainder of this APR. Selected highlights and accomplishments from these activities are summarized here.

⁹ <http://www.trb.org/TRBAVSMForum/AVSMForum.aspx>

- After three years researching the complex interactions of future mobility technologies and services, DOE’s Office of Energy Efficiency and Renewable Energy (EERE) published a series of six SMART Mobility Capstone reports summarizing the Consortium’s research methods, results, and insights. In conjunction with the publication of these Capstone reports, the EEMS Program and SMART Mobility Laboratory Consortium convened a series of webinars during 2020 to discuss the findings and answer questions about the research. The Capstone reports, as well as the webinar presentations, recordings, and transcripts, may be downloaded at the following URL:

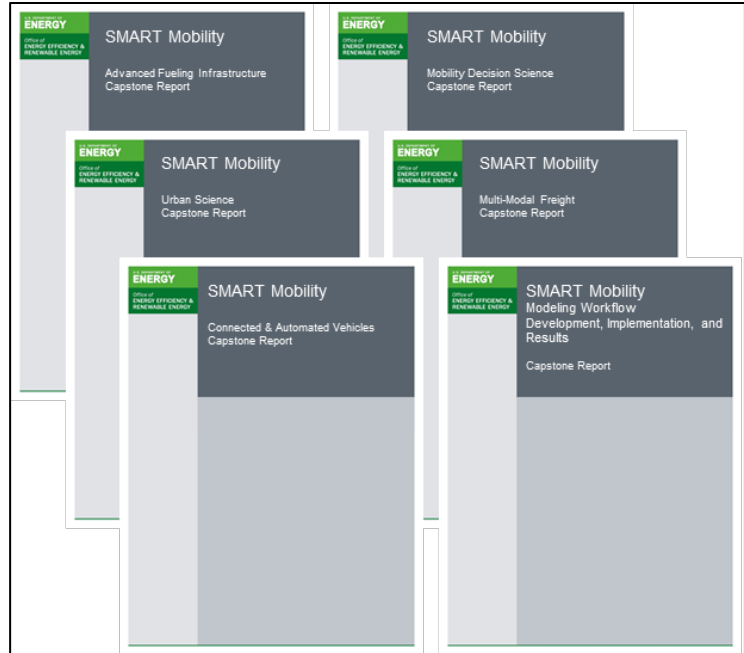


Figure 1 SMART Mobility Capstone Reports were published in FY2020.

<https://www.energy.gov/eere/vehicles/downloads/eems-smart-mobility-capstone-reports-and-webinar-series>

- Through carry-over work in the SMART Mobility Laboratory Consortium, Lawrence Berkeley National Laboratory (LBNL) led research to develop and field-test an integrated traffic signal control algorithm that incorporates trajectory planning for connected and automated vehicles. This project successfully developed algorithms that improved traffic throughput and time delays while reducing overall energy consumption, and demonstrated results using a combination of simulation and a hardware-in-the-loop (HIL) test track. With cooperative signal control combined with trajectory planning, overall vehicle speeds in the test loop increased by 29%, while vehicle energy consumption was reduced by 27%. (I.1.2 – Cooperative Adaptive Cruise Control (CACC)/Platooning Testing; Measuring Energy Savings, Interaction with Aerodynamics Changes and Impacts of Control Enhancements)

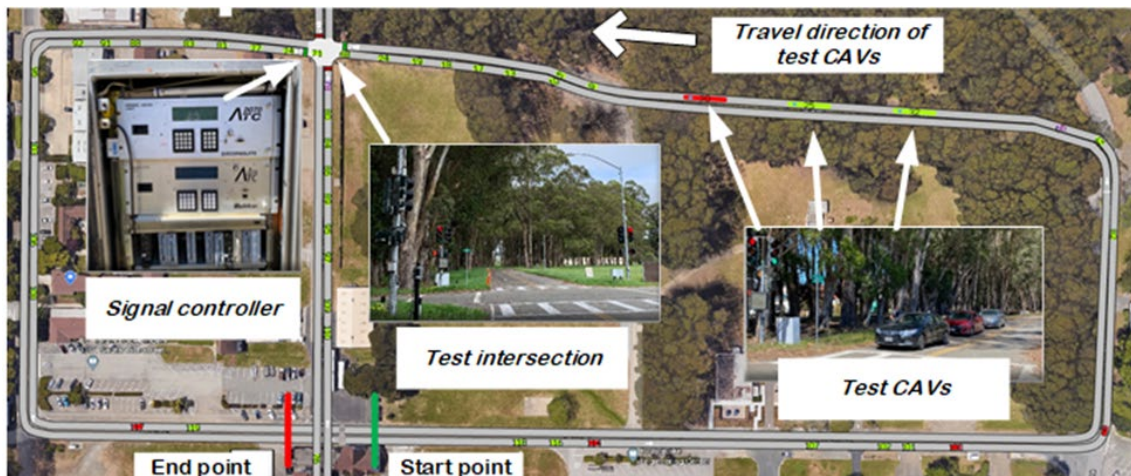


Figure 2 Hardware-in-the-Loop (HIL) Test Track.

- The National Renewable Energy Laboratory (NREL) led work through the SMART Mobility Laboratory Consortium to continue to improve the mobility energy productivity (MEP) metric, which quantifies the energy, cost, and time associated with transportation to access opportunities. In FY2020, baseline MEP calculations were extended to 100 cities in the United States, while the computational methodology for MEP was automated. Furthermore, these MEP calculations were made accessible through a web-based visualization tool, helping to disseminate this important metric to a large number of stakeholders. (I.1.4 – Urban Science)

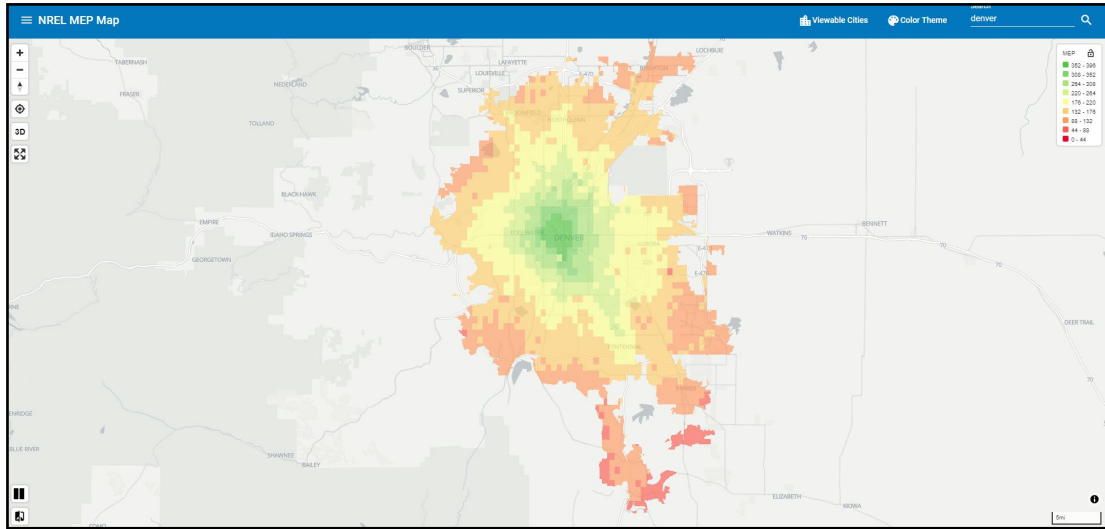


Figure 3 Web Visualization of MEP Calculation.

- In the first phase of SMART Mobility, the Consortium developed two implementations of the SMART Mobility Modeling Workflow, built on the POLARIS and BEAM agent-based transportation system models developed by Argonne National Laboratory (ANL) and the Lawrence Berkeley National Laboratory (LBNL), respectively. These models were originally applied to the Chicago and San Francisco metropolitan areas. In FY2020, the SMART Mobility Consortium

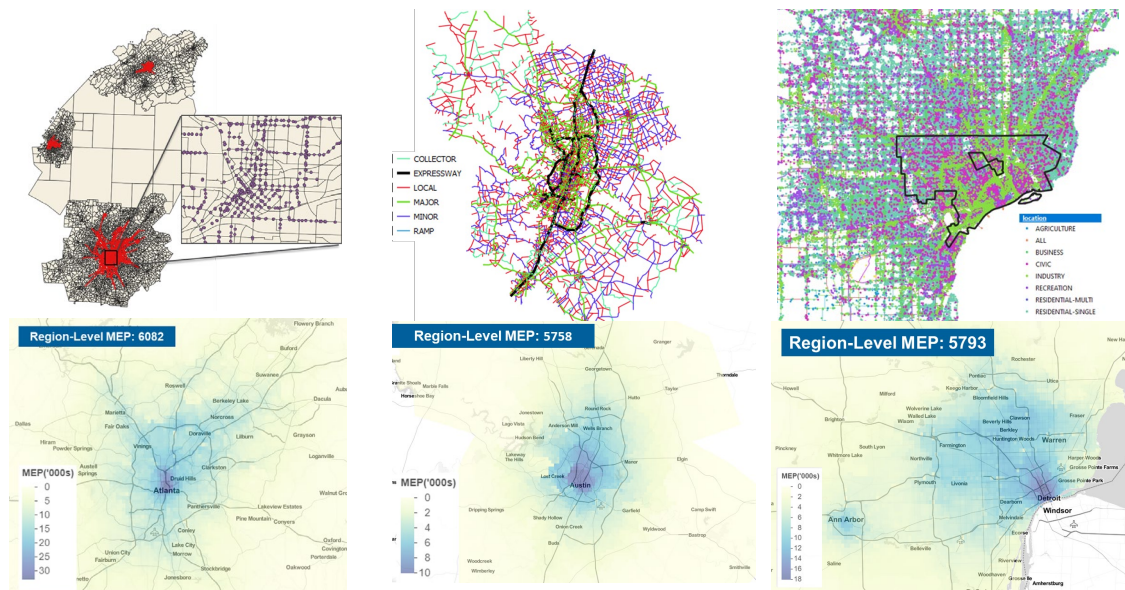


Figure 4 Visualizations of Transit and MEP in Atlanta (left); Road Network and MEP in Austin (middle); and Activity Locations and MEP in Detroit (right)

expanded the application of these models to three new cities: Detroit, MI; Austin, TX; and Atlanta, GA (POLARIS only). This effort demonstrated the applicability of the SMART Mobility Modeling Workflow to any city or region, and established new baseline models that will be used for scenario analysis in SMART Mobility 2.0. (I.1.5 – GPRA New Cities Modeling – POLARIS; I.1.6 – Transportation System Modeling of Southeastern Michigan and Austin, TX Using BEAM)

- Within the AI, HPC, and Data Analytics activity area, Pacific Northwest National Laboratory (PNNL) led research to automate the collection of multi-modal traffic data, develop traffic

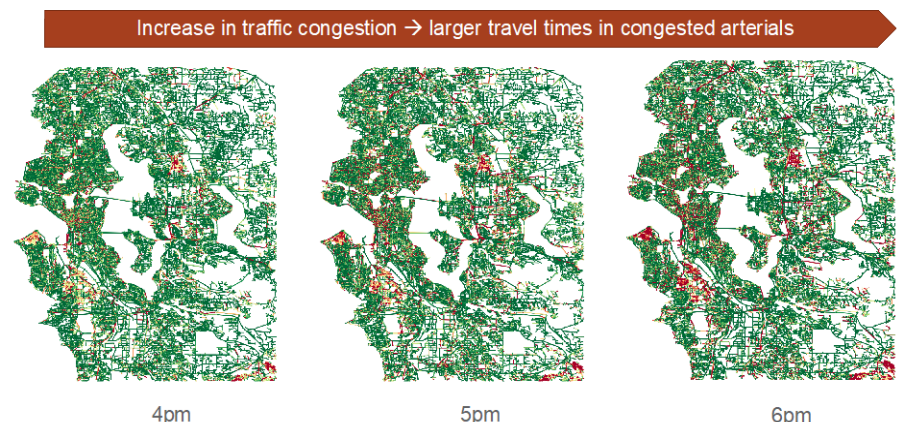


Figure 5 Visualization of the travel time estimates obtained from TranSEC for Seattle

state estimation methods, and implement a prototype tool for travel time estimation in large-scale metropolitan traffic networks. This research led to the creation of the Transportation State Estimation Capability (TranSEC) – a new approach to help urban transportation analysts discover system optimization opportunities to reduce congestion, and to help urban traffic engineers get access to actionable street-level information about traffic patterns in their cities (I.2.4 – Transportation State Estimation Capability)

- Oak Ridge National Laboratory (ORNL) led research within the Core Simulation and Evaluation Tools area to develop capabilities to accurately verify the energy benefits and emissions impacts of advanced connected and automated vehicle technologies with physical hardware in the laboratory interacting with virtual traffic environments. The team made significant progress in developing a “virtual/physical proving ground”, integrating “vehicle-to-everything” (V2X) communications capabilities, and using this platform to support connected and automated vehicle (CAV) research (e.g., through collaboration with the American Center for Mobility described in II.1.3 – Validating Connected, Automated, and Electric Vehicle Models and Simulation). (I.3.3 – Virtual and Physical Proving Ground for Development and Validation of Future Mobility Technologies)



Figure 6 ORNL CAVE Lab with Vehicle-in-the-Loop Functionality

and using this platform to support connected and automated vehicle (CAV) research (e.g., through collaboration with the American Center for Mobility described in II.1.3 – Validating Connected, Automated, and Electric Vehicle Models and Simulation). (I.3.3 – Virtual and Physical Proving Ground for Development and Validation of Future Mobility Technologies)

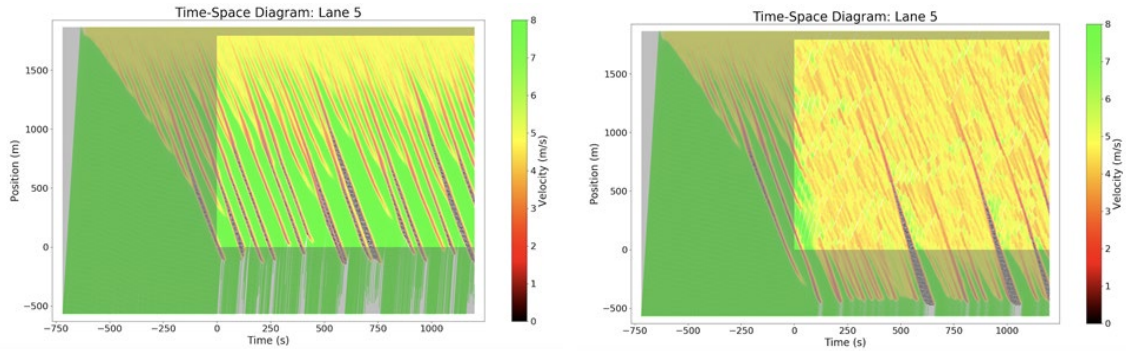


Figure 7 Space-time diagram of simulated a lane The dark region indicates segments where control is not applied. (Right) Wave formation is persistent. Left) Space-time diagram where 10% of the vehicles are controlled via RL.

- Within the Connectivity and Automation Technology R&D area, the University of California at Berkeley led a consortium of universities including Rutgers, Temple, Arizona, and Vanderbilt in the development of AI and theory-based control algorithms that smooth traffic flow and result in a 10% energy savings with only a 5% penetration of vehicles equipped with these controls. In FY2020, deployment of infrastructure hardware on the I-24 corridor in Tennessee (where the final demonstration will take place) was initiated. Computer vision algorithms were also developed to enable the extraction of full traffic-level information during the demonstration phase of the project. Additionally, the team has performed traffic flow and energy modeling to confirm that their Reinforcement-Learning (RL) control algorithms are capable of surpassing the 10% energy savings target. (II.1.2 – CIRCLES: Congestion Impacts Reduction via CAV-in-the-loop Lagrangian Energy Smoothing)
- Clemson University completed the development of anticipative vehicle guidance algorithms that result in up to a 10% average energy efficiency gain in mixed traffic depending on the penetration of the CAV controls. The team developed a novel vehicle-in-the-loop (VIL) platform and used it to demonstrate the results of their algorithms through stable co-simulation of experimental vehicles and virtual vehicles. (II.1.7 – Boosting Energy Efficiency of Heterogeneous Connected and Automated Vehicle (CAV) Fleets via Anticipative and Cooperative Vehicle Guidance)

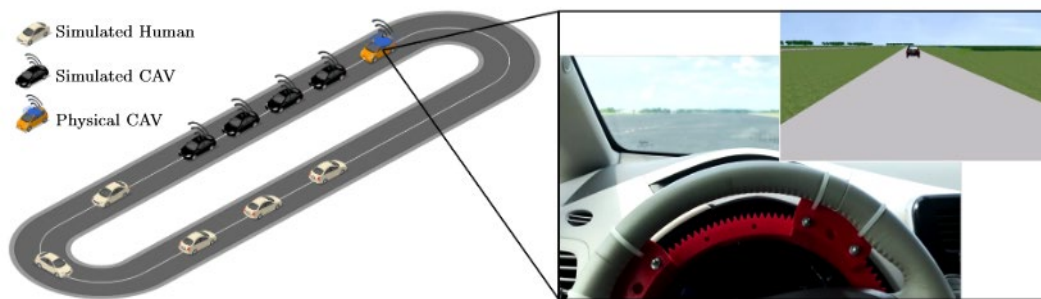


Figure 8 Vehicle-in-the-Loop Simulations: physical vehicle integrated in a string of vehicles in VISSIM.

We are pleased to submit the Annual Progress Report for the Energy Efficient Mobility Systems Program for FY 2020. Inquiries regarding the EEMS Program and its research activities may be directed to the undersigned.



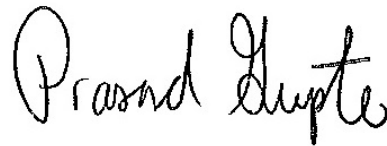
David L. Anderson
Program Manager
david.anderson@ee.doe.gov



Erin E. Boyd
Technology Manager
erin.boyd@ee.doe.gov



Heather Croteau
Technology Manager
heather.croteau@ee.doe.gov



Prasad Gupte
Technology Manager
prasad.gupte@ee.doe.gov

I Computational Modeling and Simulation

I.1 SMART Mobility

I.1.1 Experimental Evaluation of Eco-Driving Strategies (LBNL)

Wei-Bin Zhang, Principal Investigator

Lawrence Berkeley National Lab
1 Cyclotron Road
Berkeley, CA 94720
Email: wbzhang@berkeley.edu

Erin Boyd, DOE Technology Manager

U.S. Department of Energy
Email: erin.boyd@ee.doe.gov

Start Date: October 1, 2018
Project Funding: \$300,000

End Date: September 30, 2020
DOE share: \$300,000

Non-DOE share: \$0

Project Introduction

The goal of this project is to analytically and experimentally evaluate CAVs Eco-Driving strategies with regard to the energy saving benefits, impacts on efficiency, and safety of surrounding traffic. The evaluation of energy savings addresses the subject vehicle and vehicles following behind. We investigated a broad set of Eco-driving strategies in order to fully understand the potential energy-related benefits and impacts of each. Furthermore, we analytically and experimentally quantified the benefits and impacts of intersection Eco-Approach and Departure (EAD) assistant strategies.

Objectives

- Analysis of Eco-Driving strategies for a wide range of driving scenarios and applications to quantify the strategies with the largest energy savings.
- Collection of comprehensive vehicle trajectory level traffic data at the CA arterial test corridor to establish a baseline energy model for individual vehicles and the overall traffic for various traffic conditions.
- Use an instrumented vehicle (with Eco-approach and departure advisory and traffic detection capabilities) in the field to quantify realistic energy saving benefits of the subject vehicle and impacts on safety and efficiency to surrounding traffic (e.g., measures: acceleration, deceleration, headways, and Time to Collision).

Approach

Task 1. Assessment of Eco-Driving Strategies

Analysis of Eco-Driving strategies for a wide range of driving scenarios and applications will be evaluated to establish a foundational understanding of associated energy implications and assess where the biggest gains can be made.

Task 2. Field data collection at an urban arterial corridor

Portable video data collection devices are used to collect 360-degree video data at 10 signalized intersections and a number unsignalized intersections. Comprehensive vehicle trajectory level traffic data are abstracted from the video data collected to establish a baseline energy model for individual vehicles and the overall traffic for various traffic conditions.

Task 3. Data analyses

Data processing tools are developed for detection and tracking vehicles movements. Models are developed to process data to enable assessments of the fuel consumptions and emissions for vehicles traveling in traffic under real-world conditions. Data analyses will be conducted to establish a baseline energy model for individual vehicles and the overall traffic for various traffic conditions (free flow to heavy congestions).

Task 4. Field testing involving ECO approach and departure

The ECO Approach and Departure will be experimentally tested using a commercially available EAD app Enlighten developed by Connected Signals. An instrumented vehicle (with Eco-approach and departure advisory and traffic detection capabilities) and a number of conventional vehicles are used in the field to quantify realistic energy saving benefits of the subject vehicle and impacts on safety and efficiency to surrounding traffic (e.g., measures: acceleration, deceleration, headways, and Time to collision (TTC)).

Results**Task 3. Further Analyses of Unproductive fuel consumptions at signalized and stop sign Controlled Intersections Through Field Data****3.1 Unproductive Fuel Consumption at Signalized Intersections**

As we evaluate fuel saving benefits at the intersection level, it is critical to determine the level of unproductive fuel consumption that can be addressed by more situationally aware signal phase and timing. The unproductive fuel consumption for signalized intersections is the excessive fuel consumption for vehicles being stopped by traffic controls when neither vehicles nor pedestrian activities are present at the conflicting approaches.

Data analysis was conducted to assess the traffic behaviors and unproductive fuel consumption using the data collected at the test intersection located on Santa Clara St. and 4th St., in San Jose, California. The results reported in 2019 EEMS report concluded that approximately 50% of vehicles stopped at the test intersection during the red phase. During the evaluation period 70% to 80% of vehicle stops observed encountered no conflicting vehicles during the red phase. Each of these ‘unconflicted stops’ resulted in added fuel consumption during idling. These unnecessary stops are the primary cause of unproductive fuel consumption at signalized intersections, which accounts for over 15% of total estimated fuel consumption at this test intersection during observation.

Further analysis was conducted to identify various components of unproductive energy consumption and countermeasures that offer the most potential to minimize wasted fuel at signalized intersections. Eco Approach and Departure (EAD) strategies applying advanced signal status information may enable an instrumented vehicle to maintain proper speed profile to safely pass through the intersections at the end of green signal phase or when signal switches from red to green. Advanced signal status may also allow an instrumented vehicle to anticipate the change to a red light and come to a full stop with gentler deceleration. Field data was analyzed to explore the opportunities for Eco Approach and Departure to functions. Figure I.1.1.1 depicts trajectories of vehicles arriving at the southbound approach at the test intersection within a one-hour time period. As indicated by the shaded areas, the number of arrivals at the end of green and at the end of red is a small fraction of all vehicle arrivals, indicating that the opportunities for fuel savings due to Eco Approach and Departure strategies will be limited, even if all vehicles are assumed to have EAD capability.

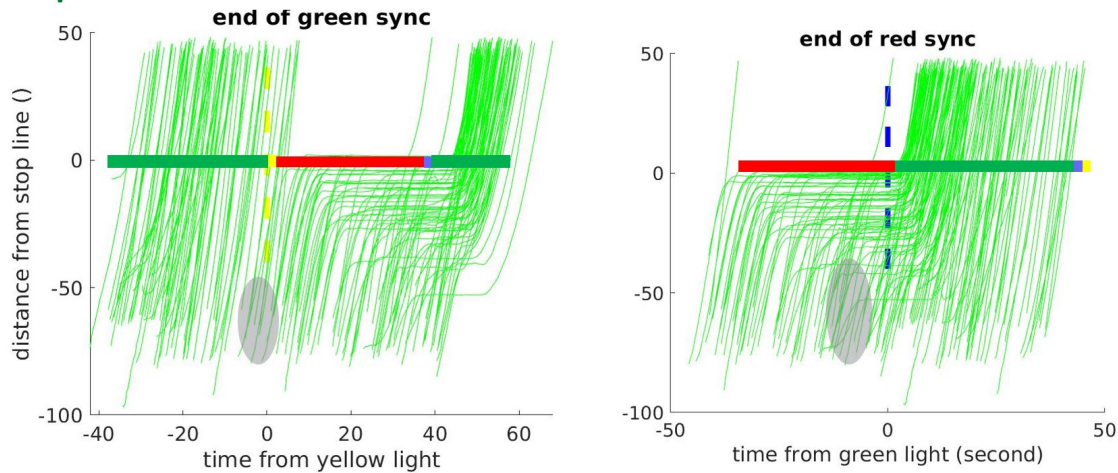


Figure I.1.1.1 The Opportunities for Vehicles to Arrive at the End of Green Phase or at End of Red Phase

The data were further analyzed to assess how to deal with remaining large majority unnecessary stops at the intersection level. Figure I.1.1.2 illustrates the trajectories of traffic during 20 signal cycles at the test intersection. The figure shows that during many of the signal cycles there were no approaching vehicles on the minor street (upper figure) when the traffic signal had stopped vehicles on the main approach (lower figure). The figure also shows that the phase length for the minor street is longer than necessary for many of the cases.

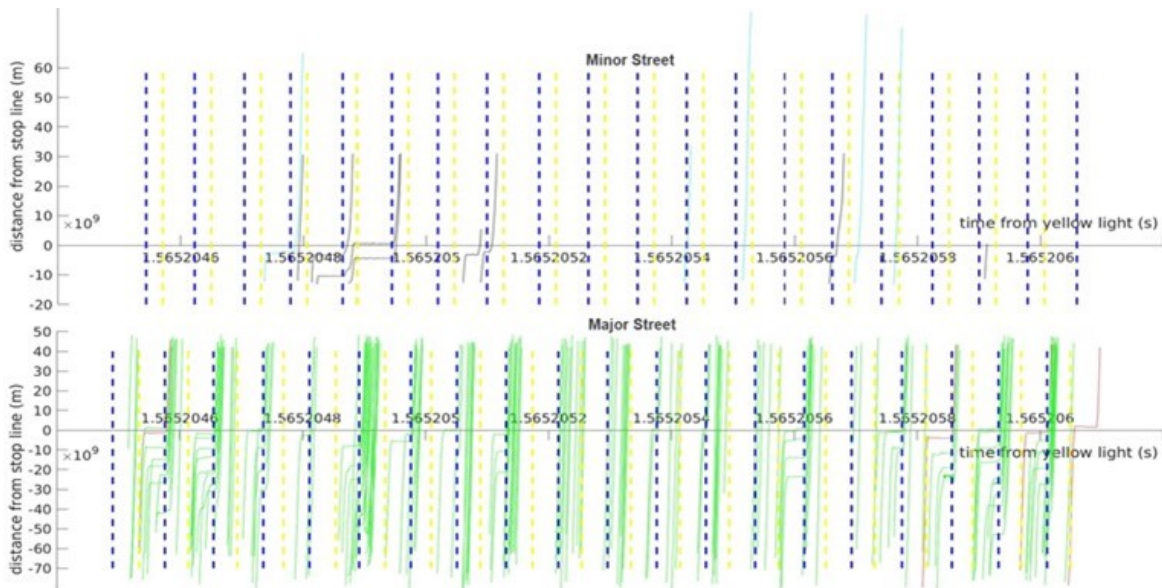


Figure I.1.1.2 Trajectories of Arriving Vehicles at Major and Minor Streets

While EAD may address a portion of unproductive fuel consumption when the signal is switched from green to red or vice versa, the unproductive fuel consumed when vehicles are stopped without the presence of any conflicting traffic should also be assessed. The study of the field data at the intersection level revealed that unnecessary stops are caused by inefficient traffic control at signalized intersections. Although adaptive traffic signal control system is used in the city of San Jose, the vehicle detection system is suboptimal because it can only detect the presence of vehicles near the stop bars. The signal control system at the test intersection was deficient with respect to vehicle approach detection, queue detection, and pedestrian detection capabilities. Due to these deficiencies, the traffic control system did not adapt traffic conditions in real-time. Note that vehicle presence detection is considered standard detection capability for adaptive traffic control system. As a

result, the traffic control was unable to adapt to real-time traffic conditions except for the presence of vehicles at the stop bar areas. The study concluded that unproductive fuel consumption can potentially be mitigated via advanced detections (e.g., latest radar and/or camera technologies) at intersections or with connected vehicle technologies that enable vehicles to communicate with intersections prior to their arrival at the intersection. Both mitigation approaches can enable the traffic controller to take into consideration the full characteristics of traffic activities in the vicinity of the signalized intersection.

3.2 Unproductive Fuel Consumption at Stop-Sign Controlled Intersections

The unproductive fuel consumption for unsignalized intersections is defined as the portion of fuel consumed by vehicles making decelerations and stops at the intersections when no vehicles nor pedestrian activities are present at the conflicting approaches. In order to estimate unproductive fuel consumption, the trajectory of slow-down-then-speed-up activity of each vehicle within the range of 40m before and after the stop sign is fed into the fuel consumption model. When there are no conflicting vehicles, if the vehicles make a stop or slows down, the extra fuel they use (i.e., unproductive fuel consumed) is compared with a reference vehicle which keeps a steady speed to cross the intersection. The vehicle behaviors are classified into complete stop (speed < 1mph), rolling stops (1 mph < speed < 5mph), and running stop signs (speed > 5mph). Data observations reported in [1] shows that at the test intersection in Pleasant Hill California, over 70% of the arriving vehicles from all approaches at this intersection do not make a complete stop. Close to 30% of all the vehicles made a full stop for this case study. Among the full stop vehicles, more than 60% of them made full stops when there were vehicles at the conflicting approaches, whereas 30%-40% of full vehicle stops were made when no vehicles appeared at other approaches. The analysis shows that the rate of rolling stops and stop sign running has an inverse relationship with the rate of conflicting vehicles, suggesting that a significant portion of the full stops made at the stop lines are likely caused by the presence of conflicting vehicles, i.e., not fully stopping was not an option. Specific to the Pleasant Hill intersection, vehicles arriving from the east and west approaches had higher rolling stop and stop sign running rate, where the rate of conflicting vehicles from South and North approaches were lower. The analysis also indicates that the unproductive fuel consumption at unsignalized intersections within the range of 40 meters before and after the stop sign can be as high as 60% of the fuel consumed at this intersection (within the assessment zone) if all vehicles make proper full stops.

Additional data were collected at five ‘four-way stop-sign’ controlled intersections in Saratoga, California. Driving behaviors were evaluated to compare with the data collected at the unsignalized intersection in Pleasant Hill. On average, drivers made full stops 35% of the time, rolling stops 53% of the time, and ran stop signs 12% of the time. Most of the full stops occurred when there were vehicles at the conflicting approaches. When no presence of conflicting vehicles, drivers stopped 13.5% of the time, made rolling stops 68% of the time, and ran stop sign 20% of the time. With other vehicles presented, drivers made full stops 50% of the time, rolling stops 42% of the time, and ran stop sign 8% of the time. With present of pedestrians, drivers made full stops 20% of the time, rolling stops 60% of the time, and ran stop sign 20% of the time. However, seven of the eight instances of a rolling stop occurred when the pedestrian was not walking in the trajectory of the vehicle. Right turns were an especially large cause of concern. When there was no direct conflict with the turn, drivers made a full stop 7% of the time, a rolling stop 78% of the time, and ran stop sign 14.8% of the time. When there was a vehicle or pedestrian blocking the path, drivers still only made a full stop 56% of the time and a rolling stop 44% of the time.

While there are some differences of the analyses results, the observation findings from these intersections are consistent. The quantitative differences are attributed to the intersection geometry designs, the traffic volume and the percentage of local driver population (i.e., the level of familiarity with the intersection and traffic patterns). These results all point to the findings that only a small portion of the vehicles make complete stops as required by the traffic laws at stop sign controlled intersections. A significant portion of the vehicles do not come to full stops. The predominant cause of the full stop is the presence of conflicting vehicles or pedestrians. Directly relevant to this study, the unnecessary stops result travel delays and unproductive fuel consumption.

The unproductive fuel consumption at unsignalized intersections can be reduced by allowing vehicles to pass through the intersection at a steady speed when no vehicles are present. Among potential remedies, signal control with intelligent vehicle and pedestrian detection can be an effective way of minimizing unproductive fuel consumption. However, most of the current unsignalized intersections do not have enough vehicular and pedestrian volumes or crash history to justify the installation of traffic signals as defined by the Manual on Uniform Traffic Control Devices (MUTCD) [3]. Roundabouts have also been viewed as a potential solution in recent years, but they are very costly and in many cases are undoable due to alignment limitations. Alternatively, yield signs are appropriate in some cases to call on drivers to slow down, defer to oncoming traffic, stop when necessary, and proceed when safe. Connected Vehicle technologies have the potential to offer more intelligent solutions to maintain safety and efficiency while reducing the unproductive fuel consumption at unsignalized intersections. Further work on innovative strategies/technologies is needed.

Task 4. Field Evaluation of Eco Approach and Departure Application

Further data analysis was conducted for the test intersection to compare fuel consumptions of vehicles with and without EAD; it confirmed that 10%-20% fuel savings may be achieved when an EAD scenario occurs. However, these scenarios occurred less than 15% of the time when the instrumented vehicles arrived at the test intersection. As a result, EAD strategies prevented stopping at the end of red phases for only ~3%-4% of arrivals, while ~10%-12% of arrivals experienced gentler deceleration at the end of the green phase. These results are considered optimal in terms of the benefits of EAD at the test intersection, as all test drivers have been advised to best utilize EAD information while maintaining safe operation. In the real world, drivers may not always pay attention to the EAD information and therefore may not take full advantage of all EAD opportunities.

The effectiveness of EAD function may also be affected by the characteristics of the arrival patterns of the traffic as well as the traffic detection capability. The EAD information is derived from the phase change prediction and the adaptive nature of signal control makes it difficult to accurately predict phase change. For adaptive traffic control system, the phase change prediction is complicated by the green phase extension optimized for arriving vehicles. The vehicle detection near the stop bars introduces significant uncertainties for the prediction. Figure I.1.1.3 shows the distributions of the green, yellow and red phases for the southbound signal. It is noted that the standard deviation of the green phase is rather big, indicating that the error for phase change prediction can be large. The large prediction error causes inaccurate EAD information, indicating that the opportunities for fuel savings due to EAD will be limited. This is true even if all vehicles are assumed to have EAD capability and may result in loss of confidence in the EAD system. EAD prediction errors may result in confidence loss in the EAD. One of the recommendations from this study is that the safety implications of large EAD prediction errors should be further studied under human factors research.

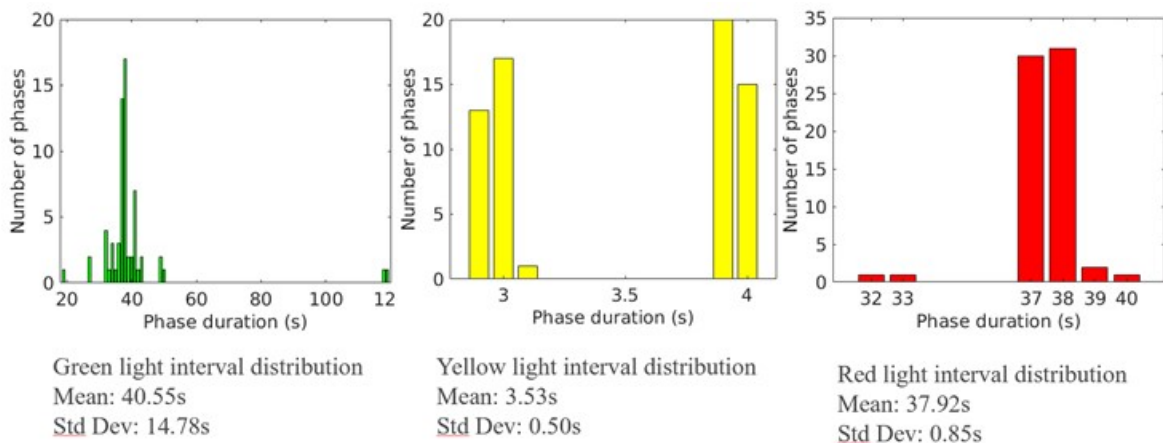


Figure I.1.1.3 Statistics of Durations of Green, Yellow and Red Phases for the Major Approach

We extended the test data to a trip-based fuel saving analysis. Assuming that average trip is 10-13 miles in length [4] and involves up to 10 intersections, the EAD may facilitate fuel saving benefits at one to two intersections. In this case, the fuel saving by EAD is less than 1% of the fuel consumed for a typical trip.

Conclusions

The following accomplishments have been made under this task:

1. Collection of additional vehicle trajectory level data at five unsignalized intersections in Saratoga California.
2. Data for one signalized intersection and one stop sign controlled intersection has been further analyzed thoroughly. Data analyses were also conducted for five additional stop-sign-controlled intersections. Conclusions have been made regarding unproductive fuel consumptions at signalized and unsignalized intersections, fuel saving benefits by EAD, and traffic control using Connected Vehicle technologies.
3. Eco Approach and Departure was evaluated based on the traffic data collection at signalized intersections in San Jose. Uncertainties introduced due to prediction error of signal phase change were also analyzed.

The key technical findings are summarized below:

Unproductive fuel consumptions at signalized intersection: Vehicle stops and idling when no conflicting vehicles were present at conflicting approach were the major cause for unproductive fuel consumption at signalized intersections. Approximately 50% of vehicles stopped at the test intersection during the red phase. For those stopped vehicle cases, 70% to 80% were stops that encountered no conflicting vehicles during the red phase, and resulted in an estimated 15% of unproductive fuel consumption at this test intersection during observation.

Benefits of Eco Approach and Departure: Analysis and field tests showed that fuel saving benefits of EAD were insignificant at both the trip and intersection levels and offer little for mitigating unproductive fuel consumption (e.g., less than 1% fuel saving for a typical trip). A more intelligent signal operation supported by advanced detection and connected vehicle technologies would be capable of addressing most of the unproductive fuel consumption at signalized intersections.

Unproductive fuel consumption at stop-sign controlled intersections: The majority of vehicles arrived at stop-sign controlled intersections did not encounter travelers at conflicting approaches and resulted in substantial unproductive fuel consumption (~30% total fuel consumption at the test intersection). Roundabouts and signal control may offer fuel saving benefits but are impractical to be deployed at the vast majority of unsignalized intersections. Additional benefits for improved coordination among vehicles using Connected Vehicle technologies should be explored.

It is important to note that the unnecessary stops that resulted in unproductive fuel consumption varied from intersection to intersection. Some of the independent factors that influenced the variance were the capacity and geographic design, the traffic control settings of the intersection, and the characteristics of traffic activities at the time when observation was conducted. As such, the analysis results reported herein represent ‘order-of-magnitude estimates’ that are specific to the test intersection.

Key Publications

1. Jiali Bao, Wei-Bin Zhang, Alex Wang, A Data-Driven Approach to a Comparative Study of Signalized and Stop Sign Controlled Intersections and Roundabouts, submitted for presentation at the 6th TRB International Roundabout Conference, Monterey, California, May 2020

References

1. USDOE Vehicle Technologies Office, Energy Efficient Mobility Systems, 2019 Annual Progress Report
2. FHWA, Why can't we have stops signs to reduce speeding along my street, https://safety.fhwa.dot.gov/intersection/other_topics/fhwasa09027/resources/Iowa%20Traffic%20and%20Safety%20FS-%20Unsignalized%20Intersections.pdf
3. FHWA, Summary of Travel Trends 2017 National Household Travel Survey
4. FHWA, Manual on Uniform Traffic Control Devices, 2009 Edition

Acknowledgements

Jiali Bao and Mike Mills of Lawrence Berkeley National Laboratory, Jacob Tsao of San Jose State University and Alex Wang, I-Ming Chen, Ching-yao Chan and Pin Wang of University of California at Berkeley made substantial contributions to the research results reported herein. The research team would also like to express appreciation for ten UC Berkeley volunteers and San Jose building managers for their assistance and help for conducting the data collection and field testing. The research team would like to thank Erin Boyd and David Anderson of United States Department of Energy for their guidance, through review and technical and programmatic assistance.

I.1.2 Cooperative Adaptive Cruise Control (CACC)/Platooning Testing: Measuring Energy Savings, Interaction with Aerodynamics Changes and Impacts of Control Enhancements (LBNL)

Xiao-Yun Lu, Principal Investigator

Building 190
Lawrence Berkeley National Laboratory
1 Cyclotron Road, Berkeley, CA
Email: xiaoyunlu@lbl.gov

David Anderson, DOE Program Manager

U.S. Department of Energy
Email: david.anderson@ee.doe.gov

Erin Boyd, DOE Technology Manager

U.S. Department of Energy
Email: erin.boyd@ee.doe.gov

Start Date: October 1, 2018
Project Funding: \$75,000

End Date: December 31, 2020
DOE share: \$75,000

Non-DOE share: \$0

Project Introduction

Intersections are nodes of traffic that dominate the performance of an urban road network in many metropolitan areas. The traffic signal control is the most common way to support the safe and efficient operation of intersections [1],[2]. In the era of Connected Vehicles (CV) and Connected Automated Vehicles (CAV), the advances of vehicle connectivity and automation have great potential to improve the capabilities of intersection controllers, reduce time delays, energy consumptions and emissions. With CAV, the controller not only has access to aggregated traffic datasets from traditional point traffic sensors but also can obtain high-resolution vehicle trajectory information from CVs and CAVs. Such rich datasets improve the controller's awareness of the traffic situations of all phases, enabling it to generate signal control plans to optimize the intersection performance [3],[4]. Alternatively, the improved intersection controller can broadcast the signal timing plans or reference vehicle trajectories via infrastructure-to-vehicle (I2V) communications [5],[6]. Upon receiving the messages, CAVs can adjust their trajectories to reduce delays due to signal control. Such proactive driving patterns are expected to improve safety, mobility, and energy efficiency of the CAVs and other traffic.

Objectives

The objectives of the project was to develop and field test an integrated intersection traffic signal control algorithm and CAV activities. This will include a cooperative intersection control algorithm that maximizes the overall intersection throughput based on the fused loop detector data, CAV data, and trajectory planning for CAVs. As a byproduct, it is expected that the delay reduction due to throughput maximization could bring energy savings and emission reduction benefits. The project proposed to test the algorithms with physical CAV, an intersection and traffic signal controller, a real-time simulation with the imbedded CAVs. The simulation will generate virtual traffic signal control and activation, road sensor, and on-vehicle sensors events. The overall systems are integrated with Vehicle-to-Vehicle (V2V) and Vehicle-to-Infrastructure (V2I) communications.

Approach

The proposed cooperative intersection control system contains a traffic signal optimization algorithm and a CAV trajectory planning algorithm. It computes the next cycle's signal plan and recommended trajectories a few seconds before the end of the current signal cycle. During the update process, the control system first

searches for the optimal phase sequence and timing using a dynamic programming approach reported in [7]. The dynamic programming approach requires future vehicle positions as the input. To this end, the trajectory planning algorithm is implemented to determine the projected vehicle positions for CAVs that lead vehicle platoons. The car-following models in [8] were used to identify the positions for CAVs and Human-driven Vehicles (HV) that follow the platoon leader. The trajectory planning algorithm does not require detailed trajectories of the preceding vehicles as the input. It is ideal for the application in the mixed traffic flow where there could be large estimation errors of HVs' future trajectories.

It adopts a dynamic programming algorithm to search for the optimal phase sequence and green time distribution for the next signal cycle. This is ideal to address the traffic flow variability associated with the mixed traffic flow. In addition, the control algorithm adopts a proportional controller to generate reference trajectories for CAVs such that they can lead a mixed vehicle platoon to pass the intersection in the next cycle without stopping. This algorithm only requires the start time of the green light and the estimation of the queue length as the inputs. Those inputs are readily available from the signal control algorithm. It does not rely on the assumption that HV trajectories can be predicted via deterministic car-following models. This makes the trajectory planning algorithm ideal to implement with the proposed signal optimization algorithm.

To test the proposed cooperative intersection controller, this study has developed a hardware-in-the-loop (HIL) tool by integrating a real-time simulation tool, a real-world intersection site, and real test CAVs. The simulation tool can generate realistic background traffic streams by using well-calibrated car-following and lane-changing models. The HIL tool includes three CAVs that are equipped with Cooperative Adaptive Cruise Control (CACC) with different powertrains which have been developed under a sister project of EEMS1.0. The presented intersection control algorithm is deployed at a real-world intersection in a 2070 signal controller. The interaction among those components is achieved via dedicated short-range communications (DSRC). The most important tool components (e.g., test CAVs, signal controller, and communication) are represented by physical systems. The HIL tool can provide test datasets that accurately reflect the effectiveness of the proposed intersection controller.

Performance evaluations are conducted as follows:

- Overall traffic throughput, time delay etc. are estimated in the real-time traffic simulation which is synchronized in time with the traffic signal and in space with the physical CAVs. It also provides an energy consumption estimated based on a simulation model.
- Energy consumption estimation are conducted in three ways:
 - Based on a simulation model for the overall traffic
 - Using fuel rate or other information from OBD II information reading on the vehicle
 - Measure the actual fuel injected into the tank with a fuel gauge in the resolution of tenth of a liter and with systematic records for each test vehicle; this is considered as the ground truth.

The Concept of Operation of the overall system is depicted as follows:

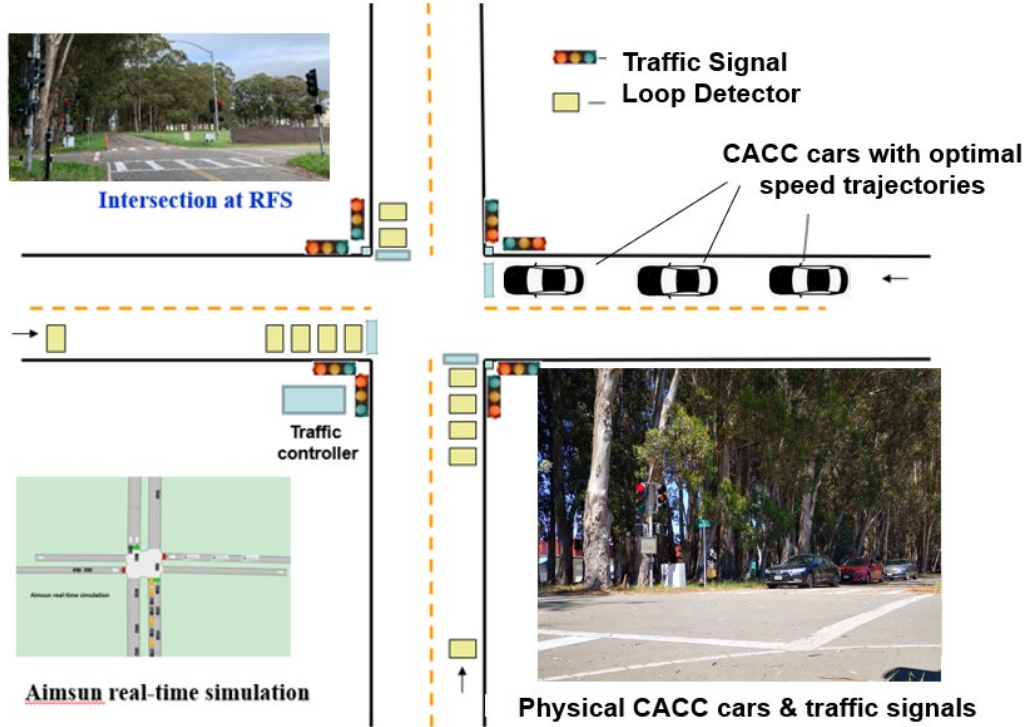


Figure I.1.2.1 The Concept of Operation for Integrated Traffic Signal Control and CAVs

Traffic Signal Optimization Algorithm

The traffic signal optimization algorithm maximizes the intersection throughput. It computes optimal signal plans based on traffic information from CAVs and fixed traffic sensors. Those traffic data sources offer real-time states (e.g., speed and position) of vehicles within the intersection region for the algorithm to estimate the future positions of those vehicles. The estimated position indicates if a target vehicle can pass the intersection at the end of a signal cycle. Such an estimation is the basis for calculating the intersection throughput. The signal optimization algorithm adopts a dynamic programming approach to compute optimal signal plans. This allows it to generate signal plans with changeable phase sequences and cycle lengths. In addition, the dynamic programming approach can be easily implemented in a parallel computing framework. This greatly reduces the computation time, making the algorithm feasible for real-time implementation.

The traffic signal optimization algorithm makes an update at the end of a signal control cycle. The input information includes the position and speed of CAVs and the number of HVs between two consecutive CAVs. The CAV information is directly obtained via vehicle-to-infrastructure communications. The HV number is provided by traffic sensors that count vehicles that approach the intersection area from upstream intersections. The algorithm outputs the optimal signal phase sequence and timing to be implemented in the next cycle. The traffic signal optimization algorithm identifies the optimal signal plan that maximizes a performance function over a control horizon T . The performance function ω is given in (1):

$$\omega_j = \omega_{j-1} + Q_j \quad (1)$$

where j is the stage (phase) ID; Q is the number of departed vehicles in a phase. For a typical four-approach intersection, the phase ID is defined in Figure I.1.2.2. The number of departed vehicles is computed by (2):

$$Q_j = \sum_{i=1}^N D_i \quad (2)$$

where i is the ID of the intersection approach; N is the total number of approaches; D is the number of vehicles departed from an approach.

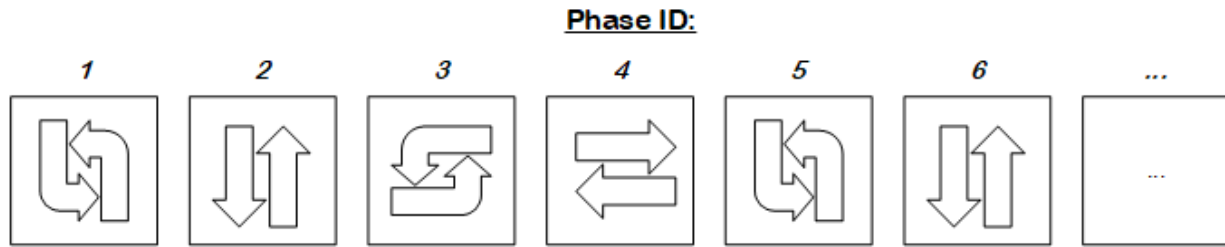


Figure I.1.2.2 The Definition of Phase ID

The dynamic programming approach is used to search the optimal signal plan. It considers individual phases sequentially. For every individual phase, the approach treats it as the last phase of a cycle and assigns different cycle lengths to it. The maximum values of the performance function under individual cycle lengths are recorded in the meantime. Such a process is repeated for the next phase by taking the performance function values of previous phases as the input.

The above optimal signal searching steps use the departed vehicle set D to update the performance function. The computation of the set relies on predictions of individual vehicles' positions at the end of the next signal cycle. If a vehicle's projected position is downstream from the stop bar, the vehicle is counted in D . To calculate the future position of a vehicle, the algorithm requires the subject vehicle's current speed v_0 and distance d_0 from the intersection, the total number of vehicles n in front of the subject vehicle, the remaining red time t_r before the green signal, and the duration of the green t_g . For the CAVs, v_0 and d_0 are directly obtained via vehicle-to-infrastructure communications. The HVs' v_0 and d_0 need to be estimated based on the information of their upstream and downstream CAVs. The estimation method was reported in [3]. The number of preceding vehicles n can be obtained from traffic sensors that provide vehicle counts upstream from the intersection [3].

Trajectory Planning Algorithm

The trajectory planning algorithm adopts a proportional controller that guides a subject vehicle to pass the intersection without stopping. This will reduce energy loss due to vehicle deceleration. The inputs of the algorithm are the length of the preceding queue and the start time of the next green signal. Those inputs are readily available from the signal optimization algorithm. The trajectory planning algorithm is depicted by (3):

$$a_{TP} = k_t \cdot (t_{eta} - t_{re}) \quad (3)$$

where a_{TP} is the acceleration of the subject vehicle; k_t is the control gain; t_{est} is the estimated time to arrive at the end of the queue; t_{re} is the remaining time before the last vehicle in the queue starts to move. With the controller, the subject vehicle will slow down and cruise at a low speed in advance before joining the queue. This will reduce or remove the queuing time for the subject vehicle and the following vehicles. This algorithm is only activated in a finite region upstream from the intersection coordinate.

Hardware-in-the-Loop Test System

The effectiveness of the proposed intersection controller was evaluated by a HIL test system. The HIL system includes a simulation environment that generates virtual traffic streams and physical test CAVs that interact with the virtual traffic on a real-world intersection. The proposed signal optimization algorithm is deployed on a 2070 signal controller, which changes the traffic lights at the test intersection. The test CAVs are equipped with CACC controllers that allow them to operate in CACC strings. The first test CAV also implements the proposed trajectory planning algorithm. When the first CAV passes the condition checks described in the

previous section, it will use the trajectory planning controller to regulate the movement. The HIL system components and the data flow among them are demonstrated in Figure I.1.2.3.

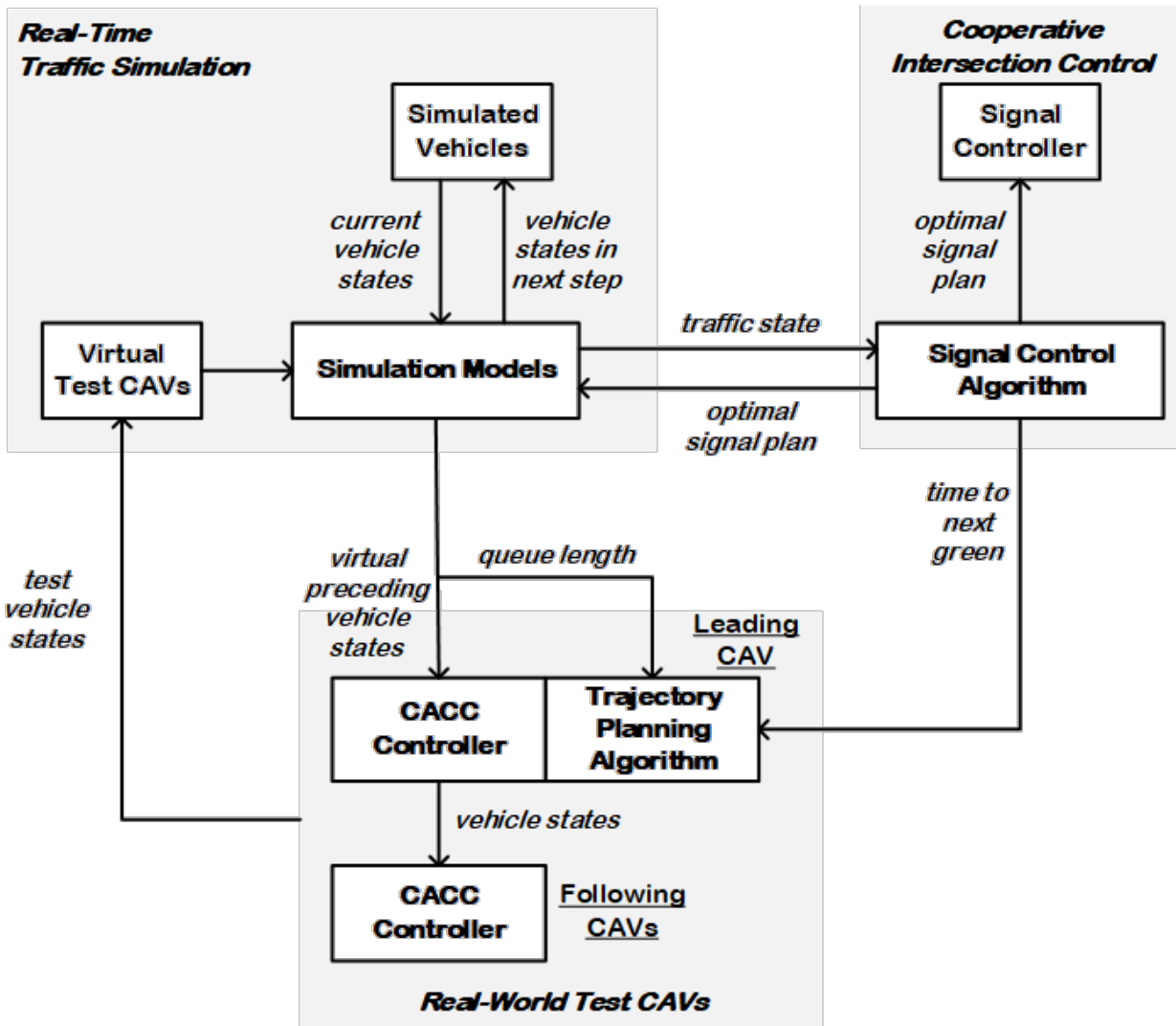


Figure I.1.2.3 HIL Components for Evaluating the Cooperative Intersection Control

The real-time traffic simulation provides virtual traffic streams in which the test CAVs can interact with simulated vehicles. Details of the simulation models can be found in [8]. The simulation uses virtual test CAVs as placeholders to represent the physical CAVs in the modeled road network. At each simulation interval, the simulation receives the location, speed, and acceleration from the test CAVs. This information is adopted to specify the speed and location of the virtual test CAVs in the simulated environment. Afterward, the remaining simulated vehicles update their movements with the new status of the virtual test CAVs considered. In the meantime, the simulation also shares the location, speed, and acceleration of the simulated vehicle that virtually leads the first test CAV. The information is the basis for the first CAV to update the movements.

The optimal traffic signal plan is also implemented in the simulation to affect the virtual traffic stream. The intersection control algorithm computes the control plan at the end of each signal cycle. Once the computation is completed, it sends the optimal signal plan to both the real-world traffic controller and the simulated traffic controller. The real and virtual controllers then implement the control plan for the next signal cycle. The intersection controller also sends the future green time to leaders of platoons so that they can develop

trajectories. The platoon leaders could be a simulated CAV or the physical test CAV. If it is the former case, the green time information is provided to the real-time simulation. Otherwise, the information is given to the test CAV.

CAV System Development

On the CAV control side, two systems have been developed to operate on the designed framework: Adaptive Cruise Control (ACC) + trajectory planning mode and CACC car-following. The former is implemented on the leader CAV to interact with any forward tracked virtual vehicle, whereas the latter is used on the follower vehicles connected with the leader CAV.

ACC + Trajectory Planning System

To control the car-following behavior of the leader vehicle, a hierarchical architecture is proposed. A high-level layer is developed that deals with the car-following and gap regulation kinematics, whereas a low-level layer deals with the vehicle longitudinal dynamics to track the reference received from the high-level system.

Low-Level Control Layer

The low-level control layer main task is to command the vehicle actuators to track the reference speed given by the high-level layer. The speed tracking structure is depicted in figure below:

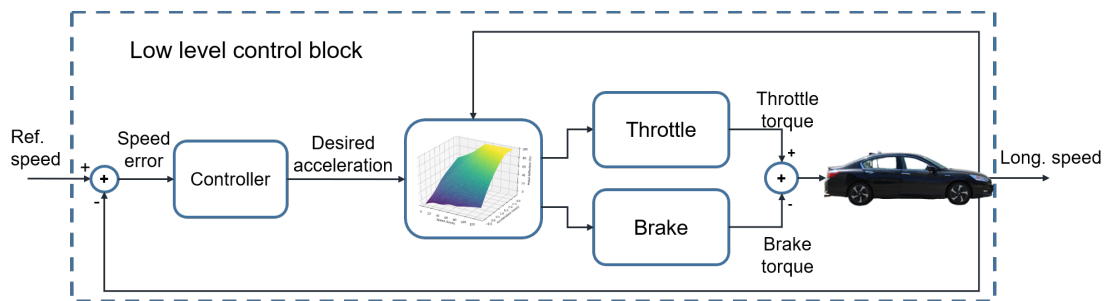


Figure I.1.2.4 Low-Level Control Layer for Reference Speed Tracking

The error between reference and measured longitudinal speed is processed by the feedback controller to generate the desired acceleration. In order to get the optimal throttle or brake application, the actuators have been accurately mapped in function of the obtained acceleration and current speed. This permits to have a 2D mapping lookup table that outputs the ideal throttle or brake in function of the measured speed and desired acceleration. These maps have been obtained through extensive open-loop testing in dynamometers. The speed tracking controller is designed to get the fastest tracking as possible, without leading to overshoot or harming the loop stability. The obtained closed-loop is subsequently tested to derive a low-level speed tracking model that is used in the design of the high-level control layer.

High-level Control Layer

In this layer, the longitudinal motion of the vehicle is handled, by combining cruise control, ACC and the trajectory planning modes. The ACC kinematics are controlled by this layer based on a constant time gap policy. Such policy proposes to keep a distance gap proportional to the vehicle speed, which not only imitates

how human drivers perform car-following, but also introduce a phase lead that increases the loop stability. The ACC structure is illustrated in the figure below:

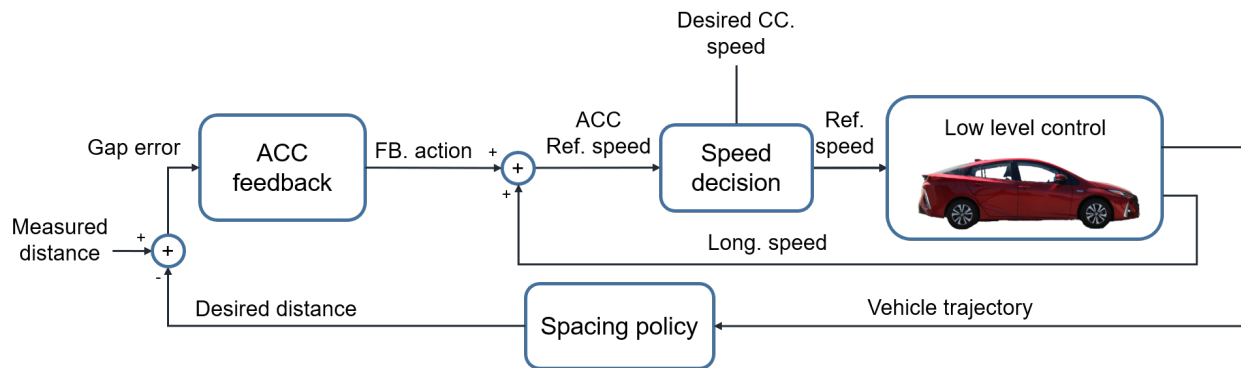


Figure I.1.2.5 ACC Block Structure

The ACC feedback controller adds the feedback (FB) action to the longitudinal speed. It processes the gap error between the distance to preceding vehicle and desired gap from the spacing policy. The ACC reference speed and desired cruise speed are fed to a speed decision algorithm that computes the reference speed for the low-level based on the headway distance to preceding vehicle. The figure below illustrates how is the headway classification regions used by the speed decision algorithm:

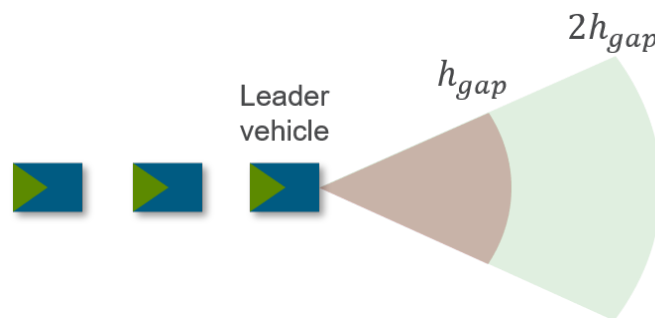


Figure I.1.2.6 Headway Regions for Cruise Control and ACC Decision Algorithm

If the virtual vehicle is farther than twice of the desired time gap h_{gap} , the vehicle will track the desired cruise speed. As soon as the subject vehicle gets closer to a virtual preceding car, the speed is reduced by penalizing in proportion of the relative speed towards such vehicle. This also guarantees a smooth transition towards the ACC car-following, once the distance is equal or less than $h_{gap}v(t)$.

In order to combine this speed decision algorithm with the trajectory planning output, the fusion is done at the desired acceleration level. The reference speed from the ACC structure in the figure above yields a desired acceleration once it is processed by the low-level layer controller, which is later combined with the trajectory planning in region prior to the intersection. The implemented logic is to take the most conservative acceleration between a_{TP} from (3) and desired acceleration within the low-level structure. Additionally, a linear increase of the gain k_t is performed before entering the trajectory planning region to guarantee a smooth transition to ACC + trajectory planning mode.

CACC System

The CACC followers in the string implement a state machine that manages the ACC and CACC operation, governed by the logic presented in the figure below:

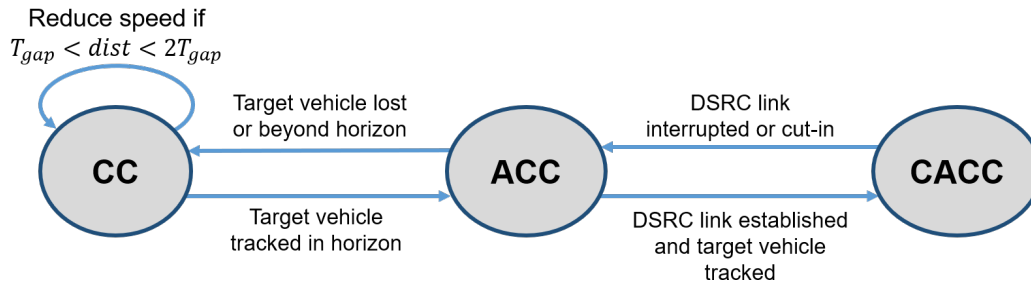
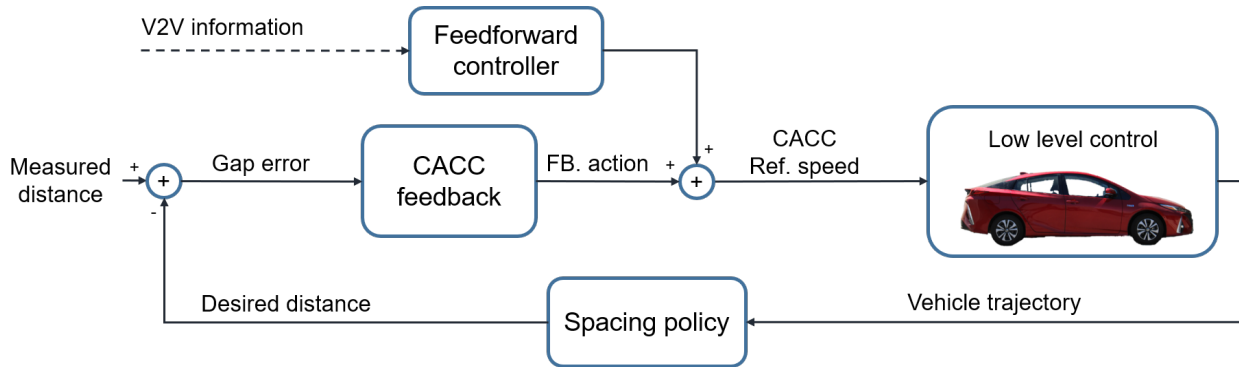


Figure I.1.2.7 Illustration of Implemented State Machine for CACC Operation

The switching logic between CC and ACC follows a similar algorithm than the leader ACC system presented above. The transition towards CACC following is performed in function of the DSRC link stability and driver’s intention to operate in such mode with the preceding vehicle. If the DSRC presents a packet drop period higher than a set tolerance time, the state machine switches the mode to ACC operation. All these transitions are performed in a smooth manner, by bounding jerk and acceleration and without losing the Headway Regions for Cruise Control and ACC Decision Algorithm closed-loop advantages. Zooming into the



CACC system, the block structure is described as follows:

Figure I.1.2.8 Headway Regions for Cruise Control and ACC Decision Algorithm

A constant time gap following spacing policy was adopted as a feature of the ACC structure. The CACC feedback (FB) block processes the gap error between measured and desired distances to generate the feedback correction. Such correction is added to the output of the feedforward controller that processes the signal received from the preceding vehicle through DSRC, in function of the set time gap [9]. This feedforward/feedback enhances the reference tracking capabilities and increases the response bandwidth towards disturbances from downstream, without decreasing the loop stability. This permits to achieve string stable behavior at shorter time gaps in comparison with ACC car-following. Finally, the CACC reference speed is sent to be tracked by the low-level control layer and manage the vehicle actuators.

Localization

In order to integrate the CACC string to the hardware-in-the-loop traffic simulation, vehicles’ trajectories are estimated and communicated in real time through DSRC to the roadside unit. For the scoped scenario, the same physical circuit is driven on all testing runs, this guarantees a fair comparison between different control strategies. Given this assumption, the vehicles localization is performed in a 1D state space, where the curvilinear coordinate describes the position of the subject vehicle over the circuit. An upper view of the

circuit map is provided in Figure I.1.2.8. The vehicles' coordinates are all estimated relative to the starting point located on the bottom part of the figure. Given that an important section of the used road is occluded with high trees, use of a GNSS sensor may introduce disturbances to the position estimation system. Instead, the vehicle longitudinal speed is filtered and integrated to estimate the curvilinear coordinate of each vehicle. For automated driving applications, model-based position estimation using its speed or angular rate measurements yields a position estimation with increasing offset with time. However, given the GNSS limitation and the pre-known length of the road section used, it has been determined that a longitudinal speed-based localization provides a sufficiently good performance, after proper filtering and calibration.

To estimate the vehicle position, the longitudinal speed is first low-pass filtered (LPF). This LPF reduces the probability of integrating high frequency noise and reduces the risk of accumulated offset over time. A linear transformation is done to the filtered speed to calibrate the coordinate estimation. Such transformation is vehicle specific and is set to guarantee that any possible scaling or offset on the vehicle speed measurement is corrected. The ground truth value for the circuit length is taken from an online accurate map application. Subsequently, several circuit runs are done with each vehicle, gathering statistical data to perform the linear transformation and match the coordinate from integrated longitudinal speed with the ground truth. On each run, the leader CAV is set to start always at the same physical position, using a landmark for alignment and ensuring replicability. The other vehicles use the same reference coordinate frame and start with a negative offset given by the radar system measured distance gap and the subject vehicle length.

Once the vehicle coordinate processing has been calibrated, the localization system has been tested extensively to assess its performance. Results show that the final coordinate measured is always estimated within $\pm 3\text{m}$ from the ground truth value of 1195 meters. In addition to a possible accumulated offset, such slight deviation might be due to non-identical cornering between runs in the four curves of the used circuit. Nevertheless, for the scoped application, the localization system performance is very acceptable.

Hardware and Software Structure for System Integration

For Vehicle Control

DSRC Radio for V2V

Cohda MK5 Dedicated Short Range Communication (DSRC) radios were used to broadcast dynamical data such as vehicle velocity, acceleration, brake level, etc., as well as control data such as position-in-platoon, radar target distance and relative velocity, boolean flags and timestamp, to the other vehicles and the Road-Side Unit (RSU). Data received on the same radio included the data sent by other vehicles and the virtual vehicle, and signal controller data from the RSU such as time remaining and distance to intersection (the RSU also sent virtual car data).

Test Scenarios

The HIL test was performed at a four-approach intersection in a closed test facility. The test intersection, the test CAVs, and the simulated test track are shown in Figure I.1.2.9. The single-lane test track has a 1960-meter loop and a 500-meter straight crossroad. The test intersection is located on the north side of the loop. Since there is no dedicated turning lane on the intersection, the turning traffic is not considered in the test. It is assumed that the intersection contains a major road and a minor road. The physical test CAVs operate on the major road. The traffic input is 800 vehicles per hour for the major road and 350 vehicles per hour for the minor road. The traffic input represents the intersection capacity measured at the 50% CAV market penetration case. The input traffic contains 50% CAV and 50% HV.

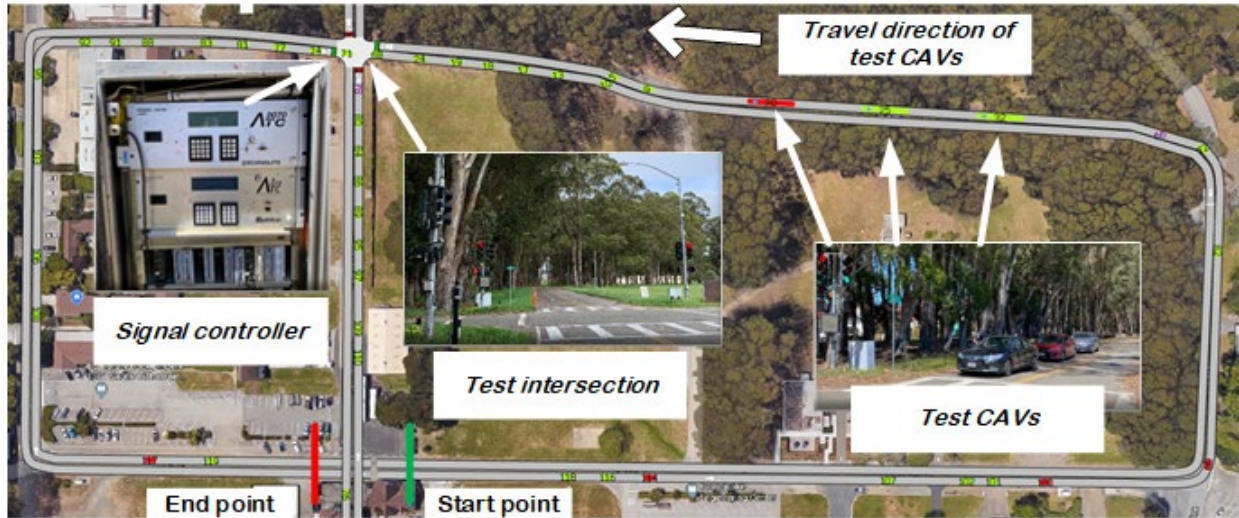


Figure I.1.2.9 HIL Test Track

The test contains a fixed time signal control case (FS), a cooperative signal case (CS), a fixed time signal plus trajectory planning case (FS+TP), and a cooperative signal plus trajectory planning case (CS+TP). The fixed time signal control case is the baseline case that offers a benchmark for evaluating the effectiveness of the cooperative intersection control algorithm. For the baseline case, the green time is 40 seconds for the major road and 20 seconds for the minor road. The yellow time is 3 seconds, and the all-red time is 2 seconds.

The research team used three physical CAVs in the test. The first and second vehicles were hybrid passenger cars. The third vehicle was a traditional gasoline car. In a test run, the traffic simulation first generated a virtual traffic stream on the test track. Afterwards, the physical CAVs started interacting with the virtual traffic while covering a test lap. The first test vehicle used an ACC controller to follow the preceding virtual car. The second vehicle followed the first in CACC mode. The third test vehicle was manually driven. When the physical CAVs finished a lap, the simulation would clear the remaining simulated vehicles on the test track and randomly regenerate a new virtual traffic stream for the next run. The vehicle trajectory and fuel consumption data obtained from a 350-meter intersection area were used for further analysis. The intersection area started 250 meters upstream from the intersection and ended 100 meters downstream from the intersection. To obtain rich data samples for evaluating the system effectiveness, the research team has completed 53 laps for the FS case, 50 laps for the FS+TP case, 98 laps for the CS case, and 101 laps for the CS+TP case. The number of test runs was smaller for the two fixed signal control cases because the traffic pattern was consistent across different test runs with a fixed signal phasing and time plan. Fifty runs were adequate to capture the random variations within the two cases.

Energy Consumption Estimation

- Simulation based on model
- On-vehicle based on CAN and OBD II information
- Actual fuel filling gauge (accuracy).

The fuel consumption results of simulated vehicles were estimated using the Virginia Tech comprehensive power-based fuel consumption model (VT-CPFM) [10]. The model provides a simple relationship between a vehicle's engine power and fuel consumption rate. The engine power is calculated based on the instantaneous speed and acceleration. As those inputs are directly accessible from the traffic simulation, this model is ideal to be integrated into the traffic simulation framework for efficient model implementation. The parameters of the VT-CPFM are listed in Table I.1.2.1.

Table I.1.2.1 VT-CPFM Model Parameters

	VT Model Parameters
Alpha 0	5.92E-4
Alpha 1	4.24E-5
Alpha 2	1.00E-6
Vehicle mass (kg)	1453
Driveline efficiency	0.92
Density of air at sea level at a temperature of 15 °C (kg/m ³)	1.23
Vehicle drag coefficient	0.30
Correction factor for altitude	1.00
Vehicle frontal area (m ²)	2.32
Rolling resistance parameters Cr, C1 and C2	1.75, 3.28E-1, 4.58

Results

Table I.1.2.2 and Table I.1.2.3 show the mobility and vehicle energy performances of simulated vehicles in the tested four scenarios. The tables indicate that the overall intersection performance could increase by 14% with the trajectory planning algorithm. The improvement due to the signal optimization ranged between 19% to 21%. When the signal optimization and trajectory planning were combined, the performance improvement reached 27% to 29%. Moreover, the minor intersection approach obtained larger benefits than the major approach. The performance improvement for the minor road was between 19% to 86%, while the improvement for the major road was 1% to 10%.

Table I.1.2.2 Mobility and Vehicle Energy Efficiency of Simulated Vehicles

Performance Metrics:	Vehicle Fuel Economy (MPG)			Average Speed (m/s)		
	All	Major	Minor	All	Major	Minor
Intersection Approach:						
FS	14.0	15.8	11.2	4.0	4.7	3.1
FS+TP	16.0	17.5	13.4	4.6	5.2	3.7
CS	16.7	15.9	18.5	4.9	4.7	5.4
CS+TP	17.8	17.1	19.8	5.2	5.0	5.7

Table I.1.2.3 Mobility and Vehicle Energy Efficiency Performance Change Regarding the Baseline Scenario

Performance Metrics:	Vehicle Fuel Economy (MPG)			Average Speed (m/s)		
	All	Major	Minor	All	Major	Minor
Intersection Approach:						
FS+TP	13.9%	10.7%	19.3%	14.6%	10.7%	21.0%
CS	18.7%	0.9%	65.2%	21.3%	0.7%	73.6%
CS+TP	27.1%	8.0%	76.6%	29.3%	7.0%	86.1%

Figure I.1.2.10 and Figure I.1.2.11 display the major road vehicle trajectories of the baseline case and the signal optimization plus trajectory planning case. Compared to the baseline case, the signal optimization algorithm could reduce the average queue length by implementing improved green time distributions. In addition, it reduced the number of cycles over a study period. This led to a decrease in the green time loss caused by phase transitions, resulting in a more efficient intersection operation. Another observation is that only a few vehicles came to a full stop even though only half of the vehicles could implement the trajectory

planning algorithm. This demonstrates that the proposed trajectory planning algorithm not only benefits the CAVs, but also the HVs that follow a leading CAV. It is interesting to observe that vehicles approaching the intersection were divided into several groups by individual CAVs that started executing trajectory planning at different positions.

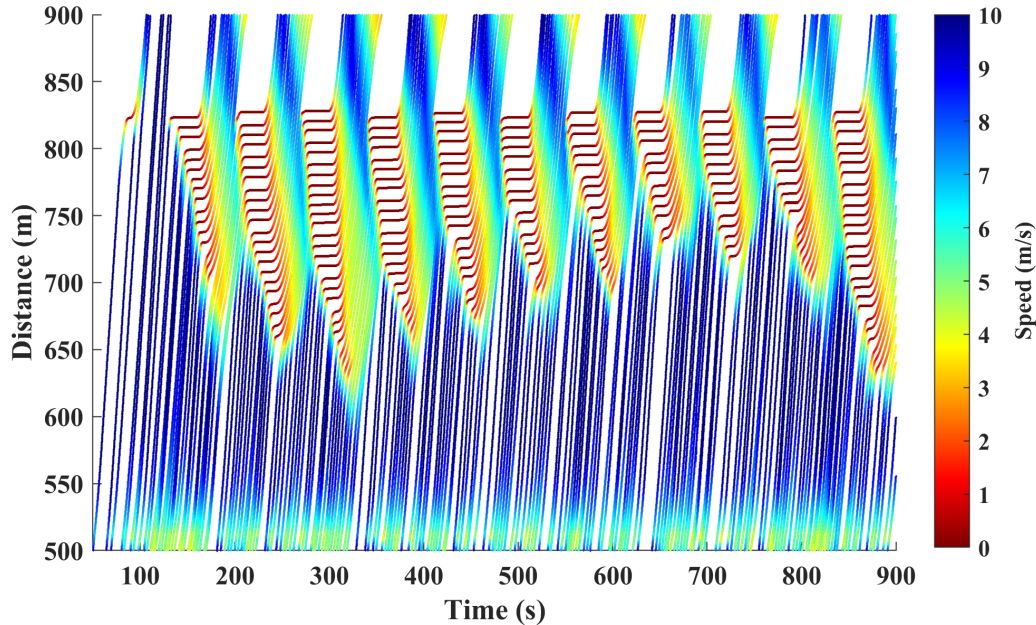


Figure I.1.2.10 Vehicle Trajectories Observed on the Major Road in the Baseline Case

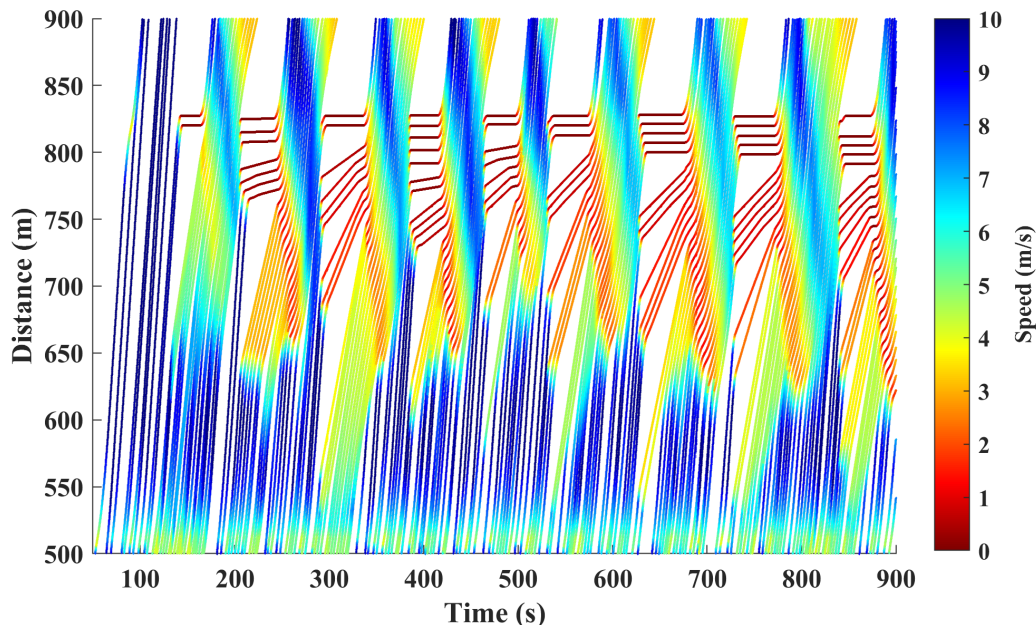


Figure I.1.2.11 Vehicle Trajectories Observed on The Major Road in the Signal Optimization Plus Trajectory Planning Case

The data of the physical CAVs were analyzed to quantify the effectiveness of the intersection control algorithm. The overall energy and mobility performance of the CAVs is demonstrated in Table I.1.2.4. Since

the three test CAVs operated in a platoon during the test, their average speeds were identical in the same test scenario. Comparing to the FS case, the TP or CS alone could slightly increase the average speed. When CS and TP were combined, the speed improvement became more noticeable. The fuel consumptions were substantially different among the three test vehicles because they used different powertrains (Car 1 is hybrid, Car 2 is plug-in hybrid, and Car 3 is a traditional ICE car). Car 1 and 2, which formed a CACC string, benefited significantly from the cooperative signal controller. On the other hand, Car 3 was manually driven because it could not perform low-speed automated car-following. It obtained greater improvement from TP than CS. The idling time of Car 1 was lower than Car 2 and 3. The extra idling time of Car 2 and 3 was observed when the three vehicles approached a slow-moving queue. Car 1 might join the queue without a full stop. But Car 2 and 3 often needed to decelerate to zero speed as they closely followed Car 1. The table shows that TP could largely reduce the idling time because it was designed to guide the test vehicles to pass the intersection without a stop. On the contrary, CS had little influence on the idling time.

Table I.1.2.4 Mobility and Vehicle Energy Efficiency Performance of Physical CAVs

	Speed (m/s) ($\Delta\%$ from Baseline)			Fuel Consumption (g) ($\Delta\%$ from Baseline)			Idling Time (s) ($\Delta\%$ from Baseline)		
	Car 1	Car 2	Car 3	Car 1	Car 2	Car 3	Car 1	Car 2	Car 3
FS	5.07	5.08	5.01	20.6	12.7	38.1	22.5	24.1	24.3
FS+TP	5.14 (+1%)	5.15 (+1%)	5.05 (+1%)	20.5 (-1%)	11.5 (-10%)	30.0 (-21%)	3.61 (-84%)	4.52 (-81%)	6.9 (-72%)
CS	5.21 (+3%)	5.18 (+2%)	5.10 (+2%)	17.2 (-17%)	10.6 (-17%)	34.7 (-9%)	22.2 (-1%)	23.6 (-2%)	23.9 (-2%)
CS+TP	5.52 (+9%)	5.55 (+9%)	5.46 (+9%)	17.5 (-15%)	10.0 (-21%)	28.9 (-24%)	4.07 (-82%)	5.50 (-77%)	7.66 (-69%)

The speed distribution of the test vehicle is shown in Figure I.1.2.12. Since the speed patterns of the three test vehicles are similar, the figure only shows the probability density estimated based on Car 1's speed samples. In addition to the high-speed peak, there is a smaller low-speed peak on the FS curve. This suggests occasional intense congested traffic conditions at the intersection when the fixed signal could not serve temporary traffic demand surges. As the TP became active, the low-speed peak was almost removed. The CS increased the probability for a vehicle to pass the intersection in nearly free flow conditions (e.g., traveling at 8 to 12 m/s). When the CS was combined with TP, the probability density curve was shifted to the right, thus further increasing the area of the high-speed region.

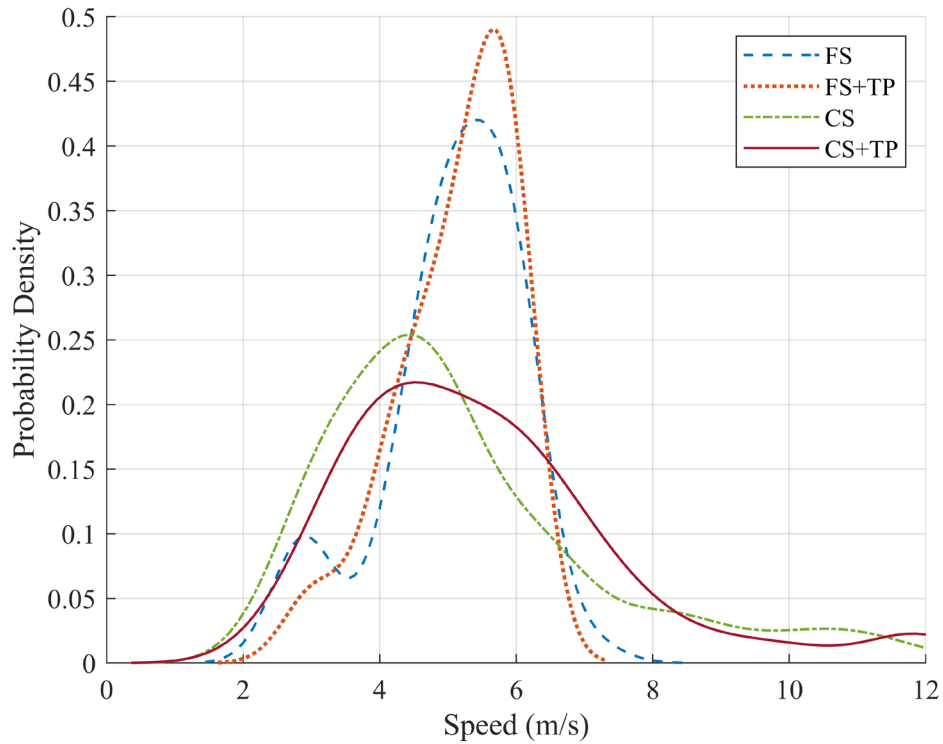


Figure I.1.2.12 Probability Density of Speed

The probability density of the fuel consumption is displayed in Figure I.1.2.13 and Figure I.1.2.14. The two figures were constructed based on the real-time fuel rate/consumption data reported by Car 1 and 2. Unfortunately, Car 3 could not output such high-resolution fuel data. The research team was only able to perform an aggregated fuel consumption analysis for Car 3 based on the gauged fuel data. The two figures show that the fuel consumption patterns are very different between Car 1 and 2, although both are hybrid vehicles. The fuel consumption of Car 1 is significantly higher than Car 2. Nonetheless, the change of fuel consumption among different test cases is consistent for both cars. As TP and CS was implemented, the probability density of the fuel shifted to the left, indicating the reduction of the fuel consumption.

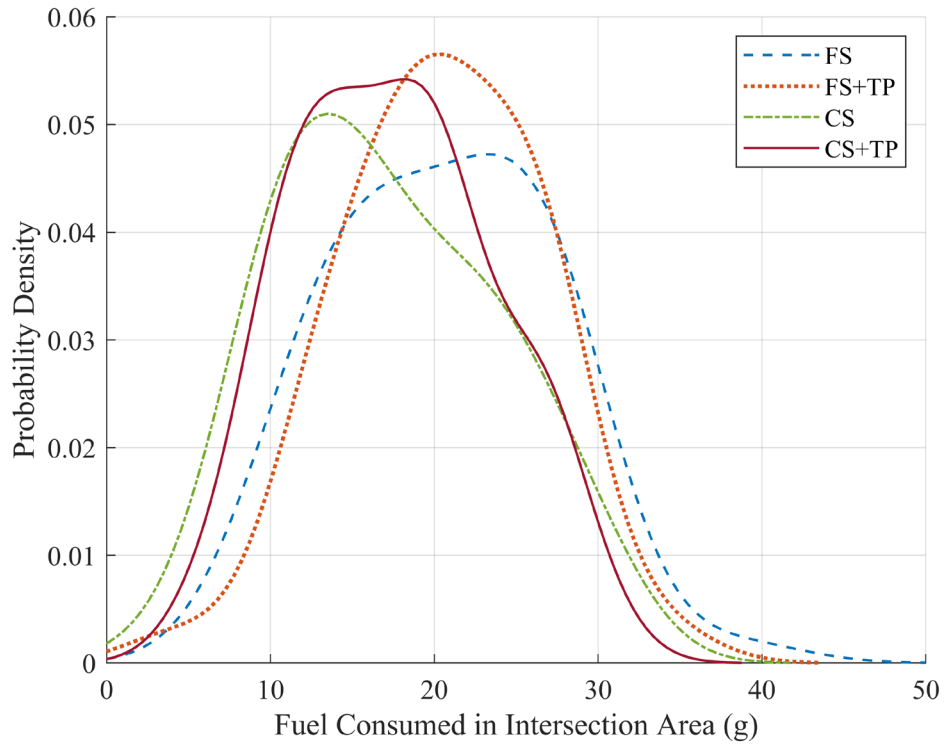


Figure I.1.2.13 Probability Density of the Fuel Consumption for Car 1

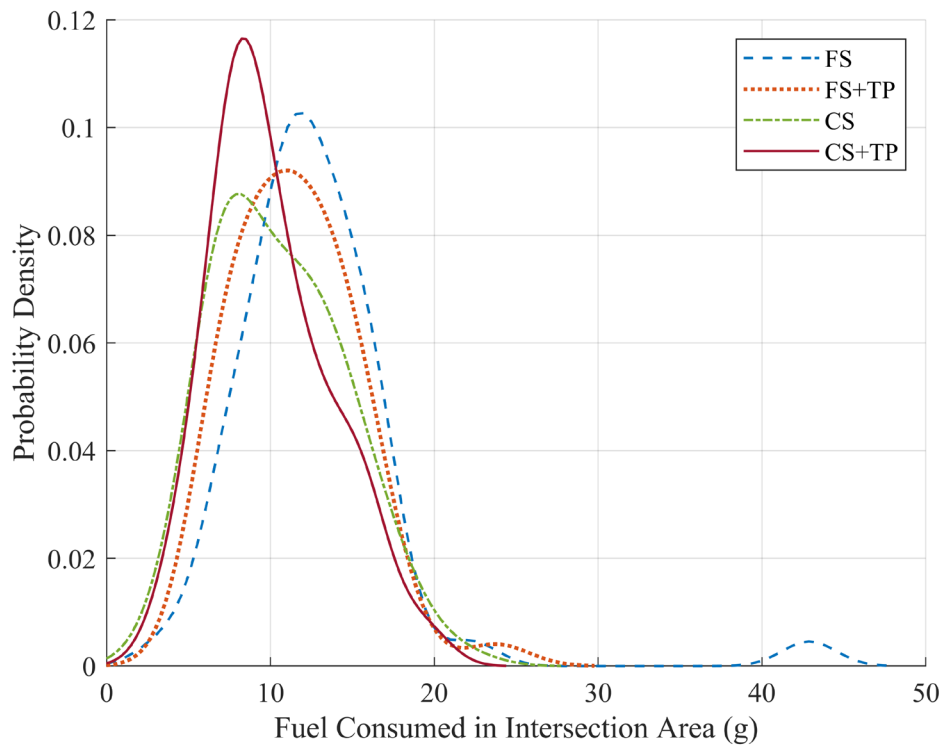


Figure I.1.2.14 Probability Density of the Fuel Consumption for Car 2

The two-sample K-S tests were performed to determine if the speed or the fuel consumption difference is significant between two different test cases. The hypothesis test results are shown in Table I.1.2.5. The speed and fuel consumption differences between FS and FS+TP are not significant, while the differences are significant between FS and CS, and between FS and CS+TP. This means that the CS and CS+TP cases could bring about statistically significant improvement compared to the baseline case. The fuel consumption differences between TP and non-TP cases (e.g., FS vs. FS+TP and CS vs. CS+TP) are not significant. It implies that the effectiveness of TP for Car 1 and Car 2 is not substantial. There are no detailed fuel consumption data for conducting the hypothesis tests of Car 3. Since the average fuel consumption reduction between TP and non-TP cases for Car 3 is between 15% and 21% (see Table I.1.2.5), it is safe to assume that TP contributes significant fuel savings for Car 3.

Table I.1.2.5 K-S Test Results between Each Two Test Cases

	Car 1 Speed H-Value (P-Value)			Car 1 Fuel H-Value (P-Value)			Car 2 Fuel H-Value (P-Value)		
	FS	FS+TP	CS	FS	FS+TP	CS	FS	FS+TP	CS
FS+TP	0 (0.74)	-	-	0 (0.81)	-	-	0 (0.41)	-	-
CS	1 (0.01)	1 (0.01)	-	1 (0.04)	1 (0.01)	-	1 (0.01)	0 (0.28)	-
CS+TP	1 (0.01)	1 (0.00)	0 (0.14)*	1 (0.02)	1 (0.01)	0 (0.69)	1 (0.00)	1 (0.04)	0 (0.40)

* The test results are significant for Car 2 and 3.

Conclusions

This research resulted an advanced intersection controller that combined traffic signal optimization and CAV trajectory planning. The controller is feasible to implement in mixed traffic that is expected to exist for many years. A HIL test system was developed to evaluate the intersection control algorithm.

Further data analysis results will be added before December 31st of 2020.

References

1. Di Febbraro, A., Giglio, D., & Sacco, N. (2015). A deterministic and stochastic Petri net model for traffic-responsive signaling control in urban areas. *IEEE Transactions on Intelligent Transportation Systems*, 17(2), 510-524.
2. Chu, T., Wang, J., Codecà, L., & Li, Z. (2019). Multi-agent deep reinforcement learning for large-scale traffic signal control. *IEEE Transactions on Intelligent Transportation Systems*, 21(3), 1086-1095.
3. Liu, H., Lu, X. Y., & Shladover, S. E. (2019). Traffic signal control by leveraging Cooperative Adaptive Cruise Control (CACC) vehicle platooning capabilities. *Transportation research part C: emerging technologies*, 104, 390-407.
4. Rafter, C. B., Anvari, B., Box, S., & Cherrett, T. (2020). Augmenting traffic signal control systems for urban road networks with connected vehicles. *IEEE Transactions on Intelligent Transportation Systems*, 21(4), 1728-1740.
5. Fayazi, S. A., & Vahidi, A. (2018). Mixed-integer linear programming for optimal scheduling of autonomous vehicle intersection crossing. *IEEE Transactions on Intelligent Vehicles*, 3(3), 287-299.
6. Kamal, M. A. S., Hayakawa, T., & Imura, J. I. (2019). Development and Evaluation of an Adaptive Traffic Signal Control Scheme Under a Mixed-Automated Traffic Scenario. *IEEE Transactions on Intelligent Transportation Systems*, 21(2), 590-602.

7. Sen, S., & Head, K. L. (1997). Controlled optimization of phases at an intersection. *Transportation science*, 31(1), 5-17.
8. Liu, H., Kan, X. D., Shladover, S. E., Lu, X. Y., & Ferlis, R. E. (2018). Modeling impacts of cooperative adaptive cruise control on mixed traffic flow in multi-lane freeway facilities. *Transportation Research Part C: Emerging Technologies*, 95, 261-279.
9. Rakha, H. A., and K. Ahn, and K. Moran, and B. Saerens, and E. Van den Bulck. (2011). “Virginia Tech Comprehensive Power-Based Fuel Consumption Model: Model Development and Testing.” *Transportation Research Part D: Transport and Environment* 16, no. 7: 492-503.
10. Naus, G. J., Vugts, R. P., Ploeg, J., van De Molengraft, M. J., & Steinbuch, M. (2010). String-stable CACC design and experimental validation: A frequency-domain approach. *IEEE Transactions on vehicular technology*, 59(9), 4268-4279.

Acknowledgements

Dr. Hao Liu (email: liuhao@berkeley.edu) of PATH, University of California Berkeley, has developed the intersection traffic signal control modeling, real-time microscopic traffic simulation with CAVs imbedded, algorithm for a single intersection Traffic Signal Control with a dynamic programming approach, V2I messages, trajectory planning for CAVs. He also conducted system integration with John Spring, designed test scenarios and systematically collected test data.

Dr. Carlos Eduardo Flores (email: carfloresp@berkeley.edu) of PATH, University of California Berkeley, has integrated the CACC system with the intersection signal control by using the SPaT signal and the speed trajectory as the reference for the CACC string of three passenger cars developed in a sister project. The ground truth location or localization of the three CACC cars is one of the critical issues for the system integration.

Mr. John Spring (email: jspring@berkeley.edu) of PATH, University of California Berkeley, provided software and hardware support and system integration in the CAC system development and field operational tests and help in driving in different test scenarios for tests on the test-track and on highways.

Mr. David Nelson (email: dnelson@path.berkeley.edu) of PATH, University of California Berkeley, provided software hardware support, ground truth measurement of actual fuel consumed, and help in driving in different test scenarios.

I.1.3 Experimental Evaluation of Cooperative ACC for Passenger Cars – Development of CACC Capability for Cars with different Powertrains (LBNL and ANL) [Task 3.1.2]

Xiao-Yun Lu, Principal Investigator

Building 190
Lowrance Berkeley National Laboratory (LBNL)
1 Cyclotron Road, Berkeley, CA
Email: xiaoyunlu@lbl.gov

David Anderson, DOE Program Manager

U.S. Department of Energy
Email: david.anderson@ee.doe.gov

Erin Boyd, DOE Technology Manager

U.S. Department of Energy
Email: erin.boyd@ee.doe.gov

Start Date: October 1, 2018	End Date: September 30, 2020	
FY19 Project Funding: \$400,000	DOE share: \$400,000	Non-DOE share: \$0

Project Introduction

Road congestion and traffic jams have become major issues on the road transport sector [1], not only for the increased time drivers spent stuck in traffic, but also the elevated amount of energy consumption, emissions and noise that these generate. With the increasing market penetration of vehicle longitudinal automation and ranging sensors, technologies such as Adaptive Cruise Control (ACC) are becoming more and more common. These systems are designed mainly as a driver assistance system for some levels of comfort and safety by releasing the car-following task from the driver. However, in a macroscopic traffic scope, these systems have no positive impact on road congestions. On the contrary, there is even evidence that ACC vehicle-following does not satisfy the string stability condition [2], which means that speed and acceleration disturbances are amplified as they propagate upstream of the ACC string. This is not only unsafe due to the risk of rear-end collisions, but also due to the traffic shockwave that a string of ACC vehicles would create. Such a string unstable property is mainly due to the cumulative delays in the string from downstream to the upstream.

The addition of Dedicated Short-Range Communication (DSRC) links was proposed to augment the vehicle perception and improve the vehicle response at even shorter distance gaps. First demonstrations of longitudinal automation, radar sensors and DSRC links were demonstrated in late 90's by the name of highway platooning [3]. However, to safely achieve the very short constant distance-gap following, dedicated lanes were required to limit speed variations and restrict interaction with other vehicles. A more flexible constant-time gap following strategy was introduced later named Cooperative Adaptive Cruise Control (CACC), intended for use on public road where interactions with other vehicles were possible [4].

A significant amount of progress has been done to increase CACC capabilities to improve traffic throughput and stability. Nevertheless, two conditions have been found necessary to get the most benefit of CACC implementations: 1) The controlled string must be composed of identical vehicles, and 2) High market penetration rates are required [5]. If higher penetration rates are desired, it is strictly required then to remove the identical vehicles restriction. Some recent efforts such as the Grand Cooperative Driving Challenge 1 & 2 have showed the potential of vehicle cooperation on different types of vehicles from different manufacturers which meant to have different control designs for different vehicles. Nevertheless, they showed performance was very conservative and left room for further improvement in terms of higher performance with shorter time

gaps and better speed and distance tracking. Besides, to the authors' knowledge, there is no previous work that considers CACC strings of vehicles of not only heterogeneous dynamics, but also different powertrains. In addition to this, given the short gaps kept on a CACC car-following, the handling of cutting-in vehicles still remains a major challenge despite previous efforts on solving this problem [6], given the abrupt distance gap change and lack of communication with the cutting-in vehicle.

Objectives

In order to solve these issues, to accelerate wide application and market penetration, to further extend CACC positive impact on traffic flow, the following objectives are set for this project:

- Develop a generic CACC design strategy that could be applied to any road vehicle that is feasible in onboard sensor reading and control actuation regardless of vehicle types (passenger car, buses and medium/heavy-duty trucks) with a variety of powertrains.
- Investigate requirements for high performance CACC strings, considering heterogeneous dynamics and powertrains.
- Extend CACC capabilities for shorter time gaps and full speed range, without leading to unsafe maneuvering.
- Study system string stability for different time gap preferences.
- Improve the handling of cutting in/out vehicles either in front of leader or follower vehicles.
- Yield a configurable framework where the driver can interface with the system and select the desired control mode and time gap, as well as the performance-comfort factor.
- Validate the proposed architecture with tests on highway and closed tracks.

Approach

The proposed generic CACC architecture is based on a modular hierarchical approach, where high and low-level control layers are implemented with complementary tasks. The former deals with the gap regulation kinematics, by processing target perception and Vehicle-to-Vehicle (V2V) communications. The latter deals with reference speed tracking and vehicle dynamics, by commanding the vehicle proprioceptive sensor reading and actuators. The approach proposed in this work is developed and tested over three different vehicles: 2014 Hybrid serial Honda Accord, 2017 Hybrid parallel Toyota Prius Prime, and 2013 Ford Taurus with internal combustion (IC) engine. The general software and data flow architecture is illustrated in Figure I.1.3.1 below:

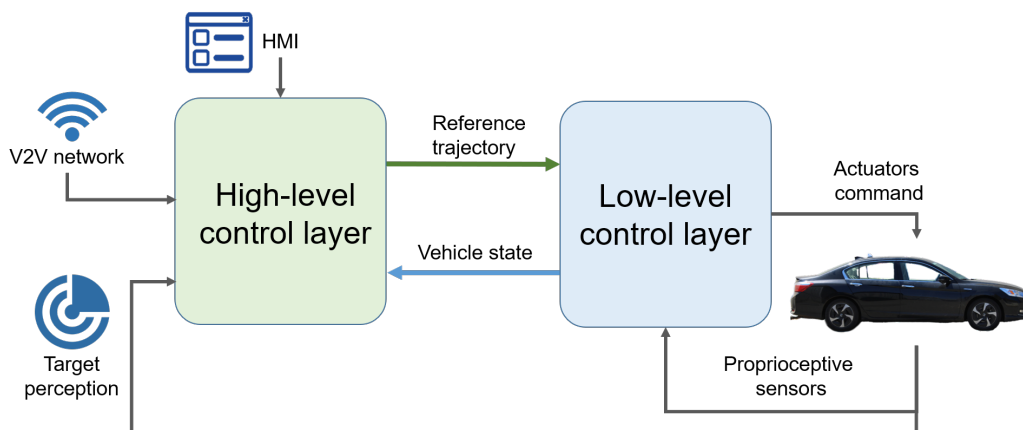


Figure I.1.3.1 Software Architecture for the CACC Control Implementation

One can see that the high and low-level control layers interact closely in a hierarchical framework, where the high level generates the reference speed trajectory to be tracked by the low-level, whereas the low level communicates the vehicle state for the high-level to regulate the car-following kinematics. The physical system structure and its instrumentation is described in the following section, which sets the base of the aforementioned architecture.

Vehicle Instrumentation and Overall System Structure

The core of the overall system structure is the PC-104, which runs a QNX real time operative system (see Figure I.1.3.2). The real-time execution permits to guarantee that processing of Controller Area Network (CAN) inputs, execution of control algorithms and commands writing are delivered within the desired scheduling period. This is essential to guarantee an optimal implementation of the CACC architecture. A Linux laptop is used to communicate with the PC-104 through ethernet in a client-host architecture. This permits the passenger to trigger, stop and monitor the system functioning. The wireless DSRC technologies are enabled by a Cohda box with an external omni-antenna, which also has an embedded GPS for time synchronization and positioning. The DSRC wireless links are used not only for exchanging control variables, but also for synchronizing the controlled vehicles. This is fundamental to guarantee that all variables are logged with the same time reference frame.

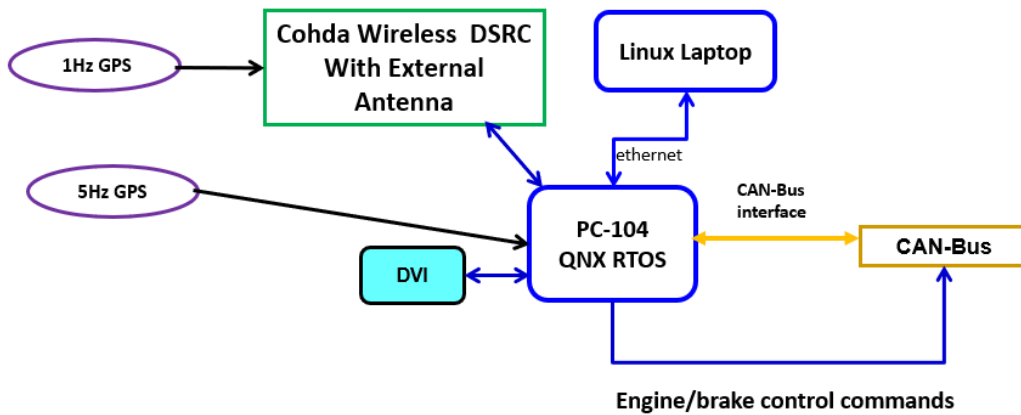


Figure I.1.3.2 CACC System Structure Represented as Block Diagram

The PC-104 sends and receive all the required messages for full CACC capabilities via connection to the vehicle CAN bus. The data from proprioceptive (wheel encoders, Inertial Measurement Units) and exteroceptive sensors (radar-based target detection) is received via CAN at different frequencies, requiring the PC-104 to handle the various processes in real-time. The actuation commands are also written to the CAN bus towards the vehicle ACC system and vary in function of the vehicle used, as well as the available method for applying the required acceleration.

Low-level control layer

The low-level control layer main purpose is both to generate the desired acceleration and command the vehicle actuators. This is done to track the reference longitudinal speed received from the high-level control layer. Its control structure is as depicted below:

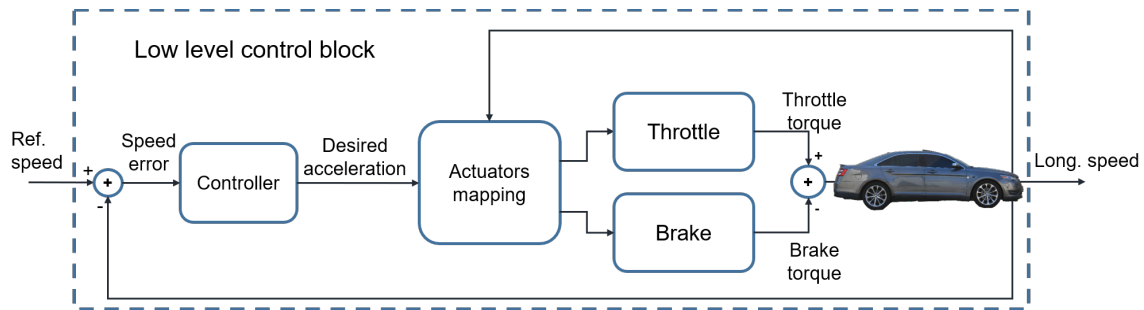


Figure I.1.3.3 Low Level Block Structure for Speed Tracking

The difference between reference and longitudinal speed is processed by the controller to yield the desired acceleration. This input is fed to a comprehensive actuator map that describes the powertrain response to longitudinal acceleration commands. Not only does each vehicle have a different acceleration envelope, but the response to an acceleration command varies by vehicle and powertrain type as well. For the three vehicles used in this project, longitudinal acceleration commands, both positive and negative, were achieved through one of two ways: 1) direct pedal override through analog voltage injection, or 2) ACC acceleration command override through a CAN bus in the middle. A more detailed explanation of these two approaches is presented in the figure below:

Veh. Model	Powertrain Type	Acceleration control through ACC & CAN Bus	Acceleration control through acceleration pedal deflection	Deceleration control through ACC & CAN Bus	Deceleration control through brake pedal deflection	Comments
2017 Toyota Prius	Hybrid Parallel	Yes	Yes, through direct analog voltage.	Yes	N.A.	Control through pedals show less delays
2014 Honda Accord PHEV	Hybrid Serial and Parallel, both modes	N.A.	Yes, through direct analog voltage.	N.A.	Yes, through CAN messages.	Control through pedals show less delays
2013 Ford Taurus	IC Engine	Yes, for speed over 19 mph; max accel. 2 m/s ²	Yes, through direct analog voltage.	Yes, for speed over 19 mph; max decel. -3.1 m/s ²	N.A.	Control through pedals show less delays

Figure I.1.3.4 Vehicle Lower-Level Properties and Available Command Systems

For the direct pedal override method, the powertrain response map for longitudinal acceleration consists of a surface plot of pedal position vs. vehicle acceleration vs. vehicle speed (see Figure I.1.3.5). This map is acquired from targeted dynamometer testing covering a wide range of vehicle speed and acceleration points and provides a lookup table for the required pedal position to achieve a desired acceleration from the vehicle, given the current vehicle velocity. This method applies to either accelerator or brake pedal for positive or negative acceleration, respectively. For the ACC acceleration command override, the powertrain response mapping consists of an entirely different plot. Since the ACC acceleration command is already in units of

acceleration, the desired acceleration from the CACC controller can be directly requested from the vehicle. However, it is necessary to know the acceleration envelope of the vehicle with ACC acceleration control. More specifically, what is the minimum and maximum acceleration capability through ACC acceleration override at any given vehicle speed. This map is obtained through targeted dynamometer testing, aimed at covering the acceleration limits of the vehicle at a wide range of vehicle speeds, and may be less than or equal to the absolute acceleration limits of the vehicle with driver inputs to the pedals.

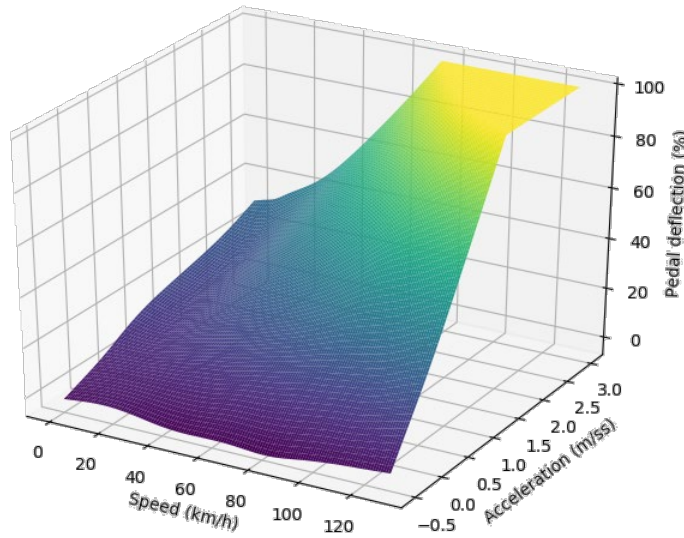


Figure I.1.3.5 Vehicle Throttle Pedal Map Surface in Function of Speed and Acceleration

Regarding the speed tracking proportional controller, the main objective is to yield a fast and consistent tracking of the reference speed, with no response overshoot. Once the actuators mapping and controller are developed, the structure is excited with different reference speed profiles to model the closed-loop frequency response of each vehicle. In the figure below, the modeled frequency response is presented for each of the three vehicle platforms. Such models were obtained through extensive closed-loop testing by exciting different frequency regions of the expected response bandwidth, as shown in the left plot of figure below.

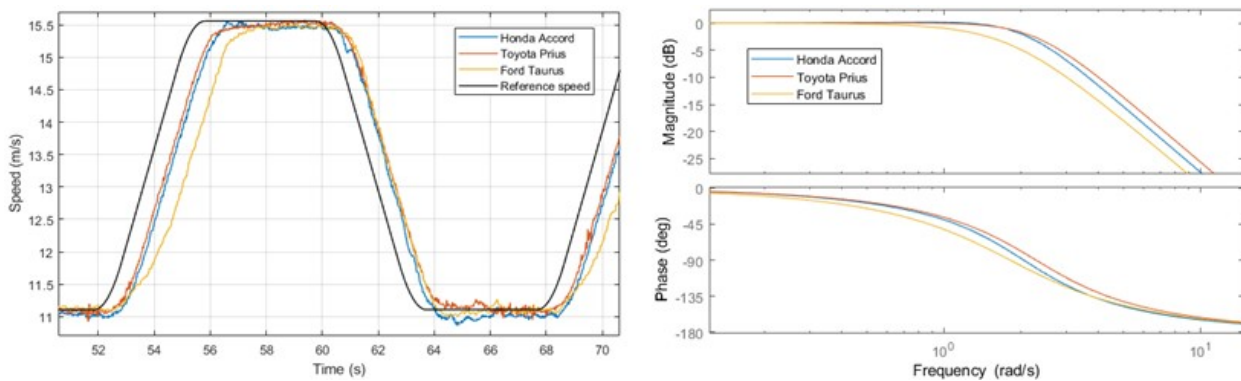


Figure I.1.3.6 Time and Modelled Frequency Response (Left and Right) of Vehicles' Low-Level

An important feature to highlight from the observed performance of each vehicle is that the speed response results consistent regardless the actuator that is used to close the loop. A slight difference in the throttling and braking dynamics is observed for the Ford Taurus, given that a powertrain based on Internal Combustion Engine (ICE) presents slower dynamics than a hybrid powertrain. A consistent response ensures that the low-level response is predictable and can be represented with a linear model with high accuracy. Considering these

experiments and other extensive closed-loop testing of the low-level speed tracking system, the following model parameters have been fitted:

Table I.1.3.1 Identified Low-Level Parameters and Acceleration Range for Each Platform

Vehicle name	Response bandwidth, ω_n (rad/s)	Damping factor, ξ	Max. deceleration (m/s ²)	Max. acceleration (m/s ²)
Honda Accord	2.046	0.64	-7.0	3.0
Toyota Prius	2.284	0.68	-4.0	3.0
Ford Taurus	1.812	0.79	-3.0	2.0

where the speed response of the low-level structure of the “i-th” vehicle in a string is defined by the expression:

$$Gp_i(s) = \frac{V_i(s)}{V_{ref,i}(s)} = \frac{\omega_n^2}{s^2 + 2\xi\omega_n s + \omega_n^2};$$

which dynamics form and parameters are used in the design of the high-level gap regulation layer. As can be observed in the Figure I.1.3.7, although the low-level design has been done to minimize spectral difference between vehicles’ responses, hybrid vehicles present faster dynamics than the Internal Combustion Engine (ICE) vehicle. Among the hybrid vehicles, the Toyota Prius show a slightly higher faster response, given its serial hybrid nature instead of parallel hybrid as the Honda Accord.

High-level control layer

Regarding the gap-regulation control layer, a state machine architecture is implemented. Transition between states is managed in function of the perceived target and the stability of the V2V link with the preceding vehicle, as described in the figure below:

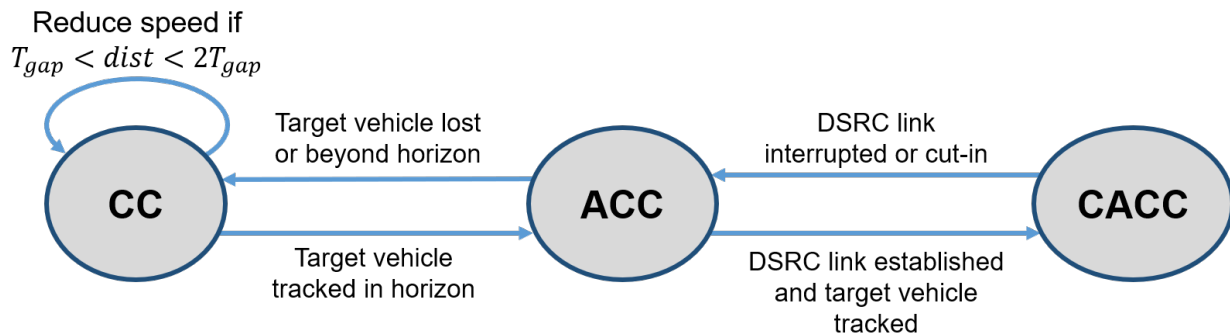


Figure I.1.3.7 Illustration of Implemented State Machine for CACC Operation

Three states are implemented: Cruise control (CC), ACC and CACC. For the sake of clarity, the leader of a CACC string will only implement CC and ACC states. All vehicles initialize executing the CC state, which follows a desired cruise speed. If the target perception system detects a vehicle with a relative distance between $T_{gap}V_i$ and $2T_{gap}V_i$; the relative speed is penalized for safety purposes and to ensure a smooth transition between CC and ACC. Once the target vehicle enters the T_{gap} region, ACC car-following is activated, where T_{gap} is the desired time gap to be kept towards the preceding vehicle.

If the subject vehicle is not the leader of a CACC string, the driver can trigger the transition towards CACC if the DSRC link is established and stable with the preceding vehicle. In the case that communication packets drop for a period higher than a tolerance time, or a cutting-in vehicle is detected between subject and preceding

vehicle, the car-following is degraded back to ACC until the link is recovered and the driver chooses to switch back to CACC. In case there is not a target detected due to a cut-out or it is too far away, the state machine switches to CC, tracking the desired cruise speed until a target is found. All transitions between states are performed in a smooth manner, limiting speed, acceleration and jerk variables to guarantee a comfortable driving.

ACC structure

The ACC structure is based on a feedback control loop to ensure a robust rejection of disturbances and the control approach is designed to handle different levels of gap and performance settings. The figure below depicts the proposed ACC structure:

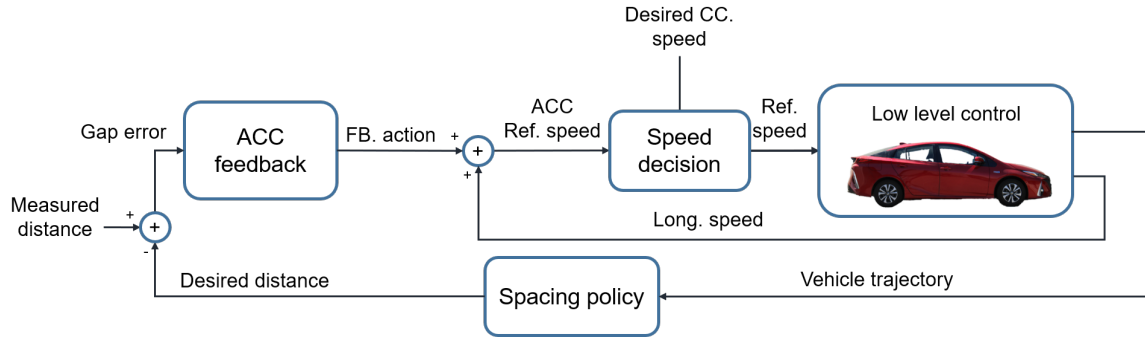


Figure I.1.3.8 ACC Block Structure

The adopted spacing policy is constant time gap, which proposes to hold a distance gap proportional to the vehicle speed, added to a fixed safety distance. The difference between the desired and measured distance gap is fed to the ACC feedback controller to compute the correction to be applied. This feedback action added to the vehicle longitudinal speed produces the reference speed to close the ACC control loop. Finally, a speed decision block is added that represents the state machine that manages transitions and reference speed generation towards the low-level control block.

CACC structure

Regarding the CACC structure, the communication link with the preceding vehicle permits a faster response towards speed variations coming from downstream. For this purpose, a feedforward controller link is added to the feedback structure to handle the V2V information. An illustration of the proposed structure is provided below:

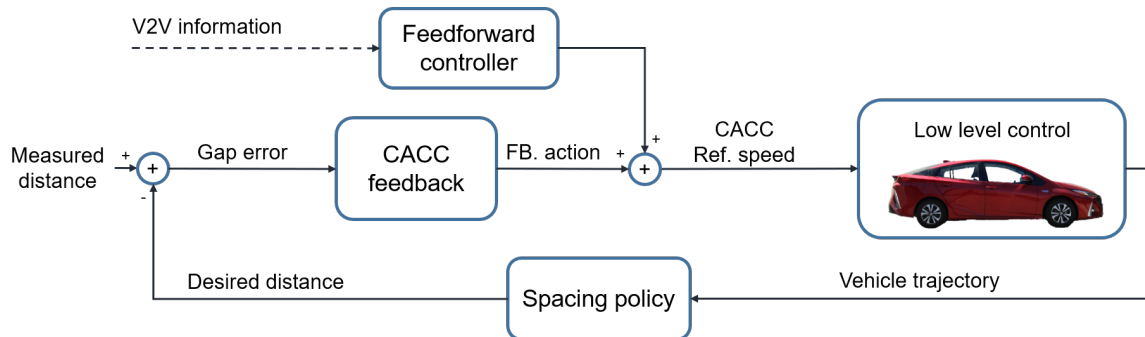


Figure I.1.3.9 CACC Block Structure

It can be observed that, as for the ACC structure, the gap error fed to the feedback controller is calculated as the difference between the spacing policy desired distance and measured gap. The feedback action is added to the feedforward controller output, which generates the reference speed to be tracked by the low-level control layer. The design of feedforward, feedback and spacing policy blocks is done in function of the operation

mode selected for the CACC algorithm. Two CACC modes of operation are proposed in this framework, comfort-CACC and high-performance-CACC.

Regular-CACC

This mode is intended for a more conservative operation where larger distance gaps are previewed and supports human interruption of the preceding vehicle control algorithm. For this mode, a constant time gap spacing policy is used, where the time gap h is used for values equal or higher than 0.6s, agreeing with [7]. The feedforward control on every vehicle is based on a predecessor-only topology and it applies a first order low pass filter to the preceding vehicle longitudinal speed $V_{i-1}(s)$, where the pole is placed in $\omega = -1/h$. Since the variable used on feedforward is the vehicle measured speed, the preceding vehicle can be either automated or manually driven, which makes this framework more flexible and conservative.

For the feedback controller design, a Linear Parameter Varying (LPV) structure is implemented, where two parameters are used to schedule the resulting controller from the designed polytopic forms. Figure I.1.3.10 illustrates how the control output is computed given the designed structure and two scheduling parameters: performance factor $\rho(t)$ and time gap $h(t)$.

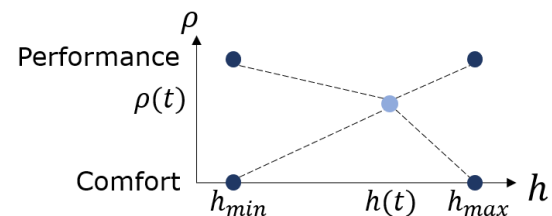


Figure I.1.3.10 LPV Representation of Feedback Control Design

The parameter ρ goes from 0 to 1, meaning from very smooth to a more aggressive tracking and it is a value chosen by the driver in function of the desired performance. Hence, a pair of conservative and aggressive controllers is designed for the minimum and maximum expected CACC time gap. Each of the dark blue dots is a controller designed using optimal \mathcal{H}_∞ metrics. For this purpose, the closed loop functions: complementary sensitivity, disturbance sensitivity and control effort; are shaped with the optimal controller frequency response and using template functions. As a general guideline for template functions selection, shorter time gaps require a higher closed loop bandwidth (which may reduce loop robustness), whereas comfort controllers require a control effort response of lower magnitude and bandwidth. It is important for all designed controllers to yield a complementary sensitivity, or string stability function, which infinity-norm or peak value of its singular values is less or equal to 1. This ensures that speed and acceleration disturbances are not amplified as they propagate upstream.

High-performance CACC

The second mode for CACC operation is high-performance CACC. Time gaps set for this mode are in the range of $h \in [0.1, 0.6]$ s. A variable time gap (VTG) spacing policy for the full speed range is used on this mode [8], aiming to get shorter distance gaps. This spacing policy proposes to have a linear increase of the desired time gap from an initial to target value as the speed increases, as visible in the left figure below:

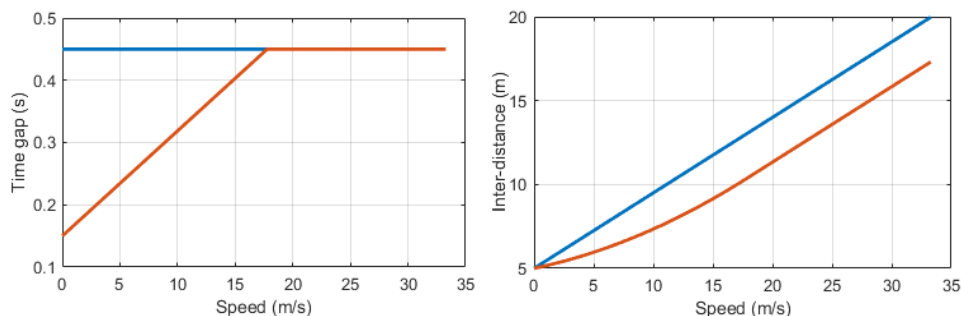


Figure I.1.3.11 Comparison Between CTG and VTG Spacing Policies on Time Gap (Left) and Spacing (Right)

In this figure, the VTG (orange line) is compared with CTG following (blue line). As the right figure shows, by starting at a shorter time gap, the VTG approach guarantees the same dynamic response of the target time gap, while keeping shorter inter-distances than with constant time gap car-following.

In this mode, no human interaction through the vehicle pedals is assumed, given that follower vehicles use the reference longitudinal speed of its preceding vehicle in feedforward, which loses validity if a driver interferes with the low-level speed tracking. To get the best performance, all vehicles of index 3 and higher implement a leader-predecessor following strategy, while the second vehicle in the string can only perform preceding-only following. Given that the evaluated platforms accounts with different dynamics and even powertrains, each vehicle low-level layer responds differently to an identical stimulus. For this reason, the dynamics ratio between linked vehicles must be considered on the subject vehicle feedforward controller structure. An illustration of such feedforward structure is presented below:

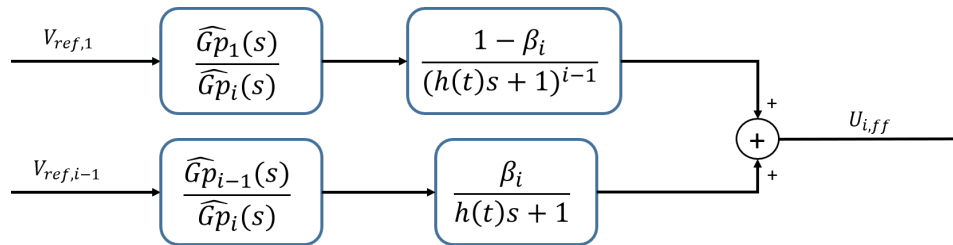


Figure I.1.3.12 Feedforward Control Structure for High-Performance CACC

Each vehicle implements two two-stage links that are added to generate the feedforward action (excepting vehicle of index 2). The first stage of each link processes the received reference speed with the ratio of both vehicles identified dynamics (leader-ego or preceding-ego). The second stage low-pass filters the outputted signals in function of the set time gap, in addition to the DC gain β_i used to mix the leader and predecessor V2V processed signals in a complementary manner. The selection of such gain is done in function of the subject and preceding vehicles' low-level dynamics, following the guidelines proposed in [8, Shaw]. These suggest that vehicles of faster response bandwidth should be more coupled to their predecessors, whereas vehicles with more limited response bandwidth should be more coupled to the leader signal to gain response speed capabilities. Regarding the CACC feedback controller, the design method explained in the previous section is used considering the time gap LPV parameter in the scoped range for this mode.

Time gap planning algorithm

To illustrate the motivation of a closed loop time gap planning algorithm, an illustration of a cutting-in scenario is presented in the figure sequence below:

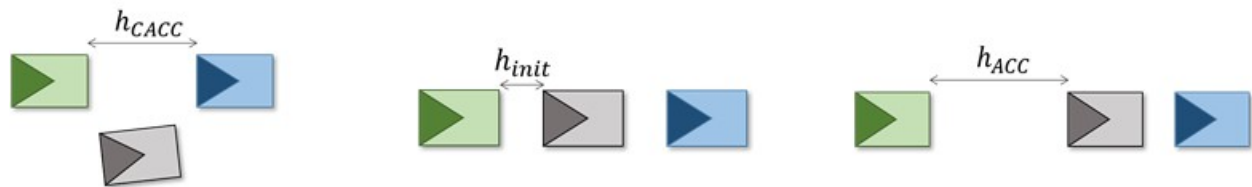


Figure I.1.3.13 Illustration of Time Sequence of Cutting-In Scenario (Left to Right)

Initially, a non-CACC-string vehicle (gray) cuts between ego (green) and leader (blue) vehicles, which are performing CACC with a time gap of h_{CACC} . When the vehicle enters the subject vehicle lane at an equivalent inter-distance of h_{init} seconds, the state machine transitions to ACC car-following to execute the gap opening maneuver at $t = t_0$. The transition from h_{init} to the desired ACC time gap h_{ACC} must be performed in a safe and comfortable way. This is performed by planning a time gap profile time vector $\bar{h}(t)$ that is utilized in the control structure to enforce the maneuver in closed loop. This approach can be used not only for cutting-in

vehicles, but also cut-out and changes on-the-fly of the driver gap settings. Based on the work of [7], this algorithm aims to transition in closed loop from an initial time gap value to the target one, while bounding the vehicle longitudinal motion within the desired constraints. The proposed planning algorithm can be used on the ACC structure and both CACC operation modes. The algorithm consists of the sequential execution of the following steps at the maneuver trigger time:

1. Derive bounds for longitudinal speed, acceleration and jerk, given the desired performance factor.
2. Estimation of the initial time gap using formula: $h_{init} = \frac{d(t0) - std}{v(t0)}$; where std , $d(t0)$ and $v(t0)$ represent the safety distance, measured distance and speed at the trigger time, respectively.
3. Assuming that the preceding vehicle is driving at constant speed, the distance gap to be added or reduced to reach the target time gap h_{target} is estimated.
4. A profile of jerk steps is planned that yields the desired inter-distance increase/decrease, guaranteeing that speed, acceleration and jerk remain within bounds. Such jerk profile is integrated twice over time to obtain a longitudinal speed profile vector $\bar{v}(t)$.
5. The final time gap profile vector is calculated with the speed profile using the formula:

$$\bar{h}(t) = \frac{V_{init}h_{init} - \int_{t_0}^t (v(\tau) - V_{init}) \cdot d\tau}{v(t)}$$

Examples of gap opening profiles are presented in the figure below to show the algorithm versatility applied on different levels of gap settings:

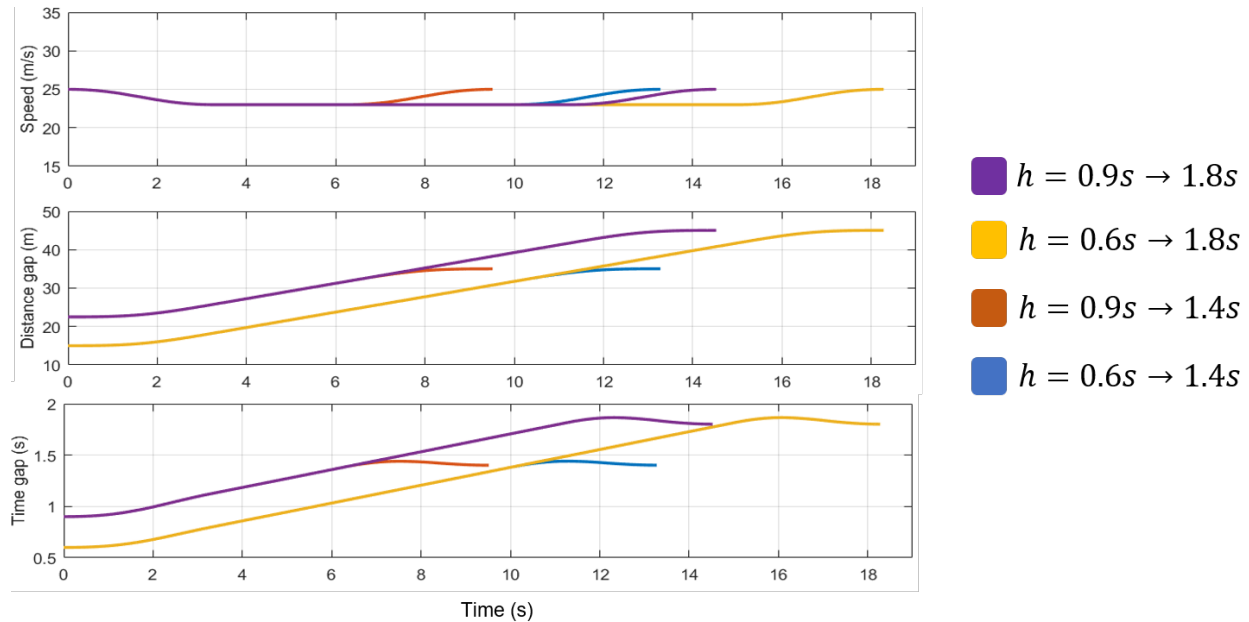


Figure I.1.3.14 Planned Speed, Distance and Time Gap Profiles for Different Time Gap Values

For the presented figure, longitudinal motion variables have been constrained as follows: $|j(t)| \leq 0.8 \text{ m/s}^3$, $|a(t)| \leq 1 \text{ m/s}^2$ and $23 \text{ m/s} \leq |v(t)| \leq 25 \text{ m/s}$. One can observe how the speed profile converges to the initial value after increasing the distance gap. Despite the different levels of h_{init} and h_{target} , the algorithm proves useful to generate the required gap change plan. Finally, the planned time gap profile is used to adapt

the spacing policy block on the outer feedback loop, as well as the feedback and feedforward controllers, from the starting time until the target time gap is reached. It is worth to mention that even if the relative speed with cutting-in vehicle is non-zero, by performing the maneuver on closed loop the safe car-following operation is maintained and the speed error is mitigated by the feedback controller.

Results

The proposed architectures have been validated on the three different vehicle platforms, over highway and test tracks. The developed ACC algorithm is demonstrated with highway test scenarios. Results for both modes of CACC operation are provided after, for highway and test tracks testing. Finally, results from the system for handling of cutting-in vehicles are depicted.

Leader vehicle ACC

The ACC control structure performance has been tested on highway traffic on freeway I-580, over the Toyota Prius platform. The figure below shows the speed of target and subject vehicle in the upper plot, while lower plot shows the target and measured time gap. The speed of target vehicle is estimated from radar relative speed measures.

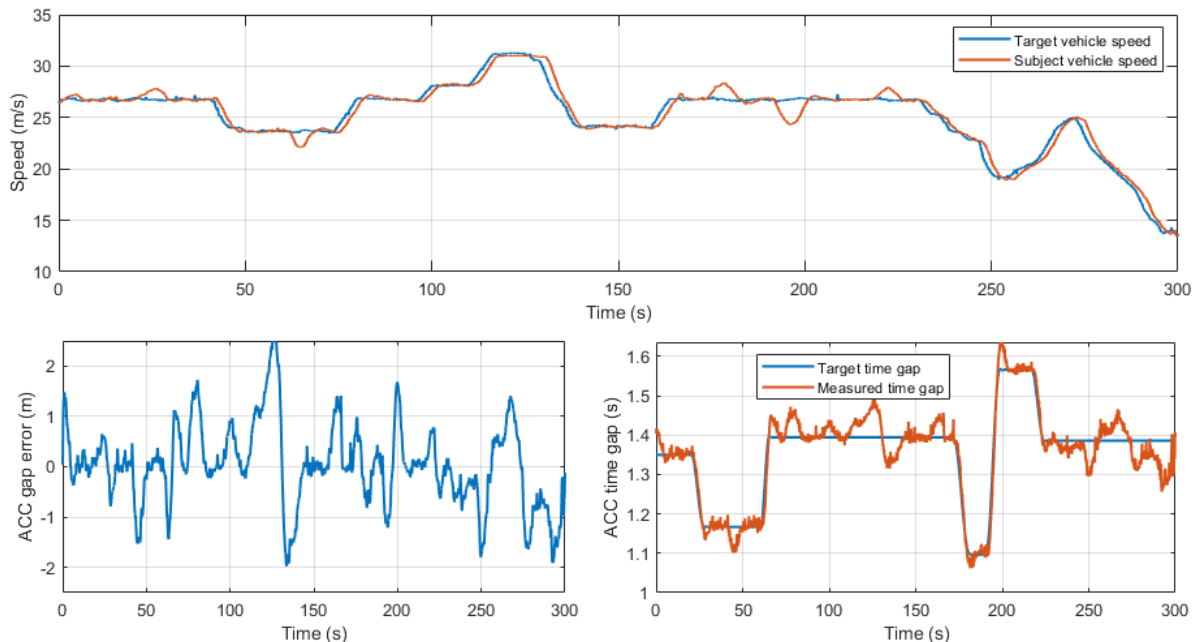


Figure I.1.3.15 ACC Structure Testing on Highway Traffic

As can be observed, the controlled vehicle tracks efficiently the target vehicle speed changes without amplifying or increasing significantly the speed disturbances coming from downstream. In addition, changes on the user time gap settings are also accurately tracked in a smooth way without leading to uncomfortable behavior. The ACC gap error was observed to remain below two meters, which shows the algorithm accuracy to perform car-following despite target vehicle speed and time gap changes.

Regular-CACC tested on highway

For the regular-CACC testing scenario, a two-vehicle string is performed in highway I-80, having the Ford Taurus and Honda Accord as leader and CACC follower, respectively. The leader vehicle is manually driven for the entire run, while the subject vehicle applies the regular-CACC car-following starting with a time gap of 0.6s. The upper plot shows the speed evolution of both leader and follower vehicles, whereas lower plots illustrate the CACC gap error and time gap (left and right plots, respectively). As can be appreciated, the

subject vehicle tracks more accurately the changes on leader vehicle speed, comparing to the ACC case. The error magnitude is mostly kept below 3 meters for the steady operation of CACC. However, when the time gap setting was changed towards 0.9s and 0.45s, the gap error magnitude is seen to increase as a product of the gap change maneuver. At $t=300$ s and 340s, one can observe a short separation of the subject vehicle speed from leader speed due to the gap settings modification, which is shortly mitigated once the car-following system stabilizes at the new target time gap. It is visible that the CACC system is robust both to changes in the target time gap and leader vehicle speed changes, even at different accelerations of the leader vehicle. Nevertheless, when the leader vehicle speed shows high frequency changes—e.g., $t=450$ s—, these disturbances are slightly amplified by the subject vehicle. This string instability is solved when the high-performance CACC framework is used instead.

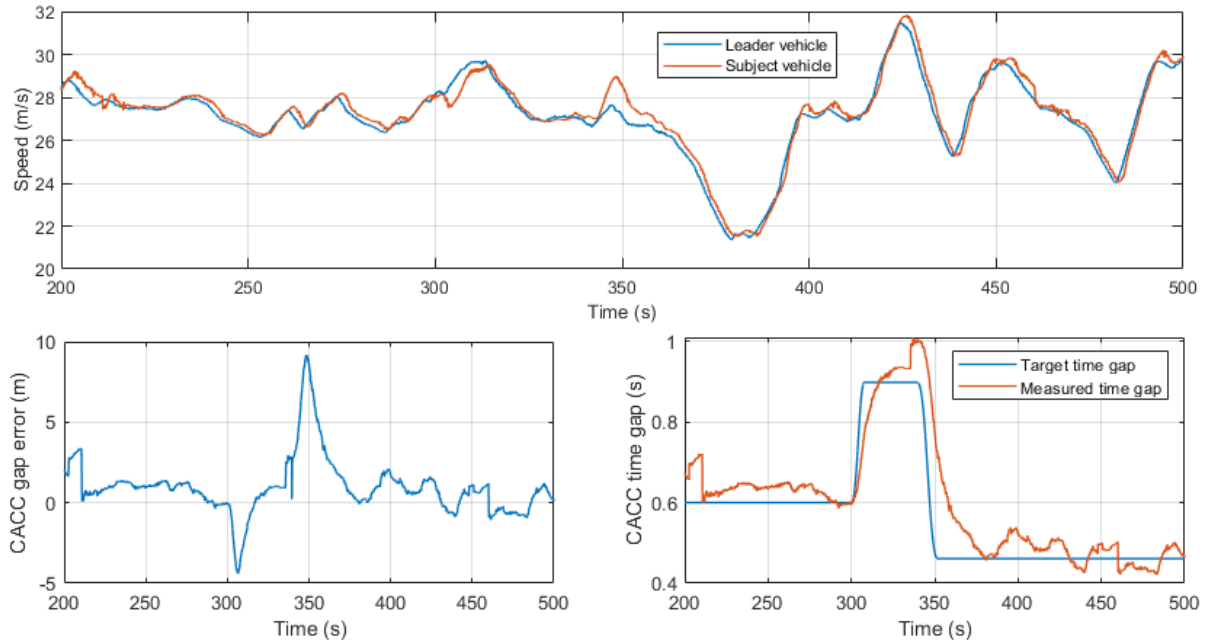


Figure I.1.3.16 Regular-CACC Testing. Speeds, Gap Error and Time Gap Variables

High-performance CACC

For testing the performance-CACC operation mode, several tests were conducted in Crows Landing Airport facilities, which accounts with a two-mile long closed test track, avoiding interaction with other vehicles for car-following at short gaps. Two profiles for the string exogenous input (leader reference speed) are designed to assess the algorithm performance: 1) speed steps, and 2) a random phase multisine profile to excite different frequency regions.

Speed profile based on jerk steps

The speed steps profile designed is based on jerk steps, which produce a second order polynomial to oscillate between 24.5 m/s and 9 m/s, with a maximum acceleration magnitude of 1.5 m/s². The vehicles are ordered from leader to second follower as: Ford Taurus, Toyota Prius and Honda Accord. The 1st follower performs predecessor-following, whereas the 2nd follower drives on a leader-predecessor following topology. The speed changes are tracked more accurately and rapidly by the followers, comparing to the regular-CACC case. The speed propagation in upstream direction results string stable, which is visible in the speed oscillations being damped and attenuated by the second and third vehicles. The VTG spacing policy set for this run goes from

0.25s at zero speed, to 0.45s at velocities higher than 18 m/s which is the threshold between urban and highway speeds. Regarding the spacing gap error, it is seen to be controlled correctly and smoothly.

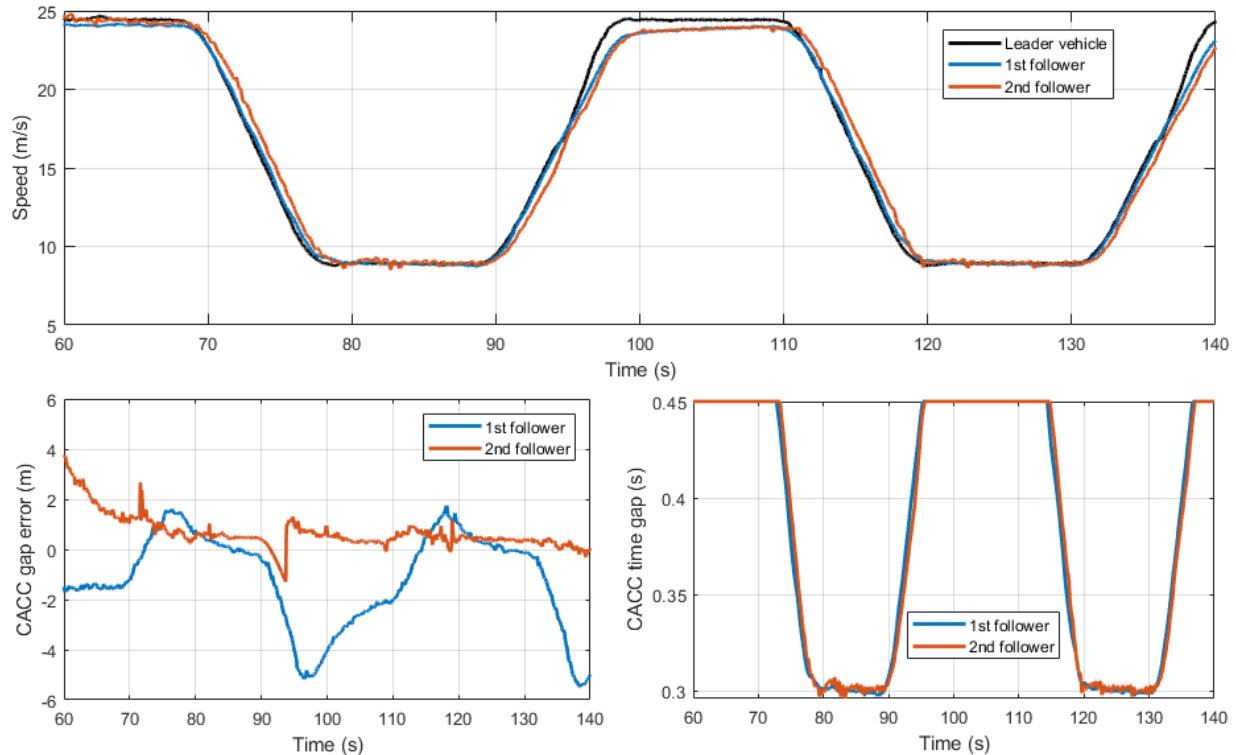


Figure I.1.3.17 Speed Variations Scenario Based on Jerk Steps Profile

However, a negative tracking error peaks were observed in the second vehicle. The 1st CACC follower gets closer than desired when the leader vehicle speeds up at a rate of 1.5 m/s^2 . The reason being that the Taurus presents a slower speed tracking transient response when throttling than braking (please refer to Figure I.1.3.5). In this work, the Taurus braking dynamics were considered as the low-level model for the design of the CACC followers' feedforward controllers due to its faster dynamics, which reduces the risk of tracking overshoot. Since the 1st follower is both using the leader reference speed and using the Taurus' braking dynamics for its low-level model for all types of speed changes, the CACC vehicle's feedforward controller over-estimates the leading Taurus' throttling performance and therefore gets closer than it should. Nevertheless, the feedback controller corrects this disturbance and regulates the spacing gap error to equilibrium.

In the case that leader vehicle reduces its speed, the error magnitude is considerably lower given that the assumed low-level model matches the real behavior of the real vehicle (both based on braking behavior). For the second follower, the gap error performs better than for the first follower as a product of the more accurate model representation of these two vehicles' low-level responses.

Multisine profile

This setup is designed to study more accurately the string stability performance of the CACC formation. The profile is composed by the addition of different frequency sine signals with random phase. This generates a signal which is rich in spectral energy on the frequency region of interest. This profile also emulates the way normal traffic scenarios evolve in a dense traffic. For this case, the VTG policy goes from 0.1 to 0.2s at higher speeds. The vehicle ordering from leader to last is as follows: Ford Taurus, Honda Accord and Toyota Prius

The CACC algorithm performs very well tracking the leader speed changes, even in a more coupled manner than the previous case. The propagation of speed oscillations results are even more coupled than in the previous case, because of the shorter time gaps that are set. Despite very short time gaps, string stable performance is observed where the CACC followers dampen the leader vehicle speed changes as expected. Very few non-uniform propagations (see $t=85s$ and $t=125s$) are observed caused by disturbances in the leader vehicle low-level response. The spacing gap error results are good with almost no significant variations, which demonstrates the algorithm accuracy.

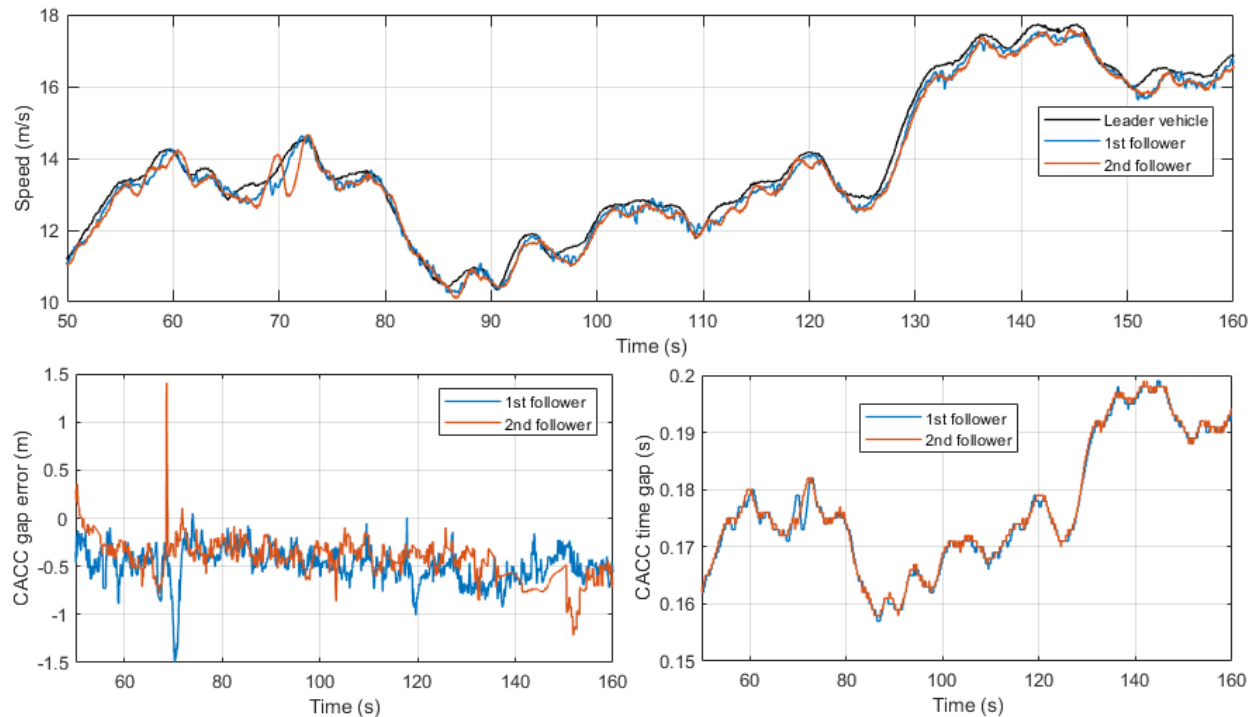


Figure I.1.3.18 Multisine Scenario Testing for High-Performance CACC

Cutting-in vehicle handling

To assess the performance of the cutting-in vehicle handling system, the Ford Taurus is set to be driving in a constant speed of 20 m/s, which renders more visible the designed algorithm performance by ensuring no speed disturbances are introduced by the leader. The Toyota Prius performs CACC with the leader at 0.9s of time gap. A third manually driven vehicle is set to cut-in and out in front of the CACC follower, triggering the cut management system. For this scenario, lower figures show gap errors and time gaps for both ACC and CACC.

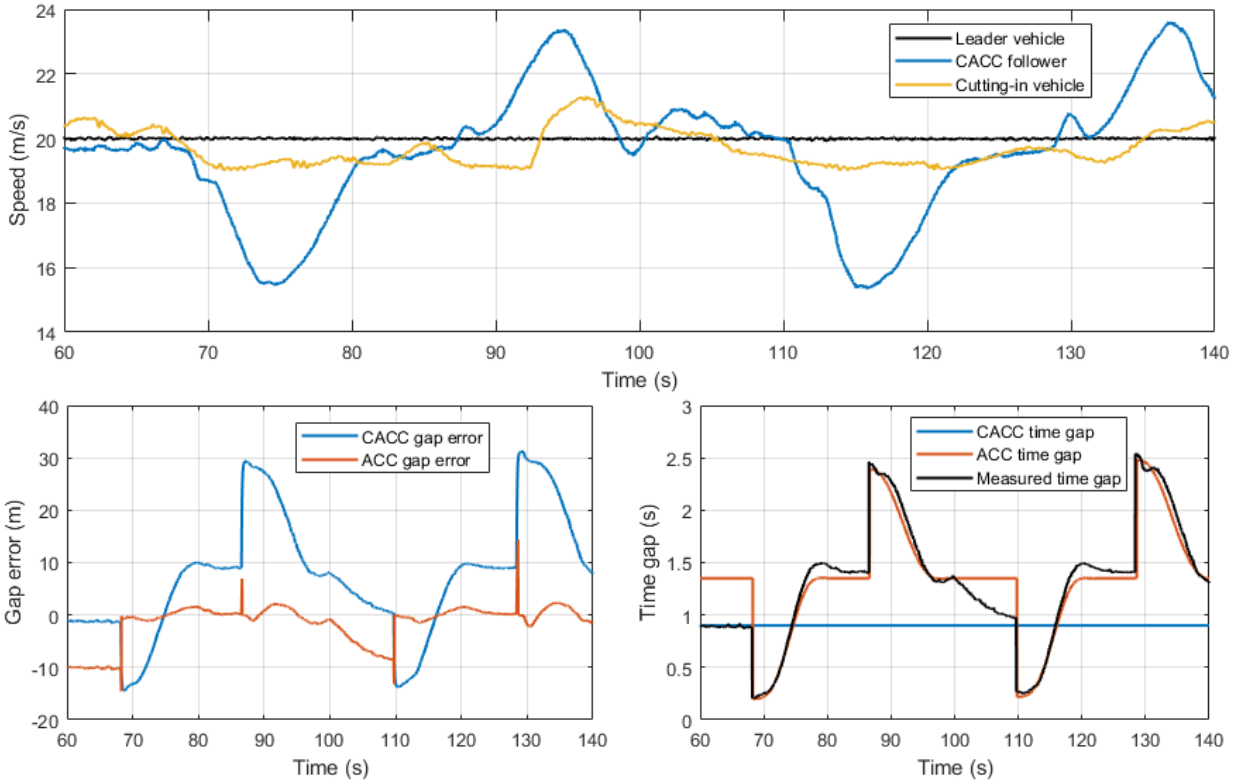


Figure I.1.3.19 Cutting-In Vehicle Testing Scenario on CACC String

At $t=68\text{s}$, the third vehicle cuts in front of CACC follower at a gap of 0.2s . The system switches instantly to ACC and adapts its structure time gap in function of the planned time gap profile towards $h_{\text{target}} = 1.35\text{s}$. The adaptation is visible in the gap error plot, where at the trigger time the ACC error goes almost to zero and stays low until the state machine switches back to CACC. One can observe the gap opening performance on how the measured time gap tracks correctly the planned profile. At $t=86\text{s}$, the vehicle cuts-out and the target perception systems tracks again the string leader, which triggers a gap-closing maneuver from 2.45s to 1.35s . Both closed loop maneuvers remain within the desired acceleration and jerk limits, as the speed plot shows. Once the vehicle stabilizes around the target ACC time gap value, the driver selects to switch back to CACC mode at $t=100\text{s}$, which induces the vehicle to accelerate to close the gap to the original CACC time gap of 0.9s . The switching is also visible in the gap error, specifically when the CACC gap error converges to zero and the ACC gap keeps decreasing for not being regulated. The same steps are repeated when the vehicle cuts in again at $t=110\text{s}$, just at the time that the CACC stabilizes the tracking. This demonstrates the algorithm usability and robustness to several cut-ins.

Highway CACC testing with three vehicles

The developed CACC algorithm has been also tested in highway I-80 with three vehicles to validate its performance when dealing with public traffic situations. The Taurus is driven manually as a leader, the Honda Accord is set on regular CACC and Toyota Prius implements the high-performance CACC.

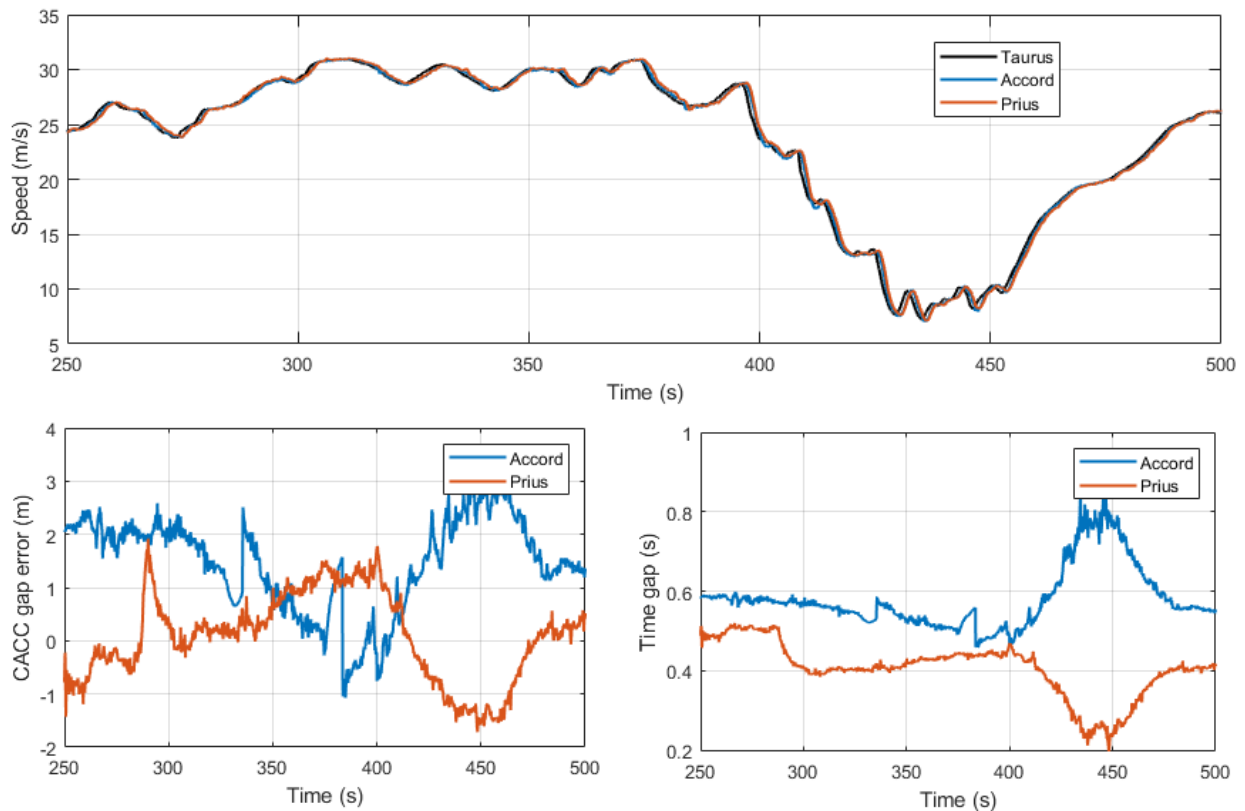


Figure I.1.3.20 CACC Vehicle Testing of Three Vehicles on Public Highway

Upper plot shows the speeds evolution along time, whereas lower left and right plot depict the CACC gap errors and measured time gaps, respectively. The second vehicle (Accord) is set to track a time gap of 0.6s, while the third (Prius) starts following at 0.5s and closes to 0.4s at $t=290$ s. The CACC follower vehicles are observed to track accurately the speed changes of their respective predecessors. Moreover, they do so without amplifying the oscillations coming from downstream, showing string stable performance. This behavior is observed not only at high speeds, but also at low speeds as reached after $t=400$ s. The vehicles are also observed to respond safely to relatively strong decelerations without showing high deviations or significant tracking errors. One can see that after $t=400$ s during the moderate braking, the high-performance CACC is seen to have lower tracking error than the regular-CACC vehicle, given the advantage of using the preceding's reference speed. The CACC system robustness is also demonstrated when the car-following has to recover from a target perception measurement error, as observed in Accord's gap error and time gap evolutions at $t=335$ s and 380s.

Conclusions

The research framework and validated developments have yielded an advanced ACC/CACC system that considers vehicles of different dynamics and powertrains. Among the research contributions of this project, one can highlight:

- Development of a hierarchical architecture for car-following, where the low-level layer deals with longitudinal speed tracking dynamics, while high-level regulates the car-following kinematics.
- Each of the three low-level speed tracking systems performed very accurately, demonstrating that use of actuators mapping enhances the acceleration/deceleration tracking capabilities.

- A feedback control design based on an LPV (Linear Parameter Variation) structure permits not only selecting the degree of comfort/aggressiveness in function of the intended use case, but also adapting to the desired time gap.
- The inclusion of feedforward controller to process the V2V information can significantly increase the tracking speed and response bandwidth, without diminishing the loop stability.
- The best results are obtained with the high-performance CACC mode. This shows that using the reference velocity of either preceding or leader + preceding vehicles helps achieve string stable CACC even at very short time gaps.
- Despite having heterogeneous dynamics in the string caused by different vehicle types and powertrains, the use of leader-predecessor topology enhances the performance and response capabilities, leveraging the knowledge of all vehicle response dynamics.
- The time gap planning algorithm provides a framework to modify optimally the gap settings, as well as to handle both cutting-in and cut-out vehicles.

It is also important to highlight that all developed algorithms have been tested and validated in highways and closed test tracks, as well as in high speeds and stop-&-go situations. It has been concluded as well that the best vehicle ordering should increase the response dynamics bandwidth, avoiding actuators saturation in any of the CACC followers.

Key Publications

1. Flores, C., Muñoz, J., Monje, C.A., Milanés, V., & Lu, X. Y. (2020). Iso-damping fractional-order control for robust automated car-following. *Journal of Advanced Research*.

References

1. Künzli, N., et al. (2000). Public-health impact of outdoor and traffic-related air pollution: a European assessment. *The Lancet*, 356(9232), 795-801.
2. Stern, R. E., et al. (2018). Dissipation of stop-and-go waves via control of autonomous vehicles: Field experiments. *Transportation Research Part C: Emerging Technologies*, 89, 205-221.
3. Rajamani, R., & Shladover, S. E. (2001). An experimental comparative study of autonomous and co-operative vehicle-follower control systems. *Transportation Research Part C: Emerging Technologies*, 9(1), 15-31.
4. Shladover, S. E., Nowakowski, C., Lu, X. Y., & Ferlis, R. (2015). Cooperative adaptive cruise control: Definitions and operating concepts. *Transportation Research Record*, 2489(1), 145-152.
5. Liu, H., Shladover, S. E., Lu, X. Y., & Kan, X. (2020). Freeway vehicle fuel efficiency improvement via cooperative adaptive cruise control. *Journal of Intelligent Transportation Systems*, 1-13.
6. Milanés, V., & Shladover, S. E. (2016). Handling cut-in vehicles in strings of cooperative adaptive cruise control vehicles. *Journal of Intelligent Transportation Systems*, 20(2), 178-191.
7. Nowakowski, C., O'Connell, J., Shladover, S. E., & Cody, D. (2010, September). Cooperative adaptive cruise control: Driver acceptance of following gap settings less than one second. In *Proceedings of the Human Factors and Ergonomics Society Annual Meeting (Vol. 54, No. 24, pp. 2033-2037)*. Sage CA: Los Angeles, CA: SAGE Publications.

8. Flores, C., Milanés, V., & Nashashibi, F. (2017, October). A time gap-based spacing policy for full-range car-following. In 2017 IEEE 20th International Conference on Intelligent Transportation Systems (ITSC) (pp. 1-6). IEEE.

Acknowledgements

Dr. Carlos Eduardo Flores (email: carfloresp@berkeley.edu) of PATH, University of California Berkeley, has developed the system modeling, simulation, control design/implementation/tuning/, Diver Vehicle Interface, field operational test, and data analysis.

Dr. Eric Rask (ex-staffer) and **Dr. Simeon M. Iliev** (email: iliev@anl.gov) of Argonne National Laboratory, developed the engine torque mapping and provided support on lower-level control actuations of all three vehicles.

John Spring (email: jspring@berkeley.edu) and **David Nelson** (email: dnelson@path.berkeley.edu) of PATH, University of California Berkeley, provided software and hardware support and system integration in the CAC system development and field operational tests and help in driving in different test scenarios for tests on the test-track and on highways

I.1.4 Urban Science (National Renewable Energy Laboratory)

Stanley E. Young, Principal Investigator

National Renewable Energy Laboratory
15013 Denver West Parkway
Golden, CO, 80401
Email: stanley.young@nrel.gov

Prasad Gupte, DOE Technology Manager

U.S. Department of Energy
Email: prasad.gupte@ee.doe.gov

Start Date: October 1, 2019	End Date: September 30, 2020	
Project Funding: \$3,247,590 (includes \$500,000 for INRIX mobility data and \$25,000 for synthesis report support)	DOE share: \$3,247,590	Non-DOE share: \$0

Project Introduction

Fiscal year (FY) 2020 was a bridge year for the Energy Efficient Mobility System (EEMS) Systems and Modeling for Accelerated Research in Transportation (SMART) Mobility Consortium, with the SMART 1.0 project wrapping up and SMART 2.0 research portfolio being formulated. Normally, APRs are project-specific with respect to SMART individual efforts; however, as a bridge year, this APR is comprehensive across the various SMART 1.0 projects that had remaining work in FY 2020, as well as some pre-SMART 2.0 projects that were initiated.

FY 2020 SMART work leveraged and expanded existing analysis, models, and tools toward an effective virtual test bed for advanced transportation systems, vehicle technologies, alternative fuels, and infrastructure. Proposed activities were coordinated through DOE's SMART Mobility Consortium, including the established laboratory organization related to the five SMART Mobility Pillars. The five pillars performed the following research: (1) work on connectivity and automation focused on testing and quantifying potential technology-specific and aggregate transportation system energy impacts of these technologies; (2) mobility decision science efforts focused on understanding the decision-making process as it relates to the transportation energy user faced with a multitude of transportation-as-a-service options; (3) urban sciences activities aimed at understanding the implications of increasing urbanization on transportation and mobility; (4) advanced fueling infrastructure co-optimization efforts to increase understanding of how vehicles and emerging alternative fueling infrastructures interact, to inform optimal co-deployment of vehicles and fuels; and (5) the multimodal freight efforts focused on the complex interrelationships that arise when integrating multimodal transportation system models for freight movement, supporting a reduction in the inefficiencies at the modal interfaces and a corresponding reduction in energy use.

A portion of the overall FY 2020 supported the development of modular tools for smart city planning applications, including (but not limited to) transportation energy infrastructure planning, workplace charging, economic analysis, gap/opportunity analysis for electric-drive people and goods movement, and other potentially meritorious tools for smart city transportation energy planning. To the extent possible, these projects supported potential collaboration and real-world analytical/modeling efforts that leverage complementary investments from other federal agencies, such as the U.S. Department of Transportation's (USDOT's) Smart City Challenge. A multi-lab consortium, utilizing the core strengths of each participating organization, is required to tackle the breadth of this topic.

This work built on previous work to support VTO's expansion in focus from single-vehicle technologies to broader system-level transportation issues, consistent with the program's evolution from foundational exploratory and prioritization analyses to applied vehicle systems modeling and simulation. As noted, the overall objective is to identify new promising areas for hardware and software technology research, development, and demonstration.

Because FY 2020 was a bridge year, this APR is organized with highlights of the various projects from SMART 1.0 that were wrapped up, as well as pre-SMART 2.0 projects that were initiated. The following sections discuss objectives, methods, and results for each of the highlighted initiatives, with an emphasis on results, deliverables, and publications.

Multimodal Energy Analysis for Freight

PIs: Kyungsoo Jeong and Alicia Birky

FY 2020 objectives included completing a publication of results. The project addressed reviewer comments and completed final revision of a Freight Mobility Energy Productivity (F-MEP) paper for journal acceptance.

A journal paper on the multimodal freight energy model was drafted, including a summary of sampled and estimated sub-Freight Analysis Framework (FAF)-level truck origin–destination tables obtained from INRIX data analysis and a description of the methodology used.

Summary of Results

The intercity F-MEP metric paper presented at the 2020 Transportation Research Board (TRB) Annual Meeting was revised and subsequently published in *Transportation Research Record* in June. The intracity F-MEP methodology, refined to include measures of circuitry, was accepted for presentation at the 2020 International Symposium on Transportation Data & Modeling (ISTDM), rescheduled for June 2021. The draft multimodal freight energy model paper was accepted for a poster presentation at the 2021 TRB Annual Meeting, scheduled for January 2021.

A methodology was developed to estimate truck origin–destination matrices using global positioning system (GPS) trip data obtained from INRIX. Analysis revealed that each trip record cannot be used directly because some trips are extremely short or have endpoints that are unlikely to be freight pickup or delivery locations. To improve the accuracy of the estimates, land use data, including fueling and trucking parking locations, were overlaid on trip start and end locations. When combined with stop dwell times, this enabled chaining of trips where probability distributions indicated the endpoints likely were not freight origins or destinations. The resulting truck flows between counties were combined with FAF truck flows to update origin–destination matrices for the Chicago metropolitan area (see Figure I.1.4.1). Identifying chaining of freight truck trips from large GPS data sets can help develop fine-tuning freight demand or simulation models. However, GPS data have inherent limitations on the sampling approach and size. Thus, the proposed approach needs to incorporate physical and operational characteristic data from trucks.

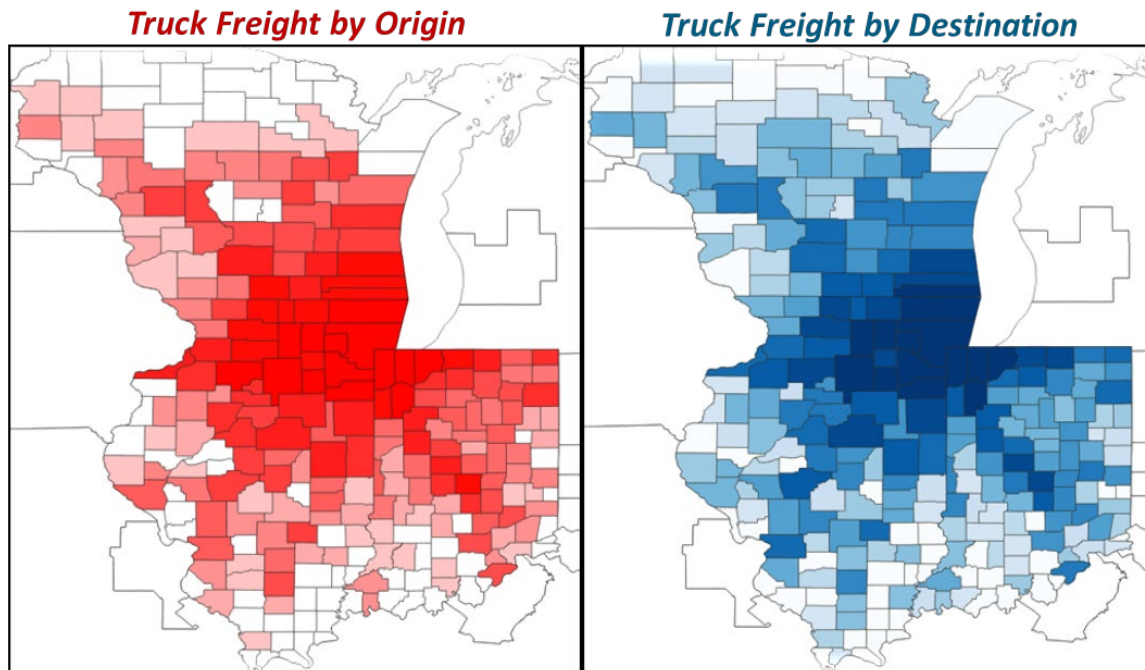


Figure I.1.4.1 Truck Freight Flows for Chicago Area by Origin and Destination

Key Publications

1. Jeong, K., V. Garikapati, Y. Hou, A. Birky, and K. Walkowicz (2020). “Comprehensive Approach to Measure the Mobility Energy Productivity of Freight Transport.” *Transportation Research Record* 2674(7):29–43. doi:10.1177/0361198120920879.
2. Jeong, K., V. Garikapati, Y. Hou, A. Birky, and K. Walkowicz (forthcoming). “A Novel Metric for Urban Freight System Using Data Fusion: Freight Mobility Energy Productivity Metric.” Accepted for presentation at the 2020 International Symposium on Transportation Data & Modeling (deferred to ISTDM 2021 due to COVID-19).
3. Jeong, K. and A. Birky (forthcoming). “Multimodal Freight Energy Model for Emerging Freight Technology Analysis.” Accepted for presentation at the 2021 TRB Annual Meeting.

Urban Typology Analysis

Pls: Patricia Romero Lankao

The objective of Urban Typology Analysis is to enhance the value of SMART Mobility efforts by making relevant outcomes transferable among cities with similar characteristics; create a multidimensional typology of adoption and impacts of emerging technologies in urban areas leveraging geographic information system (GIS) for reuse and sharing; and enable researchers, practitioners, planners, Smart Cities, and transportation and energy professionals to estimate future automated, connected, efficient (or electrified), and shared (ACES) impacts for planning and infrastructure investments.

Summary of Approach

This project used an urban systems approach to distill information about social, economic, techno-infrastructure, environmental, and governance (SETEG) factors to create clusters of similar census block groups without an explicit spatial dependency. These clusters, referred to as micro-urban social types (MUSTs), were then used to explore relationships with mobility and transportation technology adoption, initially at the scale of the State of New York (Rames et al., 2020), and then expanded to nine U.S. states

(California, Colorado, Illinois, Missouri, New York, Ohio, Oregon, Pennsylvania, and Texas) plus the District of Columbia. Data inputs to the MUST analysis encompass a total population of anywhere from 600 to 3,000 people. Initially, 13 independent variables are used in this analysis. Sources include the American Community Survey 5-year data (2012–2016) for age (% over 65), gender (% female), race (% white), education (% with bachelor’s degree or higher), household income, home tenure (% homeowners), and population density. They also include the Center for Neighborhood Technology for road intersection density, employment access, and combined housing and transportation costs as a percentage of income (H+T Affordability Index) and the U.S. Environmental Protection Agency’s Environmental Justice Screening and Mapping Tool (EJSCREEN) for particulate matter (PM_{2.5}) levels, cancer risk from air toxics, and respiratory hazard index from air toxics. These variables were normalized to a common scale using a min-max scaling approach. Then, agglomerative clustering using Ward’s criterion was used to identify five clusters, or MUSTs (named after astrological signs to be as neutral as possible).

The generation of MUSTs and identification of city types set us up for the Typology Transfer. This process captures the potential for transferring results, such as specific output from an agent-based model (ABM), from one city to another based on MUST and city type. The process began with a variable of interest, the mobility energy productivity (MEP) metric, which has both a baseline value and a future simulated value for one city (City A), and a baseline value for a second city of the same city type (City B). The values were upscaled or downscaled to match the spatial resolution of the MUST analysis. Then, they were assigned to each of the individual geographic units, which received both a MUST cluster assignment and a MEP value assignment. The values for each of the n MUST clusters were divided into p quantiles (we use $p = 5$ quantiles). This produced a grid with each MUST cluster as a row and each column as a quantile. The values in the tables can be the mean or median for that quantile. This table was calculated for both the baseline values and the future values for City A and for the baseline values for City B. The change between the baseline and future values in City A became the Typology Transfer Multiplier Matrix (TTMM). Multiplying the City B baseline value table by the TTMM generated a final table with the estimated future values of the variable of interest for City B. Note that the scaling factors from the TTMM can be applied to every geographic unit in the City B study area, and then visualized with mapping.

Results

Five clusters (MUSTs) were generated based SETEG data: (1) Pisces, representing 18% of the population, has very high income, H+T Index, education, and home and car ownership and low levels of density and risk from air pollutants; (2) Virgo, representing 5% of the population, has middle income, high education, low home ownership, very low H+T Index and car ownership, and very high levels of density and risk from air pollutants; (3) Aries, 10% of the population, has very low income, H+T Index, education, and home and car ownership; very high density; and high risk from air pollutants; (4) Taurus, 32% of the population, has low income and education, medium H+T Index, low home ownership, high car ownership, high density, and medium risk from air pollutants; and (5) Libra, 35% of the population, has middle income, education, and H+T Index; high car ownership and density; and very low risk from air pollutants (see also Romero-Lankao et al., 2020, under review).

The MUSTs typologies were the basis for Typology Transfer of BEAM and Polaris ABM modeling results, projecting MEP metric scores onto the New York City region. See Figure I.1.4.2 for representative results.

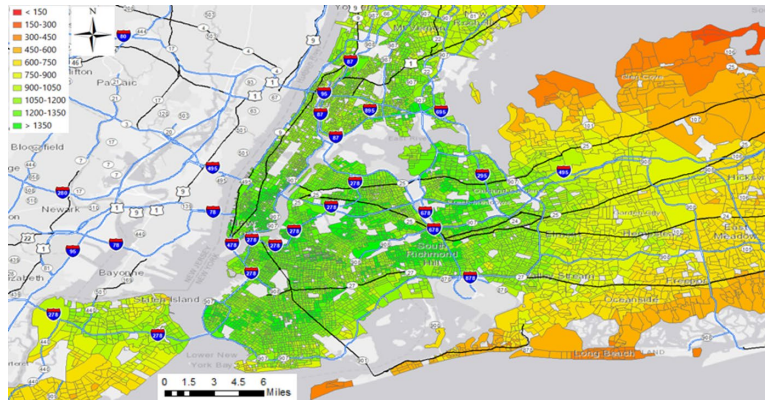


Figure I.1.4.2 Spatial Representation of MEP Values Using the POLARIS/Chicago Typology Transfer Multiplier Matrix Applied to New York City

Conclusion

The framework suggested here offers a unique opportunity to incorporate socio-spatial variables as they relate to electric vehicle (EV) adoption, mode choice, and other mobility outcomes, and generating clusters that share similarities within and across cities. This helps bring socio-spatial context to the forefront when interpreting outputs, such as the MEP metric, from ABMs. For example, it helps interpret the results of ABMs within relatable contexts of socioeconomic types. It expands the possibilities for tailoring ABM results and interpretations to specific community needs and data availability.

Key Publications:

1. Rames, Clement, Alāna Wilson, Daniel Zimny-Schmitt, Carolina Nero, Joshua Sperling, and Patricia Romero Lankao (2020). “A Data-Driven Mobility-Energy Typology Framework for New York State.” Accepted to *Environment and Planning B: Urban Analytics and City Science*.
2. Romero Lankao, Patricia, Alāna Wilson, and Daniel Zimny-Schmitt (2020). “Inequalities in Micro-Urban Social Factors, EV Adoption, and Mobility in U.S. Cities.” Submitted to *Nature Urban Sustainability* (Accepted for oral presentation at TRB 2020 Annual Meeting)
3. Zimny-Schmitt, Daniel, Alāna Wilson, and Patricia Romero Lankao (2020). “An Examination of the Effects of Socio-Demographics and City Size on Mobility Energy Contexts and Outcomes.” In preparation for *Environment and Planning A*.
4. Wilson, Alāna M., Daniel Zimny-Schmitt, Patricia Romero Lankao, Sperling Joshua, and Yi Hou (2020). “Linking Agent-Based Transportation Model (ABM) outputs with Micro-Urban Social Types (MUSTs) via Typology Transfer for Improved Community Relevance.” In preparation for *Transportation Research Part B: Methodological*.

Urban Science Capstone Report

Pls: Stanley E. Young and Andrew Duvall

The Urban Science Pillar focuses on maximum-mobility and minimum-energy opportunities associated with emerging transportation and transportation-related technologies specifically within the urban context. Such technologies, often referred to as ACES, have the potential to greatly improve mobility and related quality of life in urban areas. Although all the pillars share some commonalities, Urban Science strives to model, analyze, and gain insights from the perspective of human settlements (the “city”) as a living organism. This is especially critical as the United States is one of the most urbanized countries, and as more and more of the global population migrates to urban areas (UN DESA, 2019). Note that the urban mobility system, more so than suburban or rural systems, consists of a rich mixture that goes beyond roads and vehicles and includes

significant investments in public transit, private mobility services (such as taxis and transportation network companies [TNCs]), significant parking reserves, and curb management practices, not to mention the abundance of emerging on-demand micromobility services for the movement of people and goods such as e-bikes and scooters, which make the urban space a dynamic laboratory for mobility. Urban spaces also concentrate employment, markets, services, and attractions, which are the destinations for most trips. The concentration of human activities and ensuing density also creates the need and emphasis for space efficiency in urban environments, which is not a constraint in suburban or rural contexts. This rich mixture of transportation and mobility infrastructure and practice, combined with global urbanization trends, make urban spaces a critical focus of research for developing energy-efficient mobility systems.

For the purpose of discussion, the insights of the Urban Science research are organized into the following four thematic areas:

- Changes and Impacts on the Urban Traveler
- Development of the Mobility Energy Productivity Metric
- Urban Infrastructure & Built Environment Synergy with Mobility
- The Signal Control Network as the Urban Mobility Nerve Center.

Key Publications

1. All SMART Capstone reports, including for Urban Science, can be accessed at: <https://www.energy.gov/eere/articles/understanding-next-revolution-transportation-doe-publishes-results-3-year-smart>

References

1. United Nations Department of Economic and Social Affairs (UN DESA) (2019). *World Urbanization Prospects: The 2018 Revision* (New York: United Nations).

Energy Equivalence of Safety

Pls: Zijia Zhong, Lei Zhu, and Stanley Young

Transportation safety, as a critical component of an efficient and reliable transportation system, has been extensively studied with respect to societal economic impacts by transportation agencies and policy officials. However, the embodied energy impact of safety, other than induced congestion, is lacking in studies. This research proposes an energy equivalence of safety (EES) framework to provide a holistic view of the long-term energy and fuel consequences of motor vehicle crashes, incorporating both induced congestion and impacts from lost human productivity resulting from injury and fatal accidents and the energy content resulting from all consequences and activities from a crash. The method utilizes a ratio of gross domestic product (GDP) to national energy consumed, in a framework that bridges the gap between safety and energy, leveraging extensive studies of the economic impact of motor vehicle crashes. The energy costs per fatal, injury, and property-damage-only crashes in gasoline gallon equivalents in 2017 were found to be 200,259, 4,442, and 439, respectively, which are significantly greater than impacts from induced congestion alone. The results from the motor vehicle crash data show a decreasing trend of EES per crash type from 2010 and 2017, due primarily in part to a decreasing ratio of total energy consumed to GDP over those years. In addition to the temporal analysis, we conducted a spatial analysis addressing national-, state-, and local-level EES comparisons by using the proposed framework, illustrating its applicability.

Key Publications

1. Zhu, L., S. E. Young, and C. M. Day (2019). “Exploring First-Order Approximation of Energy Equivalence of Safety at Intersections.” Presented at the *2019 International Conference on Transportation & Development*, 6–12 June 2019, Alexandria, Virginia.

2. Zhong, Z., L. Zhu, and S. E. Young (2020). “Approximation Framework of Embodied Energy of Safety: Insights and Analysis.” (In progress).

Automated Mobility Districts Modeling Toolkit

Pls: Lei Zhu, Venu Garikapati, and Stan Young

The Automated Mobility District (AMD) toolkit is built using the Simulation of Urban MObility (SUMO) package for travel simulation and the Future Automotive Systems Technology Simulator (FASTSim) for energy analysis. The toolkit is designed with rapid implementation goals in mind to enable cities to effectively assess and evaluate benefits (or the lack thereof) of various emerging mobility alternatives. The major features and contributions of the toolkit are:

1. It is an open-source, multimodal shared automated mobility and energy simulation tool, integrating pedestrian behaviors, shared automated vehicles (SAVs), and regular traffic
2. Although the toolkit is capable of simulating an array of emerging mobility options, initial testing has been carried out for AMDs or geofenced deployments of low-speed automated shuttles
3. Multiple travel modes, including (1) regular car, (2) walk, (3) on-demand door-to-door ridesharing, and (4) on-demand fixed-route ridesharing are simultaneously implemented. Primarily, two on-demand ridesharing modes (door-to-door and fixed-route) and their interaction with regular car and walk modes are modeled.

FY 2020 efforts focused on the integration of an optimization module (Aziz et al., 2020), as well as a mode-choice model into the AMD toolkit (Zhu et al., 2020a; 2020b). The capabilities of the AMD toolkit have also been extended to simulate shared automated vehicles as first- and last-mile (FMLM) connections to transit (Huang et al., 2020).

SAVs as an FMLM Connection Mode

Although the effectiveness of FMLM connections to transit has been the subject of many research endeavors, literature on the impacts of using SAVs as an FMLM connection is rather sparse. Filling this gap, National Renewable Energy Laboratory (NREL) researchers, in collaboration with researchers from the University of Texas at Austin, applied the AMD toolkit to the Austin transit network with multiple AMDs (Figure I.1.4.3), focusing on the operations of SAVs as an FMLM solution to transit connectivity. This work extends the capabilities of the AMD toolkit by incorporating complex operations of the transit system, as well as the multidimensional interactions between pedestrians, SAVs, and transit.

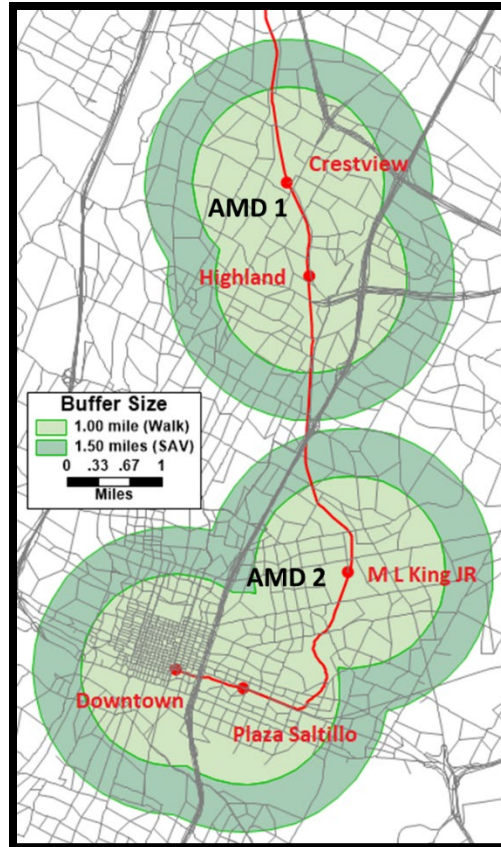


Figure I.1.4.3 Austin Red Line and Amds

Results

With SAVs serving FMLM requests in their designated AMDs, an estimated 3.71% of current person-trip-making could shift from private-car modes to the SAV-and-ride mode, leading to a 10-times increase in the use of transit with stable walk-and-ride mode share. SAV use slightly raises systemwide vehicle miles traveled (VMT) while slightly lowering average vehicle occupancy, owing primarily to SAVs' empty-vehicle travel (between customers). It was observed that SAVs were utilized more when train service was more frequent. Lower train headways also lowered SAV onboard time, wait time, and average trip length. Average walking times were quite stable across scenarios, at most 4 min for both SAVs and transit.

AMD Optimization Module

The optimization module developed and integrated into the AMD toolkit can be used for the operational planning of AMDs. The optimization module takes input from baseline scenario outputs from the micro-simulation model (i.e., SUMO), and then builds on top of the baseline scenario to optimize for operational planning under various scenarios.

Results

From simulation conducted using the optimization module, it was observed that both travel cost and energy consumption increase with AMD demand level. Whereas travel costs (within a given demand scenario) decrease with increasing shuttle battery range, it was interesting to find that energy consumption is higher when vehicles with longer range are deployed. The additional energy consumption can be attributed to a higher number of start/stops of the longer-range shuttle buses.

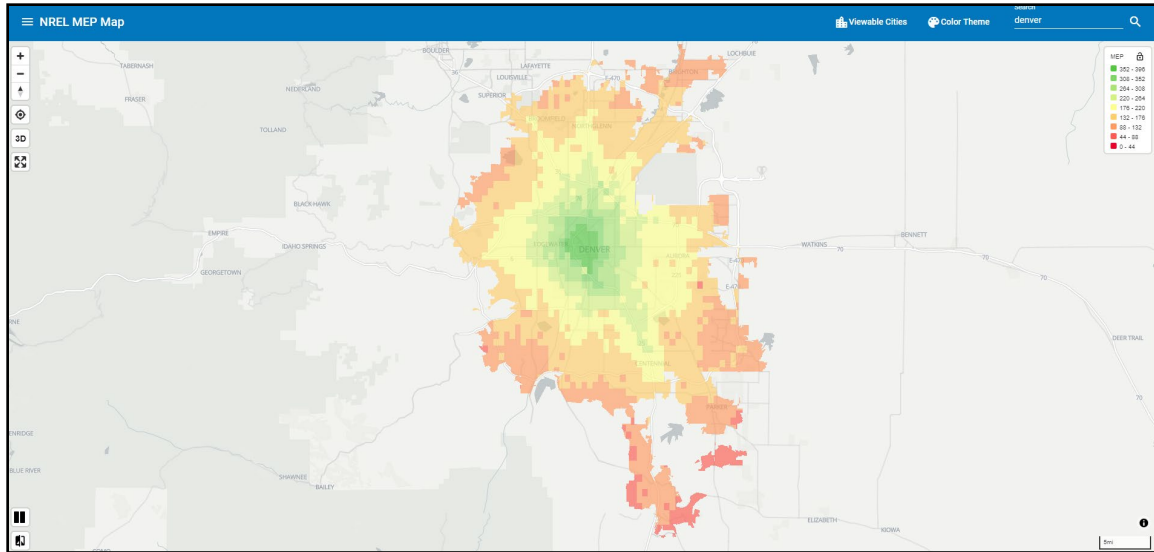


Figure I.1.4.5 Web Visualization Prototype to Display MEP Scores

In addition to this, the MEP team began a complete rewrite of the MEP code to improve run times. The previous MEP implementation relied on a combination of parallelized R scripts and PostGres spatial queries. R is an effective scripting language for exploratory data science, but it is difficult to optimize for general-purpose computing tasks, and given MEP’s multidomain computations, this became a challenge. Scala was chosen for MEP code rewrite in order to leverage Apache Spark, a very popular open-source library for distributed scientific, graph analytical, and machine-learning compute jobs. Over the next year (as a part of SMART 2.0 efforts), aforementioned improvements will be made to the MEP code to cut run times in half or shorter (with current run times at ~4 hours).

In other MEP-related work, and in conjunction with a Technology Integration project, MEP was correlated to parking availability in a major metro area. The work explores associations of parking, mobility, and energy and presents comparative analyses to inform enhanced urban productivity and the utilization of urban space. These analyses shed light on the importance of parking in understanding mobility and future energy-efficient mobility pathways. Significant potential exists for cities to reshape parking to promote new energy-productive and efficient urban movement, enhance asset and land utilization, and improve mobility affordability and access.

Key Publications:

1. Hoehne, C., J. Sperling, S. Young, V. Garikapati, and S. Qian, (2020). “Parking as a lens to the urban soul: exploring associations of parking, mobility, and energy.” Presented at the *ITS World Congress ALL-ACCESS*, 8 October 2020. <https://www.itsamericanevents.com/its-all-access/en-us/education-sessions/session-details.1846.45427.novel-data-sources-and-efficiency-metrics-for-the-new-age-of-mobility.html>.

TNC Willingness to Pool

PI: Venu Garikapati

Pooling of TNC rides is an effective solution to reduce congestion and travel cost, but pooled rides still represent a small percentage of the total trips served (and miles driven) by TNCs relative to single-occupancy (and without customer) vehicle miles. Both TNCs and cities alike will benefit from understanding what factors encourage or deter pooling a ride-hailing trip. An analysis was conducted using the Chicago transportation network provider data to identify the extent to which different socioeconomic, spatiotemporal, and trip characteristics affect willingness to pool (WTP) in ride-hailing trips.

Results

The dependent variable of interest for this analysis is the proportion of trips for which passengers expressed a WTP between two Chicago census tracts in a given 15-min time bin (regardless of whether or not these trips were successfully pooled). This variable, represented by the purple trace in Figure I.1.4.6, shows recurring trends by day of the week. Exploration of the WTP trend revealed that the proportion of trips in which TNC customers indicated a WTP was highest midweek and lowest on Saturdays (with tick marks on the x-axis indicating the first and third Sundays of each month).

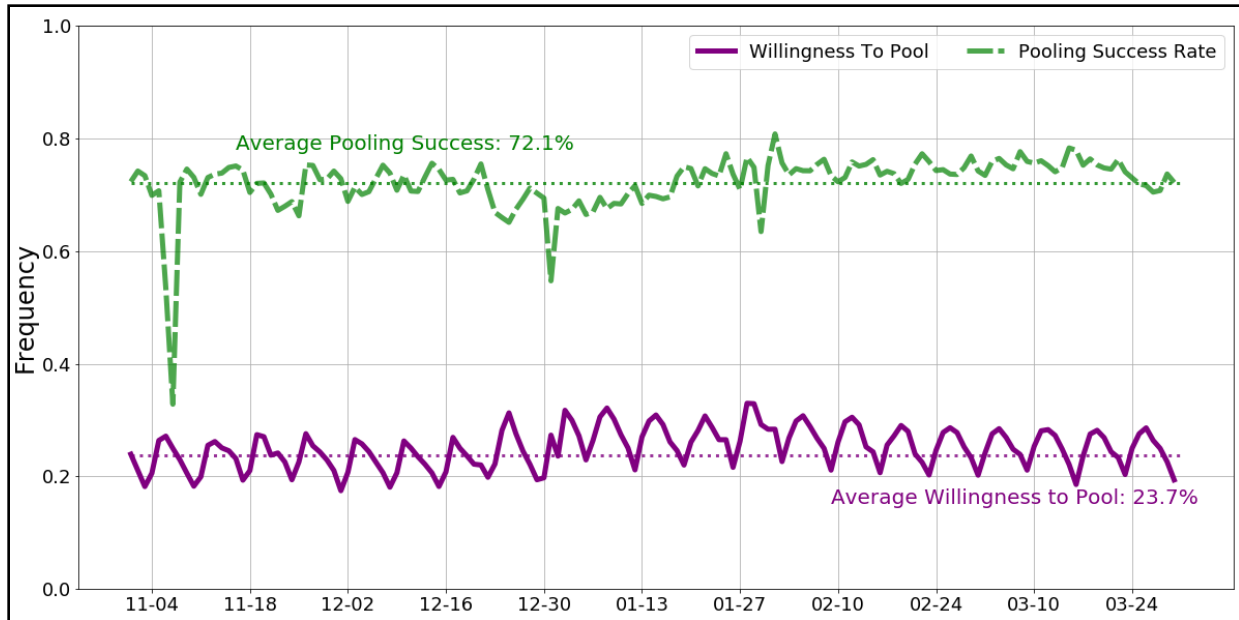


Figure I.1.4.6 Willingness to Pool and the Pooling Success Rate of Authorized Trips Over Time

Multivariate linear regression and machine-learning models were employed to understand and predict WTP based on location, time, and trip factors. The results show intuitive trends, with income level at drop-off and pickup locations and airport trips as the most important predictors of WTP. It was observed that trips starting or ending in zones with high population or job density have a lower WTP ratio. Controlling for all other factors, the elasticity of the distance variable shows that ride-hailing trips with longer trip length have a higher WTP ratio. All else being equal, if a ride-hailing trip is requested during nighttime, the WTP ratio decreases by 2.12%. Safety or an increased value of time at late hours could be possible explanations for this effect.

Key Publications

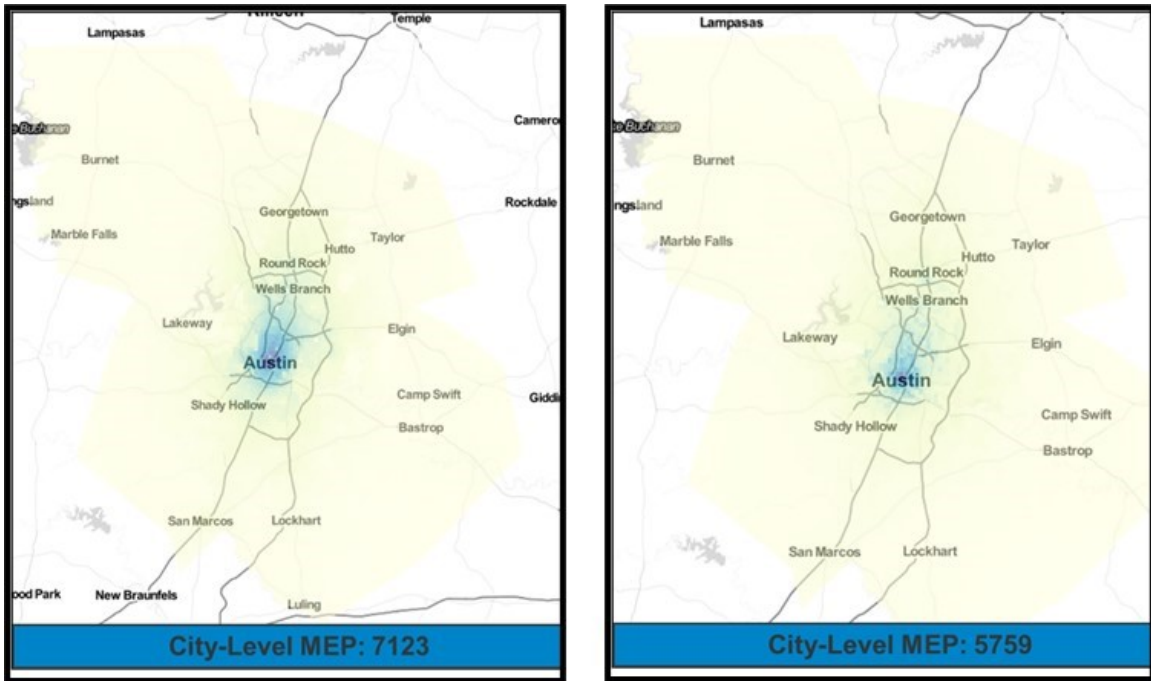
1. Hou, Y., V. Garikapati, D. Weigl, A. Henao, M. Moniot, and J. Sperling, (2020). “Factors Influencing Willingness to Pool in Ride-Hailing Trips.” *Transportation Research Record* 2674(5):419–429. <https://doi.org/10.1177%2F0361198120915886>.

New Cities BEAM and POLARIS Modeling – (SMART 1.5)

PI: Venu Garikapati

MEP team worked with Argonne and Lawrence Berkeley National Laboratory workflow teams to compute MEP scores for Austin (BEAM and POLARIS), Detroit (BEAM and POLARIS), and Atlanta (POLARIS) metro regions. In July 2020, an initial iteration of MEP calculations was carried out and both workflow teams were notified of a few anomalies in the MEP input data. A revised set of MEP computations (with new and refined input data) was carried out in September 2020 for all the new workflow cities. MEP scores for Austin for both the workflows is shown in Figure I.1.4.7, whereas Figure I.1.4.8 shows a comparison of pixel-level

(normalized) MEP scores between BEAM and POLARIS. From Figure I.1.4.8, a high degree of correlation can be observed between MEP scores from BEAM and POLARIS workflows for the Austin metro area.



BEAM – Austin

POLARIS – Austin

Figure I.1.4.7 MEP Scores for Austin

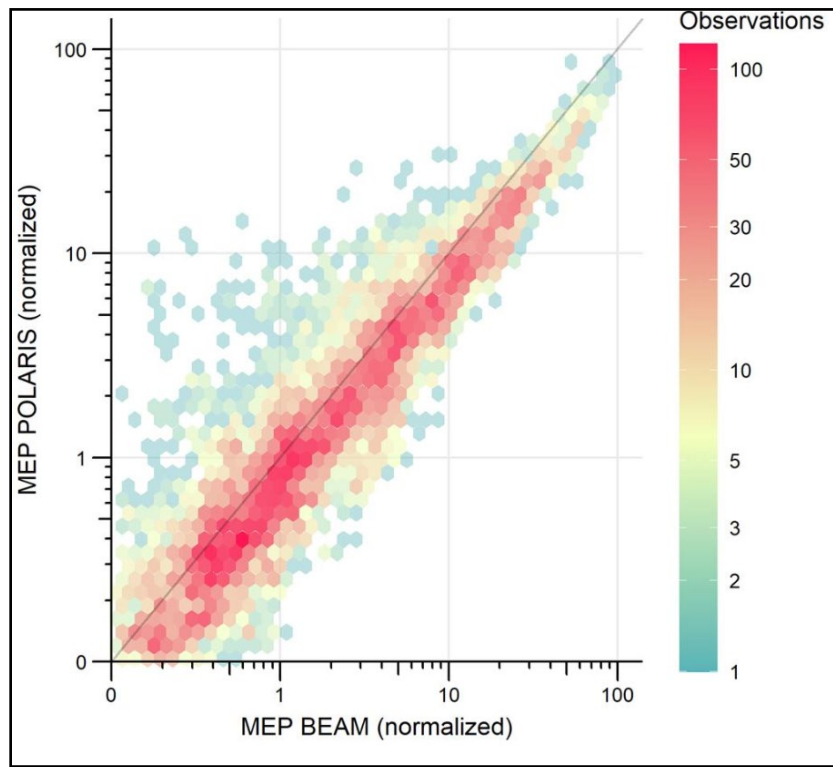


Figure I.1.4.8 Comparison of Pixel-Level BEAM and POLARIS MEP Scores for Austin

INRIX Trip Data and Travel Trends Portal

PIs: Stanley Young and Joseph Fish

Access to leading industry mobility data sets was enabled through a collaborative effort between DOE and USDOT, resulting in both aggregated data summaries delivered through a web portal to various agencies in the federal government and highly detailed, trip-based disaggregated data. Funded by EERE through this task, the web portal provided trip trend aggregate summaries of number of trips, trip length, and vehicle miles traveled for light-duty vehicles, medium-duty fleet, and heavy-duty freight. The portal provided 200 federal seat licenses with aggregate trips statistics at the state and metropolitan-area level (as well as other countries) and is the only know source of seasonally adjusted mobility data.

The disaggregated trip data delivered to NREL is a sample of approximately 10% of all vehicle trips in the United States—over 14 billion records in the first 6 months of 2020. Each data record contains the origin and destination in geodetic coordinates, as well as vehicle class (light, medium, and heavy duty). Trip data have been shared with EEMS researchers from other SMART Consortium labs through the Livewire platform. To date, the INRIX trip data represents over 99% of the data files accessed and downloaded through the Livewire system, supporting both COVID-19 and EEMS research.

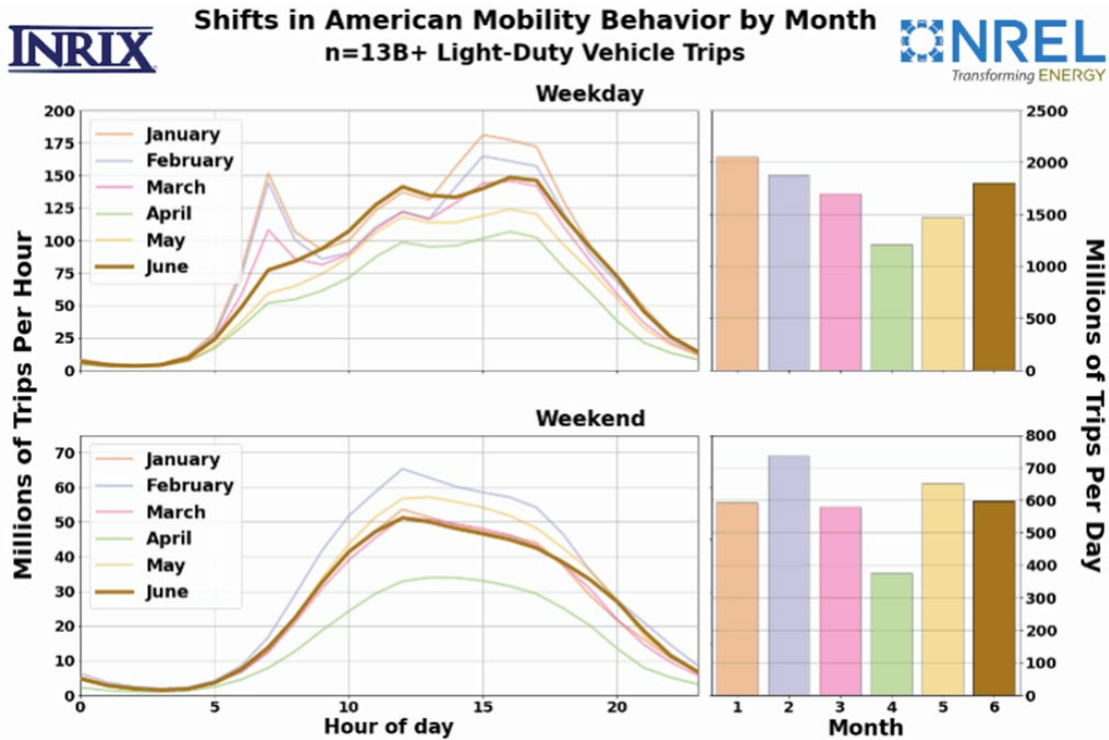


Figure I.1.4.9 Temporal Mobility Pattern Shifts Resulting from COVID-19

SMART CAVs Truck Platooning

PI: Michael Lammert

The FY 2020 effort focused on maximizing the value of previous SMART- and Federal Highway Administration-funded test track campaigns by doing detailed analysis of the airflow measurements made during those testing efforts. The transient wind-velocity measurements were used to assess the wake-shedding behavior experienced by trucks in various platoon formations, utilizing advanced analytics of data from fast-response (100–200-Hz) multi-hole pressure probes. This analysis is intended to examine aerodynamic flow features and their relationship to energy savings during close-following platoon formations. Spectral analysis

was used to identify the frequency content of the wind-velocity signals to identify the vortex-shedding behavior from a forward truck trailer, which dominates the flow field encountered by the downstream trucks. The changes in dominant wake-shedding frequencies correlate with the previously reported follower-truck fuel savings. The third truck in a platoon experiences a lower wake-shedding frequency than the second vehicle in either a two- or three-truck platoon. All followers experience a reduction in wake-shedding frequency at following distances less than 20 m—the same zone where lead trucks experience fuel savings/drag reductions and where followers experience a reduction in platooning benefits. The mechanisms by which the unsteady wake could be driving the reduced follower fuel savings/drag reductions were explored. Additionally, we investigated the heat rejection system sensitivity to intentional lateral offsets over a range of intervehicle spacings using four anemometers positioned across the grill of the following truck, as well as aligned and multiple offset positions to evaluate the sensitivity of the impact. An intentional lateral offset in truck platooning was considered as a controls approach to mitigate reduced cooling efficacy at close following scenarios where the highest platoon savings are achieved.

Key insights include:

- Wake shedding is a complex but predictable phenomenon that impacts the energy consumption of platooned vehicles and potentially can be controlled to further maximize achieved real-world savings of a promising technology for mitigating the energy consumption of freight transportation.
- The experimental results clearly show that offset driving is effective at bringing cooling airflow rate from 56% with an aligned platoon back up to 75%–80%, with minimal impact to fuel savings from platooning. These test outcomes indicate a plausible controls strategy to mitigate reduced cooling flow during hot-weather truck platooning while still enabling the highest-energy-saving, close-following scenarios.

Key Publications:

1. Zhang, C. and Lammert, M., "Impact to Cooling Airflow from Truck Platooning," SAE Technical Paper 2020-01-1298, 2020, <https://doi.org/10.4271/2020-01-1298>.
2. Holden, J, Ficenc, K, Lammert, M, and McAuliffe, B.R., "Analysis of the Unsteady Wakes of Heavy Trucks in Platoon Formation and their Potential Influence to Energy Savings." *SAE WCX 2021* submission 21SS-0332.
3. Zhang, C., M. Lammert and McAuliffe, B.R., "Impact of Lateral Alignment for Cooling Airflow during Heavy Truck Platooning." *SAE WCX 2021* submission 21HX-0060.

Employer-Provided Mobility

PI: Andrew Duvall

Work on employer-provided mobility continued on a trajectory to identify how employers were exploring alternative ways to access potential workers by providing mobility and/or commuting options as benefits of employment. Following the pandemic, this effort shifted to attempt to better understand the rapidly emerging work-from-home and telework phenomena observed throughout the nation.

This shift resulted in the production of a paper to provide an overview of new research into telework impacts and implications for potential energy and cost savings. The study explores the future of mobility, work, and value of alternative uses of commute time toward understanding of multifaceted dynamics, impacts, and opportunities to reshape sustainable mobility, quality of life, and workforce norms. Telework is not new, yet it has been greatly expanded in scope by the pandemic, estimated at 31% of the early March 2020 employed workforce by April 2020. This poses unique opportunities to explore how new telework behaviors for large segments of the workforce may transform energy and economic savings potential, with important mobility and other system-level implications. The analyses in this paper build upon recent surveys that estimate 63% of U.S.

jobs require significant onsite presence, with 37% able to be performed remotely. Savings estimated in Colorado equal 28% of household VMT, or 52.7 million round-trip VMT and 2.1 million gallons of gasoline. Nationally, estimated savings are 7.7 quadrillion Btu of energy annually. Mobility and quality of life co-benefits in sustained high levels of remote work may include new access to job choices, location-based affordability in living expenses, and beneficial value, use, and productivity of time that had previously been spent commuting. New burdens (childcare) and economic impacts (unemployment) cannot be overlooked, with more analysis needed. Questions are identified on infrastructure modernization and workforce mobility transitions, with a goal of informing future research, planning, and decision-making.

The paper was accepted for presentation by the Transportation Research Board.

Key Publications:

1. Duvall, A., J. Sperling, A. Wilson, S. Young, and D. Zimny-Schmidt (2021). "Assessing U.S. Current and Future Impacts of Telework During the COVID-19 Pandemic." Accepted for presentation at the *Transportation Research Board Annual Meeting*.

EV TNC Data Collection

PI: Matthew Moniot

The Advanced Fueling Infrastructure team continued data collection and analysis of personally owned and personally driven electric vehicles in TNC contexts. In total, over 50,000 miles of driving were collected across 11 unique TNC drivers recruited by NREL using physical Geotab telematics devices.

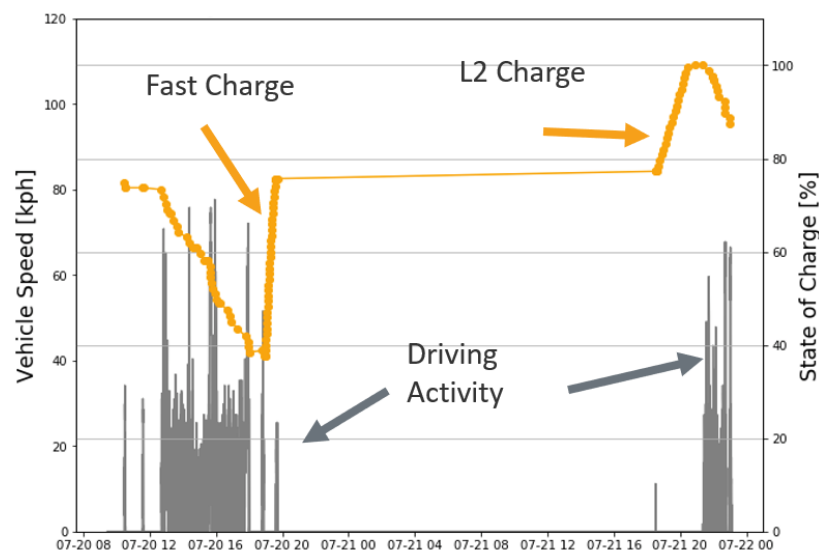


Figure I.1.4.10 Sample Telematics Streams Providing Insight into Driving and Charging Behavior

FY 2020 efforts concluded the Geotab analysis and also facilitated NREL researchers to engage with the WestSmartEV FOA project in Salt Lake City. This FOA project included a data collection component specifically for owner-operated EVs in TNC vocations. Comparisons between trends in the Geotab data and the WestSmartEV data (collected using an app in lieu of a telematics device) show strong agreement. The following bullets summarize findings from the FY 2020 EV TNC analysis:

- Locations where charging would be timely and convenient (inferred from state of charge dropping below 30%) are often found to be charging deserts.
- Drivers with access to home charging rarely fast charge. Out of the over 2,356 charging events observed in the telematics data set, only 5.6% of events occurred at fast-charging stations. This

finding is the opposite of research from the University of California, Davis, which found that drivers of fleet rental vehicles (such as Maven Gig) almost exclusively fast charge. A stark dichotomy is emerging between drivers with access to home charging and those that almost exclusively rely on the public infrastructure.

- App-based telematics are a plausible approach for collecting vehicle data in support of EV TNC research. Although physical on-board diagnostic devices produce higher-frequency data, most analysis questions can be answered with the app-based telematics vendor used by PacifiCorp (FlexCharging). App-based collection is preferable for drivers where physical installation of a device is challenging or for vehicles with no on-board diagnostic port (such as the Tesla Model 3s).

Follow-on work analyzing additional EV TNC data is planned through an NREL role in support of the awarded WestSmartEV@Scale FOA project being led by PacifiCorp (DE-EE-9224)

Curb Topology

Pls: Alejandro Henao

The Urban Science Pillar refers to the competition for space at curbsides near concentrated activity as “topology,” defined as exploration of interactions and demands for public right-of-way space at the curb. Vehicles and activities that demand use of these public spaces have expanded beyond traditional on-street car parking, public transit stops, and traditional freight delivery to include on-demand mobility activities (ride-hailing, car share, bike share, e-scooter, and other dockless micromobility), and increased “microfreight” arising from the rapid expansion of e-commerce (parcel deliveries and food deliveries).

FY 2020 efforts focused on publishing the research effort in two peer-reviewed journals, disseminating the results during several conferences and initial setup of curb modeling using the SUMO open-source traffic microsimulation software. Results, lessons learned, experiences, and partnership created during the curb topology research have been leveraged to continue research on curb management under SMART 2.0.

Results:

Curbside activity has not traditionally been represented in transportation network modeling in high fidelity. The expert interviews show that cities are having to adapt to growing curbside demand because prevailing practices are becoming increasingly untenable (from parking to curb management). The cities’ variability on current status (e.g., policies, pricing, data management) and different priorities (e.g., safety, mode shift, revenue) require an optimization model with metrics incorporated to optimally allocate and manage curbside space. This research has developed mathematical models that account for curbside activity (demand) and developed initial setup using SUMO.

Key Publications

1. Butrina, P., S. Le Vine, A. Henao, J. Sperling, and S. Young (2020). “Municipal Adaptation to Changing Curbside Demands: Exploratory Findings from Semi-Structured Interviews with Ten U.S. Cities.” *Transport Policy* 92:1–7. <https://doi.org/10.1016/j.tranpol.2020.03.005>.
2. Kong, Y., S. Le Vine, A. Henao, and S. Young (2020). “A Framework for Optimal Allocation of Curbside Space.” *Journal of Transport and Land Use* (submitted).

I.1.5 GPRA New Cities Modeling - POLARIS

Joshua Auld, Principal Investigator

Argonne National Laboratory
9700 South Cass Avenue
Lemont, IL 60439
Email: jauld@anl.gov

David Anderson, DOE Program Manager

U.S. Department of Energy
Email: david.anderson@ee.doe.gov

Start Date: January 1, 2020

End Date: September 30, 2020

Project Funding: \$1,530,000

DOE share: \$1,530,000

Non-DOE share: \$0

Project Introduction

The first phase of the SMART Mobility program led to the development of a modeling workflow centered around two travel demand simulators—POLARIS and BEAM. The workflow linked models of long-run processes (land use changes, vehicle markets, EV charger deployment) to day-to-day travel decisions in the travel demand simulators, to micro-scale decisions regarding vehicle movements. Ultimately the modeling workflows generated vehicle movements and energy consumption, which were used in the estimation of a Mobility Energy Productivity (MEP) metric to characterize the effect of a scenario in terms of energy and mobility in a single metric. The scenario analyses in SMART 1.0 were necessarily limited to the context in which the models were initially deployed, namely Chicago (POLARIS) and San Francisco (BEAM). However, it is known that travel demand and mobility vary greatly depending on local context, such as geographic conditions, infrastructure availability, socio-demographics, cultural factors, and so on. Therefore, it was of interest to extend the deployment of the SMART mobility workflow to additional cities to both determine the transferability of the modeling approach and to understand how different scenarios impact regions differently and therefore help to generalize the key findings of the consortium. In this project, therefore, the research team sought to deploy the POLARIS workflow to three additional cities and evaluate the baseline MEP and other metrics for each city. The project involved local stakeholders for each region, including the local Metropolitan Planning Organizations (MPO) who are tasked with developing travel demand models in each region, as well as local university or industry partners to help develop the models. Each instance of the POLARIS workflow was then calibrated and validated for the local region. Finally, the validated baseline model was used to estimate regional mobility and energy metrics as well as the MEP metric for each region.

Objectives

The goal of this project was the implementation of baseline models for the Atlanta, Austin, and Detroit metropolitan regions using the POLARIS SMART Mobility Workflow. The research team calibrated the models and validated them against local data and conditions to demonstrate the feasibility of deploying the SMART Mobility workflow in additional regions. Additionally, team sought to compare mobility, energy, and MEP results for two common cities between both SMART workflows. Ultimately the comparisons across tools and against baseline conditions demonstrates the usefulness of the workflow and supports future forecasting efforts using the workflow in each region—allowing the SMART Mobility consortium to generalize findings from future scenarios to multiple regions across the country.

Approach

In this project, the approach to developing each model began with engaging the local MPO and other partners to obtain the data necessary to construct and run a POLARIS model of each region. This includes data on the transportation system (road and transit network, traffic controls, transit schedules), land use and traffic analysis zoning systems, population information from Census and MPO, employment data, vehicle registrations, traffic

counts, EV charging location, and any other information necessary to implement the SMART Mobility workflow. Some of the data obtained for the project was publicly available (such as census data, transit schedules) or readily available from MPO data repositories. In many instances, however, data was obtained directly from MPO contacts after implementing Data Use Agreements. Data from the Southeastern Michigan Council of Governments (SEMCOG) and CAMPO/TxDOT was obtained in this manner. Where data was not available locally, it was licensed from commercial data providers such as CoStar, for a commercial real estate database, or from IHS/Polk through NREL for vehicle registration data. A full description of the data obtained and used in the project is shown in Table I.1.5.1.

Table I.1.5.1 Data Sources used in Model Construction

Dataset	Availability	Source	Purpose
Network files	NDA	CAMPO, SEMCOG	Roadway characteristics
	On request	ARC	
GTFS files	Public	Web (all cities)	Transit infrastructure
	NDA	SEMCOG - SMART Bus	
Census	Public	Census.gov (all cities)	Construct population
HH Travel Survey	On request	ARC	Update travel behavior models
	NDA	CAMPO, SEMCOG	
Zoning file	On request	ARC	Zone geography, employment, population
	NDA	CAMPO, SEMCOG	
Land use	Licensed	CoStar (all cities)	Land use for activity locations
Vehicle registration	Gov. license	NREL (all cities)	Vehicle fleet definition
Freight/Visitor trip tables	On request	ARC	Origin/destination flows of trips
	NDA	CAMPO, SEMCOG	
Traffic counts	NDA	CAMPO	Traffic simulation validation
	Public	SEMCOG	
Vehicle probe data	NDA	CAMPO/TxDOT	Traffic and routing validation

The datasets described above were processed for each city using multiple tools to create a functional POLARIS baseline model of the physical system. The tools used include:

- POLARIS network editor, which imports network files describing the links in the road network, converts them to POLARIS format, corrects network topology errors and imputes missing data, synthesizes intersection controls, and gives a graphical interface to make manual corrections to the network. This process results in a network compatible with the POLAS simulator for each city.
- GTFS importer, which modified the POLARIS network created by the network editor to include transit links and schedules as described in GTFS input files, as well as a walk network that connects the transit links to the road network.
- QGIS, an open-source GIS tool used to connect land use information, census population data, and TAZ files from MPOs for importation through the network editor, and to visualize other imports not currently viewable through the network editor.
- Biogeme and SAS, statistical modeling tools used to estimate new behavioral models using local household travel survey and other data.

The above tools were combined with the data sources described in Table I.1.5.1 to create a baseline physical model for each city. The models were extensively tested and corrected to identify missing data, topological errors, key missing links that would form network bottlenecks, and incorrectly specified intersection controls. After the model construction process was completed, a POLARIS-compatible physical model was available for each model region. Example visualizations of the models can be seen in Figure I.1.5.1.

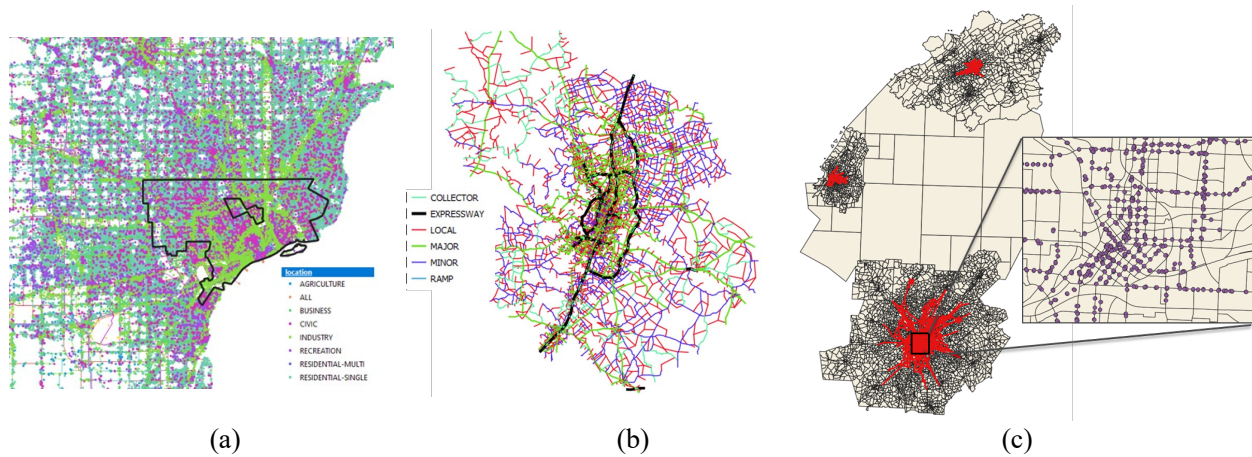


Figure I.1.5.1 Visualizations of (A) Activity Locations in Detroit, (B) Road Network in Austin, and (C) Transit in Atlanta

Using household travel survey data for each region, the core ABM behavioral model files were calibrated to local conditions through an iterative process of adjusting constant values in the utility equations for each choice model until distributions of choice outcomes from the POLARIS simulation matched local observations from the travel surveys. This process allowed the research team to adapt the default Chicago parameter settings to be representative of travelers in each model region. Adapted models include activity generation, timing, mode choice, and destination choice.

In each model region, the team also collected and analyzed data related to freight vehicle and external traveler movements. External trip volumes and MD/HD freight external trips were generated from Origin-Destination trip tables obtained from each MPO. The freight and passenger trip tables were distributed to specific activity locations within each zone based on land use types and given departure times drawn from diurnal curves estimated from survey data, Federal Highway Administration modeling guidance, traffic counts, and other sources as appropriate. Finally, local delivery trips using the delivery touring model from ORNL that was applied to e-commerce deliveries estimated from the POLARIS workflow. The delivery trips and the disaggregated freight and external passenger trips were then added back into POLARIS for each run of the model as fixed trip tables to represent the background traffic.

The model results for each region, after final calibration and validation runs, to NREL to run through the MEP estimation process to demonstrate Mobility Energy Productivity results.

Results – Atlanta

The Atlanta model includes 20 counties of the Atlanta metropolitan area along with Chattanooga and Knoxville regions in Tennessee. The modeled area comprises 7,820 traffic analysis zones (TAZ); 5,873 of these zones belong to the Atlanta metropolitan area. The surface network consists of 72,832 road links controlled via 6,052 signalized intersections and 38,671 stop signs. The 6.6M persons simulated in the model live in 2.7M households—with 5.3M of this population located in Atlanta metropolitan area. The population synthesis process ensured that the synthesized household characteristics (such as income, house type, number of vehicles, household size) and person characteristics (such as age, race/ethnicity, education, employment) match closely with the distribution obtained from the American Census Survey (ACS). The population synthesis process resulted in a weighted-average absolute percentage error of 2.6% for household level

marginals. In terms of the characteristics of the light duty vehicles (LDV), 48% of the household-owned vehicles are cars with ~37% SUV and 15% pickups. In the region, 98.5% of the LDVs have conventional powertrain and 1.2% are hybrid electrics.

The individual behaviors were calibrated against household survey data obtained from ARC to match the activity generation rate, activity start time, duration, distance traveled, and modes used for travel. POLARIS simulation of the region produced an average rate of 3.55 activities per day per person, including the return home activities, while the rate observed from the ARC survey was 3.47. Overall, the activity generation rate matched well against the survey for different activity types with the exception of a slightly lower rate of school and pick-up/drop-off activity (Figure II.1.5.2 [a]). Also, the rate of return home activity is slightly higher in the simulation compared to what was observed in the survey, indicating lower representation of complex tours in the simulation compared with the survey. As shown in Figure II.1.5.2 (b), the departure time distribution matched quite closely across the simulation and the survey for the PM peak period. On average, the distance traveled by different activity categories compared well.

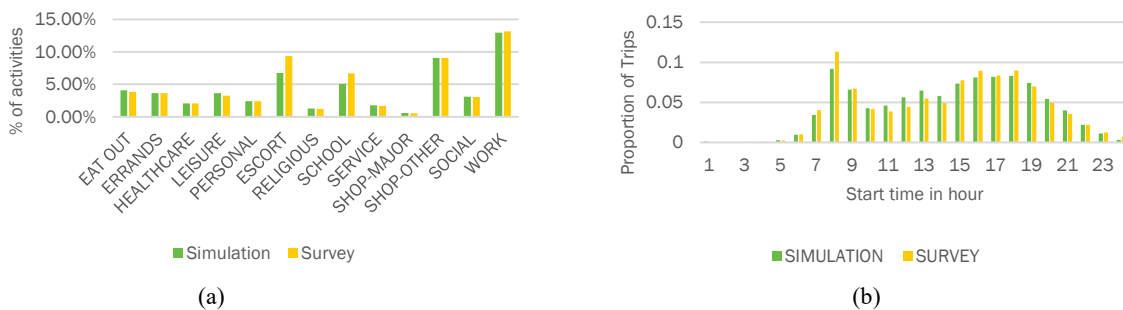


Figure I.1.5.2 Behavior Model Calibration for (A) Activity Generation and (B) Departure Times

A comparison of the distance distribution for work activity shows that the simulation closely follows the curve obtained from the survey (Figure II.1.5.3 [a]). Finally, the bulk of the trips are taken by auto, followed by walk and transit, with the simulation replicating the survey mode share closely with a highest percentage point difference of 2% for high occupancy vehicle mode (Figure II.1.5.3 [b]).

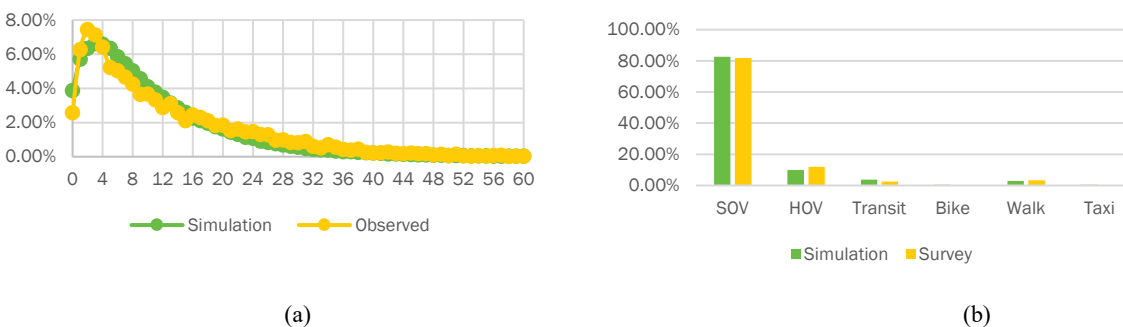


Figure I.1.5.3 Behavior Model Calibration for (A) Work Trip Length and (B) Mode Share

While comparing passenger demand, the POLARIS simulation of the Atlanta model included 2.2M freight trips and 1.1M external SOV trips. The model also accounts for the household e-commerce demand that was converted to delivery tours. Figure I.1.5.4 (a) presents the concentration of households participating in e-commerce demand in the region. In general, the percentage of households participating in e-commerce is high in the outskirts, as compared with the city center, which might be due to the lower penetration of in-store options in the suburbs compared to those in the city center. Finally, the number of vehicles in the network was plotted against those observed across the values in the survey. As can be seen from Figure I.1.5.4 (b), the simulation curve follows the curve obtained from the survey data quite closely, with a low morning peak. It

can be noted that the vehicle count does not include freight vehicles or external trips since they are not accounted for in the household travel survey.

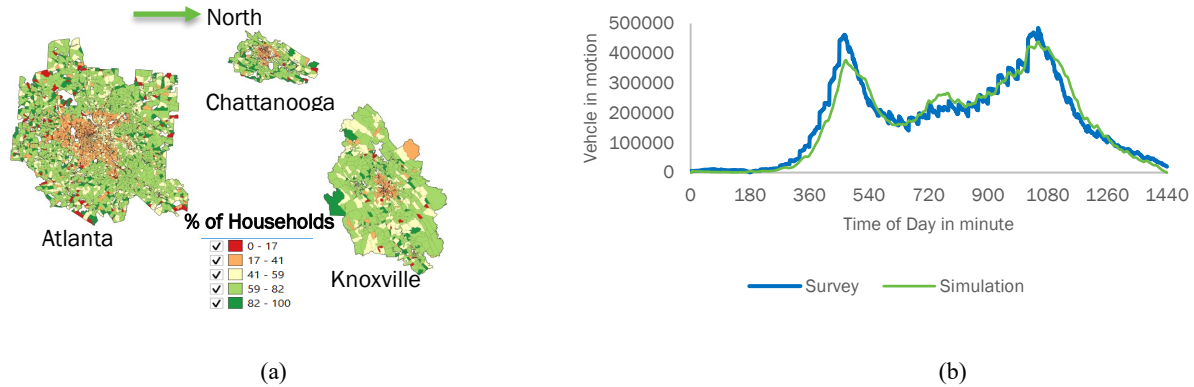


Figure I.1.5.4 (a) E-Commerce Demand and (b) Vehicle In-Network

Results – Austin

The Austin, Texas, area comprises six counties in the Capital Area Metropolitan Area Metropolitan Organization (CAMPO). The network contains 16,000 links and 10,435 nodes, 2,600 of which are signalized. In addition, the network has 8,600 stop signs. The network is divided into 2,161 TAZs, comprising an area of 5,380 square miles. With respect to demographic characteristics, the CAMPO area population is 1.88M across 800K households. The population synthesis was performed based on the CENSUS data controlling for different household characteristics (income, number of vehicles, household size) as well as person characteristics (age, ethnicity, education level). Comparing the marginal distribution of household characteristics against the census data shows that distributions have a weighted-average absolute percentage error of 1.3%. For the baseline scenario, vehicles are created based on the registration data: 44% are cars, 20% are pickups, and 36% SUVs. With respect to powertrain types, most of the vehicles in Austin area are conventional (97.4%) while hybrid electric vehicles comprise most of the remaining vehicles (2.2%).

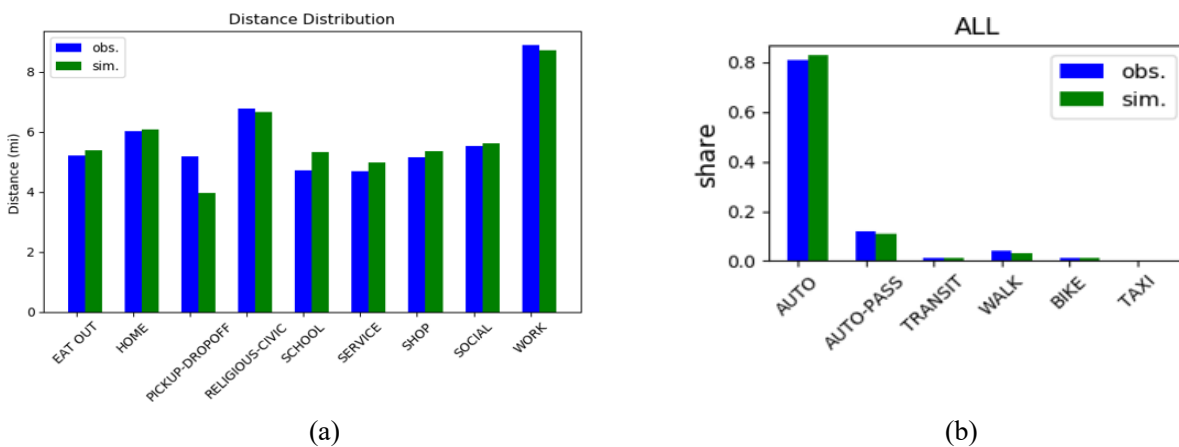


Figure I.1.5.5 The Graph Depicts (a) Average Distance Per Activity Type and (b) Overall Mode Shares

For individual behavior data, activity generation, start times, mode choices and destination choices were calibrated against the Texas Household Survey. The POLARIS model was able to replicate key aspects observed on the survey, such as the number of activities performed, the observed mode shares, and average traveled distance per activity type, except for a somewhat higher rate of return-home activities: similar to what

was found in the Atlanta results. Figure I.1.5.5 confirms some of these results, with (a) showing the average distance per activity type and (b) depicting overall mode shares.

Figure I.1.5.6 (a) shows the number of vehicles in motion over the 24-hour simulation period, compared to the same curve obtained from the Texas Household Survey. In general, the two curves follow closely with each other, except for minor differences in peak congestion in POLARIS. In Figure I.1.5.6 (b), the network speeds from POLARIS are validated against INRIX data. The graph compares average speeds over time across the links with speed observation from INRIX in 2017. The speeds overall match across the 24-hour period with very similar average speeds at peak time. POLARIS slightly underestimates the average speed between the peaks.

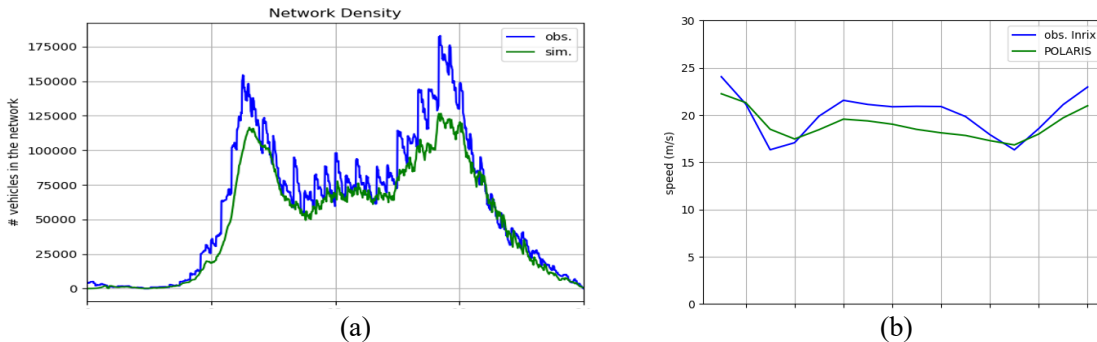


Figure I.1.5.6 Austin Network Results Showing (a) Vehicles-In-Motion Over Time and (b) the Network Speeds Over Time

Results – Detroit

The Detroit model region includes seven counties in the southeastern Michigan region surrounding Detroit. The area comprises 2899 traffic analysis zones with a total population of 4.7 million, with home and work locations of the population distributed over 145,510 activity locations derived from land use data and building files. The road network in the Detroit model includes 28,438 links, 2,781 signalized intersections, and 22,275 stop signs. The road network is connected to a transit network that contains 12,522 links and 21,971 stops across five agencies (3 bus, 2 light rail) by 47,412 walking links. The results of the population synthesis procedure show that simulated marginal distributions have a weighted-average absolute percentage error of 1.3% for household marginals, indicating close replication of the baseline population. In the Detroit region 3.6% of personal vehicles are hybrids and 0.3% are xEV, while the rest are conventional. As in Atlanta and Austin, the individual behavioral models were calibrated against survey data from the local MPO and SEMCOG. POLARIS generated an average of 3.49 trips per person per day, which is close to the observed value of 3.77. The overall %RMSE in activity generation counts for the whole population was 5.0%, indicating close correspondence between generated and observed activity patterns. Additional behavioral model validations are shown in Figure I.1.5.7.

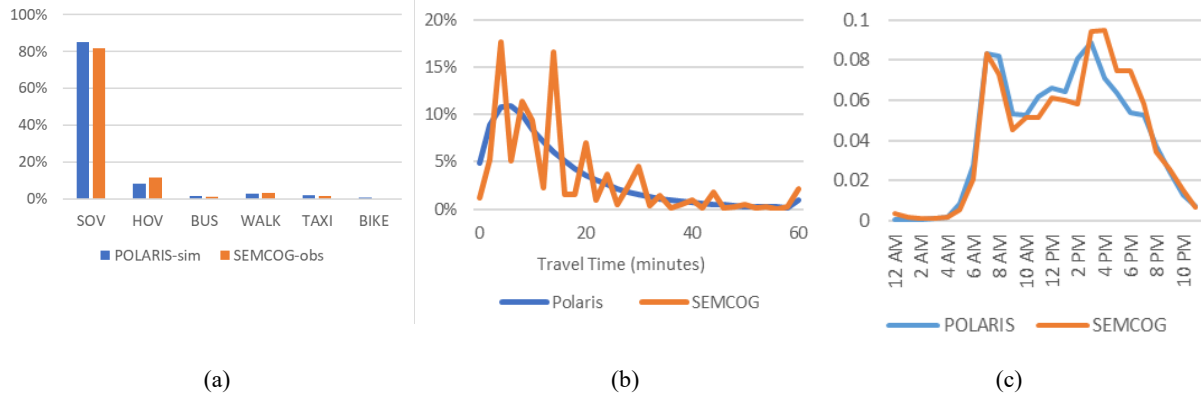


Figure I.1.5.7 Behavior Model Calibration for (a) Mode Shares, (b) Discretionary Trip Lengths, and (c) Departure Times

The models were also validated against data sources that were not used in the model calibration procedure. First, in Figure I.1.5.8 (a), the count of passenger vehicles in motion throughout the day is compared against counts derived from the SEMCOG Household Travel Survey. This figure is significant in demonstrating model performance as it is highly sensitive to misspecifications in any of the model components as well as in the dynamic traffic assignment in POLARIS. Overall, the simulated vehicles in network curve matches closely to the observed. Validation was also performed against daily traffic counts obtained from SEMCOG and Michigan DOT. This validation demonstrates the proper performance of not only the ABM in generating the correct number of trips, but also the routing and traffic flow model in assigning trips to correct links. This result is shown in Figure I.1.5.8 (b), and displays an R2 value of 0.7 between simulated and observed counts.

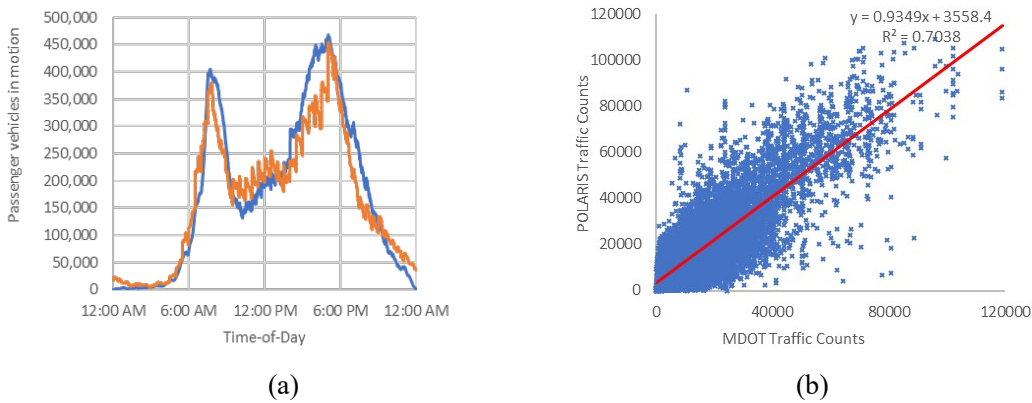


Figure I.1.5.8 Model Validation Results: (a) Passenger Vehicles in Network and (b) Link Traffic Counts Comparison

Results – Comparison

Figure I.1.5.9 compares the distribution of MEP results for each city, while Table I.1.5.2 shows key performance indicators and mobility metrics. Overall, each city has quite similar MEP values ranging from 5,758–6,082, although the mobility and energy characteristics differ somewhat in each region. The Atlanta model has a higher percentage of freight travel, given its status as a freight hub and proximity to the Port of Savannah, while Detroit and Austin have lower shares of freight trips and miles. Austin, due to its smaller size and more compact geography, has a lower average travel distance per person of 29.4 miles while Detroit and Atlanta are higher at 36.7 and 37.5, respectively, likely owing to the more decentralized nature of each metropolitan area. Finally, all cities have a high dependence on auto travel, with non-auto trip shares ranging from 8.1% in Austin to 11.0% in Atlanta—a factor likely contributing to the lower MEP scores compared to more transit-oriented regions that have been studied. Finally, travel efficiency (in productive miles per KWH

of energy) was lowest in Atlanta due a combination of less efficient vehicles in the private fleet mix, higher share of freight trips, and a lower travel speed than observed in Detroit.

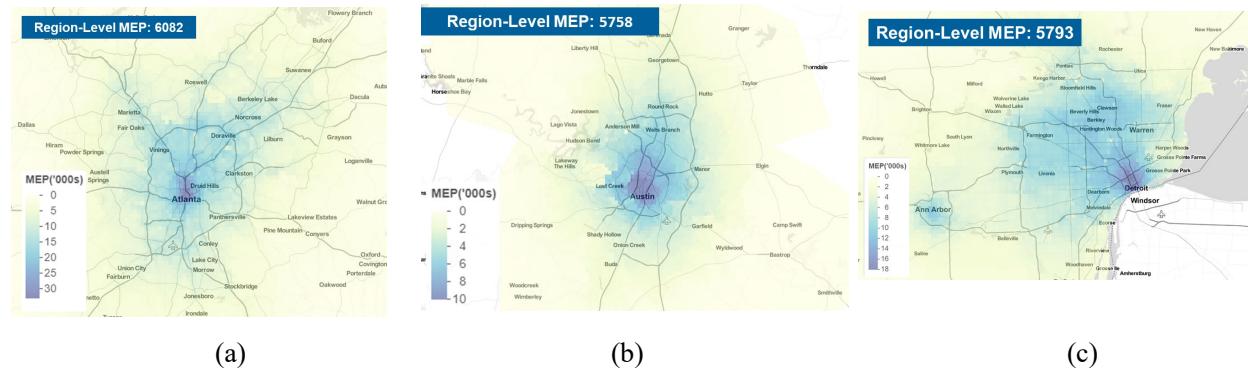


Figure I.1.5.9 MEP Results for: (a) Atlanta, (b) Austin, and (c) Detroit

Table I.1.5.2 Summary Results Comparison for All Cities

Metric	Unit	Greater Atlanta	Austin	Detroit
Total trips (freight trips)	million trips	26.2 (2.2)	7.6 (0.4)	17.6 (0.9)
Total trips (auto-based)	million trips	16.0	5.1	12.6
Productive-miles of travel	million miles	247.3	55.3	165.6
Productive-hours of travel	million hours	10.1	2.26	5.6
Vehicle miles traveled	million miles	199.8	46.4	138.1
Vehicle hours traveled	million hours	7.1	1.85	4.5
% non auto travel	%	11	8.1	9.20%
Avg. vehicle travel speed	MPH	28.1	25.1	30.6
Total energy	GWh	317.3	68.7	169.7
travel efficiency	prod.mi/KWh	0.78	0.81	0.97
Per capita Person-miles of travel	miles	37.5	29.4	36.7
Per capita Person-hours of travel	hours	1.5	1.2	1.2
Per capita Vehicle miles traveled	miles	30.3	24.6	30.2
Per capita Vehicle hours traveled	hours	1.1	0.99	1.0

Conclusions

An implementation of the POLARIS SMART Mobility Modeling Workflow was created for three new metro areas: Greater Atlanta, Austin, and Detroit. Each model was extensively calibrated to match local conditions as observed in household travel surveys and other field data, and then validated against available ground count, speed, and other data, as available, for each region. Each model exhibits acceptable fit in terms of speed and traffic counts and can replicate baseline conditions when compared with modeling reports from each MPO and other baseline data. The MEP metric for each city was successfully evaluated, demonstrating acceptable performance of the modeling workflow.

Acknowledgments

The researchers would like to acknowledge the support given for this project in both data access and project oversight by local partners, including Guy Rousseau at the Atlanta Regional Council; Gregory Lancaster at the Capital Area MPO; Christeen Pusch at Texas DOT; Ed Hard at the Texas Transportation Institute; and Archak Mittal, Richard Twumasi-Boakye, and James Fishelson at Ford Motor Company.

I.1.6 Transportation System Modeling of Southeastern Michigan and Austin, TX Using BEAM

Zachary Needell, Principal Investigator

Lawrence Berkeley National Laboratory
1 Cyclotron Road
Berkeley, CA 94720
Email: zaneedell@lbl.gov

David Anderson, DOE Program Manager

U.S. Department of Energy
Email: david.anderson@ee.doe.gov

Start Date: October 1, 2019
Project Funding: \$550,000

End Date: September 30, 2020
DOE share: \$550,000

Non-DOE share: \$0

Project Introduction

During the 2020 fiscal year, the BEAM (Behavior, Energy, Autonomy, Mobility) model was extended to two new cities while developing new data pipelines and modeling capabilities that allow both faster deployment to new cities and richer and more detailed representation of individual behavior in all cities. BEAM was developed at Lawrence Berkeley National Laboratory in large part through the SMART Mobility activities of the DOE Vehicle Technologies Office, EEMS Program. Between the conclusion of the first three-year SMART Mobility research phase (SMART 1.0) and the beginning of a second three-year research phase (SMART 2.0), BEAM work focused on deployment to new cities, in part to allow for easier comparison between BEAM and POLARIS modeling results, and on integration of new capabilities that will be further expanded upon in SMART 2.0.

Over the course of FY20, BEAM was successfully deployed in Austin, TX, and Detroit, MI. This was done using only publicly available data, producing outcomes largely compatible with other models developed in close coordination with local planning organizations that make use of proprietary data and model outputs. This deployment process was largely automated, developing a capability that will make further model deployment faster and easier (indeed, this process was used to deploy BEAM to the New York City metropolitan area in other work). In addition, various improvements were made to the core BEAM codebase, making the model faster and more accurate.

Objectives

The work proposed for FY20 had several primary objectives, all focused towards developing a version of BEAM with more capabilities that is more readily deployable and produces more carefully validated outputs. These objectives include:

Develop a deployment pipeline to new cities

The initial deployment of BEAM to the San Francisco Bay Area relied on some data products that were initially developed by local planning agencies and gradually updated over the past several years. One long term goal for BEAM is for the model to be deployed to a large and representative set of U.S. metropolitan areas, allowing for national-scale analysis of emerging transportation trends. This scope will be made much easier if an initial model implementation could be developed in any U.S. city by relying only on nationally available open-source datasets. While an automated process to produce a fully calibrated model is infeasible, the outcome of such a deployment pipeline is still a useful starting point for more detailed manual calibration, which can be continued until the model outputs reach a sufficient level of precision when compared to reference values.

Integrate non-work activities

One primary driver of differences in results between BEAM and POLARIS in SMART 1.0 was the fact that BEAM only simulated commute trips. Adding these non-work (discretionary) activities to BEAM was a primary goal of FY20, which would allow for a more realistic representation of travel patterns and energy use, along with more realistic sensitivity of travel behavior to value of time and cost assumptions.

To allow for more flexibility based on individual project's objectives, two distinct methods for integrating discretionary activities into BEAM were used—one fully internal to BEAM that can be initially calibrated using publicly available data such as the National Household Travel Survey, and one relying on ActivitySim—a more detailed open-source day activity planning model that is already in use by many metropolitan planning organizations across the United States.

Reduce model run time

Relatively long model run time is a resource constraint that slows the development and deployment speed of BEAM and reduces the number of model runs that can be accomplished on a fixed budget. Exploratory work was performed in FY20 aimed at reducing runtime, primarily through reducing the number of iterations required to reach user equilibrium. Additional exploratory work was done on evaluating faster road network routing and assignment algorithms, primarily directed towards defining the feasible scope of achievements that could be achieved to this end in SMART 2.0.

Produce calibrated model in Austin and Detroit

In SMART 1.0, the fact that BEAM and POLARIS were modeling different cities (San Francisco and Chicago, respectively) made it difficult to understand to what extent differences in results were driven by different modeling assumptions, different model capabilities, or fundamental differences between the cities being studied. One goal of the FY20 work was to deploy these two models to several common cities (chosen to be Austin and Detroit) to allow for better comparisons between the two models. On the BEAM side, this process involved using the newly-developed fast deployment pipeline in these two cities and then performing initial model calibration using publicly available datasets. Once this initially calibrated model was complete, initial comparisons were performed to POLARIS outputs.

Approach***Develop a deployment pipeline to new cities***

The general BEAM deployment pipeline is intended to allow for full end-to-end development of a BEAM implementation in a new city, with both work and non-work activities. To do this, a multi-step process was used, where a synthetic population of agents was produced, an initial BEAM implementation was used to seed initial travel times and costs to a more detailed BEAM implementation, and then the more detailed implementation was fully calibrated in order to produce a final version that could be used to evaluate baseline or long-term future scenarios.

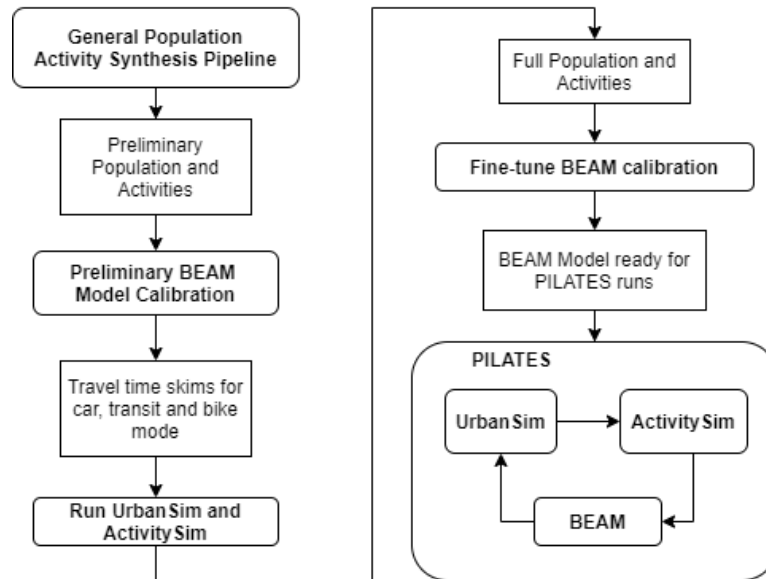


Figure I.1.6.1 BEAM Deployment Pipeline, Involving Population Synthesis, Calibration of a Preliminary Model Including Discretionary Activities Generated in BEAM, and Then Calibration of a Final Implementation Using Discretionary Activities Generated in Activitysim

As described in Figure I.1.6.1, this process consists of several stages. To start, a synthetic population of agents is generated for the study area making use of the open source SynthPop tool [1], which uses publicly available data published by the American Community Survey to generate individual agents and households, along with information on demographics and vehicle ownership, at the census block group level. Given this population, individual work locations are generated for each employed agent using home/work commute data provided by the Census Transportation Planning Package, another publicly available national dataset.

With this initial population generated, a first version of BEAM is run to generate equilibrium traffic conditions. This initial version of BEAM makes use of an internal discretionary activity choice model that was also developed in FY20 and is described in more detail below. This initial pre-calibration step produces detailed travel time matrices, or skims, that can be fed to ActivitySim [2], a more detailed activity planning model that requires accurate skims as inputs and simulates individual activity choice in more detail than BEAM’s internal module does. The fact that ActivitySim requires realistic skims in order to produce realistic activity plans is what requires the first version of BEAM to be run.

Once both ActivitySim and BEAM are fully calibrated to a base year, reproducing travel times, travel distances, and mode splits observed in external reference datasets, the new city’s BEAM implementation is ready for detailed scenario analysis, including long-term land use evolution by linking with UrbanSim. If detailed land use evolution and intra-household activity planning are not required, as was the case for a rapid COVID response modeling project done by the BEAM team in New York City, one benefit of this framework is that it can be cut off before ActivitySim integration, instead relying solely on BEAM’s internal activity planning module to model behavioral responses to changes in transportation system performance.

Integrate non-work activities

As described above, during FY20 two separate methods for generating discretionary activities were integrated into BEAM—one that is entirely internal to BEAM and one making use of the open source ActivitySim software package.

1. Internal module:

The internal discretionary activity model developed in BEAM during FY20 treated non-mandatory trip-making as a nested set of decisions of whether to travel and where to travel. In this initial implementation, all discretionary travel was represented as a single-destination subtour originating from one of a traveler's mandatory activity locations. Through a nested logit framework and day-to-day learning, agents end up taking more trips and longer trips when generalized travel costs are low and are more likely to choose destinations for these trips in areas that are more accessible via their available modes of transportation.

As the model is implemented, for every mandatory activity, the agent has a choice of whether or not to make a non-mandatory subtour (trips to and from a non-mandatory activity). The likelihood of making one of these subtours depends on the expected maximum utility of travel to and from a sample of relevant locations over all available modes. If the agent does choose to make this subtour, the actual destination is chosen in a similar manner—based on the expected maximum utility of travel to a destination over all available modes. Iteration to iteration, agents have the ability to try different timing of activities and different activity types, eventually learning full-day trip-making patterns that maximize their all-day utility. This simplified framework is intended to allow BEAM to produce realistic travel and congestion patterns throughout the day, even if it does not capture some details relating to activity scheduling and intra-household activity planning. The realistic skims produced by BEAM using this internal activity module can then be adopted by ActivitySim to simulate these factors in more detail.

2. ActivitySim:

The internal discretionary activity model developed in BEAM during FY20 focused on generating subtours as the primary lever for making travel demand more responsive to travel costs and transportation supply, not including other levers such as intermediate stops, joint activities, and pickup/dropoff trips. To capture these more nuanced behaviors, the BEAM team chose to rely on a widely-used and validated open-source external model, ActivitySim, rather than implementing similar behaviors internally to BEAM.

To generate individual activities, ActivitySim requires a population of agents and households, the locations of possible jobs and opportunities for activities, and a set of skims defining travel times and generalized costs between pairs of locations. The synthetic population used in ActivitySim is equivalent to the one generated by SynthPop for BEAM, and the locations of jobs and opportunities are taken from a database maintained by collaborators at the UrbanSim team, primarily populated with data collected from the American Community Survey and the Longitudinal Employer-Household Dynamics survey. The skims used by ActivitySim are generated by BEAM, where the characteristics of every trip simulated in BEAM are collected and aggregated by origin zone, destination zone, time of day, and mode. This collection allows ActivitySim to estimate the generalized cost associated with any possible travel option achievable by its simulated travelers. Once ActivitySim is fully calibrated given these inputs, the travel demand it simulates is passed back to BEAM in the form of plans. These plans define, for every agent, the location, start time, and end time of every activity the agent participates in over the course of the day. In SMART 2.0, the coupling between ActivitySim and BEAM will be further strengthened, allowing more iterative handoffs between the two models as well as implementation of more features in BEAM that are already simulated in ActivitySim, such as joint trips.

Reduce model run time

To help define the scope of work for SMART 2.0 and put bounds and priorities on achievable performance improvements, the BEAM team produced initial implementations of several improvements designed for faster routing and faster convergence. To allow for faster road network routing (construction of street paths from an origin to destination), the Graphhopper engine was implemented in BEAM [3], allowing for BEAM to use static contraction hierarchies to reduce the computational burden of calculating routes.

In addition to this implementation, the BEAM team also experimented with the RoutingKit framework that allows for the use of customizable contraction hierarchies [4] for street routing. This framework not only allows for faster routing calculations, but it also is flexible enough to allow for quasi-efficient traffic

equilibrium to be estimated after only the first iteration using the Frank Wolfe method, rather than requiring 5-10 iterations of BEAM to reach these relaxed link-level travel times. This shortcut could reduce the number of iterations required to reach equilibrium, and therefore total BEAM runtime, by 25%-50%. Both of these functionalities are currently implemented as trial versions, and final versions will be implemented early in SMART 2.0.

Produce calibrated model in Austin and Detroit

The generalized deployment pipeline for BEAM defined above produces a model that can run in a given city using only widely available public data, without the need for a great deal of manual intervention. The model produced, however, will not necessarily produce realistic outputs in terms of travel times, mode splits, and origin/destination flows. Given a model produced by this deployment pipeline, arriving at realistic outputs requires a manual calibration process. The degree of precision reached in calibration depends on the time and resources devoted to this process, which can be decided based on the degree of precision needed in modeling outputs in order to answer the underlying research questions.

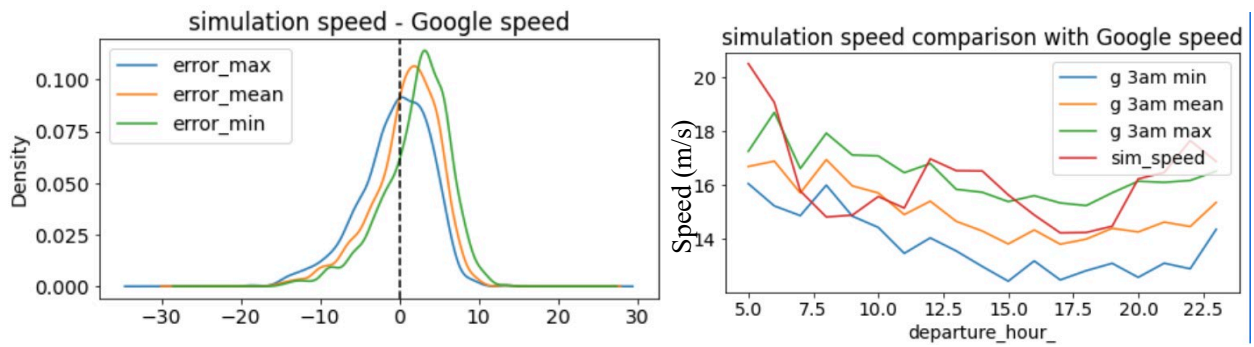


Figure I.1.6.2 Speed Calibration Values for Austin

The initial calibration produced in FY20 was a two-stage process, with activity participation rates and trip origin/destination flows calibrated in ActivitySim and mode choice and traffic network performance calibrated in BEAM. In both cases, calibration was achieved by adjusting behavioral parameters within the choice models contained in ActivitySim and BEAM such that the output travel behavior better matched expectations as observed in public datasets such as the National Household Travel Survey. In addition, road network travel times in BEAM were calibrated against travel times estimated by the Google Maps API over the course of a full day in both Austin (Figure I.1.6.2) and Detroit (Figure I.1.6.3). To do this, several global traffic flow parameters were adjusted within BEAM’s traffic simulation module until mean travel speeds fell within expected ranges in both cities.

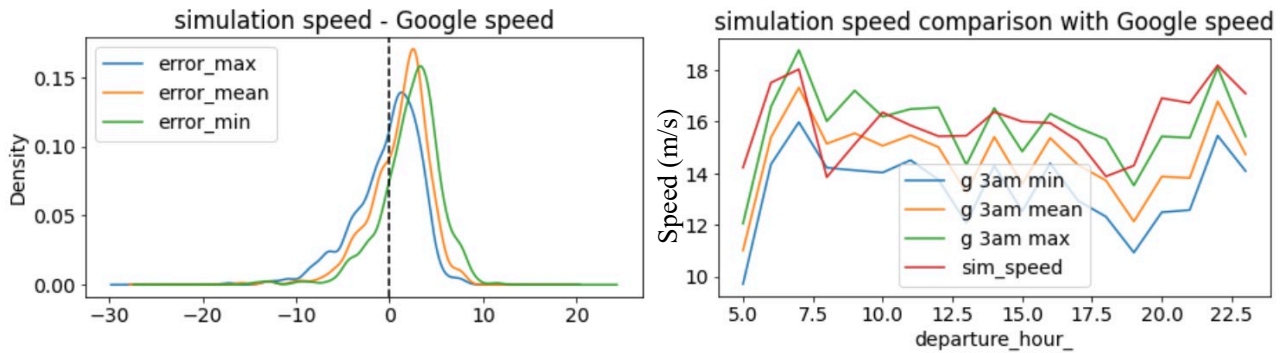


Figure I.1.6.3 Speed Calibration Values for Detroit

In SMART 2.0, additional work would be focused on easing some steps of this calibration process, allowing calibration to be performed with less time with less manual oversight, but this manual process provided important understanding as to the most important factors and potential hurdles in this process.

Results

A primary outcome of the FY20 BEAM work is calibrated BEAM implementations in the Austin and Detroit metropolitan areas. These baseline model implementations define the detailed daily travel behavior of hundreds of thousands of individual travelers in each of these cities. These disaggregate outputs can then be summarized in terms of aggregate metrics relating to the total car speed, vehicle miles traveled (VMT) per capita, person miles traveled (PMT) per capita, and energy use per capita (Table I.1.6.1) as well as the mode split (Table I.1.6.2), which can be compared to survey results and other estimates of ground truth values.

Table I.1.6.1 Summary Statistics in Austin and Detroit

Value	Austin	Detroit
Car Speed	32.1	34.5
VMT/Capita	26.7	24.7
PMT/Capita	31.4	37.1
Energy/Cap (MJ)	79.5	86.0

Table I.1.6.2 Aggregate Mode Split in Austin and Detroit

Value	Austin	Detroit
Bike	5%	0%
Car	84%	92%
Drive Transit	0%	0%
Ridehail	7%	0%
Walk	2%	4%
Walk Transit	2%	3%

In both these cases, model outputs can be presented at a much more disaggregate level as well, down to the level of origin/destination flows, speeds on individual links of the road network, or crowding levels on individual public transit vehicles. The process of a more detailed comparison between BEAM and POLARIS, another agent-based travel demand model developed using DOE resources, remains ongoing, but initial comparisons have proven fruitful. At a high level, there is great agreement between the two models in terms of travel times, origin/destination flows, activity participation rates, and modal splits. The differences that have

been found between the two models are still under investigation, but they are expected to give insight into fundamental differences between the capabilities and best use cases of the two models as well as point to individual model components that should be adjusted.

Conclusions

Over the course of FY20, the BEAM model was extended to two new cities, Austin and Detroit, yielding calibrated agent-based travel demand models in these two locations that can be used to evaluate short- and long-term transportation scenarios and that can be directly compared to model outputs produced by the POLARIS model at Argonne National Laboratory. In developing these two model implementations, the BEAM team took care to develop an integrated model deployment pipeline, greatly reducing the effort and time that will be required to deploy BEAM to further cities in the future. Further, the software infrastructure developed in BEAM relating to coupling with the ActivitySim day planning model and faster road network routing engines such as Graphhopper will enable great improvements to the accuracy, capabilities, and speed of BEAM over the next three years of planned work.

While the primary tasks defined for BEAM in FY20 were oriented towards tool development rather than research, one high level conclusion of this year of work is that it is possible to implement an agent activity-based travel demand model in a new city using only widely available public data, and for that model to produce reasonably well calibrated outputs over the course of several months of work. Regional planning agencies and other government entities often need to rely on consultants or proprietary software to build the models they use to answer long term planning questions, so the fact that an open source model such as BEAM can produce useful outputs without requiring proprietary data suggests that the next generation of travel demand models may be more widely accessible to local stakeholders, better modeling the transportation impacts of emerging transportation technologies and doing so in a way that can provide the broadest possible insights to the broadest set of communities. These goals are also reflected in the planned scope of work for BEAM over the duration of the SMART 2.0 project.

References

1. X. Ye, K. Konduri, R. M. Pendyala, B. Sana and P. Waddell, "A methodology to match distributions of both household and person attributes in the generation of synthetic populations," in 88th Annual Meeting of the Transportation Research Board, Washington, DC, 2009.
2. E. Gali, S. Eidenbenz, S. Mniszewski, L. Cuellar and C. Teuscher, "ActivitySim; large-scale agent-based activity generation for infrastructure simulation," Los Alamos National Laboratory. (LANL), Los Alamos, NM (United States), 2008.
3. P. Karich and S. Schröder, "Graphhopper," [Online]. Available: <https://www.graphhopper.com/>. [Accessed 11 November 2020].
4. J. Dibbelt, B. Strasser and D. Wagner, "Customizable contraction hierarchies," in International Symposium on Experimental Algorithms, 2014.

Acknowledgements

The following individuals and teams contributed to the results presented in this report: DOE Vehicle Technologies Office: Energy Efficient Mobility Systems Program including David Anderson, Erin Boyd, Prasad Gupte, and Heather Croteau. The BEAM Development and Research Team: Zachary Needell, Colin Sheppard, Rashid Waraich, Haitam Laarabi, Michael Zilske, Andrew Campbell, Art Balayan, Justin Pihony, Rajnikant Sharma, Bhavya Latha Bandaru, Kirill Mitin, Carlos Caldas, Dmitry Ogurtsov, Nikolay Ilin. LBNL collaborators: Tom Wenzel, Anna Spurlock, Tom Kirchstetter, Mike Mills. UC Berkeley: Paul Waddell, Max Gardner, Tim Lipman, Xiao-Yun Lu, Alex Bayen, Joan Walker. SMART Mobility: NREL (Jeff Gonder, Aaron Brooker, Jake Holden, Eric Wood, Stan Young, Venu Garikapati, Chris Gearhart), ANL (Aymeric Rousseau, Josh Auld)

I.2 Artificial Intelligence, High Performance Computing, and Data Analytics

I.2.1 HPC-Enabled Artificial Intelligence for Connected and Automated Vehicle Development

Robert Patton, Principal Investigator

Oak Ridge National Laboratory
PO Box 2008
Oak Ridge, TN 37831
Email: pattonrm@ornl.gov

Peter Graf, Principal Investigator

National Renewable Energy Laboratory
15013 Denver West Parkway
Golden, CO 80401
Email: peter.graf@nrel.gov

Erin Boyd, DOE Technology Manager

U.S. Department of Energy
Email: erin.boyd@ee.doe.gov

Start Date: October 1, 2018
Project Funding: \$1,500,000

End Date: September 30, 2020
DOE share: \$1,500,000

Non-DOE share: \$0

Project Introduction

The goal of the HPC-CAVs project is to explore and develop the application of advanced AI and high-performance computing (HPC) throughout the connected and autonomous vehicles (CAVs) pipeline. The present state-of-the-art in AVs utilize AI primarily in visual image processing, and classical algorithms elsewhere. We are investigating the entire pipeline. Also, as DOE-sponsored research, our mandate is to understand the implications for energy usage and broader sustainability, not just the safe operation of a vehicle. We have developed a series of tools (described briefly below) that explore various avenues, mostly in the single-vehicle context. Going forward, our mission now is to scale these tools up, link them, and apply them to DOE-relevant cases.

Objectives

This project seeks to achieve the following objectives: 1) increase affordability, convenience, safety, and energy productivity of mobility, 2) reduce transportation fuel use/GHG emissions, 3) validate safety of automated vehicles through accelerated simulation environments, and 4) explore and validate innovative vehicle control strategies at the system level.

To demonstrate the achievement of these objectives, this project will:

- Demonstrate HPC-based ability to analyze large data sets from prototype self-driving vehicles and discover higher performance and resilient operating algorithms in an expedited cadence.
- Develop and demonstrate new machine learning based algorithms for vehicle operating controls that are capable of scaling to “Level 5” autonomous vehicle capabilities.
- Develop a virtual test environment capable of safely evaluating autonomous vehicle operating controls over millions of miles and scenarios/environments expected to be encountered. There is expected

applicability to advanced conventional vehicles by examining electronic controls for powertrain functions.

Questions to be addressed:

1. How do we leverage machine learning for perception and control of a single autonomous vehicle given the constraints / objectives of safety, destination arrival, and energy efficiency? (FY19)
2. How do we leverage machine learning for perception and control of multiple autonomous vehicles given the constraints / objectives of safety, destination arrival, and energy efficiency? (FY20)
3. How do we leverage machine learning for perception and control of multiple autonomous vehicles in a connected environment given the constraints / objectives of safety, destination arrival, and energy efficiency? (FY21)

Approach

For FY20, ORNL and NREL explored a wide range of machine learning challenges for autonomous vehicles and developed key capabilities that address these challenges.

From ORNL, some of the key findings were:

- Data sets for developing perception do not capture a wide range of lighting conditions
- Imitation Learning for Driving shows significant progress but the robustness (how well does it handle edge cases?) needs more evaluation
- A quantitative evaluation metric is needed; assessing driving behavior is still too subjective
- Synthetic imagery data sets are needed; real world data sets do not cover the full range of
- What level of perception accuracy is needed to safely and efficiently drive a vehicle?
- How do we improve the synthetic data sets?

From NREL, some of the key findings were:

- Reinforcement Learning (RL) aware tools need to be developed across the CAV spectrum
- Multi-agent learning and curriculum learning need more attention within the CAV spectrum
- Distributed (driving) vs centralized (power systems) control: how to balance these approaches?

Each of these findings are critical to address or resolved in order to achieve the objectives.

Results

Below is an overview of the results achieved for FY20.

Driving Simulator for HPC (ORNL)

To enable AI for CAVs at scale, ORNL successfully ported CARLA (<http://carla.org>) to ORNL's Summit, which contains 27,000 GPUs and can enable many millions of miles of simulated driving per day, which enables scaling the methodology to very large cases. ORNL is now using this capability to develop a new AI system called Gremlin as described below.

AI for Autonomous Vehicle Evaluation (ORNL)

ORNL is creating a new AI system called Gremlin that will generate a large number of driving scenarios in CARLA to evaluate the driving behavior of any given perception / control algorithm. We have successfully completed the first experiments with Gremlin. Based on the initial results, Gremlin begins identifying certain failure scenarios and then generates more failure scenarios similar based on what it finds for additional testing. Eventually, Gremlin identifies and converges to a new set of scenarios where the autonomous vehicle fails completely. This was an exciting initial result, and we are now developing post-process analytic capabilities to automatically analyze the results of Gremlin and convey the results in a more human-friendly manner. To date, ORNL has successfully run Gremlin on a single node of Summit using 6 GPUs and have now progressed to scaling this code to use more nodes of Summit.

Synthetic Data Generation for AI Development (ORNL)

ORNL has developed software code that leverages CARLA's Roaming Agent to generate realistic RGB imagery and corresponding ground truth semantic segmented and LIDAR images. This data is being curated to create a single data set useful for imitation learning, perception algorithm development, and test and evaluation. This initial version of data set consists of:

- 3 towns in CARLA (Town 1, 3, and 4)
- ~23M images / 507 GB (shown in the Table below for Town 1)
- 8 combinations of weather and sun position (Clear / Hard Rain / Soft Rain / Wet, and Noon / Sunset)
- 2 hours of driving per combination per city.

No pedestrians / No traffic, currently only static objects such as buildings, traffic signs, etc.

- 200 x 90 image resolution (for comparison, CityScapes has a resolution of 2048 x 1024).

Table I.2.1.1 Statistics of Synthetic Data Set collected for CARLA Town 1

Town 1	Weather	Sun Position	RGB Files	RGB GB	SEG Files	SEG GB	Topdown Files	Topdown GB	LIDAR Files	LIDAR GB
	Clear	Noon	229,275	6.92	229,273	0.78	229,541	1.28	229,271	12.48
	Clear	Sunset	200,472	5.21	200,471	0.67	200,715	1.11	200,471	12.53
	Hard Rain	Noon	219,416	5.35	219,415	0.75	219,619	1.19	219,407	12.40
	Hard Rain	Sunset	188,670	4.66	188,669	0.64	188,934	1.04	188,663	12.50
	Soft Rain	Noon	219,512	6.79	219,512	0.76	219,772	1.26	219,508	12.51
	Soft Rain	Sunset	195,304	4.55	195,301	0.67	195,546	1.14	195,300	12.53
	Wet	Noon	216,306	6.86	216,305	0.73	216,497	1.19	216,301	12.47
	Wet	Sunset	196,470	5.53	196,468	0.66	196,662	1.06	196,466	12.43
Totals			1,665,425	45.89	1,665,414	5.65	1,667,286	9.27	1,665,387	99.84
Total GB	160.65									
Total Files	6,663,512									

AI for Autonomous Vehicle Perception (ORNL)

We have completed applying the evolutionary deep learning framework, MENNDL, to data provide by GM to test the hypothesis that object detection can be improved. Initial results have been shared with GM. Unfortunately, MENNDL currently does not achieve state of the art results for two reasons: 1) MENNDL does not create the necessary neural structures that are needed, and 2) MENNDL is not able to leverage pretraining techniques that are currently used to achieve state of the art results. However, we are now questioning the

rationale of the community and industry’s approach to AI for CAV perception based on our new findings with end-to-end driving. We have been experimenting with end-to-end driving neural networks where the networks are taking in semantic segmented images and the output is driving controls (steering, brake, and throttle). We are explicitly training the network for driving controls, but we are also implicitly training it to perform perception. We are not using MENNDL for this right now, but hopefully soon now that we’ve tackled some technical problems between MENNDL and CARLA running on Summit. The chart below shows that based on simple driving behavior metrics that we created, we have found that training accuracy/loss values (blue/red lines on chart; the lower the better) do not in any way correlate to driving behavior metrics (yellow line on chart; the higher the better). In other words, we are not guaranteed to improve driving behavior simply because we improved our training accuracy on the network. We confirmed these results visually as well from video we created from the CARLA scenarios, so we trust that the evaluation metric we created is accurate. So, based on this, we are wondering now if this same “phenomenon”, for lack of a better word, occurs when training a network explicitly for perception accuracy when it is combined with a separate control system. Based on the results shown in the chart (which surprised us), we have these questions: Are our results simply isolated to end-to-end driving networks?, Does a perception network with 90% pixel level accuracy actually drive better than a perception network with 75% pixel level accuracy?, If not, then should we be trying to design / train a perception network to achieve improved driving behavior at the system level rather than trying to achieve a 100% perception accuracy at the neural network level? We haven’t seen any research on this or evidence to suggest an answer to these questions and we are interacting with our GM collaborators to determine who may have done this or know someone who has. As a result, we recommend investigating the development of perception neural networks using system level metrics for training rather than pixel level accuracy values. Between MENNDL, CARLA, Gremlin, and Summit, we have some pieces in place now to begin investigating these questions.

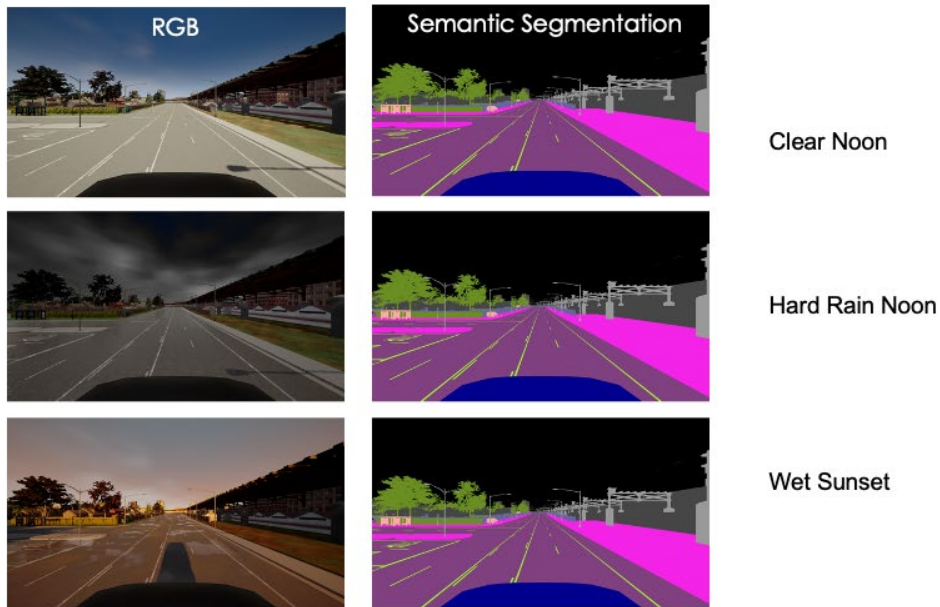


Figure I.2.1.1 Synthetic Imagery Examples

Finally, General Motors licensed MENNDL from ORNL during FY20.

Reinforcement learning (RL) in CARLA

Reinforcement learning (RL) is the central theme of the NREL side of this project. The following figure illustrates the canonical structure of RL, in which an agent learns to act correctly via many iterations of action, feedback (“reward”), and adjustment of the controller (“learning”).

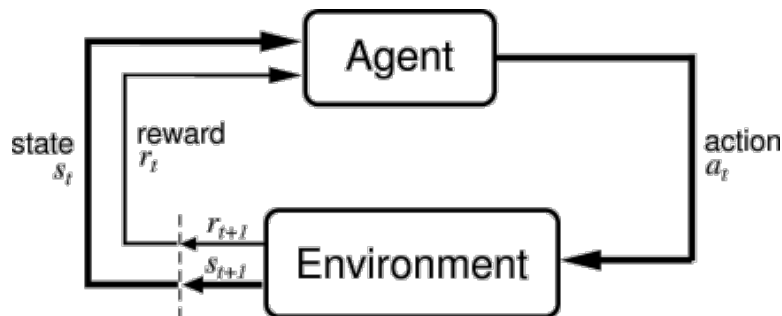


Figure I.2.1.2 Canonical Structure of Reinforcement Learning

To facilitate RL studies at scale with CARLA, we have developed various “AI Gyms” (an AI gym is a generic interface that allows a simulation tool to be used for RL studies within a variety of learning algorithms) that allow for RL in CARLA, including waypoint following, driving based on semantically segmented and other images.

Imitation learning (IL) in CARLA

By allowing the CARLA “autopilot” to simply drive around, we gather “expert” driving controls corresponding to camera images that are then used to directly (i.e., by supervised learning) map images to control actions. The IL studies have been performed at ORNL.

IL to RL in CARLA

We pass the neural network trained by imitation learning at ORNL to the reinforcement learning frameworks implemented at NREL. The pretrained network accelerates the RL training. The RL training improves the results of the IL. This ongoing work represents a form of “transfer learning”. Transfer learning is a central theme of much of our work. In transfer learning, an agent trained in one setting (usually a simpler setting) is used to “warm start” further training in a different (usually more complex setting). This is a powerful concept: learning steps should be chained together; learning should occur in appropriate stages; each stage of learning should occur in the most efficient (i.e., simplest) setting that it can, then passed on to a more advanced step. In this particular study, we designed the IL and RL neural networks to be identical, so the network “weights” learned by IL can be directly used as the starting point for RL.

KRoad

Another central theme of this project is “modularity”, which refers, generically, to breaking a task into component parts. The purposes of modularity are manifold: isolating a process in the simplest possible setting; breaking a complex task into small parts; writing computer code that can be readily repurposed and/or extended. The theme of modularity in CAVs control comes from the fact that the state-of-the-art AV “pipeline” consists of a series of somewhat well-defined steps (principally: global planning, perception, local path planning, path following). A particular observation is that several of the modular steps in the CAVs pipeline do not require the perception phase, so do not require the complex, rendering-based CARLA simulator. To that end, we have implemented the “2D” dynamic bicycle model (DBM) within a flexible python framework (the “FactoredGym”) allowing for a mixing and matching of driving scenarios, physical models, and learning algorithms.

Path following in KRoad

We are using KRoad to perform a detailed study of RL for the path following problem and comparing the results to several state-of-the-art classical controllers.

KFlow

SUMO is a well-used microscopic traffic simulator. *Flow* is an add-on package for SUMO that allows for RL in SUMO. However, the “driver model” in SUMO/Flow is very rudimentary (e.g., no steering, just instantaneous lane changes). To heighten the realism that we can achieve with Flow, we have integrated KRoad and Flow, resulting in an ability to perform RL studies using realistic physics-based driving within the macroscopic traffic simulator SUMO. We are calling this integrated capability KFlow.

3D to 2D to 3D for Faster Development Turnaround Time

We are integrating KRoad and CARLA such that CARLA maps can be exported to KRoad, where 2D learning can occur in a fast environment, and the resulting controller then operated in 3D in CARLA. Eventually these can become pretrained models that are refined in CARLA based on more complex inputs (e.g., sensor data rather than waypoints). The following figure illustrates the flavor of this “mixed-mode” simulation and learning. The left part is KRoad, and the right part is CARLA, but they are the same road layout.

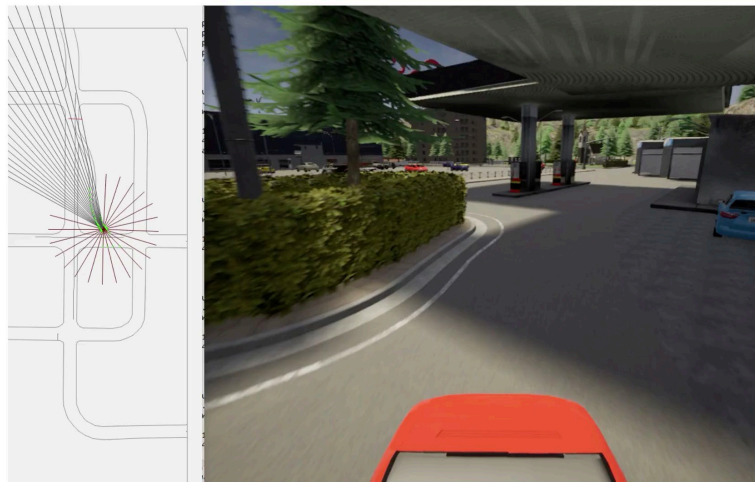


Figure I.2.1.3 Mixed Mode Simulation and Learning

Highway ramp metering with Flow

We have conducted a RL study regarding the potential for RL-based controllers to be used in highway ramp metering. The results indicate that RL controllers are superior to the industry standard baseline ALINEA algorithm. Results of this study have been submitted for publication. The following figure is representative of the simulation domain.

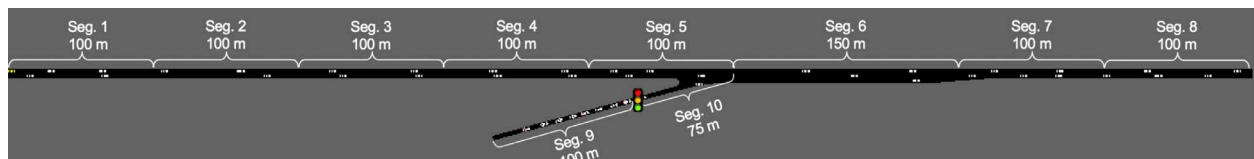


Figure I.2.1.4 Simulation Domain

Parking and Curbside applications with Flow and KFlow

Parking and curbside applications are of great interest to avoid congestion and save energy in urban environments. We are using Flow and KFlow to study and hopefully optimize vehicle movement in such scenarios. Because these are typically scenarios that occur in specific spatial locations, it is more feasible to imagine a situation where autonomous vehicles can coordinate their movements, even let their movements come under the control of a centralized system. For that reason, these studies are early use cases for emphasizing the ‘connected’ (V2V or V2I) aspect of this project.

The following figure summarizes the tools NREL has so-far developed and applied to this project

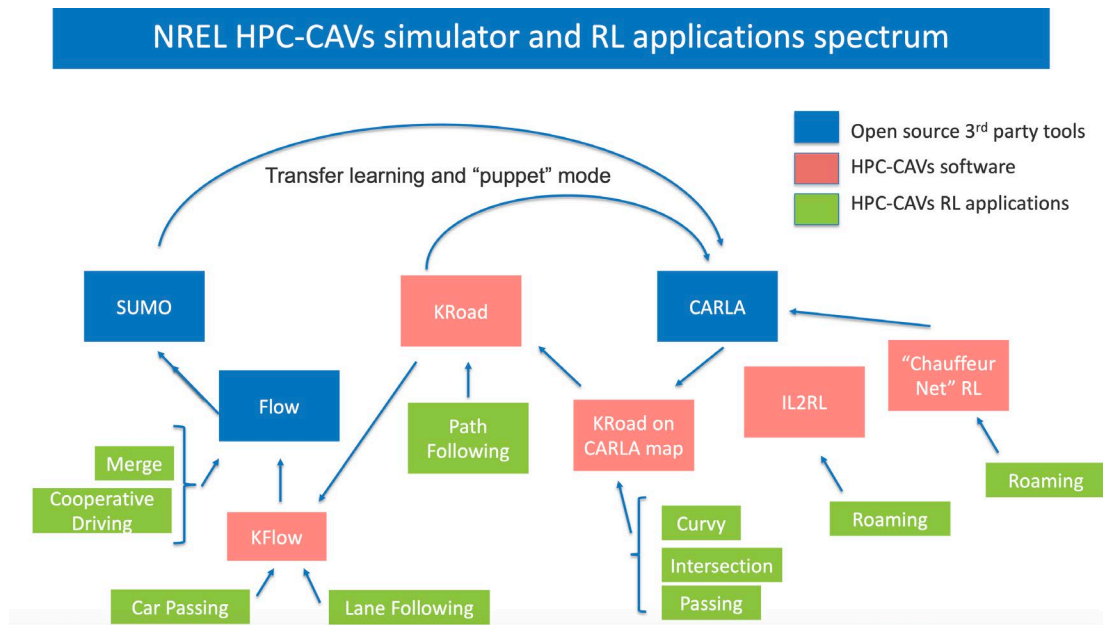


Figure I.2.1.5 Summary of Project Tools: NREL HPC-Cavs Simulator and RL Applications Spectrum

Computing Allocations (ORNL)

2019 – 2020 ALCC Project (Started on July 1, 2019 and Completed on June 30, 2020)

Title: Advances in Artificial Intelligence to Improve Sensory Perception

We are partnered with GM to further develop MENNDL for perception tasks and we were allocated 200K compute hours on ORNL’s Summit.

2019 – 2020 NREL Supercomputer (“Eagle”) Allocation (FY 2020)

Title: HPC for Connected and Autonomous Vehicle Control

Reinforcement learning (RL) is very computationally intensive, especially when coupled to the rendering-based CARLA simulator. We were allocated 78,000 Allocation Units (AUs – each AU is roughly 2-3 CPU hours) and used 77,000. These hours were used for studies of RL across our spectrum of RL-capable simulation tools.

2020 – 2021 ALCC Proposal (Started on July 1, 2020 and will be Completed on June 30, 2021)

Title: Evolutionary Multi-scenario Simulation Environment for Autonomous Vehicle Testing

We are partnered with GM to develop Gremlin for automated testing of autonomous vehicle perception and control tasks, and we have been awarded 150K compute hours on ORNL's Summit.

2020 – 2021 NREL Supercomputer (“Eagle”) Allocation (FY 2021)

Title: HPC for Connected and Autonomous Vehicle Control

Reinforcement learning (RL) is very computationally intensive, especially when coupled to the rendering-based CARLA simulator. These hours will be used for continued extensive studies of RL across our spectrum of RL-capabled simulation tools. We have been allocated 200,000 Allocation Units (AUs). Particular emphasis for FY21 is in scaling RL to large processor counts only available in National Lab facilities.

Conclusions

While significant progress has been made toward the development and application of machine learning for autonomous vehicles, the current findings have uncovered additional key questions relating to the testing and evaluation of autonomous systems, the fragility of machine learning to the wide range of driving conditions and have identified gaps in current simulation systems that limit additional machine learning development.

Key Publications

1. Robert Patton, Shang Gao, Spencer Paulissen, Nicholas Haas, Brian Jewell, Xiangyu Zhang, Peter Graf, “Heterogeneous Machine Learning on High Performance Computing for End to End Driving of Autonomous Vehicles”, 2020 Society of Automotive Engineers World Congress Experience, April 2020. <https://doi.org/10.4271/2020-01-0739>
2. Yi Hou, Xiangyu Zhang, Peter Graf, Charles Tripp, and David Biagioni, “A Cyber-Physical System for Freeway Ramp Meter Signal Control Using Deep Reinforcement Learning in a Connected Environment”, submitted to IEEE transactions on Intelligent Transportation Systems, November 2020.

Acknowledgements

This research used resources of the Oak Ridge Leadership Computing Facility at the Oak Ridge National Laboratory, which is supported by the Office of Science of the U.S. Department of Energy.

I.2.2 Ubiquitous Traffic Volume Estimation through Machine Learning Procedures (NREL)

Venu Garikapati, Principal Investigator

National Renewable Energy Laboratory
15013 Denver West Parkway
Golden, CO 80401
Email: venu.garikapati@nrel.gov

Erin Boyd, DOE Technology Manager

U.S. Department of Energy
Email: erin.boyd@ee.doe.gov

Start Date: September 1, 2019
Project Funding: \$500,000

End Date: September 30, 2021
DOE share: \$500,000

Non-DOE share: \$0

Project Introduction

High-quality traffic volume data is critical for transportation planning, operations, and travel-energy calculations. However, vehicle count data from roadside sensors is very sparse owing to high capital cost of installing, and on-going maintenance of electronic sensor equipment. This project aims to bring to market a first of its kind traffic volume data product that provides accurate estimates of traffic volumes across the entire road network for all times (*24x7*) and all locations (*100% coverage*). This product greatly improves the coverage and quality of traffic volume information by combining commercial probe traffic data with traditional traffic measurement using state-of-the-art machine learning techniques. Commercial probe traffic data has already revolutionized travel time and speed reporting both for government agencies as well as general travelers (through applications such as Waze and Google Maps). With the escalating ratio of probe vehicles in the traffic stream, now approaching 1 in 10, the number of observed probes can be combined with other data using machine learning (ML), to produce estimates of traffic volume with a high degree of statistical confidence. Combining the vehicle probe data with other data (speed, weather, and a sensor-based calibration network) using ML methods provides the opportunity to scale quality volume measures network-wide cost effectively. Conventional sensor-based vehicle counts, be it radar, pneumatic tubes, or inductive loops, represent the current state-of-the-art. Such devices provide volume data at sparse locations and are too expensive to scale. NREL's method provides a complete operational picture of traffic flow everywhere on the network and at all times and does so at a greatly reduced cost compared to adding additional sensors. The basic method has been demonstrated by NREL in collaboration with the I95 Corridor Coalition and the University of Maryland (UMD), under a grant from the Federal Highway Administration (FHWA). The results have prompted the FHWA to investigate applications for estimating average annualized daily traffic (AADT) to complement existing data collection. At full scale deployment, this technology can provide a measure of central tendency of traffic volume, as well as monitor the roadways in real-time for perturbations resulting from unusual events.

The commercial partner on this project TomTom, Inc., is one of the major suppliers of in-car location and navigation products and services. TomTom's products include portable navigation devices, in-dash infotainment systems, fleet management solutions, maps and real-time services. The Traffic and Travel Information department at TomTom collects and evaluates anonymous location information from connected devices and connected cars enhanced by external sources. These data are on the one hand used for live traffic information and on the other hand stored in a database for further evaluation. The live traffic data allow precise measurement of travel times or current speeds on the road network and can be enhanced by additional information required for various in-car applications. The historic probe vehicle data allow broad and detailed analyses on precise time-dependent behavior of traffic flow over complex road structures. TomTom possesses a massive store of probe vehicle data (from hundreds of millions of probes), which is a key input to the volume

prediction algorithm being discussed here. Over the years, TomTom was kept informed of NREL's work on ML-based volume estimation methods. Encouraged by the performance of the algorithms, TomTom is partnering with NREL to bring the lab-developed ubiquitous volume estimation methods to market. TomTom also operates a mature commercial traffic data visualization system which can be easily adapted to support large-scale deployment of the proposed product.

This project comprises three phases spanning over two years. While the first two phases of the project focus on methodological and prototype visualization efforts, the final phase of the project will focus on integrating NREL developed technology into TomTom's product environment.

Objectives

The primary objective of this project is to increase the observability of traffic volume information in the nation. With increasing proliferation of technology in the form of automated, connected, electrified, efficient, and shared vehicle systems, it is critical now more than ever to have an accurate understanding of how much traffic is on the roads for each hour of the day, and each day of the year everywhere on the network. Such information has enormous utility in transportation as well as energy domains. Transportation planners can use this information to check the adequacy of existing transportation infrastructure. Traffic operations personnel can make use of this information to effectively re-route the traffic in case of unexpected network congestion events. The energy community can benefit from more accurate estimates of travel related energy and emissions.

The end goals of the project are:

1. To develop machine learning based estimation models that can theoretically accurately predict traffic volumes anywhere, anytime, and for any functional road class (freeway, arterial, major/minor collector etc.). Acceptable error bounds (for the estimation models) have already been established based on feedback from various state DOTs. The project team will strive to develop models that meet the set error thresholds.
2. To test the spatial transferability of the volume estimation models and determine the feasibility (or the lack thereof) for utilizing a traffic volume model estimated in one state to estimate traffic volume in a different state.
3. To develop anomaly detection methods that can identify erroneous input data and tag the data for review and/or deletion. Identifying bad data upfront will help develop models that perform better.
4. Extend the models developed in step one to generate additional model outputs such as Average Annual Daily Traffic, and energy consumed at the level of roadway segment.

Building on all of these activities, the final outcome of the project is a web-based traffic volume estimation product that provides hourly traffic volumes across all the roads in a state or region, accessed either visually (as in thematic maps) or through an API call for a specific roadway and time for machine-to-machine communication. Mechanisms will be built into the system for periodic self-calibration (every week, every month etc.) based on reference data available through publicly maintained traffic volume sensor locations. The data will be seamlessly integrated into the commercial partner's (TomTom's) product environment and provided as a service to State DOTs and planning entities.

Approach

Average hourly volumes are modeled as a function of commercial probe data, weather information, and roadway characteristics. Use of machine learning for traffic volume estimation is a nascent field but one that is gaining rapid traction. Contributing to this body of knowledge, Hou et al. [1] demonstrated the advantage of using machine learning for hourly traffic volume estimation. In particular, Hou et al. [1] highlighted the superiority of a tree-based ensemble learning method namely Extreme Boosting Machine (XGBoost) in

estimating traffic volumes using probe data. XGBoost belongs to the boosting family of machine learning models driven by a meta-algorithm to boost a weak learner into a strong one to reduce bias and variance in model predictions. As a part of FY20 efforts on the project volume estimation models were developed for upper functional road class (interstates, freeways/expressways, and principal arterials) in CO, NC, and PA. In addition to this, spatial transferability exercises were carried out to explore the feasibility of applying the model developed in one state to predict traffic volumes in a different state.

The model performance is evaluated in terms of the coefficient of determination (R^2), mean absolute error (MAE), and error to maximum flow ratio (EMFR), defined as:

$$R^2 = 1 - \frac{(\hat{V}_i - V_i)^2}{(\bar{V}_i - \bar{V})^2},$$

$$MAE = \frac{1}{N} \sum_{i=1}^N |V_i - \hat{V}_i|,$$

$$EMFR = \frac{1}{N} \sum_{i=1}^N \frac{|V_i - \hat{V}_i|}{V_{max}},$$

where V_i is the observed volume, \hat{V}_i is the estimated volume, V_{max} is the maximum observed traffic volume at the location where V_i is observed, and N is the total number of observations. These criteria were chosen for model evaluation to demonstrate the predictive accuracy of the model from multiple perspectives. Coefficient of determination R^2 (bounded between 0-1) reflects the proportion of variance in the dependent variable that can be captured from the set of independent variables used in the model estimation. MAE, and EMFR are model performance measures that compare the predicted volumes against observed traffic flows on a roadway segment. While high R^2 values (>0.9) reflect a good model fit, low MAE, and EMFR values mean that the model is able to predict observed volumes closely. Particularly, EMFR values within 10% are considered good enough to potentially support traffic operations.

Results

Independent Freeway Volume Estimation Models for CO, NC, and PA

From Table I.2.2.1, it can be observed that the baseline models developed using data from CO, NC, and PA) perform quite well in terms of the model evaluation criteria. R^2 for models from all states is above 0.9, and the MAE for all the models is on the lower end. The EMFR for each model is within acceptable ranges for use in traffic operations purposes. While an R^2 closer to 1.0 reflects that the independent variables included in model are able to capture a higher proportion of variance in the dataset, a low MAE conveys that each individual prediction of the model is closer to the observed hourly traffic volume. EMFR compares the error in each hourly traffic prediction to the maximum traffic flow observed on each roadway segment. While MAE ensures the closeness of a prediction to observed values, EMFR gives us an indication of percent deviation of each predicted volume from the maximum flow observed on the roadway, which helps determine the health of the model in comparison to the specific roadway segment for which the model is applied. To put these results in perspective, the ideal values for the evaluation criteria are $R^2 \rightarrow 1$; $MAE \rightarrow 0$; $EMFR \rightarrow 0\%$.

Table I.2.2.1 Independent Model Results

State	R^2	MAE	EMFR (%)
Colorado	0.91	357	5.3
North Carolina	0.92	257	6.4
Pennsylvania	0.91	194	5.7

Spatial Transferability Exercise between Colorado, North Carolina, and Pennsylvania

Hourly traffic volume data pertaining to interstates, freeways, and principal arterials was selected to test the feasibility and accuracy of spatial transferability between CO \leftrightarrow NC, and NC \leftrightarrow PA. Two transferability models were constructed for each state pair. For example, the volume estimation model was trained on data

from CO and applied to predict hourly traffic volumes (for freeways, interstates, and arterials) in NC. The second model is the mirror opposite; a model trained on NC volumes to predict CO volumes. Results of this are presented in Table I.2.2.2. From Table I.2.2.2, it can be observed that model trained on CO data and applied on NC upper functional class roadways has an R^2 of 0.71, and a MAE of 577. The model trained on NC data and tested on CO road segments performs even worse. This result is not completely unexpected, given the disparity in traffic volumes, weather conditions, and probe penetration rates between both these states. The model performance between NC and PA spatial transfer is much better than that of CO↔NC spatial transfer.

Table I.2.2.2 Results from Spatial Transferability Exercises

State	Train → Test	R^2	MAE	EMFR (%)	Train → Test
CO ↔ NC Spatial Transferability	CO → NC	0.71	577	15.6	CO → NC
	NC → CO	0.67	704	13.6	NC → CO
NC ↔ PA Spatial Transferability	NC → PA	0.89	217	6.1	NC → PA
	PA → NC	0.79	403	10.3	PA → NC
NC + PA Meta Model	NC + PA	0.91	266	5.5	NC + PA

Comparing the case where NC based model is applied to PA, and PA based model is applied to NC, the former model performs better than the latter. The model trained on PA data systematically underpredicted volumes on the NC roadways (as seen in Figure I.2.2.1a and Figure I.2.2.1b). The highest observed volume across the PA dataset was ~4,500 vph. When the PA model is applied to NC dataset, the highest prediction (irrespective of the type of roadway) that the PA model is able to generate on NC roads is ~4,300 vph, whereas the highest observed volume on NC roads is ~7,500 vph. For any road segment in NC with volumes higher than the highest observed volume in the PA dataset, the prediction from the PA volume estimation model peaks out at the highest observed volumes used for training the model, and hence will result in an error due to the bounding issue. Based on this as well as model estimation results from other states, we conclude that unlike traditional statistical models, XGBoost models cannot extrapolate predictions beyond the bounds of the observed data.

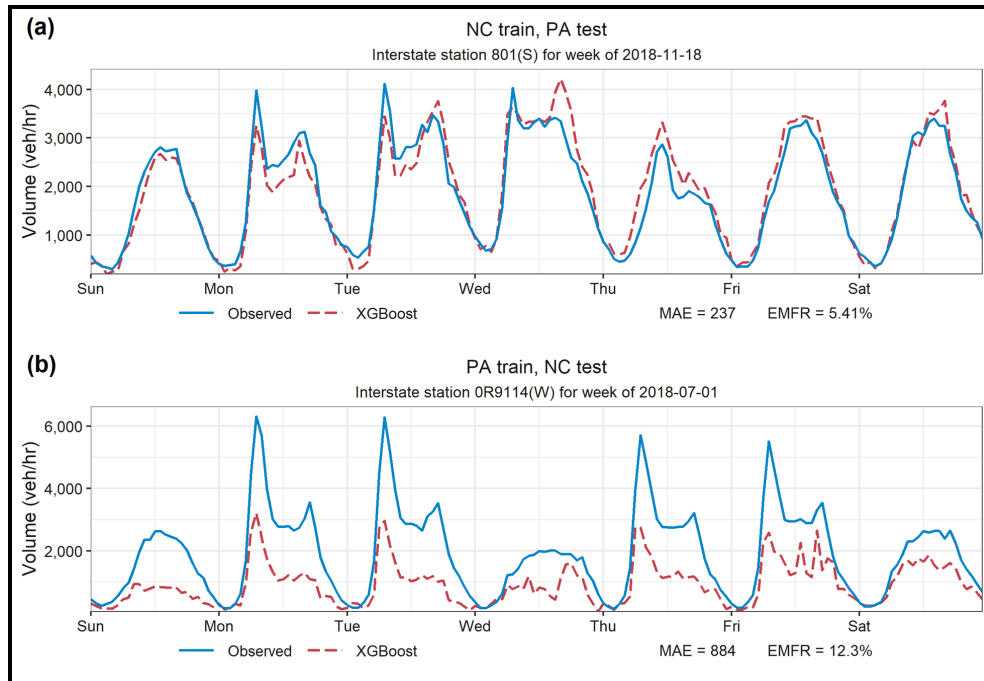


Figure I.2.2.1 Predicted Versus Observed Hourly Volumes for a Typical Week For (A) The Model Trained on NC and Tested on PA (Thus Displayed are PA Predicted Volumes), and (B) The Model Trained on PA and Tested on NC (Thus Displayed are NC Predicted Volumes)

Since accounting for all other inconsistencies (i.e., similarity in weather, date range, average volumes, and probe penetration rates) bolstered the shortcoming of the bounding issue with XGBoost model predictions, an additional analysis was undertaken to explore the advantage of combining data from two states. To do this, data from each state was split into an 80:20 (training: testing) sample while keeping data from individual stations bundled together. The 80% training data from both states were bundled together to form a combined dataset for training the meta-model. The resulting model was applied on the 20% testing sample from NC and PA. Results of the meta-models presented in the last row of Figure I.2.2.1 which shows that the meta-model performs better than any of the single-state spatially transferred models. The performance of the meta-model is comparable to the performance of the independent state models (Figure I.2.2.2). While the EMFR for independent NC and PA models are 6.4 and 5.7% respectively, the combined meta-model has an EMFR of 5.5%. As seen in Figure I.2.2.2, for the same roadway segment shown in Figure I.2.2.1b, the meta-model was able to improve upon the predictions of the PA ↔ NC model.

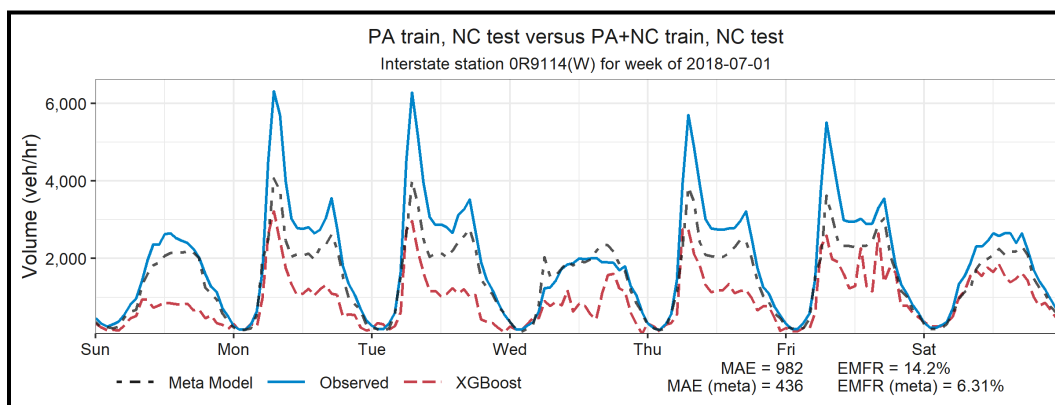


Figure I.2.2.2 Predicted Versus Observed Hourly Volumes for a Typical Week for the Model Trained on PA and Tested on NC (Thus Displayed are NC Predicted Volumes) with the Meta Model (PA+NC Train) and Test on NC

Conclusions

Data from the metropolitan region of Denver, Colorado, the state of North Carolina, and the metropolitan region of Harrisburg, Pennsylvania were used for developing volume estimation models. While each of the states provided the ground truth data for model estimation and validation, probe vehicle data for all states was sourced through TomTom. Baseline models were developed for hourly volume estimation (for interstates, freeways, and principal arterials) in each of the states. This was done with the dual intent of extensively exploring the ground truth data from each state, as well as testing the power of probe data in estimating traffic volumes. A machine learning model namely XGBoost decision tree was used to develop volume estimation model with hourly traffic volumes as the dependent variable, and probe data, weather information, and roadway characteristics as the independent variables. Independent model estimation results exhibit excellent goodness of fit measures ($R^2 > 0.9$; EMFR $\sim 6\%$) and are shown to predict traffic volume patterns in the respective states quite accurately. The model estimation results also show that probe vehicle data plays a critical role in the performance of the models. With confidence in the independent model estimations, spatial transferability exercises were carried out between state pairs CO-NC, and NC-PA. The spatial transferability exercises revealed several interesting insights.

- When transferring a volume estimation model from one state to another, it is extremely important to have temporal consistency. In other words, if a model applied in CO is being transferred to NC, it is important to have ground truth data for model development and validation for the same (or similar) time period. This is not a big issue if data from both states is available for multiple years. However, probe data does come with a price tag, so it is prudent to have temporal consistency for good spatial transferability.
- Transferring a model between states with similar weather and traffic characteristics will result in a better spatial transfer. This finding can be extended to say that it would be a good idea to develop ‘traffic typologies’ to identify clusters of regions or states for good spatial transfers.
- Through exploration of the model predictions, it was found that XGBoost (or tree learning methods in general) cannot extrapolate model predictions outside the bounds of observed data. This has a significant impact on spatial transferability, particularly when the transfer is from a state with low observed traffic volumes to a state with higher observed volumes. To overcome this issue, a meta-model was developed with data from NC as well as PA.
- Last but most importantly, the meta-model was observed to have the excellent performance (across all evaluation criteria) and is shown to overcome the bounding issue identified with spatial transfers. Though most of the lessons learnt from the spatial transferability exercise seem obvious, cumulatively they provide a guidebook that states and vendors can follow in developing and transferring volume estimation models across cities and states.

Key Publications

1. Kasundra, Kevin, Venu M. Garikapati, Christopher Hoehne, Yi Hou, and Stanley Young. *On Spatial Transferability of Machine Learning based Volume Estimation Models*. Selected for presentation at the 100th TRB Annual Meeting, Washington, DC., 2021.
2. Hou, Yi, Venu Garikapati, Christopher Hoehne, Kevin Kasundra, and Stanley Young. *State-wide Traffic Volume Estimation for Non-freeway Roads Using Probe-vehicle Data and Machine Learning Methods*. In preparation for submission to: Journal of Traffic and Transportation Engineering.

References

1. Hou, Yi, Stanley E. Young, Kaveh Sadabadi, Przemyslaw Sekula, and Denise Markow. *Estimating highway volumes using vehicle probe data-proof of concept*. No. NREL/CP-5400-70938. National Renewable Energy Lab. (NREL), Golden, CO (United States), 2018.

Acknowledgements

- The PI would like to acknowledge the efforts of the NREL team (Yi Hou, Chris Hoehne, Kevin Kasundra, and Stan Young) in the development of the volume estimation models using machine learning techniques.
- The project team offers their thanks to John Auble and his team at TomTom, Inc. for their continued support and encouragement in commercializing the NREL-developed volume estimation algorithm.

I.2.3 Transportation Data Analytics (Big Data Systems for Mobility (BDSM))

Jane Macfarlane, Principal Investigator

Lawrence Berkeley National Laboratory
1 Cyclotron Road
Berkeley, CA 94720
Email: jfmacfarlane@lbl.gov

Eric Rask, Principal Investigator

Argonne National Laboratory (ex-staffer)
9700 South Cass Avenue
Lemont, IL 60439

Prasad Gupte, DOE Technology Manager

U.S. Department of Energy
Email: prasad.gupte@ee.doe.gov

Start Date: October 1, 2017
Project Funding: \$3,900,000

End Date: September 30, 2020
DOE share: \$3,900,000

Non-DOE share: \$0

Project Introduction

The purpose of this program is to develop the data science and high-performance computing (HPC) supported computational framework needed to build next-generation transportation/mobility system models and operational analytics. In order to represent real-world urban systems, the models and analytics must scale both in spatial and temporal complexity. We will build on previous work in transportation systems, electrical grid analytics, and atmospheric modeling that has been developed within the partnered laboratories.

This work will focus on four key objectives that underlie critical transportation modeling challenges:

- Develop transportation system modeling approaches that permit parallel implementation or are limited by computational complexity and can be implemented on HPC,
- Develop methods for capturing and adjusting for data velocity and veracity across both temporal and geospatial scales,
- Understand the appropriate role of machine learning, agent-based models, and streaming analytics including feedback mechanisms, extensibility, and propagation of data veracity through those systems, and
- Develop mechanisms for semantically tuning lower-level learning systems in order to create robust automated solutions.

Objectives

By leveraging high-performance computing and big data analytics we will increase our understanding of transportation systems. Specifically, current transportation planners in urban areas do not have adequate tools for understanding the complex dynamics of their cities. Our objective is to create an ability to rapidly model urban scale transportation networks using real-world, near real-time data to optimize traffic for mobility, energy and productivity. Specific goals include:

- Learn patterns in the real-world data to inform our modeling with the goal of understanding how to respond to transient events such as accidents, emergency response and transportation network changes
- Investigate the drivers of those patterns and how we might impact those patterns to optimize modelling transportation networks for energy consumption in addition to the traditional emphasis on throughput.
- Develop control strategies for large-scale urban transportation networks through tractable computational simulations that can describe emergent behavior of vehicle dynamics
- Provide urban scale modeling tools that can integrate into urban planning and design processes and tools.

Approach

1. Define Appropriate Role of HPC in Transportation Planning
 - Determining the best use of HPC capabilities in the Transportation Planning field
2. Automated Collection, Modeling and Validation of Data Using HPC
 - Higher level algorithms that operate on historical data to predict future dynamics
3. Develop HPC Network Models
 - Modeling of urban scale transportation networks
4. Couple Data Ingestion into Modeling Platform
 - Define a common platform for the data ingestion and modeling tools. This includes data ingestion and preprocessing methods for raw data cleaning, error detection and correction, and missing data imputation
 - Real-world data will eventually come from the Connected Corridor program supported by CalTrans in Los Angeles.

Results

Task 1: Define Appropriate Role of HPC in Transportation Planning

The key focus of this task was to ensure the DOE computing facilities and embedded skill sets in high-performance computing are being used effectively to lend valuable insights to the transportation planning community. As such, the challenges of large-scale urban transportation modeling, as well as the challenges associated with next generation data acquisition systems (e.g., infrastructure and mobility sensing), in which big data analytics techniques transform raw sensed data into structural enhancements of transportation models, were chosen as core research objectives.

A lot has been accomplished in the three years of the BDSM project. The BDSM work efforts focused on building the core functionality of the Mobiliti parallel discrete event simulation platform. The Mobiliti simulation is being validated with a variety of industry and city transportation network data and will be used to develop scenarios that standard traffic assignment techniques cannot address. In addition, two core **real-world data sources** have been investigated - inductive loop data from the California highway system and GPS data from mobile devices (HERE Technologies probe data). These core data sources are driving and machine learning instantiation of a DCRNN model for predicting traffic speeds and flows at five-minute increments on the entire California highway system. Interest has been expressed, by two operational transportation groups, for installing this DCRNN model into real-world environments. Deployment of DCRNN methods within an

actual Traffic Management Center (TMC) for validation and improvement of incident detection capabilities and further identification of new applications will allow practitioners to understand the value of these next-generation techniques.

We have established strong relationships with the City of San Jose, San Francisco County Transportation Authority (SFCTA), San Diego Association of Governments (SANDAG) and the City of San Diego. We use our relationships with these organizations to not only validate the need for the research but also to understand real world applications and scenarios that would benefit the transportation community. The project was designed to focus on the LA region due to the relationship with the University of California- Berkeley (UCB) Connected Corridor (CC) which is implementing a real-time infrastructure sensing system across 5 cities in the LA Region. Recently, the UCB CC program has completed its Data Hub and we are working to integrate the CC data collection process into the platform we have developed for data analytics and urban scale simulation. The City of San Jose intends to make our work in Dynamic Traffic Assignment and urban scale simulation a foundational element in the planning processes going forward with a plan to integrate our findings into their Decision Support System design.

Task 2: Automated Collection, Modeling and Validation of Data Using HPC

Traffic Forecasting and Diffusion Convolutional Recurrent Neural Network (DCRNN)

Traffic forecasting approaches are critical to developing adaptive strategies for mobility. Traffic patterns have complex spatial and temporal dependencies that make accurate forecasting on large highway networks a challenging task. Diffusion Convolutional Recurrent Neural Networks (DCRNNs) have achieved state-of-the-art results in traffic forecasting by capturing the spatiotemporal dynamics of the traffic. Despite the promising results, DCRNNs for large highway networks remained elusive because of computational and memory bottlenecks. The effort to build a DCRNN for a very large highway network that is significantly larger than previous examples in the literature was a significant contribution from this project. To accomplish this, a graph-partitioning approach was used to decompose a large highway network into smaller networks and train them simultaneously on a cluster with Graphics Processing Units (GPU).

We forecast the traffic of the entire California highway network with 11,160 traffic sensor locations simultaneously (a first, as far as the project investigators are aware). The very large number of sensors is also important as we intend to extend these techniques to probe-based data as well. This example highway model can be trained within 3 hours of wall-clock time using 64 GPUs to forecast speed with high accuracy. Further improvements in the accuracy are attained by including overlapping sensor locations from nearby partitions and finding high-performing hyperparameter configurations for the DCRNN using DeepHyper, a hyperparameter tuning package. We demonstrated that a single DCRNN model can be used to train and forecast the speed and flow simultaneously and the results preserve fundamental traffic flow dynamics Figure I.2.3.1. It can be observed that the speed and flow forecast values closely follow the fundamental flow diagram with three distinct phases of congestion, bounded, and free flow. This forecasting pattern of DCRNN shows that the model has learned well-known properties of traffic flow. These prediction capabilities support the

overall goals of the project allowing for advanced highway traffic monitoring systems, where forecasts can be used to adjust traffic management strategies proactively given anticipated future conditions.

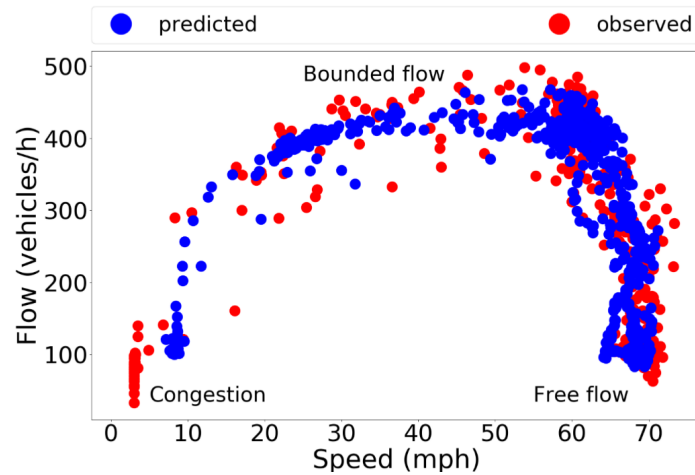


Figure I.2.3.1 Predicted Flow and Speed with Observed Flow and Speed Plotted in the Form of a Fundamental Traffic Flow Diagram, Demonstrating that the Model has Learned the Fundamental Diagram Behavior

For modeling the California highway network, data from the PeMS system was used. It provides access to real-time and historical performance data from over 39,000 individual sensors. The individual sensors placed on the different highway lanes are aggregated across several lanes and are fed into vehicle detector stations. The official PeMS website shows that 69.59% of the $\approx 18K$ stations are in good working condition. The remaining 30.41% do not capture time series data throughout the year and are excluded from our dataset. Thus, the final dataset has 11,160 stations for the year 2018 with granularity of five minutes. The data includes timestamp, station ID, district, freeway, direction of travel, total flow, and average speed (mph). For the experimental evaluation, ANL's Cooley, a GPU-based cluster at the Argonne Leadership Computing Facility, was used. It has 126 compute nodes, where each node consists of two 2.413 GHz Intel Haswell E5-2620 v3 processors (6 cores per CPU, 12 cores total), one NVIDIA TeslaK80 (two GPUs per node), 384 GB RAM per node, and 24 GB GPU RAM per node (12 GB per GPU). The compute nodes are interconnected via an InfiniBand fabric. The input data for different partitions (time series, and adjacency matrix of the graph) were prepared offline and loaded into the partition-specific DCRNN before the training started.

Transfer Learning with Graph Neural Networks for Short-Term Highway Traffic Forecasting

We have shown that deep-learning-based traffic forecasting methods can be successful at capturing traffic flow dynamics and can accurately predict speeds and flows. However, these methods require a large amount of training data, which need to be collected over a significant period of time. This can present a number of challenges for the development and deployment of data-driven learning methods for highway networks for which historical data has not been previously collected. We used transfer learning techniques to approach this problem. With transfer learning, a model trained on one part of the highway network can be adapted for a different part of the highway network. As described earlier in this report, a diffusion convolutional recurrent neural network (DCRNN), was developed for using historical data that was collected by Caltrans PeMS [*]. The DCRNN learns location-specific traffic patterns. The new modified model that includes transfer learning methods, TL-DCRNN, can learn from several regions of the California highway network and forecast the traffic on the unseen regions of the network with high accuracy. Specifically, we demonstrated that the TL-DCRNN can learn from San Francisco regional traffic data and can forecast traffic in the Los Angeles region and vice versa.

Task 3: Develop HPC Network Models

Urban Scale Transportation Network Simulation

A key area of development for this project was the development of a platform that will enable urban-scale simulation in reasonable compute times. Mobiliti is a distributed-memory, parallel simulation framework that runs on high-performance computing platforms. Over the life of the project, the core foundation of the parallel discrete event simulation was augmented to include more transportation related features. This included: adding vehicle controllers to implement dynamic vehicle rerouting behavior; developing improved maps for both San Francisco and Los Angeles metropolitan areas; and improving the demand models all the while maintaining parallel scalability to achieve high performance on distributed, parallel computing platforms.

Mobiliti is structured as a distributed parallel discrete event simulation, with actors that pass events among each other. The model includes link actors that are responsible for mediating vehicle dynamics. Vehicles are modeled as events that are passed among link actors. The link actors implement the movement of vehicles within the network as they move from their origin to their destination. In order to capture the behavior of vehicles that change their routes in response to unexpected or emergent congestion, we have added vehicle controllers, another class of actors that are responsible for servicing dynamic vehicle re-routing requests. Link actors periodically send updates about their congestion state to the vehicle controllers, which update their knowledge about the current status of the road network. Vehicles with active routing enabled can periodically check with a local vehicle controller to determine if a new route should be taken given this information.

In addition, the simulator can read a scenario input file that modifies the traversal time on the specified links at the specified times to mimic the impact of a traffic incident. Researchers can evaluate new scenarios by supplying their own files that modify the properties of the road network. We further enhanced the instrumentation of the simulator to capture relevant metrics such as vehicle controller behavior (number of reroute check requests, number of route calculations, number of vehicle diversions), vehicle behavior (differences in trip routes, times, distance, and fuel), and link behavior (impact on storage occupancy and utilization ratios).

We demonstrated how researchers might use the simulator to evaluate the impact of varying degrees of dynamic rerouting with an experiment that simulated a hypothetical traffic incident that caused a major slow down on the US-101 freeway in San Francisco (Figure I.2.3.2 below).



Figure I.2.3.2 Hypothetical Incident Location in Red

We did a parameter sweep for different penetrations of vehicles with dynamic rerouting capability and showed how major alternative arterials were able to absorb the diverted traffic off of the US-101 freeway. Figure I.2.3.4 and Figure I.2.3.5 below show the impact of dynamic rerouting on flow rates for the road network around the traffic incident.

This was a demonstration of the type of experiment mobility researchers can conduct with our simulator. Further details about these types of experiments will be reported in a paper that we have submitted for publication. We have also improved various other aspects of the link model, including the addition of a link storage capacity constraint that captures upstream spillback as links become congested.

In addition to capturing link dynamics accurately, it is important for the Mobiliti simulator to be able to take advantage of the most realistic road network data and demand data available for accurate results. To this end, we have implemented additional software modules to load and clean map data from HERE Technologies and trip data from both the SFCTA's newest CHAMP6 demand model and the LA SCAG data set. These improvements have increased the spatial resolution of the simulated trip legs by specifying trips using multi-level traffic analysis zones for origin and destination node selection, as well as the temporal resolution by specifying start times at the granularity of minutes rather than multi-hour time periods. Furthermore, the new model includes metadata to associate multiple trip legs to the same persons and the purpose of each trip leg, which will enable researchers to model electric vehicle charging choices and vary the time spent at each stop.

We have also improved other aspects of the simulator such as the quality of the link actor partitioning, which is important to achieve scalable performance for parallel execution. Even though dynamic rerouting is very computationally expensive due to the large cost of each new routing calculation on large graphs, we have successfully run our simulator for the San Francisco Bay Area (1.1 million nodes and 2.2 million links with 22 million trip legs) with dynamic re-routing enabled in just a few minutes of parallel execution on up to 512 cores of the Cori computer at NERSC. (See Figure I.2.3.3.)

Dynamic Traffic Assignment

The BDSM project began with a goal of integrating traffic assignment capabilities into the platform. Traffic assignment tools are often the core focus of city planners as it represents an optimization of traffic flow across the network—in some sense a best outcome for travelers. The complexity of the computational methods often limits the capabilities of these tools. Consequently, planners break the day into time segments, ranging from 2 hours to 4 hours, in order to be able to run scenarios in a reasonable time frame—e.g., a day scenario may take on the order of 24 hours of compute time. Our first step was to parallelize the traffic assignment in order to take advantage of the independence associated with routing the travel demand. The platform was designed so that the traffic assignment algorithms could directly access the same network and travel demand models that the Mobiliti has access to for a full day simulation run. Because a typical traffic assignment has no notion of time, an approach for addressing the time dynamics of the traffic was developed. This approach created an initial time step of interest, (e.g., two hours), assembled the travel demand for the initial two hours, and used a Frank-Wolfe algorithm to find an optimized assignment for the time step. Recognizing that the travel demand in that two-hour period would not be fully serviced in the two hours, the algorithm determines the residual travel demand at the end of the period. This residual demand represents the trips that started during the period but did not realize their goal destination. The residual demand is then added to the next two-hour time period and the optimization is run again. Several key modifications of this approach have been implemented including: updating the method to partially reassign routes during DTA optimization iterations in order to select better available paths through the network; truncating routes before link re-weighting to ignore each vehicle's impacts on links traversed after the current time segment; implementing a line search to identify an optimal step size (replace method of successive averages) for each iteration of Frank-Wolfe algorithm; and parallelizing the line search algorithm and link weight updates. This has significantly improved the



Figure I.2.3.4 Traffic Flow without Rerouting



Figure I.2.3.5 Traffic Flow with Rerouting

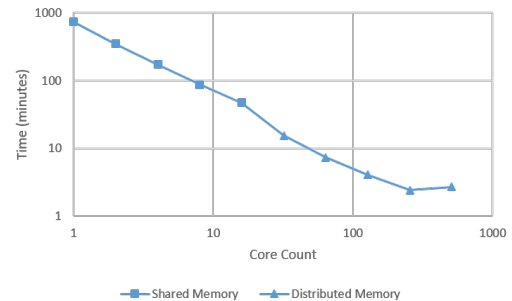


Figure I.2.3.3 Simulation Parallel Scaling with 100% Active Vehicle Rerouting Penetration on Cori

computational performance of this optimization algorithm. Due to the improved computational performance, we can improve the fidelity of temporal aspects by reducing the time step to 15 minutes. We are now able to run a DTA scenario (full Bay Area network with a 15 million trip leg demand across the day) at 15-minute time intervals and generate full-day results in a matter of minutes.

Energy Modeling:

To estimate the energy impacts of a particular drive trace, a data-driven methodology to estimate vehicle energy/fuel usage was developed to provide a fast and reasonably accurate estimate of the energy usage of a particular driving pattern (Speed versus Time), which will ultimately be predicted using a similar process to the DCRNN traffic predictions discussed above. To these ends, representative vehicles were chosen from Argonne’s Dynamometer Database and used as a trial set for a simple, data-driven energy consumption prediction based on vehicle speeds and accelerations for a particular drive cycle. Figure I.2.3.6 highlights the vehicles used for a preliminary (and BEV/Conventional) assessment of the techniques.



	2015 BMW i3 EV	2018 Mazda CX-9	2012 Ford Focus ST	2018 Chevrolet Bolt EV	2017 Ford F-150	2017 Toyota Highlander
Technology	22 kWh 360 V Li-Ion, direct drive, EV	Turbocharged I4, 4 valve per cylinder	Turbocharged I4, 4 valve per cylinder, direct injection	60 kWh, ~400V, Li-Ion, direct drive EV.	Twin-turbocharged and intercooled DOHC 24-valve V-8, VVT, aluminum block and heads, port & direct fuel injection	DOHC Atkinson cycle, Direct Injection V6, all aluminum, VVT-i.
Motor/Engine	25 kW (168 bhp)	2.5-liter SkyActive, 89 x 100 mm, 2,488 cc, 13.0:1, 186 kW (250 hp) @5000 RPM, 310 lb-ft @ 2,000 rpm (420 N-m)	EcoBoost 2.0L I4, 2000cc, direct injection, 184kW @ 5500rpm, 360Nm from 1750 - 4000rpm, Compression ratio: 9.3:1 Bore x stroke: 87.5/83.1mm	Permanent magnetic drive motor 150 kW (200hp) 266 Nm (266 ft-lb)	EcoBoost 3.5L v6, 3500cc, direct injection, 280 kW (375 HP) at 5000 rpm, 637 N-m (470 lb-ft) at 2250-3500 rpm, Compression ratio: 10.5:1 Bore x stroke: 92.5/86.6 mm	3.5 litres (3,456 cc), 24-valve DOHC V6 engine 207 kW (278 HP) at 6000 rpm and 359 N-m (265 lb-ft) at 4600 rpm.
Transmission	1 speed direct drive	6-speed automatic	6-speed automatic/manual	1 speed direct drive	10 speed automatic	8-speed shifttable automatic
Battery	60Ah (18.8 kWh)	-		60 kWh 350 V lithium-ion		
City/Hwy [mpg]	137 MPG-e (25 kW-hrs/100 mi)/ 111 MPG-e (30 kW-hrs/100 mi)		29 City / 32 Hwy	128 City / 110 Hwy	City: 16-19 / Hwy 21-26	20 City / 26 Hwy

Figure I.2.3.6 Preliminary Vehicles Assessed for Data-Driven Estimation Technique

Using the laboratory data and specific information about the vehicle, evaluated speed traces can be mapped into a scatter of speed/tractive force points which correspond to the cycles evaluated within previous laboratory testing. This process is summarized below in the left (speed vs. time) and right (tractive load versus speed) subplots in Figure I.2.3.7 below.

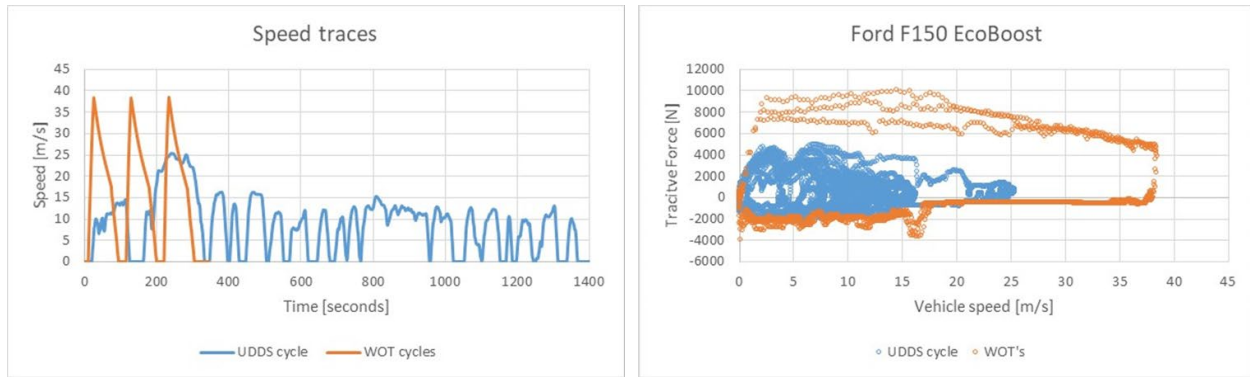


Figure I.2.3.7 Example Speed Vs Time and Corresponding Tractive Force Vs Speed Plots for Two Example Drive Cycles

If sufficient data is provided from laboratory testing, the entire speed/force chart can be supplemented with an expected instantaneous fuel or battery energy usage, which can then be used to sum energy across various time-steps and calculate overall energy/fuel usage.

A variety of data-driven, machine learning based methods were assessed for this prediction but ultimately a boosted decision tree methodology, based on XGBoost, was used for its fast response and accuracy for the candidate datasets used. Future work may refine or modify this methodology, but high accuracy results are still expected for a range of techniques. Training data for the proposed estimation was taken from laboratory testing across the UDDS, Hwy, and US06 drive cycles, supplemented by “Wide-Open-Throttle”, maximum acceleration-based tests to provide the maximum operational envelope for a particular vehicle. While all vehicles evaluated showed very accurate energy estimates across a range of drive cycles, Figure I.2.3.8 below highlights results for a Chevrolet Bolt Electric Vehicle. Even for drive cycles not used in training, the proposed method predicts the energy consumption within less the 1% of actual, well within a reasonable error for integration into the Mobiliti platform.

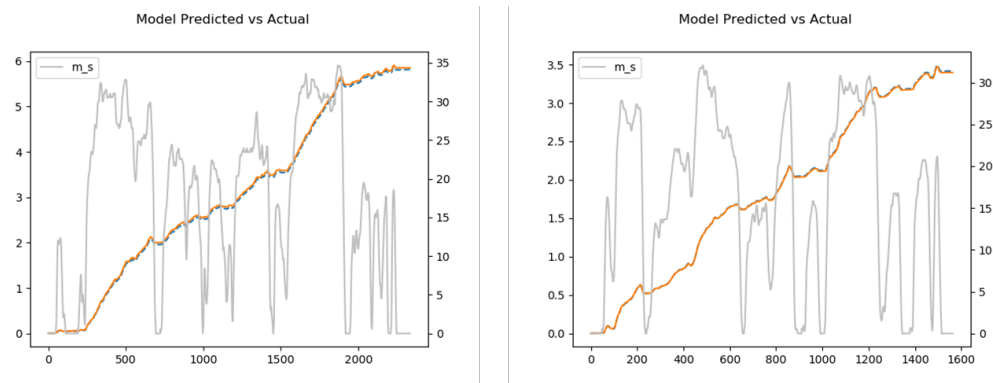


Figure I.2.3.8 Chevrolet Bolt Predicted Versus Actual Energy Consumption

Ultimately, these data-driven predictions will enable us to better understand the energy implications of a particular link’s driving dynamics as predicted by traffic flow trends generated by the DCRNN prediction capabilities discussed above. Overall, the initial results showed a 1.5% error for a conventional gas-powered vehicle and 0.5% error for an electric vehicle.

Task 4: Couple Data Ingestion into Modeling Platform

This task is focused on integrating the data-driven learning models into the simulation capabilities. While the models themselves can provide significant value to the community, our specific goal was to inform the simulation capabilities with these models in order to improve the foundational elements of the simulation.

Specifically, link travel dynamics are often significantly simplified in many meso simulations and a travel time is computed for the link, often using the BPR function. These simplifications make these types of models inadequate for predicting energy consumption. The DCRNN model provides specific dynamics as a function of the time of day reflective of the fundamental diagram overall and including more detailed drive cycle dynamics that were encapsulated in the sensor data it was derived from. Our intent is to integrate this capability into the link agents in the Mobiliti platform so that the link dynamics are reflective of the data that we see in the real world and also so that the routing agent can take advantage of the predictive capability of the DCRNN model to provide improved routing solutions for the vehicles that approach congestion. We have completed initial DCRNN link model integration, in which DCRNN Server actors are instantiated in bounded neighborhoods of the network. Link Actors periodically send status updates to DCRNN Servers and DCRNN Servers periodically execute a TensorFlow model to infer link speeds and send updates back to constituent Link Actors. The Link Actors can then use the DCRNN inferred speed to override a defaulted BPR delay model. This integration will now allow the platform to consider future congestion in the route planning algorithms. With this capability, more realistic dynamic responses can be simulated, and next generation transportation management techniques can be proposed and investigated.

Conclusions

The BDSM project work efforts have been focused on building the core functionality of the Mobiliti parallel discrete event simulation and to achieve a data-driven approach, two core **real-world data sources** have been investigated - inductive loop data from the California highway system and GPS data from mobile devices (HERE Technologies probe data). Using the inductive loop data, a machine learning instantiation of a DCRNN model for predicting traffic speeds and flows at five-minute increments on the entire California highway system was created using HPC resources. Initial efforts have been made to deploy the DCRNN in an actual TMC (with a TMC partner) for validation and improvement of incident detection capabilities. Evaluation of funding opportunities to support it are underway. We have demonstrated transfer learning at this initial highway level and can use this model interchangeably between Los Angeles and San Francisco. We are extending this approach to include GPS data which we will use to extend its application deeper into the road network graph. Our initial work to use machine learning to evaluate and predict the geospatial, temporal device data has shown promising results. Specifically, Temporal Convolution Networks had been applied and appear transferable for our initial traffic estimation problem. Automated hyper-parameter search and tuning has been developed and allow efficiencies that will be foundational to our future work. Initial efforts are underway to consider data veracity issues associated with big data feeds from a variety of mobile devices. Algorithms to detect and correct poor data quality are being developed for both ingestion at real-time and quasi real-time. Our urban simulation work has leveraged an existing code base for grid simulation and has allowed us to build urban-scale simulations of the Bay Area and LA Basin road networks with run times on the order of minutes. We support simulating the SFCTA and LA SCAG demand models that specify 20M and 41.6M vehicle trips, respectively. We have demonstrated the capability to simulate and evaluate the impact of active dynamic routing at metropolitan scale. We have also improved our link model to include a storage capacity constraint. This type of behavior is much more reflective of real-world urban dynamics. Energy modeling has been tied to the foundational simulation mechanisms and models fuel consumption using the dynamometer derived data from ANL. NREL has provided additional input to this initial model and on-going improvements to this model are underway.

Key Publications

1. Mobiliti: Scalable Transportation Simulation Using High-Performance Parallel Computing IEEE Intelligent Transportation Systems Conference; Cy Chan, Bin Wang, John Bachan, and Jane Macfarlane
2. "Transfer Learning with Graph Neural Networks for Short-Term Highway Traffic Forecasting." 2020 International Conference on Pattern Recognition (ICPR), Mallick, Tanwi., Balaprakash, Prasanna., Rask, Eric., Macfarlane, Jane.

3. Graph-Partitioning-Based Diffusion Convolution Recurrent Neural Network for Large-Scale Traffic Forecasting, TRB 2020: Tanwi Mallick, Prasanna Balaprakash, Eric Rask, Jane Macfarlane, Accepted for Transportation Research Record
4. Assessing the Equity Implications of Localized Emissions Impacts From Transportation Using Dynamic Traffic Assignment A Case Study of the Los Angeles Region, Submitted to DTA 2020: Jessica Lazarus, Ioanna Kavvada, Ahmad Bin Thaneya, Bin Wang, and Jane Macfarlane
5. Assessing the Equity Implications of Localized Congestion and Emissions Impacts of Four Traffic Assignment Scenarios in the Los Angeles Basin, TRB 2020: Jessica Lazarus, Ioanna Kavvada, Ahmad Bin Thaneya, Bin Wang, and Jane Macfarlane
6. A traffic demand analysis method for Urban Air Mobility," by Bulusu, Vishwanath; Onak, Emin; Sengupta, Raja; Macfarlane, Jane, Submitted to Special Issue on Unmanned Aircraft System Traffic Management) IEEE Intelligent Transportation Systems Transactions.
7. Kanaad Deodhar, Colin Laurence, Jane Macfarlane. 2019. Creating "Mode Shift Opportunity" with Metropolitan Scale Simulation, SCC 2019 Conference Portland OR,

I.2.4 Transportation State Estimation Capability (PNNL)

Robert Rallo, Principal Investigator

Pacific Northwest National Laboratory

Richland, WA

Email: robert.rallo@pnnl.gov

Prasad Gupte, DOE Technology Manager

U.S. Department of Energy

Email: prasad.gupte@ee.doe.gov

Start Date: October 1, 2017

End Date: December 30, 2020

Project Funding: \$1,800,000

DOE share: \$1,800,000

Non-DOE share: \$0

Project Introduction

Traffic congestion is a worldwide problem that results in increased travel times, high fuel consumption and excessive emission levels. A recent report (<https://inrix.com/press-releases/2019-traffic-scorecard-us/>) highlights that, on average Americans spend 99 hours waiting on congested roads, costing them nearly \$88 billion in 2019. Transportation system providers need improved situational awareness tools to guide transportation network management decisions aimed at reducing the impact of congestion to increase the efficiency of urban mobility systems. However, efficient operation is challenging due to the limited coverage of traffic sensors (i.e., partial observability) and the complex dynamics of urban traffic [1],[2].

To address the above challenges, PNNL has developed the Transportation State Estimation Capability (TranSEC), a computational tool that provides a scalable implementation of data-driven traffic state estimation. Our approach combines data assimilation with traffic flow analysis to provide data-informed estimates of the network state. PNNL's TranSEC solves travel time estimation in large-scale metropolitan networks [3],[4] using multiple sources of heterogeneous and sparse traffic data. Examples of traffic information that can be integrated in TranSEC include aggregated data (e.g., UBER travel times), point data (e.g., loop counters), and probe-like data (e.g., transit systems). Using any combination of the above information, the tool provides traffic status estimations without needing the full information of traffic flows at the street level. The approach has been demonstrated for large metro areas such as Los Angeles and Seattle.

Background. TranSEC emerged as a logical outgrowth from the VTO/EEMS funded Big Data Systems for Mobility (BDSM) project. BDSM's objective was to develop the data science and HPC supported computational framework for next-generation transportation/mobility system models and operational analytics, working to ensure that models and analytics scaled across spatial and temporal complexities. Key BDSM objectives included developing methods for capturing and adjusting for data velocity and veracity across both temporal and geospatial scales, and exploring roles for machine learning and streaming analytics, including extensibility and propagation of data veracity.

PNNL's role in pursuit of these objectives was to develop scalable methods and infrastructure for the near real-time ingestion, integration and analysis of heterogeneous traffic data to support LBNL/ANL modeling efforts. This included identifying traffic optimization opportunities, data and associated measurements that could inform models and serve for model parameterization and validation in various real-world scenarios, and addressing questions related to road link capacities (e.g., nominal and effective) and effective usage under differing yet common scenarios (speed limits, time of day, construction, weather, special events, accidents, etc.)

Objectives

The aim of this project is to develop a data-driven approach that efficiently adapts to local traffic patterns to provide current and localized estimates of traffic flow patterns and behaviors using a combination of streaming

and historical data. TranSEC differentiates from other traffic monitoring methods by its ability to integrate and analyze sparse and incomplete information at multiple aggregation levels to provide near real-time traffic estimates at the street level. The approach in TranSEC builds on earlier work developed at PNNL on scalable data analytics, transportation systems, electrical grid analysis and modeling. Specific objectives include:

- Develop scalable algorithms for scalable traffic state estimation from sparse heterogeneous data
- Identify relevant data sources to validate the estimation method in large metropolitan networks
- Develop efficient UQ (uncertainty quantification) methods to characterize the uncertainty of the estimates
- Implement a web-based tool to demonstrate the approach to relevant stakeholders.

Approach

The technical approach implemented in TranSEC covers four R&D areas:

- 1. Define the role of HPC and data analytics in transportation planning and operations**
 - a. Determine the best use of HPC capabilities in the transportation field with emphasis on data-driven traffic state estimation via graph analytics and large-scale optimization
- 2. Automate collection, correction and validation of multi-modal traffic data**
 - a. Identify sources of real-world multi-modal data relevant for traffic state estimation.
 - b. Assess the accuracy-complexity trade-off of diverse anomaly detection and missing data imputation methods to ensure operation close to real time
 - c. Develop optimized ingestion pipelines for each data modality
- 3. Develop traffic state estimation methods that can scale from commodity computing to HPC resources**
 - a. Develop a scalable data-driven methodology for traffic state estimation
 - b. Provide relevant accuracy and uncertainty quantification metrics for validation
- 4. Implement a prototype tool for travel time estimation in large-scale metropolitan networks**
 - a. Develop a web-based tool to demonstrate the data-driven traffic state estimation approach
 - b. Refine the tool by collect feedback from relevant stakeholders.

Results

Task 1: Define the role of HPC and data analytics in transportation planning and operations

Demonstrate scalability of the traffic state estimation method in large-scale metropolitan networks. We have developed and validated a distributed implementation of the traffic state estimation algorithm which outperforms the initial serial solver without introducing significant accuracy loss. The main achievements include:

- Completed the exploration of two distributed strategies for scaling the TranSEC travel time estimation solver, namely splitting across sampled trips and splitting across spatial partitions. After extensive experimentation, splitting across spatial chunks was selected as the preferred method.

- Interfaced the code with Metis, a well-known graph partitioning tool, to split large road networks into near-equal sized partitions with minimal cut edges.
- Extended the code to work in parallel with multiple road networks, each one corresponding to a spatial partition.
- Designed and implemented a heuristic approach to estimate the travel time for the links in neighboring partitions by ensuring the continuity of speeds when aligned with adjacent links.
- Completed the distributed code where the head node does the spatial partitioning, each spatial fragment is solved on a different node of the cluster and finally the head node completes the stitching of the cut links using the heuristic described above.
- The distributed approach enables TranSEC to compute travel time estimates for any metropolitan area with computational resource constraints, i.e., TranSEC can be used to estimate travel times using a laptop as well as using a supercomputer.
- The distributed solver was demonstrated on multiple geographical areas (LA and Seattle metropolitan networks) and a significant speed-up was observed over the serial case.

Scalable approach to uncertainty quantification. The use of secondary data sources avoids introducing bias during the performance evaluation of a data-driven method. However, the stochastic nature of our approach to traffic state estimation requires also the quantification of the uncertainty introduced during the mathematical optimization process. To this end, we use Monte Carlo methods to characterize the variability of the results and to provide lower and upper bounds for each estimate. The Monte Carlo approach requires running each estimation process hundreds of times to develop accurate statistics since single time execution is insufficient to fully capture the system variability. Performing this level of validation increases TranSEC’s computational requirements and justifies the need of HPC resources for the distributed execution of the solver.

The use of data at different levels of aggregation constitutes the main source of uncertainty in our formulation. For instance, using aggregate UBER data require sampling trip times from the (traffic analysis zones) TAZ-TAZ statistics which follows a heavy-tailed distribution. To facilitate sampling, we approximate the original distribution by a parameterized log-normal distribution. In addition, we also uniformly sample the trip origin and destination from the corresponding origin and destination TAZs. Further, given the complexity of the estimation process, we implemented a traditional Monte Carlo analysis as our method of choice for performing UQ analyses. The UQ workflow was implemented for the partitioned (distributed) and the non-partitioned (serial) cases. Figure I.2.4.1 shows a comparison of the estimated distributions for both the cases.

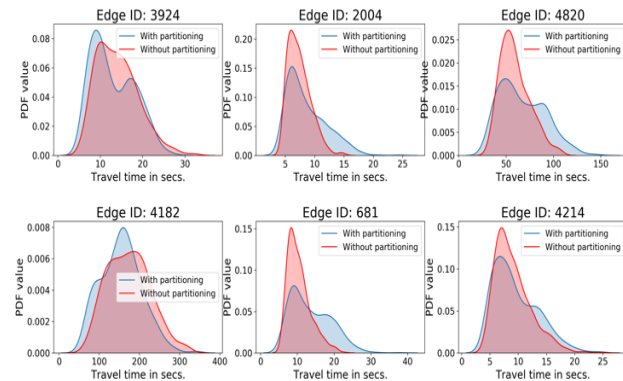


Figure I.2.4.1 Comparing the Results of Estimated Distributions of Travel Times for 6 Randomly Chosen Links in the La Downtown Network With and Without Spatial Partitioning

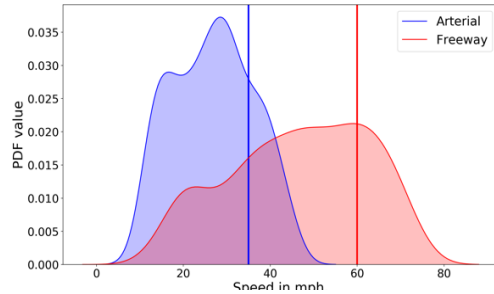


Figure I.2.4.2. Illustrating the Estimated Speed Distributions on Weekdays for a Downtown La Arterial and a Freeway Link Along with their Respective Speed Limits

network-wide formal comparison of the travel time distributions computed from partitioned and non-partitioned workflows, we developed a novel scheme involving the cumulative distribution of the Wasserstein distance between the normalized travel time distributions over the full set of the links present in our network. This workflow was applied to both the LA and the Seattle downtown areas. The cumulative distributions are visualized in Figure I.2.4.3. The results show that the spatial partitioning strategy does not affect the travel time distribution for nearly 71% of the links in the LA network and nearly 52% of the links for the Seattle network based on a stricter distance metric threshold $D = 0.75$. For a looser threshold for $D = 1.0$, this number improves to 85% and 71% respectively.

Figure I.2.4.3 shows the distributions of the estimated speeds for an arterial link with 35 mph speed limit and a freeway section (on Interstate 10), both, with the LA downtown area and for weekdays. The speed distribution was estimated from the travel time distribution, and with the knowledge of the link lengths. As seen, the estimated speeds show variation around the speed limits with a higher probability mass below the speed limit (77% and 75% respectively), in line with the weekday traffic expectations. To facilitate a

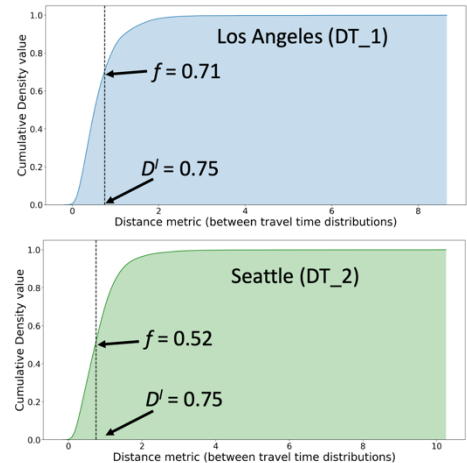


Figure I.2.4.3. Wasserstein Distance – Cumulative Distribution Function for Both Los Angeles (top) and Seattle (bottom)

Task 2: Automated collection, correction, and validation of multi-modal traffic data

Data ingestion pipeline. The main accomplishments in this task include:

- Established streaming data collection pipeline from multiple sources including:
 - Caltrans Loop Detector data via ftp protocol for various Caltrans districts that cover the L.A. basin, with main focus on district 7 that has L.A. County. Data acquisition rates are of 30 seconds for raw data and 5 minutes for Caltrans processed data.
 - Weather data from 14 cities in the L.A. Basin using OpenWeatherMap API.
 - GPS Traces for various bus services in the L.A. Basin, with data being collected every minute and with particular focus on L.A. Metro (Bus).
- Deployed a scalable time-series database (InfluxDB) to support data ingestion and querying. Also, explored InfluxDB's data visualization tool: Chronograf.
- Established data imputation (filling missing data) methodologies for near real-time data using various machine learning techniques. While some of the methodologies gave better accuracy, albeit with higher computation costs, others provided reasonable accuracy-performance trade-offs (Figure I.2.4.4).

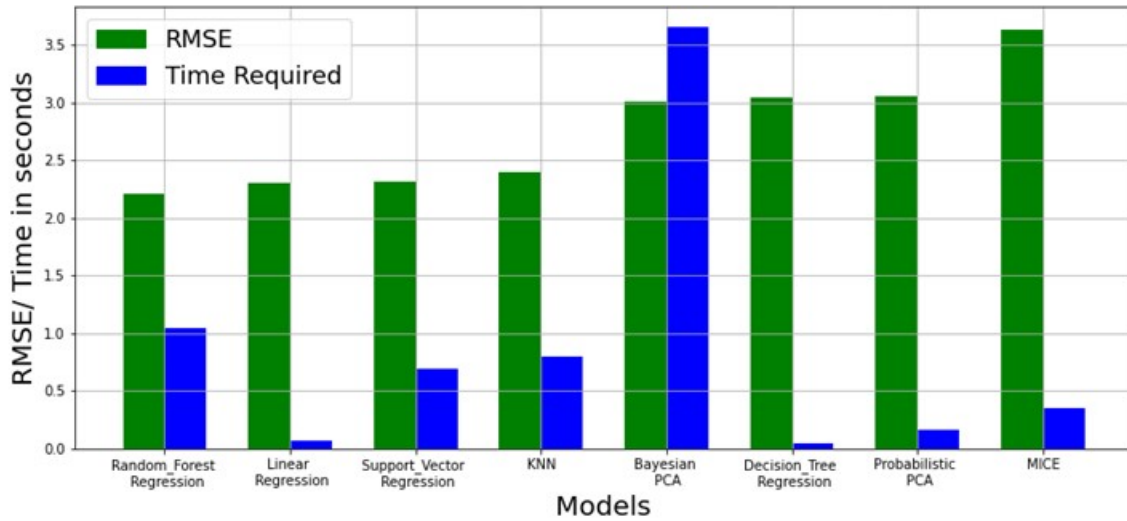


Figure I.2.4.4 Accuracy/Cost Trade-Off for Different Data Imputation Methods. Weekday 5am-10pm Using 5 Immediate Neighboring Sensors as Reference

- For the various approaches, we looked into near past data as well as neighboring detector data for imputation. Figure I.2.4.5-Figure I.2.4.8 below depict some of the results obtained using different computational cost-efficient approaches that allow real time data reconstruction:

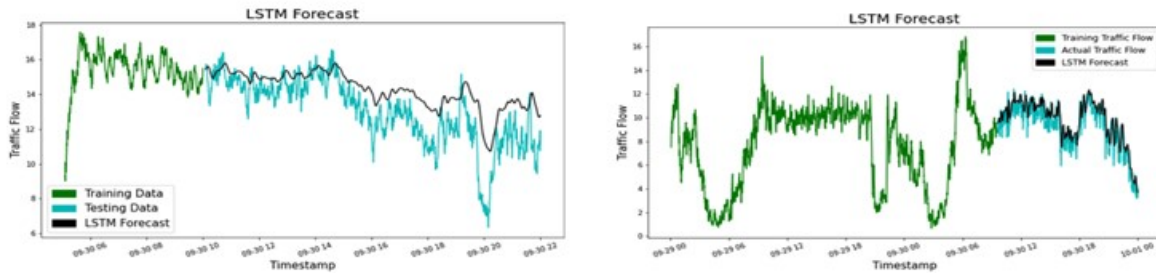


Figure I.2.4.5 Data Imputation with Long-Short Term Memory (LSTM) Neural Networks Using Two Different Sensors with Short and a Long Data Window for Model Training

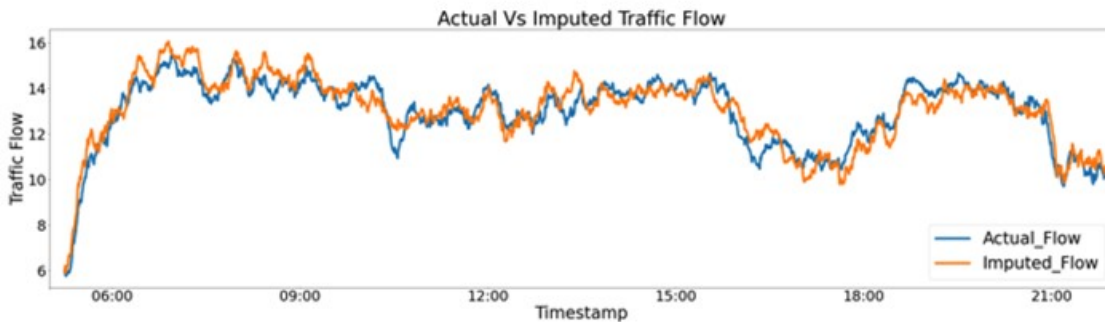


Figure I.2.4.6 Data Imputation Using a Regression Tree Algorithm

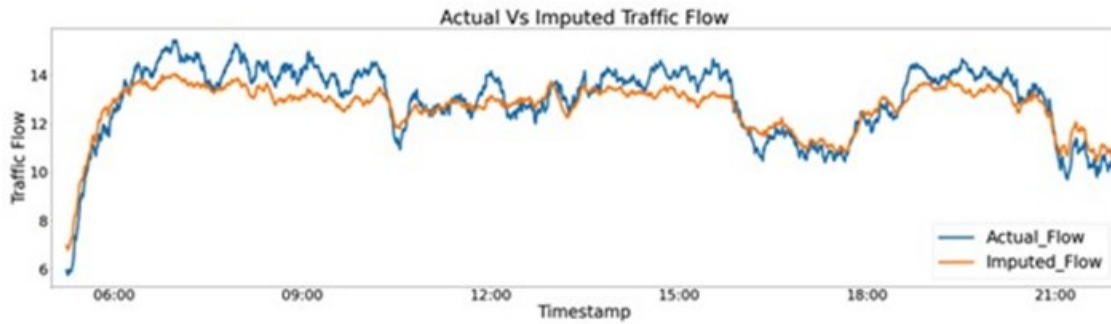


Figure I.2.4.7 Data Imputation Using a K-Nearest Neighbor (KNN) Algorithm

- Established preprocessing methods for probe-like data including GPS traces.
 - Identification and filtering of duplicate data. Bus location data are collected every minute via a REST API. An individual bus may report its trace data at intervals lower than a minute generating duplicates (i.e., same GPS traces values but with different time stamps). To remove duplicated data, we developed a multicore parallel codebase that provides the basic cleaning services for probe data.
 - Map Matching. Real world GPS traces are not always guaranteed to be mapped to the exact location where the GPS device was located (e.g., tall buildings, weak GPS signal). We have established a codebase that utilizes *Open Source Routing Machine* (OSRM) tool to map-match the GPS coordinates to the nearest road, within a certain radius from the actual recorded GPS location. The GPS trace data is discarded, if a map point is not found within the predefined radius.

Integration of additional data modalities and independent data for validation. Identified and processed additional data modalities (bus, loop detector and traffic camera) for integration with TranSEC data-driven state estimation capability. We developed different methodologies and identified appropriate tools for processing the data.

- Caltrans (District 7) – Loop Detector data. Developed a workflow for processing the data collected in near real time and mapping them onto the OpenStreetMap, using the location coordinates of the loop detector stations as well as the network representation attributes defined in the OpenStreetMap. Being able to map these data streams provides real-world vehicle flow data for baselining and extending our data-driven traffic estimation approach.
- NextBus Bus Fleet data (L.A. Area). Data are collected in near real-time. These probe-like data are useful for understanding traffic dynamics in arterial roads, where data are scarce. We developed filters to find and remove data duplicates. Duplication is due to the data aggregation process at the centralized data collection system. The code developed removes duplicates and applies the correct time stamps to the retained probe data. We also implemented a scalable map matching algorithm (*Fast Map Matching*, FMM) to map the collected data (i.e., gps coordinates) onto the open street map (i.e., specific road segments). Figure 8 shows the result of the map-matching process.



(a) Original GPS locations

(b) Map-matched route

Figure I.2.4.8. (A) Original GPS Coordinates Reported by the Bus. (B) Corresponding Map-Matched Trajectory Using FMM

- Traffic Camera Data.** We extended a “car counter” tool based on “object detection” using deep learning methods. For a given sample data feed, the tool counts the number of vehicles within a selectable region. While higher quality video feed gives more accurate result, the tool provides relatively good result for vehicle counts using low quality video data. Vehicle classification is more sensitive to the quality of the video stream. Figure I.2.4.9 shows an example of traffic camera repurposing to provide vehicle classification and vehicle counts.



Figure I.2.4.9 Vehicle Detection/Counting Within a Predefined Area of Interest (Red Polygon)

Task 3: Develop the traffic state estimation methods that can scale from commodity computing to HPC resources

The main achievements include:

- Expanded the coarse-level TAZ-TAZ travel time estimation algorithm to provide estimates at the street-level for a full metropolitan network. The basic workflow for travel time estimation using aggregated UBER movement data is outlined below:

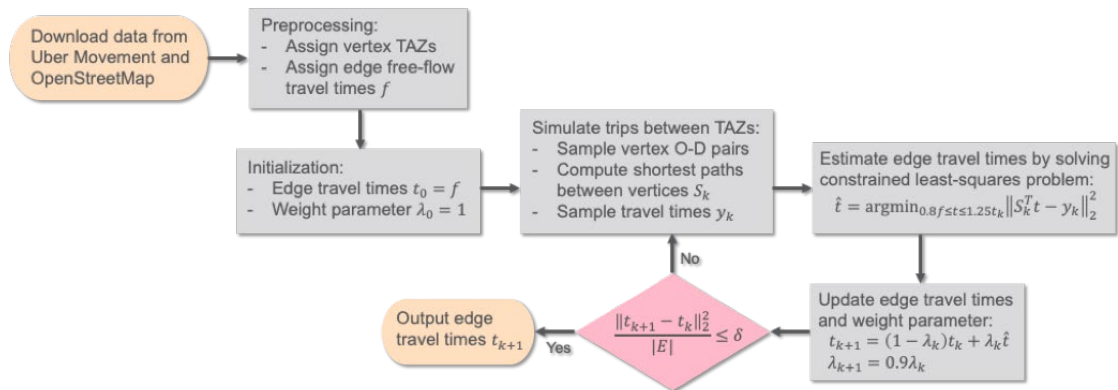


Figure I.2.4.10 Travel Time Estimation Workflow

- The new algorithm includes improved sampling strategies for trip generation from TAZ-level data. Initially, the number of trips generated for each TAZ is proportional to its size. Additional strategies that will be incorporated in the current approach include the use of metrics based on population density and land use. We will also explore the interfacing with trip demand models when these are readily available.
- The “observed” routing strategy is extracted from data during the sampling of the O-D matrix. Additional routing strategies corresponding to diverse traffic optimization targets can also be implemented in the model (e.g., shortest path, network communicability).
- The distributed solver was evaluated on two different geographical areas and a significant speed up was observed over the serial implementation. The distributed solver can estimate hourly weekday travel times the full LA metro network in 30 mins. using 1280 cores on a PNNL supercomputer whereas the serial solver takes about 19 hours on a single node.
- Travel time estimates have been demonstrated for LA and Seattle (including their associated metropolitan areas). Results shown below (Figure I.2.4.11) correspond to LA at 6pm in a weekday (upper figure) and the evolution of traffic in Seattle from 4pm to 6pm (lower figure):

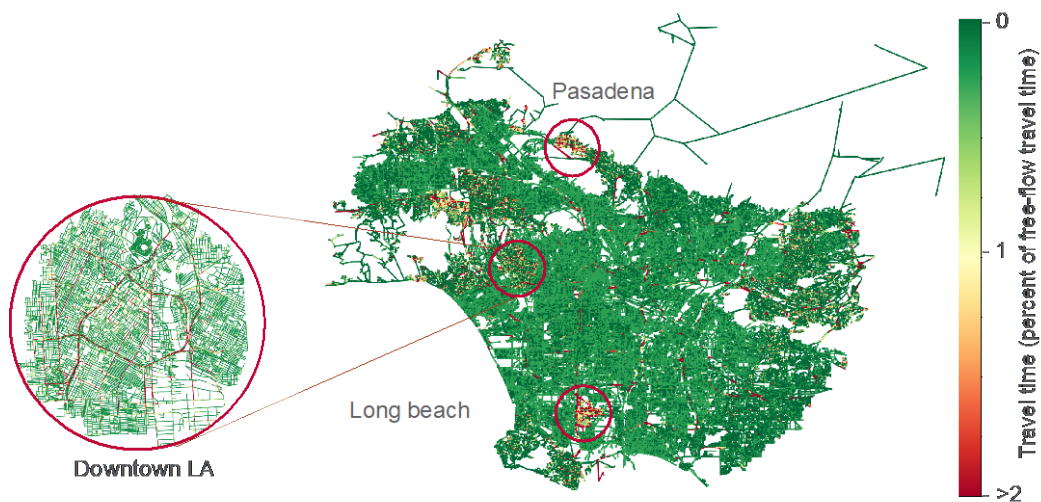


Figure I.2.4.11 Visualization of The Travel Time Estimates Obtained from Transec for the Whole LA Basin Area At 6pm on a Weekday

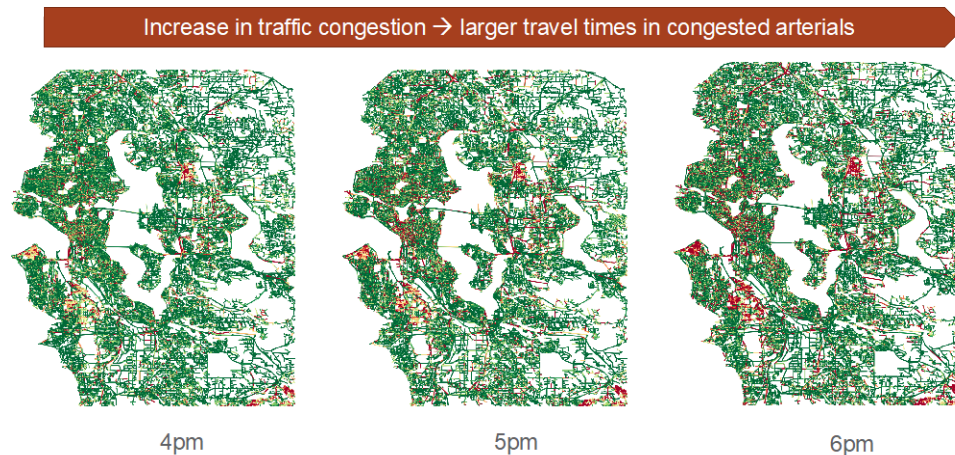


Figure I.2.4.12 Visualization of the Travel Time Estimates Obtained from Transec for Seattle and its Metropolitan Area During the Period of 4pm to 6pm

Task 4: Implementing a prototype tool for travel time estimation in large-scale metropolitan networks

Developed a web-based prototype tool (Figure I.2.4.12) that implements the TranSEC approach. The map visualization framework selected to develop the web-based tool is DeckGL, an opensource library developed by Uber. The prototype visualization tool includes the following features:

- Dropdown menu to select various traffic attributes. This allows the user to select an attribute to be shown among the edges of the map. Attributes available contain information such as the computed betweenness values, travel time, percent travel time, etc. For the latter two, the user may select an hour from 7AM - 7PM to display the appropriate values as they change.
- Edge coloring based on selected attribute. To better understand trends occurring throughout the map, each edge is assigned a color based on its normalized value, going from green (minimum) to red (maximum). The min/max values used by the tool is adjustable by the user, either via a slider or manual entry. However, the user can also hover over an edge if they wish to view a specific value, where doing so renders a tooltip with the information.
- Toggle selection to change map style. The map tile service being used for the prototype, Mapbox, provides multiple styles for displaying the map. This variety is something which the prototype passes along to the user, allowing for seamless shifting between Light, Dark, and Satellite map styles.
- Downloading GraphML files from OpenStreetMap (OSM) based on a selected bounding box. This permits a streamlined way of obtaining OSM data without needing to learn the programming interface. Using the bounding box calculated based on the current viewport, an associated GraphML file is downloaded.
- Reduce the time between attribute changes. Previously, changing an attribute/time-of-day required downloading all the graph edges, leading to undesired amounts of time spent loading redundant data. Instead, we load all the attributes on the first request so that swapping between them automatically updates the visualization shown within the browser.

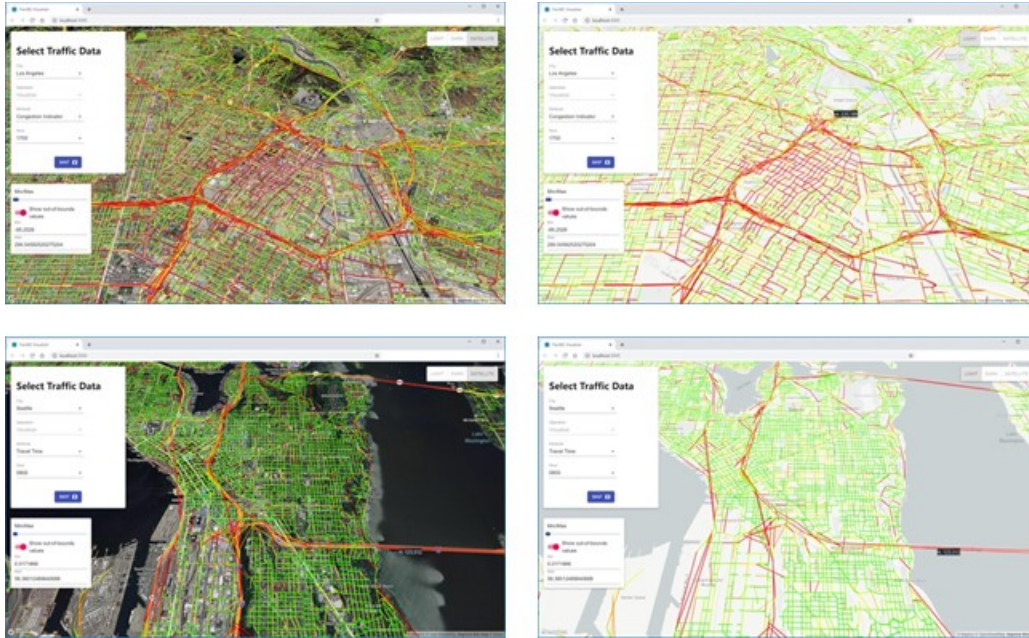


Figure I.2.4.13 Visualization of Congestion Patterns (Deviation with Respect to Free-Flow Travel Times) in Downtown LA

Conclusions

TranSEC delivers a new approach to help urban transportation analysts discover system optimization opportunities to reduce congestion. TranSEC helps urban traffic engineers get access to actionable street-level information about traffic patterns in their cities. Currently, publicly available traffic information at the street level is sparse and incomplete. Our approach facilitates the integration of traffic datasets collected from public and proprietary sources to map street-level traffic flow over time. It creates a big picture of city traffic using data analytics, optimization and leveraging the computing resources available at a national laboratory. TranSEC's data-driven approach means that as more data are acquired and processed the resulting estimates become more refined and useful over time. This kind of analysis helps traffic engineers to understand how disturbances spread across networks in near real time so that they can implement corrective strategies.

Key Publications

Conference presentations:

1. Khan A, Sathanur A, Maass KL, Rallo R, Wolf K. Street-level travel time estimation using sparse and coarse data. Northwest Transportation Conference, Corvallis, Oregon, March 11, 2020.
2. Amaya V, Deshmukh R, Rallo R, Wolf K. Near Realtime Data Collection, Storage and Data Imputation of Traffic Data. Northwest Transportation Conference, Corvallis, Oregon, March 11, 2020.
3. Sathanur A, Khan A, Maass KL, Rallo R, Wolf, K. TranSAT: Arterial travel time estimation in metropolitan networks. 2020 TRB Innovations in Travel Modeling Conference, June 14-17, Seattle, WA (accepted for presentation, event postponed due to COVID-19)
4. Khan A, Sathanur AV, Maass K, Rallo R. A Distributed Travel Time Estimation Capability for Metropolitan-sized Road Transportation Networks. *9th SIGKDD International Workshop on Urban Computing - 26th ACM SIGKDD 2020*. August 24, 2020, San Diego, CA.

Published papers:

1. Maas K, Sathanur A, Khan A, Rallo R. Street-level Travel-time Estimation via Aggregated Uber Data. Proceedings of SIAM Workshop on Combinatorial Scientific Computing (CSC20), February 11–13, 2020, Seattle WA. <https://arxiv.org/abs/2001.04533>

References

1. Gallotti, R. and M. Barthelemy (2014). "Anatomy and efficiency of urban multimodal mobility." Scientific Reports **4**(1): 6911.
2. Olmos, L. E., S. Çolak, S. Shafiei, M. Saberi and M. C. González (2018). "Macroscopic dynamics and the collapse of urban traffic." Proceedings of the National Academy of Sciences **115**(50): 12654–12661.
3. Maas K, Sathanur AV, Khan A, Rallo R. Street-level Travel-time Estimation via Aggregated Uber Data. *Proceedings of SIAM Workshop on Combinatorial Scientific Computing (CSC20)*, February 11–13, 2020, Seattle WA. <https://arxiv.org/abs/2001.04533>
4. Sathanur AV, Amatya V, Khan A, Rallo R, Maass K. Graph Analytics and Optimization Methods for Insights from the Uber Movement Data. *Proceedings of the 2nd ACM/EIGSCC Symposium on Smart Cities and Communities*; Portland, OR, USA. 3358625: ACM; 2019. p. 1–7.

I.2.5 Real-Time Data and Simulation for Optimizing Regional Mobility in the United States (ORNL, NREL)

Jibonananda Sanyal, Principal Investigator

Oak Ridge National Laboratory
Bethel Valley Road
Oak Ridge, TN 37831
Email: sanyalj@ornl.gov

Wesley Jones, Principal Investigator

15013 Denver West Parkway
Golden, CO 80401
Email: wesley.jones@nrel.gov

Prasad Gupte, DOE Technology Manager

U.S. Department of Energy
Email: prasad.gupte@ee.doe.gov

Start Date: October 1, 2018
Project Funding: \$4,000,000

End Date: December 30, 2020
DOE share: \$4,000,000

Non-DOE share: \$0

Project Introduction

Highway congestion wastes over three billion gallons of fuel each year and causes seven billion hours of lost productivity. Highway congestion costs freight movers approximately \$63 billion dollars per year, ranging from \$5,600–\$30,000 per truck (and is increasing). Research has shown the ability to introduce near-real time traffic monitoring and adaptive signal control (including small numbers of connected vehicles) can yield up to 30% reduction in congestion. Deploying this approach at a regional scale, that has high-volume and transient traffic, extreme data volumes, and potentially 100,000 vehicles, sensors, and control devices requires High Performance Computing (HPC). We created a ‘Digital Twin’ of the Chattanooga region with simultaneous pairing of both the virtual and physical world providing real-time situational awareness. This Digital Twin will be the basis of a cyber physical control system with high-speed bidirectional communication and control of the highway infrastructure and connected vehicles in the ecosystem to achieve a 20% energy savings in a region. If successful, the results of this project could be replicated region-by-region to commercialize the approach across the entire U.S., so that over the next 10 years, this project accelerates a reliable intelligent mobility system implementation to reduce overall mobility-related energy consumption by 20% and recover \$100 Billion of lost productivity in congestion.

The availability of real-time data from vehicles and the deployment of supporting infrastructure such as high-speed fiber networks has opened up an unprecedented opportunity to bring together high-performance computing, advanced mobility simulations, and existing transportation expertise to create a platform that could have a decadal impact in transforming regional mobility in the United States. We propose to optimize the movement of both people and freight in and around Chattanooga, TN, a representative urban/suburban region, by leveraging high performance computing, data analytics, and machine learning. Near real-time insights provided by the integration of data from emerging mobility technologies and services can inform all phases of strategic planning, design, operation, modernization, and decommissioning of ageing/legacy systems. Lessons learned and capabilities developed and deployed for regional mobility can be applied to optimize mobility nationally deploying region-by-region.

Objectives

The project will drive energy-efficient mobility science and technologies from early stage HPC-based R&D through demonstration to commercialize the optimization of mobility, energy efficiency, and productivity in a

regional traffic domain. Although there is emphasis in this project on real-time traffic management, the models and data will be immensely beneficial for planning transportation infrastructure. With the proper approach, preparedness for future population of connected and autonomous vehicles (CAVs) will be achieved, yet benefits will come in the nearer term from accelerated intelligent infrastructure impact on the operation and movement of conventional vehicles. The project will develop and deploy approaches and capabilities that are scalable to larger and more densely populated regions, ultimately to national scale.

A key goal is to demonstrate the ability to deliver a 20% decrease in energy consumption through the Realtime Digital Twin and Cyber Physical Control of the transportation system.

Approach

The functional capability of the “Digital Twin” is being built in several phases:

Digital Twin Phase One—Phase one established observability. It ingested and reflected the point-in-time state-of-the-system on both the signalized arterials as well as the regional highway and principal arterial system. This took in data from signals, sensors, safety, as well as integrates a modern probe data traffic feed from Waze and TomTom. Showing real-time speeds is particularly essential. Visualization of the data feeds to reflect the volume and velocity without abstracting away details allows us to meet and potentially go beyond existing analytics packages like RITIS and Iteris IPEMS. The majority of this work happened in year one. Year two saw the release of enhancements to the situational awareness capability in the form of a release of CTwin 1.1.

Digital Twin Phase Two: a) Simulation and Modeling—Phase two integrated modeling—specifically an arterial model (Shallowford Road) for within Chattanooga, TN, with real-time data inputs. The real-time data will feed the models, and the models will provide operational insight (not control, that is next during Phase Two – part b). Relevant metrics were reported in near real-time. The arterial model was able to inform the state-of-operation and suggested changes which fed into Phase Two – part b). This work started in year one and went into year two.

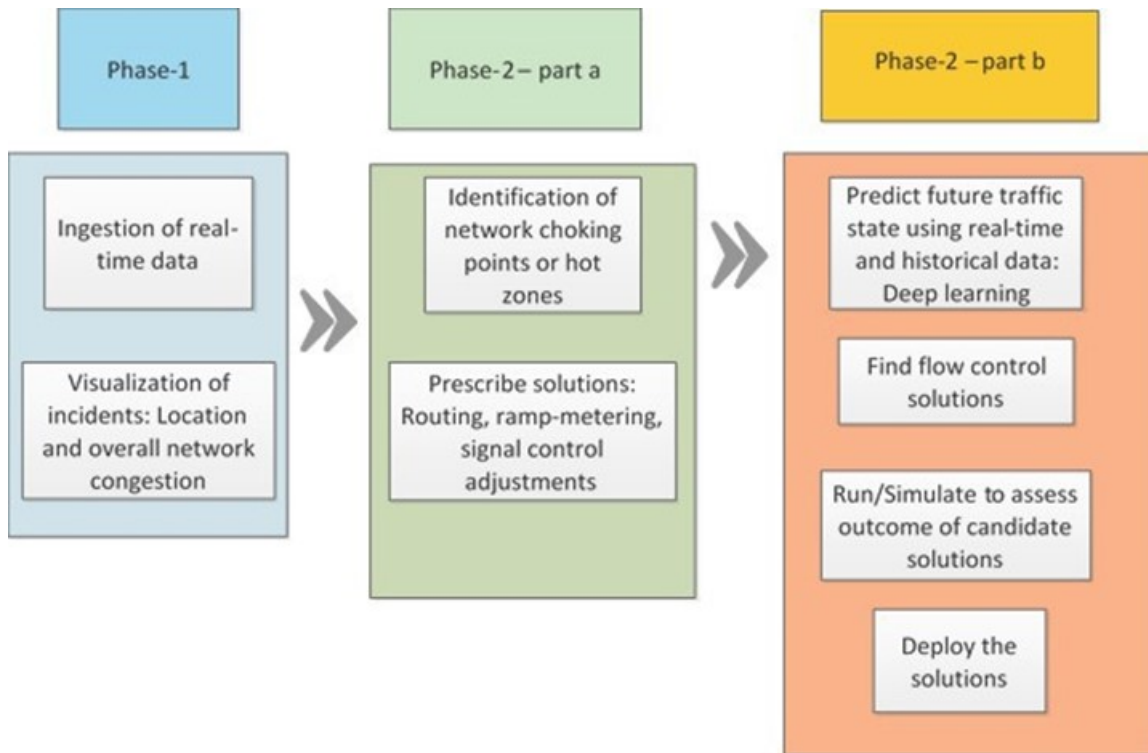


Figure I.2.5.1 Phased Workflow

Digital Twin Phase Two: b. Cyber-physical control—Building on Phase Two – part a, the feedback loop was implemented using a hardware-in-the-loop approach. This implementation demonstrated automated responses to perturbations in the network. The perturbations were perceived through real-time data from GridSmart and through changing signal timing. Also, the modeling can look forward to known events and simulate ahead of the fact to inform/insight into operations in the coming hours (e.g., perhaps in response to incidents, etc.). Most of this work was done during the latter part of year 2.

Through CTwin, we observed the traffic state in real-time through traffic data from several sources to include GridSmart, Waze, and SmartWays live CCTV footage. Through an emergent collaboration with Siemens Mobility Inc., we were able to instantiate proprietary software to allow the communication and change in traffic signal settings in real-time. A model-predictive control algorithm enabled the determination of new signal timing values that was inputted to the controllers in the field through the software. The resulting traffic changes were observed and recorded as discussed. We also observed the effects of an incident on I-75 that was located a few miles North of the Shallowford Road exit as a substantial drop in traffic volumes on the off-ramp.

Results

We now describe the results and progress made by quarter:

FY20Q1 Milestone: Identify system controls approach and develop methods for controlling signals along a corridor.

The objective of this milestone was to investigate and develop methodologies to control traffic signals along the Shallowford Road corridor in Chattanooga. More specifically, this milestone was aimed at designing control approaches along with mechanisms to enable cyber-physical deployment towards the end of FY-20 based on the simulation results that optimize traffic mobility and energy efficiency. To this end, the research team continued developmental efforts on various tasks involved with simulation calibration and validation for

baseline conditions along with quantifying energy usage for the Chattanooga region. This team also in parallel worked towards enhancing and the situational awareness (SA) tool while also focusing efforts on various data science activities that encapsulate aspects of traffic flow prediction (passenger and freight) and traffic safety analysis.

Key Activities

In this quarter, the team primarily focused on improving modeling and simulation efforts focused towards representing Shallowford Road corridor, that also involved setup, validation and calibration of the VISSIM model. The goal was to setup a framework that can simulate the corridor-level traffic dynamics along the 8-intersections on Shallowford Road along with ability to test various signal control strategies (e.g., demand response plans or coordinated signal timings) that optimize mobility and energy usage. Furthermore, the other focus in this quarter also involved in refining the SA tool to further account real-time data feeds and better represent current and historical system conditions in the Chattanooga region. Following key activities are included in this quarter.

1. Modeling setup in VISSIM for corridor-level traffic microsimulation along Shallowford Road.
2. Investigate and identify traffic control optimization strategy at corridor-level that can be both tested and implemented as a pilot.
3. Exercising pipelines to generate baseline energy usage in Chattanooga region with RouteE.
4. Interface with the M-60 traffic controller for SPaT data access for eventual cyber-physical control and deployment.
5. Refining the Situational Awareness tool to better integrate real-time data streams along with provide analytical capabilities for historical insights.
6. Exploratory analysis of data science activities that include help in building the ubiquitous traffic flow prediction algorithm leveraging traffic sensors in Chattanooga along with traffic safety analysis to help inform incident detection patterns.

FY20Q2 Milestone: Complete prototype design of data science algorithms for observability and measurability of traffic system performance focused on mobility and energy.

The objective of this milestone was to investigate and develop data science algorithms geared towards traffic system measurability and predictability to impact congestion and energy usage in Chattanooga region. A focus was also on identifying a methodology to control traffic signals along the Shallowford Road corridor in Chattanooga for the purposes of improving the traffic performance and reducing energy consumption. Further, this milestone was aimed at conceptualizing control approaches along with mechanisms to enable cyber-physical deployment towards the end of FY-20 based on the simulation results that optimize traffic mobility and energy efficiency. To this end, the research team continued calibration and validation of the simulation baseline conditions. The work also quantified energy usage for the Chattanooga region. The team successfully tested a set of new timing values entered through the Siemens software. Most notably, the team executed a controlled experiment to change the minimum green time on all signals along the Shallowford Road stretch. The experiment used a Python program that interacted directly with the traffic hardware. The team worked in parallel on activities to enhance the situational awareness (SA) tool, encapsulate aspects of traffic flow prediction (passenger and freight), and traffic safety analysis.

In this period, Jibo Sanyal presented two invited talks about the project. The first talk was at the National Association of State Energy Officials in Washington DC. The second was at a Smart Cities meeting organized by ORAU.

Key Activities:

In this quarter, the team primarily focused on design and development of data science algorithms geared towards traffic system measurability and predictability to quantify performance and baseline congestion and energy usage in Chattanooga region. The goal of these algorithms is to ingest traffic sensor data in the region to build data-analytical insights of the current system to be able to further measure and predict anticipated traffic states at scale leveraging high-performance computing. The key focus in Q2 is to design and prototype these algorithms for various data science related efforts that optimize mobility and energy-usage in the system. Furthermore, modeling and simulation efforts are also undertaken towards representing Shallowford Road corridor in a VISSIM model to simulate the corridor-level traffic with ability to test various signal control strategies (e.g., demand response plans or coordinated signal timings) that optimize mobility and energy usage. The other focus in this quarter also involved in refining the SA tool to further account real-time data feeds and better represent current and historical system conditions in the Chattanooga region. Following key tasks are included in this quarter. Note that some of these tasks had initial work done in earlier quarters.

1. Design and prototype data science algorithms that include help in building the ubiquitous traffic flow prediction algorithm leveraging traffic sensors in Chattanooga along with traffic safety analysis to help inform incident detection patterns.
2. Based on corridor-level simulation results, signal timing optimization strategy is deployed to test and evaluate a pilot soft-control strategy using existing Siemens software for traffic mitigation.
3. Interface with the M-60 traffic controller for SPaT data access for eventual cyber-physical control and deployment. Directly manipulate the minimum green time on all traffic signal controllers in Shallowford Road corridor using a cyber-physical program.
4. Refining the Situational Awareness tool to better integrate real-time data streams along with provide analytical capabilities for historical insights.

FY20Q3 Milestone: Design and development of cyber physical control approaches that prototype real-world deployment with traffic controllers for energy and traffic mobility optimization along the Shallowford corridor in Chattanooga region.

The objective of this milestone was to investigate and develop methodologies to control traffic signals along the Shallowford Road corridor in Chattanooga. More specifically, this milestone was aimed at designing control approaches along with mechanisms to enable cyber-physical deployment towards the end of FY-20 based on the simulation results that optimize traffic mobility and energy efficiency. To this end, the research team worked on interfacing mechanisms with the Siemens m60 controllers deployed in the city. Three tests were conducted to ascertain the feasibility of sending control signals to the devices and determine the checks and bounds that are required. Discussions were held with Siemens to identify a native mechanism to control signals using their implementation of NTCIP protocol. Data science activities related to computing of ATSPM, object detection for freight flow, volume estimates, and energy estimates continued.

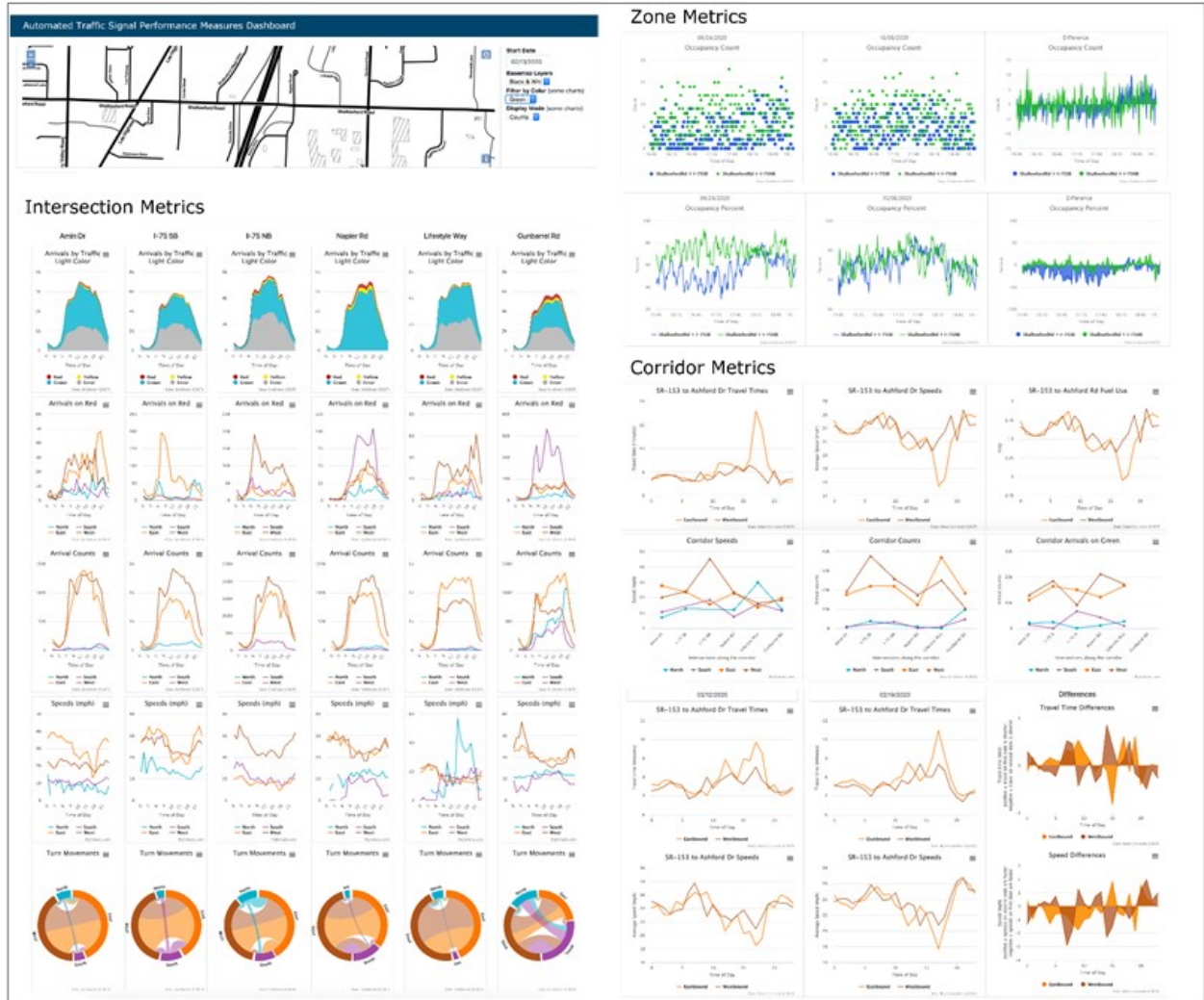


Figure I.2.5.2 Various Interactive Charts Displaying Some Atspms

Key Activities:

In this quarter, the team primarily focused on control design, approaches to control implementation, simulation calibration, developing network fundamentals diagram, and data science activities around object detection from video feeds, computing and dashboarding ATSPM, and RouteE energy estimation and validation. More specifically:

1. Work on developing the cyber-physical control approach for Chattanooga progressed and three experiments were conducted to understand and establish the bounds of the control algorithm values to be employed, observe how the signals in the city intersections responded to control signals, and identify the methodology for conducting a controlled experiment.
2. Specifics of how to compute the bounds on safe values for the signal controllers was identified.
3. A real-time online Model-Predictive Control running in the cloud was developed to generate optimal signal timing vales for the control.
4. Both microscopic and mesoscopic simulation have been tested and compared for the Shallowford Road network which is comprised of four signalized intersections.

5. A methodology for creating a summary of the regional traffic dynamics using a network fundamental diagram (NFD) was developed.
6. To support monitoring and analyzing the results of traffic signal timing experiments, we developed a dashboard prototype for Automated Traffic Signal Performance Measures. This dashboard combines data from two different sources, Waze and GridSmart, and provides an explorative view of various metrics which can be derived from these data. The corridor tab simultaneously shows Waze corridor data and GridSmart data.
7. The computational framework for running the You-Only-Look-Once (YOLO) model on GPU-accelerated nodes was investigated.
8. Improvements to the traffic volume to achieve even higher accuracy than the previous iteration was accomplished, enabling real time energy estimation.

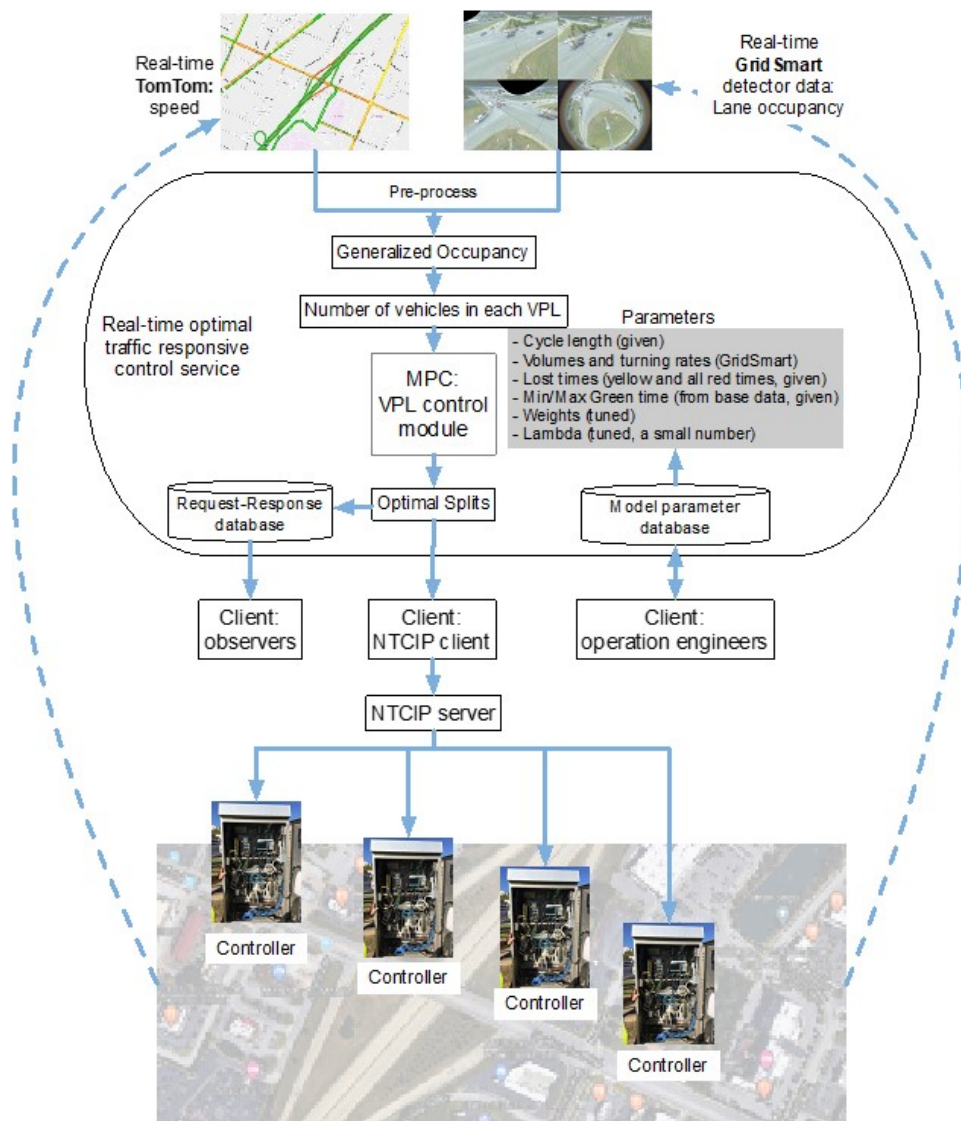


Figure I.2.5.3 Real-Time Traffic Signal Control System Structure

FY20 Q4 Milestone: Test pilot prototype of near real-time cyber-physical control along corridor informed by situational-awareness, simulation, and optimization.

The key accomplishment in the final quarter of the project was to execute the near-real-time cyber-physical control in the City of Chattanooga. The objective of this experiment has been to overcome the key technical challenges of communication, computation of new signal timing values, and demonstrate the actuation of physical signals in the real-world.

Significant rigor was put into vetting the automation approach. With everybody working remotely because of COVID-19 conditions, a major requirement was ensuring that nothing detrimental to the safety or integrity of operations would happen. We were successful in that regard.



Figure I.2.5.4 Remote Setup of Control Experiment: VPN Tunnel into City of Chattanooga from Remote Desktop Interfaces to Run Control Algorithms in the Cloud and Obtain New Values to Send to On-Street Controllers

Key Activities:

In this quarter, the team primarily focused on implementation of the control strategy in a demonstration in the City.

1. The model-predictive control was enhanced to be responsive to provide new signal timing values while running in the cloud.
2. Engagement with Siemens matured, and a Siemens developed NTCIP server implementation was shared with the project team which was then installed in the city of Chattanooga and cyber-physical code was written to interface with the on-street controllers.
3. For the execution of the control, we continued to develop multiple closed loop control strategies for optimizing signal timings along the Shallowford Rd corridor at eight intersections beyond the MPC implementation.
4. Historic TomTom probe data was used to understand how the MPC model controlled the traffic and ultimately influenced the energy along the corridor of Shallowford Road.
5. The framework of RouteE was used to estimate the gallons of gasoline equivalence (gge) per vehicle per mile to get a normalized understanding of energy consumed due to traffic flow.
6. We ran our experiment for four days (21 September 2020 – 24 September 2020) during the peak hours of 4:15 pm to 7:30 pm EST.

7. A time zone mismatch between the cloud server and the Chattanooga time zone resulted in a sub-optimal responsive system during those days. However, the MPC was sufficient at bounding its split timings in such a way that didn't cause any detriment to traffic. Further, compared to some weeks we actually significantly increased the speeds for improved energy.
8. The successes of the effort include understanding of how to execute cyber-physical control under real-world setups which positions us strongly to investigate advanced approaches in the next phase.

Chronological listing of major activities in FY20:

- Jibo Sanyal presented a lunch keynote at the Tennessee Sustainable Transportation Forum & Expo, 2019, Knoxville
- On October 31, 2020, CTwin version 1.0 was released
- On November 5, 2019, Anne Berres presented visualization work from CTwin at the 9th International Visualization in Transportation Symposium at the NAS Building in Washington, DC
- In November 2019, ORNL and NREL submitted two joint journal papers for a Transportation Research Record Special Issue on Visualization in Transportation
- From October to December 2019, ORNL developed a proof-of-concept which indicates that incidents can be detected in radar detection sensors (RDS) data up to 5 minutes faster than 911 calls were made
- On December 12, 2020, Haowen Xu presented a poster on project work at the American Geophysical Union (AGU) Fall Meeting
- On January 23, 2020, CTwin version 1.1 was released which included several enhancements to the tool
- On February 6, 2020, Jibo Sanyal presented an invited talk at the National Association of State Energy Officials, Washington DC
- Initial experiments in February demonstration of up to 16% energy improvement in the city
- On February 20, 2020, ORNL and NREL started engaging with Siemens in preliminary meeting, with many follow-up meetings throughout the rest of the fiscal year. This eventually led to the inclusion of Siemens in discussions on NTCIP controller access, control experiments, as well as the establishment of a formal partnership for the next iteration of the project
- In April 2020, an abstract by Haowen Xu et al. was published for the American Association of Geographers' Annual Meeting (the meeting itself did not take place due to COVID)
- From February to April, ORNL developed a prototype implementation which derives Advanced Traffic Signal Performance Measures (ATSPM) from GridSmart and Waze data
- Between April and June 2020, a team of NREL and ORNL team members developed a method to backfill missing Waze corridor data for a relevant corridor to enable comparisons between the February experiments and later experiments
- On April 30, Anne Berres presented the ATSPM dashboard as well as other project work at DOE Computer Graphics Forum (DOE CGF) 2020
- On July 23, 2020, Jibo Sanyal presented an invited talk at TennSMART Consortium meeting virtually

- Experiment week (September 21-24) - the cyber physical control experiments were executed on the four consecutive days, Monday to Thursday, during the evening rush hours of 4:15 pm to 7:30 pm
- Jibo Sanyal was invited to conduct a panel at the Global Smart Cities Week focused on DOE and related efforts in the Chattanooga area.

Conclusions

The above sections summarize all activities in the project in FY20. The second year of development of the various activities delivered key artifacts of situational awareness, data insights, simulation estimates of energy savings, and cyber-physical actuation of on-street hardware. The project team has learned a lot from the engagements and is excited to pursue and mature the activity to deliver significant energy savings for the region.

Key Publications

1. Jibo Sanyal, Invited talk at TennSMART Consortium meeting, 23 July 2020, virtual.
2. Jibo Sanyal, Invited talk at SOS24 Workshop, Swiss National Supercomputing Centre, St. Mortiz, Switzerland, 23–26 March 2020 (cancelled)
3. A. Todd and J. Sanyal, 2020: Classification of light and heavy-duty vehicles from live traffic cameras. CoDa 2020 Conference (Poster). Santa Fe, NM. Feb 25–27, 2020.
4. J. Severino, A. Nag, Y. Hou, J. Ugirumurera, J. Cappellucci, J. Holden, W. Jones and J. Sanyal, “Development of automated pipeline for time-resolved link-wise vehicular energy consumption in the Chattanooga, TN road network”, CoDA 2020, Santa Fe, NM, February 25–27, 2020.
5. Jibo Sanyal, Invited plenary, ORAU Council of Sponsoring Institutions: Critical Infrastructure Systems and Resiliency, 9 March 2020
6. Ugirumurera, Juliette, et al., "High Performance Computing Traffic Simulations for Real-Time Traffic Control of Mobility in Chattanooga Region", No. NREL/PO-2C00-75009, Presented at the 2019 Tennessee Sustainable Transportation Forum & Expo, 1–2 October 2019, Knoxville, Tennessee.
7. Anne Berres, Haowen Xu, Sarah Tennille, Srinath Ravulaparthi, Ambarish Nag, Jibonananda Sanyal, “Traffic Flow Performance Analysis through Visual Analytics”, DOE Computer Graphics Forum (DOECGF), 28–30 April 2020, Santa Fe, New Mexico.
8. Haowen Xu, Jibonananda Sanyal, Anne Berres, “Optimization of Network Datasets for Web-based System using Composite Bezier Curves”, American Association of Geographers Annual Meeting, 6–10 April 2020, Denver, Colorado.
9. Jibo Sanyal, Invited talk, National Association of State Energy Officials, Washington DC, 6 February 2020
10. Jibo Sanyal, Invited Keynote at TennSMART Consortium meeting, 9 April 2019, Nashville TN
11. Jibo Sanyal, Plenary panelist at Sustainable Fleet Technology Conference, 6–8 August 2019, Durham NC
12. Srinath Ravulaparthi, invited talk at Smart Cities Digital Twin Workshop at GA Tech, 2019.
13. Anne Berres, Srinath Ravulaparthi, Jibonananda Sanyal, “Transportation Systems Analysis and Visualization: A Multi-Scale and Multi-Variate Approach to Shopping Districts”, 9th International Visualization in Transportation Symposium, 5–6 November 2019, Washington DC.

14. Jibo Sanyal, Lunch keynote at Tennessee Sustainable Transportation Forum & Expo, 2019, Knoxville
15. Alisa Alering, "Real-time Answers for Traffic Jams", Science Node, Jan 21, 2019, <https://sciencenode.org/feature/Real-time%20answers%20for%20traffic%20jams.php>
16. Fish, Young, et al., "Old problems, new solutions: leveraging big data, machine learning and high-performance computing for transportation planning and operations at scale", talk to be presented at Colorado Transportation Symposium, April 21, 2021.
17. J. Severino, Y. Hou et al. "Real-time data pipeline for time-resolved link-wise vehicular energy consumption in the Chattanooga, TN road network." Transportation Research Board Annual Meeting, Washington D.C., 2021. (Submitted)
18. Wang, Qichao, et al., "Offline Arterial Signal Timing Optimization based on Virtual Phase Link Model", Transportation Research Board Annual Meeting, Washington D.C., 2021. (Submitted)
19. Wang, Qichao, "Regional Optimal Traffic Signal Timing under Oversaturated Condition", CO/WY ITE seminar, October 2020. (In preparation).
20. A. Wang and H. Wang, Decision making for complex systems subjected to uncertainties – a probability density function control approach, in Handbook of Reinforced Learning, Springer-Verlag, 2020.
21. H. Wang, M. Zhu, W. Hong, C. Wang, G. Tao and Y. Wang, Optimizing signal timing control for large urban traffic networks using an adaptive linear quadratic regulator control strategy, IEEE Trans. on Intelligent Transportation Systems., 2020.

I.3 Core Simulation and Evaluation Tools

I.3.1 Livewire Data Sharing Platform (NREL, PNNL, INL)

Lauren Spath Luhring, Principal Investigator

National Renewable Energy Laboratory
15013 Denver West Parkway
Golden, CO 80401
Email: lauren.spathluhring@nrel.gov

Chitra Sivaraman, Principal Investigator

Pacific Northwest National Laboratory
902 Batelle Boulevard
Richland, WA 99354
Email: chitra.sivaraman@pnnl.gov

Ron Stewart, Principal Investigator

Idaho National Laboratory
2525 Fremont Avenue
Idaho Falls, ID 83402
Email: ron.stewart@inl.gov

Erin Boyd, DOE Technology Manager

U.S. Department of Energy
Email: erin.boyd@ee.doe.gov

Start Date: October 1, 2018
Project Funding: \$850,000

End Date: September 30, 2021
DOE share: \$850,000

Non-DOE share: \$0

Project Introduction

Before the advent of the Livewire Data Platform, there was no recognized sharing platform for mobility-related data used by academic and national lab researchers. The energy efficiency and mobility data landscape is complex. A range of human and technical obstacles can limit data accessibility and prevent collaboration among research institutions. Researchers may lack expertise or the capabilities they need to effectively share project-generated or relevant datasets. They may lack resources—like required infrastructure or enough time to prepare metadata—to share project-generated data effectively. Not least, researchers may be inclined to resist sharing data, even data funded by the government, viewing data instead as a competitive advantage.

To successfully navigate these challenges, the Livewire Data Platform was developed to meet the needs of the energy efficiency and mobility research community. Originally focused on the EEMS research community, Livewire has since broadened its scope to provide opportunity for relevant energy efficiency and mobility researchers to share or access data. There are no fees associated with using Livewire to access data and no cost to data owners who wish to store up to 10 terabytes of data. Currently, data available via Livewire includes that from the D.O.E. Lab System, partner institutions such as Carnegie Mellon University and the American Center for Mobility, and other public and private sources of mobility data.

Livewire provides a data management platform, allowing easy and secure data sharing for the community to collaborate, eliminating barriers to transportation data sharing and discovery.

Livewire accomplishes this through three broad tasks:

1. Maintaining and enhancing the data management platform and exposing datasets
2. Building complex data management capabilities
3. Addressing human factors limiting data sharing.

Objectives

Livewire’s objective is to remove barriers to sharing data, allowing energy efficiency and mobility researchers to focus on their research. This includes providing a:

- Secure platform that enables data sharing and discovery
- Community that builds partnerships and collaboration rather than competition
- System that allows shared data to grow in size and complexity as Energy Efficient Mobility Systems (EEMS) evolve.

After an initial “soft” launch in FY19, the Livewire team created project goals for FY20, including launching the platform and making it available to a wider community online at livewire.energy.gov; shifting the emphasis from development to growth of projects, datasets, and users; and tracking the impacts and benefits of the platform. Moving forward, the platform will continue to collect, preserve, and disseminate energy efficiency and mobility research data while the Livewire team refines the capabilities and provides operational support to data owners.

Approach

Livewire has achieved its initial goal of facilitating easy and secure data sharing within the EEMS research community, and the platform continues to evolve and leverage existing assets to support new and ongoing research efforts. These foundational capabilities include leveraging Pacific Northwest National Laboratory’s successful Wind Energy Technologies Office-funded Atmosphere to Electrons data store (a2e.energy.gov) to host transportation and mobility data and using the National Renewable Energy Laboratory’s Transportation Secure Data Center and Fleet DNA, as well as the federal government’s API Umbrella (api.data.gov), for application programming interface (API) management.

In addition to expanding the platform’s features, the Livewire team is focusing on addressing the human challenges and administrative barriers to sharing data. Through conversations with data owners, the team evaluates and gathers data needs, inventories data that users would like to include, and initiates outreach for new data and users. Looking ahead, Livewire will build on these outreach efforts by establishing an EEMS Data Working Group to:

- Improve the team’s understanding of perspectives from the EEMS research community
- Help drive decisions about platform needs and features
- Strengthen data partnerships among researchers in the EEMS community.

Throughout this effort, the Livewire team maintains and is extending existing successful projects, such as Fleet DNA and the Transportation Secure Data Center.

Results

Platform Development

Livewire priorities in FY20 were to grow its capabilities and enhance its usability, and the Livewire team implemented several key features to support these goals. For example, the team created a new project search page that groups datasets by project and provides filtering capabilities that were previously unavailable,

enabling users to more easily discover relevant data. In addition, the team-built user and group management capabilities as well as the ability to drag and drop files for easy upload to the platform.

Livewire’s design and development teams also updated Livewire’s search page (see Figure I.3.1.1) to include the following search and filtering features, which are essential for any data repository:

- An updated user interface for a less cluttered page
- A link to a new project page where users can view the full project description and standard citation language, where available
- A free-form search field
- The ability to filter by participating organization, data access, and keyword
- Contact and participating organization information.

When a registered user is logged into Livewire, that user can now also see dataset names, as well as links to access datasets associated with a project.

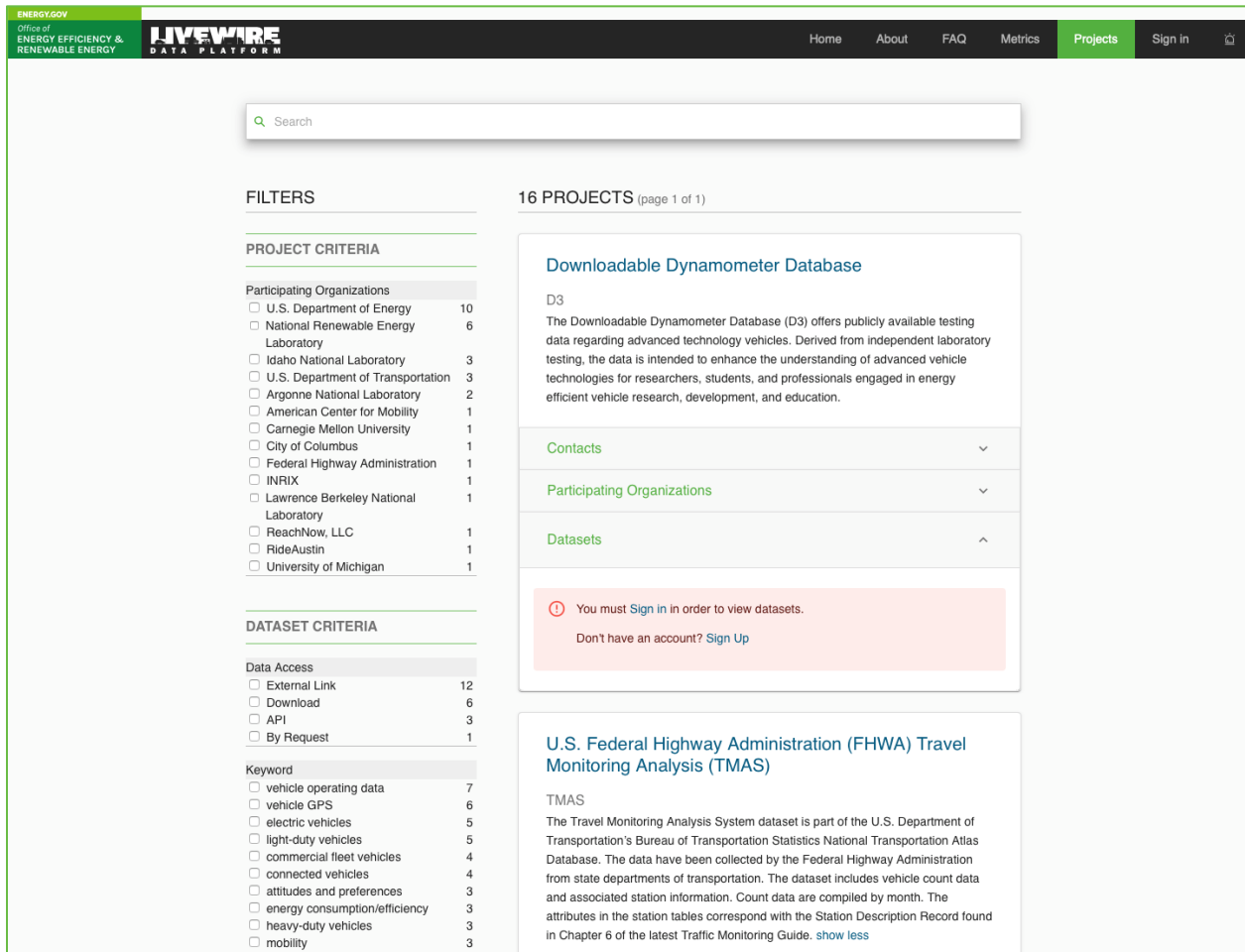


Figure I.3.1.1 Livewire Data Platform Search Page (<https://Livewire.Energy.Gov/Project-Search>)

Other features prioritized by the Livewire team in FY20 enable data owners or principal investigators to manage their own data. Logged-in data owners that choose to store their data on Livewire can add to their data

through the platform's interface, dragging and dropping files that match the user-defined naming convention (see Figure I.3.1.2).

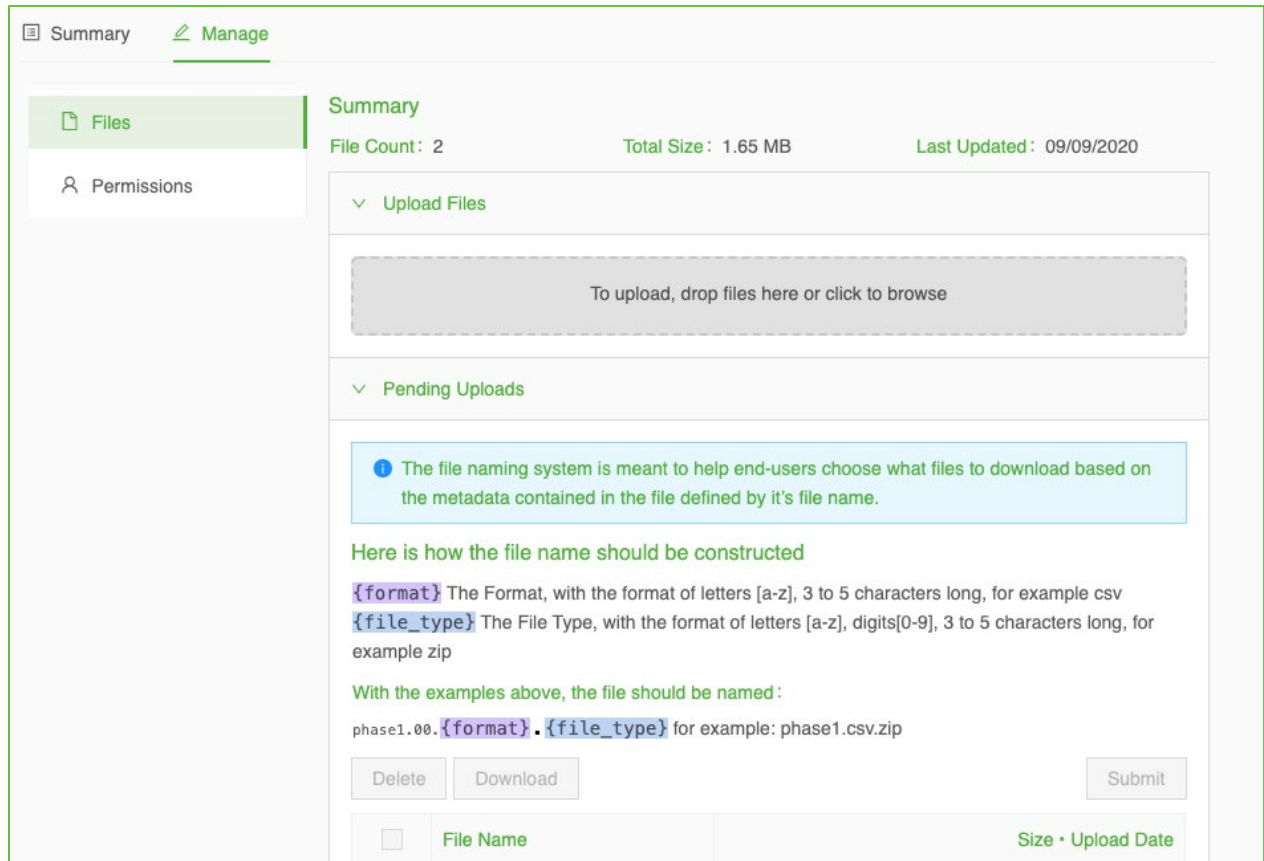


Figure I.3.1.2 Livewire Data Platform File Upload (<https://Livewire.Energy.Gov/Project-Search>)

In addition, new group and user management capabilities allow data owners to control who can download or even see their data. While most projects are accessible to the entire Livewire community, data owners may choose to restrict access to their data at the project or dataset level, which may make some data owners more inclined to use the platform (see Figure I.3.1.3 and Figure I.3.1.4).

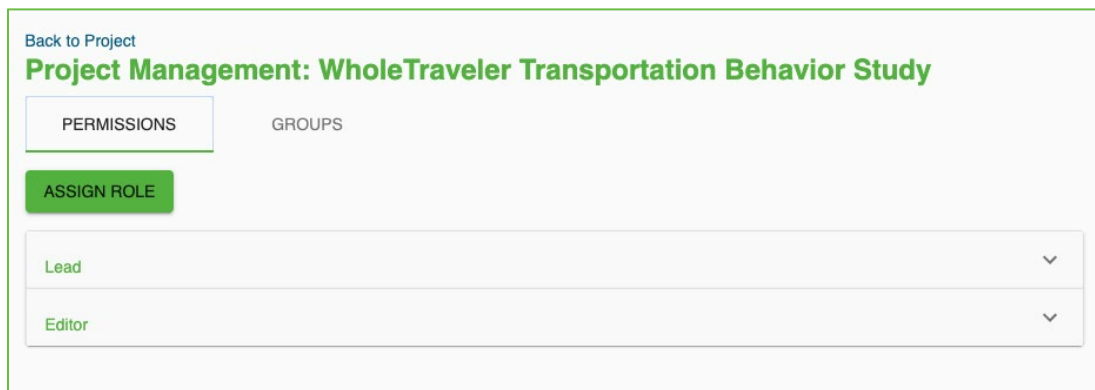


Figure I.3.1.3 Livewire Data Platform User and Group Management

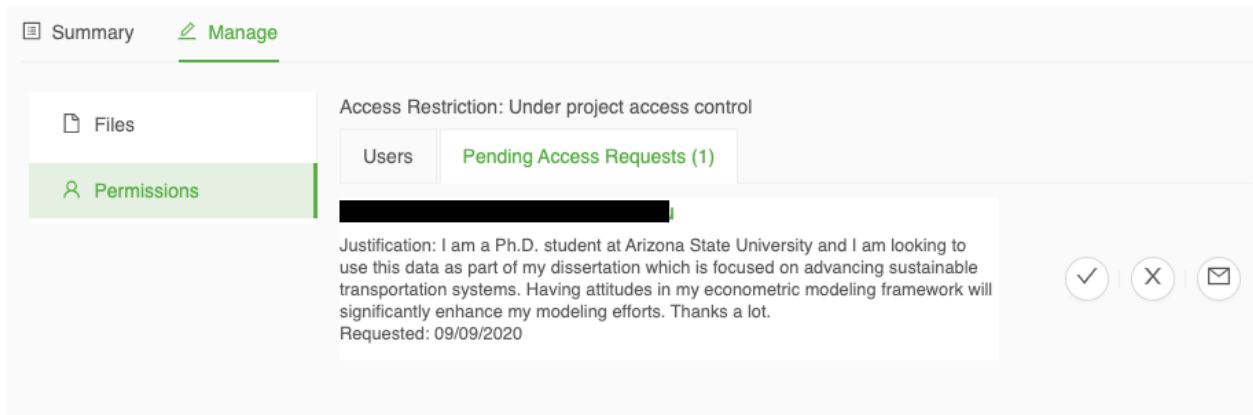


Figure I.3.1.4 Livewire Data Platform Access Management Interface

Schema and Metadata

Livewire relies on metadata, which describe dataset characteristics, to support relevant features of the platform, including user-facing capabilities, dataset analysis, and data quality characterization. In FY20, the Livewire team focused on evolving metadata standards and conventions for projects included on the platform.

The team created “high level” metadata—which describes projects and associated datasets—for each project and dataset on Livewire. These JavaScript Object Notation (JSON) files are used to drive the platform’s user interface (see Figure I.3.1.5).

The screenshot displays the Livewire Data Platform interface for the dataset "ANONYMIZED LOGGER DATA FY16 TO FY18". The page includes a summary, API details, and a map showing geographic locations. A yellow callout bubble highlights a PDF document titled "Livewire Data Platform: Data Dictionary" with the subtitle "U.S. Department of Energy/University of Michigan Energy Impact of CAV's Project De-identified Dataset". A blue callout bubble highlights a JSON file titled "umcav.json" with the following content:

```

1 {
2   "conformsTo": "https://livewire.energy.gov/schemas/v0.1",
3   "identifier": "umcav",
4   "title": "Impact of Connected and Automated Vehicles",
5   "shortName": "DOE-UM CAV Project",
6   "description": "The University of Michigan (UM) project \"Energy Impact of Connected and Automated Vehicles\" funded by the U.S. Department of Energy's (DOE) Office of Energy Efficiency and Renewable Energy's Vehicle Technologies Office (VTO). The project ran from FY 2016 to FY 2018. Aftermarket data loggers were installed in approximately 500 privately-owned vehicles in the Ann Arbor, Michigan, area based on vehicle owners volunteering to participate in the study. The data describe the energy consumption of the vehicles, speed, powertrain operation, vehicle location, and other parameters at 1-second intervals while the vehicles were operating. The purpose of the data collection was to discern whether coordination between vehicles and traffic signal phase and timing controllers, instituted by UM as part of the project, would make an appreciable difference in vehicle fuel efficiency. UM consented to share the vehicle data with DOE's National Labs to further VTO Energy Efficient Mobility Systems research efforts. Although access to the full project dataset is restricted to the immediate project team, by agreement with the UM researchers, an anonymized or \"de-identified\" version of the dataset is being shared within the DOE mobility research community. The identification process performed by UM removes identifying information (e.g., VIN) and trims the beginning and ending portions of each record within the dataset.",
7   "contactPoint": [
8     { "fn": "Matthew Shirk", "hasEmail": "mailto:matthew.shirk@inl.gov", "hasOrg": "Idaho National Laboratory" }
9   ],
10  "participatingOrganizations": [
11    { "name": "U.S. Department of Energy Vehicle Technologies Office (DOE VTO)" },
12    { "name": "University of Michigan (UM) Department of Mechanical Engineering" },
13    { "name": "Argonne National Laboratory (ANL)" },
14    { "name": "Idaho National Laboratory (INL)" }
15  ],
16  "accessLevel": "public",
17  "accessRestriction": "none",
18  "dataset": [
19    { "identifier": "umcav.ds0",
20      "title": "Anonymized Logger Data FY16 to FY18",
21      "shortName": "DOE-UM CAV Dataset",
22      "description": "The dataset originates from the University of Michigan (UM) project \"Energy Impact of Connected and Automated Vehicles\" funded by the U.S. Department of Energy's (DOE) Office of Energy Efficiency and Renewable Energy's Vehicle Technologies Office (VTO). The project ran from FY 2016 to FY 2018. Aftermarket data loggers were installed in approximately 500 privately-owned vehicles in the Ann Arbor, Michigan, area based on vehicle owners volunteering to participate in the study. The data describe the energy consumption of the vehicles, speed, powertrain operation, vehicle location, and other parameters at 1-second intervals while the vehicles were operating. The purpose of the data collection was to discern whether coordination between vehicles and traffic signal phase and timing controllers, instituted by UM as part of the project, would make an appreciable difference in vehicle fuel efficiency. UM consented to share the vehicle data with DOE's National Labs to further VTO Energy Efficient Mobility Systems research efforts. Although access to the full project dataset is restricted to the immediate project team, by agreement with the UM researchers, an anonymized or \"de-identified\" version of the dataset is being shared within the DOE mobility research community. The identification process performed by UM removes identifying information (e.g., VIN) and trims the beginning and ending portions of each record within the dataset.",
23      "accessLevel": "non-public",
24      "accessRestriction": "community"
25    }
26  ]
27 }

```

Figure I.3.1.5 Livewire Data Platform Metadata

Additionally, the project team prototyped new automation tools to create and share detailed, or “low-level,” metadata for four datasets. Using such automation tools will standardize metadata creation and capture aspects of data quality, including structure, content, and relationships; size and completeness; statistical measures of distribution and skew; and some aspects of reasonability. In the long run, the team will use these tools to create detailed metadata for all data on Livewire.

Livewire’s metadata schema also evolved over FY20. The team created a detailed matrix for assigning project- and dataset-level access restrictions. This visual representation of access levels, restrictions, and visibility will guide metadata creation of future Livewire projects and datasets.

Growth and Metrics

Following Livewire’s launch, it was important for the team to establish baseline metrics and define and agree upon acceptable metrics for growth leading up to Livewire’s June 30, 2020, Go-No/Go decision. Because Livewire is different from a traditional U.S. Department of Energy (DOE) research and development project, it can be difficult to measure growth and progress, as progress is not always linear. To account for this, the team

decided to evaluate Livewire's success based on quarterly growth in three areas: usage, engagement, and impact.

Usage metrics reveal how many people use a platform, and the team agreed that Livewire should demonstrate quarterly growth in at least one usage metric:

- Number of files
- Amount of data stored (in gigabytes)
- Number of projects
- Number of datasets
- Number of registered users
- Number of user domains.

From the December 31, 2019, baseline to September 30, 2020, Livewire showed growth in all of these areas, increasing the number of projects shared on the platform from 9 to 16, the number of datasets from 38 to 116, and the amount of data stored (in gigabytes) by nearly 5,000%. Registered users of Livewire come from 21 organizations, and data shared on the site comes from a range of sources and institutions, from the DOE lab system to EEMS researcher partners to other sources relevant to the energy efficiency and mobility research community.

Where usage metrics highlight how many people use the platform or how many projects are on the platform, engagement metrics illustrate how users interact with Livewire, providing insight into their interests and use of the platform. The Livewire team committed to reporting on and demonstrating growth on at least two engagement metrics each quarter:

- Pageviews
- Web users
- Time spent on the site
- API users
- API hits
- Number of users downloading data
- Datasets downloaded
- Number of files downloaded
- Size of files downloaded
- Number of publications citing data found on Livewire.

Because of the unpredictable nature of website traffic and researcher needs, growth in engagement metrics is not always linear; however, Livewire showed growth in at least two of these areas each quarter.

The final metric that Livewire records is impact, which demonstrates the effect Livewire has had on a user's work. Recorded and presented quarterly in the form of a testimonial from a Livewire user, impact shows how Livewire has enabled a user to accomplish something they could not have done without the platform.

In addition to these quarterly metrics for measuring growth, the team established three metrics for determining the viability of the platform at the June 30, 2020, Go/No-Go decision. These metrics, based on growth since the December 31, 2019, baseline was established, were:

- 50% increase in projects contributing data (12 projects)

- 100% increase in datasets (62 datasets)
- 50% increase in users (48 users).

Livewire successfully met or surpassed each of these targets, and the platform was deemed viable, continuing onto year three of the project's lifecycle.

Conclusions

As a targeted catalog of transportation- and mobility-related data, the Livewire Data Platform aims to empower researchers and community planners to easily store, share, and secure data to support projects and decision making. In FY20, the Livewire team supported this goal by building out new features and schemas that eliminate barriers to sharing data on the platform, an important step for fostering a spirit of collaboration in the EEMS community. As a result, the platform has seen steady growth as more researchers discover the timesaving and security benefits of storing data on Livewire. The Livewire team will build on this early success through targeted outreach, ongoing conversations with data owners, and the development of tools and processes designed to provide an optimal user experience, with a goal of spreading the word on the benefits of using Livewire and continuing to shape the platform into the leading data resource for research critical for an affordable, efficient, safe, and accessible transportation future.

Acknowledgements

The Livewire Data Platform team would like to thank the many EEMS researchers who provided input, feedback, and datasets for the initial launch of the platform.

I.3.2 Core Modeling, Simulation and Evaluation (ANL)

A. Rousseau, Principal Investigator

Argonne National Laboratory
9700 South Cass Avenue
Lemont, IL 60439
Email: arousseau@anl.gov

David Anderson, DOE Program Manager

U.S. Department of Energy
Email: david.anderson@ee.doe.gov

Erin Boyd, DOE Technology Manager

U.S. Department of Energy
Email: erin.boyd@ee.doe.gov

Start Date: October 1, 2018	End Date: September 30, 2021	
Project Funding: \$2,000,000	DOE share: \$2,000,000	Non-DOE share: \$0

Project Introduction

The U.S. Department of Energy (DOE) Vehicle Technologies Office (VTO), along with national laboratories, performs research to advance vehicle powertrain technologies, including internal combustion engines, batteries, electric machines, light-weighting, fuels and lubricants. The rise of connected and automated vehicles (CAVs) and smart mobility technologies has the ability to change traveler mobility choices as we currently know them, leading to potentially dramatic impacts on both mobility and energy. CAVs also enable higher traffic density at highway speeds with fewer transients, which allows for smaller vehicle-to-vehicle gaps—especially in the case of coordinated driving.

Given the large number of transportation and vehicle technologies, vehicle classes and operating conditions (vehicle trip profile, temperature etc.), tens or hundreds of thousands of combinations must be considered. Since it would not be possible to test and evaluate every possible combination, VTO has been relying on vehicle system modeling and simulation to estimate the potential of each technology at a system level to provide R&D guidance to VTO managers (on, for example, battery power and energy requirements) as well as maximize the potential of each technology.

Assessing the impact of new technologies across a wide range of scenarios requires the development of new systems simulation tools and workflow (e.g., HPC) and processes (e.g., vehicle-in-the-loop) supported by test data (e.g., road load changes with varying gap distances for varying vehicle types).

Objectives

This project focuses on the following main objectives:

- Enhance Autonomous vehicle models to accurately simulate the latest technologies and their impact on vehicle performance, energy consumption and cost.
- Integrate and deploy the new processes and tools through AMBER to support all DOE SMART activities
- Develop new workflows that support the activities of the Systems and Modeling for Accelerated Research in Transportation (SMART) Mobility Consortium.
- Quantify the impact of advanced technologies on energy and cost on real world cycles (Livewire).

- Develop experimental process, conduct direct road load measurements and analyze the results to provide an empirical road load model of platooning vehicles under various gaps, vehicle sizes, vehicle position offsets and configurations.
- Development of an experimental platform to quantify the energy use impacts of connected and automated vehicles technologies.

Approach

- **AMBER & Autonomie:** Altogether four releases were deployed this year. Three were AMBER releases with Autonomie as follows: 2020, 2020 Update 1, and 2020 Update 2. The fourth release was a legacy Autonomie release to support users until they migrate their models and processes to AMBER/Autonomie.
- **On-track Platooning:** A novel experimental approach is taken to directly measure road load changes of each vehicle using axle torque sensors and other data to understand the aerodynamic impacts of vehicles driving in platoon formation at different gaps, speeds, and different vehicle types/sizes.
- **Vehicle-in-the-Loop (VIL):** Uses simulated data as input to the vehicle's control, effectively "linking" the vehicle to a test environment this approach allows broad research topics into vehicles enabled by automation and/or connectivity on a chassis dynamometer.
- To enhance the VIL task, members of the EcoCAR Advanced Vehicle Technology Competitions section are collaborating to accelerate the implementation of connectivity technology and automated control overrides by developing flexible hardware systems for generating V2X signals from real and simulated vehicles and infrastructure

Results

Autonomie and AMBER

- Released an incremental version of legacy Autonomie REV16SP7 based on feedback from OEMs. In addition, this release was updated to work with the latest versions of modelling tools such as Matlab, Simulink, Stateflow. Toolchains including new releases of the visual studio, dot net browser, and Infragistics were also upgraded.
- Provided compilation support on Autonomie legacy vehicles to support the Systems and Modeling for Accelerated Research in Transportation (SMART) Mobility Consortium.
- Major improvements in GUI includes the following,
 - Added new vehicle warnings.
 - Refactored Autonomie models and extensible markup language (XML) library files prompted by the additional warnings.
 - Improved the performance of the Edit a Vehicle workflow (e.g., signal loading is faster).
 - Combined the Edit a Vehicle and Run a Vehicle workflows into a single new workflow.
 - Added changes to the Eval, Build, and Save workflow from the Run a Vehicle workflow.
 - Created an import legacy vehicle on the startup feature to enable external users to migrate to AMBER.
 - Began development of a legacy process import feature.

- Created a Matlab backend to allow the import of legacy processes with user-defined movable steps. Created a new XML specification for movable steps.
- Assured the quality of our AMBER and Autonomie software.
 - Developed additional regression tests to validate the integrity of a release.
 - Refactored existing regression tests to make the software more maintainable and modular.

Functional improvements

Each release brings the software closer to the ultimate goal of providing a seamless process that enables use of Autonomie models and results with RoadRunner, Aimsun, and POLARIS (Figure I.3.2.1).



Figure I.3.2.1 The Energy for Transportation Workflow

This report highlights just a few of the major features developed during this time. AMBER now provides users the ability to save changes that they make to a vehicle as a macro file. This feature allows users to save vehicle transformations. Using prerecorded macros that are shipped with the release, any user can change a vehicle from a two-wheel drive to a four-wheel drive, a gasoline to a diesel, an automatic to a manual, or a conventional to a belt-integrated starter generator (BISG) with just a few clicks.

Another new feature that supports our project is the Large-Scale Study Workflow. This workflow will allow the configuration of large-scale studies such as the Vehicle Technologies Office (VTO) analysis and real-world energy impacts. Studies with up to a million vehicles can be designed and run from the user interface shown in Figure I.3.2.2. Making modifications to the study will be significantly faster, requiring only some quick changes through the user interface (UI). The user defines a tree of simulations based on the selected technologies. Branches can be selectively added to the tree to represent all of the technology combinations that will be simulated. This number of combinations grows exponentially as time frames, vehicle architectures, fuels, other vehicle, and powertrain technologies are added.

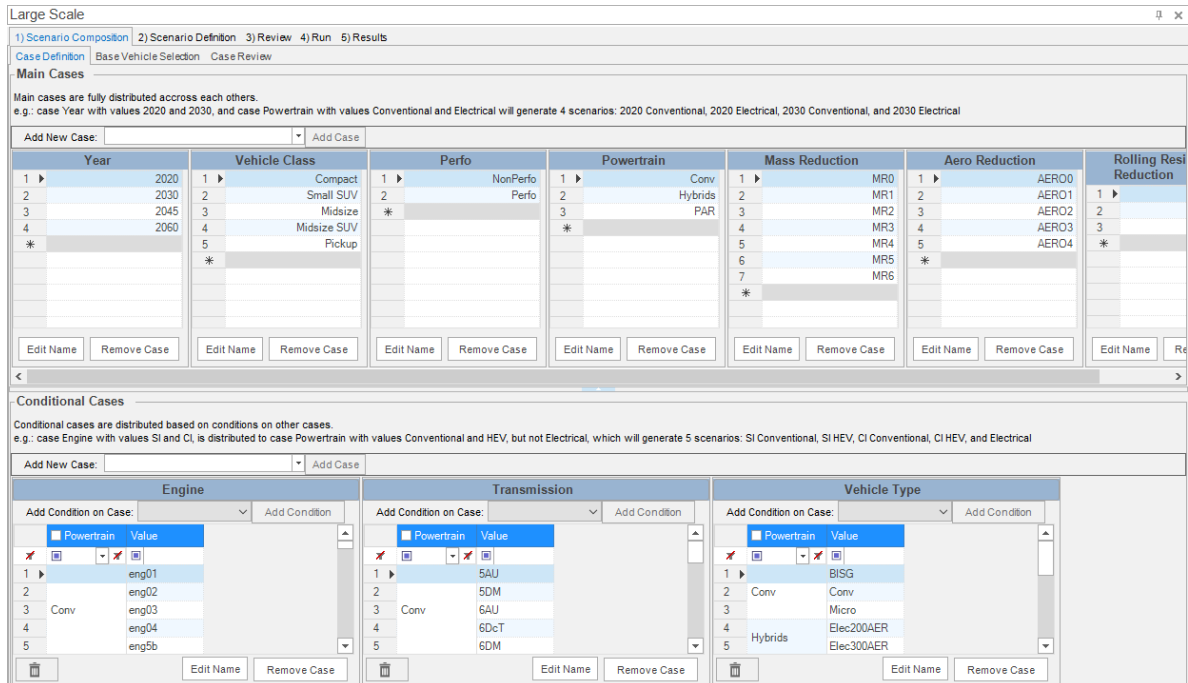


Figure I.3.2.2 Main Tab of the Large-Scale Workflow

Essentially, all large-scale studies are parametric studies and involve changing the parameters of a vehicle. However, previous tools had limitations on the type of parameters that could be changed. Only scalar parameters could be set directly, but because Autonomie models have vectors and matrices, which calibrate the model, the need arose to change the vectors and matrices. Many users have pointed out the benefit of being able to change such parameters in the UI in both a tabular form and even in a graphical form. For this reason, a vector and matrix tabular editor was added to the Autonomie parameter tab. This feature had not been integrated before because of the complexity of the problem; however, because AMBER had been designed with a “separation of concerns” in mind, the architecture could be updated with these new parameter types.

New reference vehicles and model improvements

Light-duty vehicles

We have added a new vehicle architecture similar to that of the Acura MDX to Autonomie. This architecture has a motor integrated to a dual clutch transmission (DCT) and a second motor on the rear axle. A new control model was developed for this architecture, as it differs from any existing hybrid vehicle’s control logic in Autonomie.

Heavy-duty vehicles

New reference vehicles for single-unit trucks have been developed. We now cover both automatic transmissions (ATs), automated manual transmissions (AMTs).

As part of improving the vehicle sizing process in Autonomie, we added new requirements to verify the capability to negotiate grades at highway speed and the ability to launch the vehicle on an inclined road with up to 20% grade (Figure I.3.2.3). These two requirements highlighted the need for a multi-speed transmission for electric powertrains. New reference vehicle models are now in Autonomie as examples for electric, series hybrid, and fuel cell hybrid trucks with a transmission.

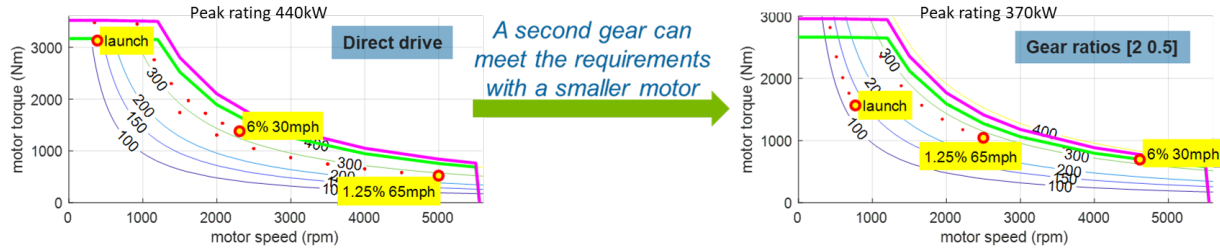


Figure I.3.2.3 A 2-Speed Gearbox Can Help Reduce the Motor Size and Still Meet the Performance Requirements

Large differences in transmission ratios, as we see in this two-speed example, is known to be a potential durability issue for trucks, so further work on optimizing the gear ratios and final drive ratio will be carried out as part of ongoing activities. We have also updated component cost calculation methods as part of this year’s work. This update provides the capability to switch between different cost conventions, and users can bring in their own cost functions easily without updating any of Autonomie’s native files.

Direct On-Track Aero/Roadload Measurements for Multi- and Mixed-Vehicle Platoons

In the last FY, the goals were to develop the hardware and controls necessary to acquire high quality data to resolve the road load changes in a computer-controlled, three-vehicle platoon at various gap distances. In order to complete the final project goals of a generalized platoon road load equation, the rate of data collection must be increased dramatically. This required improving the robustness and ease of use of the control and data acquisition system. A better data acquisition system was developed with improved GPS and gap sensors integrated into the system.

COVID-19 restrictions presented two major challenges: 1) there can be no second operator in test vehicles during testing—only one person per car (the driver), and 2) staff could not travel to test tracks that required overnight travel. The first challenge was overcome by integrating a touch screen display which presents all the operator functions to the driver without taking their eyes off the road. The second challenge was partially mitigated by doing system controls checkout on closed Argonne roads. See Figure I.3.2.4 to see the heads-up display being utilized on a closed road at ANL.



Figure I.3.2.4 Improved Data Acquisition and Control System with Heads-Up Control Touch Panel

A nearby (45 min from ANL) track was contracted to do the final testing, but in September after the contract was completed, we were informed that the track, that has been in operation for more than 20 years, was now being closed for at least two years due to COVID-19. COVID-19 limitations notwithstanding, testing will resume in the spring of 2021 at a test track suitable for efficient, high-quality data collection (likely TRC in Ohio). In parallel to the testing effort, a collaboration was established with a major OEM whereas ANL will do experimental testing and the OEM plans to simulate the very same conditions with computational fluid

dynamics. The ANL data will be helpful for the OEM to validate their modeling runs and ANL/DOE will benefit with interpolated results and results not practical to test at the limit of small gap distances. This collaboration will also help in the generalized equation development planned for FY2021.

Vehicle in the Loop Core Capability Developments

Performing standard vehicle testing with the new challenges introduced by the level of automation in driving is not optimal and yields to a virtualization of the testing methods by the means of X-in-the-Loop approaches. Among them Argonne has focused on the Vehicle-in-the-Loop approach (VIL) which allows broad research topics into vehicles enabled by automation and/or connectivity on a chassis dynamometer. This approach relies on the ability to use simulated data as input to the vehicle's control, effectively "linking" the vehicle to a test environment.

Since the validity of this core capability is a key enabler for experimental testing of automated vehicles, in the past FY, Argonne validated the response and repeatability of the longitudinal control override on dynamometer against on-road tests. The tests were conducted at the three-mile oval Navistar Proving Ground in Indiana. The results showed high correlation for the gap and acceleration distribution.

In order to evaluate the energy impacts of automated functionalities, a "link" between the research vehicle and emulated environment is required. Following the successful validation of the VIL core functionalities on-track, the environment simulation capabilities were expanded to enable the dynamic integration of aerodynamic and accessory loads during chassis dynamometer testing. The inclusion of the hardware and associated control increases the fidelity of the VIL system and allows the characterization of the energy impact encountered of varying lead vehicle distance, cornering, and automated vehicle sensing and computational loads. To enable possible research with mixtures of human and automated operators, connections were established between Argonne's two chassis dynamometer testing facilities, enabling collaborative testing to occur in real time. To provide flexibility in the simulation, multiple emulated environments, including Aimsun and the open source driving simulator, CARLA, were directly integrated as possible research environments.

As the US vehicle fleet varies heavily in available category (car / truck), and available powertrains (conventional / xEV), a flexible VIL research fleet requires similar distribution of technologies. Additionally, varying research efforts require varying points of integration between the research vehicle and emulated environment. To support this desired flexibility, over six additional vehicles of varying levels of electrification and category have been integrated in addition to the baseline research vehicle, a 2017 Toyota Prius Prime. For many vehicles within the fleet, vehicle communication network overrides allow direct control of perception and longitudinal control functionality. Additionally, to enable non-invasive integration of current and future research vehicles of interest, methods were developed to utilize a robot driver for applying direct pedal inputs, greatly simplifying and expediting vehicle integration to the emulated environment. In both cases, the same external automated controller is used: in the first case, the controller implements a direct acceleration command, while in the latter the command is converted into pedal commands using maps developed from prior high-fidelity experimental correlations.

VIL EcoCAR Collaboration

As part of the VIL task, members of the EcoCAR Advanced Vehicle Technology Competitions section are collaborating to accelerate the implementation of connectivity technology and automated control overrides. By leveraging EcoCAR competition hardware, resources, and industry connections, this subtask aims to develop flexible hardware systems for generating V2X signals from real and simulated vehicles and infrastructure, in addition to overriding automated commands in Argonne's 2019 Chevrolet Blazer.

In the last FY, EcoCAR collaborated with GM to achieve axle torque override capability on the Chevrolet Blazer through direct intervention on the vehicle's CAN networks. In addition, the team worked towards developing a hardware system using Cohda's MK5 Dedicated Short Range Communication (DSRC) radios to enable generation of both Basic Safety Messages (BSM) and Infrastructure-to-Vehicle (I2V) messages in both

test track and dynamometer environments. Bench testing of multiple MK5s has been completed and a unit is integrated and functioning on the Blazer. The hardware system has the capability to read real-time vehicle information like speed, acceleration, and steering wheel angle from many modern GM vehicle CAN busses, package that information into Basic Safety Messages (BSM) and broadcast the BSM packets. This capability can be seen in the figure below, which shows a snapshot of the real time BSM packet visualization.

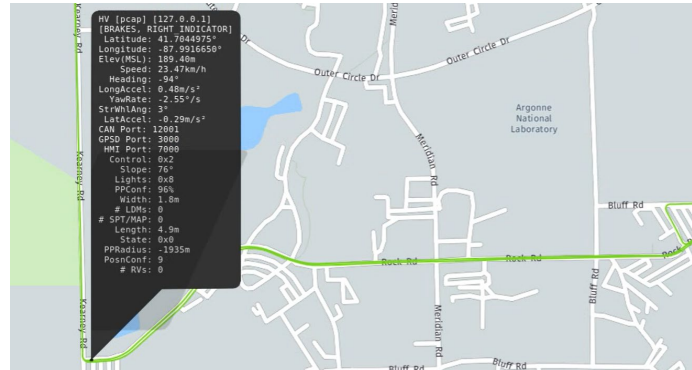


Figure I.3.2.5 Realtime Visualization of BSM Packets

The next phase of the project will involve the development of a portable connectivity interface that can be used to enable V2X connectivity on other vehicles in the VIL fleet in addition to the generation of BSM packets from simulated vehicles during VIL simulations. Now that basic ACC overrides are established on the Blazer, the next steps will involve full characterization of the override responses and integration of the system and test vehicle into the wider VIL environment.

Conclusions

Many users of legacy versions of Autonomie still exist and require features to enable them to migrate to the updated and enhanced AMBER/Autonomie. Features such as an automated vehicle import, a process library import feature, and new workflows such as Edit and Run a Vehicle are helping to ease the transition for these users. Supporting the legacy version of Autonomie also provides OEMs with the time to migrate their models and processes to AMBER/Autonomie in a structured, orderly manner. AMBER/Autonomie is the cornerstone of vehicle energy analysis at Argonne and at DOE. The new features implemented in AMBER/Autonomie are focused on enabling DOE to continue to run large-scale studies, such as SMART, with millions of simulation runs.

Experimental research efforts saw significant progress on Argonne's VIL development, with multiple emulated environments and research platforms demonstrating a path for flexible, precise, and repeatable experimentation of Connected and Automated Vehicles. On-track road load testing project made significant progress on a thorough upgrade to the measurement and control system for mass data collection, but circumstances related to the pandemic restricted testing and development of data until the spring of 2021,

Finally, the EcoCAR collaboration with GM achieved the axle torque override capability on the Chevrolet Blazer through direct intervention on the vehicle's CAN networks. In addition, a hardware system using Cohda's MK5 Dedicated Short Range Communication (DSRC) radios was successfully developed to enable generation of both Basic Safety Messages (BSM) and Infrastructure-to-Vehicle (I2V)

Acknowledgements

P. Sharer, R. Vijayagopal, K. Stutenberg, M. Duoba, T. Crain, T. Wallner (ANL)

I.3.3 Virtual and Physical Proving Ground for Development and Validation of Future Mobility Technologies (Oak Ridge National Laboratory)

Dean Deter, Principal Investigator

Oak Ridge National Laboratory (ORNL)
1 Bethel Valley Road
Oak Ridge, TN 37831
Email: deterdd@ornl.gov

Erin Boyd, DOE Technology Manager

U.S. Department of Energy
Email: erin.boyd@ee.doe.gov

Start Date: October 1, 2018
Project Funding: \$1,150,000

End Date: September 30, 2021
DOE share: \$1,150,000

Non-DOE share: \$0

Project Introduction

Emphasis on pushing the state of the art of advanced transportation technologies, specifically connected and automated vehicles (CAVs), has recently gained significant momentum in both government and industry. The Department of Energy’s SMART Mobility program is attacking the “transportation as a system” problem from multiple angles. Therefore, modeling, simulation, and analysis form the backbone for future prediction of the impacts of various technologies on mobility for the nation, in the form of the Mobility Energy Productivity (MEP) metric. A need has been identified to experimentally evaluate these solutions to ascertain the validity of their respective claims, as well as to generate critical data to feed back into SMART Mobility–developed tools for more detailed analyses. An advanced hardware-in-the-loop (HIL) platform capable of bridging the gap between analytical models and real-world hardware provides the intermediary to identify the most promising technologies that should be fully verified at the vehicle system level.

Model-based design has become the industry standard for developing vehicle supervisory and powertrain control systems. However, this approach misses the complexity of the interactions of physical hardware in real-world driving conditions. The novel approach proposed by ORNL advances the state-of-the-art research by exercising actual hardware in real-world traffic situations, in which the vehicle is expected to be operated, to capture the subtle effects of communication timing/latencies, actual powertrain energy consumption, emissions, and other dynamic phenomena. The ability to subject actual hardware to simulated real-world conditions allows diverse scenarios to be simulated for enhancing strategies and algorithms, as well as responding to micro- and macro-level traffic environments that current high-level traffic network models fail to capture. In addition, this framework provides a repeatable, cost effective environment for rapid development and validation of CAV technologies, including their respective vehicle controls and communication protocols. This capability offers the benefit of absolute safety, since the control algorithms are evaluated thoroughly in a controlled HIL laboratory environment before being targeted to an actual test vehicle for on-road or track testing.

Objectives

The objective is to accurately verify the energy benefits and emissions impacts of these advanced technologies with actual powertrain hardware physically installed in the laboratory and subjected to virtual traffic conditions for research. This approach presents the opportunity to research, develop, and evaluate a large matrix of CAV technologies over a greater, customizable design space at a time when vehicle-to-vehicle (V2V) and vehicle-to-infrastructure (V2I) hardware has not even been completely developed or is not available for full-scale testing.

ORNL will investigate early stage “smart” technologies as a system, regardless of the powertrain architecture or actual physical design selected by the researchers. Multiple research facilities within ORNL will be virtually connected to develop a novel and flexible approach to examine multiple hardware components in a variety of powertrain configurations and traffic environments in real-time, high-fidelity, traffic simulations while subjecting actual powertrain(s) to emulated real-world traffic conditions. This approach will allow for the development of control strategies and algorithms specifically targeted at advanced vehicle technologies, as well infrastructure controls.

Approach

Task 1: “Virtual-Physical” Proving Ground (VPPG)

In light of VTO’s efforts to tackle difficult questions regarding current and future smart vehicle technologies and their impact on mobility, the EEMS program and SMART Mobility consortium are trying to analyze many different CAV and SMART Mobility technologies to identify the most promising and efficient methods for future transportation and corresponding infrastructure. This work has highlighted a real need for cross-collaboration among different scientific skill sets to produce a well-analyzed and validated answer that starts in modeling and simulation and ends in validated HIL and vehicle-level laboratory experiments. This end-to-end process provides data to improve the modeling activities. ORNL is addressing this need by bringing together its various skill sets for use in the Virtual-Physical Proving Ground.

Objective: Establish and verify a capability to test and validate in HIL and VIL including V2X hardware the analytical results of current and future SMART Mobility and EEMS modeling, simulation, and analysis, as well as other relevant VTO programs. This testing and validating can provide data to improve modeling activities.

End-of-Project Goal: The end goals of this task are to (1) establish a standardized platform to allow for running multiple modeling and simulation types on multiple ORNL HIL platforms; and (2) apply this new standardized platform to ORNL’s modeling and simulation tasks of vehicles controls from SMART 1.0 in a HIL environment, and apply these HIL methodologies to other DOE-developed traffic simulation tools.

Subtask 1.1: Standardized Virtual Proving Ground Framework.

The goal of Task 1.1 is to allow flexibility in creating combinations of modeling, simulation, HIL, and vehicle-level testing. This task focuses on establishing a standardized framework that allows for the integration of multiple HIL -based research capabilities within ORNL, as well as provisions for connectivity with other national laboratory facilities, tools, and capabilities. This will allow for greater flexibility and for ease of integrating required formats, including macro traffic simulations and high-fidelity vehicle environment simulations. This flexibility to integrate many different modeling and simulation software is an important aspect of Task 1.1 because of the many different DOE tools that are being developed by DOE laboratories, as well as industry tools already in use both within the DOE laboratory system and by industry partners. Once the framework is completed, ORNL will begin to integrate a small selection of EEMS and/or SMART Mobility tools and data sets into a verification tool and as a high-fidelity data collection effort for more robust, validated models as part of subtask 2.3. Data will be collected by a fully instrumented RAV4 mule vehicle on Bethel Valley road at ORNL’s main campus. Then, ORNL’s digital twin of the main campus will be used to replicate the scene and traffic experienced by the test vehicle on the real road. Lastly, the ORNL RAV4 mule vehicle that drove the real route will be deployed in the CAVE lab to virtually drive through the digital twin of Bethel Valley.

Subtask 1.2: Virtual Proving Ground Applied to HD Platooning.

As part of an ORNL Laboratory Directed Research and Development project, a traffic network is being constructed of Interstate I-40 in the Knoxville area. This task will apply the framework developed in Task 1.1 to better understand the impacts of platooning in real-world traffic conditions on both urban and rural highway systems. Test track data from the SMART Mobility CAV Pillar for platooned HD vehicles will be leveraged to establish the aerodynamic parameters for first, second, and third trucks. Cummins will assist in getting a

current-production X-15 Class 8 engine and after-treatment package coupled with an Eaton Smart Advantage Ultra-Shift transmission operational in the VSI laboratory. Using HIL techniques this powertrain hardware will be “virtually” installed in the platooned vehicles to fully characterize fuel consumption and emissions impacts of platooning in a host of various traffic conditions and interactive traffic objects. To perform realistic testing in the HIL environment, basic sensors (radar and line/lane detection) and communications used for traditional platooning applications will be emulated and integrated into the optimized platooning control.

Subtask 1.3: Virtual Proving Ground Applied to Open-source tools.

While commercial simulation tools are often more feature rich, further developed, and user friendly, they are extremely expensive and often less flexible than their open-source counterparts. Due to the expense and flexibility, open-source tools are often favored by academia, research institutions, and national laboratories. Once ORNL has integrated its current selection of commercial virtual environment simulation tools (IPG Car/TruckMaker, dSPACE ASM, VIRES VTD, and PTV Vissim) into the VPPG, the team will then begin to integrate a selection of open-source tools into the VPPG as well. The three packages are CARLA (an open-source virtual environment), SUMO (an open source microtraffic simulation), and ROS/Autoware (an open source perception and control stack). Once these links are established, ORNL will then utilize them in a laboratory setting to work out any real-time or HIL concerns with these very new and flexible software packages. This is critical as open-source software packages often have bugs associated with strict computation time steps. Once this task is complete it will be applied to the SMART Mobility project within Subtask 2.3.

Task 2: (V2X) Communication Modeling, Development, and Validation

Currently, V2V, V2I, and other vehicle communications (V2X) are in their infancy. What final V2X infrastructure and capabilities look like is an ever-changing landscape. This situation emphasizes the need for development and testing platforms that are extremely flexible, programmable, and able to go back and forth from the modeling/simulation space to real hardware testing. ORNL’s VSI Laboratory, Vehicle Research Laboratory, and CAVE Laboratory are extremely well suited for fulfilling this need. With the virtual vehicle environment established in Task 1, V2X hardware will be tested while tied to a virtual vehicle in a real-time HIL environment or can be tied to an entire vehicle or powertrain in the test cell. This testing is all done in an extremely flexible environment that allows for low- to high-fidelity data streams, quick programming changes, and repeatable laboratory results.

Objective: Expand the capabilities of the EEMS program to not only test V2X hardware in simulation, but also allow for using HIL methodologies and virtual environments to test V2X hardware in real time.

End-of-Project Goal: The end goals of this task are to (1) establish a high-fidelity HIL model of common dedicated short-range communications (DSRC) to be run virtually on ORNL’s simulation platforms, and (2) using ORNL’s HIL systems, have two DSRC units working in real time. One will be tied to a virtual traffic object and a second tied to a physical powertrain in the VSI Lab for subtask 1.2 or a vehicle in the CAVE Lab in subtask 2.3. The units under test will react to its virtual vehicle environment based on data coming in on the real-time DSRC hardware signals.

Subtask 2.1: Integration of V2X Communications Hardware into Virtual Proving Ground Framework.

Subtask 2.1 enhances the Virtual Proving Ground with a communications-focused testing platform consisting of multiple V2X communication hardware development units integrated into several ORNL vehicle test facilities and HIL-enabled test facilities such as the VSI, CAVE, and Vehicle Research. The Vehicle Research Lab is a traditional chassis dyno lab that is used for fuels and emissions work that will be added to the network of systems, so two full vehicles could run in the loop. This approach enhances the overall Virtual Proving Ground capability with the ability to understand V2X hardware integration, communication, latency, controls delays, reliability, interference issues, and so on. This is achieved either through virtual communications or physical communications depending on lab proximity. For instance, the Vehicle Research and Security laboratories are within physical communications distance, but the VSI laboratory is not and must rely on a virtual link.

Subtask 2.2: Light-Duty Virtual Proving Ground for V2X Evaluation.

As a means of proving the capability established in Task 2.1, the team will collaborate with the American Center for Mobility (ACM) staff. The objective of Subtask 2.2 is to replicate “virtual versions” (i.e., digital twins) of the ACM facilities and communications network so that CAV technologies and control strategies can be quickly and easily verified in a safe, secure setting before vehicle deployment. Since actual vehicle components will be exercised through modeling, simulation, and HIL approaches, a full understanding of the expected energy and communications impacts can be achieved. These enhancements to the digital twin will allow this project’s communication models, hardware, and degradation experiments to be verified at ACM in collaboration with the ACM Model Validation project. Working closely with ACM staff, the approach presented here can cost effectively expand the possible design space of new and emerging technologies with a higher degree of accuracy (due to HIL principles) while providing insight into test plan development for full vehicle/system testing. Specifically, the utilization of the virtual replica of ACM facilities allows for current and future co-development and targeted, preliminary testing that optimizes scenario definition and track usage. Utilizing the work done in Subtask 1.3, the replicated communications network will also be integrated with CARMA modules similar to the ones used by ACM in order to allow the ORNL mule vehicle to communicate with the virtual roadside units mirroring ACM’s layout.

Subtask 2.3: Connected Laboratory Coordination Testing.

As a part of the DOE SMART Mobility 1.0 consortium, ORNL has developed an approach for optimizing CAV control and coordination. This modeling framework can be adapted to different traffic scenarios and can be used in a real-time system, given its analytical, closed-form solution. The approach taken to coordinate vehicles has been used to assess the impact of full penetration of optimally coordinated CAVs across different traffic scenarios. Applying this concept to vehicle HIL can validate the fuel-saving trends that have been found through simulation and/or provide feedback for model development. To this end, actual V2X communication, between the vehicles located in various ORNL HIL laboratories and a central coordinator, will improve a real-time optimal merging coordination algorithm. A chassis dynamometer (CAVE lab) and HIL components will interact through a traffic simulation with virtual vehicles. All the “vehicles” will receive control inputs from the centralized coordinator according to the optimal controller computations. The vehicles and powertrains located in the various HIL dyno laboratories will be operated by both real and virtual drivers that will follow the instructions given by the central coordinator. A minimum of two laboratories will be connected in this testing, but more can be added depending on project resources.

Results

Subtask 1.1: Standardized Virtual Proving Ground Framework.

As part of the fundamental tool creation, ORNL developed Simulink libraries, vehicle model templates, and MATLAB scripts to aid developing vehicle models. The Simulink libraries include powertrain component models (e.g., engines, transmission, and final drive) and controllers (e.g., TCM and TCM) appropriate for desktop simulations and HIL testing in the VSI laboratory. The Simulink libraries also include a longitudinal Model Predictive Control (MPC) driver capable of closely following a reference velocity based on vehicle parameters. The MPC driver can be used to follow drive traces or integrated into a controller for automated vehicle applications. Using the Simulink libraries, ORNL built vehicle model templates to provide a starting point for HD Platooning work (see Task 1.2) and Automated Vehicle Merging of On-Ramps (see Task 2.3).

Building on the work performed for first year setup and installation, the second year of work was primarily developing foundational tools and solid application platforms. To complete this task, the team deployed the dSPACE SCALEXIO racks as well as the dSPACE Automotive Simulation Models (ASM) platform. ASM provides workflows, models, and visualization capabilities necessary for virtual vehicle environment integration tasks. The targeted labs for platform deployment and research were the Vehicle Systems Integration (VSI) lab as well as the Connected and Automated Environment (CAVE) lab. Both lab deployments leveraged

a similar path for integration, with model development being at the forefront followed by a rigorous testing and validation task.

In the VSI lab, the team leveraged a medium-heavy duty powertrain utilized in a previous DOE FOA that included a 6.7 Cummins ISB, Alison 3000 transmission, and associated drive components. A medium duty model was developed and integrated in the dSPACE ASM environment for testing with powertrain installed on the dynamometer. Real-time torque from the powertrain on the dynamometer was measured and fed to the model for torque actuation of the virtual vehicle, while the driver used analog signals to interact with the powertrain (matching the configuration on a real vehicle). In this configuration, the virtual driver and vehicle coupled with the powertrain under test were able to successfully navigate a rigorous handling track in real-time (Figure I.3.3.1). This is a critical step for medium- and heavy-duty powertrains in the VSI lab and enables virtual integration via dSPACE ASM with any powertrain following proper parameter estimation and initialization.



Figure I.3.3.1 Dspace ASM Virtual Vehicle-In-The-Loop (Left) Fully Integrated and Navigating a Handling Course Using Feedback from the Powertrain Under Test (Right)

In a similar fashion to the powertrain-in-the-loop-VSI setup, a pure vehicle-in-the-loop deployment was completed and tested in the CAVE lab. For this testing, a 2019 Toyota RAV4 Hybrid was mounted to the RotoTest wheel dynamometer shown in Figure I.3.3.2. Torque and steering feedback provided from the wheel dynos and vehicle CAN actuate the virtual vehicle, while the vehicle model in the SCALEXIO rack provides road load feedback to the vehicle and driver. In this configuration in the CAVE lab, a real driver can drive the virtual vehicle using real actuation from the accelerator, brakes, and steering outputs to feed the vehicle in simulation and associated visualization. This capability is a direct complement in the light-duty space to the VSI lab as well as a powerful deployment of the RotoTest system.



Figure I.3.3.2 CAVE Lab Setup with Full Vehicle-In-The-Loop (VIL) Functionality, Including Steering, Integrated with Virtual Vehicle Environment

Subtask 1.2: Virtual Proving Ground Applied to HD Platooning.

To evaluate the impact of platooning on fuel economy, ORNL developed a model of a Class 8 truck. The model includes longitudinal dynamics, automated manual transmission, fuel flow prediction, and can be easily modified to simulate different loads. Depending on the application, the model can be quickly configured to run desktop simulations or HIL testing in the VSI laboratory. ORNL validated the model by comparing desktop simulation fuel economy to VSI HIL testing results. The next step will be correlate truck following distance to aerodynamic drag and use the models to simulate platooning scenarios.

Subtask 1.3: Virtual Proving Ground Applied to Open-source tools.

To perform integration of these open-source packages into the VPPG, one must understand where the packages fit into the VPPG structure and how will they connect to adjacent portions. The most universal piece of the structure is the Robot Operating System (ROS). ROS is an open-source suite of middleware files built upon the Ubuntu Linux operating system. With ROS installations on multiple machines in a network, one can quickly build basic communications functionality between these machines via ethernet. In the VPPG structure this feature is desirable because multiple machines will be required due to the computation complexity of each program involved such as virtual vehicle environments, microtraffic simulation, as well as sensor data processing. In this structure, ROS is the common software on each machine that will enable the fast, effective ethernet communication between all the machines on the distributed network utilizing a master node that controls all information flow from various nodes that publish out or subscribe to information. However, ROS only provides the tools to set up this communication; furthermore, the necessary software to broadcast relevant information to the network is typically handled by the open-source software tool (i.e., CARLA, SUMO, Autware) developers. This software developed using the ROS libraries is a critical tool in the communication between various tools of the VPPG.

The first package of ROS software to examine was the bridge developed for the CARLA simulator by the CARLA development team. The initial setup of this software utilized a single machine running an instance of CARLA and its associated CARLA-ROS bridge which provides the software to stream vehicle and sensor information to the ROS network. The CARLA-ROS bridge also provides launch files that set up the ROS nodes and broadcast information out to the local network, spawn an ego vehicle in the CARLA server, and

provide the user a manual control interface for the ego vehicle. This process provided a basic ROS functionality check by performing an internal broadcast of ROS topics from CARLA to the ROS network and sensor data from the ego vehicle lidar and camera was visualized in the ROS visualization package (Rviz).

The ROS-bridge setup was enhanced by distributing the ROS network over multiple machines at ORNL via an ethernet switch. The configuration ran the CARLA server and clients on a simulation PC while connected to a local network with a central sensor processing PC (Autonomous Stuff Spectra Graphics Processing Unit). On the Spectra's installation of Ubuntu, lidar data from the CARLA ego-vehicle was visualized in Rviz shown in Figure I.3.3.3.

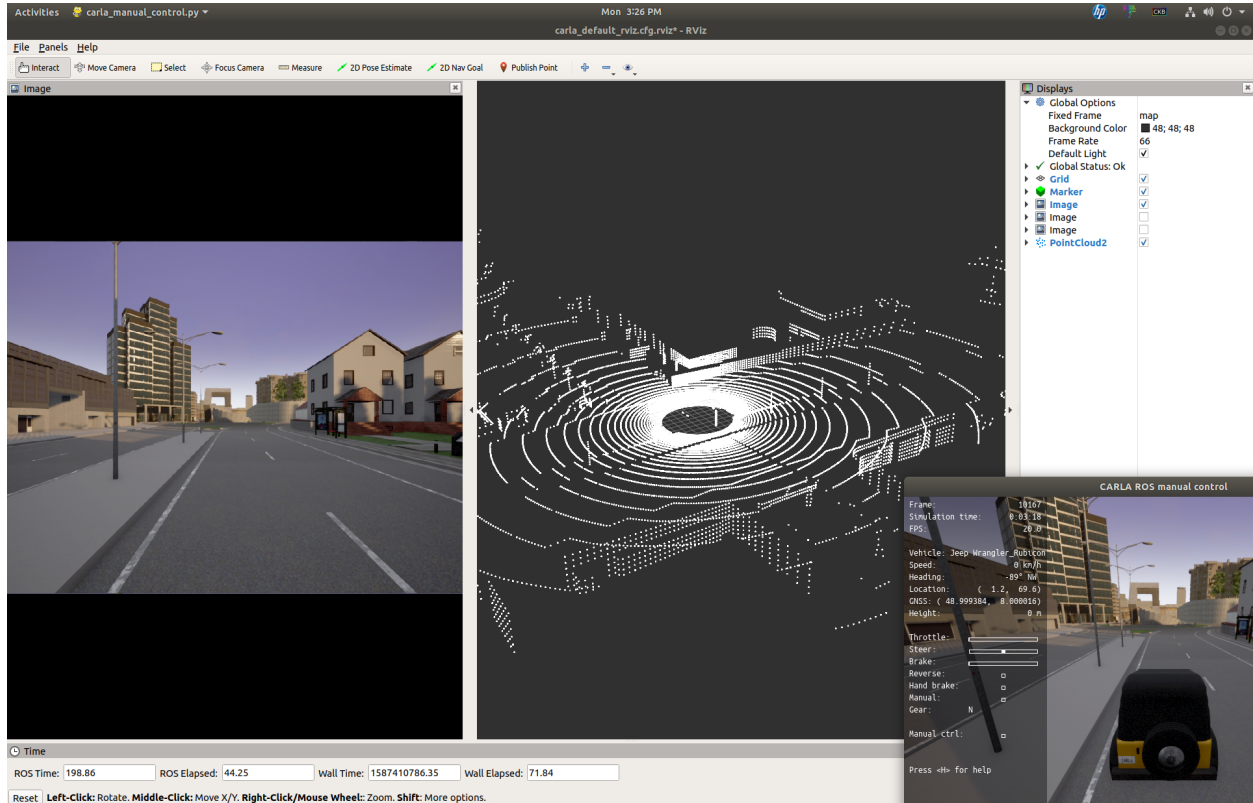


Figure I.3.3.3 Snapshot of Rviz Displaying Camera and Lidar Point Cloud Data from the Ego-Vehicle Operating in the CARLA Server. The Manual Control User Interface and Relevant Commands are Shown in the Bottom Right

In addition to the CARLA-ROS bridge, the CARLA development team also provides an interface between the CARLA simulator and Autoware, an open-source software package for autonomous driving technology built upon ROS. This CARLA-Autoware bridge enhances the CARLA-ROS bridge by providing the necessary information from a vehicle in CARLA to meet the control requirements of the Autoware software package. The CARLA-Autoware bridge was also checked for functionality on a single machine. Furthermore, the configuration was expanded to multiple machines by setting up an Autoware PC to communicate, through the CARLA-Autoware bridge, with a remote CARLA server through a router on a simulation PC. The Autoware control data and CARLA ego-vehicle perception data are plotted in Rviz on the Autoware machine in Figure I.3.3.4. Important characteristics of these multiple PC configurations were the possible latency and bandwidth limitations. These characteristics were studied using the network tool Wireshark while the CARLA-ROS and CARLA-Autoware bridge configurations were executed. No noticeable latency was noted for most of the packets transmitted for this setup. Some instances of dropped, retransmitted and long wait times between packets were noted in the Wireshark, but these instances were infrequent over the entire communications trace.

The bandwidth usage was noted to be ~250 MB/s on a 1 Gbe connection (~25% utilization). This statistic was recorded while broadcasting data from 1 lidar and 1 camera through the CARLA-ROS bridge.

Additionally, during simulations with the multi-machine CARLA-Autaware bridge, an instability was noted in Autaware during dynamic maneuvers (i.e., turns and lane changes). Experiments were performed with test setups that used a local build of Autaware and a docker image that integrated Autaware and the CARLA-Autaware bridge which was provided by the CARLA team on their GitHub. The docker image of the CARLA-Autaware bridge was noted to be more stable than the local build and much simpler to implement on different machines due to the nature of containerized applications using Docker.



Figure I.3.3.4 Left: The CARLA Server with an Ego Vehicle Making a Right Turn. Right: The Autaware Rviz Configuration Displays All the Relevant Sensor Data to Localize the Ego Vehicle and Follow the Green Waypoints

Subtask 2.1: Integration of V2X Communications Hardware into Virtual Proving Ground Framework.

No work was performed for this subtask in FY2020.

Subtask 2.2: Light-Duty Virtual Proving Ground for V2X Evaluation.

As shown in Figure I.3.3.5, virtual replica of the ACM facilities has been implemented and verified in various virtual environment simulation tools including Virtual Test Drive (VTD), IPG CarMaker, and PTV VISSIM. Real V2I communication network at ACM has been modeled and replicated in these virtual environments as well, see Figure I.3.3.6. With the integrated digital twin of ACM track and actual communication network, communication models can be verified and impacts of communication (such as latency, packet drops) on the CAV applications can be fully understood. Therefore, a high-fidelity proving ground is developed for rapid evaluation of CAV technologies and control strategies in a safe, secure setting before vehicle deployment. Currently, a speed harmonization algorithm [1] has been implemented into the simulation tools with the ACM digital twin to demonstrate the virtual proving ground.

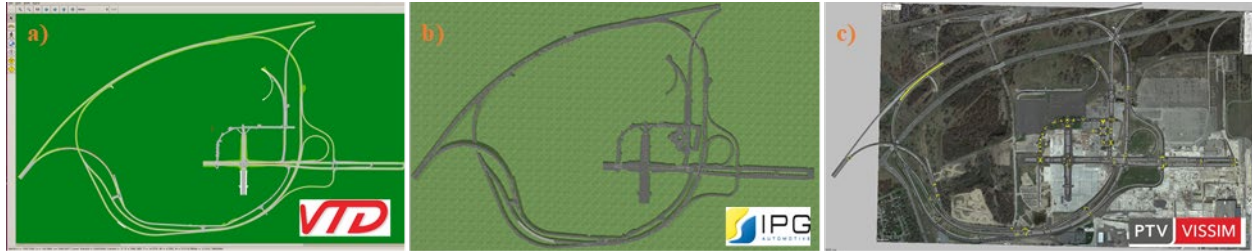


Figure I.3.3.5 Virtual Replica of the ACM Track in: A) VTD; B) IPG Carmaker; C) PTV VISSIM

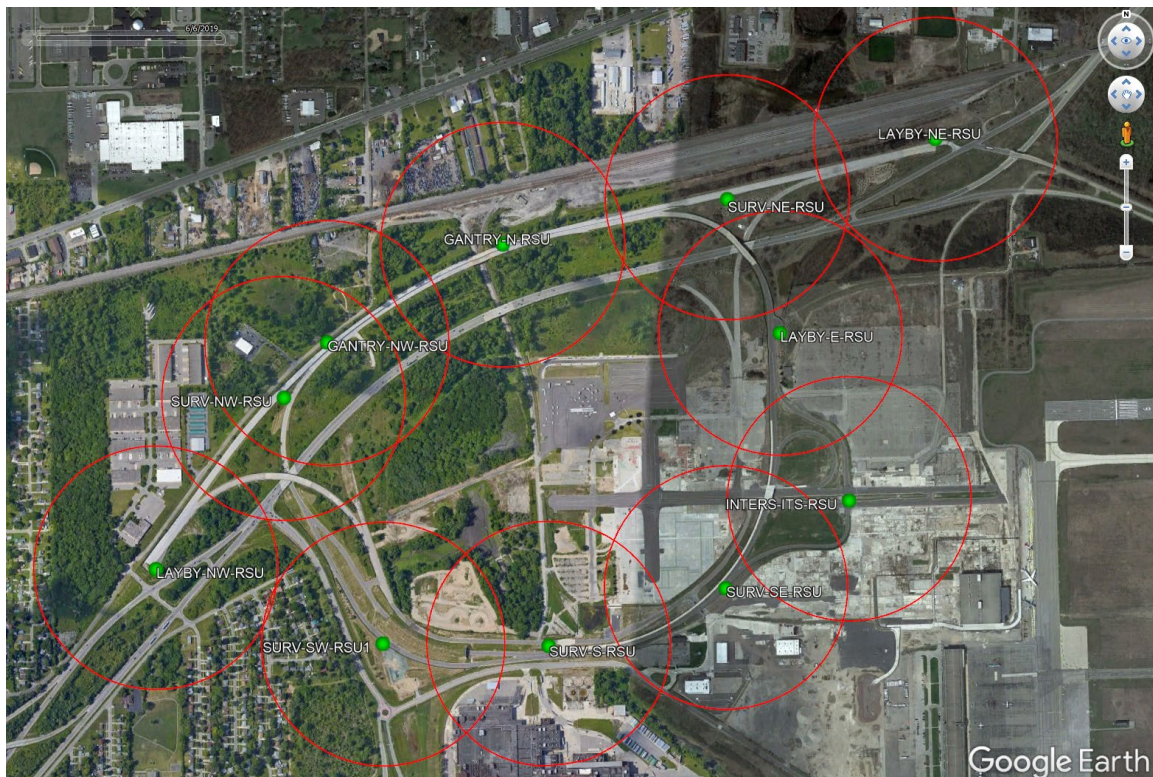


Figure I.3.3.6 Communication Network Replica of ACM Track. Green Dots: Location of Rsus; Red Circle: Communication Range

Subtask 2.3: Connected Laboratory Coordination Testing.

ORNL started developing vehicle models to predict fuel consumption for vehicle merging scenarios in the virtual environment. Using the tools and libraries developed in Task 1.1, ORNL modelled an EV and began work on a conventional vehicle model. The models include mapped-based engine, motor, and battery models for predicting energy usage and to meet real-time requirements. The EV and conventional vehicle (once completed) can be adapted to simulate a variety of vehicle classes with the same powertrain architecture. Future work includes completing the conventional vehicle model and HEV model development.

The real-time cooperative and automated vehicle merging algorithm [2],[3] previously developed by ORNL has been integrated with the ACM track digital twin (from Task 2.2) and prepared for experiments validation on the CAVE lab and HIL lab. Three subtasks have been accomplished. First, the merging algorithm has been efficiently implemented in the external driver model of VISSIM in C++ codes. Second, a real-time co-simulation framework of the IPG Carmaker (vehicle dynamics and 3D environment), and VISSIM (traffic simulation and merging algorithm) has been developed as shown in Figure I.3.3.7. At each simulation time step, the merging algorithm receives current speed and position of all vehicles from VISSIM and coordinates

the arrival time of all CAVs within the merging control zone. The optimal speed guidance of these vehicles is calculated and sent to VISSIM. Any of the vehicles within the control zone can be selected as the ego vehicle, whose vehicle and powertrain dynamics are simulated in IPG. The rest background vehicles are simulated by VISSIM. At each time step, performance of the ego vehicle and background vehicles are shared and synchronized between IPG and VISSIM. Third, the co-simulation framework has been validated on the SCALEXIO real-time control system, which is the same system used in CAVE lab and HIL lab. After this validation, the co-simulation framework will be ready for the actual experiment environment. Figure I.3.3.8 shows a screenshot of the SCALEXIO implementation. The IPG simulated vehicle dynamics is compiled and executed on the SCALEXIO real-time control system, VISSIM is running on a PC-desktop, and the synchronization between the two are established through Ethernet. To replicate dynamics of an actual vehicle, powertrain simulation model of a Chevy Bolt has been developed, calibrated, and implemented on the SCALEXIO.

Conclusions

This being the second year of a three-year project focused on tools development, a large portion of the work performed was mostly setup for the more application or validation driven work that will occur in year 3 of the project. However, there was significant accomplishments in the areas of bridging the gap between pure simulation and hardware application utilizing HIL methodologies and techniques. The integration of the Vehicle Systems Integration and Connected and Automated Vehicle Laboratories in the VPPG was a big step forward in this project to allow for realistic energy consumption, powertrain/vehicle dynamics, and controls development; both from a vehicle and coordinated controller perspective. This addition to the VPPG will allow for year three’s more application focused subtasks to fully exercise the experimental and simulation space.

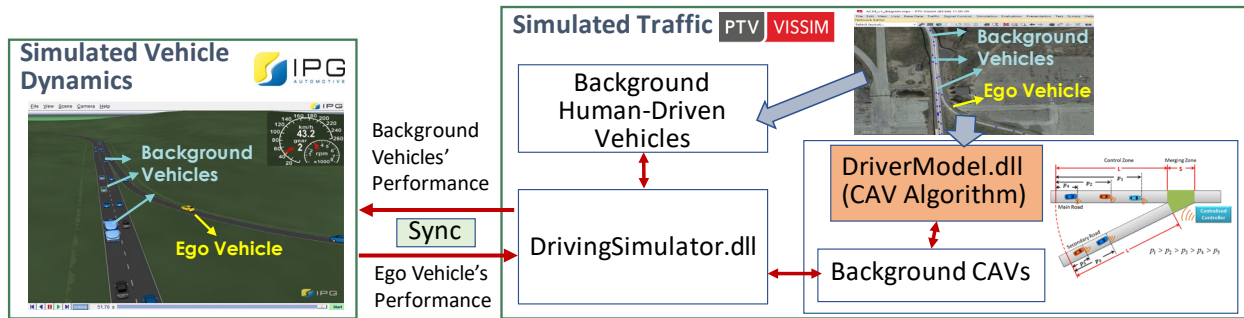


Figure I.3.3.7 Diagram of IPG Carmaker and VISSIM Co-Simulation

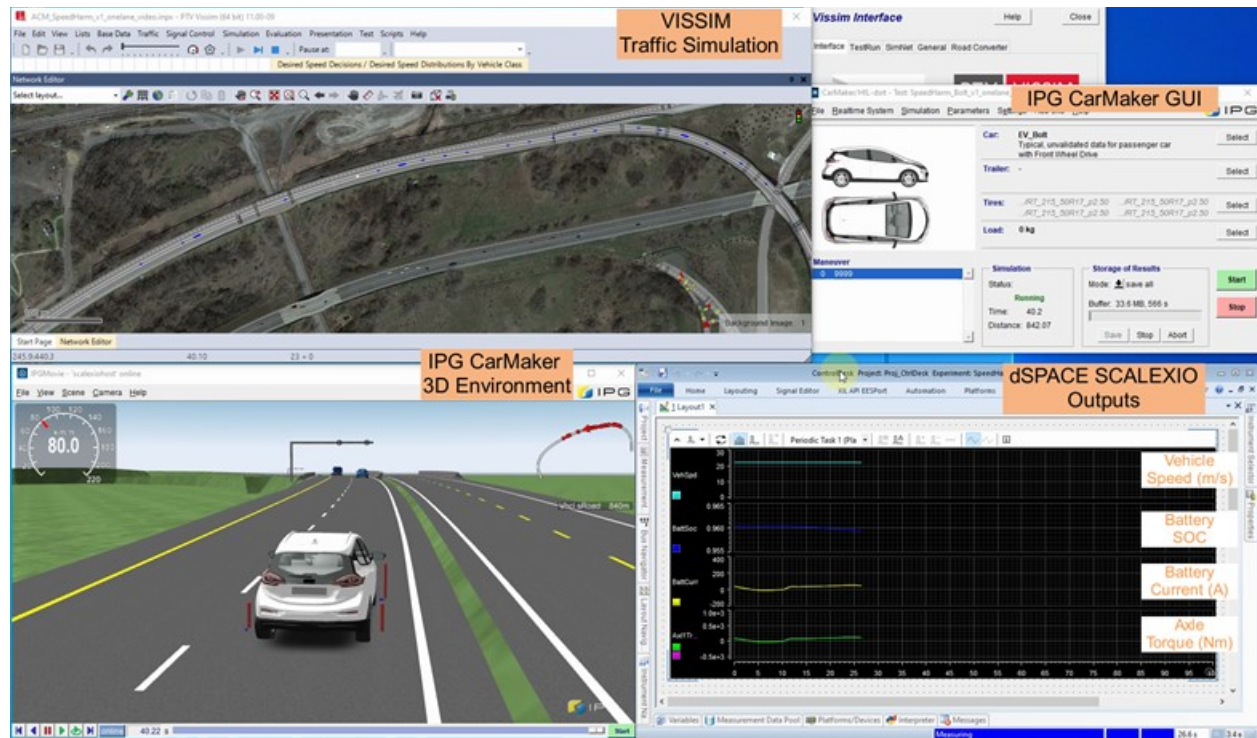


Figure I.3.3.8 IPG Carmaker and VISSIM Co-Simulation on SCALEXIO Real-Time Control System

References

1. A. A. Malikopoulos, S. Hong, B. B. Park, J. Lee and S. Ryu, "Optimal Control for Speed Harmonization of Automated Vehicles," in *IEEE Transactions on Intelligent Transportation Systems*. doi: 10.1109/TITS.2018.2865561
2. J. Rios-Torres and A. A. Malikopoulos, "Automated and Cooperative Vehicle Merging at Highway On-Ramps," in *IEEE Transactions on Intelligent Transportation Systems*, vol. 18, no. 4, pp. 780–789, 2017. doi: 10.1109/TITS.2016.2587582
3. J. Rios-Torres and A. A. Malikopoulos, "Impact of Partial Penetrations of Connected and Automated Vehicles on Fuel Consumption and Traffic Flow," in *IEEE Transactions on Intelligent Vehicles*, vol. 3, no. 4, pp. 453–462, Dec. 2018. doi: 10.1109/TIV.2018.2873899

Acknowledgements

ORNL would like to thank David Anderson and Erin Boyd as the DOE EEMS Program Manager and Technology Manger, respectively and their continued support on this project.

I.3.4 DOE/DOT Automated, Connected, Efficient, and Shared (ACES) to Human-Centric Mobility Metrics -Identifying Common Metrics, Research Methodologies and Collaboration Opportunities across DOT-DOE Mobility Portfolios (NREL)

Joshua Sperling, Principal Investigator

National Renewable Energy Laboratory
15013 Denver West Parkway, MS 1625
Golden, CO 80401-3305
Email: joshua.sperling@nrel.gov

Alejandro Henao, Principal Investigator

National Renewable Energy Laboratory
15013 Denver West Parkway, MS 1625
Golden, CO 80401-3305
Email: alejandro.henao@nrel.gov

Erin Boyd, DOE Technology Manager

U.S. Department of Energy
Email: erin.boyd@ee.doe.gov

Start Date: October 1, 2017
Project Funding: \$155,000+

End Date: October 1, 2020
DOE share: \$155,000

Non-DOE share: \$0

Project Introduction

The purpose of this project was to encourage, formalize and institutionalize cooperation across the U.S. Department of Transportation (USDOT) and the U.S. Department of Energy (DOE) mobility research portfolios by:

1. Identifying common metrics research, analysis, and modeling methodologies
2. Identifying collaboration opportunities between offices and partners (including state and local governments).

Rapid technology development and new, innovative business models are spurring fundamental changes in the way people and goods move through the nation's transportation system. These changes could have significant implications for personal mobility, safety, systemic congestion, economic competitiveness, infrastructure design and planning, transportation cost and efficiency, and energy consumption. In particular, the changes brought by advances in automation, connectivity, and shared-use transportation represent an intersection of research challenges of interest to both the USDOT and DOE and present an opportunity to foster the safe advancement of system efficiency and mobility.

Automated, Connected, Shared, Efficient Mobility Research, or ACES, is the joint USDOT-DOE effort established to take on this challenge. ACES establishes a baseline of research knowledge across USDOT and DOE in order to avoid duplicative actions, and to better identify opportunities for USDOT and DOE to collaborate on research that can safely advance the mobility of goods and people while optimizing system efficiency.

By fulfilling the objectives of ACES and an emphasis on new integrated mobility metrics, both departments will be better positioned to accelerate their respective secretarial priorities, confirm that research activities by both departments are relevant and complementary to public, private, and stakeholder's interests, and ensure that research dollars are used more effectively and efficiently through a transparent and collaborative process.

USDOT and DOE each have long-standing programs that overlap the ACES space to varying degree and with different emphasis (e.g., an emphasis on safety for DOT and an emphasis on energy efficiency for DOE). Furthermore, the organizational structures within each department are built around varying frameworks of transportation modes, market sectors, and technological maturity. A critical challenge for this effort is addressing the fact that many of these new technologies and approaches are not necessarily constrained by traditional organizational boundaries. As a result, an understanding of what can drive better coordination and collaboration between the departments is especially important. As an example, we focused on the review of and potential for new human-centered mobility metrics, rather than vehicle-centered mobility metrics, and the implications.

Objectives

The overall purpose of this project started with conducting an interrelated set of activities that worked to encourage, formalize and institutionalize cooperation across DOT and DOE mobility research portfolios by: identifying **common metrics**; identifying **common research, analysis, modeling methods**; and identifying **collaboration opportunities** between offices and partners (including state and local governments). From the state of the practice summary and joint workshops, the team then undertook a scoping study issue paper (Q1), discussion paper with case studies (Q2), conference paper (Q3) and journal article for dissemination on human-centered mobility metrics (Q4). The main effort this year focused on the role of occupancy and human-centered metrics.

Approach

The full project included five different tasks, that are listed below. Before FY20, Task 1 and Task 2 were completed. The NREL activities in this fiscal year included Task 3, 4, and 5, with efforts that focused on building on the state of practice summary and gaps identified:

Task 1 – State of practice summary: this task focused on initial identification of areas of current research and deployment activities being undertaken by both DOT and DOE individually in the technology-enabled mobility ecosystem. (prior to FY20)

Task 2 – DOE/DOT Joint Workshop – Based on the results of the state of the practice summary, a working meeting was convened to discuss issues identified in the state of the practice summary, including interest in new metrics and focus on occupancy. (prior to FY20)

Task 3 – Scoping study new mobility metrics paper: The scoping study focused on developing an issues paper that reviewed the literature and prepared an outline on issues and opportunities for DOE and DOT to advance the state of the practice in ways that bring together congestion, mobility, and energy efficiency objectives for transportation through leveraged efforts, common metrics, and initial case studies.

Task 4 – Mobility metrics extended discussion paper with case study contexts: Upon review of the scoping study results, the team moved forward to develop an extended report that addressed some of the key issues identified in the issue paper and building on discussions as part of a Transportation Research Board (TRB)-side workshop; with focus on potential real-world applications via case studies and data-driven opportunities with analysis and scenarios, identified in the scoping study.

Task 5 – Scenario Analysis: Informed by earlier efforts, the team applied human centric metric concepts with data, distributions, and scenarios for a journal article on new metrics and related factors via parameter distribution analysis on key challenges and opportunities.

Results

A short summary of Task 1 and 2 is below. Please refer to prior APR for additional information.

Task 1 and 2 – State of practice summary and DOE/DOT joint workshop

The state of the practice summary report is limited to a “snapshot” of ACES research activities occurring at USDOT and DOE. This baseline is a useful start to better inform collaborative opportunities between the departments, and to identify research gaps where there is a common interest in exploring solutions.

The State of the Practice Summary:

- Provides an initial scan and summary of existing research in each department;
- Identifies where interdepartmental collaboration currently exists;
- Proposes where future collaboration is appropriate;
- Highlights research gaps where there is a common interest; and
- Identifies the need for: common and complementary metrics, and a greater understanding of base case assumptions to enhance future modeling efforts.

Based on these results and contextual understanding of the status quo, the departments identified areas of mutual interest beyond current efforts, and to help further the potential for positive outcomes that enhance both system efficiency and mobility across all modes of transportation.

The results of tasks 3, 4 and 5 are described next.

Task 3 – An issue paper, entitled: “*Measuring what really matters in transportation: new metrics to help guide the future of Automated, Connected, Efficient, and Shared (ACES) Mobility*” was developed and discussed at a side event for the Transportation Research Board Annual Meeting in January 2020. Feedback was incorporated to sharpen towards a five-page brief paper.

This issue (or discussion paper) explores key terms and new metrics, incorporating occupancy and other human movement factors, that could enable reduced infrastructure utilization by vehicles and mitigate congestion, while increasing the asset’s utilization by the number of people served. If we can increase average occupancy, we can reduce impacts to infrastructure while moving the greatest number of *people* possible. Metrics pertaining to individual mobility, such as vehicle occupancy, space efficiency, asset utilization and productivity are noted. Opportunities to enhance the network’s productivity include greater use of higher occupancy vehicles, higher asset utilization, or increased mobility infrastructure productivity by enabling more use of other modes, such as walking, bicycling and transit (that require less land per person-mile traveled than single occupant auto). These shifts have co-benefits of enhancing efficiencies, affordability, mobility choices, and are likely to also address broader goals of reducing congestion, emissions, costs, and lost productivity. Initial definitions and proposed human-centered units of analysis include the following:

- **Occupancy** – Number of travelers inside a vehicle. Typically, a static measurement. Vehicle occupancy allows calculation of person miles traveled (PMT) and vehicle miles traveled (VMT). *Occupancy is currently informed by household survey data.*
- **Utilization** – Persons per hour per area of infrastructure used. For example, i) a total of X_1 travelers used a defined area (e.g., a 1-mile highway stretch with 4 lanes of 12’ width) within an hour, ii) a total of X_2 travelers used a parking space (with a defined area) within an hour. *Current metrics focus on traffic flow at the vehicle level without accounting for people and without measuring infrastructure.*

- **Productivity** – Amount of desired outcome (i.e., something accomplished) per unit cost. An example in this case is ‘mobility’ and an example of unit cost is ‘energy used’ [PMT per unit of energy or unit of infrastructure]. *Current metrics relate to the vehicle without reference to people benefitting.*
- **Efficiency** – Using fewer resources (e.g., efficiency of space, energy, money, time) to generate the same desired outcome. *Current metrics reference VMT per unit of energy.*

Quantity of People Who Can Travel Per Hour Per Lane Via Various Modes of Transportation

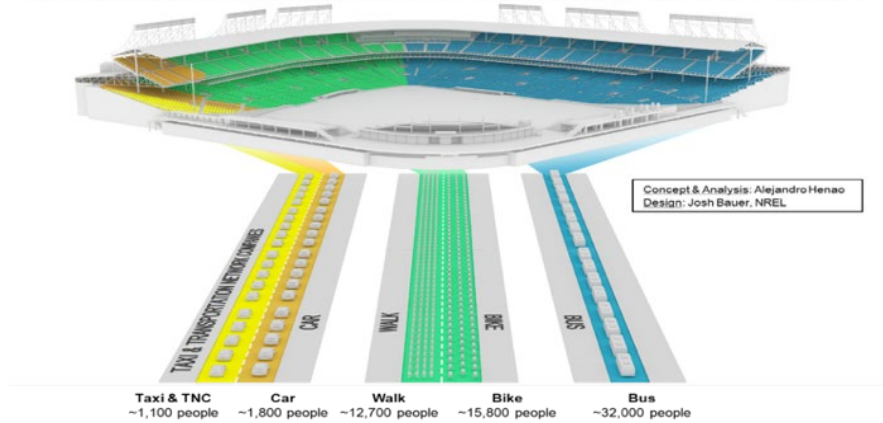


Figure I.3.4.1 Road Capacity for People

Notes: Car: 1,200 VPHPL, taxi/TNC: 1,200 VPHPL, bus: 800 VPHPL; average speed for car: 30–40 mph, taxi/TNC: 30–40 mph, bus: 15–20 mph, bike: 10 mph, walk: 3 mph; mileage-weighted vehicle occupancy for car: 1.5, taxi/TNC: 0.9, bus: 40; space per person for walker: 15 ft², biker: 40 ft².

*[*Key Message: five equal lanes have widely ranging impacts in terms of moving people to their destination]*

Task 4 – A more in-depth and detailed paper with case study contexts was developed in summer 2020, complementing the discussion paper in Task 3.

Titled: *A Long-Term View on Human-Centered Metrics to Guide the Future of Mobility*. This paper explores long-term implications of sharing assets, higher occupancy and utilization of transportation assets as key elements to create a sustainable transportation system—from economic, environmental, and equity perspectives. Table I.3.4.1 highlights a review of current metrics and new human-centered metrics, with implications of their adoption, and Table I.3.4.2 highlights the current occupancy goals and a baseline for selected U.S. cities.

Table I.3.4.1 Characterizing Current and Emerging Metrics for Integrated Mobility

	Current Metrics	New Human-Centered Metrics	Opportunities with New Metrics
Traffic	Vehicle Oriented: <ul style="list-style-type: none"> • VPHPL • Level of Service (LOS) 	1. Person oriented: <ul style="list-style-type: none"> • Person movement per hour per lane • PMT/VMT • Mobility Infrastructure Productivity (MIP) 	<ul style="list-style-type: none"> • Moving more people (or goods) with lower cost, lower energy, pollution, emissions, and congestion <p>Increase affordability and accessibility through higher occupancy and utilization</p>
Energy	Vehicle specific: <p>Miles per gallon (MPG)</p>	Mode specific: <p>Mobility Energy Productivity (MEP) as mobility benefits per energy/cost/time inputs; as location-specific metric integrating destination accessibility by multiple modes</p>	<ul style="list-style-type: none"> • Increase access to essential (i.e., jobs, food, healthcare) and non-essential (i.e., social) activities • Land use development (i.e., mixed, density) and/or increase multimodality
Life-Cycle	Life-cycle energy/CO2 intensity of Modes Per Vehicle Miles Traveled	Life-cycle energy/CO2 intensity of Modes Per Passenger Miles Traveled (requiring occupancy)	<ul style="list-style-type: none"> • Higher utilization of assets <p>Lower emissions, costs, and congestion for human-perspective benefits</p>
Economy	Infrastructure Investments based on gross domestic product (GDP) and VMT	Infrastructure Investments based on full-economy implications (in addition to GDP; safety, health, air quality, energy dependency, etc.) and PMT/VMT	<ul style="list-style-type: none"> • Higher return of investment • Include additional economic outputs • Minimizing maintenance issues <p>Lower congestion and increase affordability across varying populations.</p>
Traffic	Vehicle Oriented: <ul style="list-style-type: none"> • VPHPL • Level of Service (LOS) 	2. Person oriented: <ul style="list-style-type: none"> • Person movement per hour per lane • PMT/VMT • Mobility Infrastructure Productivity (MIP) 	<ul style="list-style-type: none"> • Moving more people (or goods) with lower cost, lower energy, pollution, emissions, and congestion <p>Increase affordability and accessibility through higher occupancy and utilization</p>

Table I.3.4.2 Occupancy Goals of Selected U.S. Cities

City	State	Occupancy Goal	Baseline
Columbus ¹	Ohio	Decrease SOV commuting by 10% by 2020	82% of commuters drive alone in 2016
Denver ²	Colorado	Reduce SOV commuters to 50%	73% of commuters drive alone in 2019
Seattle ³	Washington	Statewide commuter reduction goals	26% SOV commute rate in 2019, down from 35% in 2010
Austin ⁴	Texas	By 2039, reduce SOV commute trips to 50%	74% of commuters drive alone in 2019
Portland ⁵	Oregon	By 2040, reduce vehicle miles traveled per person by 10% compared to 2015	12.7 VMT per person per day in 2015
Boston ⁶	Massachusetts	By 2030 reduce driving alone by 50%; reduce regional VMT by 5.5% below 2005 levels by 2020	37.6% of commuters drive alone in 2017
Los Angeles ⁷	California	By 2028, shift 20% of all trips from SOVs to public and active transit	-

Table References:

- ¹ Smart Columbus, <https://smart.columbus.gov/playbook-assets/future-mobility/decreasing-the-82-percent-sov-rate-in-columbus>
- ² City and County of Denver, www.denvergov.org/content/denvergov/en/mayors-office/programs-initiatives/mobility-action-plan.html
- ³ Commute Seattle, <https://commuteseattle.com/modesplit/>, Seattle Chamber of Commerce, <https://www.seattlechamber.com/home/membership/community-news/detail/2016/06/04/interested-in-reducing-single-occupancy-vehicle-use-at-your-company>
- ⁴ City of Austin, <http://www.austintexas.gov/department/austin-strategic-mobility-plan>
- ⁵ Oregon Metro, https://www.oregonmetro.gov/sites/default/files/2018/07/02/draft2018RTP_publicreviewweb.pdf

- 6 City of Boston, https://www.boston.gov/sites/default/files/file/document_files/2017/03/go_boston_2030_-_4_goals_and_targets_spreads.pdf
- 7 LA Incubator, https://laincubator.org/wp-content/uploads/LA_Roadmap2.0_Final2.2.pdf

Figure I.3.4.2 shows analyses and mapping with the National Household Travel Survey on occupancy levels by state. For total occupancy, the states with the lowest averages are Rhode Island (1.58), Vermont (1.59), and Montana (1.68). The highest are Utah (2.3), Washington DC (2.0), and Kentucky (2.0). All other states are below 2. Utah stands out with distinctly high occupancy using this metric. To account for the influence of household size on average trip occupancy, the average number of non-household individuals appears also in Figure I.3.4.2. The states at the low end shift a bit, with New Hampshire at 0.19, Rhode Island and Oregon at 0.21, and Delaware at 0.22. At the high end, Washington DC is distinctly high at 0.44, followed by Utah at 0.38, and Kentucky at 0.34. These NHTS variables demonstrate the value of this dataset for exploring vehicle occupancy nationally.

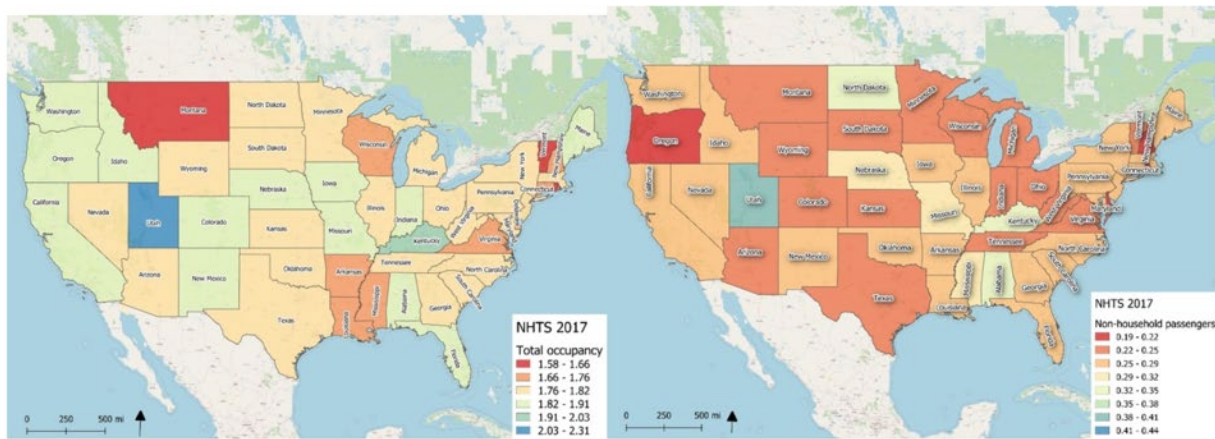


Figure I.3.4.2. Mean Occupancy Value for Trips by State (Left); and Mean Occupancy Value of Non-Household Members on Trips by State (Right) (NHTS, 2017)

Task 5 – A draft journal article, entitled: “Towards Human-Centric Mobility, Energy, and Cost Metrics for Transportation Systems”, presents three new metrics and related data for scenario analysis. While there are multiple metrics that can be developed to analyze transportation projects, this paper attempts to better understand the importance of three different areas of interest for metrics (traditional versus human-centered) as shown in Figure I.3.4.3.

Table I.3.4.3 Traditional vs Proposed Metrics for Review of Integrated Mobility, Energy, and Costs

Area	Traditional Vehicle-Centric Metric	New Human-Centric Metric	Area
Road Capacity	Vehicles per hour per lane (VPHPL)	Person movement per hour per lane (PPHPL)	Road Capacity
Energy Use	Miles per gallon (MPG)	Person energy intensity for transportation (PEIT); or as the energy use per person distance traveled	Energy Use
Affordability	Price per gallon of gasoline	Price or total costs per personal transportation (PPMT)	Affordability

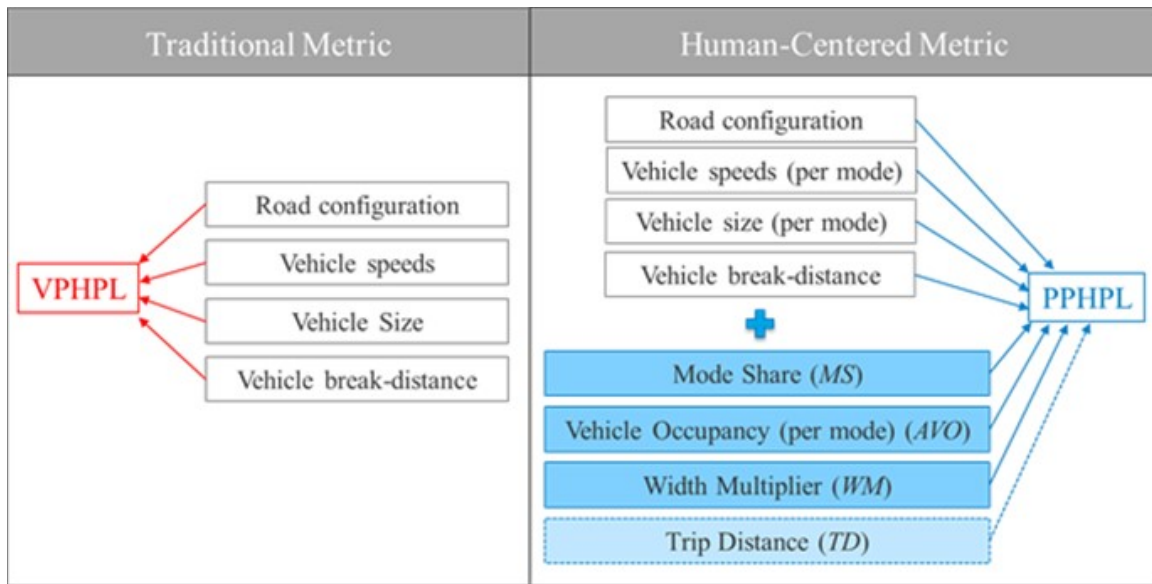


Figure I.3.4.3 Below Shows a Comparison of a Traditional Vehicles Per Hour Per Lane (VPHPL) Metric Compared to a New Proposed Persons Per Hour Per Lane (PPHPL) Metric

Using data distributions for individual parameters, Figure I.3.4.4 below shows the results of the metrics both for traditional VPHPL and the proposed PPHPL where we can see that including key factors influences the types of metrics that offers a more human-centered understanding of system performance. This is using national data on private vehicles, transit and walk/bike modes.

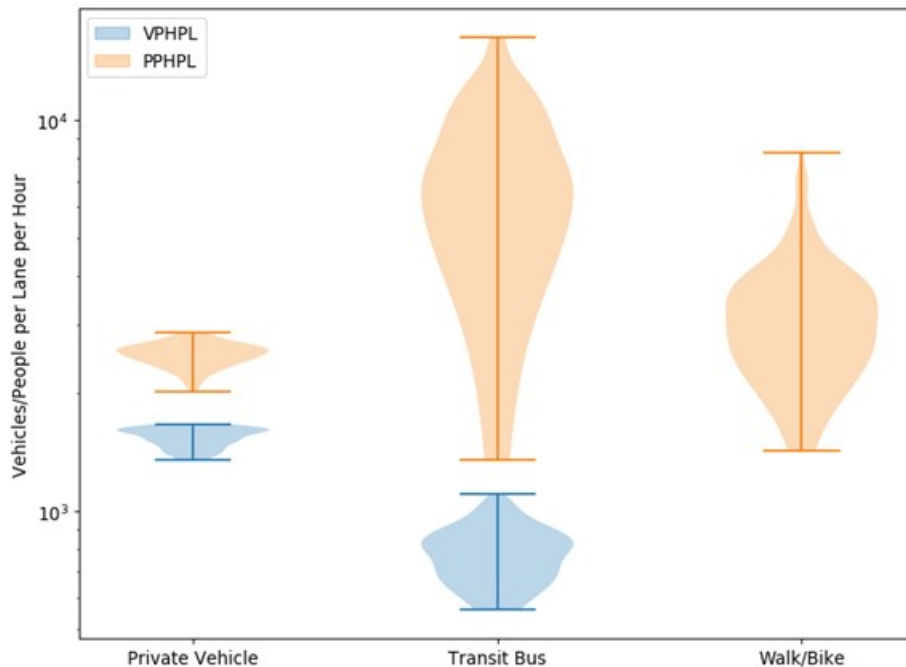


Figure I.3.4.4. Diagram on VPHPL Versus PPHPL, Considering Key Parameters Shaping PPHPL

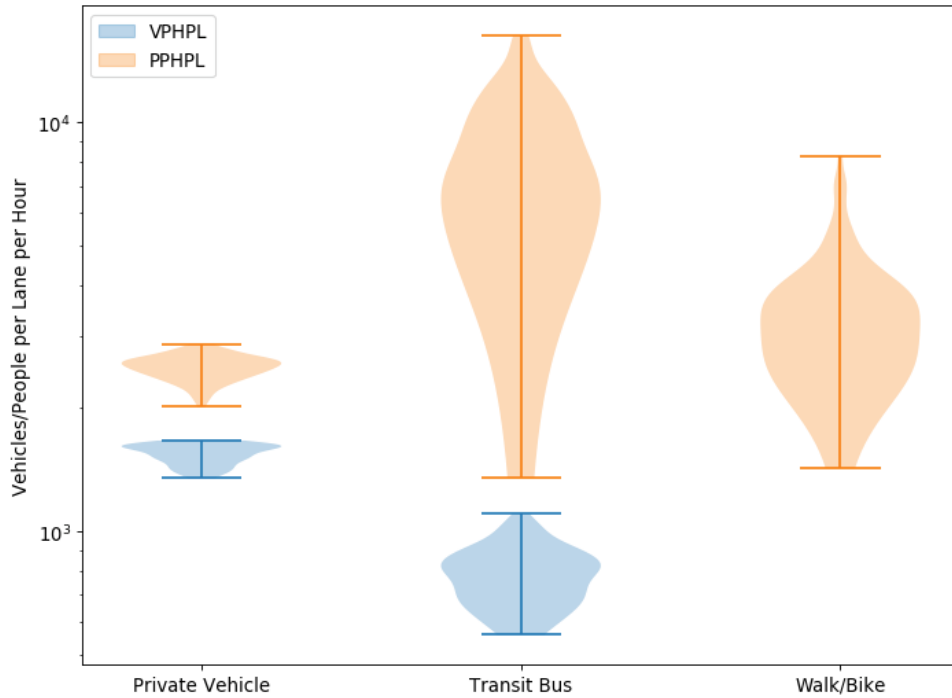


Figure I.3.4.5. Violin Plots of Road Capacity Metrics for Private Vehicles, Transit Bus and Walk/Bike

Similarly, we developed a metric named person energy intensity for transportation (PEIT), to calculate the distributions of energy use per person, considering parameters of quantity of travel, mode share, vehicle energy efficiency, and average vehicle occupancy. We then show sensitivity analysis to understand how much the metric change by varying the individual parameter one standard deviation in which the road capacity metric could increase (e.g., higher average vehicle occupancy). The results are presented in Figure I.3.4.6, Figure I.3.4.7, and Figure I.3.4.8.

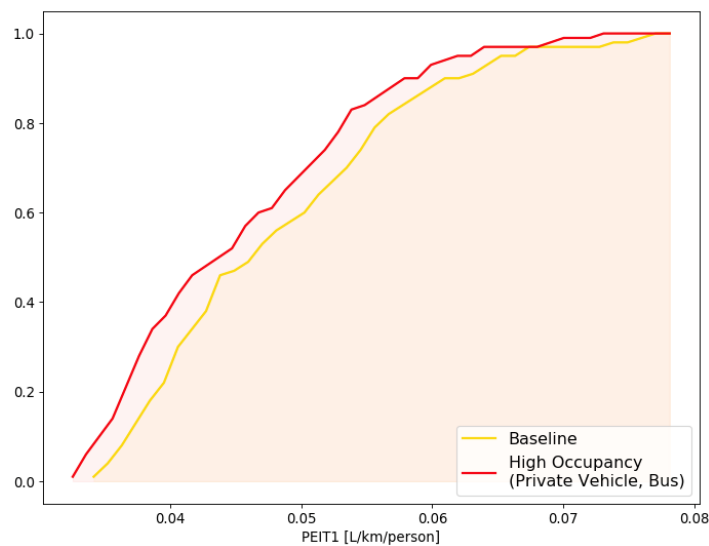


Figure I.3.4.6 Cumulative Distribution Function of PEIT by Increasing Vehicle Occupancy for Private Vehicles and Buses by One Standard Deviation

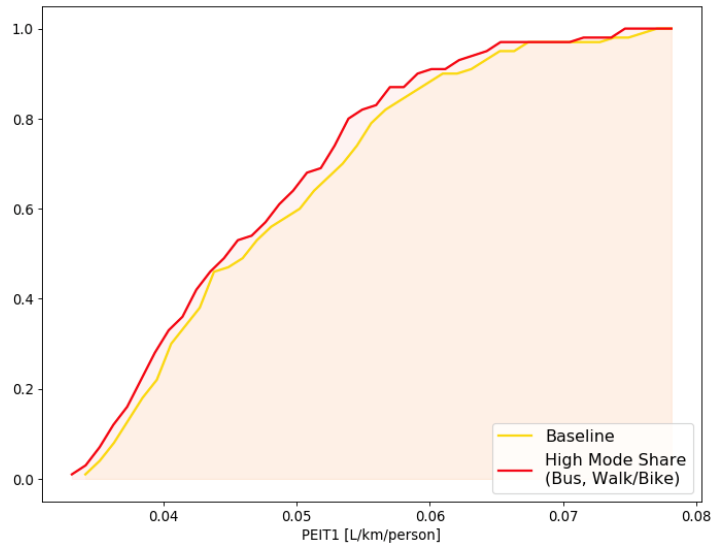


Figure I.3.4.7 Cumulative Distribution Function of PEIT by Increasing Mode Share of Walk/Bike and Bus by One Standard Deviation

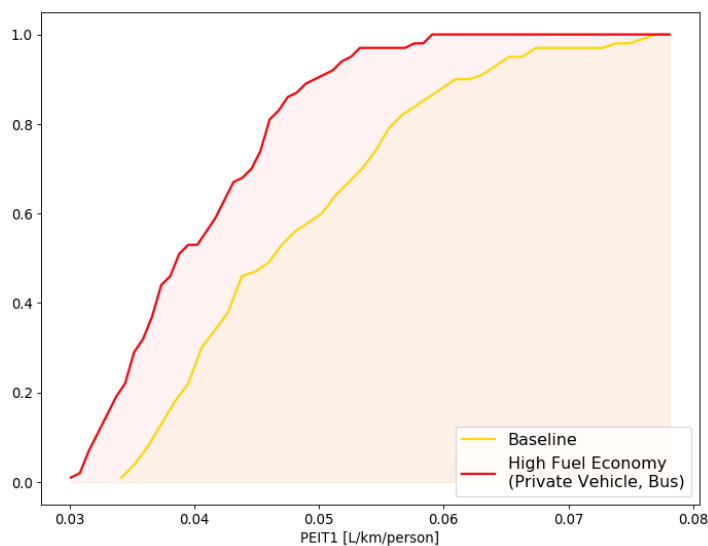


Figure I.3.4.8 Cumulative Distribution Function of PEIT by Increasing Vehicle Energy Efficiency (or Fuel Economy) by One Standard Deviation for Private Vehicles and Buses

Scenario analysis was also conducted on affordability and costs, considering direct and indirect costs for transportation. A baseline, low efficiency and high efficiency scenario is considered, using an existing cost model and adapting to our parameter distributions. The unique contribution of these results is that traditional affordability metrics tend to focus on vehicle ownership and operation as the primary driver of cost. Traditional affordability metrics tend to focus on vehicle ownership and operation as the primary cost. To develop a more comprehensive, human-based metric, it is necessary to look at additional internal and external variables that may impact decision making from the perspective of total cost. For this metric, we rely heavily on the “transportation cost and benefit” work to establish a baseline for person and mode-specific travel costs (Litman, 2011). We used the original cost categories from the model and updated the inputs to account for current market situation.

Table I.3.4.4 Average Out of Pocket Costs Per Traveler Mile (Note: Annual Fixed Costs for Car and Bicycle Travel are Distributed Proportionately Across Annual Miles Traveled)

Lever	Mode	Baseline	Low Efficiency	High Efficiency	Explanation	Source
Annual Miles	Average Car	13,500	20,000	7,000	Average total annual miles per driver used for baseline. Males aged 35-54 drove the most (low efficiency scenario). Females 65+ drove the least (high efficiency scenario).	FHWA, 2018
	Bicycle	2,332	332	4,332	Average miles traveled used for baseline. Two thousand miles variation to represent bikers for recreational purposes and super users for both utilitarian and recreational purposes	Allen, 1974
	Walk	329	29	629	Average miles walked used for baseline. Three hundred miles in each direction to account for casual/recreational walkers and pedestrian dependent citizens.	NHTS, 2017
	Diesel Bus (passenger miles)	1,459	152	2,554	Average transit trip distance used for baseline miles (assuming a transit commuter travelling 4 day per week and 48 weeks per year. We assumed an infrequent transit user traveling 20 round-trips per year (low efficiency scenario), and transit user for commuting and other purposes, traveling 7 days per week and 48 weeks per year (high efficiency)	APTA, 2019
Vehicle Occupancy	Average Car	1	1	4	Average passenger occupancy or load factors used for baseline. Excluding automated vehicles, a passenger car must have at least a driver, so the low efficiency scenario assumed one passenger. For a high efficiency scenario, we assumed full capacity of four adults in a vehicle.	FHWA, 2018
	Bicycle	1	1	1.1	One passenger per bike for baseline and low efficiency scenario. For the high efficiency scenario, we assumed every 10th trip was taken by a tandem bicycle or a cargo bike with a child passenger.	N/A
	Walk	1	1	1	For all three scenarios, occupancy is one person	N/A
	Diesel Bus	10.5	5.1	16.8	Average national transit bus occupancy factors were used for baseline. For the low and high efficiency scenarios we relied on the lowest and highest ridership averages for U.S. transit agencies.	FHWA

Table I.3.4.5 Average Out of Pocket Costs Per Traveler Mile

Average Car	Bicycle	Average Car
\$4,284.00	\$193.93	\$4,284.00
\$1,008.00	\$11.17	\$1,008.00

(Note: Annual fixed costs for car and bicycle travel are distributed proportionately across annual miles traveled)

Table I.3.4.6 Internal and External Costs Per Vehicle Mile Traveled and Per Person/Passenger Mile Traveled

	Average Car	Bicycle	Diesel Bus	Walk	Cost Type
Occupancy Lever	2.2	1	13	1	
Miles lever	12500	2332	43647	500	Distribution
Vehicle Ownership [see fixed costs to left]	\$0.34	\$0.08	\$0.00	\$0.00	Internal-Fixed
Internal Parking [see fixed costs to left]	\$0.08	\$0.00	\$0.00	\$0.00	Internal-Fixed
Vehicle Operation	\$0.21	\$0.03	\$3.14	\$0.07	Internal-Variable
Travel Time	\$0.18	\$0.49	\$4.22	\$1.58	Internal-Variable
Internal Crash	\$0.15	\$0.10	\$0.05	\$0.10	Internal-Variable
Internal Health Ben.	\$0.00	-\$0.12	\$0.00	-\$0.30	Internal-Variable
External Variable (External crash, External health benefit, Operating subsidy, External parking, Congestion, Road facilities, Land value, Traffic services, Transport diversity, Air pollution, GHG, Noise, Resource externalities, Barrier effect, Land use impacts, Water pollution, waste)	\$0.53	-\$0.10	\$10.81	-\$0.29	External variable
Total cost per vehicle mile	\$1.49	\$0.49	\$18.22	\$1.15	
Total vehicle cost per year	\$37,264.82	\$2,291.30	\$1,590,444.13	\$1,152.14	
Total cost per person mile	\$0.68	\$0.49	\$1.40	\$1.15	
Total cost per person per year	\$16,938.55	\$2,291.30	\$2,769.35	\$1,152.14	

	Average Car	Bicycle	Diesel Bus	Walk	Cost Type
Assume average round trip on transit of 7.6 and 5 round trips a week for 52 weeks at \$1.67 per trip (APTA 2020)					
	Average Car	Bicycle	Diesel Bus	Walk	
Average User Price per Vehicle Mile	\$0.63	\$0.12	\$0.44	\$0.07	
Average User Price per vehicle per year	\$7,875.00	\$281.49	\$868.40	\$33.39	
Average user price per person mile	\$0.29	\$0.12	\$0.44	\$0.07	
Average user price per person per year	\$3,579.55	\$281.49	\$868.40	\$33.39	

For comparison across modes and scenarios, see Figure I.3.4.9, Figure I.3.4.10 and Figure I.3.4.11.

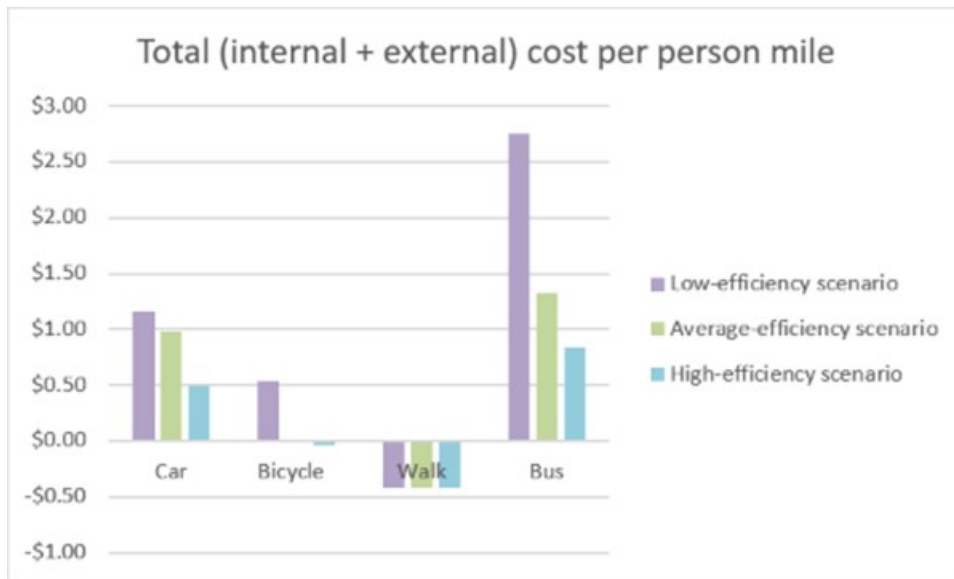


Figure I.3.4.9 Full Cost Per Mode Per Mile for the Three Efficiency Scenarios, Affordability Metric

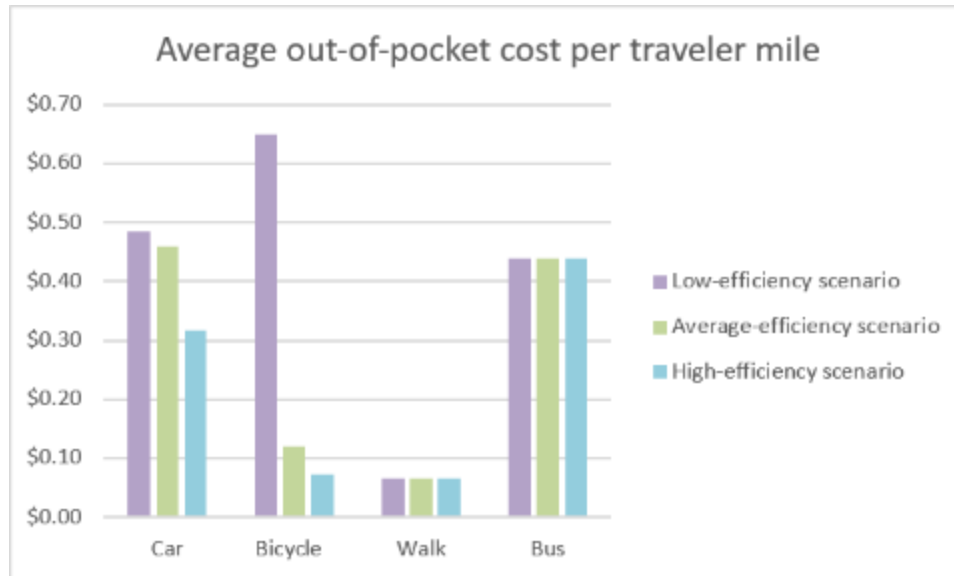


Figure I.3.4.10 Direct Out-Of-Pocket Costs to a Traveler, Per Traveler Mile, for the Three Efficiency Scenarios, Affordability Metric

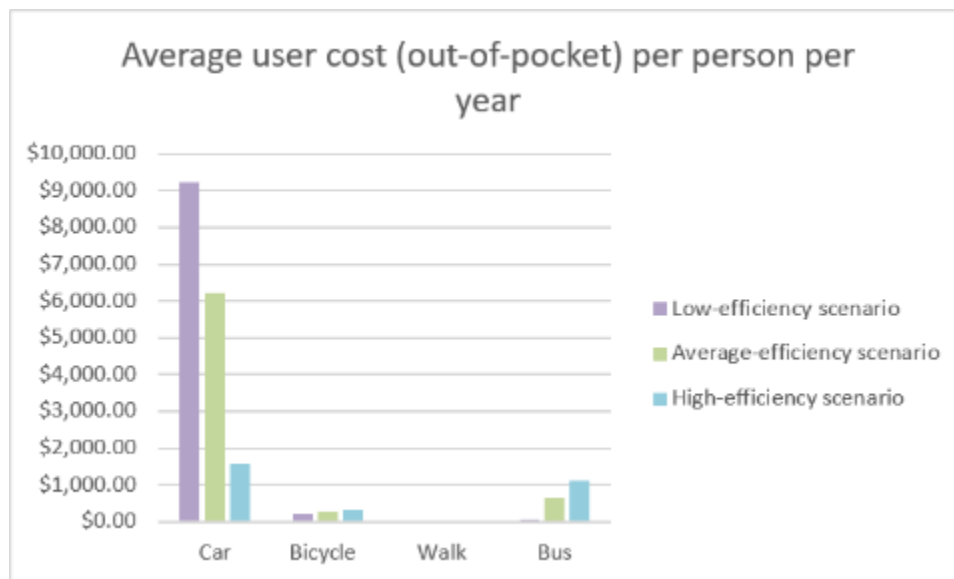


Figure I.3.4.11 Average Out of Pocket Cost Per Person Per Year for the Three Efficiency Scenarios, Affordability Metric

Overall, these results build on the earlier efforts, with the team applying human centric metric concepts with data, distributions and scenarios for a journal article focused on implications of new metrics and related factors via parameter distribution analysis on key challenges and opportunities.

To summarize efforts for tasks 3, 4, and 5, we include a list below of the key deliverables and outcomes:

- 4-page Brief Issue Paper ‘Occupancy Scoping Study’
- Three stakeholder workshops: DOE-DOT ACES, TRB Side Event / Workshop, and briefing with Volpe Chief Economist & US DOT-DOE
- Focus groups/interviews to inform survey design on understanding COVID-19 safe transit recovery

- 40-page discussion paper with case studies on measuring what matters at a human scale
- Research papers under development:
 - A long-term view on human-centered metrics to guide the future of mobility
 - COVID-19 impacts and opportunities
 - Comparing current versus new metrics with interactive data, metrics, scenario analysis
- Conference presentations under development:
 - BEEC Virtual Conference talks on future human-centered mobility metrics & COVID-related research.

Conclusions

Future work on energy and transportation interests should continue to help develop definitions, metrics and goals for automated, connected, efficient/electric and shared transportation technologies and how they relate to system efficiency and mobility, as the movement of people and goods. Common goals and co-designing new metrics across agencies—as outlined in the written products—can help guide work that is organically inclusive of each other’s priorities. Moving ahead, stakeholders can help address specific data needs and data-exchange mechanism(s) to encourage mobility service providers or technology companies to share meaningful data that planners, modelers and analysts desire. There are ongoing efforts to facilitate data exchange, and successful examples should be considered and replicated as needed.

The potential opportunities and implications resulting from better integration of occupancy are numerous, and include the following:

1. Informing investments in, management of road, curb, and vehicle uses to enhance mobility asset utilization.
2. Filling gaps in discussions on new mobility choices: ridehailing, carsharing, micromobility, and telework.
3. Filling gaps in discussions on the impacts of automation, articulating new types of risks in the C/AV era.

Key Publications

1. *In-preparation*: Henao, A, Wilson, A, Atnoorkar, S, Nobler, E, Weigl, D, Shankari, K, Sperling, J, Lian S, Stanford, J, & S. Smith. Toward Human-Centric Mobility, Energy, & Cost Metrics for Transportation Systems.
2. *In-preparation*: Weigl, D, Henao, A, J. Sperling, Wilson, A, Nobler, E, Atnoorkar, S, Shankari, K, Lian, S, Stanford, J and S. Smith. Measuring what matters in transportation at a human scale: a discussion paper on new metrics to help guide Automated, Connected, Efficient and Shared (ACES) Mobility. Accepted to BECC, 2020.
3. *In-preparation*: Atnoorkar, S, Weigl, D, Henao, A, Wilson, A, Nobler, E, Shankari, K and J. Sperling. Mobility and Energy Impacts with COVID-19: Travel Behavior Scenarios and Cases of Bike Share, Transit and Mode Choices in Philadelphia and Pittsburgh.
4. Duvall, A, Sperling, J, Wilson, A, Young, S and D. Zimny-Schmitt. 2020. Assessing U.S. Current and Future Impacts of Telework During the COVID-19 Pandemic. Manuscript Accepted for 2021 TRB Annual Meeting.

5. Alejandro Henao, Erin Nobler, Alex Schroeder, Josh Sperling, Alana Wilson, Dustin Weigl, NREL; Scott Lian, Joe Stanford, Scott Smith, US DOT Volpe Center. Internal Discussion (or Issue) Paper: Measuring What Matters in Transportation at a Human Scale: A Discussion on New Metrics to Help Guide an Integrated Future for Automated, Connected, Efficient, Shared (ACES) Mobility. (4 to 5 page ‘Brief’ version is available as well)
6. Volpe and NREL. Automated, Connected, Efficient, and Shared (ACES) Mobility Research State of the Practice Summary: Identifying Common and Complementary Metrics, Research Methodologies, and Collaboration Opportunities across the U.S. Department of Energy (DOE) and U.S. Department of Transportation System (USDOT)’s Efficiency and Mobility Research Portfolios

References

See package of written products (attached by email in submission) for references.

Acknowledgements

This manuscript has been prepared by the National Renewable Energy Laboratory (NREL) and with inputs from Volpe National Transportations Systems Center (Volpe), for VTO project # 10338.10. We acknowledge the support from USDOT’s Office of the Secretary of Transportation – Research (OST-R), and DOE’s Vehicle Technologies Office (VTO). A special thanks to US DOT’s Shawn Johnson; and US DOE’s Erin Boyd, David Anderson, and Danielle Chou. Volpe’s chief economist, Don Pickrell, along with multiple NREL colleagues, and participants in our project workshop hosted alongside of TRB 2020 with the American Council for an Energy Efficient Economy (ACEEE) we’re all helpful in informing final written products developed. A special thanks to Dustin Weigl, Swaroop Atnookar and K. Shankari at NREL for a software package developed for an interactive metric calculation for PEIT that can now be demonstrated. The team filed SWR-21-13 so others can experiment with the interactivity, launching a notebook in the cloud. This is a novel aspect of the project that may lead to new software IP by NREL.

I.3.5 RoadRunner — A Simulation Tool for Energy-Efficient Connected and Automated Vehicle Control Development

Dominik Karbowski, Principal Investigator

Argonne National Laboratory
9700 South Cass Avenue
Lemont, IL 60439
Email: dkarbowski@anl.gov

Erin Boyd, DOE Technology Manager

U.S. Department of Energy
Email: erin.boyd@ee.doe.gov

Start Date: Oct. 1, 2019
Project Funding: \$1,200,000

End Date: Mar. 31, 2022
DOE Share: \$600,000

Non-DOE Share (in-kind):
\$600,000

Project Introduction

Automotive engineers traditionally use drive cycles (vehicle speed as a function of time) to represent the actions of human drivers when simulating and testing vehicle powertrains in the design phase. However, this approach is not suitable for connected and automated vehicles (CAV): Speed is a control variable that is adjusted based on the surrounding environment that the vehicle senses or communicates with. Since we found no tool dedicated to energy efficiency research in the context of advanced powertrain, connectivity, and automation technologies, we at Argonne have been developing RoadRunner to address this market need. RoadRunner was instrumental in our research on energy-focused CAV control as part of the SMART 1.0 program.

RoadRunner is a framework for simulating multiple vehicles with full powertrain models and their interactions with their environment. RoadRunner uses powertrain models from Autonomie, Argonne's established vehicle energy-consumption simulator, but adds new capabilities, such as multi-vehicle simulation, models of road characteristics, causal models of human driving, V2X ("vehicle to everything") communications, and sensors.

The goal of this project is to improve the technical quality of simulations and the user experience of RoadRunner, so that it meets the needs of automotive R&D engineers, and to create a first release of RoadRunner at the end of the project.

The cooperative research and development agreement (CRADA) partner, Hyundai, will collect real-world driving data using vehicles that log signals from the powertrain, dashcam, radar and GPS receiver. Hyundai will also provide customer driving data. We will process the data and then validate newly developed scenarios and models, with a focus on modeling the human driver. We will incorporate this work into a rich library of default controller models, predefined vehicles, and scenarios for the public release of RoadRunner. We will improve usability by developing a graphical user interface, and we will prepare the final release, license, documentation, and marketing materials for the initial beta release.

Objectives

The objective of the project is to bring RoadRunner closer to commercialization, with a robust first release that can be demonstrated outside the development team. This will be achieved through several steps and goals as described below.

Collection of real-world driving data. Our CRADA partner, Hyundai, will collect and share with Argonne two datasets that help characterize human driving. First, Hyundai will provide a sample of recorded driving

data from U.S. customers, and second, they will provide data from a specially instrumented vehicle to be driven around southeastern Michigan over several months. These two datasets are complementary: the customer data provides a large number of real-world situations for a variety of drivers, geographical locations, vehicles, and powertrain types, while the data from the instrumented vehicle's camera and geographical coordinates will provide better context from the surrounding environment.

Development of a driving data analytics framework. As we will receive a large amount of driving data from Hyundai, a data analytics framework is needed to make sure the data can be easily used for model development. The framework will include automated data processing, quality checks, driving regime identification, traffic signal state extraction from video feeds, and addition of road attributes (e.g., speed limits, signs, etc.) via map-matching, etc.

Development and validation of a high-fidelity dynamic driver model. Our CRADA partner, Hyundai, identified human driver modeling as an essential feature of RoadRunner, as it provides a realistic baseline for research and development related to advanced driver assistance systems (ADAS) and CAVs. We will draw from the data provided by Hyundai to identify the most appropriate models and will calibrate the models using the data.

Preparation for release. In order for RoadRunner to be useful beyond its developers, it needs to have the features of professional software: an easy-to-install release, a graphical user interface (GUI) with a good set of features, documentation, and training materials. RoadRunner will also provide default models and scenarios for users to run out of the box. RoadRunner will include models of human drivers as well as CAV technologies such as adaptive cruise control (ACC), cooperative ACC (CACC), V2X communications, intersection eco-approach, and so on.

Approach

Real-world driving data collection/exchange with Hyundai

Real-world driving data is needed to develop and validate a high-fidelity dynamic human driver model in RoadRunner. As part of this project, Hyundai will share two types of driving data with Argonne: customer driving data and on-road testing data. The customer driving data provides a statistically significant variety of driving types and situations but lacks accuracy (e.g., low sampling rate, rounded-off GPS signals for privacy). However, Hyundai will also collect driving data with instrumented vehicles that log signals from the powertrain, dashcam, lidar, and GPS receiver, with Argonne's input on testing scenario design. The on-road testing data provide richer information with higher accuracy about the surrounding environment (e.g., video records) that is not included in the customer driving data.

On-road testing of the instrumented vehicles has been delayed due to COVID-19. Instead, in FY20 we focused on customer data. Since the entire dataset cannot be shared with Argonne, we formulated "data requests;" i.e., we identified the sample from which we will be able to draw maximum statistically useful data for validation. As shown in Figure I.3.5.1, this back-and-forth data request process has four steps. First, Hyundai provides a population description table that summarizes the entire population of vehicles saved in the dataset, along with key attributes (e.g., vehicle specification, approximate home location, average daily travelled distance). No temporal data is shared at this point. Second, Argonne analyzes the data, identifies influential factors (e.g., vehicle type, geographical area), develops a sampling method, and provides a list of vehicles and time frames for which temporal data is requested. Third, Hyundai extracts the data corresponding to that request, and finally, Argonne performs the analysis.

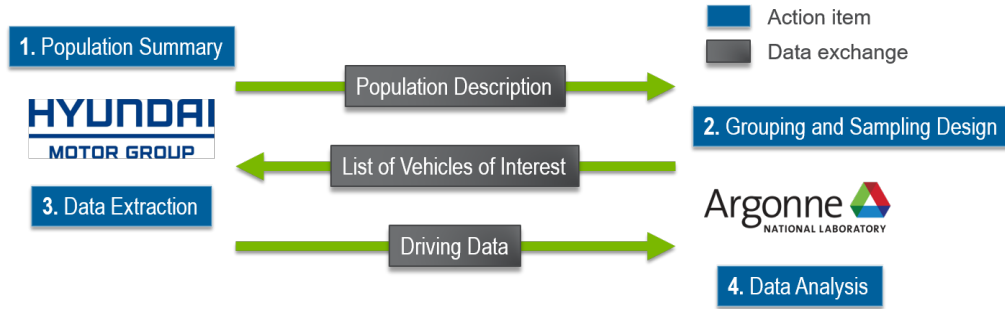


Figure I.3.5.1 Back and Forth Data Request Process Between Hyundai and Argonne

Data analytics framework

As we will receive a very large amount of driving data from Hyundai, a data analytics framework is needed to improve data quality, increase data richness (e.g., identify driving regimes), and accelerate data analysis. As shown in Figure I.3.5.2, the data analytics framework aims to build a labeled database through a multi-step automated process.

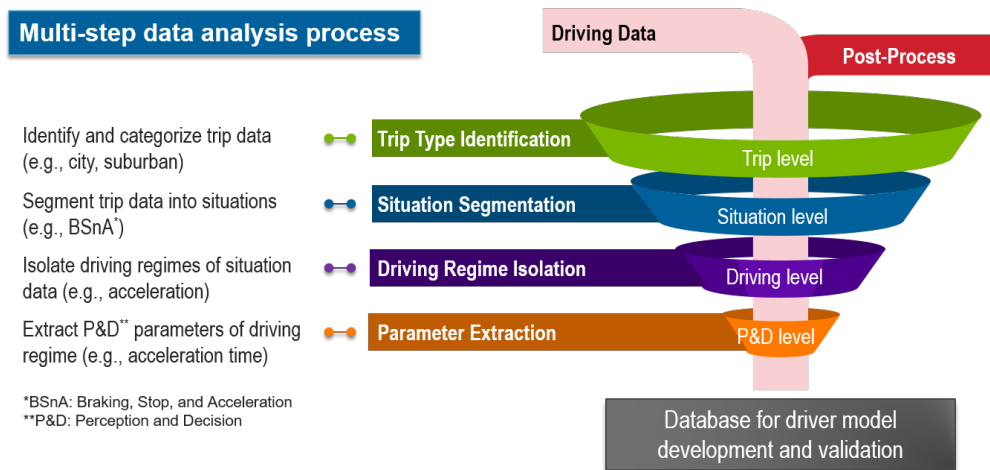


Figure I.3.5.2 Multi-Step Data Analysis Process in the Data Analytic Framework

The multi-step data analysis process involves multiple analysis levels: trip type identification, situation segmentation, driving regime isolation, and parameter extraction. The trip type level process identifies and categorizes trip data into three types—urban, suburban, and rural—to capture the differences in driving on different types of roads. As each trip consists of different situations, the situation level process segments the trip data into pre-defined situations, such as braking, stop, and acceleration (BSnA). The driving level process further divides each situation and isolates driving sub-regimes (e.g., acceleration regime in the BSnA situation), and the human perception and decision (P&D) level process extracts the P&D parameters of each driving regime data (e.g., acceleration time and distance), required for the human driver model. The data analytics framework automatically tags these extracted human P&D parameters with multiple labels (e.g., acceleration time and distance in a BSnA situation due to a red traffic light on a suburban road), and the labeled dataset is used to develop and validate the human P&D model.

High-fidelity dynamic human driver modeling

A good human driver model is critical in the development and evaluation of CAV and ADAS technologies, especially the automated driving controls for which it serves as a baseline. As part of SMART 1.0, in FY19 we

initiated the development of a new high-fidelity dynamic human driver model that consists of a P&D model and an action model, as shown in Figure I.3.5.3. The human P&D model captures the cognitive process occurring in the human brain, while the action model captures human driving behaviors affecting the state of the vehicle based on Newtonian laws of motion. The action model is based on analytical optimal solutions minimizing jerk (the derivative of acceleration) energy; its accuracy was validated with the assumption of a perfect human P&D model that provides the human P&D parameters directly extracted from a small sample of driving data.

Thanks to the large dataset provided by Hyundai, further development of the model focuses on:

- Building and completing a data-driven human P&D model that can estimate human P&D parameters using surrounding environment information
- Capturing a large variety of driving behaviors resulting from several factors (e.g., vehicle, region, and trip types).

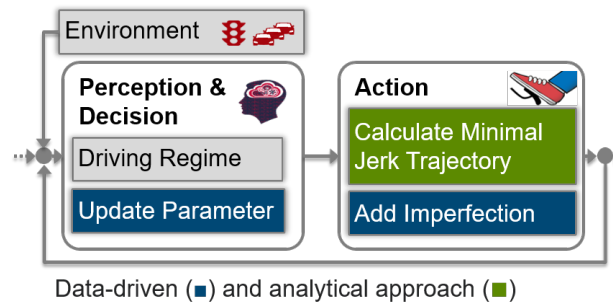


Figure I.3.5.3 Schematic Diagram of a High-Fidelity Dynamic Human Driver Model

Results

Real-world driving data collection and sampling

Due to COVID-19, driving data collection from a dedicated instrumented vehicle has been postponed to FY21. As a result, our focus shifted to the customer driving data and to how to define a subset of validation data to sample from the very large master Hyundai database.

Geographical location and vehicle type

We considered two factors influencing human driving behaviors: geographical location and vehicle type. As a result, we created five geographical location clusters by population size [1] and elevation: large metropolitan areas (e.g., Chicago-Naperville-Elgin), small metropolitan areas at higher and lower elevations (e.g., Albuquerque and Omaha), and rural areas in hilly and flat states (e.g., Colorado and Illinois). Each area is defined by cartographical boundary data provided by the U.S. Census website [2] (see Figure I.3.5.4).

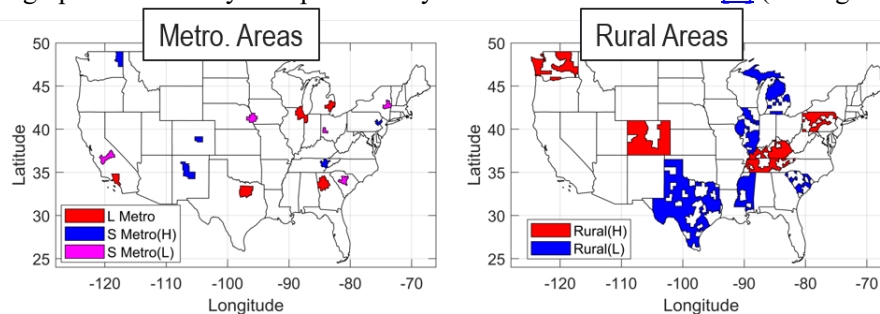


Figure I.3.5.4 Selected Areas of All Geographical Location Clusters: Metropolitan Areas (Left) and Rural Areas (Right)

Similarly, we also created six vehicle type clusters by powertrain (conventional engine with or without turbo, EV) and vehicle class (sedan, SUV, luxury/high-performance). For sampling, the most frequent vehicle model is selected in each cluster to control for vehicle-to-vehicle variability. The selected vehicle model has the capability to collect data about the preceding vehicle (e.g., distance to preceding vehicle).

Division into sampling “groups”

By combining all 25 areas and 6 vehicle models, we defined 102 “groups” and assigned a unique number to each group in ascending order, as shown in Figure I.3.5.5. As the number of available luxury/high-performance vehicles and EVs is much lower than the other models, each type defined only one group regardless of location.

	L_Metro					S_Metro_H					S_Metro_L					Rural_H					Rural_L				
	LA_CA	CHI_IL	DAL_TX	ATL_GA	DET_MI	ALB_NM	SPO_WA	CS_CO	KNO_TN	ALL_PA	FRE_CA	COL_SC	OMA_NE	ALB_NY	DAY_OH	RUR_PA	RUR_KY	RUR_TN	RUR_WA	RUR_CO	RUR_TX	RUR_MI	RUR_SC	RUR_MS	RUR_IL
Conv_sedan_wT	1	2	3	4	5	6	7	8	9	10	11	12	13	14	15	16	17	18	19	20	21	22	23	24	25
Conv_sedan_woT	26	27	28	29	30	31	32	33	34	35	36	37	38	39	40	41	42	43	44	45	46	47	48	49	50
Conv_SUV_wT	51	52	53	54	55	56	57	58	59	60	61	62	63	64	65	66	67	68	69	70	71	72	73	74	75
Conv_SUV_woT	76	77	78	79	80	81	82	83	84	85	86	87	88	89	90	91	92	93	94	95	96	97	98	99	100
Luxury	101																								
Electric	102																								

Figure I.3.5.5 Definition of 102 Groups by 25 Areas and 6 Vehicle Modes

Following this group definition, we can determine the desired number of vehicles of interest for each group by considering the number of available vehicles in the dataset and the maximum limit of data size. Data size (D_{size}) can be estimated by the following equation:

$$D_{size} = n_{avg,d} \times t_{avg,d} \times f_{samp} \times n_{sig} \times w_{avg,var.} \times n_{day} \times n_{veh}$$

where $n_{avg,d}$ is average number of daily trips, $t_{avg,d}$ is average daily trip time in minutes, f_{samp} is sampling frequency in Hz, n_{sig} is the number of data signals, $w_{avg,data.}$ is average data width in bytes, n_{day} is the number of days, and n_{veh} is the number of vehicles. Note that average daily observations per signal is $n_{avg,d} \times t_{avg,d} \times f_{samp}$.

Development of multi-step data analysis process

As part of the analysis process, we developed pattern recognition algorithms for trip type identification and for situation segmentation. To validate these models, we used a dataset with geolocation, the Safety Pilot Model Deployment (SPMD) dataset [3].

Trip level process: trip type identification

The Urbanization Perceptions Small Area Index (UPSAI) [4] is a machine learning model developed using neighborhood description data from the 2017 American Housing Survey [5] combined with U.S. census tract boundary data. UPSAI can predict the likelihood of the neighborhood type for a given area (e.g., urban, suburban, and rural) described by the average household. Using the predicted UPSAI likelihood allows us to define the neighborhood type (i.e., road type) where a vehicle is driven. As the on-road testing data contains accurate GPS coordinates, we can identify the trip type as urban, suburban, or rural by simply checking which tract-level area (formed by polygons) includes the recorded GPS coordinates. For example, the trip type can be considered suburban if GPS coordinates (yellow points) are in blue areas, as shown in Figure I.3.5.6. On the other hand, the customer driving data contains inaccurate GPS coordinates (rounded-off values due to privacy), so we performed a statistical analysis using the SPMD dataset to look for the factor that can identify the trip type and determine its threshold. Figure I.3.5.6 shows that two distributions (average speed and cruise average speed) of suburban trip data spread out more widely, and the corresponding mean values are higher, than in urban trip data. This is an expected result, as suburban roads have higher maximum speed limits and longer distances between intersections.

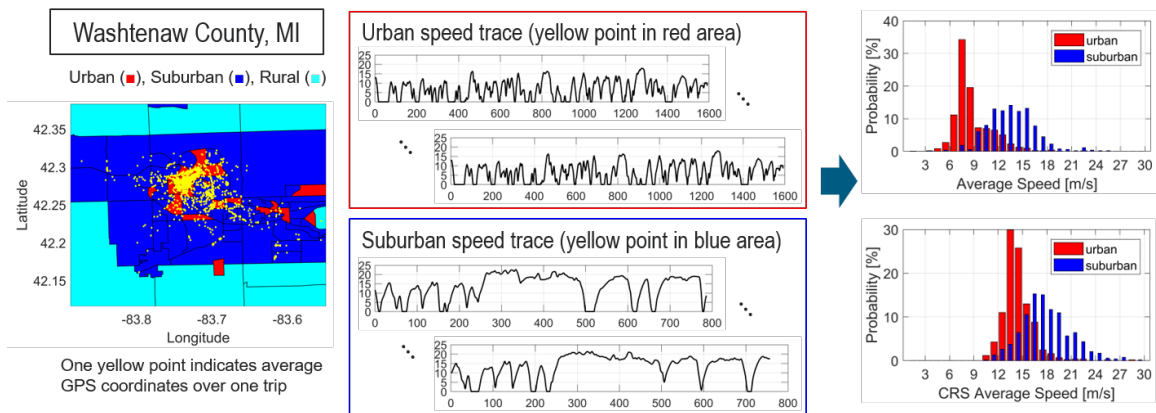


Figure I.3.5.6 UPSAI-Based Neighborhoods in Washtenaw County, MI (Left) and Statistical Data Analysis (Right)

Situation level process: situation segmentation

We categorized each trip into one of three situation clusters based on whether vehicle speed decreases and then increases due to these road events: (1) braking, stop, and acceleration (BSnA), (2) braking and acceleration (BnA), and (3) cruise (CRS). BSnA is the situation where, due to a red traffic light, stop sign, etc., the vehicle decelerates to stop, waits for a while, and then accelerates. BnA is the situation where the vehicle decelerates and then accelerates without a stop, due to an upcoming red traffic light that switches to green before the vehicle reaches it, curved roads/roundabouts/speed bumps, etc. CRS is the situation where the vehicle maintains a specific constant speed with little variation. Both BSnA and BnA situations can be sub-divided into four conditions: free-flow (FF), car-following (CF), turning (turn), and car-following and turning (CFnTurn); the CRS situation can be divided into two: FF and CF.

We developed a BSnA and BnA situation segmentation algorithm with three steps, as shown in Figure I.3.5.7.

Step 1. Road event timing search

- Find local extremes (i.e., maximums and minimums) and sort them into “influential” or “uninfluential.”
- Select influential local minimums at which there is a significant speed decrease and increase.

Step 2. Slice and dice

- Define beginning of braking and end of acceleration based on the selected influential local minimums
- Break entire trip data into smaller parts at situation level.

Step 3. Labeling

- Classify each situation-level data item into pre-defined situations.

The CRS situation can be easily isolated by defining the time interval during which speed variation is held to a minimum for specified conditions (e.g., +10 s at + 10 m/s).

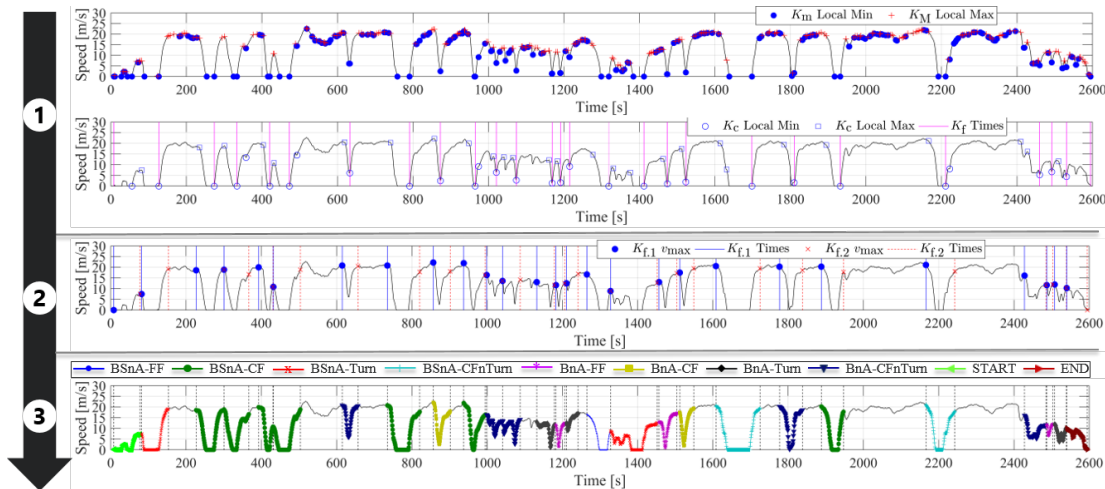


Figure I.3.5.7 Step-By-Step Bsna and Bna Situations Segmentation Algorithm

To test the situation segmentation algorithm, we used a map-matching algorithm to extract road attributes (e.g., speed limit, intersection type and position) of GPS coordinates in the suburban trip data of the SPMD dataset. We augmented this information with the post-processed driving data and overlapped the speed traces on a 3D plot of Google Earth, as shown in the top and bottom of Figure I.3.5.8, respectively. The test result shows that by using only driving records, the situation segmentation algorithm can identify road events that induce the speed decrease and increase and categorize these into pre-defined situations.

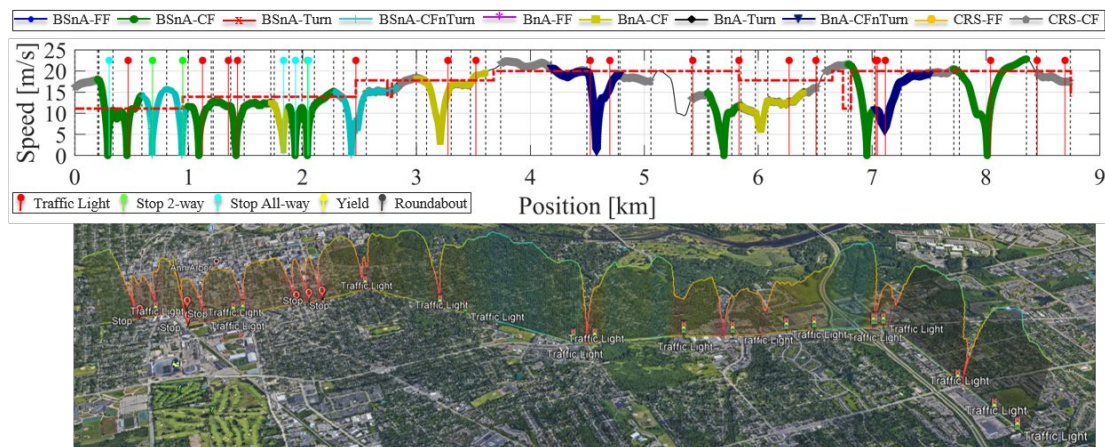


Figure I.3.5.8 Situation Segmentation Algorithm Test Result

Driving and P&D level process: driving regime isolation and P&D parameter extraction

As both BSnA and BnA situations consist of braking and acceleration regimes, and the cruise situation itself represents the cruise regime, we can isolate each regime from situation-level data. We then extract the human P&D parameters, i.e., the boundary conditions ($v_0, v_f, s_f - s_0, t_f - t_0$) of collected trajectories, where $s, v,$ and t are position, speed, and time, respectively, and subscript 0 and f indicate initial and final, respectively (e.g., v_f is the final speed of the trajectory). Given $s_0 = t_0 = 0$, both v_0 and v_f (e.g., cruising speed, turning speed) are related to environmental factors such as the maximum speed limit and curvature of the road, whereas both t_f and s_f (e.g., acceleration time and distance) are related to human factors such as driving style. To estimate t_f and s_f , we introduced two variables representing driving style: constant desired acceleration (a_d) and aggressiveness (k_a). Following the kinematic formula $v_f^2 = v_0^2 + 2a_d s_f$, we can calibrate a_d by minimizing the sum of the squared errors between the observed and estimated values. Desired time interval (t_d), which is one missing variable in the kinematic formula, can be computed by $t_d = 2s_f / (v_0 + v_f)$. As shown in Figure I.3.5.9, a correlation exists between the desired and actual time intervals. Thus, assuming a simple linear regression model, we can calibrate the slope k_a in the same way as in the a_d calibration. A lower value of k_a indicates aggressive driving behavior because the acceleration/braking time interval decreases, given the same other parameters.

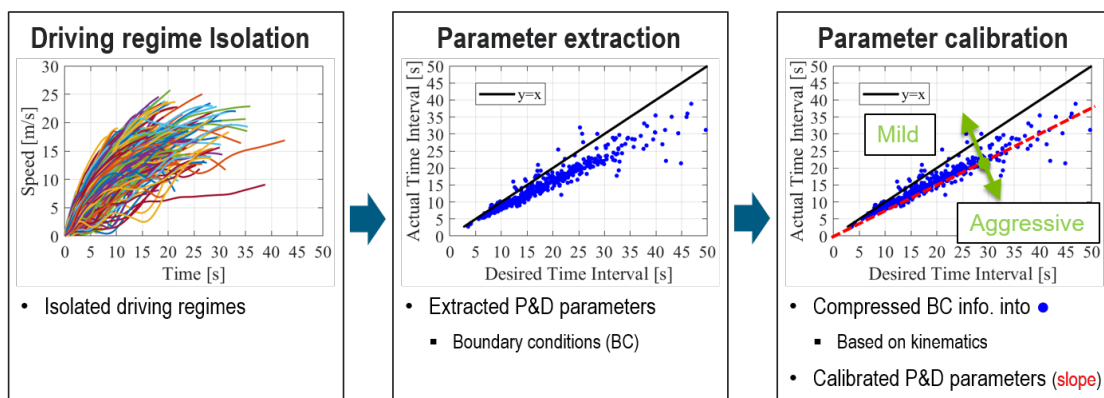


Figure I.3.5.9 Acceleration Regime Calibration Example

RoadRunner core and interface development

We improved the RoadRunner core (i.e., structure and code) by adding new features such as customizable I/Os and parallel simulations. Customizable I/Os accommodate different control system architectures enabled by connectivity and automation (e.g., engine torque and mechanical brake torque demands, gear number for conventional vehicles). A new message-passing interface enables distribution of simulations across multiple cores of a computer, and it accelerates a large-scale simulation study without requiring additional hardware or software by using clusters, distributed computing toolboxes, and other tools.

We also improved the RoadRunner interface by implementing AMBER [6] functions and classes for the simulation process to synchronize the workflow format with AMBER. The structure of the a run files was updated to make it easier for the user to define multiple scenarios in the structure of the metadata files that run RoadRunner simulations. An API-like command-line interface was also added. This enables better back-end communications with the graphical user interface (GUI) and allows the use of RoadRunner in customized workflows, such as large-scale studies. Based on the improved workflow, we created a prototype GUI in AMBER, which allows the user to change parameters and run simple simulations, as shown in Figure I.3.5.10.

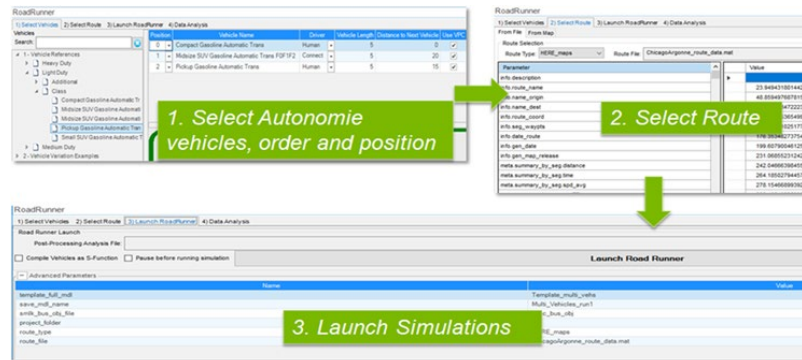


Figure I.3.5.10 Roadrunner GUI in AMBER

Conclusions

The objective of the project is to bring RoadRunner, a tool dedicated to energy efficiency research in the context of advanced powertrain, connectivity, and automation technologies, closer to commercialization. This entails the development of a release with graphical user interface and a library of default models useful for outside users as well as the development of a high-fidelity human driver. The driver modeling effort is enabled by the data collected and provided by the CRADA partner, Hyundai.

Due to COVID-19, on-road data collection with a dedicated instrumented vehicle was postponed. In the meantime, Hyundai is sharing samples of customer driving data. Our first focus in FY20 was to define a method of characterizing which subset of data should be share (e.g., which vehicles, in which area, for how long). Based on a table summarizing key attributes for each vehicle in the Hyundai database, we formulated a grouping and sampling method that precisely identifies the data that will provide a statistically representative dataset for modeling. Secondly, we developed a data analytics framework to post-process the data and implemented several pattern recognition algorithms to identify, for example, urban vs. rural driving, and to divide the trips by driving regimes. We can then directly use the labeled data to develop and validate the human P&D model. Finally, we improved the RoadRunner core source code for greater flexibility and customization and developed a first prototype of the RoadRunner interface for better usability.

In FY21, we will complete and use the data analytics framework to build a labeled customer driving dataset, and, using this dataset, we will calibrate the human P&D model. We will also adapt it to data from on-road testing. We will complete a model library that includes human driver and CAV models. We will further develop the graphical user interface for the first RoadRunner release.

Key Publications

1. Han, J., Karbowski, D., Kim, N., and Rousseau, A. "Human Driver Modeling Based on Analytical Optimal Solutions: Stopping Behaviors at the Intersections." ASME. Letters Dynamic Systems Control. January 2021; 1(1): 011010.

References

1. U.S. Census Bureau. Metropolitan and Micropolitan. Retrieved 2019. Accessed from <https://www.census.gov/programs-surveys/metro-micro.html>.
2. U.S. Census Bureau. Cartographic Boundary File. Accessed from <https://www.census.gov/geographies/mapping-files/time-series/geo/carto-boundary-file.html>.
3. Safety Pilot Model Deployment. (2014). Safety Pilot Model Deployment Data. (Dataset). Provided by ITS DataHub through Data.transportation.gov. Accessed from <http://doi.org/10.21949/1504482>.

4. Bucholtz, S., Molfino, E., and Kolko, J. “The Urbanization Perceptions Small Area Index: An Application of Machine Learning and Small Area Estimation to Household Survey Data.” Working paper. 2020. Accessed from <https://www.huduser.gov/portal/AHS-neighborhood-description-study-2017.html#overview-tab>.
5. U.S. Census Bureau and U.S. Department of Housing and Urban Development. (2019). Metropolitan Area Oversample Histories: 2015 and Beyond.
6. Rousseau, Aymeric, Sylvain Pagerit, Paul DeLaughter, Michael Juskiewicz, Phillip Sharer, and Ram Vijayagopal. “AMBER: A New Architecture for Flexible MBSE Workflows.” In IEEE VPPC. Belfort, France, 2017.

Acknowledgements

We would like to acknowledge Jihun Han, Namdo Kim, Yaozhong Zhang (ANL); Jason Lee, Yong Sun, Shihong Fan, and Jinho Ha from Hyundai-Kia America Technical Center, Inc. (HATCI) as well as Seoungwoo Ha, Jaesung Park, and Ji-hye Kim from the Data analytics Team 1 of Hyundai Motor Group, for coordinating the collection of data used in this project.

II Connectivity and Automation Technology

II.1.1 Energy-Efficient Maneuvering of Connected and Automated Vehicles (CAVs) with Situational Awareness at Intersections (SwRI)

Sankar Rengarajan, Principal Investigator

Southwest Research Institute
6220 Culebra Road
San Antonio, TX 78238
Email: sankar.regarajan@swri.org

Heather Croteau, DOE Technology Manager

U.S. Department of Energy
Email: heather.croteau@ee.doe.gov

Start Date: October 1, 2019

End Date: December 31, 2022

Project Funding: \$4,214,135

DOE share: \$3,207,135

Non-DOE share: \$1,007,000

Project Introduction

The increased development of Connected and Automated Vehicle (CAV) systems, currently used for safety and driver convenience, presents new opportunities to improve the energy efficiency of vehicles. Southwest Research Institute (SwRI) recently concluded a project that demonstrated 20% reduction in energy consumption on a Toyota Prius Prime 2017 plug-in hybrid by leveraging information streams enabled via connectivity—Vehicle-to-Vehicle (V2V), Vehicle-to-Infrastructure (V2I) and Vehicle-to-Everything (V2X). The effort was part of the Next Generation Energy Technologies for Connected and Automated on-Road Vehicles (NEXTCAR) program funded by the Advanced Research Project Agency-Energy [1]. The energy consumption gains were achieved by a combination of vehicle dynamics and powertrain control algorithms with a focus on SAE L1 and L2 automated vehicles where a human is still responsible for safe operation. The increased traction gained by the Mobility-as-a-Service (MaaS) movement is stimulating investment in the development of L4 and L5 automated vehicles. A life cycle assessment by the University of Michigan [2] indicates that subsystems in such highly automated vehicles could increase vehicle primary energy use and GHG emissions by 3–20% due to increases in power consumption, weight, drag, and data transmission. The application of NEXTCAR style technologies on such highly automated vehicles could not only improve their energy consumption but also provide additional opportunities for energy savings given the improved sensing and actuation capabilities of such vehicles.

From a technical standpoint, this program aims to answer and address three fundamental questions:

1. While technologies like eco-driving in CAVs have shown great potential for energy savings, how do these savings translate with respect to different types of powertrain - Internal Combustion Engine Vehicles (ICEV), Hybrid Electric Vehicles (HEV), Plug-In Hybrid Electric Vehicles (PHEV) and pure Electric Vehicles (EV) as well as different levels of automation—L0 through L4 vehicles?
2. Existing studies show that significant improvement in energy consumption is possible even with limited levels of automation such as cruise control [3],[4]. Programs like NEXTCAR integrate V2V and V2I connectivity with simple automation mechanisms and proved that benefits up to 20% is feasible. While such improvements were achieved at an individual vehicle level, what is the effect of these ‘smart’ vehicles at a system level under realistic traffic scenarios?
3. Can infrastructure mobility solutions contribute to more than safety and help in achieving system-level energy benefits?

Objectives

The primary objective of this project is to develop and demonstrate CAV technologies that enable $\geq 15\%$ reduction in energy consumption at a system level without negatively impacting traffic flux as shown in Figure II.1.1.1.

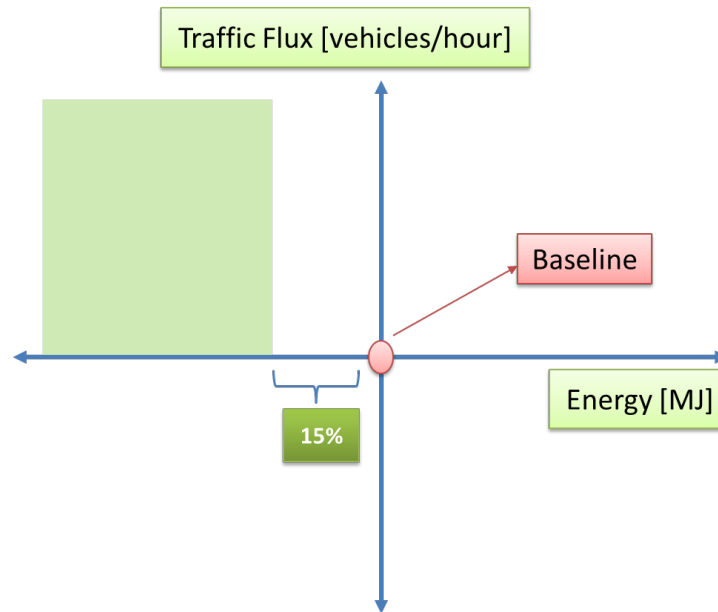


Figure II.1.1.1 Program Objective

Approach

In order to better understand the impact of CAV based energy saving technologies on different vehicle platforms, a vehicle mix as shown in Figure II.1.1.2 has been selected. These six vehicles form the ‘ego’ vehicle set and are chosen based on powertrain type and automation levels. V2X connectivity is a common theme across the ego vehicles.

		<i>Automation Levels</i>						
		L0	L1	L2	L2+	L4		
<i>Powertrain</i>	ICE	Hyundai Elantra				Chrysler 300		Hyundai contribution
	HEV							Continental contribution
	PHEV			Toyota Prius Prime				SwRI contribution
	EV			Kia Soul	Tesla Model 3	Easy Mile EZ 10		

Figure II.1.1.2 Ego Vehicle Set

The ego vehicle set needs to be tested under realistic traffic scenarios. Generating repeatable traffic scenarios for on-road testing is challenging and at times, not feasible. Some traffic patterns are dangerous and weather patterns add to noise factors. Further, it becomes unclear whether calibrations and control strategies are producing the desired effect or whether environmental factors are influencing results. Therefore, the team is building a traffic simulator as part of this effort. An urban corridor in Columbus, Ohio as shown in Figure II.1.1.3 is currently being modeled and calibrated for realistic traffic flow patterns in the PTV Vissim environment. The traffic simulator will be integrated with a high-precision vehicle hub dynamometer to test the ego vehicles in a controlled environment.

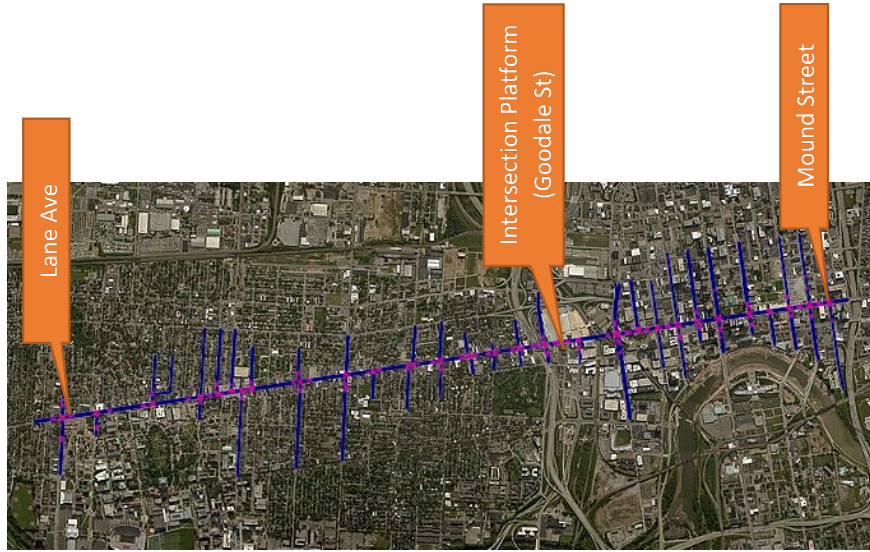


Figure II.1.1.3 Urban Corridor in Columbus, Ohio (High Street)

The intelligent intersection platform concept built by Continental, one of the project team members, is shown in Figure II.1.1.4. The intersection platform uses conventional automotive sensors such as radars, cameras, and a Dedicated Short-Range Communication (DSRC) radio. The system can accommodate other sensors such as LIDAR as well. The intersection platform leverages these sensors in conjunction with an environment model to develop a comprehensive scene understanding akin to a ‘virtual’ traffic police. In addition to scene understanding, the system is also able to create ‘proxy’ Basic Safety Messages (BSMs) and Personal Safety Messages (PSMs) on behalf of non-connected entities. This information can be sent to connected vehicles via the DSRC road-side unit mounted on the stack. While the intersection stack was primarily aimed for safety applications and augmenting sensor info for L4 vehicles, the ego vehicle set in this program will receive the messages from the intersection platform and optimize their approach. Energy savings enabled via the intersection stack will be quantified.

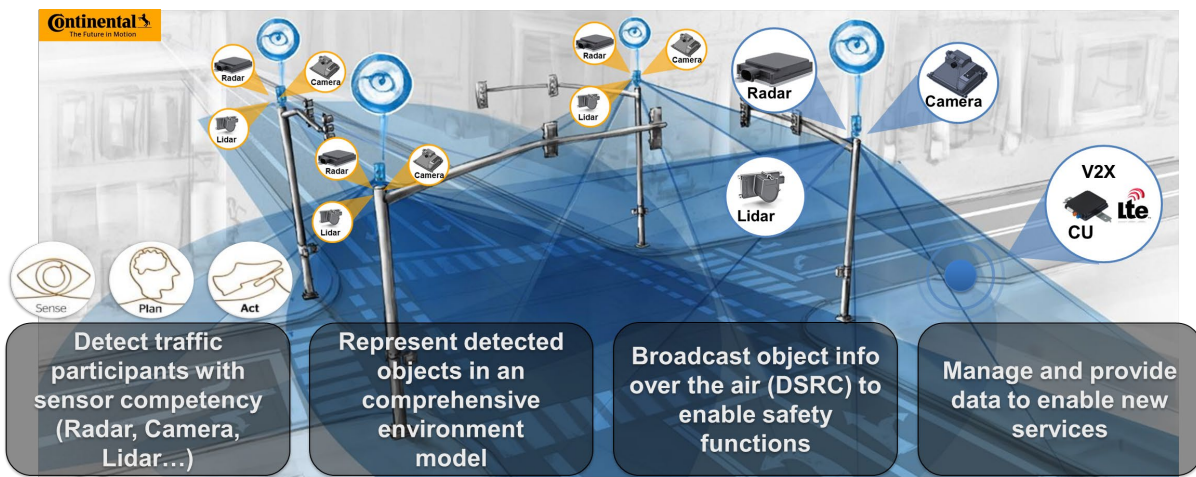


Figure II.1.1.4 Intelligent Intersection Concept

Figure II.1.1.5 describes the overall technology that is being built as part of this program and how the above-mentioned technologies blend together. L0-L3 vehicles use an advisory system to guide a human driver while L4 vehicles can directly integrate the information into their trajectory planning module and optimize their approach. Frost & Sullivan, the Tech-to-Market (T2M) partner for the program, will bring market forecast

studies that will be used to tune three key parameters for the study – (1) Vehicle powertrain mix (2) V2V and V2I penetration and (3) Vehicle Automation. Energy consumption impact at a system level will be studied under different scenarios by tuning these parameters.

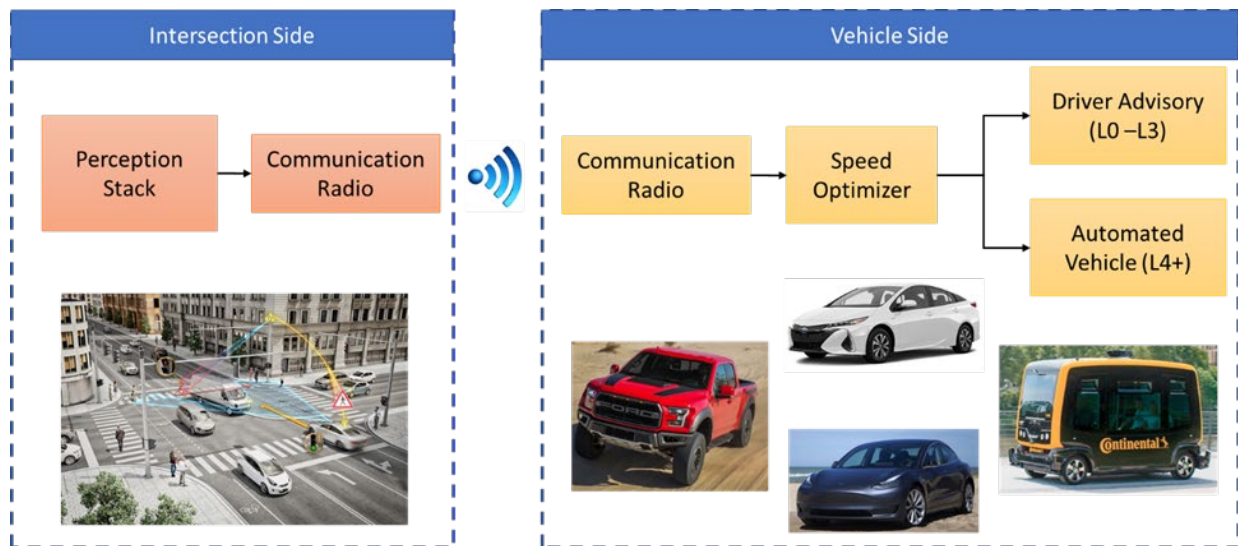


Figure II.1.1.5 Technology Approach

The focus of this budget period (10/01/2019 – 12/31/2020) is on simulation study. A summary of milestones in this budget period along with their corresponding status is shown Table II.1.1.1

Table II.1.1.1 Milestone Summary (as of Q4)

Milestone	Description	Type	Due	Completion Status
Road network for traffic simulation validated	Road network for traffic simulation complete.	Technical	Q5	100%
Macroscopic traffic simulation validated	Demonstrate relevant metrics from simulation within 10% of measured value.	Technical	Q5	75%
Traffic simulation with intersection functionality validated	Completion of the initial version of traffic simulation with intersection-based traffic mix. This will be validated with real data recorded at intersections.	Technical	Q5	100%
Vehicle & powertrain models for energy consumption on transient drive cycles validated	Completion of initial vehicle and powertrain models for the vehicle mix selected for the program. Validation will be using dynamometer or Environmental Protection Agency (EPA) published (effective) fuel consumption on standard test cycles.	GO/NO-GO	Q5	100%

Traffic Simulation

The road network and basic traffic control strategies of the selected corridor in Columbus, Ohio, has been modeled in the traffic simulation environment. In order to realistically model the traffic flow patterns in the simulation, traffic flux [vehicles/hour] and average corridor speed [miles/hour] is required. The team is fusing data from camera footage provided by City of Columbus, Continental intersection stack, public cameras at intersections, and navigational services such as Google Maps to calibrate the simulation for realistic traffic flow patterns.

The City of Columbus provided the traffic signal phasing and timing patterns for the corridor and traffic camera video footage from a few intersections. The signal timing patterns have been integrated into the simulation at every signalized intersection location. An example of such a program is shown in Figure II.1.1.6. This signal controller has five signal groups, where each group is a unique timing scheme for a traffic signal. The "signal sequence" selects the red-green-yellow traffic light pattern for a signal. The cycle length for this example is 76, meaning these patterns repeat every 76 seconds. The green bars, yellow rectangles, and red lines are pictorial representations of the time lengths assigned to each traffic light in seconds. For example, the signal pattern "1", "12th SL" is green between 0 and 44 seconds, yellow for three seconds thereafter, and red for the remainder of the cycle length. These programs are also communicated to eco-driving vehicles as signal phasing and timing information.



Figure II.1.1.6 Signal Phasing and Timing Pattern (High Street Corridor Sample)

Modeling representative traffic densities for an entire network requires calibrating the number of vehicles entering the simulation at every street and the routes these vehicles take to eventually exit the simulation. The latter has been accomplished by introducing decision points at every intersection, as shown in Figure II.1.1.7. When a vehicle reaches a decision point, it is assigned a path based on the "relative flow" (RelFlow). For example, northbound vehicles approaching the intersection in Figure II.1.1.7 enter vehicle routing decision (VehRoutDec) "11." For every 10 vehicles, two are directed to turn right, two are directed to turn left, and six will continue straight. If the vehicles do not exit the simulation after this intersection, they will approach another decision point, and the process repeats.

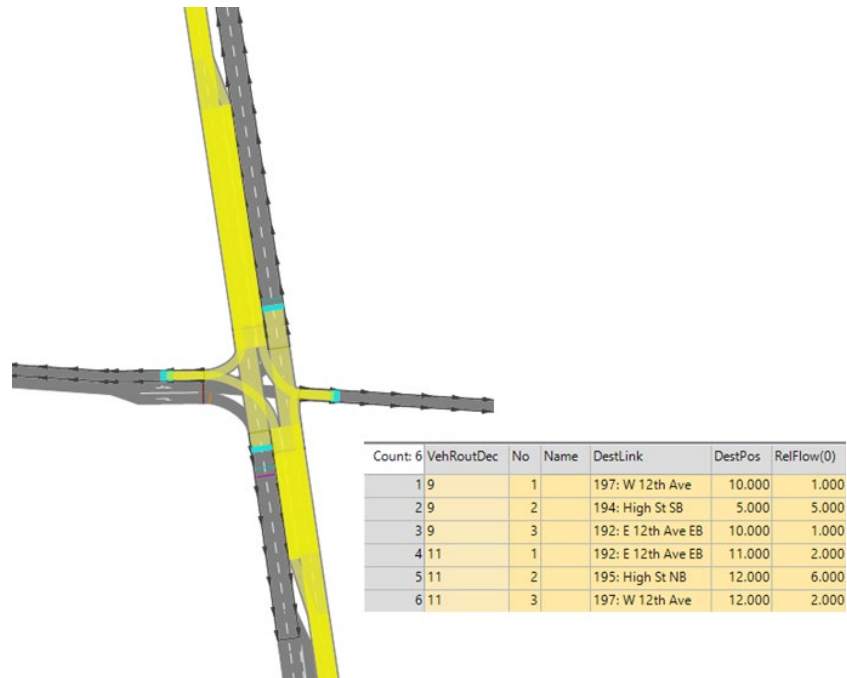


Figure II.1.1.7 Vehicle Routing Decisions

Figure II.1.1.8 shows a sample camera feed from the High Street corridor that is being analyzed by the team for capturing traffic flux information and understanding queue sizes at various traffic lights.



Figure II.1.1.8 Camera Feed High Street

Vehicle Simulation

In order to understand energy consumption impact, high-fidelity powertrain models are required. Since the focus of the program is not building powertrain models, existing models were leveraged when available. The models were validated via vehicle chassis dynamometer data or EPA certification numbers. The acceptance criteria for the energy estimation models is given below:

- Energy consumption within 10% for regulatory cycles
- Nice to have: Meet Normalized cross-correlation power (NCCP) criteria [5].

Appropriate permissions were obtained to leverage a validated Hyundai Elantra GT-Suite model developed by SwRI for a prior program that was funded by Hyundai, one of the project team members. The Toyota Prius Prime vehicle simulator developed by SwRI for the NEXTCAR program will be used for this project. The model has been validated using multiple regulatory and real-world drive cycles. The remainder of the powertrain models were built and validated as part of the program. The vehicle models have been developed leveraging data available on the OEMs websites, EPA certification and fuel economy database [6],[7],[8],[9],[10], and chassis dynamometer and road test data obtained from various source including SwRI’s Energy Storage System Evaluation & Safety (ESSES) consortium [11].

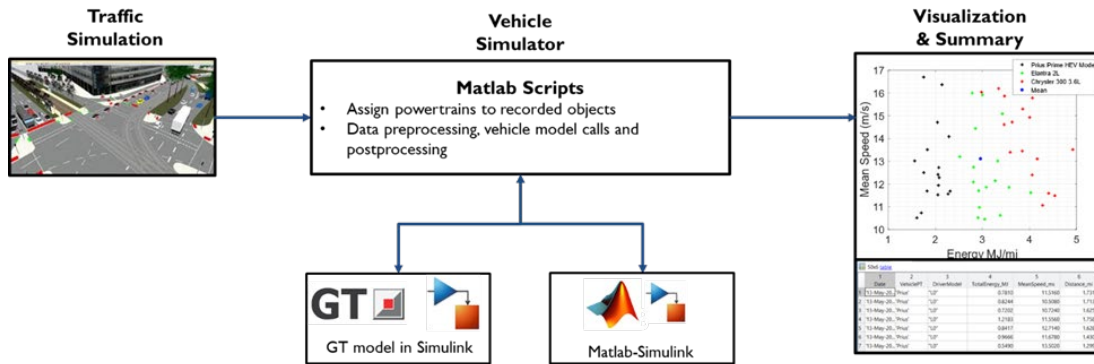


Figure II.1.1.9 Energy Estimation Framework

The team also developed the energy estimation framework (refer Figure II.1.1.9) to process and visualize the results. Figure II.1.1.10 depicts a sample plot which is generated by the framework. The plot contains distance normalized energy consumption on the x-axis and distance normalized trip time on the y-axis, for each vehicle that is part of the traffic simulation environment. Energy and trip time numbers for each vehicle present in the traffic simulation environment is calculated for all powertrains in the mix. These numbers are then weighted based on the share of each powertrain type in the mix to obtain weighted average numbers for the corridor for the baseline case and eco-driving case. Further, calculation of energy and trip time numbers for ego vehicles and neighboring vehicles in eco-driving run is done separately, to analyze the effects of ego vehicle on neighboring vehicles. Trip time in [min/mile] is used as an equivalent representation of vehicle flux shown in Figure II.1.1.10

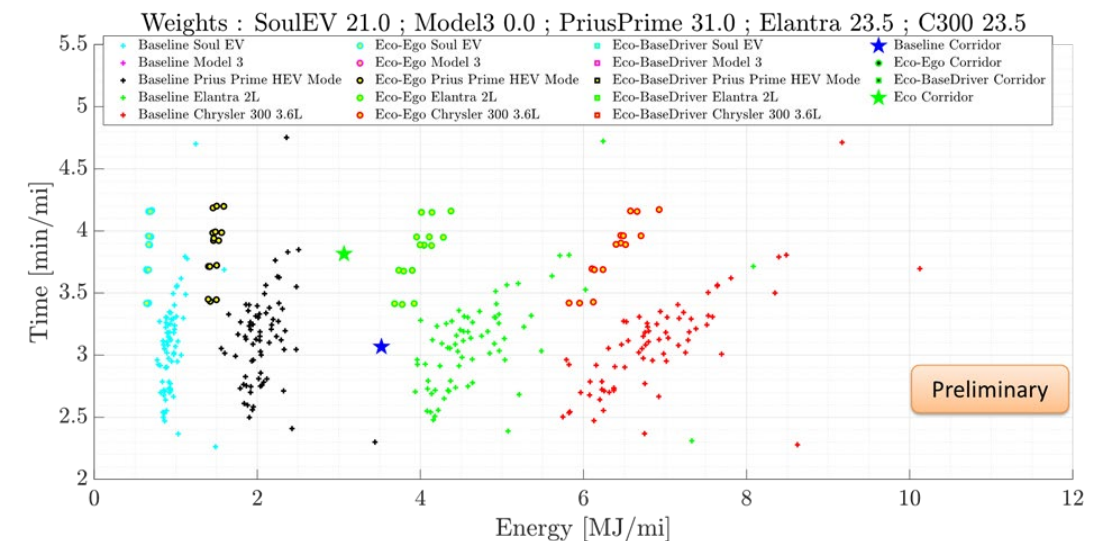


Figure II.1.1.10 Sample Output of the Energy Estimation Framework Summarizing Energy Consumption Based on Powertrain Mix, Driver Model and Cav Penetration

Tech to Market (T2M)

From a T2M perspective, the team is working on forecasting studies and a literature survey focused on passenger acceptance. Public sector engagement was delayed due to COVID-19.

Results

Traffic Simulation

The target velocity profile and travel time for a vehicle traveling the entire length of High Street has been estimated by querying the Application Programming Interfaces (APIs) of Google Maps. The result of such a query is shown in Figure II.1.1.11. This figure shows the nominal speed of a vehicle traveling at 9 AM on a typical Wednesday, starting at the southern end of the modeled corridor and continuing north. Note the map overlay below the speed trace, which was included to display Google's color-coded traffic visualization, with orange signifying "medium amount of traffic." Travel times are "typically" 10-26 minutes, with a "best guess" of around 16 minutes. The mean speed is roughly 22 kph (~13 mph). The speed limit is generally 56 kph (~35 mph), with several slower zones between some intersections. As there are over 28 signalized intersections in this route, the mean speed is expected to be lower than the possible maximum (traveling continuously at the speed limit).

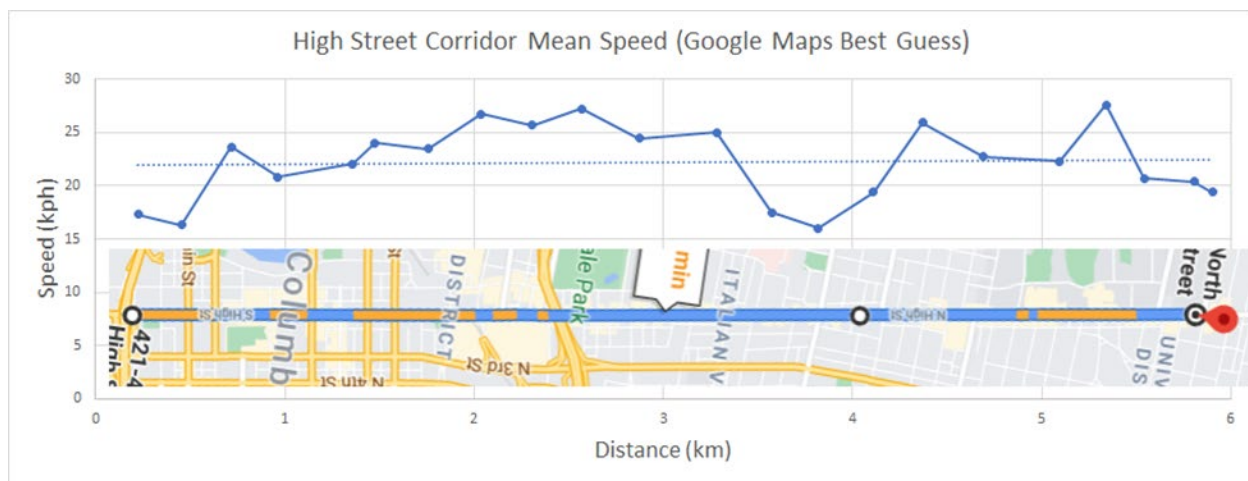


Figure II.1.1.11 Google Maps Estimation for High Street Nominal Speeds

The first pass at calibrating the corridor using parameters outlined above produced results shown in Figure II.1.1.12. This figure is a normalized histogram of trip times for default Vissim vehicles traveling the entire length of the High Street corridor, from the southernmost to the northernmost points of the simulation. The vehicles have an average trip time of 13.5 minutes and a mean speed of 27.2 kph (~17 mph), with travel times ranging from roughly 11-16 minutes. This is somewhat faster than the trip times predicted by Google Maps, likely indicating localized slowdowns in the real world that could be included in the simulation for a more accurate representation. The team will continue to improve the traffic simulation to match real world scenarios.

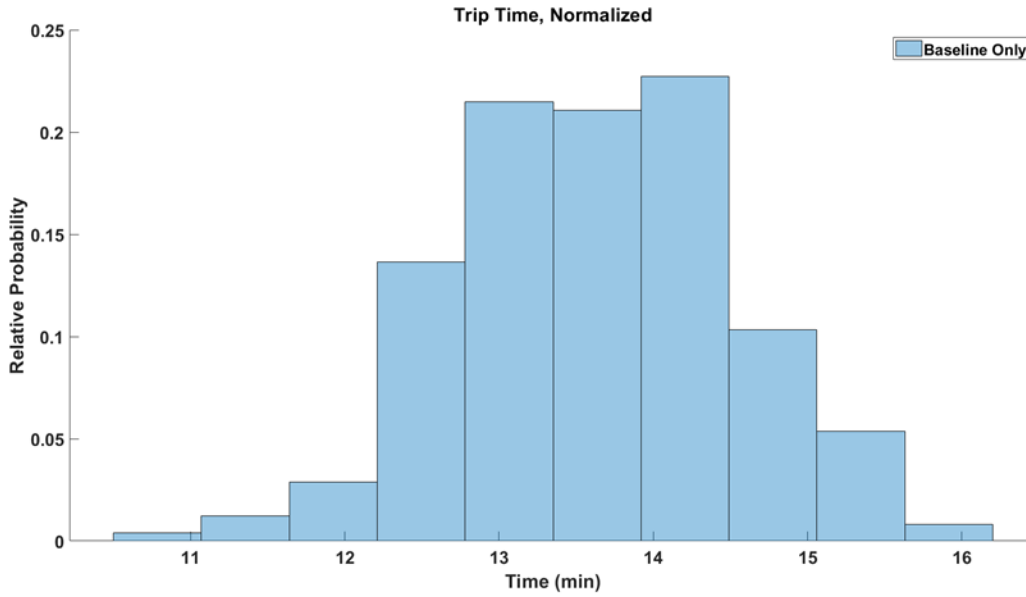


Figure II.1.1.1.12 Trip Time Histogram of Vehicles in Traffic Simulation Navigating High Street Corridor

Vehicle Simulation

The Elantra model has been validated to match EPA certification application fuel economy values [7].

Table II.1.1.2 Fuel Economy (Miles per Gallon) Comparison for Hyundai Elantra

	EPA Certification [10]	SwRI Model	% Error
FTP75 Bag 1	35.2	33.9	-3.6
FTP75 Bag 2	36.7	37.4	1.9
FTP75 Bag 3	40.0	40.3	0.7
FTP75 Weighted	37.1	37.3	0.3
US06 City	20.1	21.8	8.4
US06 Highway	38.1	39.9	4.7
US06	31.7	33.4	5.5
HwFET	52.4	52.6	0.4

The 2016 Chrysler 300 powertrain consists of a 3.6L V6 engine and an 8-Speed ZF transmission. The powertrain specification of the 2014 Dodge Charger tested and benchmarked by the EPA [10],[9] matches the specification of the vehicle that will be used in the program. The approach was to first develop a model for 2014 Charger and validate it with the available data. The validation was done by comparing the fuel economy

values with certification document values [12]. Further, the team computed the NCCP values for the Dodge Charger model based on the available EPA benchmarking data. The numbers are summarized in Table II.1.1.3. The parameters (final reduction ratio and road load coefficients) were then changed to match 2016 Chrysler 300, and the fuel consumption values were compared to EPA certification values [6]. As shown in Table II.1.1.4, the fuel consumption values match well with EPA values.

Table II.1.1.3 NCCP Values for Dodge Charger Model

	FTP 1	FTP 2	FTP 3	HwFET 1	HwFET 2	HwFET 3	US06 1	US06 2	US06 3
Vehicle Speed	0.98	0.99	0.99	0.99	0.99	0.99	0.99	0.99	0.99
Wheel Force	Not available	0.91	0.91	0.88	0.88	0.88	0.93	0.94	0.95
Engine Speed	0.88	0.88	0.88	0.99	0.98	0.98	0.98	0.96	0.98
Engine Torque	0.90	0.92	0.92	0.91	0.90	0.88	0.93	0.96	0.97

Table II.1.1.4 Fuel Economy (Miles per Gallon) Comparison for Chrysler 300

	EPA Certification	SwRI Model	% Error
FTP75 Bag 1	21.4	21.6	0.6
FTP75 Bag 2	21.5	21.0	-2.5
FTP75 Bag 3	24.7	24.9	0.6
FTP75 Weighted	22.3	22.1	-0.8
US06 City	14.0	15.2	8.2
US06 Highway	27.5	26.5	-3.4
US06	22.6	22.7	0.5
HwFET	36.1	34.2	-5.4

The Toyota Prius Prime vehicle simulator developed by SwRI for the NEXTCAR [1] program is being used for this project. The model has been validated using multiple standard and real-world drive cycles. The fuel consumption was within 5% and the change in SOC over the trip was within 1% (refer Figure II.1.1.13).

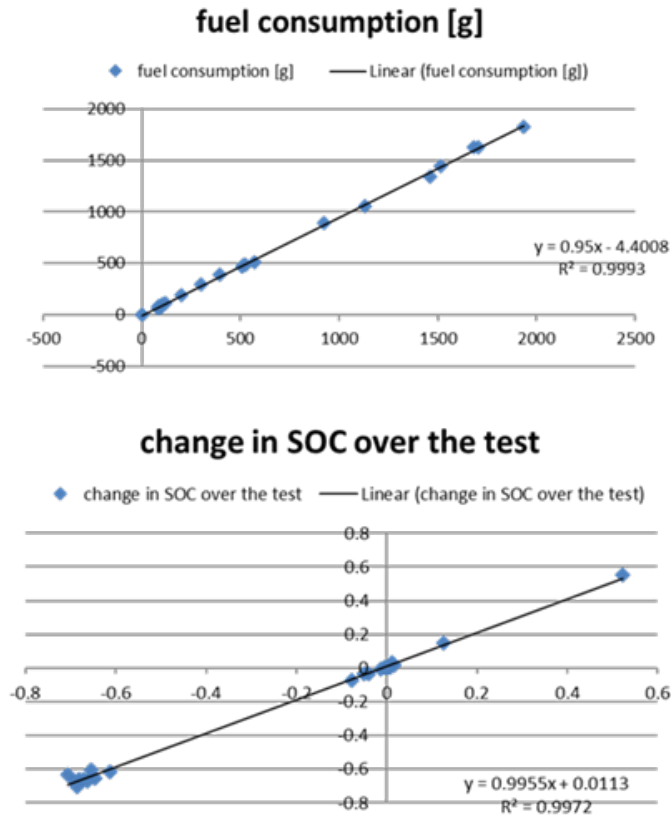


Figure II.1.1.13 Comparison Between Measured and Predicted Fuel Consumption and Delta SOC (Battery Usage) Across 17 Different Drive Cycles (Each Dot Represents a Drive Cycle)

The team leveraged the Kia Soul EV and Tesla Model 3 benchmarking data collected as part of SwRI’s ESSES consortium [11] to develop the model. This included detailed benchmarking of energy storage system at cell and pack level. Further, some chassis dynamometer and road tests were also conducted, during which CAN-bus data was recorded. The energy storage data collected as part of ESSES along with certification information published on EPA’s website [12] was used to develop the model. To validate the model, the team used the CAN-bus data recorded during the chassis dynamometer testing. Table II.1.1.5 and Table II.1.1.6 compare the energy consumption of the Kia Soul EV model and Tesla Model 3 powertrain model with the test data. The positive energy consumption mentioned in the table considers energy consumption during traction and does not include regeneration. The net energy consumption includes energy regenerated. Both parameters are within the criteria mentioned earlier. The reference data for UDDS and HwFET cycle comparison for the Tesla Model 3 (shown in Table II.1.1.7) was based on the certification document publicly available from EPA(Tesla Inc. n.d.) which did not include the positive energy consumption. The model was validated using the data from WLTP cycle on a chassis dynamometer at SwRI. A summary of NCCP values for the vehicle models are in Table II.1.1.7 and Table II.1.1.8. The NCCP values for both models suggest a good agreement between the test and simulation results for the evaluated cycles. After obtaining more test data, the team plans to simulate scenarios comparing results with other standard cycles from dynamometer runs to further improve the model.

Table II.1.1.5 Energy Consumption Comparison for Kia Soul EV

Test #	Cycle Contents	Simulation [$\frac{kWh}{100mi}$]		CAN Data [$\frac{kWh}{100mi}$]		Difference [%]	
		Net	Positive	Net	Positive	Net	Positive
1	1st 1200s UDDS	18.8	25.7	19.1	26.2	-1.6	-1.7
2	Part UDDS	20.5	27.2	20.8	27.1	-1.7	0.3
3	1x HwFET +	22.2	24.5	23.0	25.2	-3.5	-2.9
4	1x HwFET +	22.2	24.6	22.9	24.6	-3.0	0.2
5	Part HwFET	24.4	26.3	24.2	25.5	0.7	3.3
6	US06 – 1 Full + 1 Partial	32.8	39.1	32.3	39.4	1.6	-0.7

Table II.1.1.6 NCCP Values for Kia Soul EV

Test	#1	#2	#3	#4	#5	#6
Vehicle Speed	0.999	0.999	0.999	0.999	1.000	0.999
Battery Terminal Voltage	0.997	0.996	0.996	0.999	0.998	1.000
Battery Current	0.968	0.957	0.967	0.918	0.916	0.945
Battery SOC	0.996	0.997	0.995	0.994	0.998	0.994

Table II.1.1.7 Energy Consumption Comparison for Tesla Model 3

Drive Cycle	Simulation [$\frac{kWh}{100mi}$]		CAN Data [$\frac{kWh}{100mi}$]		Difference [%]	
	Net	Positive	Net	Positive	Net	Positive
UDDS*	15.0	24.9	14.5	-	3.5	-
HwFET*	17.6	20.1	16.3	-	8.0	-
WLTP	19.5	27.8	19.8	27.9	-1.5	-0.4

* Reference numbers for UDDS, HwFET are average of last 2 runs part in certification document which indicate warmed conditions to better represent the data used as basis for simulation.

Table II.1.1.8 NCCP Values for Tesla Model 3

	WLTP
Vehicle Speed	1.000
Battery Terminal Voltage	0.983
Battery Current	0.999
Battery SOC	0.966

Conclusions

The focus of FY20 was on simulation study. The team finished road network modeling of the High Street corridor based in Columbus, Ohio for the traffic simulation framework. The City of Columbus provided the team with signal timing and phasing patterns for the High Street corridor and camera footage from a few intersections. This information along with data from the Continental intersection platform deployment and Google Maps is currently being used to calibrate realistic flow patterns in the traffic simulation. The team has completed powertrain model validations for all the vehicle platforms. An energy estimation framework that interfaces between the traffic simulation and powertrain models has been established to understand system level impact in a succinct fashion. From a T2M perspective, the team started work on forecasting studies and a literature survey focused on passenger acceptance. Public sector engagement was delayed due to COVID 19. The team is compiling a list of DOTs, cities, and infrastructure providers to interview in the near future.

References

1. S. Rengarajan, S. Hotz, J. Sarlashkar, S. Gankov, P. Bhagdikar, M. C. Gross and C. Hirsch, "Energy Efficient Maneuvering of Connected and Automated Vehicles," in SAE Technical Papers, 2020.
2. J. H. Gawron, G. A. Keoleian, R. D. De Kleine, T. J. Wallington and H. C. Kim, "Life Cycle Assessment of Connected and Automated Vehicles: Sensing and Computing Subsystem and Vehicle Level Effects," *Environmental Science & Technology*, vol. 52, no. 5, 2018.
3. R. E. Stern, S. Cui, M. L. Delle Monache, R. Bhadani, M. Bunting, M. Churchill, N. Hamilton, R. Haulcy, P. Hannah, W. Fangyu, P. Benedetto, B. Seibold, J. Sprinkle and D. B. Work, "Dissipation of stop-and-go waves via control of autonomous vehicles: Field experiments," *Transportation Research Part C: Emerging Technologies*, vol. 89, 2018.
4. U.S. Energy Information Administration, "Study of the Potential Energy Consumption Impacts of Connected and Automated Vehicles," www.eia.gov
5. Y. Meng, M. Jennings, P. Tsou, D. Brigham, D. Bell and C. Soto, "Test Correlation Framework for Hybrid Electric Vehicle System Model," *SAE International Journal of Engines*, vol. 4, no. 1, pp. 2011-01, 2011.
6. FCA US LLC, "Application for Certification," 2015. [Online]. Available: iaspub.epa.gov/otaqpub/display_file.jsp?docid=36539&flag=1.
7. Hyundai Motor Company, "Application for Certification - Part 1," 2015. [Online]. Available: iaspub.epa.gov/otaqpub/display_file.jsp?docid=38646&flag=1
8. Tesla Inc., "Request for issuance of a new certificate of Conformity to include a running change – Addition of a new variant to the RWD," 2019. [Online]. Available: iaspub.epa.gov/otaqpub/display_file.jsp?docid=46584&flag=1

9. U.S. EPA, 2014 Dodge Charger Vehicles with 3.6L & 845RE Tier 2 Fuel – Test Data Package. Version 2019-04, Ann Arbor, MI: U.S. EPA, National Vehicle and Fuel Emissions Laboratory, National Center for Advanced Technology.
10. U.S. EPA, 2014 FCA HFE 845RE Transmission Mapping – Test Data Package. Version 2019-04, Ann Arbor, MI: U.S. EPA, National Vehicle and Fuel Emissions Laboratory, National Center for Advanced Technology.
11. Southwest Research Institute, "Energy Storage System Evaluation & Safety (ESSES) | SwRI," [Online]. Available: <https://www.swri.org/consortia/energy-storage-system-evaluation-safety-esses>
12. A. Moskalik, A. Hula, J. Kargul and D. Barba, "Investigating the Effect of Advanced Automatic Transmissions on Fuel Consumption Using Vehicle Testing and Modeling," SAE International Journal of Engines, vol. 9, no. 3, pp. 2016-01, 2016.

Acknowledgements

SwRI would like to thank DOE for funding this work and is excited to participate in building the next generation of highly efficient mobility systems. We would also like to extend our appreciation to our partners Continental, Hyundai Kia America Technical Center Inc., Frost & Sullivan and Alamo Area Clean Cities Coalition for their valuable contributions to this work

II.1.2 CIRCLES: Congestion Impacts Reduction via CAV-in-the-loop Lagrangian Energy Smoothing (The Regents of the University of California)

Alexandre Bayen, Principal Investigator

Institute of Transportation Studies, University of California, Berkeley
109 McLaughlin Hall
Berkeley CA 94720-1720
Email: bayen@berkeley.edu

Benedetto Piccoli, Principal Investigator

Department of Mathematical Sciences, Rutgers University, Camden
311 North Fifth Street
Camden, NJ 08102
Email: piccoli@camden.rutgers.edu

Benjamin Seibold, Principal Investigator

Department of Mathematics, Temple University
1905 North Broad Street
Philadelphia, PA 19122
Email: seibold@temple.edu

Jonathan Sprinkle, Principal Investigator

Department of Electrical and Computer Engineering, University of Arizona
1230 East Speedway Boulevard
Tucson, AZ 85721
Email: sprinkjm@email.arizona.edu

Daniel Work, Principal Investigator

Department of Civil and Environmental Engineering, Vanderbilt University
1025 16th Avenue South, Suite 102
Nashville, TN 37212
Email: dan.work@vanderbilt.edu

Heather Croteau, DOE Technology Manager

U.S. Department of Energy
Email: heather.croteau@ee.doe.gov

Start Date: January 1, 2020

End Date: December 31, 2022

Project Funding: \$4,991,896

DOE share: \$3,499,906

Non-DOE share: \$1,491,990

Project Introduction

The energy efficiency of today's vehicular mobility relies on the un-integrated combination of i) control via static assets (traffic lights, metering, variable speed limits, etc.); and ii) onboard vehicle automation (adaptive cruise control (ACC), ecodriving, etc.). These two families of control were not co-designed and are not engineered to work in coordination. Recent studies have shown i) limitations of controls, and even ii) negative impacts of ACC [1]. The project focuses on the technology development, implementation and prototyping, and validation of *Mobile Traffic Control* (MTC). MTC can be viewed as an extension of classical traffic control (in which static infrastructure actuates traffic flow). In the MTC paradigm, automated vehicles actuate the entire flow via their behavior, offering enhanced possibilities to optimize the energy footprint of traffic, if designed correctly.

We want to demonstrate for the first time that considerably reduced fuel consumption of all vehicles in traffic can be achieved via distributed control of a small proportion of CAVs. Compared to baseline vehicular technologies, our work offers a significant design departure: control algorithms for the CAVs consider the impact one vehicle can have on overall traffic, improving resulting overall fuel consumption. We focus on using a few vehicles as traffic controllers via CAV technology to improve the energy efficiency of traffic flow to further optimize energy efficiency. The demonstrated technology will result in energy gains exceeding 10% for all vehicles on the road, through automation of less than 5% of the vehicles in the flow. This estimate is based on our prior field experiments that demonstrated fuel consumption reductions of up to 40% on a single lane track under ideal conditions [2]; which we expect (based on model- and simulation-based estimates) to be reduced in realistic highway conditions due to lane changing and other drivers' responses to actuation.

Objectives

The objective of this project is to develop and demonstrate AI- and theory-based control algorithms that smooth traffic flow in stop-and-go traffic conditions capable of providing $\geq 10\%$ energy savings.

In this project, we will develop control algorithms using classical control theory as well as deep reinforcement learning (deep-RL) that will allow our control vehicles to cooperatively smooth stop-and-go waves in a real highway environment with live traffic. A discussion of the work sites follows:

- The classical control algorithms will be developed at Rutgers University Camden.
- Energy models for the control and non-control vehicles will be developed at Temple University.
- The testbed development, including installation of high-resolution cameras along a segment of the I-24 freeway in Nashville and development of computer vision tracking algorithms, will be done at Vanderbilt University and on I-24, in collaboration with Tennessee Department of Transportation.
- CAV controls implementation and testing will be done at University of Arizona and partially in parallel with UC Berkeley researchers at the Richmond Field Station.
- The deep-RL algorithms, as well as some of the previously mentioned work, will be developed and tested at UC Berkeley.

Approach

The work focuses on mobile actuation of multi-lane traffic. Our approach is thus to i) establish the minimum sensing and connectivity needs required for eliminating traffic waves with mobile actuation, and ii) investigate control requirements to dampen stop-and-go traffic. We will publish data sets of vehicular trajectories with fuel consumption rates to further advance the development of high-fidelity control strategies. Our approach to achieve our objectives includes i) developing mathematical models of the traffic to enhance understanding of the predictability of stop and go waves with careful investigation of lane changing models, ii) designing sensing systems and estimation algorithms to detect the traffic state using on-board vehicle sensing and/or infrastructure sensor networks, iii) designing control and machine learning algorithms to robustly dampen waves or prevent their amplification by combining lateral and longitudinal control of CAVs, iv) performing software verification of the models, sensing systems, estimation and control algorithms in simulation and on-board CAVs, and v) investigating intelligent agent design constructs for human–autonomous collectives in mixed autonomy environments.

Results

I-24 Testbed Development. Research and development for the I-24 testbed began with evaluating modern CCTV camera systems for possible deployment on roadside poles for traffic observation. A determination of high-resolution (4K) cameras, capable of individual pan-tilt-zoom control, was made. Roadside poles at a height of 110 feet were selected to minimize optical occlusion between vehicles. Six cameras could be housed

on a single roadside pole with their fields of view adjusted for complete coverage of 500 linear feet of roadway.

Testing of this proposed configuration was conducted on an existing roadside pole owned by the Tennessee Department of Transportation (TDOT). This test confirmed the feasibility of the configuration and the decision was made to move forward with it in the I-24 site design. The test also provided valuable video data for computer vision algorithm development.

The site of the I-24 testbed was chosen and refined based on roadside site layout, traffic patterns, and existing TDOT data sources. Detailed engineering design was conducted during summer 2020 and contractors were engaged to construct the roadside poles, modify communication infrastructure, and manufacture camera cluster housings with continual input from the research team.

Computing and data storage hardware is also being deployed on the testbed network. GPU-equipped servers will ingest, and process video data streamed from the testbed cameras. A storage array will hold video data for continued algorithm development and validation, in addition to resultant trajectory data. Out-of-band network access was installed via 4G cellular to enable remote monitoring and management of the system.

The validation phase of the I-24 testbed—the installation of the first three highway poles and camera clusters—was completed on August 30, 2020 (see figures below). These poles carry 18 4K resolution cameras that will soon provide continuous coverage of traffic on I-24, capturing trajectories from ~150,000 vehicles daily. We are on our way to making the largest continuous and complete trajectory dataset in existence. The cameras will also serve as an essential monitoring system to validate our phantom jam fighting and energy reduction strategies generated by the entire CIRCLES team.





Figure II.1.2.1 Images Taken from the Validation Phase of the I-24 Testbed

Computer Vision. Thus far, computer vision work has been focused on developing a novel, faster method for object tracking. Existing methods, while fairly accurate, fall far short of the testbed needs in terms of speed. A fast method is necessary to process video data as it is streamed and to provide high-fidelity estimates of vehicle positions. The core innovation of this new tracking method is to rely on a convolutional neural network for object localization within a small crop of a video frame, rather than utilizing object detectors that specialize in finding all object locations within an entire video frame. The lightweight localization network is able to run much faster than the object detector at only a small cost in accuracy.

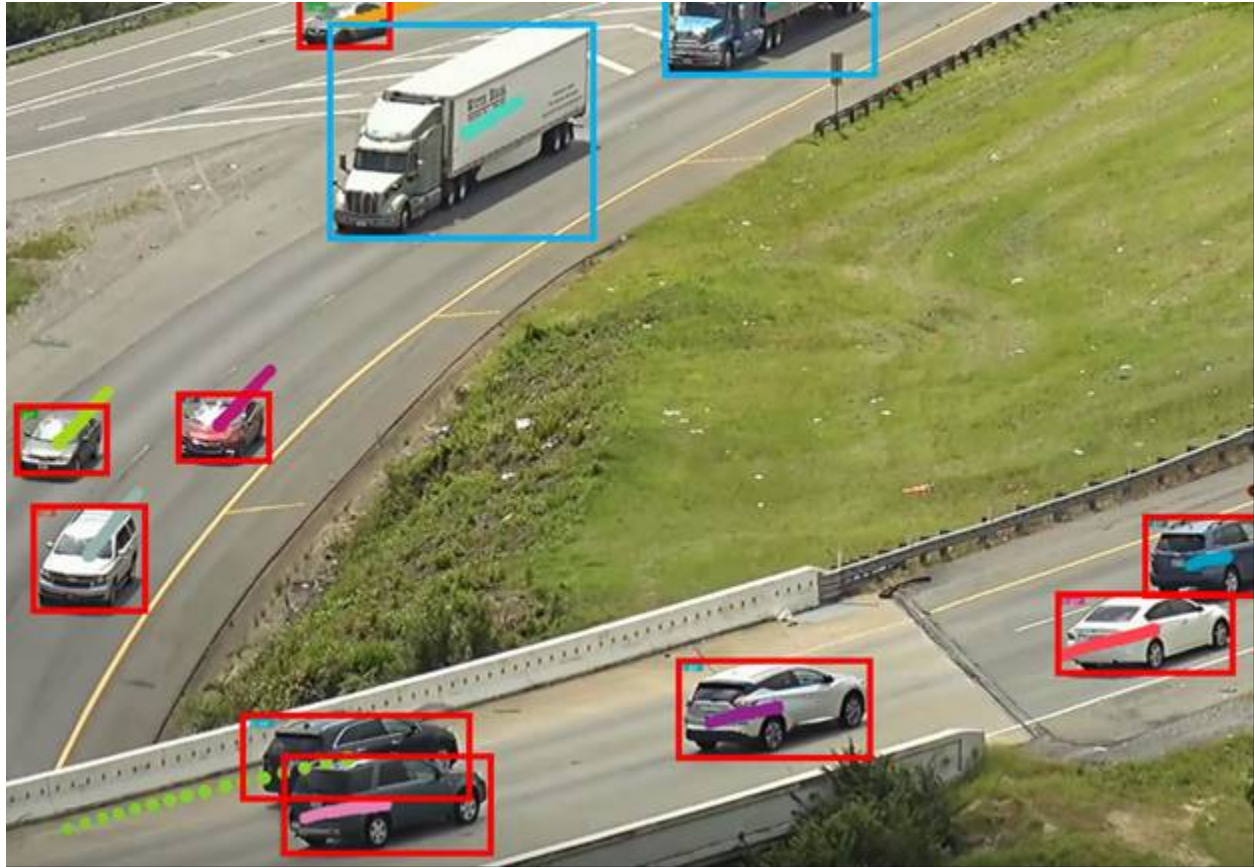


Figure II.1.2.2 Demonstration of Object Tracking with Bounding Boxes and Vehicle Speed Annotations

Computer vision algorithms have been continually developed on video data from cameras on roadside traffic monitoring poles, mimicking the setup of the I-24 testbed. This has enabled algorithms to be tuned for performance with large numbers of objects in view, which exhibit realistic vehicle dynamics within the field of view.

The current version of computer vision algorithms will be deployed on a GPU-equipped computing server on the testbed network in Fall 2020 to begin generating vehicle trajectories from the three camera poles and 18 cameras on the first phase of the testbed. These trajectory results and video data will be used to further refine the computer vision algorithms in terms of accuracy and processing speed.

Traffic Flow Modelling. To train and test wave smoothing control strategies, a subteam has been working on developing high fidelity traffic simulation models that explicitly produce non-equilibrium phenomena. Target traffic patterns, such as stop-and-go waves and traffic congestion, are evaluated and carefully tested for consistency with known phenomena on real roads. While our first quarter work focused on getting simple network set-ups to produce those target traffic patterns, our second quarter work led to our third iteration model release “Model v3.0” of a 5-lane highway with lane changing and integrated failsafe logic on a stretch

of I-210 in California. This group determines and implements several model features to meet the needs of other groups, such as the Energy Team, Mean-Field Team, RL Team, or Hardware Team. In general, we adopt an iterative approach that combines consultation with the control teams (Mean-Field & RL) for necessary simulation tools with principled mathematical formulations of the underlying desired traffic phenomena.

After releasing “Model v3.0,” our third quarter work centered on the data requirements to further enhance and calibrate a larger model on I-24 where our field tests will be located. We investigated various calibration routines and associated metrics. This resulted in the production of a conference paper submission to the annual Transportation Research Board, in which we identified an inability in current traffic simulation calibration routines to accurately calibrate phantom traffic jams from currently available data sources. Going into the future, a major focus for our group will be developing novel techniques to address this problem, incorporating explicit knowledge of the structure of traffic waves, and then applying them to our previously developed frameworks.

Energy Modelling. Based on (proprietary) energy models provided by Toyota, this subteam (including Toyota) has carefully reconstructed two simplified models that are compatible with the modeling and data framework needed by the other teams in this project. One of the fitted models (PriusEV 1.0) is for a hypothetical vehicle that possesses all the characteristics of the 2017 Prius, except for being a fully electric vehicle (rather than a hybrid vehicle). The other fitted model (Tacoma 1.0) is for an internal combustion engine 2017 Tacoma vehicle. These fitted models are fast to compute, smooth convex functions to facilitate optimization and machine learning and can be open-sourced. Both fitted models are implemented into Flow to be used in optimization as well as in our post-processing data pipeline (see Data Pipeline & Internal Leaderboard section below for more details).

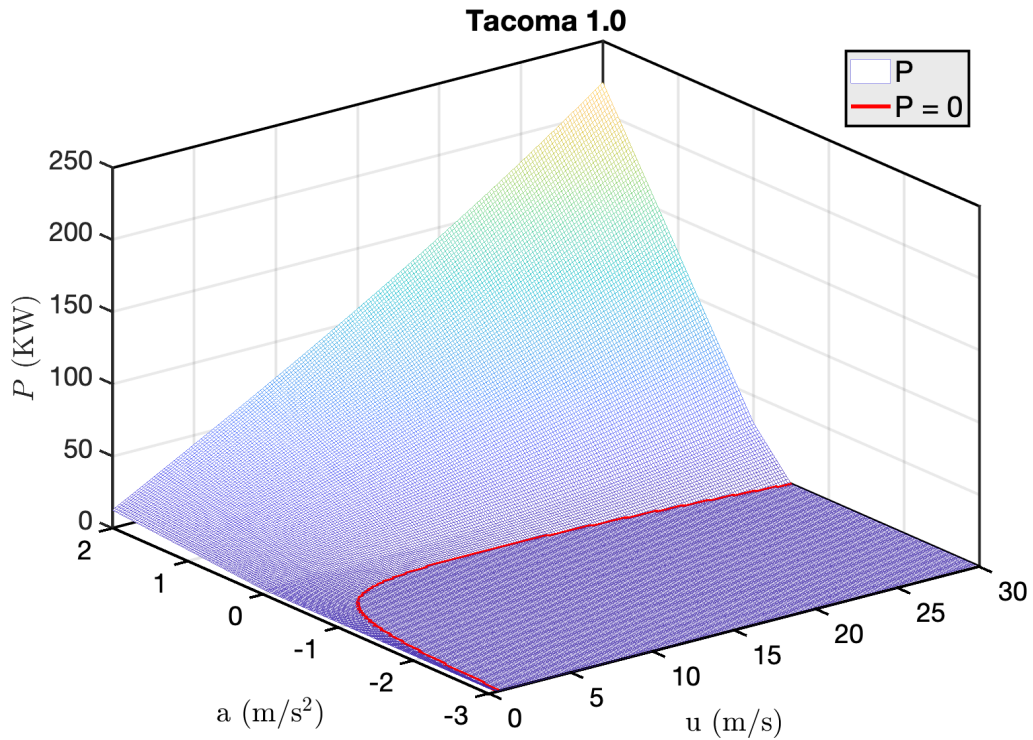
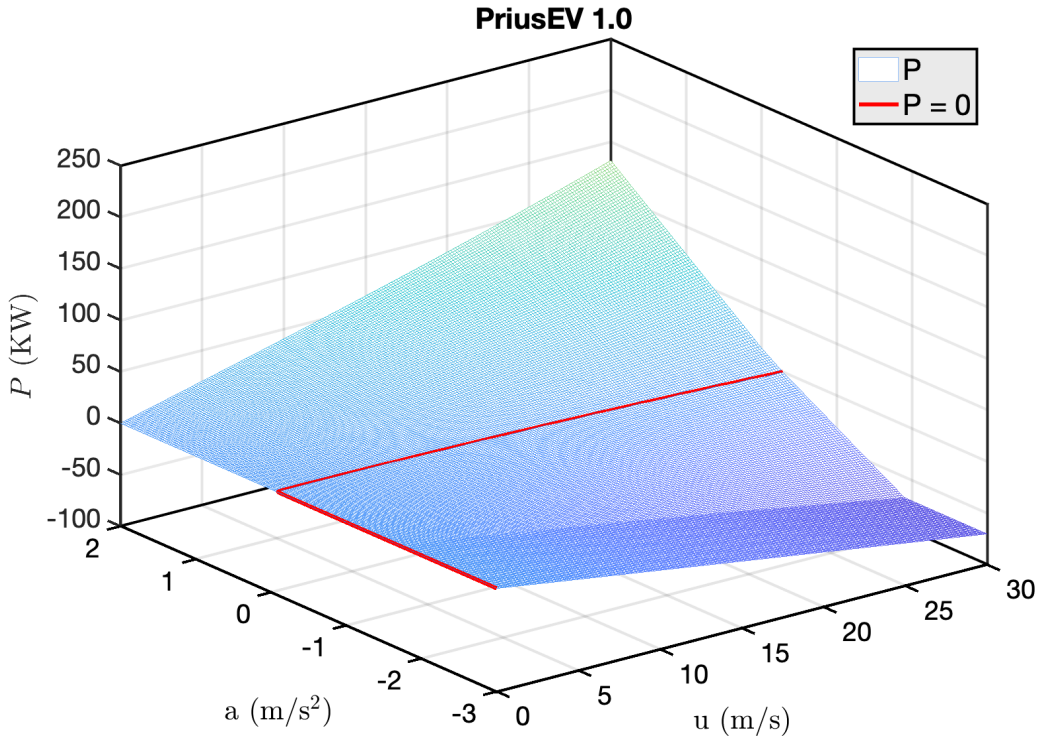


Figure II.1.2.3 Visualization of Both Fitted Simplified Models for Power Consumption as a Function of Instantaneous Vehicle Speed and Acceleration. Left: Priusev 1.0 Model for an Electric Vehicle. Right: Tacoma 1.0 for an Internal Combustion Engine Vehicle

Based on these models, the energy team is actively working with the Reinforcement Learning (RL) subteam on understanding the structural implications of using energy-based objective and reward functions in learning-based optimization. A fundamental insight is that typical optimal-energy functions tend to be much shallower in the speed direction than in the acceleration direction, rendering most off-the-shelf optimization routines inefficient. Ongoing research involves determining suitable proxies that allow for energy to be involved in the optimization, while retaining an effective RL-based methodology, as well as suitable preconditioning techniques to allow for efficient energy optimization.

The fitted simplified models have enabled the team to standardize the evaluation of controller strategies with models for both combustion engine vehicles and electric vehicles. Along these lines, the team is investigating the energy saving potential of wave smoothing in the context of different vehicle types and compositions. In particular, the team has started using Autonomie, a software developed by the Argonne National Laboratory, which encodes detailed models to calculate the fuel and battery consumption for a wide variety of vehicle types and classes given trip trajectories. The energy models in Autonomie are extremely complex, modeling many components of the vehicle (e.g., gas pedal, powertrain, etc.) as well as the driver, and thus they are excessively costly for optimization. To enable the usage by other teams, in the same spirit as the above Tacoma 1.0 and PriusEV 1.0 models, the team is developing a pipeline to systematically build simplified models from an array of Autonomie vehicle models.

ODE/PDE & Mean-Field Models. We designed control strategies in multi-line multi-population microscopic models by using a small number of autonomous vehicles (AVs) (less than 5% penetration rate) to represent Lagrangian control actuators that can smooth stop-and-go waves in multi-lane traffic flow. A multi-lane model is typically composed of two components: longitudinal dynamics for each lane and a lane-change mechanism. The lane-changing mechanism is studied to model conditions at which the regular cars change lanes. Such condition parameters include a safety threshold, incentive to accelerate, and time passed since the last lane change. Lane changes influence stop-and-go waves, and we show that the choice of safety threshold and incentive threshold matter from a modelling point of view, as the resulting behavior could be different for different parameters. This is shown in the figure below of the speed variance of the entire system for different incentive and safety thresholds on the lane-change mechanism (left side). In the experiments of Figure II.1.2.4, speed variance varies from almost 0 m/s to 6 m/s (average speed is around 8 m/s).

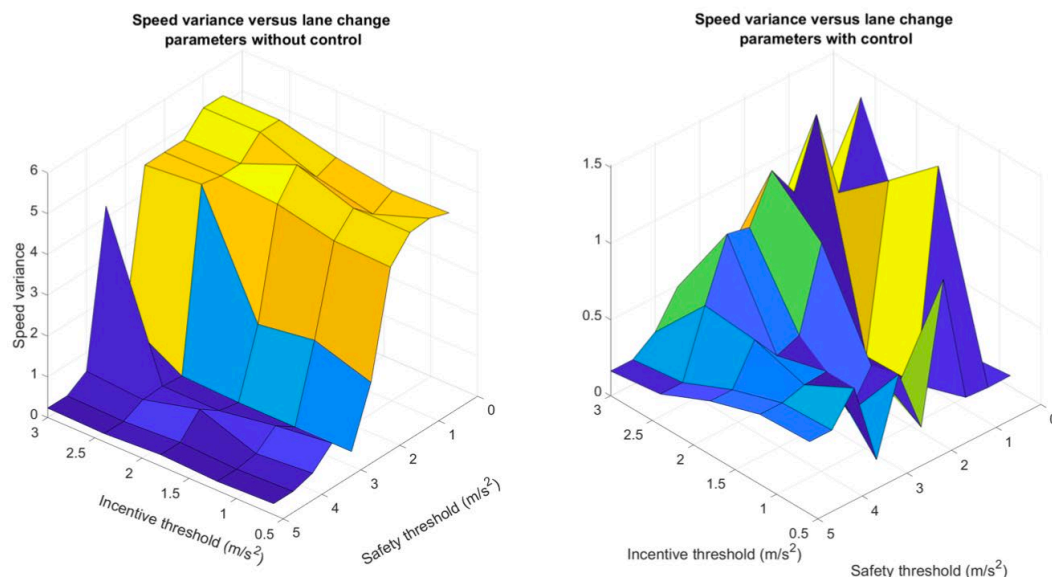


Figure II.1.2.4 Speed Variance for Different Safety and Incentive Thresholds. Left: Without Control, Right: With Control

Using our micro-model we were able to derive and study an effective controller for the AVs. The theory showing the dissipation of waves was derived in a ring-road setting. The numerical experiments were tested on a ring road and on a straight road using an in-house numerical solver (MATLAB language) and ultimately on the test network (Flow/SUMO). Despite the large influence of the lane-change thresholds on the behavior, we showed that for any lane changing threshold, a single AV can be a very effective controller for dissipating stop-and-go waves. This also sets up a good basis to derive a controller for mean field models. We simulated our results over a range of threshold values, where the incentive threshold ranged from 0.5 m/s/s to 3 m/s/s, and the safety threshold ranged from 0 m/s/s to 5 m/s/s.

We also established a macro-model consisting of a PDE coupled to several ODEs by a flux relation. This model represents the interaction between the global traffic flow and the AVs, which are represented as moving bottlenecks. We have shown that this model exhibits stop and go waves.

Finally, we established a new mean-field model that allows us to take the behavior of the well-known and well-studied microscopic models (such as the IDM) to a higher scale. The solution of this mean-field model is a density of cars $q(x,v)$ corresponding to the cars with location x and velocity v . This is obtained by considering the microscopic equations as equations on concentrated distributions that are the individual cars and showing a convergence when the number of cars goes to infinity. Both macro and mean field models are now investigated to design more controller candidates with high efficiency at low penetration rate.

Reinforcement Learning. The Reinforcement Learning team has built a variety of training procedures that we have used to smooth traffic across a few different wave settings. To test the efficacy of our approaches, we first demonstrated that using multi-agent reinforcement learning (MARL) techniques, in particular a variant of proximal policy optimization, we could completely eliminate waves on a straight road segment. We then investigated the scalability of our approach to the I-210, showing that using fully decentralized control and inputs that can easily be obtained via radar, we could learn a controller that provided a ~44% improvement in fuel efficiency at a 10% penetration rate. Time-space diagrams indicating the improvement are shown in Figure II.1.2.5 where a reduction in the number of waves (the slanted black-orange lines) is clearly visible. Furthermore, these algorithms are somewhat robust to penetration rate and network speed, as is visible in Figure II.1.2.6.

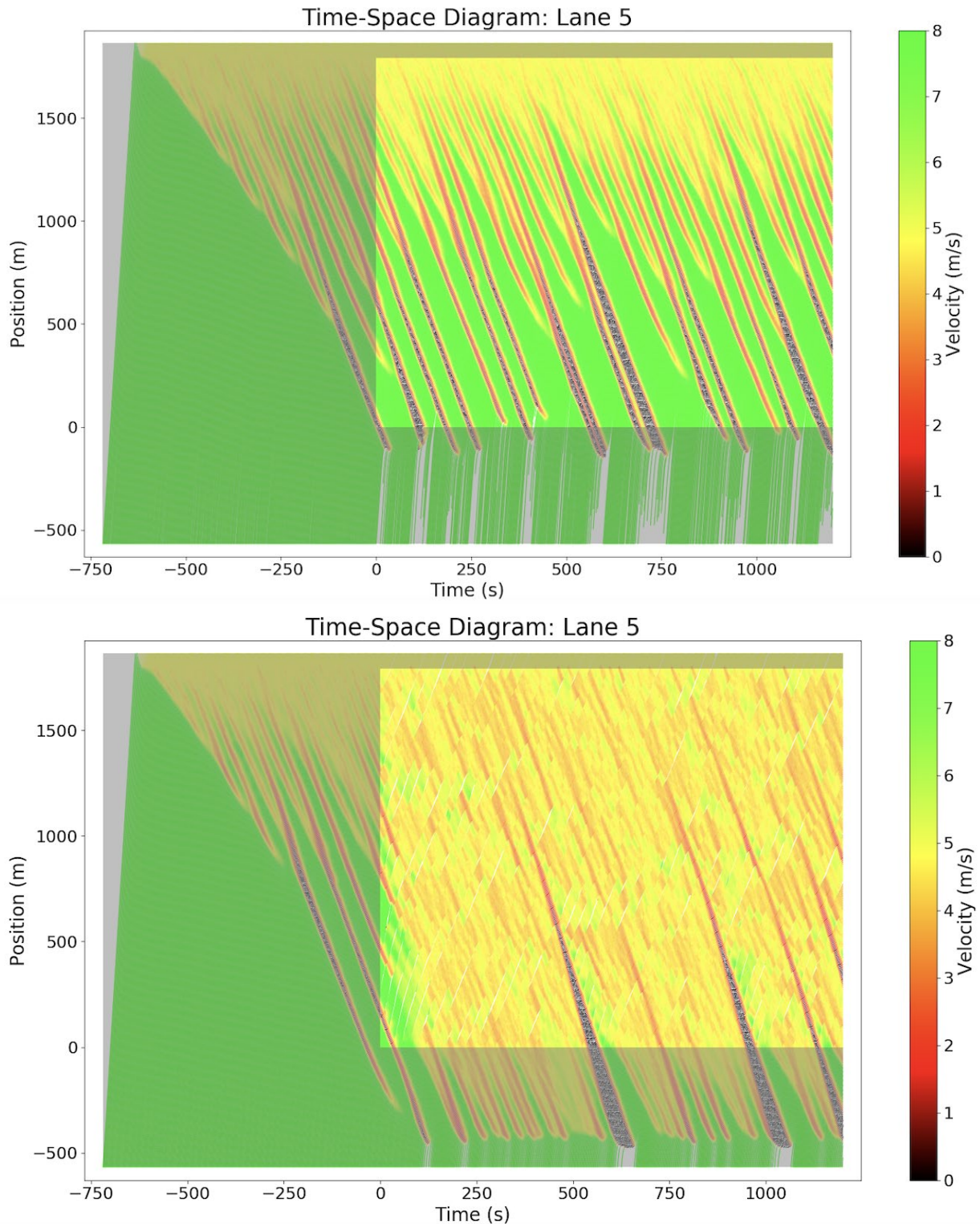


Figure II.1.2.5 (Left) Space-Time Diagram of a Lane in the I-210 in the Absence of Control. The Dark Region Indicates Segments Where Control is Not Applied. Wave Formation is Persistent. (Right) Space-Time Diagram Where 10% of the Vehicles are Controlled Via RL

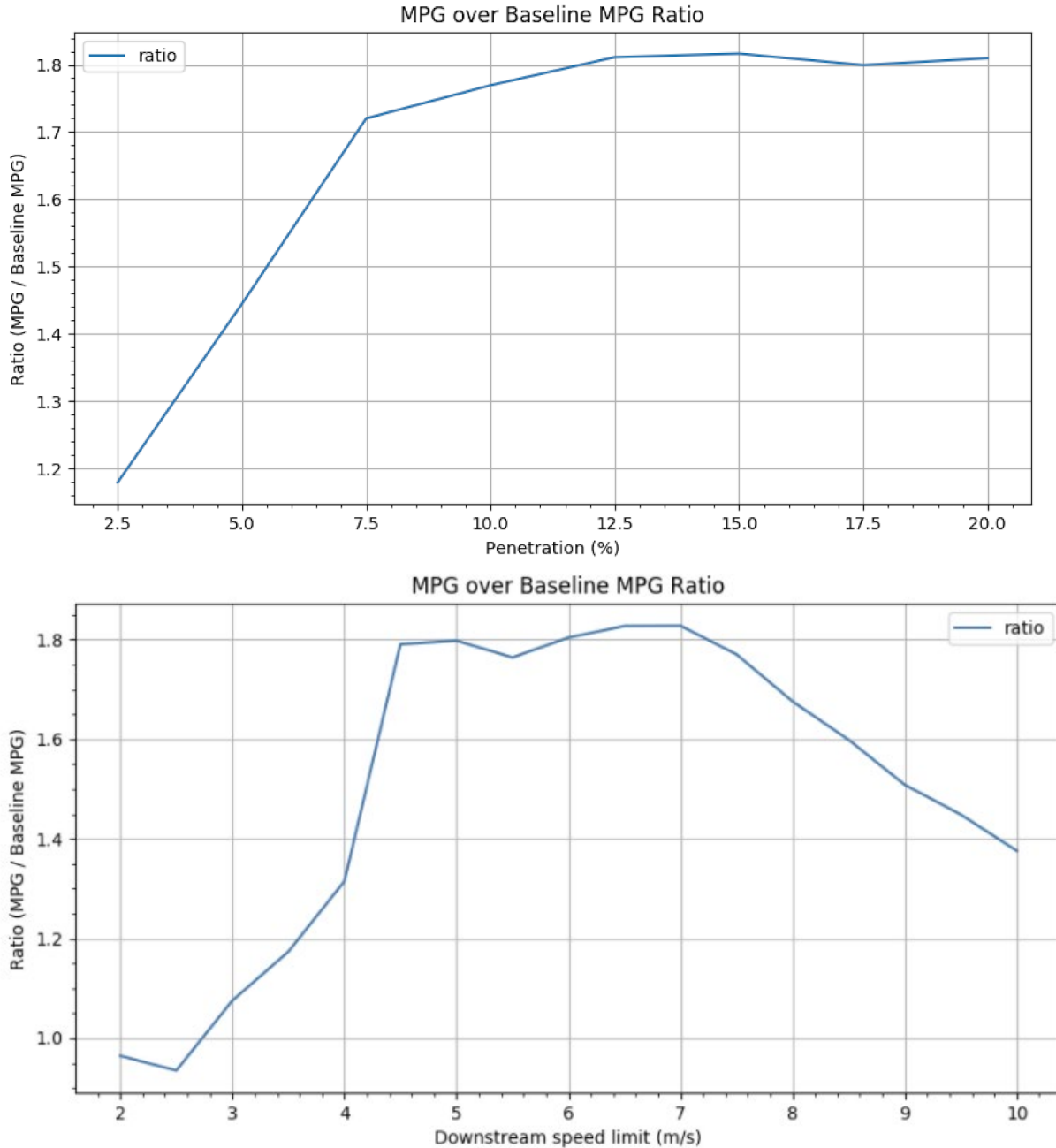


Figure II.1.2.6 (Left) Ratio of System-Level MPG of RL-Controlled to System-Level MPG of the Uncontrolled Case as a Function of Penetration Rate. At All Studied Penetration Rates, We See a Significant Improvement Over the Uncontrolled Case. (Right) Ratio of System-Level MPG of RL-Controlled to System-Level MPG of the Uncontrolled Case as a Function of Max Speed of the Network. At Most Velocities, With the Exception of Speeds Where Cars are Essentially Stopped, We See a Significant Improvement Over the Uncontrolled Case

In addition to studying multi-agent, or decentralized, learning and control methods for traffic regulation via automated vehicles, we are also studying the applicability of single agent, or centralized, methods as well. Under this setting, automated vehicles within a controllable region share local state information to a centralized policy that then assigns desired accelerations to individual vehicles, as seen in Figure II.1.2.7. This approach potentially provides insights on the performative benefits that can arise from enabling communication and cooperation between individual vehicles; however, it serves to complicate the optimization

processes as the growth of the state and action spaces degrade the RL algorithms ability to readily learn and explore via the curse of dimensionality.

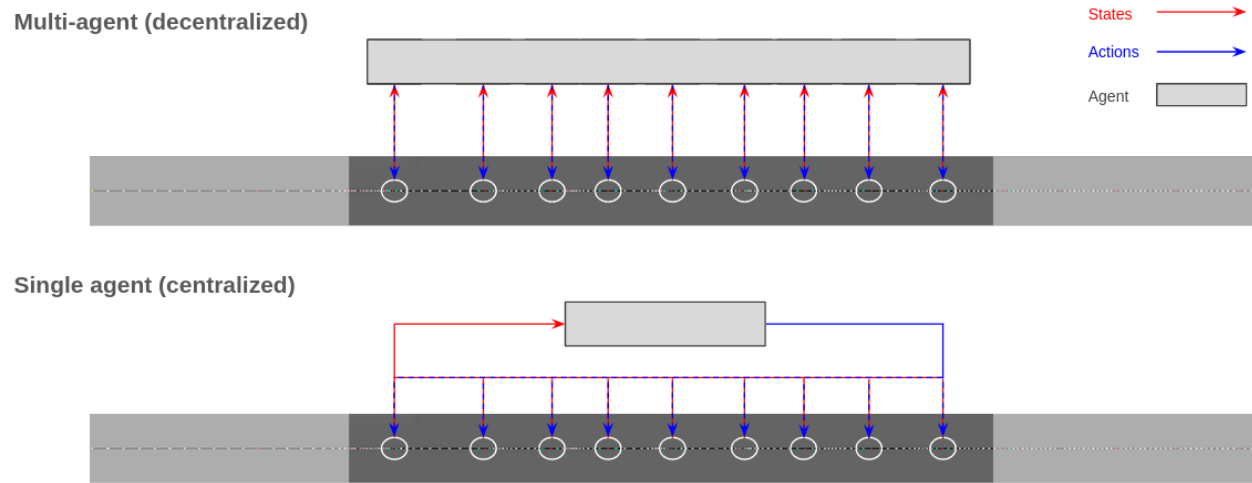


Figure II.1.2.7 Centralized and Decentralized Traffic Control Approaches Currently Being Explored by the RL Team

Under both the centralized and decentralized settings, we have found standard RL and MARL algorithms to be rather slow for the problems we aim to tackle here. For example, the control strategy resulting in the time-space diagrams presented in Figure II.1.2.7 requires millions of interactions with the simulator, or the computational equivalent of running an operation for one week on 32 CPUs. These approaches, as such, hinder progress and development, and motivate the need for more sample efficient techniques. As a result, we are in the process of examining the potential benefits of following methods:

- Advanced multi-agent RL techniques:** While we have primarily focused on a small set of MARL algorithms, there is an immense variety of new algorithms that have recently been studied. We have built a large, open-source library of modern deep MARL algorithms and are in the process of benchmarking these on standard, fast-running MARL benchmarks. The best-performing algorithms will then be tested on the I-210 to see if we can achieve performance gains over our current set of algorithms. In the process, we should be able to establish a sense of order on the relative performance of these algorithms which would constitute a useful contribution to the multi-agent research community.
- Structured exploration & hierarchical learning:** In addition to comparative performance of various multi-agent algorithms, we are examining the benefits of structured exploration methods for improving upon the performance and sample efficiency of standard MARL techniques within the context of problems in question. We will focus primarily on two forms of exploration: 1) intrinsic motivation, whereby external reward signals are augmented within the optimization procedure to produce a desired exploratory behavior (e.g., visiting a wide variety of states), and 2) hierarchical reinforcement learning, whereby decision-making and actuation are temporally abstracted to allow to more efficient exploration across large time horizons. For the latter, we have demonstrated that introducing cooperative constraints between sub-policies within a hierarchy can allow such techniques to learn very strong traffic flow control strategies using as few as 1 million interactions with the environment for relatively smaller scale tasks than we hope to explore here. Moving forward, we hope to determine whether the coupling of intrinsic motivation and hierarchical learning techniques can lead to equally as impressive control strategies in large-scale networks such as the I-210 or I-24.

- **Offline reinforcement learning:** Offline reinforcement learning focuses on extracting a controller from a fixed batch of data. As such, it bypasses the need for a simulator or even the need to construct a calibrated network. If successful, this would allow us to essentially skip the slowdown being caused by long simulation times. We are performing initial validation of the efficacy of offline reinforcement learning in the setting where data comes entirely from human driving trajectories. Our minimal viable test, whether we could extract an optimal policy from trajectories of simulated human driving has been successful; we are now proceeding to see if we can extract similar traffic smoothing controllers from publicly available human driving data.

Safety. To build safety into the development and evaluation of our autonomous vehicle controllers, we seek to establish a method of validating safety via the use of reachability analysis. Our analysis should produce safe sets that represent a set of states from which, when evolved forward for all time, our controller's action will not result in a collision. The safety is dependent on maneuvers of the leading vehicle and the controlled vehicle. Under the reachability framework, we will require our safe sets to be invariant, which will guarantee that any trajectory of the system that is within the set is able to remain in the set under any possible inputs and disturbances. To solve the reachability problem, we formulate the problem as a two-player game with a leading vehicle and subject (following) vehicle. The two-player game is an optimization problem optimizing over control input of both vehicles. The cost function of the optimization problem is the minimum distance between two vehicles at all times. The subject vehicle is governed by a controller, while the leading vehicle's input is some input that minimizes the cost function. Both vehicles are subject to input acceleration upper bound and lower bounds. We assume that the acceleration of the leading vehicle can be controlled directly, and the subject vehicle acceleration response is limited by vehicle dynamics. We also assume that both vehicles cannot drive backwards, and a speed limit is observed. The safety set is determined as a positive value set of the optimal value function. The safe set of the FollowerStopper controller is evaluated. Figure II.1.2.8 shows the safe set of the FollowerStopper.

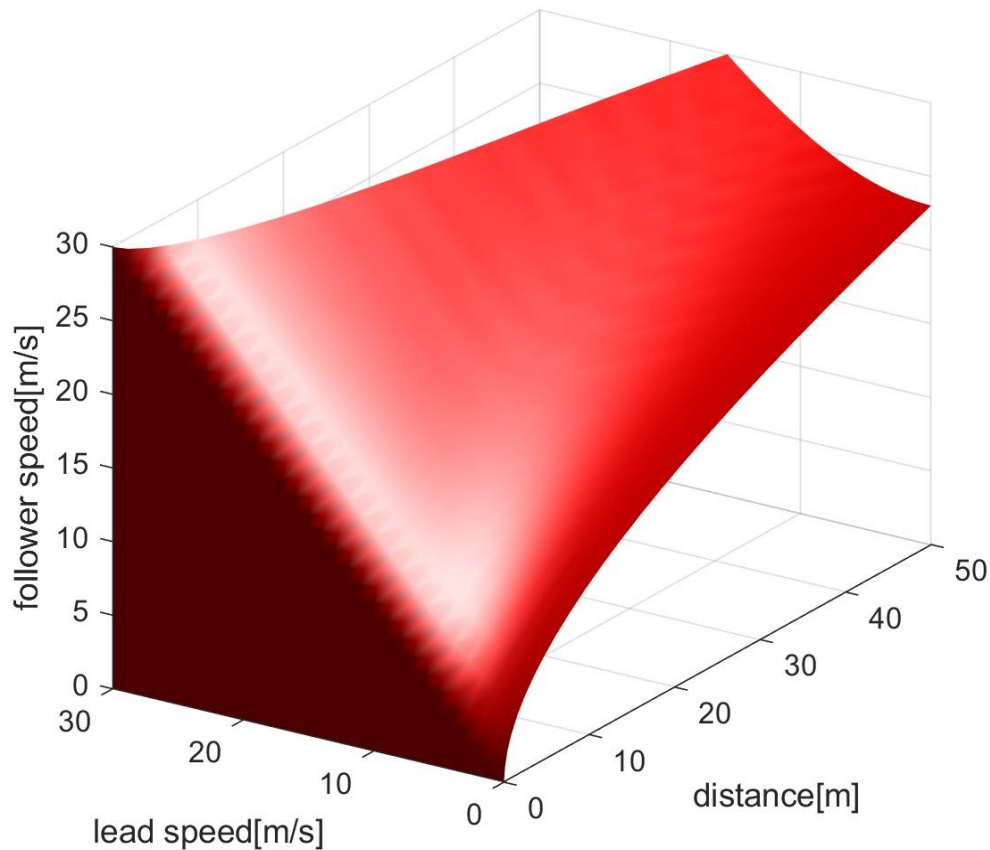


Figure II.1.2.8 Safe Set of the Followerstopper. The Safe Set is Defined in the Domain Where *Distance* is Positive, *Lead Speed* is Between 0 and 30, and *Follower Speed* is Between 0 and 30. The Red Surface Represents the Boundary of the Safety Set. The Safe Set is the Set of States Bounded by the Surface (I.E., All States Below the Surface)

Data Pipeline & Internal Leaderboard. Since we have multiple individuals from multiple sub-teams developing vehicle controllers, we have set up a data pipeline to standardize all post-processing evaluations of those controllers. Any analysis or metric that other subteams wish to standardize is implemented via this subteam. Separating these post-processing tasks from the simulations allows for quick re-computation of any new or updated analysis without having to re-run all old simulations.

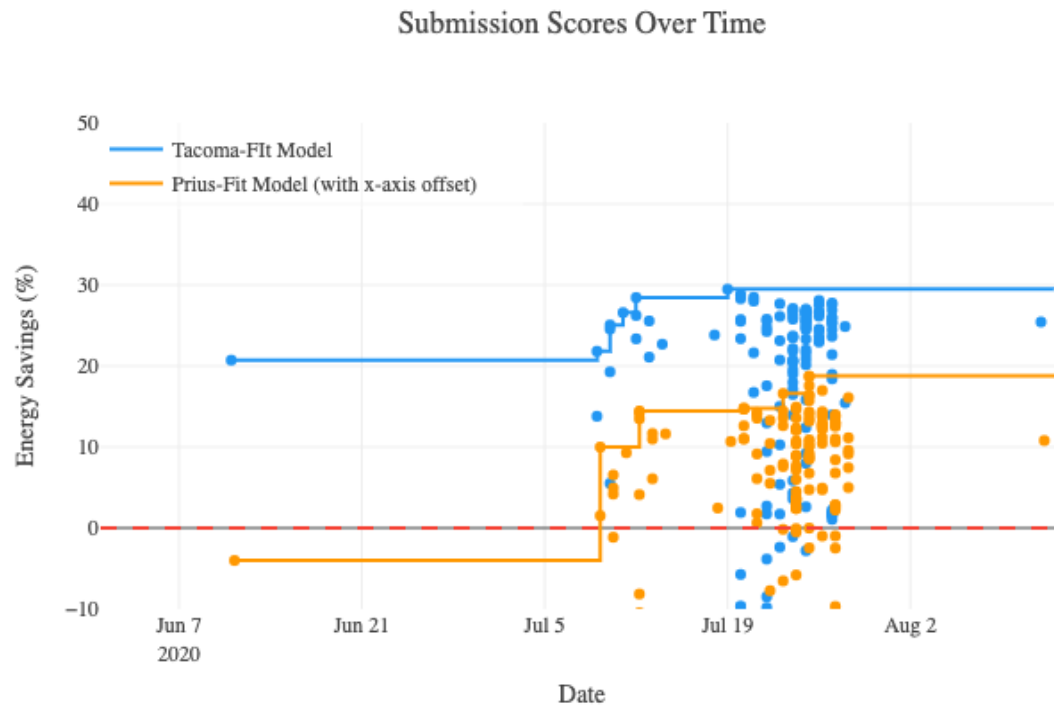


Figure II.1.2.9 A Timeline of Control Strategy Scores. Each Dot Represents a Control Strategy Score Assuming 100% Toyota Tacomas (Blue) and 100% Toyota Prius Evs (Orange) on the Road. Scores are Plotted as Percentage Improvement Relative to the Baseline (Red), and Solid Blue and Orange Lines to Show the Best Scores to Date

The results of the post-processing are then served up onto an internally facing, password protected website (see screenshot above). Every submission is displayed graphically with its energy savings score evaluated via two energy models (Tacoma 1.0 and PriusEV 1.0); they are also tabulated to display high-level metrics (e.g., system-level fuel economy using both models, inflow rate, etc.). Moreover, any row of the leaderboard table can be toggled open to display plots from various drill-down analyses to help understand the pros and cons of each submitted strategy.

Hardware. We have developed a custom library in C++ called libpanda to interface with vehicle's controller area network through OBD ports for CAN data acquisition in real-time. Libpanda is a multi-threaded C++ based library for custom Panda interface applications using the observer-based software design pattern (i.e., callbacks). Also featured in the software area are pre-made data recording utilities, simple data visualizers, startup services, and network handling services. The utilities save CSV-formatted data for downstream analysis by our data-analytic tool strym written in python for further downstream analysis of acquired data. Strym uses DBC files and CSV-formatted CAN message files as input to decode the message to produce time-series data representing specific signals, such as speed, acceleration, brake, lead distance, etc. LibPanda can be seen as a part of the stack in Figure II.1.2.10.

We created the CAN Coach, which is a system that continuously feeds time gap sensor information from the CAN bus back to the driver in near real time. Three sets of preliminary experiments are conducted in which the study vehicle follows a lead vehicle driving a specified driving profile to assess the potential of the CAN Coach to modify driver behavior. The experiments consider Normal driving (the driver is given no prompt and no feedback), Instructed driving (driver is given a prompt to drive at a two second time gap, but is not given any feedback from the CAN Coach), and Coached driving (two second prompt and CAN Coach feedback). The mean time gap errors from the 2 second target are 0.39s (Normal Driving), 0.09s (Instructed Driving), and

0.01s (Coached Driving). The standard deviation of the time gap error with the CAN Coach reduced by 72% and 68% from Normal Driving and Instructed Driving, respectively. Given this reduction of mean and standard deviation of the time gap error, we conclude that it is possible to “coach” drivers using only data from the CAN. Below shows how CAN Coach fits in the loop:

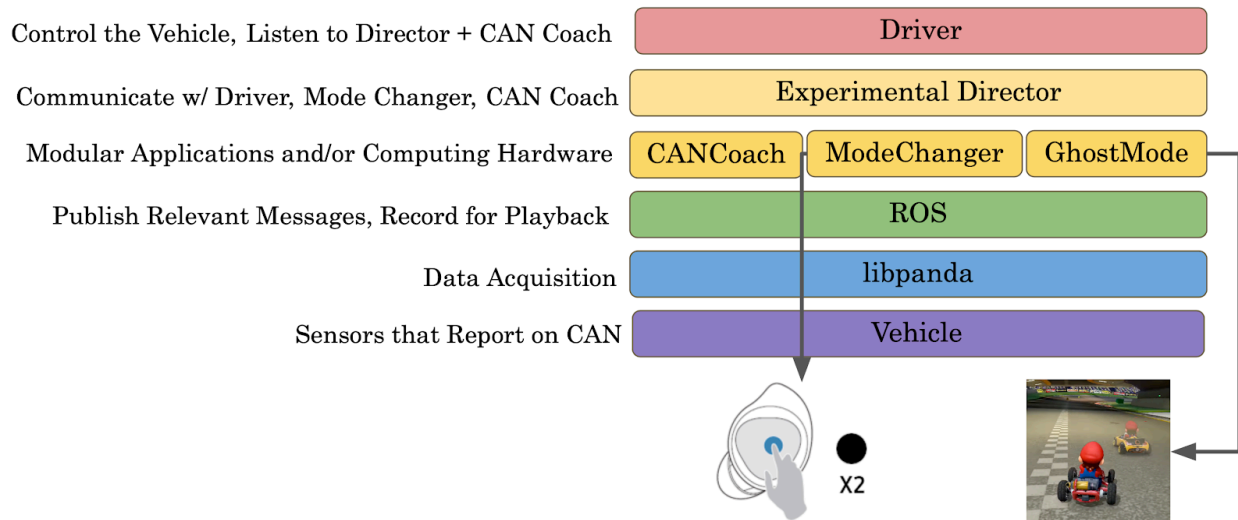


Figure II.1.2.10 A Diagram Showing Where Libpanda, ROS, and the CAN Coach Fit in the Hardware/Software Stack

In early July 2020, two PIs were near enough one another to orchestrate our first minitest: Minitest 1. Because the test involved two drivers who were in separate vehicles, it permitted us to use radio communications in lieu of person-to-person communications, and thus follow safety guidelines for social distancing.

The goal of Minitest 1 was to gather synchronized data from stop-and-go traffic conditions, explore the timescales involved in starting and stopping a test, confirm approaches for communication between vehicles, and validate the robustness of the automation we are using for data gathering from libpanda and dashcams. Postprocessing of minitest data gives us a way to test whether we can re-visualize the data in our system simulators, for later validation work to check the safety of the controllers that are developed through the theoretical and reinforcement learning-based work.

Two videos linked provide (i) a replay of the minitest, which took place on July 8, 2020, and which shows the video sets from two vehicles as well as the interesting events that took place: <https://youtu.be/pp4O0aOKy1g>, and (ii) the replay of the data gathered by the Toyota vehicle, which was extracted from the libpanda installs: https://youtu.be/bwqn2_ZLWKS.

Conclusions

As of July, we are now able to make systematic assessments of our algorithms’ energy saving capabilities in congested traffic simulations. We have a pair of energy models “in production” that we can use to compute fuel economy (aka “mpg”) and energy consumption (i.e., energy consumed normalized by distance traversed). We use fuel economy as a sanity check but compute energy savings using the energy consumption metric (evaluated with two energy models from different powertrains). **We can confirm that many of our best controllers have surpassed our Year 1 Go/No Go milestone of 10% energy savings in simulation at moderate penetration rates in traffic regimes for which strong traffic waves are present.** Future steps include: (1) calibration of the simulations not only to macroscopic flow quantities but also individual vehicle dynamics; (2) add effects caused by on-ramps, off-ramps, or road grade; (3) test the controllers against larger ensembles of simulations with heterogeneous flow states and vehicle composition.

Key Publications

Published:

1. Derek Gloude-mans, William Barbour, Nikki Gloude-mans, Matthew Neuendorf, Brad Freeze, Said ElSaid, Dan Work, “Interstate-24 MOTION: Closing the Loop on Smart Mobility,” Workshop on Design Automation for CPS and IoT (DESTION 2020) Co-located with IEEE/ACM CPS-IoT WEEK 2020, April 21, 2020, Sydney, Australia (virtual).
2. Yanbing Wang, Matt Nice, George Gunter, Maria Laura Delle Monache, & Dan Work, “Online Parameter Estimation Methods for Adaptive Cruise Control Systems. *IEEE Transactions on Intelligent Vehicles*, 2020 (in press).

Submitted:

1. Fangyu Wu, Guanhua Wang, Siyuan Zhuang, Kehan Wang, Alexander Keimer, Ion Stoica, Alexandre Bayen, “Provably Efficient, Stable, and Robust Model Predictive Control with Augmented Control Memory”, Conference for Robot Learning 2021.
2. Sadman-Ahmed Shanto, George Gunter, Rabie Ramadan, Benjamin Seibold, Dan Work, “Challenges of Microsimulation Calibration with Traffic Waves using Aggregate Measurements”, Transportation Research Board Annual Meeting 2020.
3. Nicolas Kardous, Amaury Hayat, Sean McQuade, Xiaoqian Gong, Sydney Truong, Paige Arnold, Alexandre Bayen, Benedetto Piccoli, “A rigorous multi-population multi-lane hybrid traffic model and its mean-field limit for dissipation of waves via autonomous vehicles”, Transportation Research Board Annual Meeting 2020.
4. Xiaoqian Gong, Benedetto Piccoli, Giuseppe Visconti, "Mean-field limit of a hybrid system for multi-lane multi-class traffic", SIAM Journal on Control and Optimization.
5. Felisia Angela Chiarello, Benedetto Piccoli, Andrea Tosin, "Multiscale control of generic second order traffic models by driver-assist vehicles", SIAM Multiscale Modeling and Simulations.
6. Eugene Vinitzky, Yuqing Du, Kanaad Parvate, Kathy Jang, Peter Abbeel, Alexandre Bayen, “Robust reinforcement learning using adversarial populations”, Conference on Robot Learning.
7. Matthew Nice, Dan Work, “CAN Coach: Continuous CAN-based Feedback to Change Driver Behavior”, Transportation Research Board Annual Meeting 2020.

References

1. Liang, Chi-Ying and Huei Peng, “Optimal adaptive cruise control with guaranteed string stability.” *Vehicle System Dynamics*, 32, no. 4-5 (1999): 313–330.
2. Stern, Raphael E., Shumo Cui, Maria Laura Delle Monache, Rahul Bhadani, Matt Bunting, Miles Churchill, Nathaniel Hamilton, R’mani Haulcy, Hannah Pohlmann, Fangyu Wu, Benedetto Piccoli, Benjamin Seibold, Jonathan Sprinkle, Daniel B. Work, “Dissipation of stop-and-go waves via control of autonomous vehicles: Field experiments.” *Transportation Research Part C*, 89 (2018): 205–221.

Acknowledgements

This material is based upon work supported by the U.S. Department of Energy’s Office of Energy Efficiency and Renewable Energy (EERE) award number CID DE-EE0008872. The views expressed herein do not necessarily represent the views of the U.S. Department of Energy or the United States Government.

The project PIs would like to thank Senior Engineering Manager and Project Coordinator, Dr. Jonathan Lee, for his leadership and effort in assembling this report.

CIRCLES would like to thank Dave Anderson and Brett Aristegui for their technical and project support.

Also, thanks to each of our campus deputies—Dr. William Barbour, Dr. Matt Bunting, Dr. Amaury Hayat, Dr. Sean McQuade, and Dr. Rabie Ramadan for their project management and leadership. Thanks to Dr. Ken Butts and Toyota, Mr. Brad Freeze and the Traffic Operations Division at Tennessee Department of Transportation, and Professor Craig Philip for the invaluable partnership.

Finally, the team wishes to thank all the campus administrators—Timothy Funk, Peter Gudlewski, Jason Holmes, Kristy Kruse, Jack Long, Sara Maddox, Paul Martinez, Camie Morrison, Laman Sadaghiani, Dannielle Sesay, Missy Sheehy, Wendy Turner, Elysa Weiss—for everything that they do behind the scenes

II.1.3 Validating Connected, Automated, and Electric Vehicle Models and Simulation (American Center for Mobility)

Reuben Sarkar, Principal Investigator

American Center for Mobility
2701 Airport Drive
Ypsilanti, MI 48198
Email: reuben.sarkar@acmwillowrun.org

David Anderson, DOE Program Manager

U.S. Department of Energy
Email: david.anderson@ee.doe.gov

Erin Boyd, DOE Technology Manager

U.S. Department of Energy
Email: erin.boyd@ee.doe.gov

Start Date: October 1, 2019

End Date: June 30, 2022

Project Funding: \$7,628,923

DOE share: \$6,103,138

Non-DOE share: \$1,525,785

Project Introduction

The American Center for Mobility (ACM) and its project partners—Michigan Technological University, Michigan Technological Research Institute, Oak Ridge National Laboratory (ORNL), and Argonne National Laboratory (ANL)—are engaged in a collaboration to conduct research that compares modelling of the impact on energy efficiency of vehicles using connected, autonomous, and electric technologies with empirical measurements made on-road with vehicles in controlled track environment. Control algorithms designed to improve energy efficiency have been evaluated in simulation but require supporting measurements in real world vehicle tests to validate results. The project comprises the translation of laboratory algorithms from modeling & simulation into vehicle controls in highly automated vehicle experimental platforms that are instrumented for conducting designed experiments in a controlled test track environment for generation of data that can be used to validate and iteratively refine laboratory models. This report documents the progress made in year one of this two-year project.

Objectives

The objective of this project is to test connected, automated, and electric vehicles to support updates to and validation of modeling and simulation tools.

Approach

Researchers under this collaboration are working to identify cases and ensure the analytical models are fully understood and capable of being tested. Multi-vehicle, controlled track testing will be conducted to validate the initial assumptions, programming, and expected benefits used in national laboratory simulated environments and related studies. Highly automated vehicles will be built and instrumented for collection of high-fidelity energy usage and communication information and developed to enable the rapid implementation and assessment of proposed multi- and individual-vehicle control strategies. Instrumented intersections and corridors in addition to the instrumented research vehicles mentioned above, will be used to predict the performance of various vehicle and fleet control algorithms and their effect on public behavior and transportation system performance. The researchers have selected scenarios where models with traffic can be safely and repeatably re-created in a controlled test track environment. To satisfy these requirements, tests are being designed in three categories: speed harmonization, highway mergers, and intersection transit. Data from the experiments will be fed back iteratively to models and used to validate or modify assumptions, as well as support continued model development by identifying key real-world implementation challenges.

There are five key milestones related to this overall effort:

1. Integrate national laboratory model criteria – Key data elements and their definitions to be tested and agreed upon with National Laboratories.
2. Design Experiments – Safe and repeatable experiments that estimate the energy consumption for comparison with models
3. Test Vehicle Setup – Highly automated vehicle experimental platforms with open-controller and high-fidelity instrumentation ready for testing.
4. Conduct Experiments – Orchestrate real and virtual participants in vehicle tests on track, and record measurements along with ground truth information for analysis.
5. Experiment complete – Planned experimental testing is complete and data elements meet defined file formats

Year 1 efforts have focused on milestones 1, 2 and 3, with 4, and 5 taking place in year 2. This report covers the progress for year 1 efforts.

Test Vehicle Set Up

The first major task is development and integration of the interfaces and controllers in vehicles in partnership with suppliers. A total of five vehicles, one Pacifica with an internal combustion engine (ICE), two Chevy Volt Plug-in Hybrid Electric Vehicles (PHEVs) and two Chevy Bolt Battery Electric Vehicles (BEVs) are being built for this program each equipped with a range of sensor packages, dedicated short range communications (DSRC) radios for V2V and V2I and drive by wire (DBW) systems for highly automated driving. Each is also equipped with an open-controller and is fully instrumented for testing. Three vehicles (2 Volts and 1 Bolt) have been completed and have undergone significant validation and testing for baselining and development of controls needed in preparation for the integration of the Lab’s algorithms. Two other vehicles are nearing completion (2nd Bolt and Pacifica). These have the additional Autoware ROS based automation systems.

Integrate National Laboratory Model Criteria

National laboratory researchers provided an in-depth description of their algorithms and completed a standardized specification document that detailed basic information and features of their models, parameters, signals of interest, and proposed tests. A summary document was compiled that compared the testing and data needs as well as the specification documents of each national laboratory to find common requirements between the project participants. In addition, the testing proposals from each lab were examined in detail to determine the requirements that were currently satisfied by the ACM test infrastructure and what capabilities needed to be developed by the project team.

Demonstration and Validation of Controls (ORNL)

ORNL initial efforts consider an algorithm for efficient merging [\[1\]](#), which has been adapted for speed harmonization. The algorithm has been implemented in simulation using VIRES Virtual Test Drive. Predicted results from simulation will be compared to measurements of energy consumption on test vehicles at ACM. The algorithm coordinates multiple vehicles through a centralized control algorithm to improve energy efficiency, while avoiding collisions between vehicles. Simulations suggest the algorithm can reduce the fuel consumption and overall travel times. Test vehicles need to be instrumented to communicate with a central controller via a Dedicated Short Range Communications (DSRC) service. Multiple cars are being developed to operate as autonomous connected vehicles as discussed earlier in the section with ability to communicate through DSRC radios for V2V and V2I.

Controls in the ORNL configuration include a centralized controller whereas the ANL configuration discussed later in this section involves on-vehicle controllers. In the centralized controller, vehicle movement is controlled, and commands are sent to the vehicle via DSRC. For the scenarios for on-vehicle controllers the control and optimization are integrated into an in-vehicle controller. In both cases, the labs algorithm work through a dSPACE MicroAutobox (MABx). The MABx has interfaces to DSRC, additional sensing, vehicle CAN networks and ability to control the vehicle through either an integrated Drive-by-Wire system controlling accelerator pedal, brake pedal and steering, or through an Autoware ROS L4/L5 system that does higher levels of vehicle automation.

ACM is equipped with DSRC Roadside Units (RSU) to support vehicle to infrastructure (V2I) communications. This infrastructure allows a main computer running at the facility to communicate with vehicle on the test track through the network of RSUs. Initial tests are underway to characterize the delays inherent in the hardware and software being used to relay vehicle locations and speeds through Basic Safety Messages (BSM) to the centralized controller, as well as, the messages transmitted by the centralized controller, requesting adjustments in lateral control of each vehicle.

In anticipation of tests that may press the limits of the number of vehicles, or complexity of traffic, which can be safely and repeatably operated for tests, the researchers are developing hardware and software to inject virtual vehicles into the tests through the V2I network. The virtual vehicles will operate in simulation, on a virtual test track modeled from ACM specific track segments, e.g., the highway loop with ramps. The simulation will relay the BSMs of the virtual vehicles through the V2I network and receive positions of real vehicles to be mirrored in the simulation.

Demonstration and Validation of Controls (ANL)

Researchers at ANL have developed eco-driving control algorithms for Connected and Automated Vehicles (CAVs) [2],[3],[4] and demonstrated up to 20% energy savings [5] in simulations performed in ANL's RoadRunner [6]. An eco-driving CAV adjusts its speed for maximum energy-efficiency using information from sensors, V2X communications and road preview from digital maps. As part of this collaboration, ANL controls will be implemented in ACM/MTU vehicles and demonstrated through tests on track with real vehicles. ANL controls will be installed on each vehicle MABx, and will command the accelerator and brake pedal positions (APP/BPP). The demonstration will focus on robustness in a real-world setting, verification that the controls work as planned, and validation of the energy savings demonstrated in simulation.

The focus for ANL in FY20 was:

- Testing of the vehicles (Pacifica and Bolt) on a chassis dynamometer for powertrain characterization and energy consumption modeling.
- Primary validation of Autonomie energy models for these vehicles, and integration within the RoadRunner simulation environment.
- Adaption and update of the eco-driving controllers for implementation to test vehicles.
- Development of test plans and processes to generate a virtual road model to be used on track.

Results

Vehicle Test Set-up

Vehicle Dynamics Baselineing (MTU)

Verification and tuning of the Volts and Bolts DBW system have been done at ACM. Testing of direct accelerator and brake pedal show full dynamic control without significant latency. Further testing of speed control has shown the ability to perform vehicle dynamics control from 0 – 45 mph with control of acceleration and jerk limits. Testing of vehicle dynamics has been completed on the MTU Volts and Bolts with

the MABx / DBW control system and control system and vehicle latency and dynamics fully characterized for the Bolt with similar analysis nearing completion on Volt. Location based speed control with GNSS/RTK input and closed looped velocity control has been demonstrated on the ACM Highway Loop with the Volt and Bolt. The system has been tuned to match human driving, reduce excessive acceleration and jerk and repeatably stop at virtual stop-signs and stop-lights.

Results from the vehicle dynamics baselining for the Bolt with MABx to DBW control are shown in Figure II.1.3.1 for a step input from 0 to 30% accelerator pedal input. Characterization of latency and dynamics of the entire control, actuation, and vehicle have been characterized and modelled over a wide range of inputs. The results show the MABx/DBW system to provide full vehicle longitudinal control without significant latency (<50ms). A dynamics model has been developed and shared with ANL to enable simulation of the vehicle for their code development for release and model integration in vehicle. Dynamics characterization and baselining in nearly completion on the Volt and will start on the Pacifica next quarter.

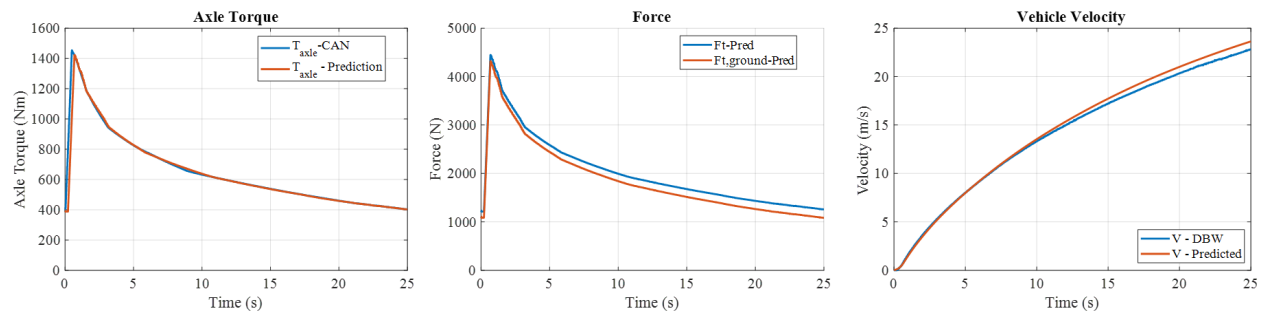


Figure II.1.3.1 Results Showing a Dynamic Test on the Bolt for a 0-30% APP Input with Comparisons of the Vehicle Dynamics Prediction/Model

Testing functionality of the navigation / location-based speed control on the 3.7km ACM highway loop with both the Volt and Bolt have been completed as shown in Figure II.1.3.2. Vehicle position is determined from the high precision GNSS/RTK via the ACM base station. The vehicle position is used as the index to a preloaded location base speed target. The sample includes seven virtual stop signs and virtual lights. The dynamic speed target is then feed from the MABx to DBW closed loop velocity control. Testing validates several functions required for the ORNL and ANL work. For ORNL as discussed above, the speed target will be generated by the central controller communicated via DSRCs via BSMs. For ANL, the MAP will be preloaded with vehicle speed limits and virtual stop-signs and lights. This information will be supplied to the ANL ECO-Driving control algorithm and the ANL control/optimization will control vehicle dynamics by direct actuation of accelerator and brake pedal inputs.

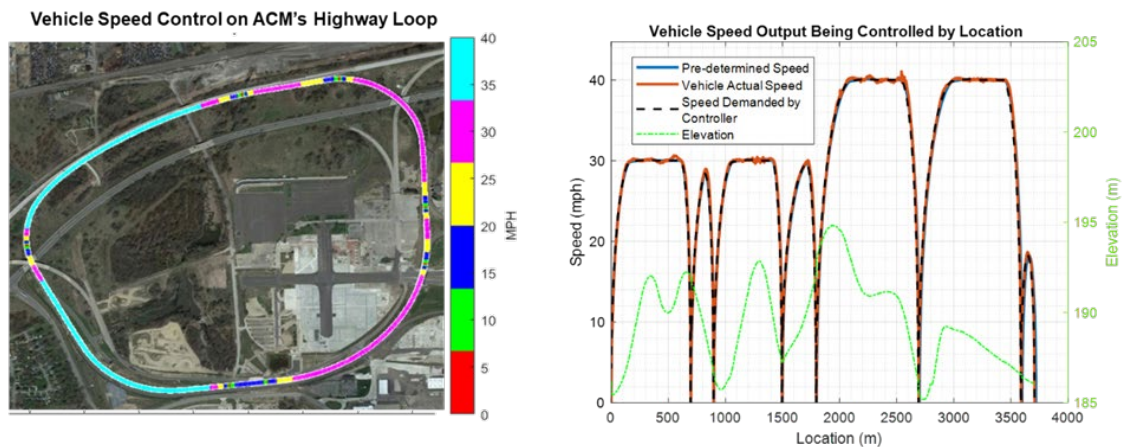


Figure II.1.3.2 Results Showing Testing and Demonstration of Navigation-Based Speed Control on the ACM Highway Loop with a GM Volt

Integrate National Laboratory Model Criteria

Demonstration and Validation of Controls (ORNL)

C++ and MATLAB code of ORNL’s merging coordination and speed harmonization algorithms have been shared with ACM via an ORNL internal project GitLab, along with flowcharts and lists of inputs/outputs of each algorithm. To evaluate complex traffic scenarios with many vehicles, the ORNL algorithms will be implemented in a mixed reality simulation fashion, as illustrated by Figure II.1.3.3. Therefore, in addition to actual test vehicles on ACM’s test track, virtual vehicles will be simulated on a high-fidelity digital twin of the ACM test track in the Virtual Test Drive (VTD) software. The virtual vehicles and test vehicles will share information through Roadside Units (RSUs) utilizing Dedicated Short-Range Communications (DSRC) adhering to the SAE J2735 protocol. Based on real-time vehicle information from virtual and actual vehicles, ORNL’s algorithms are implemented in a centralized controller which determines the speed trajectory for all vehicles within a predefined control zone. ORNL’s algorithms include a “coordinator” that coordinates the vehicle arrival sequence at the end of the control zone, and an “optimizer” that optimizes the desired speed for CAVs. The “coordinator” is critical for the merging and intersection scenarios so that vehicles coming from different lanes can be coordinated to improve energy efficiency.

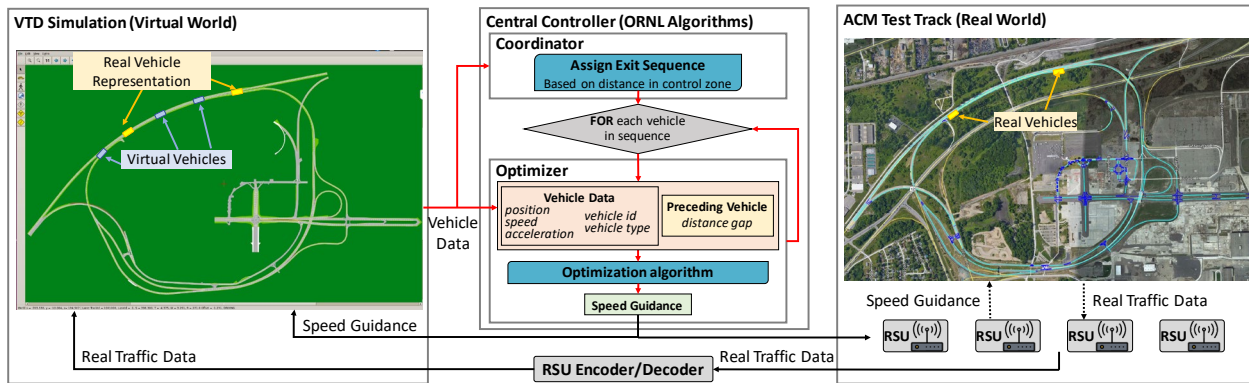


Figure II.1.3.3 Architecture of the ORNL Algorithms Implemented in Mixed Reality Simulation

Based on the mixed reality simulation architecture, ORNL created an I/O diagram that tracked the data flow through the simulation, ACM infrastructure, and test vehicles. This I/O diagram tracked the required signals for the centralized controller algorithm, sources and destinations for each signal, modifications made at each interface, engineering units as well as data type and size throughout the architecture. Additionally, ORNL have imported the high-fidelity ACM test track model into VTD. The centralized controller has been implemented in VTD to integrate the speed harmonization algorithm in the mixed reality simulation architecture. The necessary software interfaces have been developed for the centralized controller to obtain vehicle data from the virtual world and send out speed guidance. The speed harmonization algorithm is currently under evaluation and preparation for experimental validation. Since the centralized controller can be simulated entirely with virtual traffic, it will be used for comparison to better emphasize real-world traffic impacts. Figure II.1.3.4 below illustrates the speed harmonization implementation in VTD: subplot a) shows the overview of the test scenario; subplot b) is the 3D visualization of the virtual ACM test track and virtual vehicles; subplot c) shows the main GUI of VTD; subplot d) shows the execution of the centralized controller and displays the controller’s outputs (speed guidance).

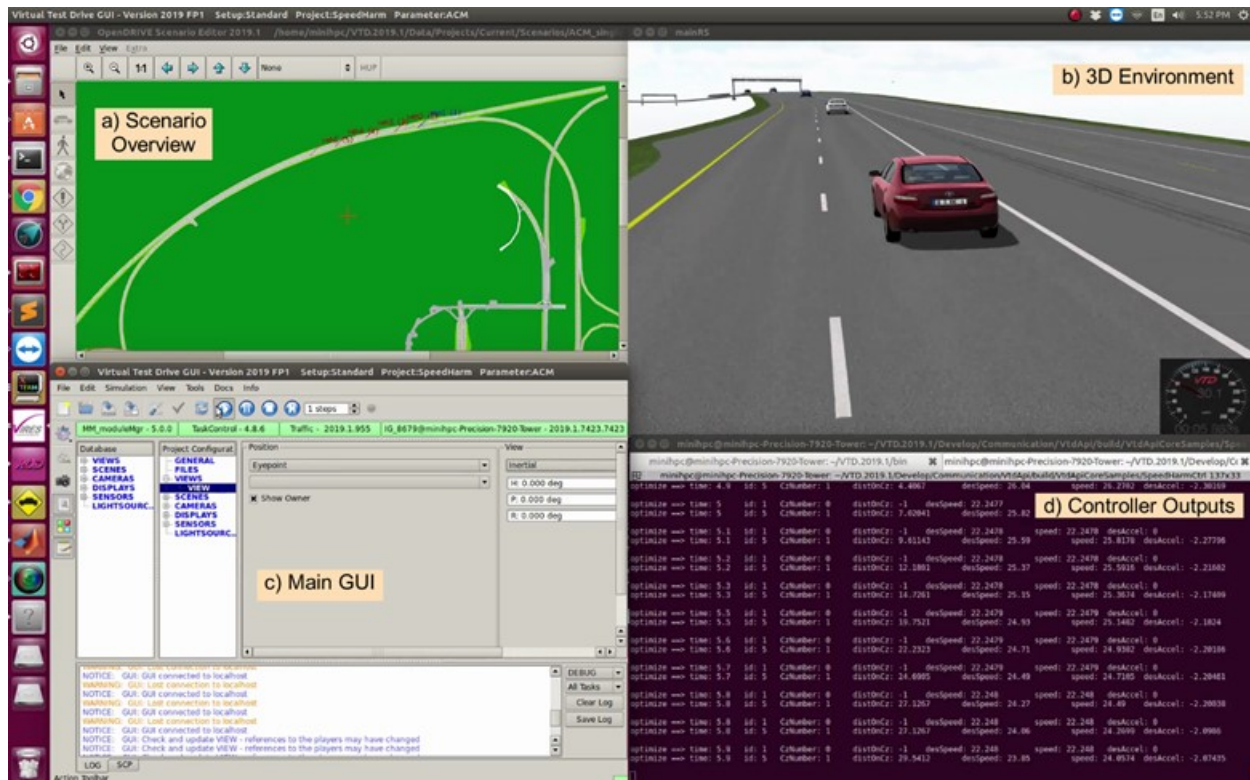


Figure II.1.3.4 ORNL's Speed Harmonization Algorithm Implementation In VTD

ORNL drafted a list of experiment scenarios including the scenario description, test maneuvers, number of vehicles, number of trials, design parameters to evaluate, and data collection. To further understand how the design parameters can affect the performance of the algorithms and energy benefits, a simulation parameter evaluation test was designed for the speed harmonization algorithm. A list of critical parameters has been identified including different speed limits and speed reductions, car-following distances, as well as number of vehicles. A vast number of simulation tests have been designed to cover different combinations of design parameters. The parameter evaluation test is currently ongoing to identify the most meaningful parameter settings and scenarios that will be studied for experimental validation.

Demonstration and Validation of Controls (ANL)

Vehicle Model Validation and Implementation

Testing of vehicles on a 4-wheel drive chassis dynamometer at ANL was completed for the Bolt and Pacifica prior to the integration of additional sensing and controls. ANL engineers instrumented the vehicles with sensors, decoded and logged key CAN messages in order to provide a comprehensive picture of the operations of the powertrain and the energy consumption. ANL developed models of the vehicles in Autonomie and validated them using the dynamometer data. The operations of the vehicle, its individual components (e.g., engine, battery, motor) and controls (e.g., gear shifting logic) were analyzed, modeled and validated in each case. Figure II.1.3.5 below shows some of the component performance maps.

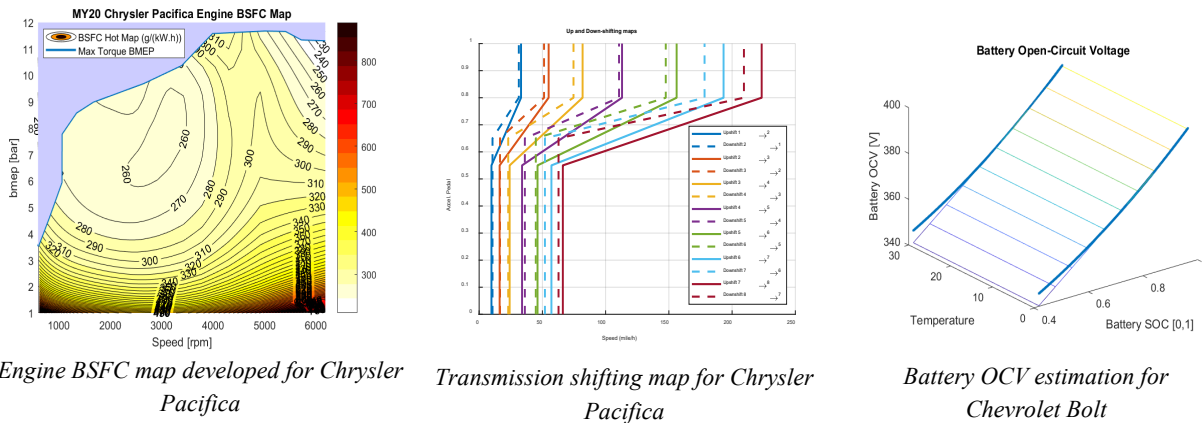


Figure II.1.3.5 Component Performance Maps for Chrysler Pacifica Integrated into Autonomie

ANL implemented models of both vehicles, including calibrated plants and controllers, in Autonomie. The validation process is iterative, and combines data analysis, model development and model calibrations. Figure II.1.3.6 below shows how a sample of the main signals in the test and in the simulations compare with each other for the UDDS driving cycle and demonstrates the successful validation of the vehicles based on Normalized Cross-Correlation Power (NCCP).

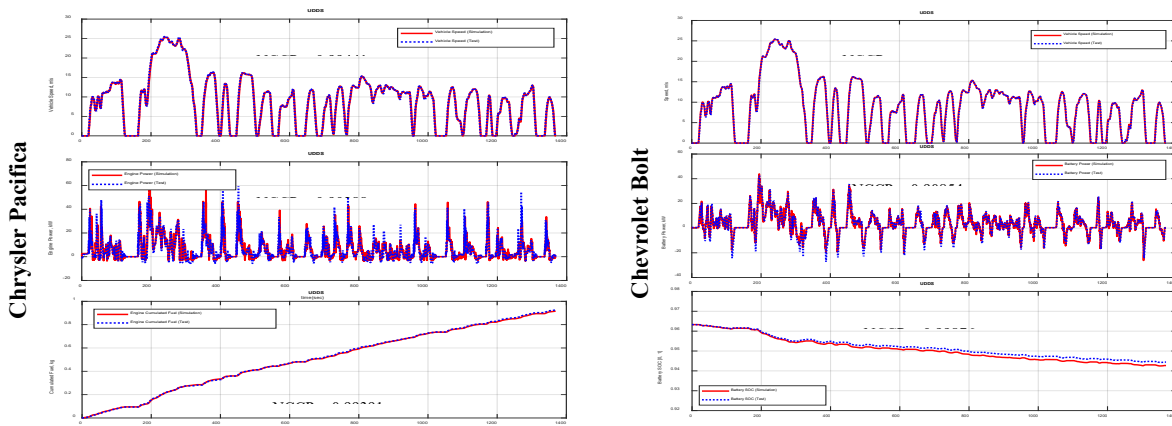


Figure II.1.3.6 Vehicle Speed, Engine Power, and Cumulated Fuel Rate for the Chrysler Pacifica, in Test and Simulation (Left); Vehicle Speed, Motor Power, and SOC for the Chevrolet Bolt, in Test and Simulation

Table II.1.3.1 and Table II.1.3.2 below list the comparison of energy consumption of simulated vs. test results of the two vehicles.

Table II.1.3.1 Chrysler Pacifica Validation

[mpg]	UDDS	HWFET	US06	NEDC	WLTC
Test Result	22.63	35.20	21.49	24.86	24.40
Simulation (error)	22.75 (+0.53%)	34.43 (-2.2%)	21.33 (-0.74%)	25.05 (+0.76%)	24.29 (-0.45%)

Table II.1.3.2 Chevrolet Bolt Validation

[Wh/mile]	UDDS	HWFET	US06	NEDC	WLTC
Test Result	183.6	202.3	284.9	196.3	222.4
Simulation (error)	182.5 (-0.6%)	207.5 (2.6%)	285.9 (+0.4%)	195.9 (-0.2%)	224.4 (+0.9%)

Using the ANL dynamometer test results as well as road testing and track testing at ACM, MTU developed reduce order energy models for the Volt, Bolt and Pacifica. These will be integrated into the vehicle controller to dynamically check vehicle operation and control relative to the baseline.

Update ANL Eco-Driving Controller for Implementation

The optimal controllers were adjusted and updated for the implementation to the test vehicles as shown in Figure II.1.3.7 below. The adaptation allows the controller to work both in a digital twin of test and simulation. A process to build “wiring harness” model, compile the controller, and quality check the results was developed for rapid, reliable, and smooth implementation. The updates were focused on three steps. First, the input/output (I/O) and outer configurations of the controller were re-organized to facilitate implementation into the dSPACE Micro-Autobox (MABx). The optimal controller inside was also adjusted based on new I/Os, and features signal processing at the input, and APP/BPP calculations at the output. The sharable input and output interface models that include signals names, type, unit, factor, range, frequency, and descriptions were exchanged with MTU, and constitute a wiring harness. ANL also developed a compilation process for the rapid implementation and control updates. Finally, additional functionalities were added for robustness, error, and quality check during or after execution, in the test and in simulation.

Test Plans Development and Generating Process

ANL developed a process to define road conditions to be tested on the track and established a digital twin in RoadRunner to simulate the vehicles and controls in the same conditions as in the track tests. This will ensure an efficient use of hardware and infrastructure resources, and that a variety of real-world conditions will be captured. In the initial round of testing, a single vehicle with ANL controls will be tested on a track with three types of virtual features: 1) Stop signs, 2) Traffic signals, and 3) Speed limit changes. A large number of independent short scenarios, or “mini-scenarios,” is preferable in order to test specific features in specific situations. However, it is not practical to do large number of short tests repeatedly. As a result, ANL developed test plans that consist of multiple mini-scenarios put back-to-back to cover one full loop of the ACM track (3.72km). Five test plans (one test = one loop) were developed as shown in Figure II.1.3.8: four combining stop signs and traffic signals, and one with speed limit changes at higher speed. The goal is to test the vehicle approaching an intersection for a range of approach speeds and relative positions in the traffic signal timing sequence. 4 to 6 intersections with traffic signal can fit into one test, with various speed limits (20, 30, 40, and 50 mph). The phases of the traffic signals must be reset when the vehicle passes at a predefined position in a mini-scenario to ensure that one mini-scenario does not impact the following ones. A segment is a minimal unit in a test plan to define the test plan. A segment will have information of distance of a segment, speed limit, intersection type, offset of traffic signal, offset reset position, and connectivity. The test plans can be shared with ACM in spreadsheet format and the spreadsheet can be transformed to the road models automatically for quick simulation in RoadRunner.

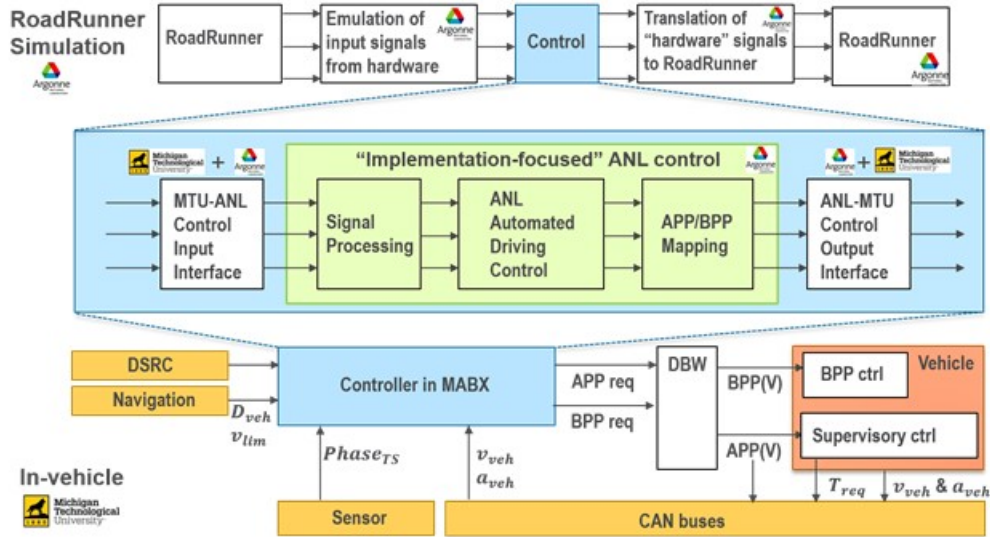


Figure II.1.3.7 Configuration of the Controller Implementation for Development of a Digital Twin

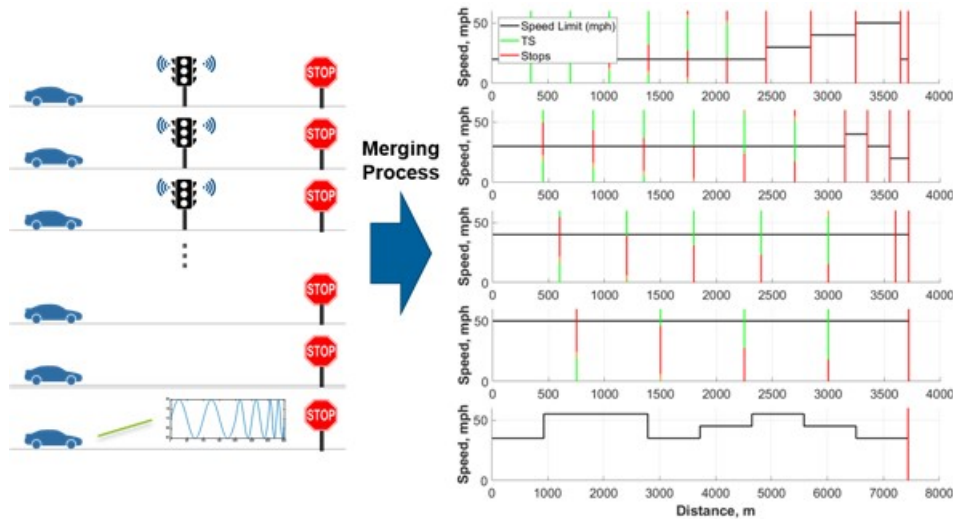


Figure II.1.3.8 Five Test Plans Developed with Multiple Types of Mini-Scenarios

Conclusions

As part of vehicle baselining, MTU performed road testing on the Bolt for vehicle baseline characterization and track testing of the Bolt and Volt with integrated MABx controlled by the DBW system. Baseline testing was completed on the Volt and Bolt to characterize vehicle dynamics response. MABX/DBW performance & latency was characterized as < 50 ms and determined to be acceptable. Additionally, MTU demonstrated MAP/Location-based speed control on the Volt and Bolt which involves a straightforward conversion for other vehicles. The I/O list for the lab’s vehicle longitudinal dynamics controller was prepared and validated in vehicle testing. Vehicle baseline characterization on ANL’s chassis dyno, for the Bolt and Volt along with road and track testing results was used to develop, calibrate, and validate real-time reduced order energy models. All of the data from vehicle evaluations of the Volt and Bolt were recorded and made available for lab use.

ORNL shared C++ and MATLAB code of merging coordination and speed harmonization algorithms with ACM as well as flowcharts and lists of I/O of each algorithm. The speed harmonization algorithm was implemented on a high-fidelity digital twin of the ACM track in VTD simulation. The speed harmonization algorithm is currently under evaluation and preparation for experimental validation. The experiments will be

implemented in a mixed reality fashion where virtual vehicles in VTD simulation share information with test vehicles on ACM track through RSUs. Also, ORNL has drafted a list of experiment scenarios considering various factors and a simulation parameter evaluation test is currently ongoing to identify the most meaningful parameter settings and scenarios for experimental validation.

ANL tested the Bolt and Pacifica on a chassis dynamometer, and validated Autonomie models that can be used in the simulation platforms for energy consumption prediction. ANL also prepared the control for implementation and developed a testing plan for the initial testing phase in FY21. The testing will consist of five full track loops with a mix of stop signs, traffic signals and speed limit changes. Full digital twins of the vehicle and track in RoadRunner, along with automated simulation or simulation-to-testing workflows enable a greater level of simulation-based testing and verification. These activities will greatly speed-up the deployment of the controls to actual vehicles that are to be tested at ACM.

References

1. Rios-Torres, Jackeline, Andreas Malikopoulos, and Pierluigi Pisu. "Online optimal control of connected vehicles for efficient traffic flow at merging roads." In *2015 IEEE 18th International Conference on Intelligent Transportation Systems*, pp. 2432–2437. IEEE, 2015.
2. Han, Jihun, Dominik Karbowski, and Namdoo Kim. "Closed-Form Solutions for a Real-Time Energy-Optimal and Collision-Free Speed Planner with Limited Information." In *2020 American Control Conference (ACC)*. Denver, CO, USA, 2020. <https://doi.org/10.23919/ACC45564.2020.9147382>.
3. Jeong, Jongryeol, Daliang Shen, Namdoo Kim, Dominik Karbowski, and Aymeric Rousseau. "Online Implementation of Optimal Control with Receding Horizon for Eco-Driving of an Electric Vehicle." In *IEEE Vehicle Power and Propulsion Conference (VPPC)*, 1–6. Hanoi, Vietnam, 2019. <https://doi.org/10.1109/VPPC46532.2019.8952220>.
4. Shen, Daliang, Dominik Karbowski, and Aymeric Rousseau. "A Minimum Principle-Based Algorithm for Energy-Efficient Eco-Driving of Electric Vehicles in Various Traffic and Road Conditions." *IEEE Transactions on Intelligent Vehicles*, July 2020, 1–1. <https://doi.org/10.1109/TIV.2020.3011055>.
5. D. Karbowski, J. Jeong, D. Shen, J. Han and N. Kim, "Eco-Driving: Energy-Focused CAV Control Development" in *SMART Mobility Connected and Automated Vehicles Capstone Report* (DOE EEMS Vehicle Technologies Office Capstone Reports, July 2020).
6. Kim, Namdoo, Dominik Karbowski, and Aymeric Rousseau. "A Modeling Framework for Connectivity and Automation Co-Simulation." In *SAE Technical Paper 2018-01-0607*, 2018. <https://doi.org/10.4271/2018-01-0607>.

Acknowledgements

John Conley (DOE-National Energy Technology Laboratory-Morgantown); David Anderson and Erin Boyd (DOE-Vehicle Technologies Office); Jeff Naber, Grant Ovist, and Ahammad Basha Dudekula (Michigan Technological University-Houghton); William Buller, Richard Chase, Joseph Paki, Miles Penhale and Colin Brooks (Michigan Technological Research Institute); Dominik Karbowski, Jongryeol Jeong, Ehsan Islam, Eric Rask, and Simeon Iliev (Argonne National Laboratory); Jackeline Rios-Torres, Yunli Shao, Dean Deter, Nolan Perry, and David Smith (Oak Ridge National Laboratory); Dennis Winslow (Intertek); and Reuben Sarkar and Beth Jakubowski (ACM).

II.1.4 Next Generation Intelligent Traffic Signals for the Multimodal, Shared, and Automated Future (Xtelligent, Inc.)

Andrew Powch, Principal Investigator

Xtelligent, Inc.
525 South Hewitt Street
Los Angeles, CA 90013
Email: andrew@xtelligent.io

Prasad Gupte, DOE Technology Manager

U.S. Department of Energy
Email: prasad.gupte@ee.doe.gov

Start Date: August 19, 2019
Project Funding: \$500,000

End Date: August 18, 2021
DOE share: \$500,000

Non-DOE share: \$0

Project Introduction

Significant energy efficiency and greenhouse reduction gains can be achieved with better management of traffic flow, but 98% of the U.S. signalized intersections still use antiquated fixed timers to dictate their timing, resulting in static systems that fail to accommodate real-time conditions.² Adaptive Traffic Control Systems (ATCS), which adapt signal timing based on real traffic conditions, have only been adopted in ~2% of U.S. intersections over the last 30 years. The primary reasons are high cost due to expensive sensor infrastructure (average \$65,000 per intersection) and limited effectiveness due to simplistic and antiquated algorithms. Incumbent ATCS technology providers consume poor quality data from local sensors like induction loops or video cameras, rely almost exclusively on centrally controlled mechanisms that stifle scalability, are significant security liabilities (single point of failure), and focus on optimizing offsets on a narrow set of road arteries, rather than the full transportation network.

This SBIR Phase 2 project engages in live-intersection research and validation of a novel ATCS algorithm to optimize traffic signal performance. The research falls under the market term “Cooperative Intelligent Transport Systems” (C-ITS), and represents a unique approach that can significantly reduce transportation network energy consumption by widely deploying the latest control algorithms in conjunction with emerging technologies to address key hurdles preventing wide-spread adoption of adaptive ITS technology: efficacy and cost.

The core algorithms are inspired by information technology network throughput maximization techniques; They are inspired by the routing and scheduling paradigms which dictate how packets of information flow efficiently over telecommunication information networks. Based on PTV VISSIM simulations, the proposed proportionally fair classes of optimization algorithms, combined with additional real-time data (connected vehicle, telecommunications carriers, mobile applications, etc.), have the potential to increase vehicle throughput through transportation networks by up to 50% over the best incumbent technologies, while substantially reducing the capital investment cost by up to 90%.

However, current benefits estimated through detailed modeling and simulation need to be validated through actual real-world experiments. Xtelligent has installed the system in live city intersections in Colorado and California and has been testing aggressively. Successful validation of this research will confirm the positive effects of the proposed high efficacy / low-cost C-ITS concept. Mass adoption of such a system across U.S. intersections could result in 373 million gallons of fuel saved, 3.7 megatons of CO₂ equivalent greenhouse gases, and 2.5 billion hours of time saved each year alone.

Objectives

The core goal from our Phase I remains: to research, develop, and evaluate the proportionally fair traffic signal control algorithm in a real-world setting. With Phase II SBIR funding, we seek to finalize system design for coordinated ATCS control, deploy across a wider city network of 100 contiguous intersections, and test the inclusion of real-time streaming vehicle location data from internet-based sources (rather than physical sensors).

We have previously demonstrated a 50% throughput improvement in PTV VISSIM microsimulation modeling environment which is expected to yield 15% improvement in energy efficiency, but the simulated environment does not provide for all of the unforeseen variables that only the real-world setting can provide. Real-world validation is also necessary before additional financial and human resources can be committed for the commercialization of the researched algorithm. The SBIR will also help us quantify the energy impact of the technology for different market penetration.

- Objective 1: Coordinated ATCS Control for Throughput Maximization:
 - Xtelligent’s novel traffic signal control algorithm will be fully tested across a complex grid of coordinated intersections while relying on in-road physical sensors. The goal is to activate up to 100 intersections simultaneously for a broad system test.
- Objective 2: Evaluate novel vehicle location data sources in combination with traditional physical sensor data as inputs to Xtelligent’s ATCS.
 - Potential data sources under evaluation include connected vehicle automotive manufacturers, telecommunications service providers, smartphone application companies, smart phone manufacturers, 3rd party traffic data aggregators, and other data sources. Each is expected to have different characteristics, including varying precision, latency, penetration, and transmission frequency. Duplicated data will need to be removed, temporal differences aligned, varying levels of accuracy/precision accounted for, and the behavior of unconnected/“unseen” vehicles inferred from the smaller population of “seen” vehicles. Based on Xtelligent’s discussions with industry partners, we anticipate 20-40% penetration of location-aware vehicles across the full population of vehicles.
- Objective 3: Performance Improvement by Supplementing Existing Physical Sensor Data with Connected Vehicle Location Data (V2I using 4g/LTE)
 - Existing Xtelligent pilot sites under SBIR Phase I and new sites anticipated under this Phase II proposal include some physical sensors already present in the roadway. These sensors suffer from two major categories of limitations: technical and commercial. From a technical standpoint, the induction loops and video systems provide limited data: binary vehicle presence information at small zones (6 ft) at the stop bar or slightly upstream and are unaware of estimated times of arrival or volumes of approaching vehicles. Critical measurements like queue length must be inferred and are not measurable by today’s sensor systems. They are primarily designed to supply data to actuated intersections and are not well-suited to high performing adaptive control. Rigorously test before/after system performance to determine energy efficiency benefit to transportation network of including this additional data.
- Objective 4: Attempt to maintain or improve system performance using only novel location data streams.
 - This objective involves Xtelligent’s unique, proportionally fair ATCS control with full reliance on streaming location data without any use of in-road, physical sensors.

- Objective 5: Evaluation of Beta/Pilot
 - Includes detailed data analysis and reporting of the live deployment data. This data will also be supplied to Argonne National Laboratory, which will then execute its subaward work to quantify the energy reduction effects of the traffic management system.

Approach

To achieve the research objectives listed above, Xtelligent first identified a set of potential pilot site partners. These transportation agencies needed to have 1) sufficient density of traffic flow, 2) NTCIP-compliant controllers for ease of implementation, 3) at least 20-100 contiguous intersections, and 4) an enthusiastic and innovation-minded set of public works/transportation staff willing to partner with this effort. The Colorado Department of Transportation, City of Greenwood Village, CO, and Fremont, CA were selected as sites.

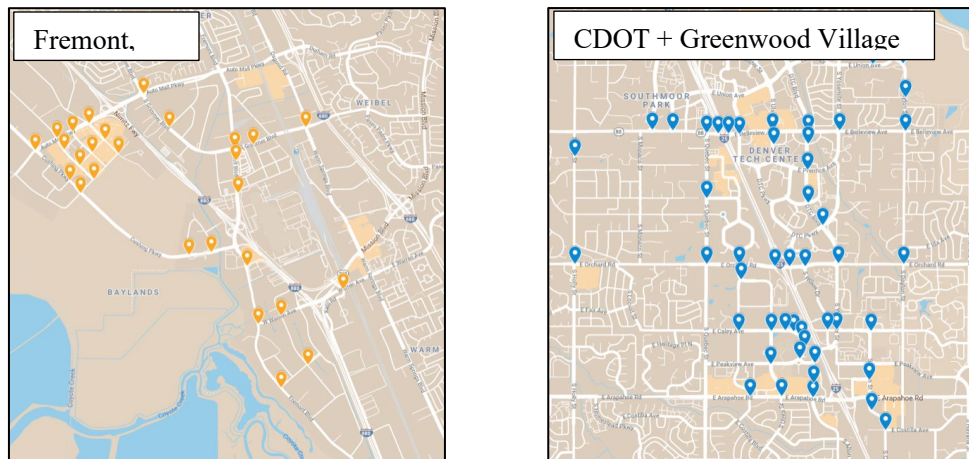


Figure II.1.4.1 Transportation Agency Pilot Sites

The next effort was also completed under Phase I of this project and involved integration with the Siemens, Intelight, and Econolite controllers across these three agencies. This integration has required, and continues to require, a significant amount of software development effort to understand the nuanced implementation of NTCIP across several controller manufacturer types, but has resulted in a smoothly interoperable system. Xtelligent also constructed an off-line signal laboratory to more quickly iterate integration development. The lab includes McCain, Intelight, Econolite, and Siemens controllers, and is accessible remotely by secure VPN. This setup has also proved helpful keeping the research team productive during the ongoing COVID-19 pandemic.

Upon system installation, we also needed to validate the limited physical sensor data available to us. While the original PTV VISSIM simulations undertaken had the benefit of perfect simulation data, traditional traffic signal systems rely on induction loop and/or video camera data, which only gives occupancy and volume information based on vehicle presence in a single sensor location—typically at the stop bar of an approach, and sometimes in an “advanced” configuration a few hundred feet from the stop bar. Extensive mathematical correlations needed to be completed comparing recorded CCTV video data with sensor data logged from the controllers. Xtelligent was able to validate these algorithms to create suitable inputs for the Proportionally Fair ATCS algorithm used in this research.

Next, in order to complete Objective 1 Xtelligent began activating its novel traffic signal control algorithm across single intersections and corridors to validate performance. The specific approach required at least 5 days of baseline data, which was compared with 5 days of adaptive testing data. This allowed for a close baseline with a sufficient number of cycles to generate statistically significant results.

In parallel with controller integration software development, Xtelligent’s leadership team began researching for appropriate internet-based location data streams to include as inputs per Objectives 2 through 4. As of October 2020, Xtelligent is working towards data partnerships with five automotive connected vehicle manufacturers, two telecommunications service providers, two traffic data aggregators, and two smart phone application companies.

The first live integrations of this data will begin during the week of October 26 and will continue through the remainder of this grant research. A third pilot site is being opened in Long Beach, CA, and should introduce a suitable pilot site for data integration given a co-located automotive OEM test fleet and telecom service provider test site.

Finally, the comprehensive set of baseline and test research data will be analyzed in detail by both Xtelligent’s research team and Argonne National Laboratory’s transportation simulation group. We will collectively be determining the results of our tests and simulating the extrapolation of these results across a major metropolis. The increase in transportation network energy productivity, greenhouse gas emissions reductions, travel time savings, throughput increases, and any other available metric will be studied and submitted in the final SBIR project report.

Results

This annual progress report represents the conclusion of the first 12 months out of a 24-month period of performance under this grant. A significant amount of foundational work has been completed to implement a real-world, in-street ATCS system to research and develop Xtelligent PF ATCS. COVID19 impacts to vehicular congestion levels and partner transportation agency priorities caused a material impact on project timeline.

Technical results to date include over 30 in-streets tests as the system design is iterated, a preliminary evaluation of real-time streaming data source quality, and the initial design of a user interface to help transportation engineers understand the performance of their transportation networks.

- A) Single intersections activations in 2019: At the end of Phase I, Xtelligent was able to demonstrate successful implementation of its PF ATCS solution in single, non-coordinated environments. Because single-intersections effectively represent a network of one node, we use green-time utilization (or the inverse, “slack ratio”) as the representative metric. Green-time utilization is the percent (%) of green-time utilized, and is correlated to throughput and traditional transportation metrics like travel time, delays, arrivals on red, level of service, etc. Key focus was ratio of green-time utilization between major through-phases (2 and 6) and side phases (4 and 8). Perfect balance would be indicated by a Slack ratio of 1.00.

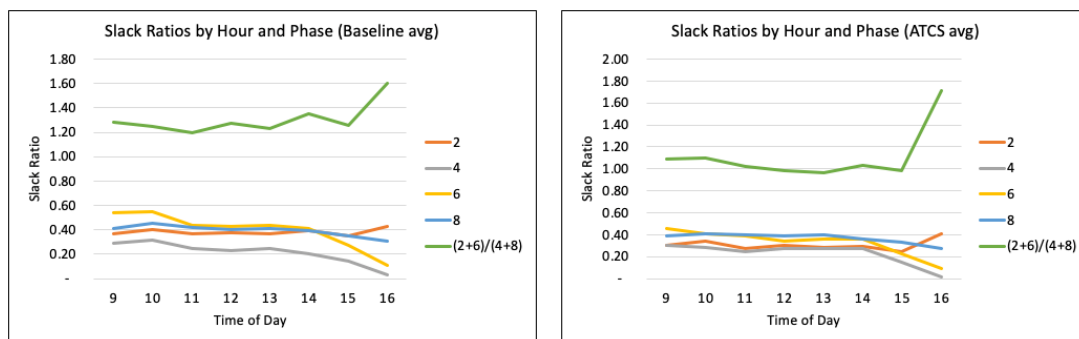


Figure II.1.4.2 Performance Improvement in Single (Non-Coordinated Intersections)*

In the charts above “Slack ratio” represents proportion of green time not utilized. Most phases exhibited 0.40 unused greentime. Baseline ratio of main phases to side phases (2+6)/(4+8) = 1.30. When activating Xtelligent’s PF ATCS, the ratio of main phases to side phases (2+6)/(4+8) = 1.09, a 21% improvement.

*Tests deactivated daily at 1600. Spike at 1600 due to restoration of city control

- B) Coordinated intersection activation testing began in summer 2020 and is still ongoing. COVID-19 has impacted traffic volumes significantly, affecting relevant real-world baselines for research validation. The deepest reduction in traffic volumes approached 80% in April 2020, and remains down approximately 30-40% depending on location. In addition, several agencies have converted their usual Time of Day (TOD) coordination plans along corridors to a free-mode policy in order to accommodate the unusual, eclectic traffic volumes. Xtelligent has successfully tested its system against this scenario, showing a 26% improvement in system performance. Our next efforts are focused on validating the system against a more robust, TOD baseline.

The below table includes Xtelligent’s PF ATCS performance data from 8/10 – 8/14 as compared to a baseline data set on the same corridor from 8/3 – 8/7, using a variant of the sum of induction loop occupancy times per phase per hour for each type of system. A reduction in hourly sum of this demand on each phase denotes a reduction in congestion and a more optimal traffic signal timing scheme. Changes in aggregate traffic volumes were also compared between baseline and ATCS weeks to account for any changes resulting from this alone.

8/3 - 8/7 Baseline (Free mode)								8/10 - 8/14 PF ATCS								
Hour	Phase					Stdev %	Avg	Hour	Phase					Stdev %	Avg	Δ
	3-Aug	4-Aug	5-Aug	6-Aug	7-Aug				10-Aug	11-Aug	12-Aug	13-Aug	14-Aug			
9	6,369	5,886	6,281	6,093	6,343	3%	6,194	9	4,370	4,251	4,148	4,452	4,492	3%	4,343	30%
10	5,951	6,373	6,633	6,554	6,619	4%	6,426	10	5,135	5,408	4,808	5,522	5,105	5%	5,196	19%
11	6,934	6,857	6,906	6,801	6,674	2%	6,834	11	4,775	4,915	4,930	6,011	5,082	10%	5,143	25%
12	6,581	6,528	6,739	6,813	6,960	3%	6,724	12	4,343	4,892	4,952	5,353	4,834	7%	4,875	28%
13	6,300	6,210	6,447	6,531	6,810	4%	6,460	13	4,604	4,759	4,885	4,693	4,933	3%	4,775	26%
14	7,088	7,590	6,929	7,089	7,446	4%	7,228	14	4,948	5,493	5,691	5,172	5,517	6%	5,364	26%
15	8,654	8,007	7,972	8,256	8,251	3%	8,228	15	5,972	6,412	5,835	6,578	5,635	7%	6,086	26%

Figure II.1.4.3 Performance Improvement from Free Mode Corridor Baseline

- C) Xtelligent has been aggressively pursuing location data partnerships in preparation for integration of these data streams into its PF ATCS test bed. Key variables for each data stream are % penetration, % accuracy, data latency, and ease of partnership. Due to non-disclosure agreements, all names must remain obscured. GDPR and similar data privacy considerations have resulted in protracted discussions. Not all data partners will be utilized—only those with technical potential to augment PF ATCS system. Preferred data streams appear to be 1-4, 5, and 10. The table below in Figure II.1.4.4 summarizes the current status of data partner evaluation.

	Data partner	% Penetration (of vehicles)	Accuracy	Latency	Partnership potential
1	Connected Vehicles: OEM 1	<1%	2m	30 sec	Medium
2	OEM 2	<1%			Medium
3	OEM 3	0-5% ¹			High
4	OEM 4	~4%			High
5	Telecom 1	30%	100m	>5 min ²	High
6	Data Aggregator 1	10%	~50m	1-15 min ³	Medium
7	Data Aggregator 2				Medium
8	Data Aggregator 3				Medium
9	Xtelligent's App	0%	2m	1s	High
10	Map Provider	>10%	2m	<10s	Medium

Figure II.1.4.4 Data Partner Current Evaluation Status

The likely first site for testing of the combined data pipelines listed above is Long Beach, CA, based on Long Beach City Council's approval of our pilot site on September 15, 2020.

Conclusions

In conclusion, Xtelligent has used the first half of its SBIR Phase II period of performance effectively to develop real-world pilot sites where it is regularly testing its PF ATCS novel algorithm. While the team underestimated the amount of time it would take to integrate with legacy infrastructure, and was also impacted strongly by the COVID19 pandemic, early test results are promising. Initial review of several data pipelines are also complete, and Xtelligent is beginning to plan integration of these data sources into its system. We look forward to providing further progress reports as we continue into our second and final 12 months of this Phase II grant period of performance.

Acknowledgements

Acknowledging Michael Lim, who has been instrumental in developing and managing our city/agency partnerships. These real-world pilot sites are instrumental to Xtelligent's DOE SBIR research, and his support has been invaluable.

II.1.5 Developing an Eco-Cooperative Automated Control System (Virginia Tech)

Hesham Rakha, Principal Investigator

Virginia Tech Transportation Institute
3500 Transportation Research Plaza (0536)
Blacksburg, VA 24061
Email: hrakha@vt.edu

Kyoungho Ahn, Co-Principal Investigator

Virginia Tech Transportation Institute
3500 Transportation Research Plaza (0536)
Blacksburg, VA 24061
Email: kahn@vt.edu

Prasad Gupte, DOE Technology Manager

U.S. Department of Energy
Email: prasad.gupte@ee.doe.gov

Start Date: October 1, 2017
Project Funding: \$1,675,265

End Date: March 31, 2021
DOE share: \$1,507,197

Non-DOE share: \$168,068

Project Introduction

The transportation sector accounts for 69% of the nation's petroleum consumption and 33% of the nation's CO₂ emissions. Consequently, any reductions in the energy consumed by the transportation sector will have significant environmental benefits. Connected Vehicle (CV) systems comprise sets of applications that connect vehicles to each other and to the roadway infrastructure using vehicle-to-vehicle (V2V) and vehicle-to-infrastructure (V2I) communications, collectively known as V2X. While Automated Vehicles (AVs) offer enhanced operation of individual vehicles, CVs produce cooperative, network-wide benefits through the exchange of information. These new technological advancements have the potential to drastically improve the efficiency and sustainability of our transportation system. Consequently, as part of the proposed research effort we are taking a revolutionary approach to developing a next-generation, vehicle dynamics (VD) Connected Automated Vehicle (CAV) system that builds on existing CAV technologies to reduce the energy/fuel consumption of internal combustion engine vehicles (ICEVs), battery-only electric vehicles (BEVs), plug-in hybrid electric vehicles (PHEVs), and hybrid electric vehicles (HEVs).

Objectives

The main project goal of this effort is to substantially reduce vehicle fuel/energy consumption by integrating vehicle control strategies with CAV applications. Specifically, the team is developing a novel integrated control system that (1) routes vehicles in a fuel/energy-efficient manner and balances the flow of traffic entering congested regions, (2) selects vehicle speeds based on anticipated traffic network evolution to avoid or delay the breakdown of a sub-region, (3) minimizes local fluctuations in vehicle speeds (also known as speed volatility), and (4) enhances the fuel/energy efficiency of ICEVs, BEVs, HEVs, and PHEVs.

Approach

We are taking a revolutionary approach by developing a next-generation CAV system (Figure II.1.5.1) that builds on existing CAV technologies to reduce the energy/fuel consumption of ICEVs, BEVs, HEVs, and PHEVs. The development of the Eco-Cooperative Automated Control (Eco-CAC) system involves the following key steps and components:

1. Develop a CV eco-routing controller that can be used for various vehicle types. This unique eco-router will use a dynamic feedback controller, employ key link parameters that capture the entire drive cycle, compute vehicle-specific link energy functions using these link parameters, and compute user-optimum routings.
2. Develop a speed harmonization (SPD-HARM) controller that regulates the flow of traffic approaching network bottlenecks identified using the Fundamental Diagram (FD) and/or the Network Fundamental Diagram (NFD). This controller will be fully integrated with the vehicle router, resulting in a unique strategic controller that can route traffic away from congested areas and regulate the flow of traffic entering congested areas using gating techniques.
3. Develop a multi-modal (ICEV, BEV, PHEV, and HEV) Eco-CACC-I controller that computes and implements optimum vehicle trajectories (ICEVs, BEVs, PHEVs, and HEVs) along multi-intersection roadways within CAVs considering dynamic vehicle queue predictions.
4. Develop an Eco-CACC-U controller that provides local longitudinal energy-optimal control in consideration of homogenous and non-homogeneous vehicle platooning of ICEVs, BEVs, PHEVs, and HEVs.

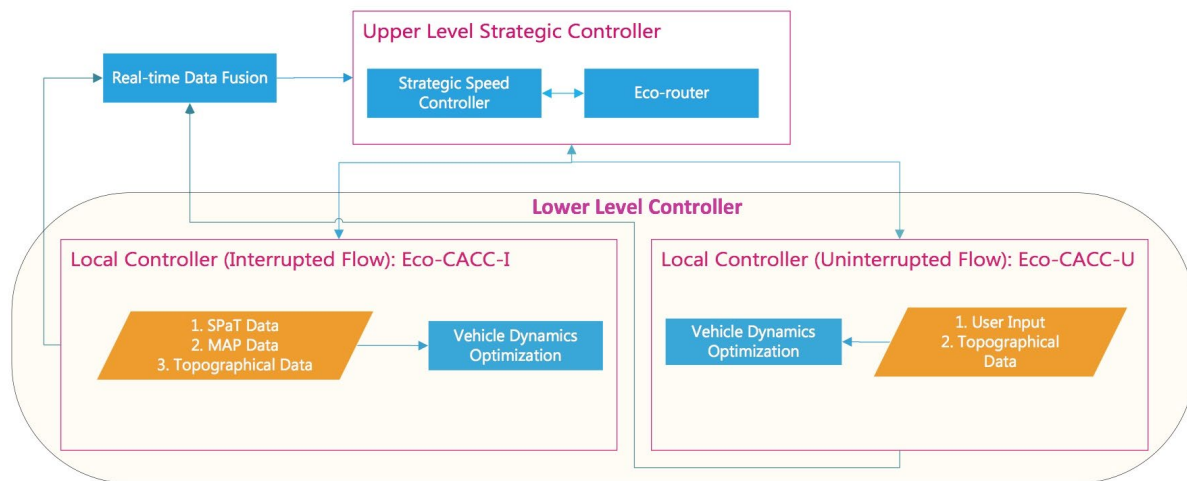


Figure II.1.5.1 Proposed Eco-CAC System

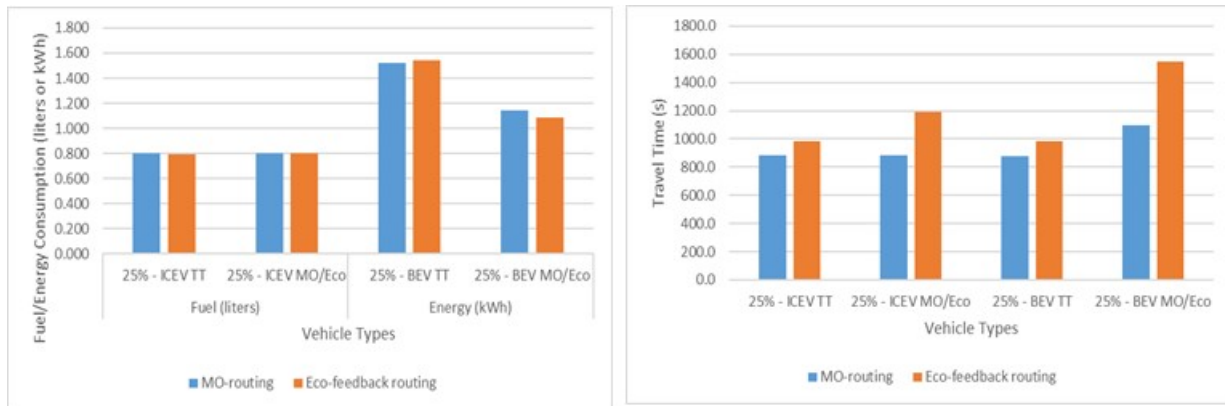
At the upper level, the strategic controller (eco-router and strategic speed controller) will compute the energy/fuel-optimum route and vehicle optimum speeds (upper and lower bounds) required to regulate the flow of traffic approaching downstream sub-networks and/or bottlenecks, thus preventing or delaying the breakdown of traffic flow and mitigating traffic congestion. This strategic controller will extend traditional eco-routing and SPD-HARM systems beyond the currently used isolated control to a fully integrated, network-wide controller that identifies bottlenecks and controls the flows approaching the bottlenecks in real-time. The eco-router within the strategic controller will develop optimum eco-routes using a vehicle-specific feedback controller. Unlike a predictive controller, a feedback controller does not require a link-specific analytical fuel consumption function, which is typically difficult to develop, inaccurate, and not vehicle-specific. Instead, the eco-router controller uses information shared by other CVs to compute the link cost estimates. In addition, a SPD-HARM controller will be developed and integrated with the eco-router to regulate the traffic flow approaching transportation bottlenecks.

At the lower level, a VD controller will operate along the routes and within the speeds recommended by the strategic controller to compute energy-efficient vehicle speeds based on local conditions using two local controllers: an Eco-CACC-I and an Eco-CACC-U controller. The Eco-CACC-I controller will compute energy-optimum vehicle trajectories through signalized intersections (i.e., interrupted flow conditions) using

traffic count and signal phase and timing (SPaT) data. The Eco-CACC-U controller will develop fuel/energy efficient platooning strategies along uninterrupted road facilities. The VD lower-level controller will use the planned vehicle routes and trajectories to anticipate the vehicle operational mode and compute the optimum VD strategies. The fully functional Eco-CAC system will be implemented in a traffic simulation environment so that it can be tested at a network level. The proposed CAV applications, testing parameters, and validation methods will be used to quantify the Eco-CAC system’s benefits.

Results

The team developed and quantified the impacts of a multi-objective Nash optimum (user equilibrium) traffic assignment on a large-scale network for BEVs and ICEVs in a microscopic traffic simulation environment. Eco-routing is a technique that finds the most energy efficient route. ICEV and BEV energy consumption patterns are significantly different with regard to their sensitivity to driving cycles. Unlike ICEVs, BEVs are more energy efficient on low-speed arterial trips compared to highway trips. Different energy consumption patterns require different eco-routing strategies for these two types of vehicles. This study found that eco-routing could reduce energy consumption for BEVs but also significantly increased their average travel time. The simulation study found that multi-objective (MO) routing could reduce BEVs’ energy consumption by 13.5%, 14.2%, 12.9%, and 10.7%, as well as ICEVs’ fuel consumption by 0.1%, 4.3%, 3.4%, and 10.6% for “not congested,” “slightly congested,” “moderately congested,” and “highly congested” conditions, respectively in a downtown Los Angeles, CA (LA) network. The study also found that the multi-objective user equilibrium routing reduced the average vehicle travel time by up to 10.1% compared to the standard user equilibrium traffic assignment for the highly congested conditions, producing a solution closer to the system optimum traffic assignment.



(a) Highly congested – Fuel/Energy consumption.

(b) Highly congested – Travel time.

Figure II.1.5.2 Fuel/Energy Consumption and Travel Time for High -Congestion, Multi-Class Routing Options

Figure II.1.5.2 compares the fuel/energy consumption and the travel time of ICEVs and BEVs for the multi-objective (MO)-routing and eco-routing options. We assigned four vehicle classes, including two 25% ICEVs and two 25% BEVs, to an LA network. Specifically, we assigned 25% ICEV travel time (TT) routing, 25% ICEV MO-routing, 25% BEV TT routing, and 25% BEV MO-routing. The same runs were repeated by replacing the MO-routing with a single objective eco-routing option. Figure II.1.5.2 shows the simulation results of the highly congested condition. The study found that both the MO-routing and eco-routing vehicles consumed very similar amounts of fuel/energy except for the BEV eco-routing vehicles, which reduced energy consumption by 5.4% compared to the MO routing. However, the study found that the MO-routing vehicles reduced ICEVs’ and BEVs’ travel time by up to 25.9% and 29.4%, respectively. The results indicate that the MO-routing can effectively reduce fuel/energy consumption with minimum impacts on travel times for both BEVs and ICEVs.

The team developed and tested speed harmonization (SH) logic coupled with the sliding mode controller (SM) on the downtown LA network, as illustrated in in Figure II.1.5.3. The network had 3,556 links, including 331 freeway links, 457 signalized intersections, 285 stop signs, and 23 yield signs, where the SH controller was not activated, which might obfuscate the improvements of the proposed controller. To get a clearer picture of the SH controller's benefits, we only evaluated the freeway sections. The simulation was conducted during the morning peak hour (7:00–8:00 a.m.), and the simulation time was set to 10,000 s (2.77 h). Table II.1.5.1 presents the margins of error in improvement percentage over the base case using the SH controller. An average travel time reduction of 20.48% was achieved. Similarly, there was a reduction in the number of average queued vehicles per link, total fuel consumption per link, and total CO₂ emissions per link of 21.63%, 2.56%, and 3.75% respectively. These results indicate that the SH controller effectively reduces vehicle delay, fuel consumption, and CO₂ emissions on the freeway links.

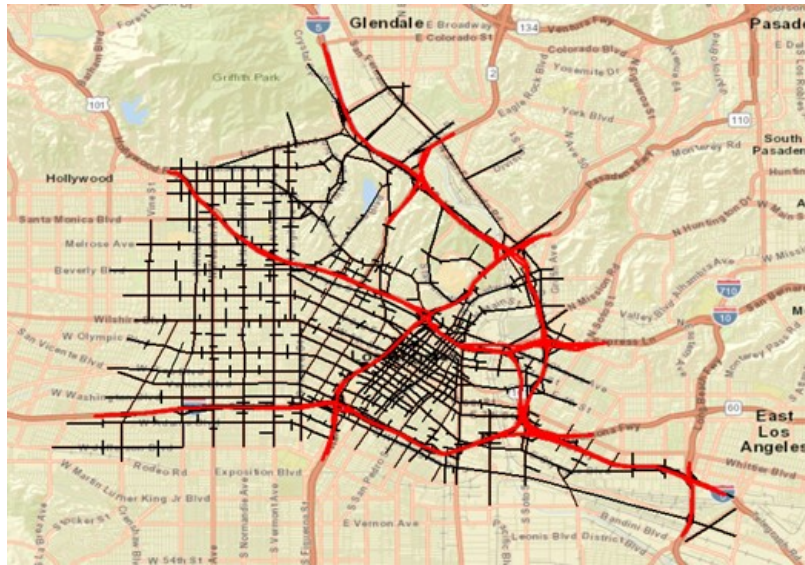


Figure II.1.5.3 LA Network - Speed Harmonization Logic Test Network (LA Network)

Table II.1.5.1 Average Freeway Benefits of Speed Harmonization Logic

	Base	SH	Improvement (%)
Average Travel Time (s/veh)	41.99	33.39	20.48
Average Queued Vehicles (veh/link)	17.09	13.39	21.63
Total Fuel Consumption (L/link)	297.29	289.67	2.56
Total CO ₂ Emissions (grams/link)	615800	592710	3.75

The team also extended our sliding mode strategic speed controller to make it more robust. Robustness is the insensitivity of the controller to non-designed effects, such as disturbances, measuring noise, unmodelled dynamics etc. The typical structure of a robust controller is composed of a nominal component, similar to a feedback linearizing or inverse control law, and additional terms aimed at dealing with model uncertainty. In the developed robust nonlinear controller, the controller is designed based on the consideration of both the nominal model and some characterization of the model uncertainties. The developed speed harmonization–based sliding mode controller was applied on freeways in the downtown LA network. The simulation results at 100% level of market penetration (LMP) of CVs showed a significant reduction in travel time (12.66%), total delay (21.27%), stopped delay (36.20%), and CO₂ emissions (2.97%). The team is currently running more simulations to test the developed controller at different LMPs and various seeds.

The team also investigated the performances of the Eco-CACC-I controllers with signal optimization using the LA network. A simulated network with two signalized intersections was tested to compare the system performance under six scenarios, as summarized in Table II.1.5.2. Compared to the basic case, the signal optimization in scenario 2 reduced fuel consumption by 17.7%. The study found that the combination of the Eco-CACC-I controller and signal optimization further reduced the fuel consumption. In particular, scenario 6 produced the maximum fuel reduction of 23.4%. We also found that the Eco-CACC-I 1S and multi-signal (MS) controllers produced very similar results by reducing fuel consumption, traffic delay and vehicle stops, but the computation speed of the Eco-CACC-I 1S controller outperformed the Eco-CACC-I MS controller. Therefore, the Eco-CACC-I 1S controller may be a better option for a large simulation network since it does not add too much computational cost. The test results also show that scenario 5 produced the most savings in traffic delay of 69.5%, and that scenario 6 can greatly reduce vehicle stops (63.8% reduction).

Table II.1.5.2 Test Results of the Eco-CACC-I Controllers with Signal Optimization

Scenarios	Fuel (liter)	Fuel Reduction (%)	Delay (s)	Delay Reduction (%)	Stops	Stop Reduction (%)
S1: Basic	0.175		79		1.6	
S2: Optimization	0.144	-17.7	31.4	-60.3	1.02	-36.3
S3: Eco-CACC-1S	0.162	-7.4	61.8	-21.8	0.97	-39.4
S4: Eco-CACC-MS	0.161	-8.0	77.9	-1.4	0.66	-58.8
S5: Eco-CACC-1S + Optimization	0.136	-22.3	24.1	-69.5	0.62	-61.3
S6: Eco-CACC-MS + Optimization	0.134	-23.4	31.9	-59.6	0.58	-63.8

The team investigated the impacts of a developed platooning logic on the LA network considering only platoons of ICEVs. Platooning is only activated on the highway stretches. For this test, an LMP of 100% was selected. The platooning logic was combined with a multi objective routing option. The findings suggest that platooning essentially results in lower fuel consumption for all the vehicles in the network even though platooning is applied only on limited stretches. Various simulations were performed using only one single seed. Various platooning configurations (detailed in Table II.1.5.3) were tested. The study utilized a limited platoon which had, on average, 25 vehicles. The RPA car-following model and collision avoidance system [1] was used for all vehicles including platooned and non-platooned vehicles. For the multi-objective routing, an update frequency of 900 s was considered. The results associated with these configurations are presented in Table II.1.5.4, which shows the average travel time, delay, and fuel consumed for all the vehicles. The results suggest a slight reduction of the consumed fuel for all the vehicles traversing the network at a cost of an increase in travel time and delays. We can therefore conclude that the efficient movement of a subset of vehicles inside a large network leads to an improved mobility for the whole network.

Table II.1.5.3 Tested Platooning Configurations

Configuration	Lanes	Platoon Length
1	All	Limited
2	All	Unlimited
3	1	Unlimited
4	1	Limited
5	2	Limited

Table II.1.5.4 Platooning Test Results with Multi-objective Routing

ID	Vehicle Count	Travel Time (s)	Delay (s)	Fuel (l)	Travel Time Change %	Delay Change %	Fuel Change %
No Platooning	143756	762.57	297.06	0.7453			
1	143755	821.18	327.79	0.6070	7.69	10.35	-18.56
2	143755	873.41	369.12	0.7226	14.53	24.26	-3.05
3	143756	802.42	312.03	0.7654	5.22	5.04	2.70
4	143755	794.53	311.83	0.7362	4.19	4.97	-1.22
5	143754	760.30	283.35	0.6711	-0.30	-4.62	-9.96

Conclusions

This project develops a novel Eco-CAC system that integrates VD control with CAV applications. The project includes eight primary tasks and their associated sub-tasks. The research team is currently testing and evaluating the developed Eco-CAC system. In particular, we have implemented the developed eco-routing system, the strategic control application, the Eco-CACC-I algorithm, and the Eco-CACC-U algorithm into a microscopic simulation environment to quantify the energy and environmental impacts of the developed technologies in mixed traffic containing Eco-CAC-equipped and non-equipped vehicles. The team developed simulation scenarios for the proposed CAV applications and is starting to conduct the simulation runs. The simulation scenarios include technology penetration rates ranging from 1% to 100% along with different congestion levels (low, medium, and high).

Key Publications

1. Bichiou, Y., Rakha, H., A., and Abdelghaffar, H. Simple Cooperative Platooning Controller for Connected Vehicles. ArXiv, <https://arxiv.org/abs/2008.04650>.
2. Bichiou, Youssef, and Hesham Rakha. Vehicle Platooning: An Energy Consumption Perspective. No. DOE-VT-0008209-C08. Virginia Polytechnic Institute and State University, Blacksburg, VA., 2020.
3. Chen H. and Rakha H.A. Developing a Hybrid Electric Vehicle Eco-Cooperative Adaptive Cruise Control System at Signalized Intersections. Accepted for presentation at the Transportation Research Board (TRB) 100th Annual Meeting, Washington DC, Jan. 25–29, 2021 [Paper: TRBAM-21-02674].
4. Ahn, K., Bichiou, Y., Farag, M., and Rakha, H.A. Multi-objective Eco-Routing Model Development and Evaluation for Battery Electric Vehicles. Accepted for presentation at the Transportation Research Board (TRB) 100th Annual Meeting, Washington DC, Jan. 25–29, 2021 [Paper: TRBAM-21-00565].
5. Chen, Hao, and Hesham A. Rakha. "Battery Electric Vehicle Eco-Cooperative Adaptive Cruise Control in the Vicinity of Signalized Intersections." *Energies* 13, no. 10 (2020): 2433. <https://doi.org/10.3390/en13102433>.
6. Abdelghaffar H., Elouni M., Bichiou Y., and Rakha H.A. "Development of a Connected Vehicle Dynamic Freeway Sliding Mode Variable Speed Controller." *IEEE Access*, pp. 1–8, 2020. <https://doi.org/10.1109/ACCESS.2020.2995552>.
7. Ahn, Kyoungcho, Hesham A. Rakha, and Sangjun Park. "Eco Look-Ahead Control of Battery Electric Vehicles and Roadway Grade Effects." *Transportation Research Record* (2020): 0361198120935445. <https://doi.org/10.1177/0361198120935445>.

8. Ahangari S., Jeihani M., Chen H., and Rakha H.A. “Investigating the Impact of an Eco-Speed-Control System for Hybrid Electric Vehicles on Driver’s Behavior using a Driving Simulator.” *International Journal of Current Research* (2020).

References

1. Rakha, H., P. Pasumarthy, and S. Adjerid, *A simplified behavioral vehicle longitudinal motion model*. Transportation Letters: The International Journal of Transportation Research, 2009. **1**(2): p. 95–110.

II.1.6 Evaluating Energy Efficiency Opportunities from Connected and Automated Vehicle Deployments Coupled with Shared Mobility in California (UCR, NREL)

Matthew Barth, Principal Investigator

University of California, Riverside – CE-CERT
 1084 Columbia Avenue
 Riverside, CA 92507
 Email: barth@cert.ucr.edu

Prasad Gupte, DOE Technology Manager

U.S. Department of Energy
 Email: prasad.gupte@ee.doe.gov

Start Date: October 1, 2017
 Project Funding: \$1,207,460

End Date: March 31, 2020
 DOE share: \$1,094,578

Non-DOE share: \$122,882

Project Introduction

With the rapid growth of information and communication technologies, Connected and Automated Vehicles (CAVs) are deemed to be disruptive with the potential to significantly improve overall transportation system efficiency, however, may increase vehicle miles traveled (VMT). Further, shared mobility systems are another disruptive force that is reshaping our travel patterns, with the potential to reduce VMT. The goal of this project was to extensively collect data from vehicles and associated infrastructure equipped with CAV technologies from both real-world experiments and simulation studies mainly deployed in California, and develop a comprehensive framework for evaluating energy efficiency opportunities from large-scale (e.g., statewide) introduction of CAVs and wide deployment of shared mobility systems under a variety of scenarios. To quantify the combined impact of CAV and shared mobility on travel behavior, traffic performance and energy efficiency, a mesoscopic simulation-based model was developed for mobility and energy efficiency evaluation considering the disruptive transportation technologies.

Objectives

As a complement to existing studies on nationwide evaluation of CAV energy impacts, this project focused on data collection efforts and CAV applications under congested traffic environments that are frequently experienced on a massive scale across the major metropolitan areas in California. Another key component of this project considered the interaction between different CAV technologies and shared mobility models, and the compound effect on energy efficiency. The outcomes from this project have helped close the knowledge gap on recognizing the potential energy impacts of a broad (regional or statewide) deployment of CAV technologies across a wide range of roadway infrastructure with varying levels of congestion and different penetration rates of shared mobility systems. In addition, the results from this project can be used to support policymakers in steering CAV development and deployment, coupled with shared mobility systems, in an energy-favorable direction. To realize these outcomes, the specific objectives of this project included:

- Data collection from both real-world implementations (including experiments, demonstrations, and early deployments) and simulation studies of CAV technologies mainly in California. The real-world data were used to model the energy efficiency from each individual CAV technology with a small fleet of equipped vehicles, while simulation data will facilitate the analysis of aggregated effects on traffic with multiple CAV technologies concurrently deployed.
- Model implementation for quantifying the impacts of CAV technologies on energy intensity (e.g., energy consumption per unit distance for different driving conditions) and for quantifying the amount of driving (measured by vehicle miles traveled or VMT) represented by each driving condition. The

models included the consideration of vehicle class, roadway type, level of traffic, penetration rate, and level of vehicle automation.

- Developing a regional or statewide energy inventory under various CAV technology deployment scenarios by incorporating datasets and models for predicting vehicle market share and vehicle usage which are tightly associated with the penetration of shared mobility systems.

Approach

This research project was divided into three phases. The first phase (data collection and processing) and second phase (model implementation) have been completed in FY18 and FY19. In FY20, the research team completed the last phase of this project.

Phase III – Energy Impact Evaluation

Framework Development

In this phase III effort, we designed and carried out simulation-based numerical experiments to estimate the system-wide impact of CAVs and shared mobility and to evaluate the energy efficiency opportunities from CAV deployments in California. The models developed in previous phases have been integrated into the framework illustrated in Figure II.1.6.1. As the simulation engine, *BEAM* loads all types of input data from different sources, including activity-travel patterns, the mode choice model, and the *RouteE* model. To provide high resolution activity input data for the *BEAM* model, *Popgen* was applied to generate socio-economic characteristics for each person and for each household in the area, the Southern California Association of Governments (SCAG) travel demand model was used to estimate the transportation system level of service for each origin-destination pair, and the *CEMDAP* model was employed to simulate daily activities and travel patterns of all individuals in the region. The modified fundamental influencing factor (FIF) mode choice model was integrated into *BEAM* to enable refined and defensible estimation of travelers’ mode choice preferences in the study area when faced with hypothetical future CAVs and shared mobility scenarios. The *RouteE* model receives the link-by-link activity output from *BEAM* to estimate the energy use for a certain vehicle route, which can be further utilized to estimate the energy consumption at any scale.

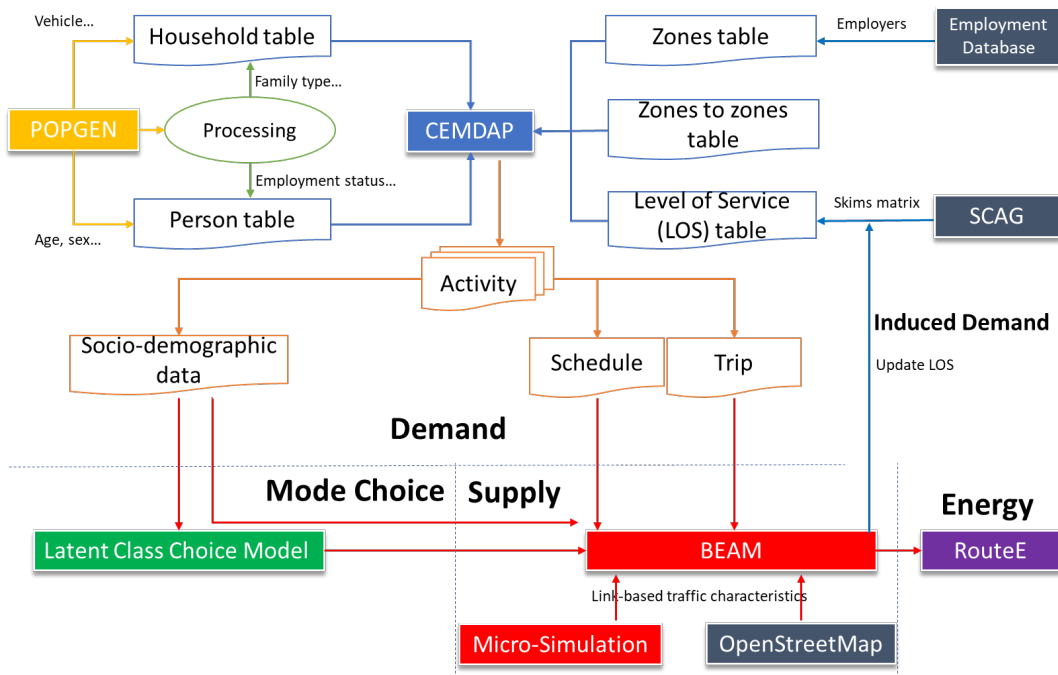


Figure II.1.6.1 Model Framework

Scenario Design

Based on the calibrated Riverside *BEAM* model, we designed scenarios to study the joint impact of CAVs and shared mobility. Note that “CAV” is a broad concept which may either refer to the cooperative automated driving technology, or the operation/business model facilitated by the technology. The scenarios have been designed to capture the potential impact of CAVs on: 1) mobility (e.g., link capacity increase); 2) system-level energy consumption; and 3) in-vehicle time utilization coupled with mode choice shift. We also examine the potential cost savings for a shared autonomous vehicle (SAV) fleet, and the potential VMT increase associated with deploying AVs without regulation. We do not directly use “CAV” and “shared mobility” as two dimensions to define scenarios, due to the overlapping area of two terms, e.g., SAV. Instead, we use terms “penetration rate of CAV technology” and “operation model of shared fleet” to disengage the technology and operation aspects of new mobility modes. Although there is correlation between the CAV technology and its operation/business model, we cannot assert that a certain penetration rate of CAV technology will always lead to a certain level of operation/business model, and vice versa. Therefore, we designed nine different future scenarios in terms of penetration rate of CAV technology and operation model of shared fleet to cover all possible combinations. The CAV technology penetration rate has three levels, low (L), medium (M) and high (H). At a low level, the penetration rate is 0% according to the current situation in City of Riverside. The CAV technology penetration rate is assumed to be 40% at medium level, and 80% at high level. We also defined operation model of shared fleet by three levels: baseline (B), popular (P) and dominant (D). Baseline level corresponds to the current operation model, penetration rate, and pricing plan of ride-hailing companies. Popular level still assumes ride-hailing vehicles are driven by human-drivers with same pricing plan, but with a higher ride hailing penetration rate. The dominant level assumes the human-drivers are ultimately replaced by shared autonomous vehicles (SAVs), which causes dramatic reduction on the cost and increase on the penetration, e.g., up to 20% of the entire vehicle population.

Statewide Energy Evaluation Model

A clustering-extrapolation model was developed to link the *BEAM* simulation with state-level energy efficiency results, considering the impact of CAVs and shared mobility. As described above, *BEAM* is a mesoscopic simulator which has been designed to realistically represent network level demand-supply dynamics. The outputs from the *BEAM* simulation along with the *RouteE* module provide a good summary of the mobility and energy statistics for given CAV and shared mobility scenarios at a regional level. However, it is difficult, if not impossible, to represent all the details of a mesoscopic model at the state-level. On the other hand, the 2017 National Household Travel Survey (NHTS) California data provides a diverse sample of socio-demographic and trip data from a total of 26,095 households in California. Based on the *BEAM* model and NHTS dataset, the research team developed an approach to extract information from the highly detailed regional level model and extrapolate it to the state level. In *BEAM*, the energy consumption per person was calculated based on the energy consumption estimates and occupancy information provided in the events file. Agent socio-demographic and household attributes are stored in different files in the *BEAM* setup. Some of the network-related attributes are found in the *BEAM* network definition. Using *BEAM* activity data and agent’s socio-demographic characteristics in the City of Riverside, a decision tree-based clustering and prediction model was employed to classify the modal shift types in the NHTS samples. Finally, a synthetic population of the state was generated using the NHTS samples and census level survey data. The estimated energy savings per person was then applied on the synthetic population to estimate the overall statewide energy savings.

Results

Impact Evaluation on Travel Behavior

We first evaluated the travel behavior results from the nine *BEAM* scenarios described above. In Figure II.1.6.2(a), we show the mode distribution of three mode groups: ‘private cars’, ‘ride-hailing’ (including single-occupancy ride-hailing and pooling) and ‘other’ modes. The other group includes walking, biking, and transit use modes. Here we use the combination of initials of the CAV technology level and operation model of shared fleet as the name of the scenario, e.g., L-B as Low (CAV penetration), -Baseline (shared fleet), M-P as

Medium-Popular, and H-D as High-Dominant. As shown in the figure, the mode choice distribution is sensitive to the ride-hailing penetration and operation model, but is not sensitive to the level of CAV technology. From baseline level to popular level, the share of ride-hailing doubles from 6.7% to 12.9%. Over half of the non-motorized travelers switch his/her mode during this transition. From popular level to dominant level, the percentage of ride-hailing reaches 60%. As the share of non-motorized travelers stays at the same level in this transition, the results suggest that over half of the private car drivers switches to ride-hailing in the SAV era. Next, we evaluated the VMT change at various CAV and shared mobility levels. As the empty trip rate of ride-hailing is significantly underestimated in the *BEAM* model, we assume a 40% empty-trip rate for all the ride-hailing vehicles according to the existing research, and generate an adjusted VMT distribution. Figure II.1.6.2(b) shows the adjusted VMT results, with a significant increasing trend in terms of the popularity of ride-hailing. From the baseline level to popular level, the VMT increases by 14%. For SAV scenarios, the VMT has a 36% significant increase over the baseline cases. Note that empty trips take about one third of VMT in the adjusted distribution as shown in Figure II.1.6.2(b), which is the main reason causing the VMT increase.

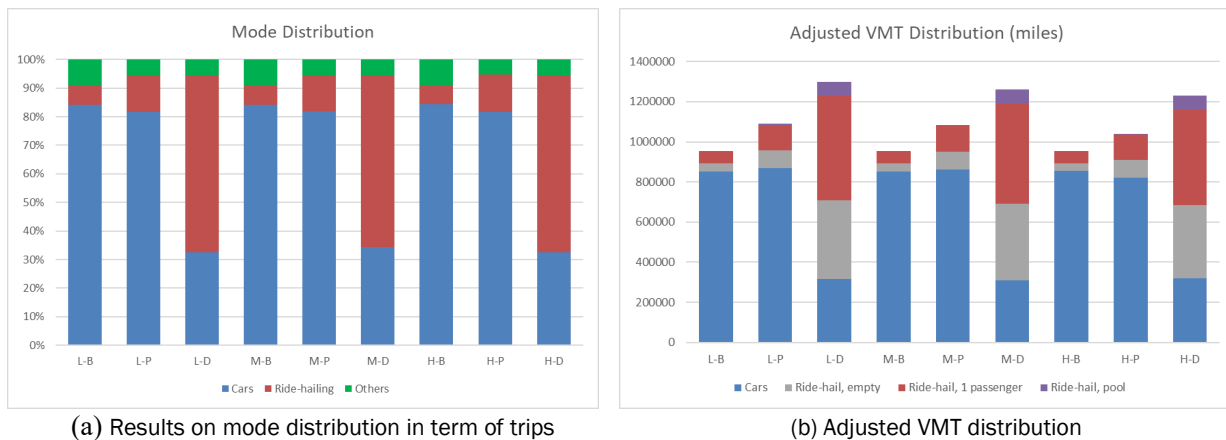


Figure II.1.6.2 Impact Evaluation on Travel Behavior

Impact Evaluation on Mobility

In Figure II.1.6.3, we use a 3D histogram plot to show the average speed for all the vehicle-based trips. Here the average speed is defined as the total trip length from car trips or ride-hailing based travelers divided by the total trip travel time from those travelers. This measure can represent the mobility performance of the road network. Due to the improved link capacity, the scenarios with higher CAV penetration have higher average speed in general. When increasing the CAV penetration rate from 0 to 80%, the average speed of baseline, popular and dominant level scenario increases by 2%, 28% and 21%, respectively. In contrast, ride-hailing and ridesharing would likely cause additional delay when keeping the CAV penetration fixed, as increased VMT would degrade the network performance, and increased pooling ratio would also bring additional pick-up/drop off delays in ridesharing. The ride-hailing induced delay is more significant at lower CAV penetration rates, i.e., the average speed reduces by 28%. At higher CAV penetration, the speed gap shrinks to 11%.

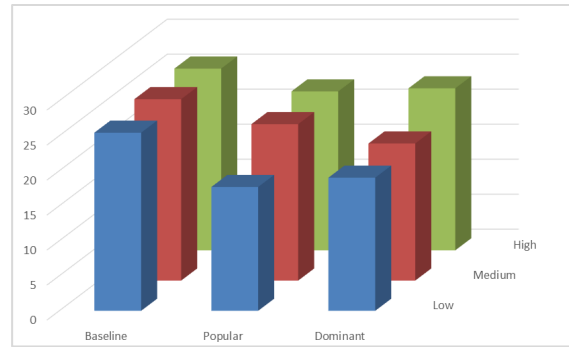


Figure II.1.6.3 Speed Histogram in a 3D View (Unit: Mph)

The ride-hailing waiting time is another performance measure in our mobility analysis. According to the results, the average waiting time is 298s for the baseline ride-hailing scenarios, and 226s for both the popular and dominant scenarios. Figure II.1.6.4 shows the ride hailing waiting time histograms for two typical scenarios—baseline, low CAV case in (a) and SAV, High CAV case in (b). In the baseline case, most passengers have to wait for over 5 minutes. In the SAV case, over a half of the passengers only need to wait for 2 minutes, as the penetration rate of ride-hailing service is higher in this scenario. By observing the distribution of trip number in a day, the SAV scenario reaches its peak volume at 6am, while the baseline scenario reaches its peak volume at noon time. This difference shows that the ride-hailing vehicles mainly serve non-commute trips in the current scenario, but SAVs will be as competitive as private cars for commute trips.

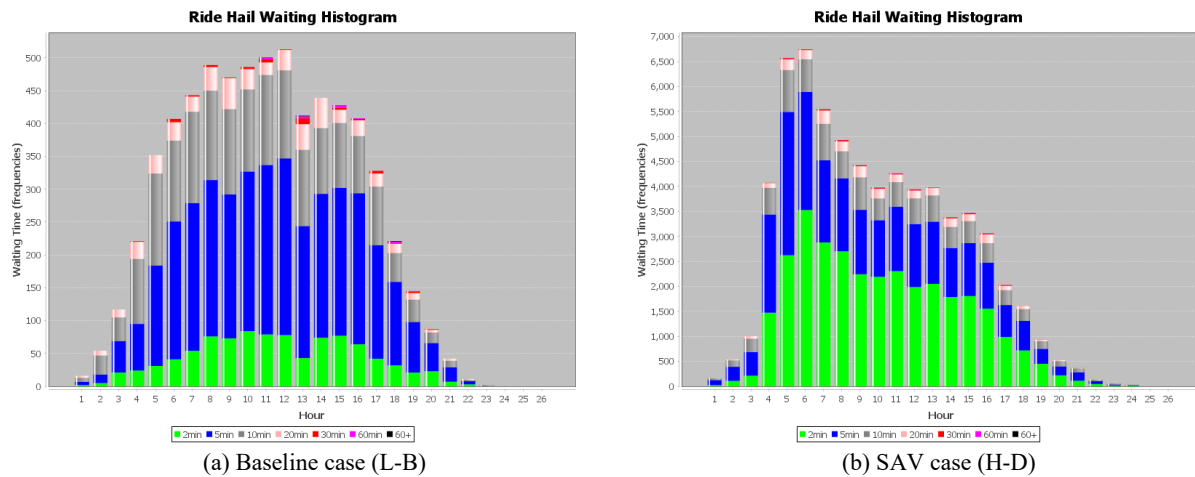


Figure II.1.6.4 Ride-Hail Waiting Time Histogram

Impact Evaluation on Energy

The system level energy consumption is determined by two groups of impact factors: 1) modal activity-related factors including VMT and link speeds, and 2) energy intensity related factors including *RouteE* CAV model and vehicle type composition. In *BEAM*, passenger cars and ride-hailing cars have different vehicle type composition in this simulation, e.g., they typically have higher penetration of electric vehicle (EV) and hybrid vehicle rate for ride-hailing cars. Figure II.1.6.5(a) shows the histogram of energy consumption for the City of Riverside network. On average, the popular and dominant ride-hailing scenarios consume 6% more energy than the baseline scenarios at the same CAV technology penetration rate. With the increase of CAV penetration rate, the energy consumption is reduced by 2% at 40% level, and then by additional 2% at 80% level. Figure II.1.6.5(b) shows an alternative scenario assuming the private cars have the same EV composition as the ride-hailing vehicles due to successful development and promotion of vehicle electrification technology. Then the impact of CAVs and ride-hailing is more significant. Compared with the baseline scenario (L-B), high penetration of CAV only (H-B) would reduce the energy consumption by 4%, and SAV only (L-D) would increase the energy consumption by 40%. The combination of the two (H-D) will consume 29% more energy than the baseline.

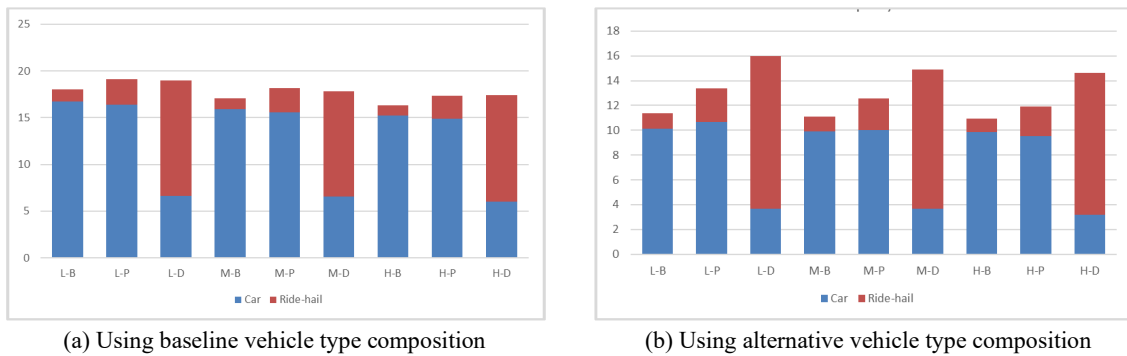


Figure II.1.6.5 Energy Consumption for the City of Riverside Network (Unit: Kwh Per Capita)

Statewide VMT and Energy Analysis

Using the NHTS sample data, we illustrated the mode-specific VMT per capita at the state-level. As CAV technology penetration has little impact on VMT, we only show the impact of ride-hailing and SAVs in Figure II.1.6.6(a). According to the NHTS sample data, non-motorized and public transit modes (labeled as “Others”) have high percentage in trip number, but the average distance per trip is much smaller than the private cars and taxi (including ride-hailing vehicles). In the popular ride-hailing scenario, the share of non-motorized and public transit modes is significantly dominated by private cars and ride-hailing. For the SAV scenario, shared autonomous fleets take over 70% of trips, with over 80% of VMT when considering addition mileage introduced by deadheading. To estimate the impact of CAV and shared mobility on energy in California, we first derived the average energy consumption rate for each vehicle types model under different CAV technology penetration rate from *BEAM-RouteE* model. Then the energy rates are then applied to the estimated VMT to calculate the state-level light duty-vehicle energy consumption. In Figure II.1.6.6(b), for each CAV penetration, the energy consumption per capita first increases slightly as non-motorized and public transit modes are replaced by cars and ride-hailing vehicles. It then drops in the dominant scenario due to the high percentage of EVs in the SAV fleet.

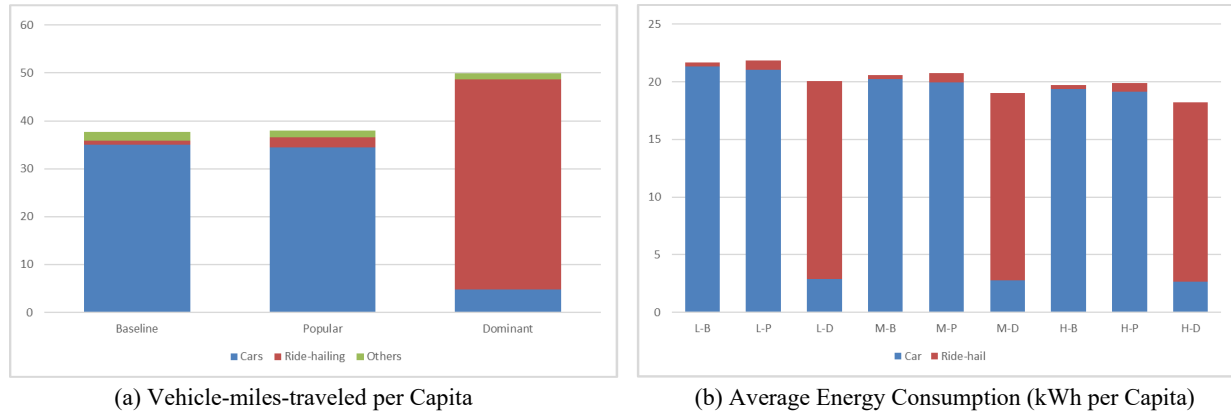


Figure II.1.6.6 Statewide VMT And Energy Analysis

Conclusions

In this project, we have created an extensive real-world data set for CAVs and shared mobility systems, and are able to model a variety of energy scenarios that vary with a variety of factors: 1) different vehicle types and fuel/powertrain technologies, 2) combinations of CAV applications, 3) various levels of automation, 4) roadway characteristics, and 5) traffic conditions. The outcomes from this project go a long way to close the knowledge gap on recognizing the potential performance and energy impacts of a broad deployment of CAV and shared mobility technologies across a wide range of roadway infrastructure with varying levels of congestion. This is useful to: 1) support policymakers in steering CAV development and deployment in an energy favorable direction; 2) increase the confidence of CAV technology investors both on the infrastructure side (i.e., transportation agencies) and on the vehicle side (i.e., OEMs); and 3) expedite the deployment of promising CAV and shared mobility applications.

Key Publications

1. D. Oswald, G. Scora, N. Williams, P. Hao and M. Barth, "Evaluating the Environmental Impacts of Connected and Automated Vehicles: Potential Shortcomings of a Binned-Based Emissions Model," *2019 IEEE Intelligent Transportation Systems Conference (ITSC)*, Auckland, New Zealand, 2019, pp. 3639–3644.
2. P. Hao, C. Wang, G. Wu, S. Tanvir, B. Sun, J. Holden, A. Duvall, J. Gonder, and M. Barth, "Evaluate the System-Level Impact of Connected and Automated Vehicles Coupled with Shared Mobility: An Agent-based Simulation Approach," accepted by TRB 2021 Annual Meeting, Washington, D.C.

Acknowledgements

This research is supported by Department of Energy Vehicle Technologies Office, under the Energy Efficient Mobility Systems (EEMS) Program. The authors would like to thank Colin Sheppard, Dr. Tom Wenzel and the BEAM development team for their support on BEAM model.

II.1.7 Boosting Energy Efficiency of Heterogeneous Connected and Automated Vehicle (CAV) Fleets via Anticipative and Cooperative Vehicle Guidance (Clemson University)

Ardalan Vahidi, Principal Investigator

Clemson University
208 Fluor Daniel Building
Clemson, SC 29634-0921
Email: avahidi@clemson.edu

Yunyi Jia, Co-Principal Investigator

Clemson University International Center for Automotive Research (CU-ICAR)
4 Research Drive
Greenville, SC 29607
Email: yunyij@clemson.edu

Beshah Ayalew, Co-Principal Investigator

Clemson University International Center for Automotive Research (CU-ICAR)
4 Research Drive
Greenville, SC 29607
Email: beshah@clemson.edu

Dominik Karbowski, Co-Principal Investigator

Argonne National Laboratory
9700 South Cass Avenue, #362
Lemont, IL 60439
Email: dkarbowski@anl.gov

Prasad Gupte, DOE Technology Manager

U.S. Department of Energy
Email: prasad.gupte@ee.doe.gov

Start Date: September 1, 2018
Project Funding: \$1,343,193

End Date: April 31, 2020
DOE share: \$1,159,987

Non-DOE share: \$183,206

Project Introduction

This project introduces novel anticipative car following and lane selection schemes for Connected and Automated Vehicles (CAVs). Our control schemes benefit from collaboration and information exchange between CAVs to save energy, reduce braking, and harmonize traffic. The proposed schemes will be implemented in traffic microsimulations at different levels of CAV penetration to analyze energy saving benefits. We will create a Vehicle-in-the-Loop (VIL) testbed to demonstrate the benefits to real CAVs driven on a test-track. Clemson has partnered with Argonne National Laboratory to integrate the vehicle guidance algorithms with Autonomie, Argonne's detailed vehicle energy utilization simulation software. Clemson has partnered with PTV to incorporate the proposed algorithms in their state-of-the-art traffic micro-simulation tool, VISSIM. Clemson has also partnered with the International Transportation Innovation Center (ITIC) to conduct experiments for evaluating the proposed technical approach with novel co-simulations of traffic and physical automated vehicles on a test track in Greenville, South Carolina.

Objectives

The three main objectives of the project are:

1. Developing anticipative vehicle guidance algorithms including perception and prediction of motion of surrounding vehicles. Designing the car following and lane selection algorithms to demonstrate >5% efficiency gain in mixed traffic with 30% CAV penetration. Generating the corresponding custom code for PTV VISSIM Traffic Microsimulation.
2. Detailed energy evaluation using high-fidelity powertrain models of heterogeneous vehicles to demonstrate >5% (10%) average efficiency gain in mixed traffic for CAV penetration >30% (60%).
3. Vehicle instrumentation and experimental testing via Vehicle-in-the-Loop (VIL) platform. Demonstrating stable co-simulation of two experimental vehicles and <10 virtual vehicles and document >5% average energy efficiency gains for the entire fleet. Documenting >5% additional average efficiency gain resulting from collaborative driving.

Approach

Anticipative Car Following Scheme

A combined probability modeling and Model Predictive Control (MPC) system is employed to boost the energy efficiency of CAVs. MPC consumes a preview of disturbances and optimizes a modeled system over a finite time horizon. In mixed traffic, CAVs using MPC communicate their intentions to other CAVs, and must predict using current and historic sensed data when interacting with human-driven vehicles. Chance constraints account for uncertainty as described in [3]. The cumulative distribution function of surrounding vehicle position is inverted to obtain the safe distance needed to avoid a collision with some safe probability. To avoid excessive conservatism and take advantage of closed-loop disturbance rejection, the safe probability decays linearly over prediction from 99.9% one step ahead to deterministic at the end of the prediction horizon — as in Figure II.1.7.1.

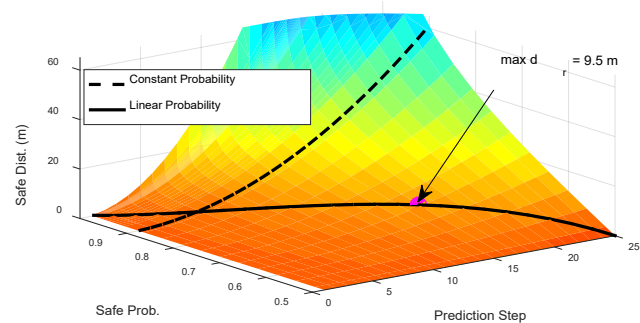


Figure II.1.7.1 Inverse Probability Density Function of Position

Single-Lane Collaborative Guidance

Centralized and collaborative approaches to connected and automated driving in a single lane were explored in collaboration with IFP Energies nouvelles. Compared to the multilane collaborative guidance, this single-lane research included more baseline algorithms, took a different approach to distributed collaboration, and more closely examined string effects. Three optimal control approaches were studied: Decentralized Hierarchical Control (DHC) where each vehicle considers only itself during optimization, Centralized Hierarchical Control (CHC) where a single leader solves for and commands the others' control moves, and Cooperative Hierarchical Control (CoHC) where each vehicle solves for its own control move while considering its neighbors in the string. The term hierarchical here refers to a control architecture where an efficient traffic-free trajectory is first computed for the whole trip, then used as a guideline for a receding horizon controller that is responsible for avoiding collisions. Publication [7] describes these and the baseline algorithms in more detail.

Multi-Lane Collaborative Guidance

Techniques for improving the collective performance of groups of CAVs on multilane roads were developed in a collaboration with IFP Energies nouvelles. The previously described multilane guidance algorithm shares intentions between CAVs that solve sequential optimal control problems (OCPs), with the solution depending on the computation order. In a new distributed approach, the CAVs share their sensitivity to constraints in order to dynamically select computation orders that reduce collective cost. Centralized optimization where one

lead agent solves a unified OCP and dictates other agents' solutions was also prototyped as a high-performing benchmark. Publication [6] and the 2019 Annual Report describe these algorithms in detail.

Anticipative Lane Selection Scheme

The NLP-based anticipative lane selection scheme (from 12) presented in the 2019 annual report was expanded to utilize two different methods for references speed assignment [10]. We call the methods rule-based speed assignment (RBSA), and harmonization-based speed assignment (HSA). The overall control framework for the two methods is outlined in Figure II.1.7.2. The RBSA technique utilizes measurements of vehicles within the field of view (FOV) of the connected and automated vehicle (CAV), to assign the lane reference speed to be the velocity of the slowest relevant neighboring object vehicle (OV). We define a relevant neighboring OV as a vehicle that is behind and traveling faster, or ahead and traveling slower than the CAV. The HSA technique, on the other hand, assigns the lane reference speed based on an estimate of the average speed in that given lane. The average speed on a lane is estimated by taking the average velocity of vehicles in the given lane and FOV of the CAV and then combining this, through a weighted average, with shared average velocities from communicating CAVs. For more details on both methods, the reader is directed to [10]. Results of extensive microsimulations comparing the two methods will be presented in the results section.

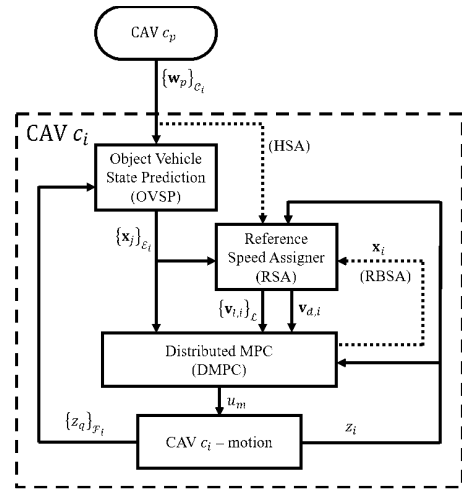


Figure II.1.7.2 Block Diagram of the Optimal Lane Selection NLP Distributed MPC Framework

Another research question that we dealt with, was whether optimal lane selection had a significant positive impact on the overall performance of mixed traffic. To do this, we performed additional microsimulations comparing mixed traffic with either CAVs that are controlled with a 2-dimensional maneuver planning MPC, or a 1-dimensional longitudinal MPC with rule-based lane selection. As the differentiating component of the two types of CAVs was their lane selection method, we designate them as optimal lane selection (OLS) CAVs, or rule-based lane selection (RBSL) CAVs. The OLS CAVs utilized the complete control framework from [9] and [10],[11], while the RBSL CAVs only applied the longitudinal control action, and utilized the built in rule-based lane selection algorithm of PTV VISSIM [26]. A summary of results for this study are presented in the results section of this report, for more detail and a complete discussion of the results please see [11].

Vehicle-in-the-Loop Testbed and On-Road Energy Consumption Estimation

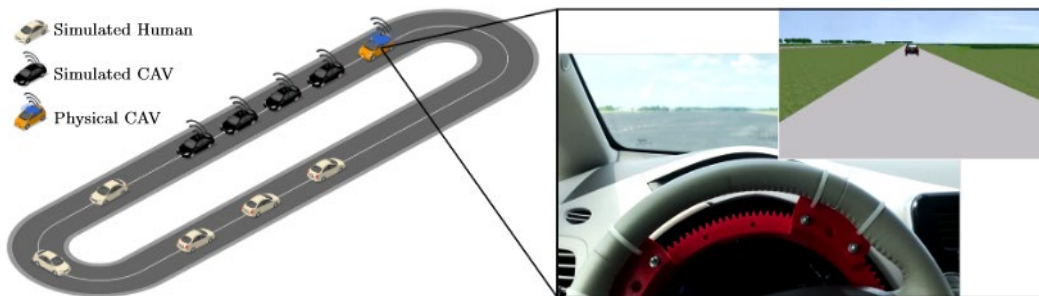


Figure II.1.7.3 Vehicle-in-the-Loop Simulations: Physical Vehicle Integrated in a String of Vehicles in VISSIM

We have constructed a VIL testbed at ITIC test track where our two real CAVs interact with virtual traffic in the VISSIM simulation, as shown in Figure II.1.7.3. The EPA US06 and EPA UDDS drive cycles were also

used in separate simulations to set the velocity profile of the simulated preceding vehicle, where the velocity trajectories of the cycles were scaled down by 40% and 15%, respectively because of the speed limits at the test track.

The energy consumption of experimental CAVs are estimated via On-Board Diagnostics (OBD-II) port accessed by our iOS application [18],[19]. We use a flow meter [20] to verify and calibrate our OBD-based fuel rate estimations on a chassis dynamometer. In order to conduct VIL verifications for the combustion engine vehicle, we ran the test vehicle on a chassis dynamometer following a preceding vehicle to characterize the full scope of the engine performance (Figure II.1.7.4). For each chassis dynamometer test, fuel volume was measured outside the vehicle and a flow meter was used throughout the run to assess dynamic estimation characteristics (see Quarterly Report 10). The energy consumption of experimental CAVs are estimated via On-Board Diagnostics port accessed by our iOS application [18],[19]. We use the flow meter data to verify and calibrate our OBD-based fuel rate estimations on the chassis dynamometer.

Table II.1.7.1 Fuel Flow in Chassis Dynamometer Testing

	Flow Meter		OBDII (basic)	OBDII (calibrated)
Test 1 1 gal (3.79 L)	3.94 liter (+4.0%)		3.60 liter (-5.0%)	3.79 liter (0.0%)
Test 2 2.5 gal (9.46 L)	10.22 liter (+8.0%)		8.58 liter (-9.3%)	8.90 liter (-5.9%)
Test 3 3 gal (11.36 L)	11.51 liter (+1.4%)		10.98 liter (-3.3%)	11.38 liter (+0.2%)

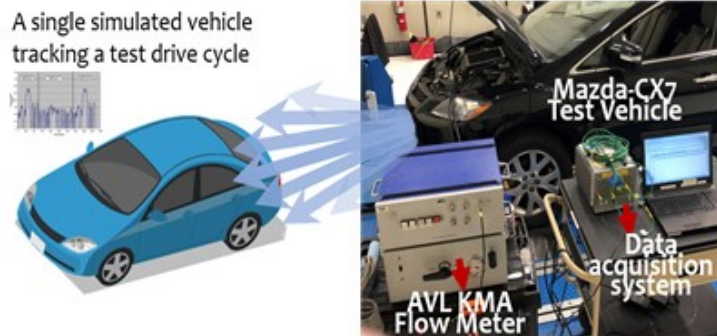


Figure II.1.7.4 Fuel Flow Dynamometer Test Setup

Vehicle-in-the-loop (VIL) Communication Setup

The communication between the physical vehicle and the simulation server has been established using cellular network at ITIC test track and Wi-Fi at chassis dynamometer. In order to apply Dedicated Short Range Communications (DSRC) to our VIL platform, we have successfully configured two iSmartWays On-board Equipment (OBE) [23] and one Road Side Equipment (RSE). We have tested the RSE-OBE communication for tuning the RSE position and measuring the packet reception/dropping rate in 1.2-mile stretch of ITIC test track facility. With 1 Hz broadcast rate and while whole test track is considered, the packet reception rate is 97% and consecutive packet drop probability is 0.1%. For 10 Hz broadcast rate, the packet receptions decline; however, while the test area is limited to the 800 m radius from the RSE, the packet reception probability is around 96% and consecutive packet drop probability is 0%.

Results

PTV VISSIM Traffic Microsimulation Car-Following Results

Realistic microsimulations were set up by imposing headway distributions sampled from highway traffic data on the Wiedemann (WIE) driver model used in VISSIM. Inflow of vehicles are varied to create a variety of traffic demands, and total penetration rate of CAVs in the fleet are varied. Figure II.1.7.5 then shows that, for a conventional SUV fleet, up to 28% fuel improvement can be realized for the whole fleet over the all-WIE driven scenario. We then show that the introduction of CAVs allows for traffic smoothening effects: the cell density plots in Figure II.1.7.6 show natural shockwaves propagating backwards through the network at 2000 veh/hour, which are subsequently dissipated as CAV penetration increases. This included some secondary effects of improved fuel economy for WIE drivers, particularly at high penetration of CAVs. Furthermore, we observe that CAVs drive with significant fuel benefit over WIE drivers in high volume scenarios: we found

between 8% and 33% fuel improvement for the CAVs over WIE drivers. This was the most significant fuel improvement source observed in the network: the majority of CAVs drive more efficiently than WIE drivers, so average fleet fuel performance increased with greater densities of CAVs. Further details are depicted in [8].

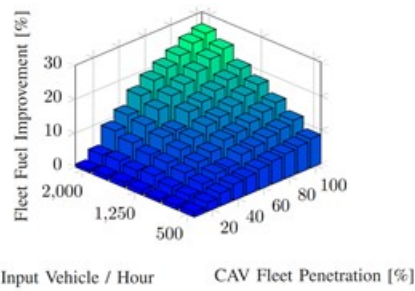


Figure II.1.7.5 Mean Fleet Fuel Efficiency Improvements Over the 0% CAV Case at Each Input Vehicle Volume/Hour

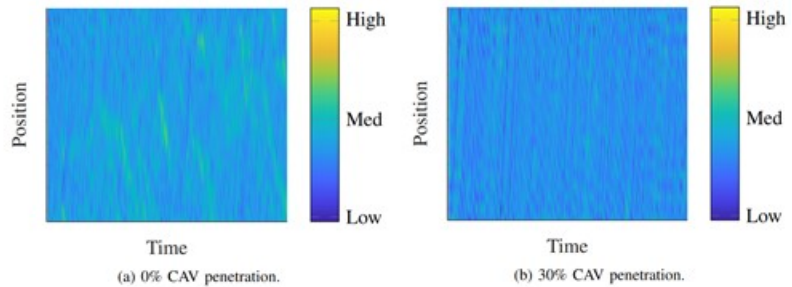


Figure II.1.7.6 Cell Density Plots Showing Dense Groups of Vehicles in the Network at 0%, 30% CAV Penetration. With the Introduction of CAVs, Shockwave Effects Were Dissipated

Finally, a similar study was done on the effects of vehicle powertrain typing and its effect on the energy performance of the fleet. Figure II.1.7.7 shows that the electric and hybridization technologies already realize some of the energy savings potentials of the smoothed driving introduced by the CAVs.

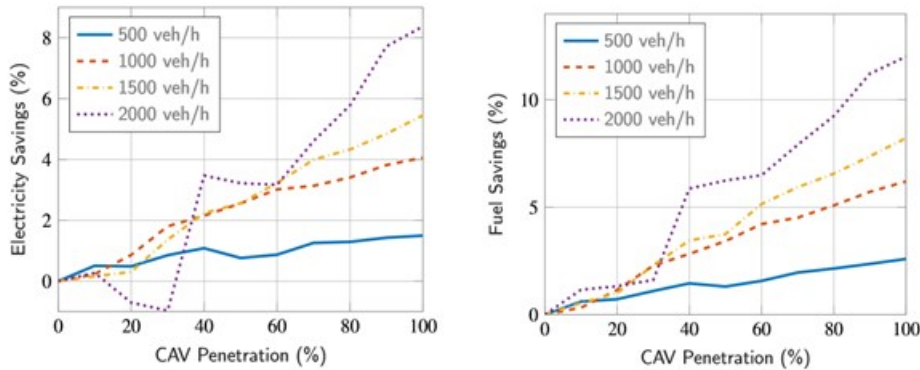


Figure II.1.7.7 Fleet Fuel Efficiency Improvements Over the 0% CAV Case at Each Input Vehicle Volume/Hour for an SUV-Sized Vehicle Electric Powertrain (Left) and Hybrid

Single-Lane Collaborative Guidance

The proposed DHC, CHC, and CoHC approaches were simulated in strings where 8 AVs followed an open-loop leader. This leader tracked either the Worldwide Harmonized Light Vehicles Test Cycle (WLTC) Low or WLTC High. Classical cruise control (ACC) with either 0.8 or 1.5 s time headway along with position constrained shrinking horizon control (PCSHC) were also simulated for comparison. Figure II.1.7.8 shows how the various systems performed in the WLTC Low scenario in terms of electric vehicle (EV) energy consumption and string length, which generally trade off against one another. The hierarchical algorithms outperformed the baselines overall, enabled by trajectory preview that ACC and PCSHC lacked. While the energy benefit of collaborative guidance was relatively small (<2%), the traffic compactness benefit was much greater. This result suggests that decentralized control is sufficient in sparse traffic where longer gaps are acceptable, with higher traffic flow demand revealing the benefits of collaborative guidance. Publication [7] provides additional results, including those obtained using the WLTC High.

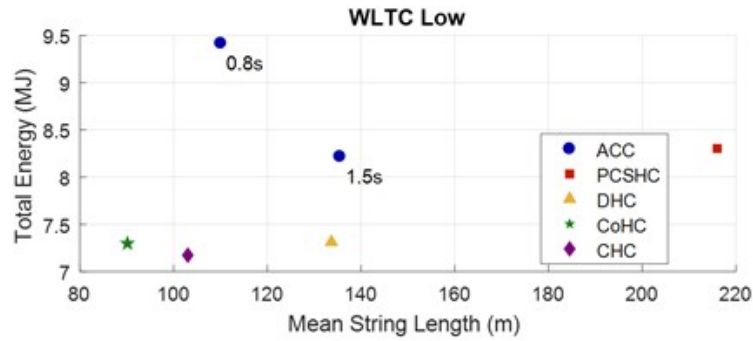


Figure II.1.7.8 Simulated Energy and String Length of 8 Automated Electric Vehicles Trailing a Drive Cycle-Bound Lead Vehicle

Anticipative Lane Selection Scheme (NLP distributed MPC framework)

The simulated traffic network is comprised of a 5000m long straight three-lane link, with a single input node and single output node as shown in Figure II.1.7.9. The input node is located on the left with the direction of travel to the right. For the first 30m of the link, vehicles are restricted from changing lanes, in order to prevent a vehicle from moving directly into the path of a neighboring vehicle that has not yet entered the network. The desired velocities of vehicles were distributed using the default speed distribution in VISSIM with a mean of approximately 87 km/hr.

Simulations were run for 30 minutes of simulation time with CAV penetration rates from 0 to 100% increasing in 10% increments and at low ($Q_L = 2000\text{veh/hr}$), medium ($Q_M = 4000\text{veh/hr}$), and high ($Q_H = 6000\text{veh/hr}$) traffic demands. The network starts the simulation empty, therefore, for evaluation purposes we omit the time from the start of the simulation until the number of vehicles on the network reaches 90% of the maximum observed number of vehicles on the network. We will refer to the remaining simulation time as the evaluation duration. Human driven vehicles (HDVs) are assumed to follow the Wiedemann-99 psycho-spacing car-following model, and the default rule-based lane selection (RBL) algorithm of VISSIM, which was originally developed by Spurmann [26]. For all future discussions, the baseline scenario will be 0% CAV penetration at the respective traffic demand with ALL vehicles being HDVs.

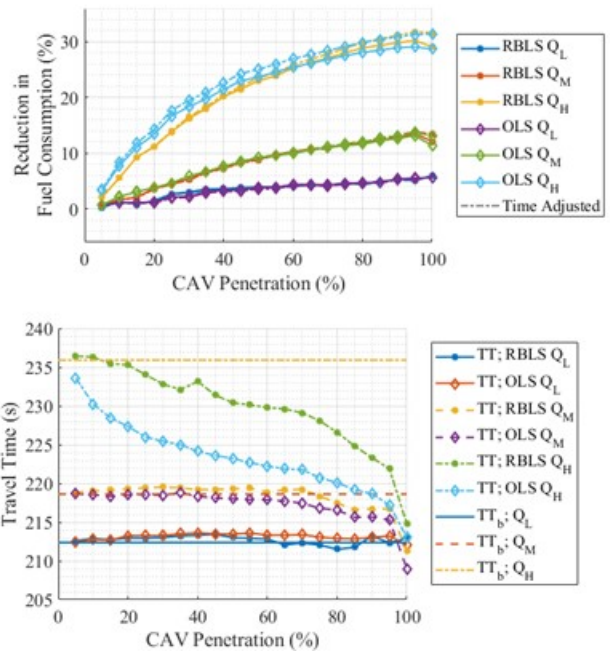


Figure II.1.7.9 Percent Reduction in Fuel Consumption (Top) and Average Travel Time (Bottom) for the Rbls and Ols Methods Compared to the Baseline of 0% Cav Penetration. Note: T_b is the Average Travel Time for the Baseline Scenario

a) Comparison of reference speed assignment methods

Figure II.1.7.10 presents the fuel consumption and travel time results as a percent reduction compared to the baseline for the two reference speed assignment methods. It can be seen that for low traffic demand there is no significant difference between the RBSA and HSA case in the overall network performance in terms of travel time and fuel consumption. At medium traffic demand, there is no significant difference in the realized fuel consumption performance, however, at high CAV penetrations, the HSA CAVs begin to outperform the RSA CAVs. Lastly, at high traffic demand, the HSA CAVs realize a significant performance benefit in terms of travel time at all CAV penetrations. However, a fuel consumption benefit is only observed at low to moderate CAV penetration ($\leq 60\%$ CAVs). For a detailed discussion of the results and comparison of the two methods please see [10].

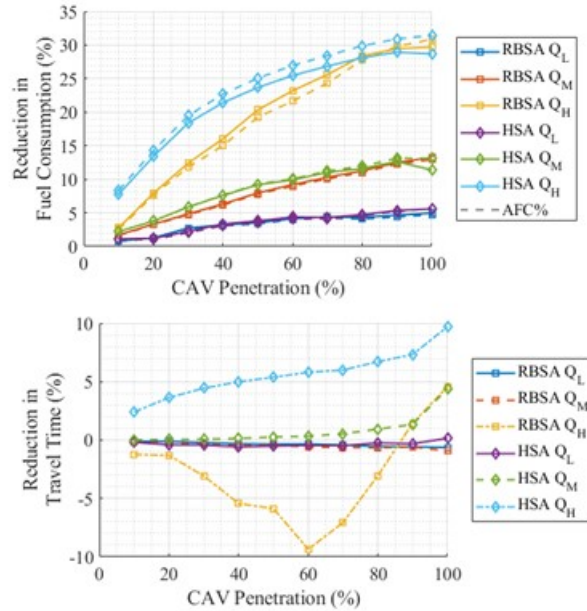


Figure II.1.7.10

b) Isolation of optimal lane selection benefits

Figure II.1.7.11 presents the fuel consumption and travel time results for both the OLS CAVs and RBLS CAVs compared to the baseline. For a brief description of the two CAV control methods please see the Anticipative Lane Selection Approach section. It can be seen that for all traffic demands and CAV penetrations there is not a significant difference in fuel consumption performance between the OLS and RBLS CAVs. However, when comparing the travel time performance, at all CAV penetrations, the OLS control scheme realizes a shorter travel time at high traffic demand. As there is generally a trade-off between travel time and energy consumption, we formulated the time adjust percent reduction in fuel consumption to compensate for this. Observing this in the top of Figure II.1.7.11, adjusting for the travel time does not significantly change the fuel consumption results. The conclusion we can draw from these results is that for the given simulation scenario the longitudinal behavior of CAVs has a much larger impact on the energy consumption of the mixed fleet of vehicles than the lateral behavior. There is ongoing research to investigate if this holds for more complex simulation scenarios with bottlenecks or a disturbance in each lane. For a more complete discussion of these results please see [11].

Instrumenting and Automating the experimental CAVs

The low-level speed control of both experimental CAVs have been improved to achieve better speed and acceleration tracking performance. To improve the performance, the first major change made to the low-level control was replacing the original polynomial surface-based calibration maps with artificial neural network (ANN)-based calibration maps. The ANN-based calibration maps fit the calibration data more precisely, thus improved the performance of the feedforward component of the controller. The second major change made was changing the feedback signal of the PID component of the controller from speed to acceleration. A Kalman filter was introduced to fuse the position information from RTK-GPS with the speed and acceleration information from the inertial navigation system (INS) to get a more precise estimate of vehicle acceleration. This change improved performance of the feedback component of the controller. As a result, the overall performance of the combined low-level feedforward-feedback controller has been massively improved, as shown in Figure II.1.7.11 and Figure II.1.7.12. In the figures, the dashed blue curve shows the actual vehicle speed and acceleration collected on the test track when the vehicles were following virtual vehicles in the front. The black solid curves show the desired speed and acceleration of the vehicle which are calculated by assuming that the deal driving environment is ideal and the acceleration command from the high-level

controller could be executed ideally. Thus, the closer the actual curve is to the desired curve, the better performance the controller can offer. The figures show that the actual speed and acceleration curves are almost overlapped with the desired ones, which indicates a satisfactory controller performance. In this test, the average absolute acceleration tracking error was smaller than 0.2 m/s^2 for both vehicles, which is a huge improvement over the previous low-level controller design.

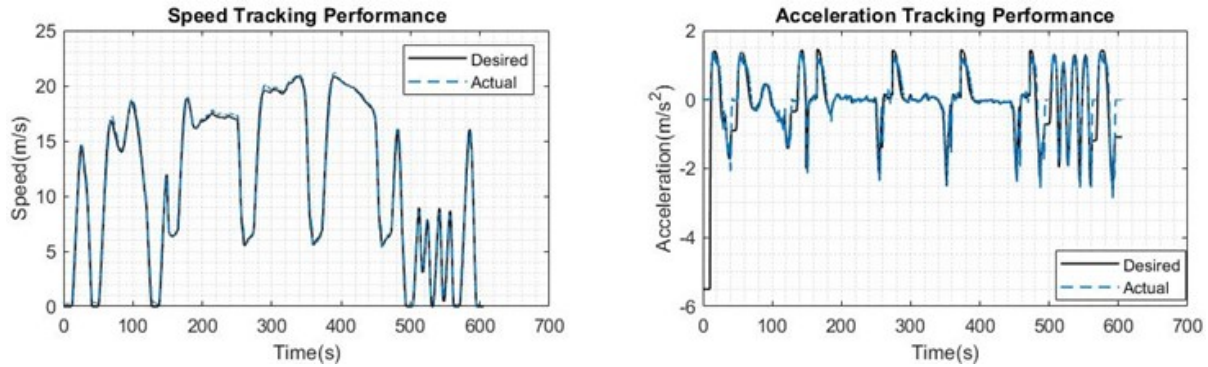


Figure II.1.7.11 Nissan Leaf Tracking Performance

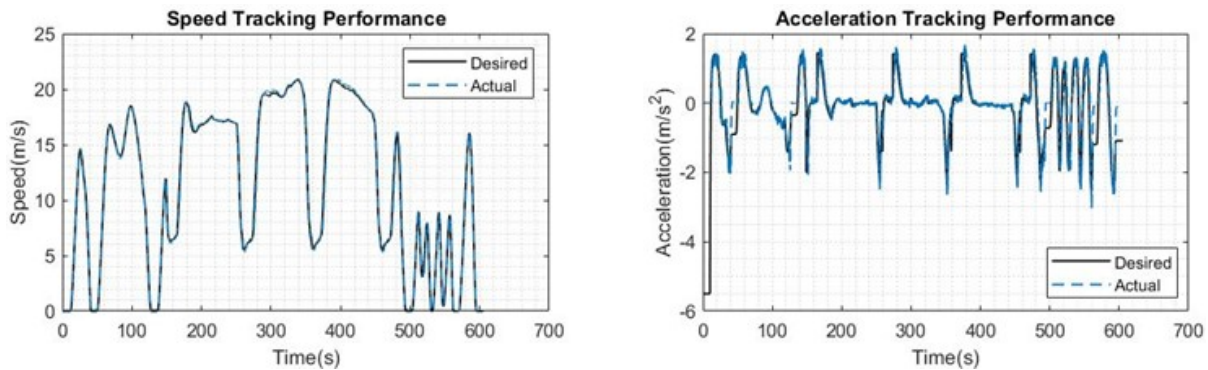


Figure II.1.7.12

Vehicle-in-the-Loop Simulation

The experimental setup as depicted in Figure II.1.7.12 was followed to embed a Mazda and Nissan into VIL simulation. The physical vehicle followed the simulated traffic using high-level controller types of Wiedemann 99 (WIE), Intelligent driver model (IDM), and MPC unconnected (MPC-U). The vehicle-to-vehicle connectivity was also added between the real and simulated vehicle extending the event horizon of the real vehicle for an MPC connected (MPC-C) case. Tables Table II.1.7.2 and Table II.1.7.3 summarize the results of the emergent VISSIM traffic scenario, US06, and UDDS studies for the Mazda and Nissan respectively. It was found that the MPC-U improved energy performance over the WIE baseline by 8 to 12% in the VISSIM scenario, and energy savings potentials were even higher in the representative cycle studies. Energy savings potentials are further improved with connectivity, which further added up to 10% greater energy performance. Overall, it was found that both modes of the MPC had comparable headway performance to the WIE baseline, indicating that traffic flow was similarly comparable. Whereas the IDM had similar energy performance, it exhibited significant loss in headway performance, and hurts traffic flow to negate any benefits. Further discussion can be found in 2019 annual report and [16].

Table II.1.7.2 Combustion Mazda RX7 - Experimental Controller Performance

		WIE	IDM	MPC-U	MPC-C
VISSIM	Avg. Headway [s]	3.47	5.73 +65.1%	3.32 -4.3%	2.75 -20.7%
	Net Fuel [L]	2.556	2.174 -15%	2.241 -12%	1.978 -24%
US06	Avg. Headway [s]	2.45	6.23 +154.3%	2.64 +7.8%	2.66 +8.6%
	Net Fuel [L]	1.006	0.840 -17%	0.746 -26%	0.684 -32%
UDDS	Avg. Headway [s]	3.39	5.94 +75.2%	2.85 -15.9%	3.53 +4.1%
	Net Fuel [L]	1.370	1.329 -3%	1.175 -14%	1.048 -24%

Table II.1.7.3 Electric Nissan Leaf - Experimental Controller Performance

		WIE	IDM	MPC-U	MPC-C
VISSIM	Avg. Headway [s]	3.96	5.81 +46.7%	2.93 -26.0%	2.82 -28.8%
	Net Energy [kwh]	4.090	3.730 -8.8%	3.766 -7.9%	3.247 -20.6%
US06	Avg. Headway [s]	2.14	5.80 +171.0%	2.76 +29.0%	2.58 +20.6%
	Net Energy [kwh]	1.286	1.230 -4%	1.064 -17%	0.963 -25%
UDDS	Avg. Headway [s]	4.22	4.39 +4.0%	2.51 -40.5%	3.15 -25.4%
	Net Energy [kwh]	1.855	1.639 -12%	1.389 -25%	1.221 -34%

Conclusions

We observe that CAVs drive with significant fuel benefit over native VISSIM human drivers in microsimulation studies: When evaluating mid-sized SUVs equipped with a conventional powertrain, we found that MPC vehicles performed at 10% higher energy efficiency over human drivers at low volume, and performed at 20% higher energy efficiency over human drivers at high volume - while improving in throughput of the road over the all-human driver scenario. Secondary effects were seen in that traffic was smoothed to dissipate shockwaves and cut wasteful braking events, and so human driver fuel economy was additionally improved. Overall, up to 25% higher fuel benefits in the entire fleet were observed in all-automated scenarios.

Further energy evaluation was conducted using electric and hybrid powertrains, modeled in Autonomie, as well. Largely due to regenerative braking which improved human driver energy usage, energy improvements because of MPC presence in the fleet were not as pronounced, though we found up to 6% improvement in energy efficiency over human drivers with electric vehicles, and we found up to 9% improvement in energy efficiency over human drivers with hybrid vehicles.

The non-linear programming (NLP) based model predictive control (MPC) lane decision algorithm was also implemented within VISSIM and fuel consumption results were obtained for CAV penetration and traffic flow rates. Experiments were conducted on both a combustion engine vehicle and electric motor vehicle to evaluate their energy and traffic performance using chance-constrained model predictive control for vehicle guidance. Both vehicles were equipped for autonomy by fitting pedal and steering actuators to control their acceleration and pose. In particular, a novel data-driven approach to vehicle pedal control was executed and fused classical methods with a feedforward map to approximate the powertrain nonlinearities.

A Vehicle-in-the-Loop environment was designed to embed a physical vehicle into virtual reality with simulated traffic. Three separate experimental scenarios were designated to cover a variety of traffic conditions: a microsimulation experiment was conducted to study emergent highway-conditioned car-following, the US06 was simulated for the preceding vehicle to stimulate aggressive acceleration, and the UDDS was simulated for the preceding vehicle to create urban conditions.

The MPC is designed to minimize commanded acceleration and error in headway tracking for each CAV. When following another MPC vehicle it leverages connectivity to better plan control decisions, and in the absence of connectivity it quantifies uncertainty in prediction of the front human driver to balance safety with traffic compactness. It was found the MPC outperformed the human-like driver models with regards to both realized headway and energy economy. Overall, the microsimulation experiment showed the MPC improved

energy efficiency by 12% and 8% for the combustion and electric vehicles when following human drivers. Benefits were even greater in the drive cycle studies, where the US06 showed 26% and 17% improved energy efficiency for the combustion and electric vehicles, whereas the UDDS showed 14% and 25% improved energy efficiency for the combustion and electric vehicles. Finally, once introducing connectivity, between 6-12% additional improvement in energy efficiency was found for the MPC compared with its unconnected variant. We also estimated secondary impacts of connectivity on traffic upstream of the ego vehicle, and found that 4.5% energy benefit was achieved for the 11 following drivers on average.

Key Publications

1. R. Austin Dollar, and Ardalan Vahidi. "Quantifying the impact of limited information and control robustness on connected automated platoons." In *Intelligent Transportation Systems (ITSC), 2017 IEEE 20th International Conference on*, pp. 1–7. IEEE, 2017.
2. R. Austin Dollar, and Ardalan Vahidi. "Efficient and Collision-Free Anticipative Cruise Control in Randomly Mixed Strings." *IEEE Transactions on Intelligent Vehicles*, vol. 3, no. 4, pp. 439–452 (2018).
3. R. Austin Dollar, and Ardalan Vahidi. "Automated Vehicles in Hazardous Merging Traffic: A Chance-Constrained Approach."* In *IFAC-PapersOnLine* 52, no. 5 (2019): 218–223.
4. R. Austin Dollar, and Ardalan Vahidi. "Predictively Coordinated Vehicle Acceleration and Lane Selection Using Mixed Integer Programming."** In *Proceedings of the ASME DSCC*, 2018.
5. R. Austin Dollar, and Ardalan Vahidi. "Automated Driving with Variational Optimal Control and Mixed Integer Programming." In review, *IEEE Transactions on Control Systems Technology* (2019).
6. R. Austin Dollar, Antonio Sciarretta, and Ardalan Vahidi. "Multi-Agent Control of Lane-Switching Automated Vehicles for Energy Efficiency." In *2020 American Control Conference*, 2020.
7. R. Austin Dollar, Antonio Sciarretta, and Ardalan Vahidi. "Information and Collaboration Levels in Vehicular Strings: A Comparative Study." Presented, *IFAC World Congress 2020*, 2020.
8. T. Ard, R. A. Dollar, D. Karbowski, Y. Zhang, and A. Vahidi. "Microsimulation of Energy and Flow Effects from Optimal Automated Driving in Mixed Traffic." *Transportation Research Part C: Emerging Technologies* 120, (2020): 102806.
9. N. Goulet and B. Ayalew. "Coordinated Model Predictive Control on Multi-lane Roads." *Proceedings of the ASME 2019 International Design Engineering Technical Conferences & Computers and Information in Engineering Conference*, DETC2019-98117, August 18–21, 2019, Anaheim, CA.
10. N. Goulet and B. Ayalew. "Impacts of Distributed Speed Harmonization and Optimal Maneuver Planning on Multi-Lane Roads." *2020 Conference on Control Technologies and Applications*.
11. N. Goulet and B. Ayalew. "Distributed Maneuver Planning with Connected and Automated Vehicles for Boosting Traffic Efficiency." *In review*, *IEEE Transactions on Intelligent Transportation Systems*.
12. X. Wang, L. Guo and Y. Jia, "Human Intervention Detection on a Retrofit Steering Actuation System in Autonomous Vehicles," *SAE Technical Paper*, 2018. (Trevor O. Jones Outstanding Paper Award)
13. X. Wang, L. Guo and Y. Jia, "Online Sensing of Human Steering Intervention Torque for Autonomous Driving Actuation Systems," *IEEE Sensors Journal*, vol. 18, no. 8, pp. 3444–3453, 2018.
14. G. G. M. Nawaz Ali, Beshah Ayalew, Ardalan Vahidi, and Md. Noor-A-Rahim, "Analysis of Reliabilities Under Different Path Loss Models in Urban/Sub-urban Vehicular Networks", to appear,

Proceedings of IEEE 90th Vehicular Technology Conference (IEEE VTC-Fall'19), Honolulu, HI, 2019.

15. G. G. M. Nawaz Ali, Beshah Ayalew, Ardalan Vahidi, and Md. Noor-A-Rahim, "Feedbackless Relaying for Enhancing Reliability of Connected Vehicles," in review, IEEE Transactions on Vehicular Technology, 2019.
16. T. Ard, L. Guo, R. A. Dollar, A. Fayazi, N. Goulet, Y. Jia, B. Ayalew, and A. Vahidi. "Energy and Flow Effect from Optimal Automated Driving in Mixed Traffic: Vehicle-in-the-loop experimental results." *Transportation Research Part C: Emerging Technologies*, in review, 2020.

* Young Author Award

** Automotive and Transportation Systems Best Paper Award

References

1. Q. Wang, B. Ayalew, and T. Weiskircher, "Optimal assigner decisions in a hybrid predictive control of an autonomous vehicle in public traffic," in 2016 American Control Conference (ACC), 2016, vol. 2016–July, pp. 3468–3473.
2. S. A. Fayazi, A. Vahidi, and A. Luckow, "A Vehicle-in-the-loop (VIL) Verification of an all-Autonomous Intersection Control Scheme," *Transportation Research Part C: Emerging Technologies, Special Issue on CAV Control*, vol. 107, pp. 193–210, Oct. 2019.
3. OBD Log iOS Application introduction, available online: <https://youtu.be/7zWhUk7hEZQ>
4. AVL KMA Mobile fuel consumption measurement system, <https://www.avl.com/-/avl-kma-mobile>
5. R. Quirynen, M. Vukov, M. Zanon, and M. Diehl, "Autogenerating microsecond solvers for nonlinear MPC: A tutorial using ACADO integrators," *Optim. Control Appl. Methods*, vol. 36, no. 5, pp. 685–704, Sep. 2015.
6. "ELM327, OBD to RS232 interpreter," ELM Electronics, 2012, available online: www.elmelectronics.com/DSheets/ELM327DS.pdf
7. iSmartWays Technology Inc., <http://www.ismartways.com/>
8. The Federal Test Procedure (FTP), <https://www.epa.gov/vehicle-and-fuel-emissions-testing/dynamometer-drive-schedules>
9. The EPA US06 or Supplemental Federal Test Procedures (SFTP), <https://www.epa.gov/emission-standards-reference-guide/epa-us06-or-supplemental-federal-test-procedures-sftp>
10. PTV Group, "PTV Vissim 10 User Manual," 2018.

Acknowledgements

The Principal Investigators would like to acknowledge the critical work of the other authors of this work: R. Austin Dollar, Tyler Ard, Ali Reza Fayazi, Longxiang Guo, Nathan Goulet, and G. G. Md. Nawaz Ali. The collaborative guidance algorithm discussion in the "Collaborative Multilane Guidance" subsection was developed jointly with IFP Energies nouvelles under the joint supervision of Antonio Sciarretta and Ardalan Vahidi.

(This page intentionally left blank)

U.S. DEPARTMENT OF
ENERGY

Office of
**ENERGY EFFICIENCY &
RENEWABLE ENERGY**

For more information, visit:
energy.gov/eere/vehicles

DOE/EE-2333 • June 2021